ACTA PHYSICA

ACADEMIAE SCIENTIARUM HUNGARICAE

ADIUVANTIBUS
L. JÁNOSSY, I. KOVÁCS, K. NAGY, A. SZALAY

HUNC TOMUM CURAVIT
I. KOVÁCS

TOMUS XXVII FASCICULI 1—4

AKADÉMIAI KIADÓ, BUDAPEST
1969

ACTA PHYS. HUNG.

ACTA PHYSICA

A MAGYAR TUDOMÁNYOS AKADÉMIA FIZIKAI KÖZLEMÉNYEI

SZERKESZTŐSÉG ÉS KIADÓHIVATAL: BUDAPEST V., ALKOTMÁNY UTCA 21.

Az *Acta Physica* német, angol, francia és orosz nyelven közöl értekezéseket a fizika tárgyköréből.

Az *Acta Physica* változó terjedelmű füzetekben jelenik meg: több füzet alkot egy kötetet.

A közlésre szánt kéziratok a következő címre küldendők:

Acta Physica, Budapest 502, P. O. B. 24.

Ugyanerre a címre küldendő minden szerkesztőségi és kiadóhivatali levelezés.

Az *Acta Physica* előfizetési ára kötetenként belföldre 120 forint, külföldre 165 forint. Megrendelhető a belföld számára az Akadémiai Kiadónál (Budapest V., Alkotmány utca 21. Bankszámla 05-915-111-46), a külföld számára pedig a „Kultúra" Könyv- és Hírlap Külkereskedelmi Vállalatnál (Budapest I., Fő u. 32. Bankszámla 43-790-057-181 sz.), vagy annak külföldi képviseleteinél és bizományosainál.

Die *Acta Physica* veröffentlichen Abhandlungen aus dem Bereich der Physik in deutscher, englischer, französischer und russischer Sprache.

Die *Acta Physica* erscheinen in Heften wechselnden Umfanges. Mehrere Hefte bilden einen Band.

Die zur Veröffentlichung bestimmten Manuskripte sind an folgende Adresse zu richten:

Acta Physica, Budapest 502, P. O. B. 24.

An die gleiche Anschrift ist auch jede für die Redaktion und den Verlag bestimmte Korrespondenz zu senden.

Abonnementspreis pro Band: 165 Forint. Bestellbar bei dem Buch- und Zeitungs-Aussenhandels-Unternehmen »Kultúra« (Budapest I., Fő u. 32. Bankkonto Nr. 43-790-057-181) oder bei seinen Auslandsvertretungen und Kommissionären.

ACTA PHYSICA

ACADEMIAE SCIENTIARUM HUNGARICAE

ADIUVANTIBUS
L. JÁNOSSY, I. KOVÁCS, K. NAGY, A. SZALAY

HUNC TOMUM CURAVIT
I. KOVÁCS

TOMUS XXVII

AKADÉMIAI KIADÓ, BUDAPEST
1969

ACTA PHYS. HUNG.

THIS VOLUME OF
ACTA PHYSICA HUNGARICA IS DEDICATED TO
PROF. P. GOMBÁS
ON THE OCCASION OF HIS SIXTIETH BIRTHDAY

Acta Physica Academiae Scientiarum Hungaricae, Tomus 27, pp. 5—10 (1969)

GENERAL FORM OF THE CENTRIFUGAL TERM IN THE ROTATIONAL SPECTRA*

By

I. Kovács

DEPARTMENT OF ATOMIC PHYSICS, POLYTECHNICAL UNIVERSITY, BUDAPEST

(Received 28. XI. 1967)

The explicit form of the centrifugal term is known so far only for the Hund's limiting cases. The present paper presents its explicit form in the intermediate case between Hund's case a) and b) for terms of any kind.

At the theoretical examination of the structure of the rotational spectra of diatomic molecules several interactions must be taken into consideration simultaneously by means of the perturbation calculation. These are the terms omitted at the separation of the wave equation, the terms of the spin—orbit, spin—spin and rotation—spin interactions, as well as the non-diagonal terms of the centrifugal term. The simultaneous taking into consideration of all these terms would make the final form of the multiplet formulae very complicated. Since the perturbation between the multiplet components and the spin—orbit interaction is commonly larger than the others, it seems suitable to consider first these interactions by means of the perturbation calculation (these give the well-known multiplet formulae) and then the remainder by a method of approach which gives the terms derived from the last interactions in additive form to the multiplet formulae already established. Such a consideration of the spin—spin interaction, as well as the interaction between the rotation and spin is already well known [1],[2]. In the case of the spin—spin interaction a number of the experimental examples showed a good agreement with the theoretical results. In the present paper the same procedure is applied for the case of the centrifugal term. By establishing the form of the centrifugal term for the Hund's case a) and b), as well as the non-diagonal perturbation matrix elements, the form of the centrifugal term may be given in this way in the intermediate cases between Hund's case a) and b), for terms of any kind and multiplicity.

Let H_0 denote the energy operator of the separable wave equation and H^p, on the one hand, the perturbation operator of the terms of higher order of magnitude neglected at the separation, which describes the perturbation

* This paper is dedicated to my friend, Academician PÁL GOMBÁS, on the occasion of his sixtieth birthday, as a mark of my high esteem and heartfelt feelings. I wish him all further success in his activities and a long life.

between the components of the same multiplet term, and on the other hand, the perturbation operator of a higher order of magnitude of the spin–orbit interaction. $\bar{H}^p$ should denote the perturbation operator of the smaller interactions (e.g. centrifugal term, spin—spin or rotation—spin interaction) to be taken into account later.

$$(H' + \bar{H}^p - W_i'')\,\psi_i'' = 0\,, \tag{1}$$

where $H' = H_0 + H^p$ and $W_i'' = W_i' + \Delta W_i'$. Here ψ_i'' is the new perturbed wavefunction, and W_i' the eigenvalue of the operator H', and this represents the well-known multiplet formulae. If $\bar{H}^p$ is small (as according to the experiments the value of the centrifugal term, the spin—spin interaction and interaction between the rotation and spin is small compared with, for instance, the spin–orbit interaction which gives the greatest part of the multiplet splitting) then $\Delta W_i'$ is also small and no great error is committed if ψ_i'' is replaced by ψ_i', the already once perturbed wave function of the operator H'. Thus, let $\psi_i'' \approx \psi_i'$. Then, since

$$(H' - W_i')\,\psi_i' = 0 \tag{2}$$

with a good approximation it can often be written (1) and (2) that

$$(\bar{H}^p - \Delta W_i')\,\psi_i' = 0 \tag{3}$$

and

$$\Delta W_i' = \int \psi_i^{*\prime}\,\bar{H}^p\,\psi_i'\,d\tau\,, \tag{4}$$

respectively.

It is known, however, that $\psi_i' = \sum_k S_{ik}\psi_k$, where ψ_k is the unperturbed wavefunction of the operator H_0 and S_{ik} the elements of the transformation matrix, arising from taking into account the operator H^p. The latter are known explicitly for the doublet, triplet, and quartet terms as functions of the rotation quantum number for all kinds of terms. By the use of this (4) can be written

$$\Delta W_i' = \sum_k S_{ik}^* \sum_l S_{lk}\,\bar{H}_{kl}^p \tag{5}$$

and

$$\bar{H}_{kl}^p = \int \psi_k^*\,\bar{H}^p\,\psi_l\,d\tau\,. \tag{6}$$

Applied to the spin–spin interaction this formula could, in many cases, excellently interpret the deviations from the usual multiplet formulae even if the terms mentioned belong not to Hund's limiting cases, but to the intermediate case. This can be seen in the cases of the $^3\Pi$ terms of the NH, PH, PF and TiO molecules, respectively, of one $^3\Delta$ term of the CO molecule and of one $^4\Pi$ term of the O_2^+ molecule [3].

As is known, with the increase of the rotation of the molecule the equilibrium nuclear distance becomes greater which is manifested in the apparent decrease of the rotational constant, or an additional term is attached to the energy expression, the form of which in Hund's case b) is as follows:

$$H_b^c(\Lambda, N; \Lambda, N) = -D\vec{R}^4 = -D\,[\vec{N}^2 - \Lambda^2]^2 = -D\,[N(N+1) - \Lambda^2]^2, \quad (7)$$

where N is the rotational quantum number in case b), Λ is the projection along the molecular axis of the resulting orbital angular momentum, and D the constant of the centrifugal term. However, (7) is exact only when the electron spin is coupled to the vector $\vec{N}$. If we want to follow the process of the suc-

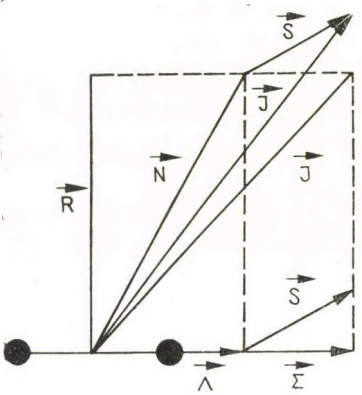

Fig. 1

cessive decoupling from the molecular axis and the coupling to vector $\vec{N}$, the perturbation calculation of quantum mechanics has to be employed. This, however, requires a knowledge of the perturbation matrix element. For its calculation let us start from (7) by expressing the vector $\vec{N}$ by vectors $\vec{J}$ and $\vec{S}$. On the basis of the Figure it can be seen that

$$\begin{aligned} H^c &= -D[\vec{N}^2 - \Lambda^2]^2 = -D[(\vec{J} - \vec{S})^2 - \Lambda^2]^2 = -D[\vec{J}^2 + \vec{S}^2 - \Lambda^2 - 2(\vec{J}\vec{S})]^2 = \\ &= -D[\vec{J}^2 + \vec{S}^2 - \Lambda^2 - 2J_\zeta S_\zeta - 2(J_\xi S_\xi + J_\eta S_\eta)]^2 = \\ &= -D\{[\vec{J}^2 + \vec{S}^2 - \Lambda^2 - 2J_\zeta S_\zeta]^2 + \\ &\quad + 4(J_\xi S_\xi + J_\eta S_\eta)^2 - 4(J^2 + S^2 - \Lambda^2)(J_\xi S_\xi + J_\eta S_\eta) + \\ &\quad + 4J_\zeta S_\zeta (J_\xi S_\xi + J_\eta S_\eta) + 4(J_\xi S_\xi + J_\eta S_\eta) J_\zeta S_\zeta\}. \end{aligned} \quad (8)$$

In the course of the detailed calculation, by making use of a few of the well-known relationships pertaining to the characteristics of quantum vectors,

the following matrix elements are given which hold good for a term of any multiplicity and type:

$$H_a^c(\Omega,\Sigma;\Omega\Sigma) = -D\{[f(J)+f(S)]^2+2f(J)f(S)+2\Omega\Sigma\},$$
$$H_a^c(\Omega,\Sigma;\Omega\pm1,\Sigma\pm1) = -2D[f(J,\Omega)+f(S,\Sigma)-1]\{f(J,\Omega)f(S,\Sigma)\}^{1/2}, \quad (9)$$
$$H_a^c(\Omega,\Sigma;\Omega\pm2,\Sigma\pm2) = -D\{f(J,\Omega)f(J,\Omega\pm1)f(S,\Sigma)f(S,\Sigma\pm1)\}^{1/2},$$

where

$$f(x) = x(x+1)-\bar{x}^2,$$
$$f(x,\bar{x}) = x(x+1)-\bar{x}(\bar{x}\pm1), \quad (9a)$$
$$f(x,\bar{x}\pm1) = x(x+1)-(\bar{x}\pm1)(\bar{x}\pm2),$$

and $\bar{x}$ is the component of x along the molecular axis. It can be seen that taking into account the decoupling of the spin also modifies the diagonal term corresponding to case a) which has been expressed so far in the form

$$-D[J(J+1)-\Omega^2]^2. \quad (10)$$

Taking into account (9) on the basis of (5) for doublet term leads to the following expression for the centrifugal term in the intermediate case between Hund's cases a) and b)

$$H_N^c(J) = -D\{J_\Lambda^2(J_\Lambda^2+1)+\Lambda^2+ \\ +2\Lambda J_\Lambda^2(S^2_{\Lambda-1/2,N}-S^2_{\Lambda+1/2,N})-4S_{\Lambda+1/2,N}S_{\Lambda-1/2,N}J_\Lambda^3\}, \quad (11)$$

where $N = J-1/2$ and $J+1/2$, respectively, the forms of S are known [4] and

$$J_\Lambda^2 = (J+1/2)^2-\Lambda^2. \quad (11a)$$

(11) is simply to be added to the well-known HILL and VAN VLECK doublet formula. ALMY and HORSFALL [5] have produced (9) for a special case, namely, that of $^2\Pi$ terms, but did not give a solution on the basis of (5), but solved the secular equation supplemented by them (i.e. (9)) directly which broke up the structure of the original HILL and VAN VLECK formula and resulted in a complicated expression difficult to handle. This is further complicated in the case of higher multiplets, and, in addition, if further corrections are taken into account (e.g. spin—spin interaction, rotation—spin interaction), the whole process has to be started again and it is rather difficult to see the actual effects of the respective corrections. These hindrances can be avoided by the application of (5), since the corrections thus calculated are given in an additive way to the well-known multiplet formulae and their respective effects can be studied separately (cf. the result shown at the spin—spin interaction). That these state-

ments are valid can be seen from the fact that with the procedure mentioned for doublet terms GILBERT [6] was not able to supply explicit formulae for the case of $^3\Pi$ terms for centrifugal corrections, only a procedure for determining the multiplet splitting constant A.

By the use of (5) and (9) the intermediate form of the centrifugal correction valid for all triplet terms can easily be given. This will be

$$H_N^c(J) = S^2_{\Lambda+1,N}\, H^c_{\Lambda+1,\Lambda+1} + S^2_{\Lambda,N}\, H^c_{\Lambda,\Lambda} + S^2_{\Lambda-1,N}\, H^c_{\Lambda-1,\Lambda-1} + \tag{12}$$
$$+ 2\, S_{\Lambda+1,N}\, S_{\Lambda,1}\, H^c_{\Lambda+1,\Lambda} + 2\, S_{\Lambda,N}\, S_{\Lambda-1,N}\, H^c_{\Lambda,\Lambda-1} + 2 S_{\Lambda+1,N}\, S_{\Lambda-1,N}\, H^c_{\Lambda+1,\Lambda-1},$$

where $N = J-1, J, J+1$, and the elements of H^c are to be taken from (9), and the explicit forms of S are already known [7]. (12) is simply to be added to the BUDÓ triplet formula. Substituting $Y = 0$ into (12) it is transformed into (7), whereas for $Y \to \infty$ it supplies the diagonal elements of (9).

The calculation may be carried out in a similar way for a quartet case. Then we obtain:

$$\begin{aligned} H_N^c(J) = {} & S^2_{\Lambda+3/2,N}\, H^c_{\Lambda+3/2,\Lambda+3/2} + S^2_{\Lambda+1/2,N}\, H^c_{\Lambda+1/2,\Lambda+1/2} + S^2_{\Lambda-1/2,N}\, H^c_{\Lambda-1/2,\Lambda-1/2} + \\ & + S^2_{\Lambda-3/2,N}\, H^c_{\Lambda-3/2,\Lambda-3/2} + 2\, S_{\Lambda+3/2,N}\, S_{\Lambda+1/2,N}\, H^c_{\Lambda+3/2,\Lambda+1/2} + \\ & + 2\, S_{\Lambda+1/2,N}\, S_{\Lambda-1/2,N}\, H^c_{\Lambda+1/2,\Lambda-1/2} + 2\, S_{\Lambda-1/2,N}\, S_{\Lambda-3/2,N}\, H^c_{\Lambda-1/2,\Lambda-3/2} + \\ & + 2\, S_{\Lambda+3/2,N}\, S_{\Lambda-1/2,N}\, H^c_{\Lambda+3/2,\Lambda-1/2} + 2\, S_{\Lambda+1/2,N}\, S_{\Lambda-3/2,N}\, H^c_{\Lambda+1/2,\Lambda-3/2}, \end{aligned} \tag{13}$$

where $N = J - 3/2, J - 1/2, J + 1/2, J + 3/2$, and the elements of H^c are to be taken from (9), while the forms of the S transformation matrix elements for $^4\Pi$ term are already known [8].

By taking all these into account the complete multiplet formulae can be written as follows:

$$F_N(J) = T_N(J) + H_N^c(J) + H_N^{SS}(J) + H_N^{SR}(J), \tag{14}$$

where $T_N(J)$ denotes the usual multiplet formula (for doublet term the known HILL and van VLECK, for triplet term the BUDÓ and for quartet term the BRANDT formulae), $H_N^c(J)$ is the centrifugal correction of a general form given just above, $H_N^{SS}(J)$ is the general form of the spin—spin interaction and lastly $H_N^{SR}(J)$ that of the interaction between rotation and spin. All the four terms refer to the intermediate case between Hund's cases a) and b).

Adopting the procedure written here the calculation for the centrifugal term of the intermediate case between Hund's cases b) and d) may also be carried out. From these the forms calculated for the p- and d-terms-complexes can be found in the author's book [9].

REFERENCES

1. I. Kovács, Acta Phys. Hung., **17,** 67, 1964, Rev. Roum. de Chim., **10,** 1173, 1965.
2. I. Kovács, Opt.-i Spektr. USSR, **12,** 17, 1962.
3. I. Kovács, Acta Phys. Hung., **12,** 67, 1960 (NH); **13,** 303, 1961 (PH); **18,** 107, 1965 (CO); Can. J. Phys., **42,** 2180, 1964 (PF); J. Mol. Spectr., **18,** 229, 1965 (TiO); Á. Budó and I. Kovács, Acta Phys. Hung., **4,** 273, 1954; I. Kovács and S. Weniger, Journ. de Phys., **23,** 377, 1962 (O_2^+).
4. E. L. Hill and J. H. Van Vleck, Phys. Rev. **32,** 250, 1928.
5. G. Almy and R. B. Horsfall, Phys. Rev., **51,** 491, 1937.
6. C. Gilbert, Phys. Rev., **49,** 619, 1936.
7. Á. Budó, Zs. f. Phys. **105,** 579, 1937; I. Kovács, Can. J. Phys., **38,** 955, 1960.
8. Á. Budó and I. Kovács, Phys. Z., **65,** 122, 1944.
9. I. Kovács, Rotational Structure in the Spectra of Diatomic Molecules. a. p. Akadémiai Kiadó Budapest, and Adam Hilger Ltd., London 1969.

ОБЩАЯ ФОРМА ЦЕНТРОБЕЖНОГО ЧЛЕНА В РОТАЦИОННОМ СПЕКТРЕ

И. КОВАЧ

Р е з ю м е

Явная форма центробежного члена известна до сих пор только в предельных случаях Гунда. В данной работе дается его явная форма в промежуточном случае между случаем Гунда *а)* и *б)* членов любого вида.

Acta Physica Academiae Scientiarum Hungaricae, Tomus 27, pp. 11—18 (1969)

RADIATIVE CORRECTIONS TO MUON DECAY WITH FINITE NEUTRETTO MASS*

By

F. CSIKOR and K. NAGY

INSTITUTE FOR THEORETICAL PHYSICS, ROLAND EÖTVÖS UNIVERSITY, BUDAPEST

(Received 23. I. 1968)

Radiative corrections to muon decay are calculated, assuming a finite neutretto mass. The corrections are shown to be free of infra-red divergences even at the end point of the spectrum.

1. Introduction

Recent measurements [1] indicate an upper limit of 1—2 MeV for the mass of the neutretto. Several authors [2] have suggested that an upper limit can be set on the neutretto mass by observing the shape of the electron energy spectrum near the high-energy end in the muon decay. In fact, the shape of the spectrum is more sensitive to the mass m_ν' of the neutretto than the end-point itself. The spectrum is given by the formula

$$P(E)\,dE = \frac{g^2 m_\mu^5}{(2\pi)^3\,12}\sqrt{E^2 - l^2}\left\{(El^2 + E - 2l^2)\left(1 - \frac{3n^4}{m^2} + \frac{2n^6}{m^3}\right) - \right.$$

$$\left. - E\left(-2m + 3n^2 - \frac{n^6}{m^2}\right)\right\} dE, \qquad (1)$$

where $m = 1 + l^2 - 2E$, and the electron energy E, as well as the electron and the neutretto masses l, n are expressed in terms of the muon mass. The spectrum (1) is shown in Fig. 1 for some values of m_ν'.

We see that for $m_\nu' = 0$ the spectrum gives a finite value for the maximal electron energy, meanwhile it gives zero for $m_\nu' \neq 0$. This seems to be extremely favourable for the determination of m_ν'. However, if radiative corrections are taken into account, the spectrum decreases for high energies even in the $m_\nu' = 0$ case. In fact, because of uncancelled infra-red divergences for $m_\nu' = 0$ the spectrum tends to minus infinity at the upper end [3] (Fig. 3).

In this note we give the radiative corrections for the $m_\nu' \neq 0$ case, and show that they are not divergent at the upper end of the spectrum, but give exactly zero.[1]

* Dedicated to Prof. P. GOMBÁS on his 60th birthday.

[1] This fact has not been observed in [7], where the same problem is treated in a certain approximation.

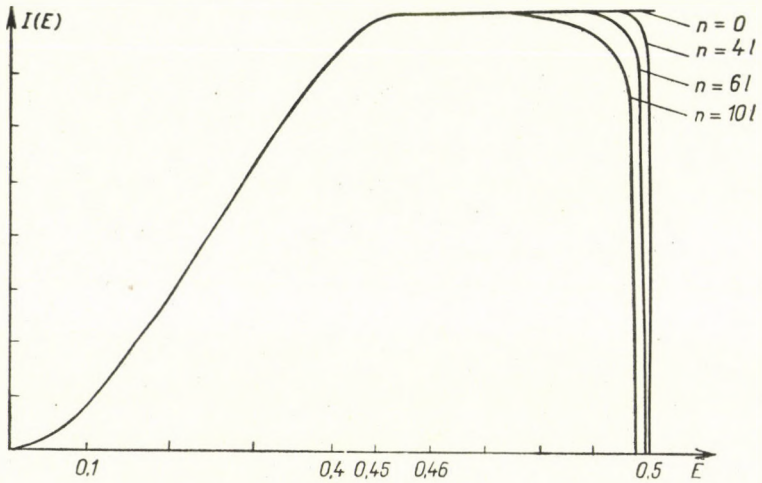

Fig. 1

2. The electron spectrum

The interaction responsible for the decay of muon is

$$H_{\text{int}} = g\left(\overline{\psi}_e \gamma_i \frac{1+\gamma_5}{2}\psi_\nu\right)\left(\overline{\psi}_\nu \gamma_i \frac{1+\gamma_5}{2}\psi_\mu\right) + \\ + ie\,\overline{\psi}_e \gamma_i \psi_e A_i + ie\,\overline{\psi}_\mu \gamma_i \psi_\mu A_i, \tag{2}$$

where $\psi_\mu, \psi_e, \psi_\nu, \psi_\nu$, are the Dirac field operators of muon, electron, neutrino and neutretto, respectively; A_i is the electromagnetic field. We use hermitic Dirac matrices, with the commutation rule $\{\gamma_i, \gamma_k\} = 2\,\delta_{ik}$ $(i, k = 1, \ldots 4)$. The graphs giving contributions to the electron spectrum up to second order in e are shown in Fig. 2.

Fig. 2a gives the uncorrected spectrum, Fig. 2b the inner Bremsstrahlung correction, and Fig. 2c the virtual photon corrections.

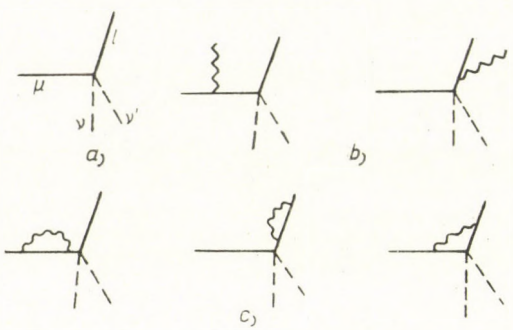

Fig. 2

It is convenient to reorder the weak part of the Hamiltonian (2) by means of a Fierz transformation (4) which yields

$$H_{int} = g\left(\overline{\psi}_e \gamma_i \frac{1+\gamma_5}{2} \psi_\mu\right)\left(\overline{\psi}_\nu \gamma_i \frac{1+\gamma_5}{2} \psi_\nu\right) + \\ + ie\,\overline{\psi}_e \gamma_i \psi_e A_i + ie\,\overline{\psi}_\mu \gamma_i \psi_\mu A_i. \tag{3}$$

In this form the neutrino part of the matrix element can be calculated independently of the rest of the matrix element. Let us calculate it in detail. The matrix element assumes the form

$$M = C_a N_a \delta^4 (q - p^\nu - p^{\nu'}) \tag{4}$$

where N_a is the neutrino part of the matrix element; $N_a = \bar{u}_\nu \gamma_a \frac{1+\gamma_5}{2} v_\nu$ and $p^{\nu'}$, p^ν mean the neutretto and the neutrino four momenta, respectively. The value of q is $p^\mu - p^e$ for the graphs of Fig. 2a, c and $p^\mu - p^e - k$ for Fig. 2b (k is the photon momentum). Summing over the spins we get

$$\sum_{Spin} N_a N_b^* = \frac{2}{E^{\nu'} E^\nu}\left(p_a^{\nu'} p_b^\nu + p_b^{\nu'} p_a^\nu - \delta_{ab} p_i^{\nu'} p_i^\nu - \right. \\ \left. - p_c^{\nu'} p_d^\nu \varepsilon_{abcd} - 2\delta_{b4}\,(b=4)\right), \tag{5}$$

where $E^{\nu'}, E^\nu$ mean the neutretto and neutrino energies, respectively. By $(b=4)$ we denote all the terms standing before, taken at $b=4$. ε_{abcd} is the Levi—Civita symbol.

Carrying out the integration over the neutrino and neutretto momenta we encounter with integrals of the following type

$$I_{ab} = \int d^3 p^\nu\, d^3 p^{\nu'}\, \delta^4 (q - p^\nu\, p^{\nu'}) \frac{p_a^\nu p_b^{\nu'}}{E^\nu E^{\nu'}} . \tag{6}$$

Using the relativistic properties of I_{ab} we easily find

$$I_{ab} = -\frac{\pi}{2}(q_i q_i + n^2)^2 \left(-\frac{2q_a q_b}{(q_i q_i)^2} + \frac{4q_a q_b - q_i q_i \delta_{ab}}{3(q_i q_i)^2}(q_i q_i + n^2)\right). \tag{7}$$

Using (7) we get integrating (5)

$$N_{ab} = \Sigma \iint N_a N_b^* \delta^4 (q - p^\nu - p^{\nu'}) \frac{d^3 p^\nu\, d^3 p^{\nu'}}{(2\pi)^6} = \\ = \frac{2}{(2\pi)^6}\left(2A q_a q_b + B\,\delta_{ab} - 2\delta_{ab}(b=4)\right) \\ \text{with} \quad A = \frac{\pi}{3}\left(1 - \frac{3n^4}{(q_i q_i)^2} - \frac{2n^6}{(q_i q_i)^3}\right), \tag{8} \\ B = -\frac{\pi}{3}\left(2q_i q_i + 3n^2 - \frac{n^6}{(q_i q_i)^2}\right).$$

Our next task would be to evaluate $C_a C_b^* N_{ab}$ for all the graphs (taking into account also the cross terms between the different graphs), to carry out the electron spin summation, to average for the muon spin and integrate over the electron direction. For the inner bremsstrahlung contribution we must average over the photon polarisation and integrate over the photon momentum, too. The calculation is rather lengthy, so we give no details, only make some remarks.

There is no problem with ultra-violet divergence, as the theory is renormalizable [5]. Nevertheless, infra-red divergences occur. They are removed in the usual way by introducing a finite photon mass λ. Naturally λ occurring in the inner bremsstrahlung correction cancels exactly against the infrared divergences in the virtual photon corrections. It is rather satisfactory that after this cancellation there remains no infrared divergence in the electron energy spectrum in the case $m_\nu' \neq 0$, to be contrasted with the case $m_\nu' = 0$. (This point will be discussed in some detail later.) Integration according to k was carried out with special care, taking the $\lambda \to 0$ limit only after the integration. Our result is

$$P(E)\,dE = \frac{g^2 m_\mu^5}{(2\pi)^3 \cdot 4}\, p dE \left\{ P_0 - \frac{\alpha}{4\pi}(A + B) \right\} = \frac{g^2 m_\mu^5}{(2\pi)^3\, 4}\, I(E)\,dE, \qquad (9)$$

where P_0 is the uncorrected spectrum, A the virtual photon correction, B the inner bremsstrahlung correction.

$$P_0 = \frac{1}{3}(l^2 E + E - 2l^2)\left(1 - \frac{3n^4}{m^2} + \frac{2n^6}{m^3}\right) - \frac{E}{3}\left(-2m + 3n^2 - \frac{n^6}{m^2}\right),$$

where $m = 1 + l^2 - 2E$; E and p are the electron energy and momentum. l, n are the rest masses of electron and neutretto, respectively, expressed in terms of the muon mass.

$$A = -\frac{4E}{p} P_0 \Bigg[L\left(\frac{-2p}{l^2 - E - p}\right) - L\left(\frac{2p}{1 - E + p}\right) +$$

$$+ \lg(E + p) \lg \frac{E - p - l^2}{l(1 - E + p)} - \frac{1}{2} \lg \frac{E + p}{E - p} \cdot \lg l \Bigg]$$

$$+ \frac{(m - n^2)^2}{m^2} \Bigg\{ \Bigg\{ \lg l \cdot \Big(4(E - 1) + 2E(1 - l^2 - 2n^2) +$$

$$+ \frac{1}{m} \Bigg\{ 4(1 - E)\, l^2 m + \frac{4}{3}(m - n^2)(3m + 4p^2) +$$

$$+ 2n^2 (3 + l^2)(1 - E) \Bigg\} - \frac{2(1 - l^2)\, n^2 (m + 2p^2)}{m^2} \Bigg) +$$

$$+\lg\frac{E+p}{E-p}\left\{m\,\frac{3l^2+2n^2-1}{2p}+\frac{1}{2p}\left\{n^2(m+2p^2)+\right.\right.$$

$$+\frac{1}{3}(3m+4p^2)(m-n^2)+2(1-E)\left[m+n^2(2E-1)+\right.$$

$$\left.\left.+(l^2+2E)(l^2+n^2-1)\right]-(1-l^2)(m+l^2+2n^2)\right\}+$$

$$+\frac{1}{2mp}\left[4n^2p^2(1-E)-n^2(1+l^2)(m+2p^2)+\right.$$

$$+2(1-E)[1-l^2]\left[2l^2(1-E)+n^2+\right.$$

$$\left.\left.+l^2(l^2+n^2-1)\right]+\frac{8E-1-{}^2}{3}(m-n^2)(3m+4p^2)\right\}-$$

$$-\frac{2n^2p(m+2p^2)}{m^2}\Bigg)-\frac{8}{3}\frac{(3m+4p^2)(m-n^2)}{m}+$$

$$+2(1-E)\left(4(1-l^2)-3n^2\right)-\frac{2n^2}{m}(m+2p^2)\Bigg\}\Bigg\},$$

$$L(x)=\int_0^x\frac{\lg|1-t|}{t}\,dt$$

where

$$B=\frac{4E}{p}P_0a+b+c+d,$$

$$a=L\left(-\frac{p}{E}\right)-L\left(\frac{p}{E}\right)-\frac{1}{4}\lg^2(E+p)+\frac{1}{4}\lg^2(E-p)-$$

$$-\frac{1}{2}\lg 2E\lg\frac{E-p}{E+p}-\frac{1}{2}L\left(\frac{E-p}{2E}\right)+\frac{1}{2}L\left(\frac{E+p}{2E}\right)+$$

$$+\lg(m-n^2)\left\{2\frac{p}{E}-\lg\frac{E+p}{E-p}\right\}+L(E+p)-L(E-p)+$$

$$+\frac{l^2}{2E}\frac{\lg(1-E-p)}{E+p}+\frac{l^2}{2E}\frac{\lg(1-E+p)}{p-E}+$$

$$+\frac{l^2}{2E}\lg\left(\frac{E+p}{E-p}\cdot\frac{1-E+p}{1-E-p}\right)-\frac{1}{2}\lg\frac{E+p}{E-p}-$$

$$-\frac{p}{2E}\lg m+\frac{1-E}{2E}\lg\frac{1-E-p}{1-E+p}.$$

$$b = \frac{4E}{3p}\left\{(2l^2 - E - El^2)\cdot\left(\frac{3n^4}{m^2} - \frac{2n^6}{m^3}\right) + \frac{n^6 E}{m^2}\right\}\left[\frac{m-n^2}{n^2}\frac{p}{E} + \right.$$
$$+\lg\frac{m}{n^2}\left(2\frac{p}{E} - \lg\frac{E+p}{E-p}\right) + \frac{m-n^2}{n^2}\left(\frac{E^2+E-1}{1-2E}\lg\left(\frac{E-p}{E+p}\cdot\right.\right.$$
$$\left.\cdot\frac{1-E+p}{1-E-p}\right) - \lg\frac{1-E-p}{1-E+p} - (1+E)\lg\frac{E+p}{E-p}\Big) -$$
$$-\frac{l^2}{2E}\frac{m-n^2}{n^2}\left\{\left(\frac{E^2+E-1}{2E-1} - \frac{2E^2+E-1}{2E}\right)\lg\frac{E+p}{E-p} + \right.$$
$$\left.\left.+E\frac{E-1}{2E-1}\lg\frac{1-E-p}{1-E+p} - \frac{1+E}{l^2}p\right\}\right].$$

$$c = -\frac{4}{3}n^6(2l^2 - E - El^2)\frac{m-n^2}{m^3}\left\{-\frac{l^2}{p}\frac{m-n^2}{2n^4}\left[\left(\frac{E^2+E-1}{2E-1} - \right.\right.\right.$$
$$\left.\left.\left.-\frac{2E^2+E-1}{2E}\right)\lg\frac{E+p}{E-p} + \frac{E-1}{2E-1}E\lg\frac{1-E-p}{1-E+p} - \frac{1+E}{l^2}p\right] + \right.$$
$$+\frac{4}{n^2} + \frac{m-n^2}{n^4} - \frac{2}{n^2}\frac{E}{p}\lg\frac{E+p}{E-p} +$$
$$+\frac{m-n^2}{n^4}\cdot\frac{E}{p}\cdot\left(\frac{E^2+E-1}{1-2E}\lg\left(\frac{E-p}{E+p}\,\frac{1-E+p}{1-E-p}\right) - \right.$$
$$\left.\left.-\lg\frac{1-E-p}{1-E+p} - (1+E)\lg\frac{E+p}{E-p}\right)\right\}.$$

$$d = -\frac{(m-n^2)^2}{3}\left\{4 - \frac{1+l^2}{m} + 3\frac{m-2E}{4p}\lg\frac{E+p}{E-p}\right\} +$$
$$+\frac{n^4(1+l^2)}{2p}\left(\frac{m-n^2}{n^2} + \lg\frac{n^2}{m}\right)\lg\frac{E+p}{E-p} -$$
$$-\frac{n^2(1+l^2)}{6p}\frac{(m-n^2)^2}{m}\lg\frac{E+p}{E-p} - \frac{n^6}{6}\lg\frac{n^2}{m}\cdot$$
$$\cdot\left(\frac{4}{m} + \frac{1}{p}\lg\frac{E+p}{E-p}\right) - \frac{2n^2(m-n^2)}{3m^2}(n^2-2m)\cdot$$
$$\cdot\left(\frac{E}{p}\lg\frac{E+p}{E-p} - 2(1+l^2) + \frac{2l^2E}{p}\lg\frac{E+p-l^2}{E-p-l^2}\right) -$$
$$-\frac{m-n^2}{36}(11n^4 - mn^2 - 4m^2)\left(\frac{4}{m} + \frac{1}{p}\lg\frac{E+p}{E-p}\right) -$$
$$-\frac{2(m-n^2)}{3m}\left(n^2(3m-n^2) - (3m-2E)m\right)\left(2 - \frac{E}{p}\lg\frac{E+p}{E-p}\right).$$

An approximate formula may be found in [7].

The spectrum (9) is shown in Fig. 3 for some values of n

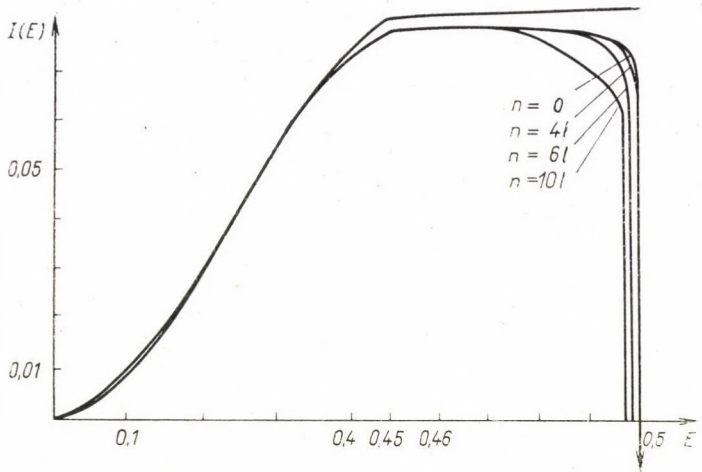

Fig. 3

3. The problem of infra-red divergences

The problem of infra-red divergences arises in an acute form in the zero neutretto mass case. In fact, taking the limit in (9), it is easy to see that at the maximal electron energy the spectrum tends to minus infinity which is evidently an unsatisfactory result. The usual explanation for this is the following [3]. Near the end-point of the spectrum the strong damping effect of virtual soft photons is only partially compensated by emission of real soft photons, owing to phase space restrictions for real emission. At the end-point real emission is completely inhibited, and so the infra-red divergent part of the virtual photon contribution fails to be cancelled by real photon terms.

Let us see how these ideas are reflected in our formulae. The interesting part of the inner bremsstrahlung correction is

$$-\frac{\alpha}{4\pi}P_0 p\left[\frac{4E}{p}\left(2\frac{p}{E}-\lg\frac{E+p}{E-p}\right)(\lg\lambda+\lg m)+\right.$$
$$\left.+\frac{2(1-E)}{p}\lg(1-E-p)-2\lg m\right]. \tag{10}$$

At the maximal electron energy $E_{\max}=(1+l^2-\lambda^2)/2$, the above expression gives a finite value, depending logarithmically on λ. In the limit $\lambda\to 0$ this value tends to minus infinity, which shows that our formula gives an unphysical result even for the emission of real photons. As is well known, the summation of the power series provided by the totality of infra-red terms would lead to a finite result [6.] Let us turn now to the $m_{\nu}\neq 0$ case. As we

mentioned before, the spectrum is finite even at the end-point. In fact, for the maximal electron energy $P(E)$ is exactly 0. The terms containing λ are of the form $\sim P_0 E\,(2\,p/E - \lg E + p/E - p)\lg\lambda$. As $P_0 \to 0$ if $E \to E_{\max}$ we see that at the maximal energy there is no need for the cancellation of the infra-red divergent terms. Neither the inner bremsstrahlung nor the virtual photon correction is divergent at the maximal energy. A probable explanation for this is that the available phase space is confined to a single point at $E_{\max}$. (In the $m_{\nu'} = 0$ case $k \neq 0$ real photons are also allowed, although in both cases the available invariant phase-space volume is zero at $E_{\max}$.) Thus, in the $m_{\nu'} \neq 0$ case we are able to give a spectrum completely satisfactory even at the end point.

REFERENCES

1. L. G. Hyman et al., Phys. Letters, **25B,** 376, 1967.
P. S. L. Booth et al, Phys. Letters, **26B,** 39, 1967.
2. J. Bachall and R. B. Curtis, Nuovo Cimento, **21,** 422, 1961.; R. Friedberg, Phys. Rev., **129,** 2298, 1963; K. Nagy, Acta Phys. Hung., **17,** 163, 1964.
3. E.g. T. Kinoshita and A. Sirlin, Phys. Rev., **107,** 593, 1957 and **113,** 1652, 1959.
4. M. Fierz, Zeitschrift für Physik **104,** 553, 1937.
5. Ja. A. Smorodinsky and He Tso-Hsiu, JETP **38,** 1007, 1960.
6. J. M. Jauch and F. Rohrilch, The Theory of Photons and Electrons (Reading, Mass. 1955).
7. G. R. Allcock, Proc. Phys. Soc., **85,** 875, 1965.
8. K. Mitchel, Phil. Mag., **40,** 351, 1949.

РАДИАЦИОННЫЕ КОРРЕКЦИИ К РАСПАДУ МЮОНОВ С КОНЕЧНЫМИ МАССАМИ НЕЙТРЕТТО

Ф. ЧИКОР и К. НАДЬ

Резюме

В работе вычисляются радиационные коррекции к распаду мюонов с предположением конечной массы нейтретто. Коррекции свободны от инфракрасных расходимостей даже при конечной точке спектра.

Acta Physica Academiae Scientiarum Hungaricae, Tomus 27, pp. 19—23 (1969)

MEASUREMENT OF THE CROSS SECTION FOR THE ISOMERIC ACTIVATION OF ^{115}In BY γ-RAYS FROM ^{24}Na SOURCE*

By

A. VERES and L. LAKOSI

INSTITUTE OF ISOTOPES OF THE HUNGARIAN ACADEMY OF SCIENCES, BUDAPEST

(Received 1. X. 1968)

The activation cross section of ^{115}In for a 150 Ci ^{24}Na source emitting 1.38 and 2.75 MeV gamma photons has been determined. The value found on the basis of the induced ^{115m}In activity proved to be 13.5×10^{-32} cm^2, being about threefold of 4.9×10^{-32} cm^2, the value determined with the aid of ^{60}Co photons.

This deviation gives evidence of the existence of higher, 1.42, 2.13 and 2.63 MeV activation levels in addition to the first 1.078 MeV, which have already been measured when using accelerators for excitation.

The isomeric activity resulting from the ^{115}In(γ, γ') ^{115m}In reaction has already been measured and studied by several authors. For its activation not only the bremsstrahlung from particle accelerators [1] but also some of the γ-emitting radioisotopes were used. The activation cross section per gamma quantum, as evaluated for the 1.17 and 1.33 MeV γ-rays from ^{60}Co [2—4] was found to lie in the range $(1.3—8.3)\times10^{-32}$ cm^2, varying with the experimental conditions. For activation with γ-rays from the 54 min half-life ^{116m}In produced by indium—gallium reactor-loop, ABRAMS et al. [5] obtained a ^{115}In activation cross section of $(1.5\pm0.3)\times10^{-31}$ cm^2. The reaction cross section is obviously dependent on the energy of the primary γ-rays of the radiation source used. The relation between the energy of the activation level and that of the primary gamma quantum is always $E_a \leq E_\gamma$, since a metastable state in any nucleus cannot be produced except by decay from a higher excited level. The isomeric activation cross-section also varies with the experimental conditions under which the Compton scattering resulting in the γ-quantum with an energy equal to that of the activation level is being produced. In addition, it depends on the number of higher levels which can be excited in the nucleus.

To extend the number of radiation sources available for the practical applications of the nuclear photo effect, like activity measurement and activation analysis [6—7], for which the effective activation cross section must be known, it seemed of interest to measure the ^{115}In activation cross section for the 1.38 and 2.75 MeV γ-rays from ^{24}Na.

* Dedicated to Prof. P. GOMBÁS on his 60th birthday.

Experimental

a) *Preparation of ^{24}Na source*

Sodium carbonate of c. p. grade, compressed to 19 mm $\times$ 44 mm cylindrical form of 19.108 g was irradiated for 71 hours in a thermal neutron flux of $4.33 \cdot 10^{13}$ n cm^{-2} sec^{-1} of the WWRS—2M reactor. One hour after termination of the irradiation the ^{24}Na activity was found to be 145 Ci. The activity measurement taken 25 hours after irradiation with the use of the Philips-type ionization chamber of the National Bureau of Measurements calibrated to $\pm 3\%$ showed 45^{+2}_{-4} Ci, in good agreement with the value predicted from the reactor flux with correction for decay time.

b) *Isomeric activation by ^{24}Na source*

Natural indium targets, each 3 g and $\varnothing$ 10 mm by 6 mm in size, were used for the activation of ^{115m}In. The ^{24}Na source was placed in a paper cup

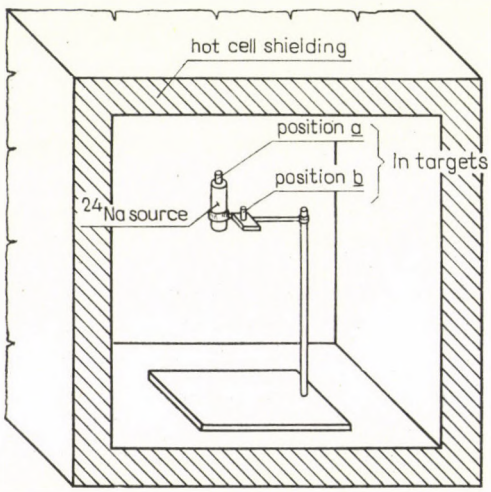

Fig. 1. The position of the indium targets during the gamma-irradiation by ^{24}Na source

located 400 mm from the bottom and at a somewhat greater distance from the top and the side-walls of the hot cell. Four indium targets were mounted around and two above the source in the arrangement shown in Fig. 1. Because of the 15h half-life of the ^{24}Na activity, the irradiation time was chosen to be, generally, 3 hours.

c) *Measurement of isomeric activity*

The irradiated samples were measured by Siemens single channel analyzer coupled to a 2 in. $\times 1\frac{3}{4}$ in. NaI (Tl) well-type scintillation counter. The energy and half-life of the measured radiation were found to be $E = 335$ keV and

$T_{1/2} = 4.5$ h, i.e. the characteristic data for ^{115m}In. The resolution of the detector, as checked with the 661 keV line of ^{137}Cs—^{137m}Ba was 13.7%. For the 323 keV line of ^{51}Cr used for the calibration of the efficiency and geometric factor of the well-type NaI (Tl) crystal and the self-absorption of the sample, the counting efficiency in the channel width used was measured as 28%. The activity measurements lasted from 5 to 10 minutes. The background in the channel corresponding to the 335 keV photopeak of ^{115m}In with a channel width of 14 V (174 keV) was found to be 32 cpm.

Discussion

The activation cross section per primary gamma quantum of the radiation source can be evaluated from the measured isomeric activity by making use of the expression

$$\sigma_m = \frac{I(\alpha+1)}{\Omega\Sigma} \cdot \frac{A}{N.a.m.} \cdot \frac{1}{f.S}, \tag{1}$$

where the first factor on the right hand side gives the isomeric activity as determined by the counting rate I in cps, the internal conversion coefficient is α and the counting efficiency is $\Omega\Sigma$. The second factor gives the number of target nuclei as determined by the atomic weight A, the Avogadro number N, the weight m and the isotopic abundance a of the target. The third factor stands for the primary γ-flux f and the saturation factor $S = 1 - \exp.(-0.693t \cdot T^{-1})$ with t being the irradiation time and T the half-life of the isomeric nucleus. The activation cross section evaluated for the primary γ-quanta of ^{24}Na with the use of this formula, gives $1.35 \pm 0.27 \times 10^{-31}$ cm^2 as compared with that of $4.9 \cdot 10^{-32}$ cm^2 obtained in an earlier measurement [8] for ^{60}Co of the same size as the ^{24}Na source and with similar indium targets. The difference of the two values can be explained by the fact that the 1.17 and 1.33 MeV γ-lines of ^{60}Co can excite, through Compton scattering, only the first activation level in indium at 1.078 MeV [9], while the 2.75 MeV lines of ^{24}Na are capable of also exciting the higher levels of 1.42, 2.13 and 2.63 MeV, the existence of which have already been shown in experiments with bremsstrahlung (Fig. 2).

The effective activation cross section under the given experimental conditions can be predicted [10—11] if one uses the formula

$$\sigma = \sum_i \Delta\Phi_{ei}\,\sigma_{ai} \left\{ \frac{n_{01}}{\mu_1} \frac{e^{\mu_1 d_2} e^{\mu_2 \varrho}}{e^{\mu_{1i} d_2} e^{\mu_{2i}\varrho}} (1 - e^{-\mu_1 d_2}) + \right.$$
$$\left. + \frac{n_{02}}{\mu_{2i} - \mu_2} \left[1 - e^{(\mu_2 - \mu_{2i})\varrho}\right] + \frac{n_{04}}{\mu_4} \left(1 - \frac{1}{\mu_4 l} + \frac{e^{-\mu_4 l}}{\mu_4 l}\right) \right\}, \tag{2}$$

where $\Delta\Phi_{ei}$ the differential cross-section for electron scattering to the i-th activation level i.e. to the range of energies corresponding to the level width.

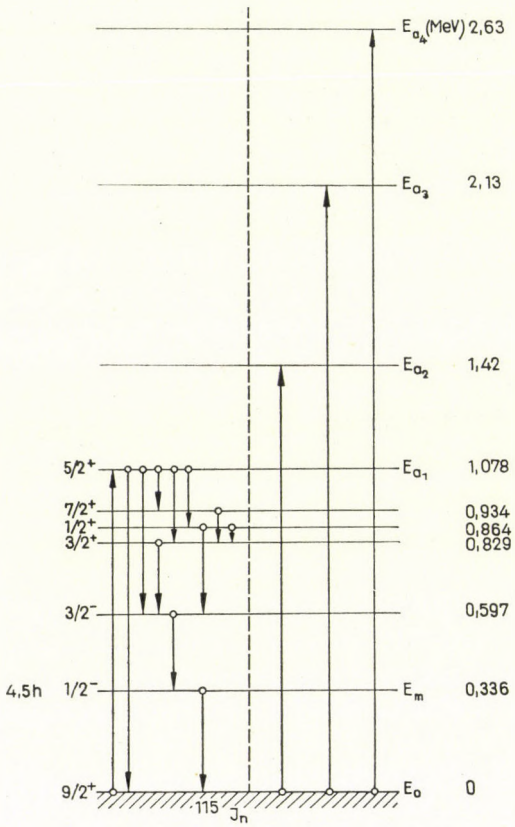

Fig. 2. The excited level scheme of ^{115}In

$\Delta\Phi_{ei}$ can be evaluated from the Klein—Nishina formula. σ_{ai} is the cross-section for resonance absorption at the i-th level. The terms in the brackets stand for the source, the absorber and the target, as determined by the electron densities n_{01}, n_{02} and n_{04}, the absorption coefficients μ_1, μ_2 and μ_4 and the thicknesses d, ϱ, l, respectively.

The cross section for excitation to the first, 1.078 MeV level in indium with subsequent decay to the metastable state was evaluated from Eq. (2), as $\sigma = 5.15 \times 10^{-32}$ cm^2 by taking the resonance level width to be $4 \cdot 10^{-3}$ eV, as estimated by GUTH [12], which gives $\sigma_a = 10^{-22}$ cm^2 for the absorption cross section.

Comparison of the value predicted for the first excited level at 1.078 MeV with the measured cross section of 13.5×10^{-32} cm^2 shows clearly that there must be an appreciable contribution to the activation from the second and possibly higher excited levels of indium. The individual contributions, however, cannot be evaluated without a knowledge of the absorption cross section and level width data involved.

REFERENCES

1. B. Pontecorvo and A. Lazard, Compt. Rend., **208**, 99, 1939.
2. G. Harbottle, Nucleonics, **12**, (4), 65, 1954.
3. N. Ikeda and K. Yoshihara, Radioisotopes, **7**, 11, 1958.
4. A. Veres, Int. J. Appl. Rad. and Isotopes, **14**, 123, 1963.
5. И. А. Абрамс, Л. Л. Пелекис, Известия АН Латв. СССР, Сер. Физ. и Техн. 1968. 1. 19.
6. A. Veres, I. Pavlicsek and M. Ozsgyáni, Standardization of Radionuclides, IAEA, Vienna 1967 p. 453.
7. A. Veres, Proc. of the Analytical Chemical Conference, Budapest, 1966 p. 360.
8. A. Veres and I. Pavlicsek, Int. J. Appl. Rad. and Isotopes, **17**, 69, 1966.
9. Э. А. Запаров, Б. С. Мазитов, Прогр. и Тез. XVIII. ежегодн. совещ. по ядерной спектроскопии и структуре ядря. Рига, 1968, 57.
10. K. Yoshihara, Isotopes and Radiation, **3**, 464, 1960.
11. A. Veres, Magyar Fizikai Folyóirat, **14**, 143, 1966.
12. E. Guth, Phys. Rev., **59**, 325, 1941.

ИЗМЕРЕНИЕ ЭФФЕКТИВНОГО СЕЧЕНИЯ АКТИВАЦИИ ЯДЕРНОГО ИЗОМЕРА ^{115}In γ-ЛУЧАМИ ^{24}Na

А. ВЕРЕШ и Л. ЛАКОШИ

Резюме

Определяется эффективное сечение активации изомера ^{115}In, относящееся к гамма-лучам энергии 1,38 и 2,75 Мэв радиоактивного источника ^{24}Na при активности 145 кюри. Из измерения активности изомера ^{115m}In данное значение получилось равным 13.5×10^{-32} см^2, что примерно в три раза больше значения полученного гамма-лучами ^{60}Co (4.9×10^{-32} см^2). Степень расхождения подтверждает, что наряду с первым активационным уровнем при 1,078 Мэв существуют и высшие уровни с энергией 1,42; 2,13, 2,63 Мэв, уже наблюденные ускорителями.

Acta Physica Academiae Scientiarum Hungaricae, Tomus 27, pp. 25—33 (1969)

ON THE KINETICS OF THE PHASE TRANSFORMATION OF CsCl CRYSTALS II*

By

I. GAÁL

RESEARCH INSTITUTE FOR TECHNICAL PHYSICS OF THE HUNGARIAN ACADEMY OF SCIENCES, BUDAPEST

Z. MORLIN

RESEARCH LABORATORY FOR CHEMICAL STRUCTURES OF THE HUNGARIAN ACADEMY OF SCIENCES, BUDAPEST

and

I. TARJÁN

RESEARCH GROUP FOR CRYSTAL PHYSICS OF THE HUNGARIAN ACADEMY OF SCIENCES, BUDAPEST

(Received 10. XII. 1968)

The kinetic curve of the $B_2 \rightleftharpoons B_1$ phase transformation observed during uniform heating may be divided into three different stages. In the first stage disk-like nuclei are formed which grow rapidly along the B_2 phase boundaries. In the second stage no nuclei are formed and the growth takes place normal to the original grain boundaries. Finally, the decrease of the transformation rate in stage III may probably be associated with the Clausius-Clapeyron type decrease of the driving force. In the framework of this visualization of the kinetic curve some previous results are also interpretable.

1. Introduction

The (CsCl type lattice) $\rightleftharpoons$ (NaCl type lattice) phase transformation in CsCl is connected with a pronounced change in the electrical conductivity [1, 2, 3, 4, 5] which gives a good opportunity to investigate the kinetics of this transformation [5, 6]. The conductivity of various sintered Johnson—Matthey specpure CsCl samples was found to be a well-defined function[1] of time when heating the samples at a constant rate above the equilibrium temperature of transformation ($T_c = 726$ °K) (Fig. 1 [6]). The aim of this paper is to present the experimental data in terms of the formal theory of phase transformation.

It will be assumed that the $B_1 \rightleftharpoons B_2$ transformation is of the nucleation and thermally activated growth type, i.e. the volume fraction of the stable phase (ξ) is given by the equation

$$\xi(t) = 1 - \exp\left[\int_0^t \left(\prod_{i=1}^{3} \int_\tau^t V_i\,(T(t')\,dt')\right) I\big(T(\tau), \tau\big)\,d\tau\right], \tag{1}$$

* Dedicated to Prof. P. GOMBÁS on his 60th birthday.

[1] It should be noted that the data were corrected for various experimental errors.

where $T(t)$ is the temperature programme of heating, $I(T(t)t)$ is the temperature and time-dependent rate of nucleation and V_1, V_2, V_3, denote the growth velocities in three mutually perpendicular directions. The growth velocity is determined by the phase boundary mobility, B, and the driving force, $\Delta G : V = B\Delta G$. The mobility depends on the temperature, concentration of dissolved impurities and the relative orientation of the adjacent phases. The temperature dependence of the mobility is characterized by an energy of activation denoted by E_M. The driving force is given by the free energy difference between the adjacent phases along the phase boundary and by the curvature and free energy of the migrating boundary (see e.g. [7]).

2. Relation between conductivity and the transformed volume

Debye—Scherrer patterns obtained by electron diffraction prove that the B_1 and B_2 phases form a two-phase aggregate in the course of the $B_1 \rightleftharpoons B_2$ transformation [8]. There are many formulae to determine the effective electrical onductivity of two-phase aggregates [9]; we :used the formula of ODALEVSKI [10] and LANDAUER [11]

$$\left(\frac{\sigma_1 - \sigma_{eff}}{\sigma_1 + 2\sigma_{eff}}\right) x_1 + \left(\frac{\sigma_2 - \sigma_{eff}}{\sigma_2 + 2\sigma_{eff}}\right) x_2 = 0\,, \tag{2}$$

where σ_1, σ_2 are the B_1 and B_2 phase conductivities, respectively, x_1, x_2 are the volume fractions of the component phases. This equation is valid for random geometry, since it was derived from the assumption that the mean electric and current field in the constituent 1 (or 2) might be determined by considering a sphere 1 (or 2) embedded in an infinite conducting medium.[2]

LANDAUER [11] has shown that Equ. (2) accounts quite fairly for the observed conductivities in equiaxial two-phase matrices even when σ_1 and σ_2 differ by a factor of 10. However, it should be emphasized that this statement is limited to random geometry. Model experiments show that for disk-like second phases perpendicular to the mean direction of the current the experimental results may deviate from the values calculated with Equ. (2) by a factor of 30 if $\sigma_1/\sigma_2 \geqslant 1$ [12].

When applying Equ. (2) to evaluate x_1 one has to take into account that σ_2 and σ_1 are inherently temperature-dependent. The actual conductivities might be determined by extrapolating from the B_2 and B_1 data using the relations

$$\sigma_2(T) = \sigma_2(T_2) \exp\left[-\frac{E_2}{h}\left(\frac{1}{T} - \frac{1}{T_2}\right)\right], \tag{3a}$$

$$\sigma_1(T) = \sigma_1(T_2) \exp\left[-\frac{E_1}{T}\left(\frac{1}{T} - \frac{1}{T_1}\right)\right]. \tag{3b}$$

[2] It is worth noting that the derivation of Eq. (2) makes use of the Maxwell equations and Ohm's law only and so it applies eq ally to metals, semiconductors and insulators.

In Equ. (3) T_1 and T_2 are temperatures at which CsCl exists in the B_2 and B_1 phase, respectively; E_1 and E_2 are activation energies of the conductivities in the respective phases.

At the evaluation of the conductivity values from the measured data corrections must be made to account for the volume change of the samples due to the transformation. Since the elastic moduli of B_1 and B_2 at the tem-

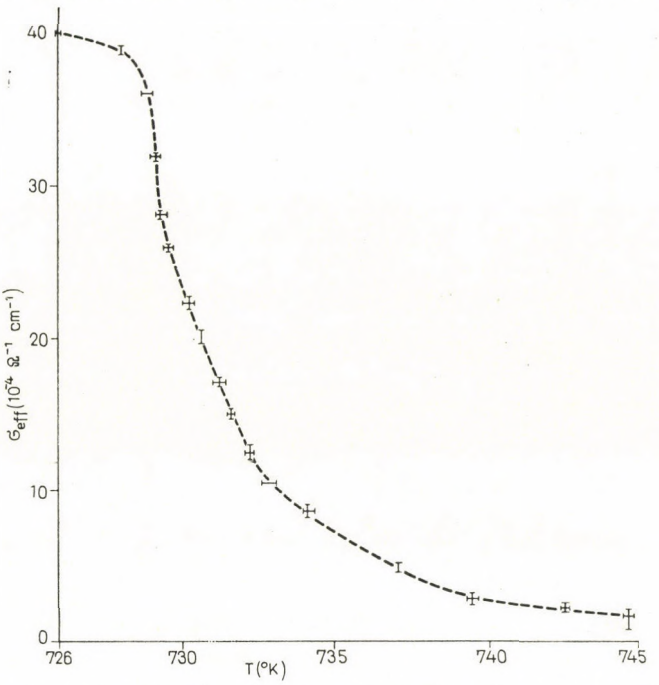

Fig. 1. The decrease of the effective conductivity in the $B_2 \rightarrow B_1$ transition. (The measurements were carried out on 8 different samples)

perature of transformation are not known equal elastic moduli were assumed for both phases. According to this assumption [16]

$$\frac{v(x_1) - v(x_2 \approx 1)}{v(x_2 = 1)} = \frac{V_1 - V_2}{V_2} x_1 , \tag{4}$$

where v denotes the volume of the sample and V the mole volume of the phase (V_1—$V_2/V_2 = 0.12$ [13]). Knowing the dimensions of the sample before the phase transformation (l_0, q_0), the effective conductivity is given by the relation

$$\sigma = \frac{T}{V} \frac{1 + \Delta l/l}{1 + \Delta q/q} \cong \frac{T}{V} \frac{l_0}{q_0} \left(1 - \frac{1}{3} \frac{V_1 - V_2}{V_2} x_1\right). \tag{5}$$

Arends and Nijboer [2] have found that E_{B_2} and E_{B_1} are 1.35 eV and 1.65 eV, respectively. σ_{B_1} (744.5) and σ_{B_2} (729) amount to $0.16 \cdot 10^{-5}$ Ohm^{-1}cm^{-1} and $40 \cdot 10^{-5}$ Ohm^{-1}cm^{-1} (Fig. 1). With these data x_1 was calculated from

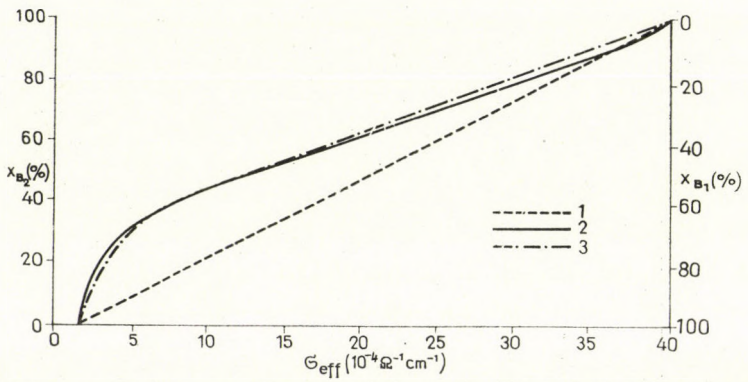

Fig. 2. Effective conductivity as a function of xb_2 or xb_1 (Curve 1 visualizes the conductivity by linear interpolation. Curve 2 was calculated from (2), (3) and (5) with temperature corrections, Curve 3 was calculated without any temperature correction

Equ. (2), (3) and (5) (Fig. 2). Since there is some disagreement in the literature about the activation energy values E_2 and E_1 those x_1 values are also given in Fig. 2 which were calculated without any temperature correction.

3. The interpretation of the kinetical curve

In Fig. 3 $\log 1/1-x_1$ is plotted against $T-T_c = a \cdot t$. The curve has three quite well separated stages. The first is parabolic, the second linear, and the third begins with a significant decrease of $\log 1/1-x_1$ with time (or with $T-T_c = a \cdot t$).

Let us first consider the second stage. It is clear that $I(T(t), t) \geq 0$, and if it is assumed that the growth velocity is not a decreasing function of $T-T_c = a \cdot t$ [3] the linearity of the kinetical curve leads to the conclusions that in this stage: i) the growth of the equilibrium phase grains is restricted to one special direction only, their growth in the other two directions being vanishingly small; ii) no new nuclei are formed; iii) the driving force is constant. This means that:

$$\log \frac{1}{1-x_1} = \text{constant} \left(\int_0^t M_0 \, e^{-E_M/kT} \, dt \right) . \tag{6}$$

In good approximation

$$\frac{1}{T} = \frac{1}{\left(1 - \frac{at}{T_c}\right)} = \frac{1}{T_c} \left(1 - \frac{at}{T_c}\right) \tag{7}$$

[3] The mobility of the grain boundaries is an increasing function of the temperature, and so the quasi-constant velocity of the phase boundary migration needed to explain the linearity of stage II would mean a compensation of the E_M determined increase of the mobility by the Clausius-Clapeyron type decrease (see later) of the driving force. At present, we do not think there is any support for such kind of assumption.

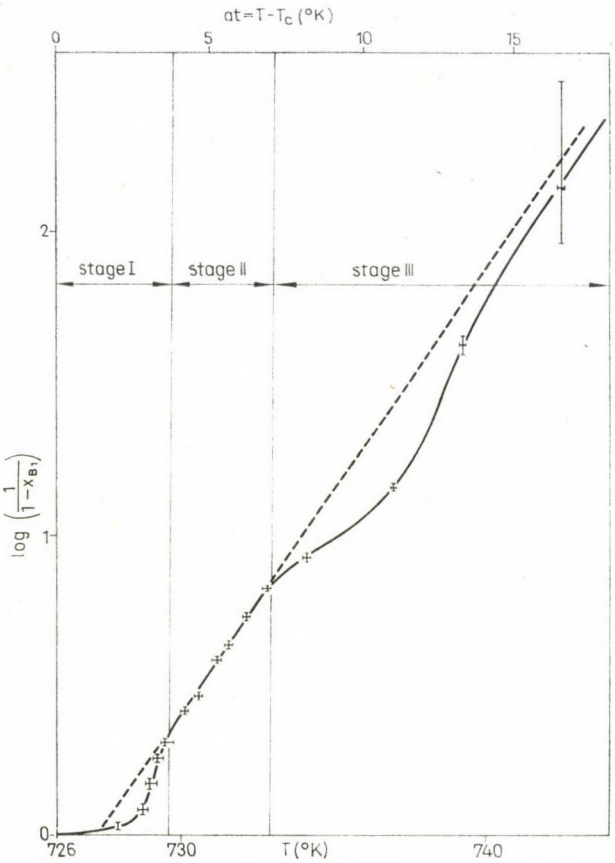

Fig. 3. The kinetic curve (the maximum possible error in log $1/1 - x_1$ and ΔT is marked by + 1)

because in the investigated temperature interval

$$\frac{\Delta T}{T_c} = \frac{at}{T_c} \leq 0{,}15\,.$$

Putting (1) into (6) and assuming that

$$\frac{E_M}{kT_c} \cdot \frac{\Delta T}{T_c} \ll 1$$

the expansion into power series yields

$$\frac{1}{1 - x_1} = \text{const}\ \Delta T \left(1 + \frac{E_M}{kT_c} \cdot \frac{\Delta T}{k}\right). \tag{8}$$

This equation accounts for the observed linearity if

$$\frac{E_M}{kT_c}\,\frac{\Delta T}{T_c} \ll 1.$$

The observed deviation from exact linearity gives an upper limit 0.6 eV for the activation energy of the phase boundary mobility. By supposing the two conductivity values to be slightly more accurate than was actually found in the experiments one obtains the value 0.2 eV for E_M. These values (0.6—0.2 eV) are quite reasonable, since the activation energy of the grain boundary migration was found to be equal or lower than that of vacancy migration in the cases investigated [14].

At first sight it appears that, in spite of our suggestion, the driving force of the phase boundary migration ought to be an increasing function of $T—T_c = a \cdot t$, since the free energy difference between the stable and unstable phase increases with increasing $T—T_c$. One has, however, to keep in mind that the phase transformation connected with a volume change gives rise to accommodation stresses. This stress field cannot be fully relaxed by plastic deformation, since the flow stress has a finite value and only the shear components of the stress tensor can initiate the flow. According to the Clausius-Clapeyron equation the stress field is connected with a change in the equilibrium transition temperature in the following way [15]

$$T_c - T_{c_0} = \frac{u_{ik}(B_1)\, u_{ik}(B_2)}{T_{c_0}\, \Delta H}\,. \tag{9}$$

In the formula, T_{c_0} and T_c are the equilibrium transition temperatures in the stress-free state and in the elastically distorted state, respectively. u_{ik} denotes the stress tensor at the phase boundary and $u_{ik}(B_1)$ and $u_{ik}(B_2)$ are the components of the distortion tensor at the B_1 and the B_2 side of the phase boundary. (The stress tensor and the displacement vector are measured with respect to the single phase matrices in the stress-free state.) ΔH amounts to 7.5 K/mole [17].

The order of magnitude of the Clausius-Clapeyron effect can be estimated with the help of the following model. Let a spherical B_2 phase be surrounded concentrically by a spherical B_1 phase, and let the boundary between them be an incoherent one. Assuming that no plastic flow takes place, and using the well-known stress field values [15, 16] one gets 100 °K for $T_c—T_{c_0}$. When plastic deformation relaxes the stress field to the value of the flow stress ($\sim$1 hg $\cdot$ mm^{-2} [18]) the change in the transformation temperature is 5 °K. According to these considerations a constant driving force results owing to an interplay between the Clausius-Clapeyron type change in the equilibrium

transformation temperature and the restricted plastic deformation of the matrix. The one-dimensional growth may be explained in the following way: in the first stage disk-like nuclei are formed in the grain boundaries of the polycrystalline B_2 phase; these nuclei grow rapidly along the B_2 phase grain boundaries; during this growth the thickness of the B_1 phase grains remains as small as that of the nuclei. At the end of the first stage the area of the original B_2 grain boundaries is covered with B_1 phase grains, whose slow growth normal to the surface of the original B_2 phase is considered to account for the one dimensional growth characteristic of the second stage.

If the nucleation rate were constant during stage I, $\log 1/1-x_1$ would be a third order parabola. If the nucleation rate were a rapidly decreasing function of time, owing to the decrease of the grain boundary area of the B_2 phase, $\log 1/1-x_1$ would be a second order parabola. A numerical test has shown that the experimental curve has an intermediate position between these two extreme possibilities.

It should be noted that the formation of disk-like nuclei in the original grain boundaries is favoured by two effects: i) disk-like nuclei indicate the smallest possible accommodation energy in the two phase aggregate, as was shown by NABARRO [19]; ii) the rapid growth along the grain boundaries might be associated with the Clausius-Clapeyron type change in the equilibrium transition temperature. (The plastic relaxation is certainly favoured by the plastic shear of the grain boundaries. This gives rise to a rather easy stress relaxation which in consequence makes the Clausius-Clapeyron type decrease of the driving force less effective in the direction parallel to the grain boundaries than in the direction normal to it.)

The decrease of the transformation rate in stage III may probably also be associated with the Clausius-Clapeyron type decrease of the driving force. To show this, let us assume that the plastic flow resulting from the accommodation stress has exhausted the lower yield point region of the matrix, and now work hardening becomes a dominant factor. When the rate of recovery does not compensate the hardening in exactly the same rate as the phase transformation goes on, a decrease or an increase might both be observable. This depends only on the relative rate of these two reactions.

4. Discussion

Let us now discuss some other experimental results supporting the model suggested.

One of us described some isothermic conductivity measurements carried out slightly above T_c [6]. The change of the conductivity was not a monotonic function of time; an increasing transformation rate was followed by a consider-

able slowing down after which the transformation rate increased again. This process which was repeated several times seems to be very similar to the "fine structure" of phase transformation observed by ARENDS [20]. These effects may be associated with the Clausius-Clapeyron type changes in the driving force (see stage III). The internal stress field which played an important role in the suggested model appears directly in the anomalous change of the lattice parameter of the phase during phase transformation observed in [8]. From the amount of the anomalous change in the lattice parameter a value of several degrees arises for T_c—T_{c_0}.

In another set of experiments, published earlier, it was shown that the transformation process is extremely structure-sensitive which means that the transformation kinetics depends strongly on the defect state of the lattice [5]. The experimental facts can easily be explained with our suggested model by considering three effects of a heat treatment slightly above T_c: i) some B_1 grains are formed; ii) the grain size of the B_2 grains decreases as a result of the driving force brought about from the decrease of the total grain boundary area; iii) the overall dislocation density decreases by annihilation, and the density of movable dislocation decreases by impurity reactions. If, after the heat treatment at the equilibrium temperature of transformation, the sample is quenched and then warmed up again (as they actually were in the experiments described in [5]), the nucleation and two dimensional growth along the grain boundaries will cover a smaller total grain boundary area than before the heat treatment. Consequently, the rate of transformation decreases. A second effect in the same line arises from the fact that plastic deformation becomes more difficult after heat treatment. This should be expected because an increase of the yield stress makes the Clausius-Clapeyron type decrease of the driving force more effective. When the increase in yield stress is extremely large the rate of transformation may become vanishingly small before obtaining a single phase matrix.

Finally, it should be mentioned that the simplest direct test of the suggested model should be given by the micrographic investigation of the phase transformation. We hope to present some results in this line in due time.

The authors are much indebted to Dr. J. ARENDS for letting them know his results about the "fine structure" of transformation before publication. It is a pleasure to thank Prof. Dr. S.LENGYEL for his helpful interest.

REFERENCES

1. W. W. HARPUR, R. L. MOSS and A. R. UBBELOHDE, Proc. Roy. Soc., **A 232**, 310, 1955.
2. I. M. HOODLESS and J. A. MORRISON, Phys. Chem., **66**, 557, 1962.
3. J. ARENDS and H. NIJBOER, Solid State Communications, **5**, 163, 1967. Phys. Stat. Sol., **26**, 537, 1968.
4. P. J. HARVEY and I. M. HOODLESS, Phil. Mag., **16**, 543, 1967.
5. Z. MORLIN, Acta Phys. Hung., **21**, 137, 1966.

6. Z. MORLIN, Acta Phys. Hung., **24,** 277, 1968.
7. J. W. CHRISTIAN, The Theory of Transformation in Metals and Alloys, Pergamon Press, Oxford, London, Edinburgh, New York, Paris, Frankfurt, 1965. pp. 471—489.
8. Z. MORLIN and J. TREMMEL, Acta Phys. Hung., **21,** 130, 1966.
9. J. A. REYNOLDS and J. M. HOUGHT, Proc. Roy. Soc., B**70,** 769, 1957.
10. V. I. ODALEVSKI, J. Tech. Phys. (UdSSR), **21,** 667, 678, 1379, 1951.
11. R. LANDAUER, J. Appl. Phys., **23,** 779, 1952.
12. I. GAAL and L. URAY, Phys. Stat. Sol., **29,** K163, 1968.
13. Gmelins Hdbch der Anorganischen Chemie, Band 25, p. 145, Verl. Chemie Gmbh. Weinheim, Berstr. und Berlin.
14. P. GORDON and R. A. VANDERMEER, Recrystallization, Grain Growth and Textures (ed. H. Margolin) 205—266, American Society for Metals, Metals Park, Ohio, 1966.
15. L. D. LANDAU and E. M. LIFSHITZ, Theory of Elasticity, Pergamon Press, London, Paris, New York, Los Angeles, 1959, pp. 9, 20.
16. J. D. ESHELBY, in Solid State Physics (ed. by F. SEITZ and D. TURNBULL) Vol. 3. pp. 79—107, Academic Press, New York, 1956.
17. W. AUER, in Landolt Börnstein Zahlenwerte und Funktionen, Bd 2. Teil 14. p 207. Springer, Berlin, Göttingen, Heidelberg, 1959.
18. W. L. PHILLIPS, J. Trans AIME, **218,** 947, 1960.
19. F. R. N. NABARRO, Proc. Roy. Soc., **52,** 90, 1940.
20. J. ARENDS, private communication.

О КИНЕМАТИКЕ ФАЗОВОГО ПЕРЕХОДА КРИСТАЛЛОВ CsCl II

И. ГАЛ, З. МОРЛИН и И. ТАРЬЯН

Р е з ю м е

Кинетическая кривая фазового перехода $B_2 \rightleftarrows B_1$, наблюдаемого при равномерном нагреве, может быть разделена на три разные фазы. В первой фазе формируются дискообразные ядра, которые быстро растут в направления фазовых граничных линий B_2. Во второй фазе ядра не образуются и рост протекает в направления, перпендикулярные к контурам первоначальных зерен. Наконец, уменьшение скорости перехода в третьей фазе вероятно можно связать с уменьшением возбуждающей силы типа Клаузиуса—Клапейрона. В рамках данного представления кинетической кривой имеется возможность для объяснения некоторых ранних результатов.

Acta Physica Academiae Scientiarum Hungaricae, Tomus 27, pp. 35—46 (1969)

THE HYDRODYNAMICAL MODEL OF WAVE MECHANICS*

THE MANY BODY PROBLEM

By

L. JÁNOSSY

CENTRAL RESEARCH INSTITUTE OF PHYSICS, BUDAPEST

(Received 19. XII. 1968)

The problem of how to extend the hydrodynamical model — described in previous publications — to many body problems is discussed and it is shown that the difficulties which arise in such an attempt are not of mathematical nature, but they reflect upon a physical problem which in our opinion is unsolved so far. It is suggested that in the correct treatment of a many body problem one should try to select between the possible wave functions such functions which are very likely in a statistical sense. This proposed selection resembles the selection of the very likely configurations in statistical mechanics.

§ 1. We have shown in a number of publications [1—5] how the wave equation describing a one-body problem can be transformed into a mathematical equivalent form, so that in the new form the variables have a good meaning in the classical sense.

It is generally believed to be impossible to carry out a similar transformation of the wave equation describing the motion of a system consisting of several particles.

We analyse the latter problem and show that there are difficulties indeed to express the many-body problem in terms of hydrodynamical variables, but these difficulties are not of mathematical nature but are connected with a physical problem which does not seem to be solved so far.

I

§ 2. The wave equation describing the motion of N particles under the influence of a potential V can be written

$$\sum_{\nu=1}^{N}\left(-\frac{\hbar^2}{2m_\nu}\nabla_\nu^2\psi + V\psi\right) = i\hbar\dot{\psi}\,, \tag{1}$$

* This article is dedicated to the 60th birthday of my good friend, Academician P. GOMBÁS, whom I sincerely wish many more years of undiminished activity. I always followed with great interest his work, in particular on the statistical methods of obtaining the stationary states of many body systems. Since many years I am wondering, whether a dynamical version of this theory could be found? It may be that the ideas developed in this article have some connection with the latter problem.

where

$$\psi = \psi_\nu(\mathfrak{r}, t), \qquad \mathfrak{r} = \boldsymbol{r}_1, \boldsymbol{r}_2, \ldots . \boldsymbol{r}_N \tag{2}$$

and ∇_ν is the nabla operator acting upon the components of $\boldsymbol{r}_\nu$.

V may be supposed to have the form

$$V(\mathfrak{r}) = \sum_\nu V_\nu(\boldsymbol{r}_\nu) + \sum_{\nu \neq \mu} V_{\nu\mu}(\boldsymbol{r}_\nu - \boldsymbol{r}_\mu). \tag{3}$$

A type of equation which somewhat resembles to the hydrodynamical relations can be obtained from (1) by writing

$$\psi = Re^{iS}, \tag{4}$$

where R and S depend on $\mathfrak{r}$ and also on the time t.

Making use of the relation (4) one finds

$$\frac{\nabla_\nu^2 \psi}{\psi} = \frac{\nabla_\nu^2 R}{R} - (\mathrm{grad}_\nu S)^2 + i\left(\frac{2\,\mathrm{grad}_\nu R\,\mathrm{grad}_\nu S}{R} + \nabla_\nu^2 S\right). \tag{5}$$

Introducing (5) into (1) one finds separating real and imaginary parts

$$\sum_\nu \mathrm{div}_\nu \varrho \mathfrak{v}_\nu + \frac{\partial \varrho}{\partial t} = 0 \tag{6}$$

with

$$\varrho = R^2 \qquad \mathfrak{v}_\nu = \frac{\hbar}{\boldsymbol{m}_\nu} \mathrm{grad}_\nu S. \tag{7}$$

(We use gothic $\mathfrak{v}$ for the velocity distribution in $3N$ dimensions).

From the real part of (5) we find

$$-\mathrm{grad}_\mu \left[\sum_\nu \left(\frac{\hbar^2}{2\boldsymbol{m}_\nu} \frac{\nabla_\nu^2 \varrho^{1/2}}{\varrho^{1/2}} + \frac{1}{2} \boldsymbol{m}_\nu \mathfrak{v}_\nu^2\right) + V\right] = \boldsymbol{m}_\mu \mathfrak{v}_\mu. \tag{8}$$

§ 3. Equations (6), (7) and (8) give a set of differential equations which can be solved for given initial conditions. These equations can be regarded as "hydrodynamical equations in a $3N$-dimensional space". Relations (5), (6) and (7) do not seem, however, to have particular physical significance as they express the motion of a physical system in a $3N$-dimensional configuration space. Such a description reveals just as little the physical significance of the process involved as the original wave equation.

II

§ 4. We obtain sets of equations referring to three-dimensional distributions by forming suitable averages. We may introduce three-dimensional densities by writing

$$\varrho_\nu(\boldsymbol{r}) = \underbrace{\int \dots \int}_{(N-1)} \varrho(\boldsymbol{r}_1 \dots \boldsymbol{r}_{\nu-1}, \boldsymbol{r}, \boldsymbol{r}_{\nu+1} \dots \boldsymbol{r}_N)\, d^3\boldsymbol{r}_1 \dots d^3\boldsymbol{r}_{\nu-1}\, d^3\boldsymbol{r}_{\nu+1} \dots d^3\boldsymbol{r}_N . \quad (9)$$

In place of (9) we can also write shorter

$$\varrho_\nu(\boldsymbol{r}) = \int\limits_{(\nu)} \varrho d^{3(N-1)}\boldsymbol{r} , \quad (10)$$

where the symbol on the right hand side of (10) is supposed to stand for the right hand expression of (9).

Similarly we may introduce

$$\varrho_\nu(\boldsymbol{r})\, \boldsymbol{v}_\nu(\boldsymbol{r}) = \int\limits_{(N-1)} \dots \int \varrho \mathfrak{v}(\boldsymbol{r}_1 \dots \boldsymbol{r}_{\nu-1}, \boldsymbol{r}, \boldsymbol{r}_{\nu+1} \dots \boldsymbol{r}_N)\, d\boldsymbol{r}_1 \dots d\boldsymbol{r}_{\nu-1}\, d\boldsymbol{r}_{\nu+1} \dots d\boldsymbol{r}_N . \quad (11)$$

Or writing short

$$\boldsymbol{v}_\nu(\boldsymbol{r}) = \int\limits_{(\nu)} \varrho \mathfrak{v}_\nu\, d^{3(N-1)}\boldsymbol{r} . \quad (12)$$

§ 5. Integrating the continuity relation (6) into $(N-1)$ coordinate vectors $\boldsymbol{r}_\nu$ $\nu = 1, 2, \dots \mu-1, \mu+1 \dots N$, i.e. integrating over all coordinate vectors with the exception of $\boldsymbol{r}_\mu$ we find that $N-1$ of the terms under the sum vanish and we obtain

$$\operatorname{div}(\varrho_\mu \boldsymbol{v}_\mu) + \frac{\partial \varrho_\mu}{\partial t} = 0 \qquad \mu = 1, 2, \dots, N . \quad (13)$$

We see thus that the three-dimensional distributions $\varrho_\mu(\boldsymbol{r})$ and $v_\mu(\boldsymbol{r})$ $\mu = 1, 2, \dots, N$ represent flows each satisfying a continuity relation in three dimensions.

III

§ 6. So as to show that the N flows so obtained have a good physical significance, we note that we may introduce current and charge densities

$$\boldsymbol{i}_\nu = e_\nu \boldsymbol{v}_\nu \varrho_\nu / c , \qquad \varrho_{\mathrm{el}_\nu} = e_\nu \varrho_\nu , \qquad \nu = 1, 2, \dots, N , \quad (14)$$

where e_ν is the electric charge carried by the ν-th particle. Forming retarded potentials

$$\boldsymbol{A}_\nu = \int \frac{[\boldsymbol{i}_\nu]}{|\boldsymbol{r}-\boldsymbol{r}'|}\, d^3\boldsymbol{r}', \quad \Phi_\nu = \int \frac{[\varrho \mathrm{e}]_\nu}{|\boldsymbol{r}-\boldsymbol{r}'|}\, d^3\boldsymbol{r}' \tag{15}$$

in the usual way, we can suppose that the electromagnetic field of the system can be derived from potentials

$$\boldsymbol{A} = \Sigma \boldsymbol{A}_\nu, \qquad \Phi = \Sigma \Phi_\nu. \tag{16}$$

Indeed the field obtained from $\boldsymbol{A}$ and Φ as given by (15) and (16) is exactly equal to the expectation values of the corresponding quantities obtained in terms of the usual operator formalism.

§ 7. Similarly we can introduce quantities like momentum and angular momentum writing

$$\boldsymbol{p}_\nu = \int \varrho_\nu \boldsymbol{v}_\nu\, d^3\boldsymbol{r}, \qquad \boldsymbol{M}_\nu = \int (\boldsymbol{r} \times \varrho_\nu \boldsymbol{v}_\nu)\, d^3\boldsymbol{r}, \tag{17}$$

and it can be verified easily that the system as a whole behaves as a system with total momentum respectively angular momentum given by

$$\boldsymbol{p} = \Sigma \boldsymbol{p}_\nu, \qquad \boldsymbol{M} = \Sigma \boldsymbol{M}_\nu.$$

We see therefore that the behaviour of the N particle system can be characterized indeed with the help of the densities $\varrho_\nu \boldsymbol{v}_\nu$ and ϱ_ν. Taking the spin of the particles into consideration we have to introduce further variables, e.g. $\boldsymbol{T}_\nu$ where $\boldsymbol{T}_\nu = \boldsymbol{T}_\nu(\boldsymbol{r}, t)$ are unit vectors characterizing the directions of spins of the various particles.

§ 8. Multiplying both sides of (8) by ϱ and integrating over N—1 coordinate vectors $\boldsymbol{r}_\nu \neq \boldsymbol{r}_\mu$ we obtain three-dimensional equations of motions of the form

$$\varrho_\mu \dot{\boldsymbol{v}}_\mu = \boldsymbol{F}_\mu \qquad \mu = 1, 2, \ldots, N, \tag{18}$$

where

$$\boldsymbol{F}_\mu = -\operatorname{grad} \int_{(\mu)} \varrho(\mathfrak{Q} + \mathfrak{R} + V)\, d^{(n-1)}\boldsymbol{r},$$

$$\mathfrak{Q} = \sum_\nu \frac{\hbar^2}{m_\nu} \frac{\nabla_\nu^2 \varrho^{1/2}}{\varrho^{1/2}}, \qquad \mathfrak{R} = \frac{1}{2} \sum_\nu m_\nu \mathfrak{v}_\nu^2. \tag{19}$$

IV

§ 9. The relations (18) and (19) have the form of three-dimensional equations of motions which describe the motion of N media simultaneously. However, there is an essential difference between the one-body problem with $N = 1$

and the more-body problems $N > 1$. Indeed, in the case $N = 1$ the wave function ψ can be unambiguously determined from the distributions $\boldsymbol{v}$ and ϱ. Therefore in the one-body problem the right hand expression (18) can be expressed in terms of $\boldsymbol{v}$ and ϱ and thus (18) together with the continuity relation (13) gives a set of differential equations which for a given initial condition can be integrated. Therefore if we describe a one-particle system by giving

$$\boldsymbol{v}(\boldsymbol{r}, 0) = \boldsymbol{v}^{(0)}(\boldsymbol{r}) \qquad \text{and} \qquad \varrho(\boldsymbol{r}, 0) = \varrho^{(0)}(\boldsymbol{r}),$$

then we can determine the motion of the system unambiguously.

§ 10. In the case of several particles the position is different. Let us consider $N = 2$.

Giving initial conditions

$$\left.\begin{aligned} \mathfrak{v}_\nu(\boldsymbol{r}_1, \boldsymbol{r}_2, 0) &= \mathfrak{v}_\nu^{(0)}(\boldsymbol{r}_1, \boldsymbol{r}_2) \qquad \nu = 1, 2 \\ \varrho(\boldsymbol{r}_1, \boldsymbol{r}_2, 0) &= \varrho^{(0)}(\boldsymbol{r}_1, \boldsymbol{r}_2) \end{aligned}\right\}. \tag{20}$$

We can determine the motion of the system in an unambiguous manner. However, if we give only

$$\left.\begin{aligned} \varrho_1^{(0)}\boldsymbol{v}_1^{(0)}(\boldsymbol{r}) &= \int \varrho \mathfrak{v}_1(\boldsymbol{r}, \boldsymbol{r}', 0)\, d^3\boldsymbol{r}, \quad \varrho_1^{(0)}(\boldsymbol{r}) = \int \varrho(\boldsymbol{r}, \boldsymbol{r}', 0)\, d^3\boldsymbol{r}' \\ \varrho_2^{(0)}\boldsymbol{v}_2^{(0)}(\boldsymbol{r}) &= \int \varrho \mathfrak{v}_2(\boldsymbol{r}', \boldsymbol{r}, 0)\, d^3\boldsymbol{r}', \quad \varrho_2^{(0)}(\boldsymbol{r}) = \int \varrho(\boldsymbol{r}', \boldsymbol{r}, 0)\, d^3\boldsymbol{r}' \end{aligned}\right\}, \tag{21}$$

then we cannot determine $\psi(\boldsymbol{r}_1, \boldsymbol{r}_2, 0)$ from the initial condition; expressing $\mathfrak{v}_\nu$ respectively ϱ in terms of $\psi = Re^{iS}$ making use of (8) we find that there exist a very large number of functions ψ satisfying (21).

§ 11. In fact the densities $\varrho_1\boldsymbol{v}_1$ and $\varrho_2\boldsymbol{v}_2$ can be taken as two three-dimensional moments of a six-dimensional distribution. A number of three-dimensional moments restrict a six-dimensional distribution only to a very slight extent. Indeed, we may approximate ψ by a step function dividing each of the coordinate axes into n sections and giving the average value of ψ in any of the $m = n^{3N}$ $3N$-dimensional cubes thus obtained. The number of conditions which can be imposed by giving the three-dimensional moments corresponding to the distribution (21) is

$$M = 8\, Nn^3 \ll m\,.$$

If we were to give some more three-dimensional fields we could increase the number of conditions but still we could not determine ψ from a number of such moments.

V

§ 12. We note that the fact that ψ depends on $3N$ space variables introduces a large ambiguity concerning the variation of the three-dimensional densities. Indeed, if we give not only $\boldsymbol{v}_\mu$ and ϱ_μ for $t = 0$ but also the time

derivatives $\dot{\boldsymbol{v}}_\mu$, then we still can construct a great manifold of ψ-functions which reproduce this extended initial condition.

Differentiating the equations of motion (18) and (19) into the time, we can eliminate with the help of the wave equations (1) the time derivatives of ψ which appear in the right hand side of the differentiated expressions. We obtain thus relations of the type

$$m_\mu \frac{d^l \boldsymbol{v}_\mu}{dt^l} = \text{function of } \psi \text{ and space derivatives integrated over the } \boldsymbol{r}_\nu, \nu \neq \mu. \tag{21a}$$

However, the left hand expressions depend for a fixed μ on the coordinate $\boldsymbol{r}_\mu$ only, while the right hand expression contains the ψ and its derivatives suitably averaged over the variables $\boldsymbol{r}_\nu \neq \boldsymbol{r}_\mu$. Therefore the right hand expressions can be taken to be 3-dimensional moments of the $3N$-dimensional distribution ψ. One can therefore find an infinite number of distributions ψ which satisfy the conditions (21a) at $t = 0$ for arbitrarily given values of the $\boldsymbol{v}_\mu$ and their time derivatives.

The fact that we can impose arbitrary initial conditions for the $\boldsymbol{v}_\mu$'s and their time derivatives means that we can prescribe the change of time of the $\boldsymbol{v}_\mu$'s themselves. I.e. *we can give* $\boldsymbol{v}_\mu(\boldsymbol{r}, t)$ *for an extended interval of time and find a* ψ*-function which corresponds to a motion in which* $\boldsymbol{v}_\mu(\boldsymbol{r}, t)$ *takes up values in this arbitrary prescribed manner.*

The above result shows that something is missing in the theory. The task of a theory is to determine the motion of a system from suitable initial conditions. Here we meet a state of affairs such that we can prescribe arbitrarily the motion of a system and the theory yields inner parameters, i.e. the wave function ψ, which leads to the motion we prescribed.

The unsatisfactory feature of the theory for $N > 1$ could be avoided in a formal way if we were to admit that the initial condition of a physical system has to be given by a $3N$-dimensional wave function or by $3N$-dimensional density distributions rather than by the averages referring to the three-dimensional space.

§ 13. So as to see the physical contents of the difficulty more clearly we give the following analogy: consider opaque bodies moving before a screen and let us observe the two-dimensional shadows which the three-dimensional bodies throw on the screen.

Studying the motion of the shadows we find that their motions cannot be determined from initial conditions. Indeed, bodies of quite different shapes may produce in one instant similar shaped shadows, but the shadows of the differently shaped bodies will change in different manner according to the shape of the moving three-dimensional body.

§ 14. To return to our original problem we can take the densities $\varrho_\mu(\boldsymbol{r})$ and velocities $\boldsymbol{v}_\mu(\boldsymbol{r})$ to represent a kind of three-dimensional projections of the $3N$ dimensional distributions $\varrho(\mathfrak{r})$ and $\mathfrak{v}_\nu(\mathfrak{r})$. If the state of the system is in fact determined by the $3N$-dimensional distribution, then the motion of the "shadows" described by the three-dimensional distributions cannot be determined from their three-dimensional initial conditions. Indeed, considering physical systems described by two wave functions $\psi_1(\mathfrak{r}, t)$ and $\psi_2(\mathfrak{r}, t)$ which lead, say at $t = 0$, to the same three-dimensional distributions. The systems starting from identical three-dimensional initial conditions will show entirely different motions for $t > 0$.

§ 15. The initial conditions giving the three-dimensional distributions at $t = 0$ do not determine the motion of a system if the equations of motions can be expressed in the form of wave equation

$$H\psi = i\hbar\dot{\psi}, \qquad \psi = \psi(\mathfrak{r}, t). \tag{22}$$

The physical problem of describing the motion of atoms seems, however, to require predictions of the motion of atoms described by three-dimensional distributions as we show presently.

Indeed, if we observe atoms we can observe their electromagnetic fields, i.e. we can observe electromagnetic fields emitted in form of radiation; we can also observe electric- or magnetic dipole moments arising if the atoms are polarized. We can further observe energy and momentum of atoms in particular if they collide with a macroscopic body. We can observe angular momentum and other similar parameters of an atom. All these quantities enumerated above can be observed more or less directly and they can be expressed using three-dimensional distributions only. Thus the features of an atom which are observed in usual experiments seem to give information at most upon the three-dimensional distributions.

§ 16. When we make the above statement we restrict ourselves to quantities which can be measured indeed by real experiments. We disregard quantities which are supposed to be "measurable" in terms of an abstract theory. To illustrate our point of view let us consider a He-atom and the supposed measurement of the positions of both of its electrons.

The wave function $\psi(\boldsymbol{r}_1, \boldsymbol{r}_2, t)$ describing a two-body configuration is supposed to give

$$P(\boldsymbol{r}_1, \boldsymbol{r}_2)\, d^3\boldsymbol{r}_1\, d^3\boldsymbol{r}_2 = |\psi|^2\, d^3\boldsymbol{r}_1\, d^3\boldsymbol{r}_2, \tag{23}$$

which quantity is supposed to give the probability to find the first particles of the system inside a volume element $d^3\boldsymbol{r}_1$, the second inside $d^3\boldsymbol{r}_2$. Taking the system, say, to consist of the two electrons of a He-atom, (23) gives the probability density of finding the electrons very near to points $\boldsymbol{r}_1$ and $\boldsymbol{r}_2$ inside the atom.

Considering real experimental conditions, we feel that it is impossible to locate by real measurements the position of even one electron inside an atom and it appears absolutely phantastic to try to make statistics of "where we find the second electron once we have found the first electron inside an element $d^3\boldsymbol{r}_1$".

§ 17. The proposition that by a series of hypothetical measurement of coordinates we can determine experimentally $\psi(\boldsymbol{r}_1, \boldsymbol{r}_2)$ seems to be absurd. Nevertheless, the wave function ψ has a good physical significance. Any real measurement will lead to the determination of moments

$$M_k = \int \psi^*(\mathfrak{r})\, \mathfrak{M}_k(\mathfrak{r})\, \psi(\mathfrak{r})\, d^{3N}\,\mathfrak{r}\,, \tag{24}$$

where $\mathfrak{M}_k(\mathfrak{r})$ is a function of $\mathfrak{r}$ or some operator acting on the wave function $\psi(\mathfrak{r})$. However, determining moments of the type (24) we obtain only very weak restrictions as to the distribution of $\psi(\mathfrak{r})$ in a $3N$-dimensional space.

We may determine the field of an atom which determination amounts to determining some moment M_k as function of the coordinate vector $\boldsymbol{r}$. In this way we obtain relations which can be written symbolically

$$M_k(\boldsymbol{r}) = \int \psi^*(\mathfrak{r})\, \mathfrak{M}_k(\mathfrak{r})\, \psi(\mathfrak{r})\, d^{3N-3}\,\mathfrak{r}\,. \tag{25}$$

The relation (25) — if $M_k(\boldsymbol{r})$ is obtained by measurement for all values of $\boldsymbol{r}$ — gives merely a three-dimensional restriction upon $\psi(\mathfrak{r})$. As explained in § 11 even a number of such restrictions are utterly insufficient for the determination of the distribution $\psi(\mathfrak{r})$ itself.

We see therefore that the empirical information we can obtain as to physical state of an atom is restricted to three-dimensional moments of ψ and therefore a useful theory must attempt to make conclusions about the motion of atoms based on information consisting of such three-dimensional moments only.

VI

§ 18. Logically there seem to be two possibilities to avoid the ambiguity involved in the more-body problems. One might suppose that the wave equation (22) gives only a *necessary condition* for the motion of $\psi(\mathfrak{r}, t)$. One might suppose that the full equations of motion have the form

$$\left.\begin{aligned} H\psi &= i\hbar\dot{\psi}\,, \qquad (a)\\ A\psi &= 0\,, \qquad (b)\end{aligned}\right\} \tag{26}$$

where the second condition is supposed to be an auxiliary condition compatible with the wave equation. If the condition (26b) is a sufficiently strong condition the solutions of (26a), (26b) reduce to a manifold of the order of that of

three-dimensional distributions. If such a condition (26b) existed, then the relations (10) and (12) together with (26b) would be sufficient to determine $\psi(\mathfrak{x})$ uniquely and thus hydrodynamical equations of motion could be obtained in the case $N > 1$ also.

§ 19. A condition of the form (26b) is obtained e.g. by requiring the wave function to be antisymmetric in certain variables. Such a condition is compatible with (26a) but it gives a very weak restriction only on the wave function. The condition that the wave function should be antisymmetric does not permit to reduce the manifold of solutions of (26a) sufficiently so as to make the solutions to correspond to three-dimensional distributions.

The ground state of an atom is uniquely determined by a variational condition. I.e. the ground state is described by the wave function for which

$$\delta \int \psi^* H\psi \, d^{3N}\mathfrak{x} = 0 . \tag{27}$$

One might be tempted to think that the auxiliary condition could be taken to be a variational condition of the type (27). The condition (26b) might require to look for the minimum of the energy among those functions ψ which lead to a given three-dimensional current charge distribution

$$\boldsymbol{v}_\mu(\boldsymbol{r}) \quad \text{and} \quad \varrho_\mu(\boldsymbol{r}) . \tag{28}$$

Thus one might try to postulate that a system which exhibits a (three-dimensional) current charge distribution (28) is to be described by that wave function ψ which leads in terms of (10), (11) to the distribution (28) and which possesses the minimum energy which is compatible with the configuration (28).

§ 20. The solutions obeying (27) together with the condition (28) obey certain differential equations which are somewhat similar to the time-independent Schrödinger equation. However, one finds that inserting as initial condition into (22) a wave function which possesses a relative minimum thus described — one finds from (22) that in the course of time the function *loses* the minimum property. Thus the conditions (27) and (28) are in general *incompatible* with the wave equation (22).

§ 21. We think it likely that conditions of the form of (26b) do not exist which are: 1) compatible with the wave equation (26) and 2) reduce the set of solutions to a sufficient degree. Whether or not this supposition is correct could be investigated in the following way.

We may suppose that the ground state of an atom — which is described at, say, $t = 0$ by a wave function $\psi_0(\mathfrak{x})$ — is a possible state. Let us consider another state which at some fixed time $t = t_1 > 0$ is described by an arbitrarily given wave function $\psi_1(\mathfrak{x})$.

The question arises whether we can find some outside perturbations which e.g. can be described by a potential

$$V(\mathfrak{r}, t) = \sum_{\nu=1}^{N} V_\nu(\boldsymbol{r}_\mu, t)\,, \tag{29}$$

such that in the interval $t = 0$ to $t = t_1$ the action of the potential makes the wave function to transform from

$$\psi = \psi_0 \quad \text{to} \quad \psi = \psi_1\,.$$

Suppose e.g. a wave equation of the form:

$$\left\{\sum_{\nu=1}^{N}\left(-\frac{\hbar^2}{2m_\nu}\nabla_\nu^2 + V_\nu(r_\nu, t)\right) + V_0\right\}\psi = i\hbar\dot{\psi}\,, \tag{30}$$

where V_0 represents the interaction between the N particles. The question arises whether we can find potentials $V_\nu(r_\nu, t)$ such that starting from an initial condition $\psi = \psi_0$ the solution of (3) will be equal to $\psi = \psi_1$ at $t = t_1$.

§ 22. The answer to the above question is not trivial for the following reason. The change $\delta\psi$ of ψ in an infinitesimal interval δt can be written

$$\delta\psi = \dot{\psi}\delta t = -\frac{i}{\hbar}H\psi\,, \tag{31}$$

we can choose the potentials V_ν at a given time t arbitrarily. Nevertheless because H contains the sum of potentials V_ν each depending on one variable only, (31) cannot be satisfied for an arbitrarily given $\delta\psi$.

In a formal way we can suppose ψ and $\psi + \delta\psi$ to represent two points in Hilbert space. We find that using potentials of the form (29) we can obtain *direct transitions* from a point ψ of Hilbert space only to exceptional points in its vicinity if we restrict ourselves to potentials of the form (29). Thus most of the points in the vicinity of a point ψ are *inaccessible* by *direct transition.*

From this it does not follow that these points cannot be reached on a round about way. In fact we think that most of the points of Hilbert space can be reached from an initial point ψ_0 as the effect of a sufficiently well chosen — rather complicated — perturbation of the form (29).

We hope to comeback to the mathematical discussion of this question in a later paper.

§ 23. The second logical possibility is to suppose that there exist no strong restrictions as to the ψ-functions which are accessible — but like in statistical mechanics the states described by ψ have very different probabilities to become realized. If there exist ψ-functions which give very likely configurations and others which give very unlikely ones, then we can postulate that a given distribution (28) is represented in most cases by a "very likely" ψ. Therefore

the motion of the system will in most cases take place in a very good approximation, in a manner to be expected in terms of a "very likely" ψ-function.

The analogy of the concept and that of statistical mechanics is a very deep one. Indeed, in statistical mechanics the motion of say a gas can be calculated exactly if the initial conditions are given, containing the coordinates and velocities of all the N atoms of the gas at $t = 0$.

From the mechanical equations of motion, the motion of the gas as a whole can be determined. However, if we give only the macroscopic density distribution and the distribution of velocity of flow, then these distributions do not determine the initial conditions for the motion of the individual atoms. Constructing sufficiently artificial initial conditions for the atoms, we come to configurations which starting from a given macroscopic initial condition behave in a very abnormal manner. With sufficient skill we can find initial conditions for the atoms which lead to an almost arbitrary prescribed macroscopic motion of the gas.

The equations of motion which give the correct macroscopic motions of a gas are obtained if we choose among the possible microscopic configurations the very likely ones. Deviations from the macroscopic equations of motions arise because of fluctuations, i.e. because occasionally there occur distributions which deviate from those which are the most likely ones.

§ 24. In the case of the ψ-function one imagines that "smoothed" functions are more likely than those which show a great deal of irregular fluctuations. It seems to be an unsolved problem which ψ's are the very likely ones.

Although we can give no method of actually selecting the "very likely ψ-functions" it seems plausible that these functions are somewhere near those possessing minimum properties of the type described in § 18. Indeed, if an atomic system is in a state possessing a great deal of energy, then it is likely to emit electromagnetic radiation and thus to reduce its energy. We expect therefore a tendency of atoms to approach states with low energy.

§ 25. We close these qualitative considerations with another remark. From the solutions of the wave equations valid for many-body systems we find — in excellent agreement with observation — the spectra of many electron systems, e.g. we find the spectrum of the He atom. A radiating He atom is a moving system and therefore we are in fact in a position to determine correctly the motion of the charge of the electrons inside a He atom.

It must be emphasized, however, that taking the superpositions of an arbitrarily large number of stationary solutions of the wave equation — we can find a combination which produces for a limited period an oscillation with an arbitrarily given frequency ν — this frequency need not be anywhere near to the optical frequencies of the He atom.

That as the result of the beat of the natural frequencies of He we can obtain a state in which an arbitrary frequency ν arises, is analogous to the

problem of the Fourier analysis. Using a large number of Fourier components we can obtain (inside a limited interval) a harmonic function with an arbitrary period ν which may differ from the periods of the terms of the series.

The state in which a He atom oscillates for a time with an unusual frequency ν contains obviously components of rather higher energy — and after a certain time the accidental phase relations between the natural frequencies which produce the beat frequency ν will disappear.

When we state that according to the theory a He atom generally emits well-defined combination frequencies only, then we make already a strong restriction on the wave functions ψ which we think likely to occur — we suppose that in the observed states the wave function of the discrete states are predominant.

REFERENCES

1. L. JÁNOSSY and M. ZIEGLER-NÁRAY, Acta Phys. Hung., **16**, 37, 1963.
2. L. JÁNOSSY and M. ZIEGLER-NÁRAY, Acta Phys. Hung., **16**, 345, 1964.
3. L. JÁNOSSY and M. ZIEGLER-NÁRAY, Acta Phys. Hung., **20**, 233, 1966.
4. M. HUSZÁR and M. ZIEGLER-NÁRAY, Acta Phys. Hung., **25**, 99, 1968.
5. M. HUSZÁR and M. ZIEGLER-NÁRAY, Acta Phys. Hung., **26**, 223, 1969.

ГИДРОДИНАМИЧЕСКАЯ МОДЕЛЬ ВОЛНОВОЙ МЕХАНИКИ

ЗАДАЧА МНОГИХ ТЕЛ

Л. ЯНОШИ

Резюме

Дискутируется проблема расширения гидродинамической модели—описанной в предыдущих работах — к задаче многих тел. Показывается, что появляющиеся в приложении трудности не математического характера, они отображают физическую проблему, не решенную по нашему мнению до настоящего времени. Оказывается возможным, что в точном решении проблемы многих тел удается выбирать из возможных волновых функций те, которые очень подобны в статистическом смысле. Предполагаемый отбор напоминает отбор очень подобных конфигураций в статистической механике.

Acta Physica Academiae Scientiarum Hungaricae, Tomus 27, pp. 47—85 (1969)

FIRST-ORDER MAGNETIC PHASE TRANSITIONS*

By

L. PÁL

CENTRAL RESEARCH INSTITUTE FOR PHYSICS, BUDAPEST

(Received 9. I. 1969)

The general properties of the first-order magnetic phase transitions between ordered structures have been investigated. The number of possible models has been limited by supposing the sensitivity of the exchange energy to the interatomic distance to be responsible for the phase transition. It is shown that the magnetic phase transition occurs as a result of a sign-change in the proper combination of the exchange parameters. The transition may be influenced by the variation of the pressure and the magnetic field. The actual phase transition is, however, hindered in both directions by the elastic energy wall, separating the free energy minima of the different phases. The T—P phase diagram has been calculated and the conditions for the existence of a triple point in the T—P plane have been investigated in the case of antiferromagnetic $\rightleftarrows$ ferromagnetic transitions. The temperature hysteresis, i.e. the difference between the upper (T_{sup}) and lower (T_{inf}) transition temperatures has been determined at different pressures and for both temperatures a linear dependence has been obtained. The character of the disappearance of the magnetic order has been also studied and it has been found that under certain conditions the order of the ferromagnetic—paramagnetic transition may be different from that of the antiferromagnetic—paramagnetic one.

The T—H coexistence curve between the ferromagnetic and the spin-flop antiferromagnetic phases has been determined. The upper and the lower phase transition temperature versus magnetic field curves are calculated and it is found that with increasing magnetic field and decreasing temperature the difference between these two curves (i. e. the hysteresis width) becomes increasingly small until at a critical field (H_t) and temperature (T_t) they end in a common point with the coexistence curve. Below T_t the variation of the magnetic field does not lead to a first-order antiferromagnetic $\rightleftarrows$ ferromagnetic transformation. The ferromagnetic phase is nothing, but the antiferromagnetic phase in a magnetic field strong enough to turn the moments parallel to the field direction. Above H_t but below H_c the variation of the temperature brings about also a second-order ferromagnetic $\rightleftarrows$ antiferromagnetic transition.

The discontinuous change of the lattice parameter and that of the sublattice magnetization have been calculated at the coexistence temperature and at both the upper and lower transition temperatures. It has been shown that the entropy change of the transition has two contributions: one of them is associated with the volume change while the other with the magnetization change. Under certain conditions the order of magnitude of both contributions may be the same.

1. Introduction

The subject of this paper is related to first-order magnetic phase transitions. The expression, first-order phase transition is used in its usual thermodynamic sense, i.e. the first derivatives of the system's Gibbs free-energy with intensive parameters (temperature, pressure, magnetic field, e.g.) exhibit a discontinuity at the critical values of these parameters. In other words, the

* Dedicated to Prof. P. GOMBÁS on his 60th birthday.

molar entropy, molar volume, molar magnetization, and other molar parameters suffer discontinuous change. In the higher-order phase transitions the molar parameters are continuous but their derivatives are discontinuous. It is worthwhile to note here that the most characteristic feature of the higher-order phase transformations is the discontinuous change in symmetry of the system with the continuous change of the state of system. This approach was very successfully developed many years ago by LANDAU and LIFSHITZ [1].

In order to systematize in a very simple way the magnetic phase transformations a "family tree" has been constructed from different types of trans-

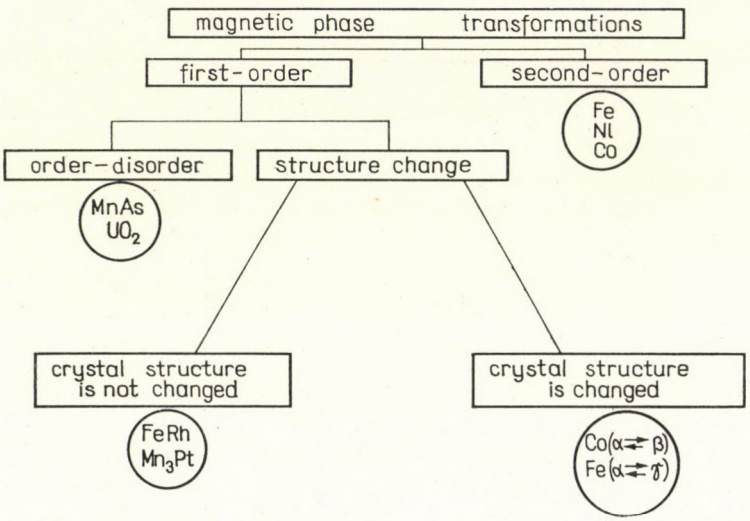

Fig. 1. "Family tree" of magnetic phase transitions

itions. This "family tree" is shown in Fig. 1. Some magnetic systems that exhibit transitions of first-order are listed in Table I. It is clear that the simplest case is when the crystal structure does not change during the magnetic structure transition and when this latter takes place between ordered magnetic phases. As substantial theoretical difficulties are associated with those phase transformations where the magnetic order disappears, such transformations will be excluded from our considerations.

It has been known since the last century that the onset of the magnetic order (e.g. ferromagnetism) results in a smaller or larger distortion of the crystal lattice (in many cases without any crystal symmetry change). This phenomenon is related to the dependence of the exchange energy on the interatomic spacing.

As a result of this dependence the free-energy of the crystal may be lowered by a distortion of the lattice in the direction of decreasing exchange-energy. The distortion will introduce to the free-energy a term in strain energy

Table I

Some magnetic systems that exhibit transition of first-order

Material	Type of the transition	Transition temperature °K	Material	Type of the transition	Transition temperature °K
MnAs	$F \rightarrow P$	318	Mn_3GaC	$AF \rightarrow F$	150
Cr_2As_2	$F_i \rightarrow P$	213	Mn_3Ge_2	$AF \rightarrow F$	113
Cr	$AF \rightarrow P$	311.7	$Mn_{0,9}Li_{0,1}Se$	$AF \rightarrow F$	71
UO_2	$AF \rightarrow P$	30.8	$(Mn_{1-x}Cr_x)_2Sb$	$AF \rightarrow Fi$	$T(x)$
$TiCl_3$	$AF \rightarrow P$	210	$RbFeF_3$	$F \rightarrow AF$	86
$MnBr_2$	$AF \rightarrow P$	2.16	Dy	$F \rightarrow S$	85
$KMnF_3$	$AF \rightarrow P$	88.3	$MnSn_2$	$AF \rightarrow AF$	73
FeRh	$AF \rightarrow P$	350	Mn_3Pt	$AF \rightarrow AF$	365

which will increase the free-energy, and thus, a compromise between distortion and exchange is reached, which minimizes the free-energy. In the case of order-disorder phase transformations (i.e. ferromagnetic $\rightleftarrows$ paramagnetic, antiferromagnetic $\rightleftarrows$ paramagnetic) the magneto-elastic coupling between the magnetic and elastic part of the system's free-energy may drastically alter the character of phase transitions. If the exchange parameter dependence on the interatomic spacing is rather strong a first-order phase transition will be observed instead of the usual second-order one.

The reason for this is quite obvious. The elastic distortion tends to stabilize the magnetic order and, thus, slows down its decrease with temperature. At a certain temperature, however, the magnetic order can find no way for decreasing smoothly to zero since the stabilizing influence of the lattice distortion ceases to act below a certain magnetic order, i.e. at a critical temperature the magnetic order and lattice distortion go to zero discontinuously. Using BEAN's formulation [2] the situation is like that of a man who has run beyond the brink of a cliff; there is no gentle way down.

Of course, not only the appearance and disappearance of the magnetic order but in many cases the structure changes in the ordered phase may also lead to a remarkable variation of the crystal distortion. In the following these structure changes will be discussed and the aim of this paper is to give an elementary introduction to the physics of these phenomena.

2. Magnetic structure and the model

First of all, we have to discuss the conditions for the existence of various magnetic structures in a given crystal lattice since our goal is to study the phase transitions between these structures. To do this in general is a very

complex task and, therefore, we have to limit our considerations to the simplest case which is probably distinct from any real situation but has a great advantage, the possibility of an elementary treatment without incurring any substantial losses in the physically important conclusions.

The stability conditions required for a given magnetic structure can be derived when we first answer the following question: what are the possible magnetic structures in a given crystallographic symmetry?

Assuming second-order character of the formation of various magnetic structures from the magnetic disorder (i.e. from the paramagnetic phase) this question can be answered in principle very rigorously.

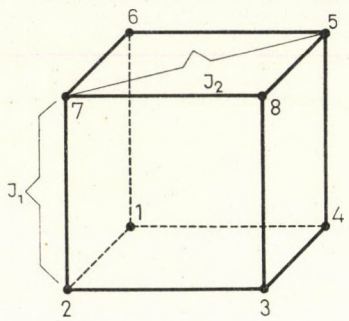

Fig. 2. Lattice points with sublattice numbers

One has to notice here that the assumption of the second-order character of the magnetic structure formation does not involve any serious restriction on the character of the phase transitions between the ordered structures. Therefore, we could start our considerations in this way.

Unfortunately, in answering the first question the problem of finding the criteria for the existence of various magnetic structures in terms of physical parameters remains still unsolved. If we want to solve this problem too, we need a more or less definite model containing important information about the exchange interactions in the crystal.

We do not want to go into the details of the method with the help of which we can answer the first question; we refer only to some basic works in this field. Originally LANDAU and LIFSHITZ [1] proposed this theory for the investigations of the ordered structures in alloys. Later DZYALOSHINSKY [3] and KOVALYOV [4] applied it to the case of magnetic phase transformations and very recently a further generalization was made by SÓLYOM [5].

This rigorous method can be used only for finding the possible magnetic structures but for the actual calculation we always need a definite model. Now we want to choose the simplest one which is still useful enough to illustrate the most important qualitative properties of the phase transformations.

In the following we shall proceed from an improved version of the model proposed by ANDERSON [6] and SMART [7]. First of all, we choose a simple

cubic lattice for the calculations and assume the exchange interaction between the localized magnetic moments to be other than zero only for the nearest and for the next-nearest neighbours. In order to ensure that within a given distance each lattice point should be surrounded by lattice points belonging to different sublattices one has to introduce a specified number of different sublattices only. If this characteristic distance is the interatomic spacing between the next-nearest neighbour atoms, eight sublattices are required. The lattice points with their sublattice number are shown in Fig. 2.

We denote by $\overline{M}_j (j = 1, \ldots, 8)$ the thermal averaged magnetic moment in the j'th sublattice and write down the internal energy of the crystal per unit volume in molecular field approximation. We get

$$U_m = -\sum_{i,j} \overline{M}_i A_{ij} \overline{M}_j , \tag{2.1}$$

where

$$\tilde{A} = \begin{pmatrix} \tilde{A}_1 & \tilde{A}_2 \\ \tilde{A}_2 & \tilde{A}_1 \end{pmatrix} \tag{2.2}$$

is the interaction matrix and

$$\tilde{A}_1 = \begin{pmatrix} 0 & a & b & a \\ a & 0 & a & b \\ b & a & 0 & a \\ a & b & a & 0 \end{pmatrix}, \quad \tilde{A}_2 = \begin{pmatrix} b & a & b & 0 \\ 0 & b & a & b \\ b & 0 & b & a \\ a & b & 0 & b \end{pmatrix}. \tag{2.3}$$

Here we used the notations

$$a = \frac{1}{4} NJ_1, \quad b = \frac{1}{2} NJ_2. \tag{2.4}$$

J_1 and J_2 are the effective exchange parameters between the nearest and the next-nearest neighbours, respectively, and N is the number of atoms in the unit volume.

Taking into account that the effective internal field

$$\overline{H}_j = -\frac{\partial U_m}{\partial \overline{M}_j} \tag{2.5}$$

$$(j = 1, 2, \ldots, 8)$$

must have the same direction as the corresponding sublattice magnetization, i.e.

$$\overline{H}_j = \lambda \overline{M}_j \tag{2.6}$$

we may get immediately the possible magnetic structures from the eigen-value equation

$$(A - \lambda \tilde{E})\, \overline{M} = 0\,, \tag{2.7}$$

where $\tilde{E}$ is the unit matrix and

$$\tilde{M} = \begin{pmatrix} \overline{M}_1 \\ \overline{M}_2 \\ \vdots \\ \overline{M}_8 \end{pmatrix} \tag{2.8}$$

is the structure matrix. One has to note that the independence of the proportionality factor λ of sublattice magnetization is valid only near the ordering temperature.

Making use of some theorems for block-matrices the eigenvalues of equation (2.7) can be easily calculated. One finds

$$\lambda_1 = 3(a+b)\,, \quad \lambda_2 = -3(a-b)\,, \quad \lambda_3 = \lambda_4 = \lambda_5 = -(a+b)$$
$$\lambda_6 = \lambda_7 = \lambda_8 = (a-b)\,.$$

The magnetic structures are determined by the corresponding eigen-vectors belonging to these eigen-values. Results of the calculations are summarized in Table II. As can be seen one ferromagnetic and three antiferromagnetic structures are possible in the frame of this very simple model. The antiferromagnetic unit cells are doubled in all three directions while the ferromagnetic one is identical with the chemical unit cell.

The eigen-value of a given structure is proportional to the ordering temperature. Of two phases that is the more stable which has a higher ordering

Table II

Eigen-values and eigen-vectors for different structures

Eigen-value	Eigen-vector	Structure	Internal energy
$3(a+b)$	$\overline{M}_1 = \overline{M}_2 = \ldots = \overline{M}_8 = \overline{M}$	ferromagnetic F	$-12(a+b)M^2$
$-3(a-b)$	$\overline{M}_1 = \overline{M}_3 = \overline{M}_5 = \overline{M}_7 = \overline{M}$ $\overline{M}_2 = \overline{M}_4 = \overline{M}_6 = \overline{M}_6 = -\overline{M}$	antiferromagnetic AF I	$12(a+b)M^2$
$-(a+b)$	$\overline{M}_1 = \overline{M}_3 = \overline{M}_6 = \overline{M}_8 = \overline{M}$ $\overline{M}_2 = \overline{M}_4 = \overline{M}_5 = \overline{M}_7 = -\overline{M}$	antiferromagnetic AF II	$4(a+b)M^2$
$a-b$	$\overline{M}_1 = \overline{M}_2 = \overline{M}_3 = \overline{M}_4 = \overline{M}$ $\overline{M}_5 = \overline{M}_6 = \overline{M}_7 = \overline{M}_8 = -\overline{M}$	antiferromagnetic AF III	$-4(a-b)M^2$

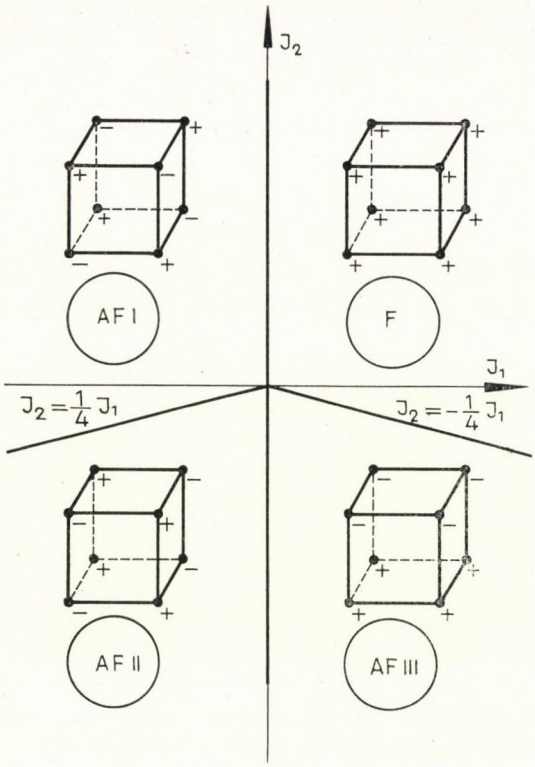

Fig. 3. Different structures and phase boundaries

temperature. The phase boundaries between the different phases are shown in Fig. 3.

Four structure changes are possible, namely

$F \rightleftarrows AF\text{I}$,	if $J_2 > 0$ and	J_1	changes its sign,
$AF\text{I} \rightleftarrows AF\text{II}$,	if $J_1 < 0$ and	$4J_2 - J_1$	changes its sign,
$AF\text{II} \rightleftarrows AF\text{III}$,	if $J_2 < 0$ and	J_1	changes its sign,
$AF\text{III} \rightleftarrows F$,	if $J_1 > 0$ and	$4J_2 + J_1$	changes its sign.

A simple phenomenological description of the structure changes can be made in the following way. One finds that during the transition certain antiferromagnetically oriented pairs transform to ferromagnetic ones and vice versa. Let 2Θ be the angle between the moments of transforming pairs in an intermediate (non-equilibrium) state and denote by m the cosine of Θ, i.e.

$$m = \cos\Theta . \tag{2.9}$$

The magnetic part of the internal energy may be written as

$$U_m = -(A+\gamma B) M_0^2 \sigma^2 - B M_0^2 \sigma^2 (2m^2-1), \qquad (2,10)$$
$$(A > 0),$$

where the parameter B which is an appropriate combination of interaction constants changes its sign during the phase transition. σ is the average relative magnetization per atom at temperature T, i.e.

$$\sigma = \frac{M}{M_0},$$

where M_0 is atomic magnetic moment at $T = 0$. The values of A, B and γ for different structure changes are listed in Table III.

When the sign of the parameter B is changing the m has to vary from $m = 0$ to $m = 1$, or vice versa; in other words phase transformation takes place. It is important to note that physical meaning can be attributed to m only in the case of antiferromagnetic $\rightleftarrows$ ferromagnetic transitions. In this case the meaning is evident; m is a measure of the bending between the moments.

It is absolutely clear that this oversimplified model cannot give practically useful results but, as we shall see later, a lot of physically interesting qualitative conclusions can be drawn from it.

The next step in perfecting the model is to exploit the sensitivity of the exchange parameters against the lattice distortions. First NÉEL [8] and later SMART [7], BEAN and RODBELL [2], KITTEL [9] and many others [10] have emphasized the importance of this sensitivity and investigated its influence on the temperature behaviour of magnetization. Now, we should like to apply some of their results to the theory of those magnetic structure transitions which are associated with lattice distortions.

Let l_c be the distance between the nearest neighbour atoms at which the parameter B changes its sign. So, one may expand A and B into a power

Table III

Parameters for various transitions

	$F \rightleftarrows AFI$	$AFI \rightleftarrows AFII$	$AFII \rightleftarrows AFIII$	$AFIII \rightleftarrows F$
A	$6NJ_2$	$-\frac{3}{2}NJ_1$	$-2NJ_2$	$\frac{3}{2}NJ_1$
B	$3NJ_1$	$N(4J_2-J_1)$	$-NJ_1$	$-N(4J_2-J_1)$
γ	0	$\frac{1}{2}$	0	$\frac{1}{2}$

series of l—l_c. For the sake of simplicity, terms higher than linear are neglected, i.e.

$$A = A_0 + \left(\frac{dA(l)}{dl}\right)_{l=l_c} (l-l_c)\,,$$
$$B = \left(\frac{dB(l)}{dl}\right)_{l=l_c} (l-l_c)\,. \tag{2.11}$$

As has already been mentioned, the dependence of exchange interactions on the interatomic spacing leads to a spontaneous distortion of the lattice. The competition between the bonding and exchange forces will determine the actual value of the distortion. Let l_0 be the distance between the nearest neighbour atoms at temperature $T = 0$ in the absence of distortion and let ε be the relative dilation at temperature $T \geq 0$.

One gets from (2.11)

$$A = A_0 + A_1(\varepsilon-\varepsilon_c) \quad \text{and} \quad B = B_1(\varepsilon-\varepsilon_c)\,, \tag{2.12}$$

where

$$A_1 = \frac{1}{3}\, l_0 \left(\frac{dA(l)}{dl}\right)_{l=l_c} \tag{2.13}$$

and

$$B_1 = \frac{1}{3}\, l_0 \left(\frac{dB(l)}{dl}\right)_{l=l_c}, \tag{2.14}$$

while

$$\varepsilon_c = 3\,\frac{l_c - l_0}{l_0}\,. \tag{2.15}$$

In the presence of lattice distortion one has to add to the internal energy an elastic energy term which in its simplest form is

$$U_e = \frac{1}{2} R\varepsilon^2\,, \tag{2.16}$$

where

$$\frac{1}{R} = -\frac{1}{V}\left(\frac{\partial V}{\partial P}\right)_T \tag{2.17}$$

is the compressibility.

The thermodynamics of the phase transition can be founded on the Gibbs free-energy per unit volume. Denoting the magnetic and the lattice entropy by S_m and S_l we can write

$$G = U_m + U_e + P_\varepsilon - T(S_m+S_l)\,. \tag{2.18}$$

This is the appropriate form of the free-energy needed in our case. In accordance with the molecular-field approximation the magnetic entropy may be expressed as

$$S_m = Nk\left\{\log 2 - \frac{1}{2}(1+\sigma)\log(1+\sigma) - \frac{1}{2}(1-\sigma)\log(1-\sigma)\right\}. \quad (2.19)$$

The lattice entropy is approximated as

$$S_l = R\alpha\varepsilon\,, \quad (2.20)$$

where

$$\alpha = \frac{1}{V}\left(\frac{\partial V}{\partial T}\right)_P \quad (2.21)$$

is the volume thermal expansion coefficient. Introducing the following dimensionless quantities

$$\Omega = \frac{A_1}{A_0}\,, \quad \omega = \frac{B_1}{B_0}$$

$$p = \frac{P}{A_0 M_0^2}\,, \quad r = \frac{R}{A_0 M_0^2}\,, \quad \tau = \frac{NkT}{2 A_0 M_0^2} \quad (2.22)$$

and

$$\Theta = \frac{R\alpha}{Nk}\,, \quad w(\sigma) = \frac{S_m}{Nk} \quad (2.23)$$

the Gibbs free-energy can be written in the form

$$G = A_0 M_0^2\left\{-\sigma^2 - [\Omega + \omega(\gamma + 2m^2 - 1)]\,\sigma^2(\varepsilon - \varepsilon_c) + \right.$$
$$\left. + \frac{1}{2} r\varepsilon^2 + p\varepsilon - 2\tau\Theta\varepsilon - 2\tau W(\sigma)\right\}, \quad (2.24)$$

where A_0 is a definitely positive quantity.

The equilibrium value of the deformation can be found from the equation

$$\frac{\partial G}{\partial \varepsilon} = 0\,. \quad (2.25)$$

One gets

$$\varepsilon = 2\frac{\Theta}{r}\tau - \frac{p}{r} + (\Omega + \gamma\omega)\frac{\sigma^2}{r} + \frac{\omega}{r}\sigma^2(2m^2 - 1)\,. \quad (2.26)$$

The change of the deformation at the phase transition point is

$$\delta\varepsilon = \varepsilon(m=1) - \varepsilon(m=0) = \frac{2\sigma^2\omega}{r} \quad (2.27)$$

the sign of which is determined by the sign of B_1. Making use of the expression (2.26) for the Gibbs free-energy one can derive the formula

$$G = A_0 M_0^2 \left\{ -\sigma^2 \left[1 + \frac{\mu}{r} (2\Theta\tau - r\varepsilon_c - p) \right] - \right.$$
$$\left. - \frac{1}{2} \frac{\mu^2}{r} \sigma^4 - 2\tau w(\sigma) - \frac{1}{2} r \left(\frac{2\Theta\tau - p}{r} \right)^2 \right\}, \tag{2.28}$$

where

$$\mu = \Omega + \omega (\gamma + 2m^2 - 1). \tag{2.29}$$

The relative sublattice magnetization per atom can be expressed from the equation

$$\frac{\partial G}{\partial \sigma} = 0. \tag{2.30}$$

After a short calculation one finds

$$\sigma = th \frac{h_{\text{mol}}}{\tau}, \tag{2.31}$$

where

$$h_{\text{mol}} = \left[1 + \frac{\mu}{r} (2\Theta\tau - r\varepsilon_c - p) \right] \sigma + \frac{\mu^2}{r} \sigma^3. \tag{2.32}$$

In the majority of cases the ratio μ/r is smaller than one and, thus, making use of the inequality

$$q = \frac{\mu}{r} (\mu\sigma^2 + 2\Theta\tau - r\varepsilon_c - p) \ll 1 \tag{2.33}$$

one may expand G into a power series of q and it seems sufficient to retain only those which are not higher than linear. To do this, first of all, we rewrite (2.31) in the form

$$\sigma = \sigma_0 + \sigma_1 q \sim \sigma_0 + \sigma_1 q_0, \tag{2.34}$$

where

$$q_0 = \frac{\mu}{r} (\mu\sigma_0^2 + 2\Theta\tau - r\varepsilon_c - p) \tag{2.35}$$

and

$$\sigma_0 = th \frac{\sigma_0}{\tau}. \tag{2.36}$$

The Gibbs free-energy is given by

$$G(\sigma, m) = G_0 (\sigma_0, 0) + q_0 G_1 (\sigma_0, m) + 0 (q_0^2). \tag{2.37}$$

A short calculation shows that the linear corrections to σ^2 and $2\tau w(\sigma)$ cancel each other out, and thus, we get

$$G_0(\sigma_0, 0) = A_0 M_0^2 \left\{ -\sigma_0^2 - 2\tau w(\sigma_0) - \frac{1}{2} r \left(\frac{2\Theta\tau - p}{r} \right)^2 \right\} \tag{2.38}$$

and

$$G_1(\sigma_0 m) = -\frac{1}{2} A_0 M_0^2 \sigma_0^2 \left(1 + \frac{2\Theta\tau - r\varepsilon_c - p}{\mu\sigma_0^2 + 2\Theta\tau - r\varepsilon_c - p} \right). \tag{2.39}$$

The second term on the right side of (2.37) can be re-expressed in the form

$$q_0 G_1(\sigma_0, m) = A_0 M_0^2 \sigma_0^2 \omega\delta\varepsilon_0 \left\{ f(m, u) + f_0(u) \right\}, \tag{2.40}$$

where

$$f(m, u) = -m^4 + \left(1 - \frac{u}{\omega} \right) m^2 \tag{2.41}$$

and

$$f_0(u) = \frac{1}{2} \left(1 - \gamma - \frac{\Omega}{\omega} \right) \left\{ \frac{u}{\omega} - \frac{1}{2} \left(1 + \gamma + \frac{\Omega}{\omega} \right) \right\}. \tag{2.42}$$

Here, we have introduced the notation

$$u = \frac{2\Theta\tau - r\varepsilon_c - p}{\sigma_0^2} + \Omega + \gamma\omega . \tag{2.43}$$

It can be seen from (2.40) that the reduced free-energy $f(m, u)$ has to be used for the investigation of phase transitions characterized by different values of γ, listed in Table III. In very fortunate cases the relative magnetization σ_0 does not vary significantly with temperature in the neighbourhood of the transition point and, thus, the parameter u introduced by (2.43) may be regarded as a linear function of temperature. In the following this linear dependence will be assumed unless the refinement of the theory requires a more realistic dependence.

3. Phase transitions with constant σ_0

Making use of the preceding model, we should like to apply it to the phase transitions between antiferromagnetic structures. In this case the first task is to find the necessary and sufficient conditions for the loss and onset of stability in the states $m = 0$ (or $m = 1$), and $m = 1$ (or $m = 0$), respectively.

The considerations are very trivial, nevertheless, a short review of them will be useful for the better understanding of the physical content of the theory.

The equilibrium value of the parameter m has to be chosen from the roots of the equation

$$\frac{df}{d\Theta} = 2m(1-m^2)^{1/2}\left(1-\frac{u}{\omega}-2m^2\right) = 0 \tag{3.1}$$

which has three solutions, namely

$$m_1 = 0; \quad m_2 = \sqrt{\frac{1}{2}\left(1-\frac{u}{\omega}\right)}; \quad m_3 = 1\,. \tag{3.2}$$

The physically allowed Θ values in these solutions have to satisfy the condition $0 \leq \Theta \leq \pi/2$.

Let us follow the variation of the parameter m in the equilibrium state with increasing u/ω. (As has already been mentioned u/ω is a linear function of temperature, if σ_0 is constant within the temperature interval under consideration.) If $u/\omega < -1$, then among the solutions (3.2) only two, namely m_1 and m_3 have physical meaning, $m = m_1$ minimizing the reduced free energy since

$$\frac{d^2f}{d\Theta^2} = \begin{cases} 2\left(1-\dfrac{u}{\omega}\right), & \text{if} \quad m = m_1 \\ 2\left(1+\dfrac{u}{\omega}\right), & \text{if} \quad m = m_3. \end{cases}$$

The second solution gives $m_2 > 1$. Therefore, it has to be excluded.

When $-1 \leq u/\omega \leq 1$, then among the solutions (3.2) satisfying the condition $0 \leq \Theta \leq \pi/2$, two, corresponding to $m = m_1$ and $m = m_3$, minimize, while the third $m = m_2$ maximizes the free energy as one can see from the expression

$$\frac{d^2f}{d\Theta^2} = \begin{cases} 2\left(1-\dfrac{u}{\omega}\right), & \text{if} \quad m = m_1, \\ -2\left(1-\dfrac{u^2}{\omega^2}\right), & \text{if} \quad m = m_2, \\ 2\left(1+\dfrac{u}{\omega}\right), & \text{if} \quad m = m_3. \end{cases}$$

The maximum between the two minima hinders the transitions. The free energy of the state $m = m_3$ is equal to that of the state $m = m_1$ at temperature $u/\omega = 0$, but the actual phase transition $m_1 \to m_3$ takes place only at that

temperature where the energy barrier between the states disappears. Since

$$f(m,\tau)=\begin{cases} 0 & , \quad \text{if} \quad m=m_1\,, \\ \dfrac{1}{4}\left(1-\dfrac{u}{\omega}\right)^2 & , \quad \text{if} \quad m=m_2\,, \\ -\dfrac{u}{\omega} & , \quad \text{if} \quad m=m_3\,, \end{cases}$$

the $m_1 \to m_3$ transition will be realized when

$$u(1\to 3)-\omega=0\,. \tag{3.3}$$

Finally, if $u/\omega > 1$, then again only two solutions, namely $m = m_1$ and $m = m_3$ have physical meaning and the free energy is minimized by $m = m_3$. The solution m_2 is imaginary and therefore must be excluded.

Now, when we follow the change of the equilibrium value of the parameter m in the direction of decreasing temperature we find quite a similar picture. At the temperature $u/\omega = 0$ the free energy of the phase $m = m_1$ becomes the same as that of the phase $m = m_3$. Transition, however, cannot be observed because the energy maximum between the coexisting phase hinders the transition process. The phase transformation actually takes place at that temperature, where the system's free energy in the state $m = m_3$ will be equal to that in the maximum. This condition is precisely

$$-\frac{u}{\omega}=\frac{1}{4}\left(1-\frac{u}{\omega}\right)^2,$$

i.e.

$$u(3\to 1)+\omega=0\,. \tag{3.4}$$

If $\omega > 0$ (i.e. $B_1 > 0$), then

$$u(1\to 3) > u(3\to 1)\,.$$

The opposite inequality is valid when $\omega < 0$. In the next sections we shall use the following notations:

$$\begin{aligned} u_{\text{sup}} &= \max\{u(1\to 3)\,;\ \ u(3\to 1)\} \\ u_{\text{inf}} &= \min\ \{u(1\to 3)\,;\ \ u(3\to 1)\}. \end{aligned} \tag{3.5}$$

The equilibrium temperature u_e where the two phases coexist lies between the upper and lower transition temperatures. (In our case $u_e = 0$.)

The ferromagnetic $\leftrightarrows$ antiferromagnetic transitions in the absence of an external magnetic field have to be treated in a similar way.

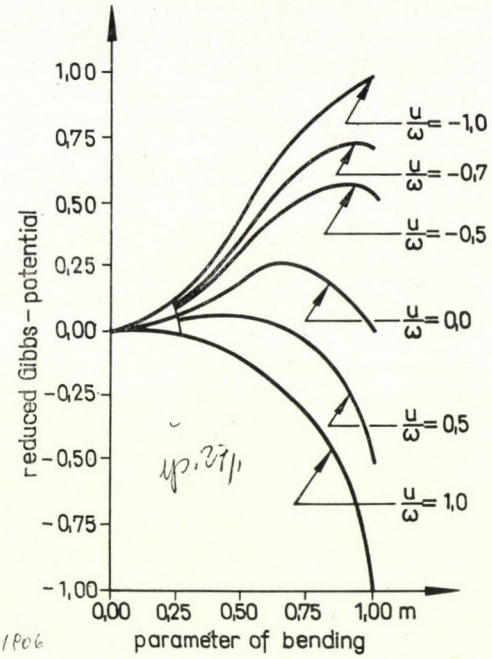

Fig. 4. Dependence of the reduced Gibbs potential on the parameter of bending for different values of u/ω

The dependence of the reduced Gibbs potential on the parameter m is shown in Fig. 4 for different values of u/ω. The variation of the equilibrium value of m with temperature in the ideal case is illustrated in Fig. 5 (see the full line).

From the equations (3.3) and (3.4) one gets

$$T_{\text{sup}} = T_e(P) - \frac{1}{2}\,\frac{\delta\varepsilon_0}{\alpha}\;;\quad T_{\text{inf}} = T_e(P) - \frac{1}{2}\,\frac{\delta\varepsilon_0}{\alpha}\,, \tag{3.6}$$

where

$$T_e(P) = \frac{1}{2}\,\frac{P}{R\alpha} + \frac{1}{2}\,\frac{\varepsilon_c}{\alpha} - \frac{1}{2}\,\frac{\Omega + \gamma\omega}{R\alpha}\,A_0\,M_0^2\,\sigma_0^2. \tag{3.7}$$

Introducing the expression for the dilation discontinuity at the transition temperature the width of the temperature hysteresis can be given in the following form

$$T_{\text{sup}} - T_{\text{inf}} = \frac{\delta\varepsilon_0}{\alpha}\,. \tag{3.8}$$

This formula is valid only if the sublattice magnetization σ_0 hardly changes in the interval $T_{\text{inf}} < T < T_{\text{sup}}$. The equivalent width in pressure is

$$P_{\text{sup}} - P_{\text{inf}} = 2R\delta\varepsilon_0.$$

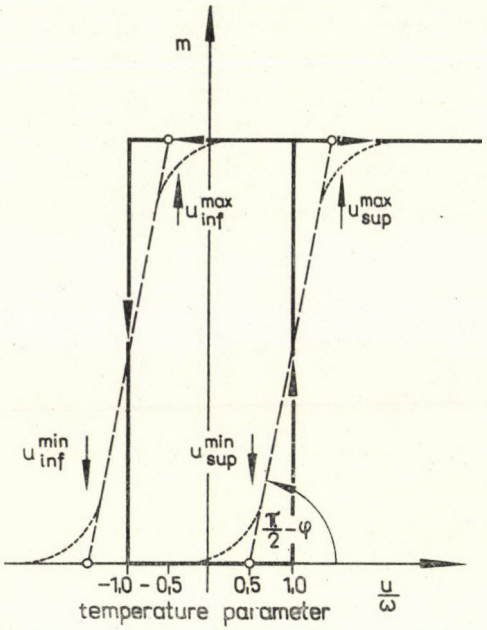

Fig. 5. Variation of the equilibrium value of m with temperature (the full line corresponds to the completely homogeneous transition while the dashed line to the inhomogeneous one)

In practical cases the sharpness of the transition is rather smoothed because of more or less inhomogeneity in internal stresses existing in any real crystal. (See the dashed line in Fig. 4.) As a result of this inhomogeneity one may expect a definite cant in the hysteresis-loop. The canting angle Φ is exactly

$$\Phi = \text{arc cotan} \frac{\langle(\delta P)^2\rangle^{1/2}}{2R\alpha}, \tag{3.9}$$

where $\langle(\delta P)\rangle^2$ is the mean square deviation of the local pressure.

From the $u_e = 0$ one may see that the coexistence temperature, i.e. the temperature where the Gibbs potentials of both phases $m = 0$ and $m = 1$ are equal, satisfies the equation

$$\frac{dT_e}{dP} = \frac{1}{2R\alpha} \tag{3.10}$$

which is exactly the same as that derived from the Clausius-Clapeyron equation if one assumes that the discontinuous change in entropy is due to the discontinuous change in lattice parameter only. The latent heat is given by

$$Q_1 = T_e R\alpha\delta\varepsilon_0. \tag{3.11}$$

In order to extend our investigations to the case of antiferromagnetic $\rightleftarrows$ ferromagnetic transitions in an external magnetic field one has to add to the Gibbs free energy (2.34) a new term expressing the interaction between the magnetic moments and field. Denoting the magnetization per atom in the sublattice a and b by $\overline{M}_a$ and $\overline{M}_b$, respectively, one can write this additional term in the form

$$G_H = -\frac{1}{2} N\overline{H}(\overline{M}_a + \overline{M}_b). \tag{3.12}$$

Let us introduce the vectors

$$\bar{l} = \frac{\overline{M}_a - \overline{M}_b}{2M_0\sigma} \quad \text{and} \quad \overline{m} = \frac{\overline{M}_a + \overline{M}_b}{2M_0\sigma}, \tag{3.13}$$

where

$$M_0\sigma = |\overline{M}_a| = |\overline{M}_b| . \tag{3.14}$$

If one neglects the magnetic anisotropy in the crystal then the vector $\bar{l}$ is perpendicular and the vector $\overline{m}$ is parallel to the external field direction. Therefore, instead of (3.12) one gets

$$G_H = -2A_0 M_0^2 \sigma hm , \tag{3.15}$$

where

$$h = \frac{1}{2} \frac{NH}{A_0 M_0}$$

and here m is the absolute value of $\overline{m}$. The role of m is the same as in (2.10) but in this case it has a definite physical meaning; m being the net magnetization of the antiferromagnetic phase. One has to note that in the majority of the practically important cases the order of magnitude of h is the same as that of μ/r. Therefore, instead of (3.15) we write

$$G_H \sim -2A_0 M_0^2 \sigma_0 hm . \tag{3.16}$$

One may expect that the presence of the external magnetic field will promote the antiferromagnetic $\rightarrow$ ferromagnetic transition. Near the coexistence temperature a relatively weak magnetic field may already produce a significant net magnetization. In other words, this means that with the increasing magnetic field the antiferromagnetically coupled moments gradually turn into the field direction, i.e. the angle between the moments decreases. However, contrary to the usual behaviour of antiferromagnets, in this case the angle between the moments decreases to a definite, temperature dependent value only at which the umberella-like antiferromagnetic structure will suddenly collapse, and thus, a simple ferromagnetic structure will be formed.

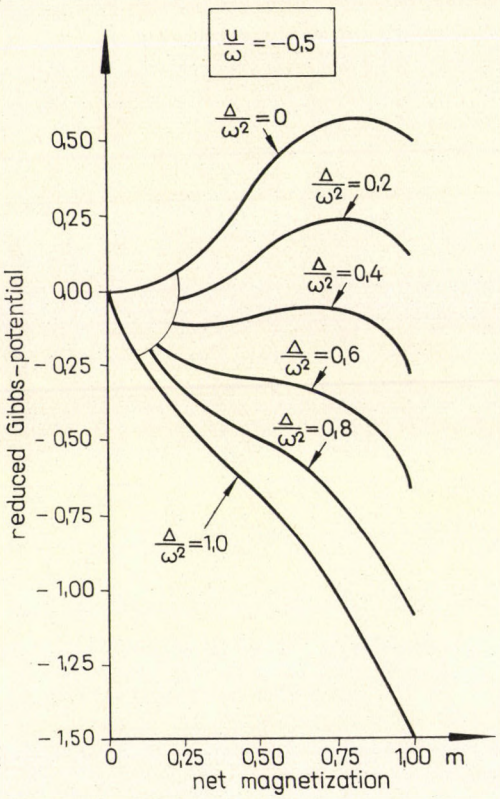

Fig. 6. Reduced Gibbs free-energy versus "magnetization" at constant temperature but different magnetic fields

If the transition is induced by temperature variation in the presence of a magnetic field the character of the variation in m will be the same as in the former case.

With help of (3.15) the reduced free energy may be written in the form

$$f(m, u, \Delta) = -m^4 + \left(1 - \frac{u}{\omega}\right) m^2 - 2\frac{\Delta}{\omega^2} m\,, \tag{3.17}$$

where

$$\frac{\Delta}{\omega^2} = \frac{h}{\sigma_0\, \omega \delta \varepsilon_0}\,. \tag{3.18}$$

The reduced free energy versus "magnetization" at a given temperature but for different magnetic fields is shown in Fig. 6, while in Fig. 7 similar curves can be seen but here the magnetic field is constant and the temperature is changing from curve to curve. The value of ω has been supposed to be positive

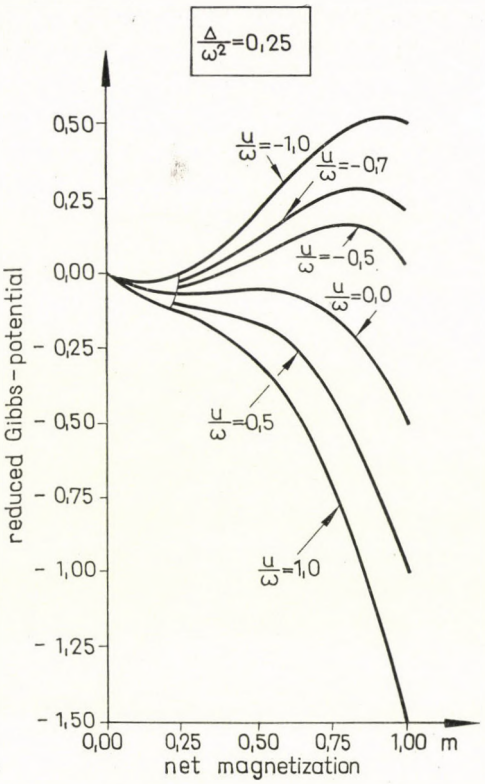

Fig. 7. Reduced Gibbs free-energy versus "magnetization" at constant magnetic field but different temperatures

and this means that the ferromagnetic state is stable at $u > 0$ in the absence of a magnetic field. It can be seen in Fig. 6 that at a given field the free energy of the ferromagnetic state is equal to that of the antiferromagnetic state. Nevertheless, the two states are energetically separated, i.e. the phase transition is hindered. A further increase in the magnetic field is needed to overcome the energy barrier of elastic origin. The situation is quite similar in the case illustrated in Fig. 7 but the role of the magnetic field is replaced here by that of the temperature.

In the following we shall calculate the field dependence of the coexistence temperature and also that of the upper and lower transition temperatures. In order to do this we have to find, first of all, the conditions for the existence of physical solutions of the equation

$$\frac{df}{d\Theta} = 2\left[-2m^3 + \left(1 - \frac{u}{\omega}\right)m - \frac{\Delta}{\omega^2}\right]\frac{dm}{d\Theta} = 0. \tag{3.19}$$

It is clear that one has to deal with the solutions satisfying the inequality $0 \leq m \leq 1$. Denote by m_1, m_2, m_3 the roots of the third-order equation

$$-m^3 + \frac{1}{2}\left(1 - \frac{u}{\omega}\right) m - \frac{1}{2}\,\frac{\Delta}{\omega^2} = 0\,, \tag{3.20}$$

and let m_4 be the solution of the equation $dm/d\Theta = 0$. Taking into account the condition

$$\frac{d^2 f}{d\Theta^2} = 2\left[-6m^2 + 1 - \frac{u}{\omega}\right]\left(\frac{dm}{d\Theta}\right)^2 + 4\left[-m^3 + \frac{1}{2}\left(1 - \frac{u}{\omega}\right) m - \frac{1}{2}\,\frac{\Delta}{\omega^2}\right]\frac{d^2 m}{d\Theta^2} > 0 \tag{3.21}$$

one can immediately find the minimizing solutions.

It is easy to show that among the roots m_1, m_2 and m_3 only one is real if u and Δ satisfy the inequality

$$\left(1 - \frac{u}{\omega}\right)\left(\frac{4\omega^2}{\Delta}\right)^{2/3} < 6\,. \tag{3.22}$$

One has to note, however, that in this case the real root is always negative.

It follows from this that only the solution $m_4 = 1$, which corresponds to the ferromagnetic state, has physical meaning. Indeed, the root $m_4 = 1$ minimizes the free energy if

$$\left(\frac{d^2 f}{d\Theta^2}\right)_{m=m_4} = 2\left(1 + \frac{u}{\omega} + \frac{\Delta}{\omega^2}\right) > 0\,. \tag{3.23}$$

This condition is always satisfied when the inequality (3.22) is true. The proof is very elementary. Replace u/ω in (3.23) from (3.22) by the quantity $1—6\,(\Delta/4\omega^2)^{2/3}$ which is always smaller then u/ω and write down the inequality

$$1 + \frac{u}{\omega} + \frac{\Delta}{\omega^2} > 2 - 6\left(\frac{\Delta}{4\omega^2}\right)^{2/3} + 4\,\frac{\Delta}{4\omega^2}\,.$$

Since

$$4x^3 - 6x^2 + 2 \geq 0\,; \quad x = \left(\frac{\Delta}{4\omega^2}\right)^{2/3}$$

for every $x \geq 0$ the statement is proved. One has to notice that the ferromagnetic state, in accordance with (3.23), remains stable for values u and Δ not satisfying the inequality (3.22).

When instead of (3.22) the inequality

$$\left(1-\frac{u}{\omega}\right)\left(\frac{4\omega^2}{\Delta}\right)^{2/3}>6 \tag{3.24}$$

is true then all three roots of (3.20) are real and it is easy to show that

$$m_1<-\sqrt{\frac{1}{6}\left(1-\frac{u}{\omega}\right)} \tag{3.25}$$

and

$$0\leq m_2\leq\sqrt{\frac{1}{6}\left(1-\frac{u}{\omega}\right)}<m_3\,. \tag{3.26}$$

Making use of these inequalities one can prove on the basis of (3.21) that the free energy is minimized by the solution $m=m_2=\tilde{m}$ and maximized by $m=m_3$. The solution $m=m_1$ has to be excluded because of its non-physical nature.

The umbrella-like solution $\tilde{m}$, which will be named simply as the antiferromagnetic solution remains stable until

$$\tilde{m}^2(u,\Delta)<\frac{1}{6}\left(1-\frac{u}{\omega}\right).$$

Instability sets in when

$$\tilde{m}^2(u,\Delta)=\frac{1}{6}\left(1-\frac{u}{\omega}\right) \tag{3.27}$$

and then the antiferromagnetic phase suddenly transforms into the ferromagnetic one.

Eliminating the net magnetization m in (3.20) with the help of (3.27) one gets a very important equation for the field dependence of the antiferromagnetic → ferromagnetic transition temperature. This equation can be written in the form

$$\frac{\Delta}{4\omega^2}=\left[\frac{1}{6}\left(1-\frac{u}{\omega}\right)\right]^{3/2}. \tag{3.28}$$

It follows from this that the local stability of the antiferromagnetic state in the presence of a magnetic field breaks down when the temperature reaches a certain critical value

$$u_{\sup}=\omega\left[1-6\left(\frac{\Delta}{4\omega^2}\right)^{2/3}\right]. \tag{3.29}$$

The onset of the stable ferromagnetic phase results in a discontinuous change of the net magnetization. Its maximal value in the antiferromagnetic state before the sudden change is

$$\tilde{m}_{\text{sup}}(\Delta) = \left(\frac{\Delta}{4\omega^2}\right)^{1/3}. \tag{3.30}$$

When the temperature is fixed and the increasing magnetic field brings about the transition one observes its start only at a certain critical value of the magnetic field, namely at

$$\Delta_{\text{sup}} = \frac{1}{3}\sqrt{\frac{2}{3}}\,\omega^2\left(1-\frac{u}{\omega}\right)^{3/2}. \tag{3.31}$$

In this case the maximal net magnetization in the antiferromagnetic state can be expressed by

$$\tilde{m}_{\text{sup}}(u) = \sqrt{\frac{1}{6}\left(1-\frac{u}{\omega}\right)}. \tag{3.32}$$

Varying the temperature and magnetic field in opposite direction the ferromagnetic → antiferromagnetic transition will be observed when

$$1+\frac{u}{\omega}+\frac{\Delta}{\omega^2}=0.$$

i.e. in a constant field antiferromagnetism will appear at temperature

$$u_{\text{inf}} = -\omega\left(1+\frac{\Delta}{\omega^2}\right). \tag{3.33}$$

where the net magnetization changes discontinuously from the value of $m = 1$ to that of

$$\tilde{m}_{\text{inf}}(\Delta) = \frac{1}{2}\left[\sqrt{1+2\frac{\Delta}{\omega^2}}-1\right]. \tag{3.34}$$

At constant temperature the stability of the ferromagnetic phase disappears when the magnetic field is lowered to

$$\Delta_{\text{inf}} = -\omega^2\left(1-\frac{u}{\omega}\right). \tag{3.35}$$

The parameter m shows a definite jump from $m = 1$ to

$$\tilde{m}_{\text{inf}}(u) = \frac{1}{2}\left[\sqrt{-\left(1+2\frac{u}{\omega}\right)}-1\right]. \tag{3.36}$$

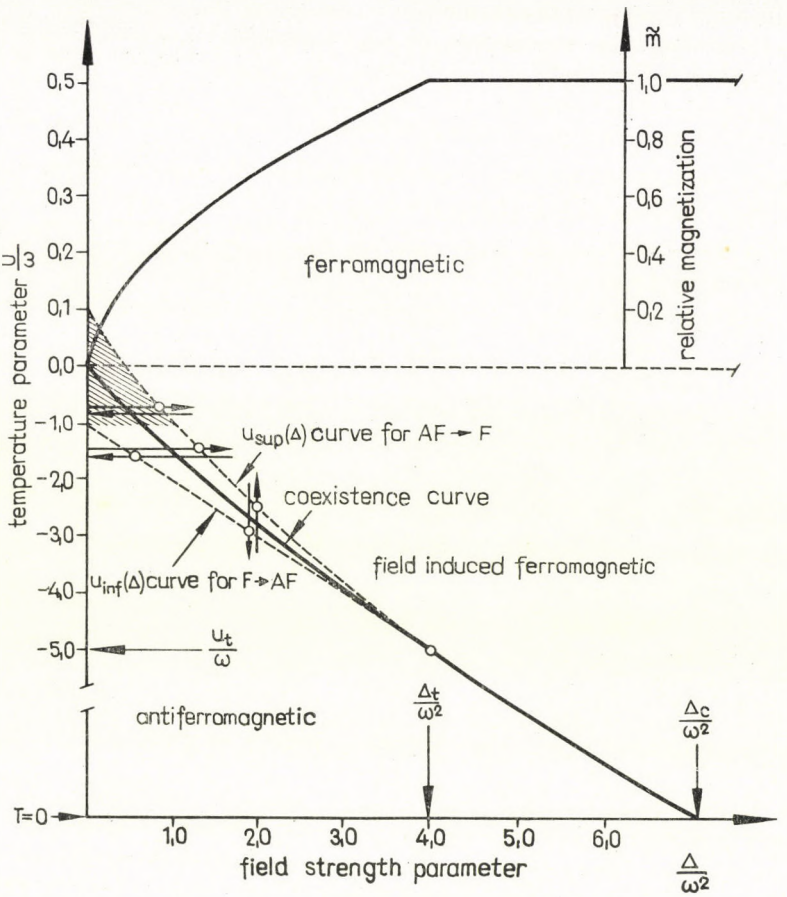

Fig. 8. $T-H$ (i.e. $u/\omega.-.\Delta/\omega^2$) phase diagram and variation of the magnetization along the coexistence curve

Since both parameters Δ_{inf} and $\tilde{m}_{\text{inf}}$ must be positive one can produce a ferromagnetic → antiferromagnetic transition with decreasing magnetic field only if $u/\omega < -1$. In other words, the magnetic field induced antiferromagnetic → → ferromagnetic phase transition is reversible only when $u/\omega < -1$. In this case, by lowering the magnetic field below the critical value Δ_{inf} the energy barrier separating the thermodynamically stable antiferromagnetic state from the ferromagnetic one disappears, making the way for the transition free.

In Fig. 8 one can see the coexistence curve $u_e(\Delta)$ between the curves $u_{\text{sup}}(\Delta)$ and $u_{\text{inf}}(\Delta)$. Along the curve $u_e(\Delta)$ the Gibbs free energy of the ferromagnetic phase is equal to that of the antiferromagnetic phase. Explicit formula for the coexistence curve cannot be given; a parametric equation, however,

can be easily derived. One finds

$$\frac{u_e}{\omega} = -\tilde{m}(2 + 3\tilde{m}),$$

$$\frac{\Delta}{\omega^2} = \tilde{m}(1 + \tilde{m})^2, \tag{3.37}$$

where $\tilde{m}$ is the solution of (3.20). The coexistence curve $u_e(\Delta)$ reaches the curves $u_{\text{sup}}(\Delta)$ and $u_{\text{inf}}(\Delta)$ in the point

$$\frac{\Delta_t}{\omega^2} = 4, \quad \frac{u_t}{\omega} = -5, \tag{3.38}$$

when u_t is higher than absolute zero.

The first-order character of the phase transition disappears in this point. It is seen that when the magnetic field is high enough, i.e.

$$4 \leq \frac{\Delta}{\omega^2} \leq \frac{\Delta_c}{\omega^2},$$

then the ferromagnetic $\rightleftarrows$ antiferromagnetic transition will be of second-order. One may expect large fluctuations of the parameter m when the transition is of second-order. In the point given by (3.38) the quantity

$$\frac{d\tilde{m}}{d\Delta} = \frac{1}{\omega^2\left(1 - \frac{u}{\omega} - 6\tilde{m}^2\right)} \tag{3.39}$$

which is proportional to the susceptibility, becomes infinite. One has to note that at fields higher than Δ_c/ω^2 the temperature variation does not result in a real phase transition, the only change is that the ferromagnetic phase transforms at $u = 0$ to a phase which is nothing but the antiferromagnetic phase in a magnetic field strong enough to turn the moments parallel to the field direction.

In the upper part of Fig. 8 the variation of the net magnetization of the antiferromagnetic phase along the coexistence curve is also shown. For fields higher than Δ_t/ω^2 the net magnetization is equal to 1.

The phase transition is always of first-order and is hindered if the parameters Δ and u satisfy the inequalities: $0 \leq \Delta/\omega^2 < 4$ and $-5 < u/\omega \leq 1$, respectively. The hindrance of the transition — as has already been pointed out — results in a definite hysteresis. The width of the thermal hysteresis depends on the magnetic field and as can be seen from the expression

$$u_{\text{sup}} - u_{\text{inf}} = 2\omega\left[1 + \frac{\Delta}{2\omega^2} - 3\left(\frac{\Delta}{4\omega^2}\right)^{2/3}\right] \tag{3.40}$$

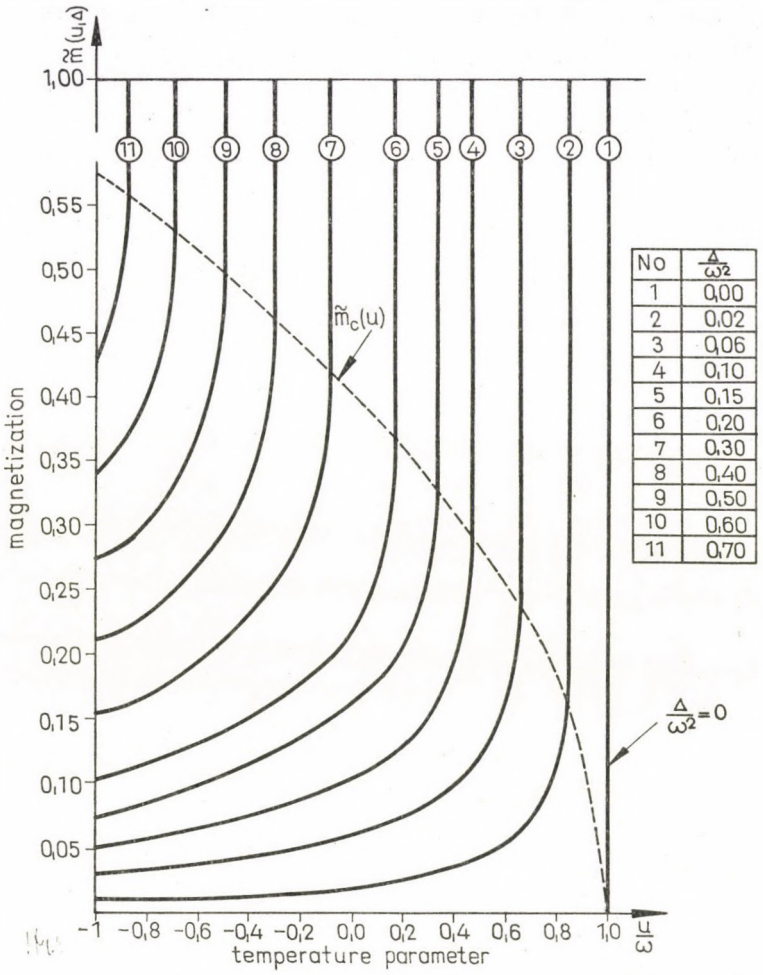

Fig. 9. Net magnetization versus temperature at different magnetic fields in the antiferromagnetic state

it decreases with increasing field and vanishes at the field corresponding to Δ_t. The same will be true for the temperature dependence of the magnetic hysteresis width since

$$\Delta_{\text{sup}} - \Delta_{\text{inf}} = \omega^2 \left[1 + \frac{u}{\omega} + \frac{1}{3} \sqrt{\frac{2}{3}} \left(1 - \frac{u}{\omega} \right)^{3/2} \right]. \tag{3.41}$$

In Fig. 8 the arrows intersecting the phase boundary illustrate the different types of phase transitions. The circles on the arrows indicate the parameters u and Δ characterizing the transition.

For the sake of completeness we show in Fig. 9 the temperature dependence of the net magnetization in the antiferromagnetic phase at various magnetic

fields. One can see on the curves that the net magnetization suffers a sudden change from $\tilde{m}_{\text{sup}} \leq 1$ to $\tilde{m} = 1$ when the temperature u reaches a critical value u_{sup} due to a given magnetic field. The dashed curve in Fig. 9 shows the function $\tilde{m}_{\text{sup}}(u)$ which gives the maximal net magnetization available in the antiferromagnetic state at constant temperature in an external magnetic field.

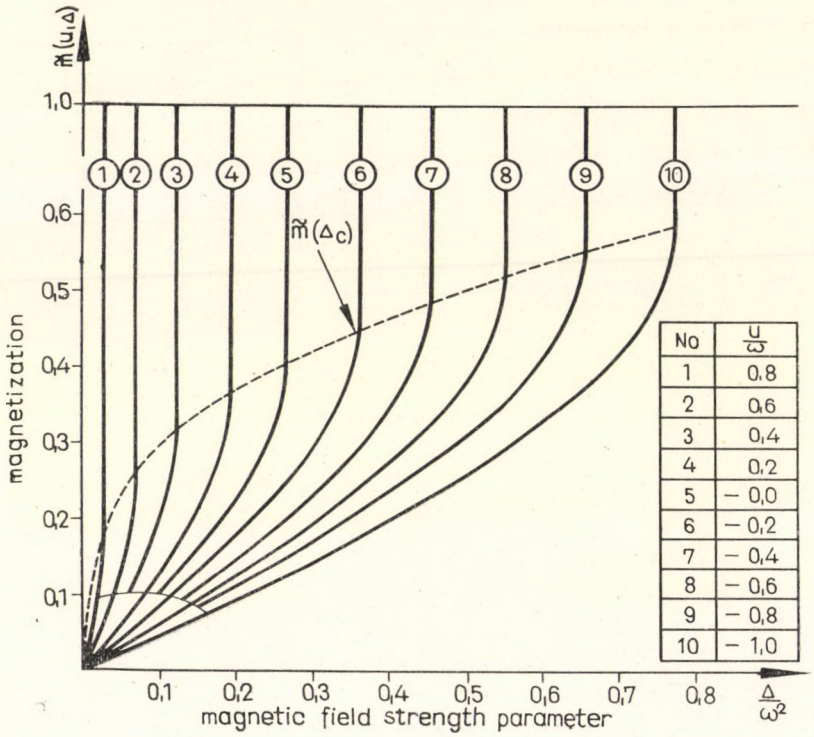

Fig. 10. Net magnetization versus magnetic field at various temperatures in the antiferromagnetic state

In Fig. 10 the magnetic field dependence of $\tilde{m}$ is illustrated for different temperatures. Contrary to the previous case, the dashed curve in this figure shows the maximum of the magnetization $\tilde{m}_{\text{sup}}(\Delta)$ available in the antiferromagnetic phase with increasing temperature but at constant magnetic field.

Finally, it seems to be useful to rewrite the most important formulae in such a way that only directly measurable quantities should occur in them. Making use of the expressions (2.27) and (3.6) one gets from (3.29) and (3.33) the formulae:

$$T_{\text{sup}}(H) = T_{\text{sup}} - 3\,(T_{\text{sup}} - T_{\text{inf}})\left(\frac{H}{H_t}\right)^{2/3} \tag{3.42}$$

and

$$T_{\text{inf}}(H) = T_{\text{inf}} - 2(T_{\text{sup}} - T_{\text{inf}})\frac{H}{H_t}, \tag{3.43}$$

where

$$H_t = 4(T_{\text{sup}} - T_{\text{inf}})^2 \frac{R\alpha^2}{NM_0\sigma_0} \tag{3.44}$$

is the critical magnetic field The critical temperature T_t can be expressed in a very simple form, namely

$$T_{\text{sup}}(H_t) = T_{\text{inf}}(H_t) = T_t = 3T_{\text{inf}} - 2T_{\text{sup}}. \tag{3.45}$$

The temperatures T_{sup} and T_{inf} may be obtained from measurements without magnetic field.

4. Variation of the average magnetization per atom

Let us examine, first of all, the correction term to the magnetization per atom. To get a self-consistent solution we write the equation (2.31) in the form

$$\sigma = \sigma_0 + \sigma_1 q = th\,\frac{\sigma_0 + (\sigma_0 + \sigma_1)\,q}{\tau} \sim \sigma_0 + (1-\sigma_0^2)\,(\sigma_0+\sigma_1)\,\frac{q}{\tau} \tag{4.1}$$

and replacing q by q_0 we get

$$\delta\sigma = \sigma_1 q_0 = \frac{\mu}{r}\,\sigma_0\,\frac{\lambda}{1-\lambda}\,(\mu\sigma_0^2 + 2\Theta\tau - r\varepsilon_c - p)\,, \tag{4.2}$$

where

$$\lambda = \frac{1-\sigma_0^2}{\tau}\,. \tag{4.3}$$

It can be easily shown that λ is a monotonically increasing function of τ in the interval $0 \leq \tau \leq 1$. One finds that

$$\lim_{\tau\to 0}\lambda(\tau) = 0 \quad \text{and} \quad \lim_{\tau\to 1}\lambda(\tau) = 1\,. \tag{4.4}$$

From (4.2) it can be seen that the value of magnetization per atom at the coexistence temperature, i.e. where

$$2\Theta\tau_e - r\varepsilon_c - p = -(\Omega+\gamma\omega)\,\sigma_0^2 \tag{4.5}$$

is not the same in the phases $m = 1$ and $m = 0$. We find

$$\delta\sigma_e(m=1) = \frac{\omega\,[\Omega + (1+\gamma)\,\omega]}{r}\;\frac{\lambda_e}{1-\lambda_e}\,\sigma_{0e}^3 \tag{4.6}$$

and

$$\delta\sigma_e(m=0) = -\frac{\omega\,[\Omega - (1-\gamma)\,\omega]}{r}\;\frac{\lambda_e}{1-\lambda_e}\,\sigma_{0e}^3\,, \tag{4.7}$$

where the subscript e indicates that each temperature dependent quantity should be taken at the coexistence temperature. The discontinuous change in magnetization per atom brings about a similar change in magnetic entropy too, which leads, obviously, to the appearance of a magnetic latent heat contribution. This is given by

$$\Omega_m = -4A_0 M_0^2 \frac{\omega(\Omega+\gamma)}{r} \frac{\lambda_e}{1-\lambda_e} \sigma_{0e}^4 T_e \,. \tag{4.8}$$

As has already been mentioned, the phase transition is hindered and, thus, the formation of the phase $m = 1$ takes place only at the temperature $\tau = \tau_{\text{sup}}$.

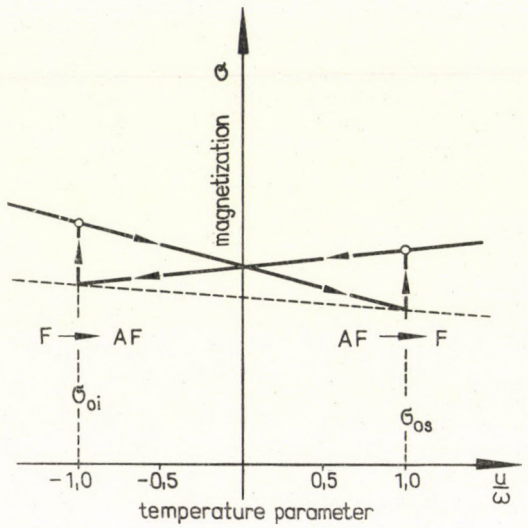

Fig. 11. Temperature dependence and discontinuous change of the average magnetic moment per atom

The change in the magnetization per atom at this temperature can be expressed by

$$\sigma(m=1, \tau=\tau_{\text{sup}}) - \sigma(m=0, \tau=\tau_{\text{sup}}) = [\Omega + (1+\gamma)\omega] \frac{\lambda_s}{1-\lambda_s} \sigma_{0s} \delta\varepsilon_{0s}, \tag{4.9}$$

where the subscript s indicates that each temperature dependent quantity should be taken at the temperature $\tau = \tau_{\text{sup}}$. A similar discontinuous change in the magnetization has to be expected at the temperature $\tau = \tau_{\text{inf}}$ where the inverse transition takes place. One gets

$$\sigma(m=1, \tau=\tau_{\text{inf}}) - \sigma(m=0, \tau-\tau_{\text{inf}}) = [\Omega - (1-\gamma)\omega] \frac{\lambda_i}{1-\lambda_i} \sigma_{0i} \delta\varepsilon_{0i}, \tag{4.10}$$

where the subscript i shows again that each temperature dependent quantity is taken at $\tau = \tau_{\text{inf}}$. The schematic behaviour of the temperature dependence of σ is shown in Fig. 11, when $\Omega = \gamma = 0$.

In Section 3 we derived a simple formula for the discontinuous change of the lattice distortion [see (2.27)]. Now, taking into account the magnetization change we should like to refine this formula. A short calculation shows that at the transition temperature $\tau = \tau_{\text{sup}}$ we should write

$$\delta\varepsilon_s = \delta\varepsilon_{0s}\left\{1 + \left(2+\gamma+\frac{\Omega}{\omega}\right)[\Omega+(1+\gamma)\,\omega]\,\frac{\lambda_s}{1-\lambda_s}\,\sigma_{0s}\,\delta\varepsilon_{0s}\right\} \tag{4.11}$$

and similarly at $\tau = \tau_{\text{inf}}$ we get

$$\delta\varepsilon_i = \delta\varepsilon_{0i}\left\{1 - \left(2-\gamma-\frac{\Omega}{\omega}\right)[\Omega-(1-\gamma)\,\omega]\,\frac{\lambda_i}{1-\lambda_i}\,\sigma_{0i}\,\delta\varepsilon_{0i}\right\}. \tag{4.12}$$

The corrections both in (4.11) and (4.12) are usually small, nevertheless, it seems useful to take into account these corrections in evaluating the parameters Ω and ω from the measured data of $\delta\varepsilon$.

Making use of the results obtained for the discontinuous change of σ the equation (4.5) giving the coexistence temperature can be also refined. It is not necessary to reproduce here the details of calculations since they are very elementary; it is better to cite the final result. The corrected equation can be written in the form

$$\tau_e = \frac{r\varepsilon_C}{2\Theta} + \frac{p}{2\Theta} - \frac{\Omega+\gamma\omega}{2\Theta}\,\sigma_{0e}^2\left\{1+(\Omega+\omega)\,\frac{\lambda_e}{1-\lambda_e}\,\delta\varepsilon_{0e}\right\}. \tag{4.13}$$

It can be seen from this that in the case of non-vanishing Ω and γ the pressure coefficient of τ_e is given by

$$\frac{d\tau_e}{dp} = \frac{1}{2\Theta}\,\frac{1}{1+\dfrac{\Omega+\gamma\omega}{\Theta}\,\sigma_{0e}\dfrac{d\sigma_{0e}}{d\tau_e}} \tag{4.14}$$

if one neglects the small correction term in (4.13). The second factor on the right side of this formula may become very large when $\Omega + \gamma\omega > 0$, since $d\sigma_{0e}/d\tau_e < 0$. Therefore, in most cases the expression for $d\tau_e/dp$ given earlier by (3.10) must be replaced by (4.14).

Now, we have to discuss in more detail the influence of the temperature dependence of σ_0 on the transition. In the preceding considerations we dealt only with the discontinuous change in σ but when doing this we always assumed the variation of σ_0 in the interval $\tau_{\text{nf}} \leq \tau \leq \tau_{\text{sup}}$ to be small. In addition to this we supposed the inequality

$$\frac{\delta\sigma}{\sigma_0} \ll 1$$

to be satisfied also in the whole temperature range $0 \leq \tau \leq \tau_{\text{sup}}$. The correction $\delta\sigma$ derived by linear approximation in q is obviously wrong near the ordering temperature, since σ_0 tends to zero, and unfortunately, $\delta\sigma$ goes to infinity. One has to note that this behaviour of $\delta\sigma$ is a direct consequence of the limited validity of the linear approximation. Nevertheless, if we want to use in our consideration corrections linear in q only, we have to indicate the temperature limit below which the linear approximation is certainly correct. This problem can be solved easily in a slightly reformulized manner by requiring the linear approximation to be valid until $\tau > \tau_{\text{sup}}$ and thence deriving a criterion for the basic parameter of the theory. Proceeding from (4.9) we get

$$\sigma_{0s}^2 \frac{\lambda_s}{1-\lambda_s} \ll \frac{1}{2} \frac{r}{\omega[\Omega+(1+\gamma)\omega]} . \tag{4.15}$$

Using this inequality one can always decide for a given set of parameters whether the linear approximation is true or not below the temperature τ_{sup}.

In order to say more about the temperature dependence of $\delta\sigma$ one should rewrite the expression (4.2) in the form

$$\delta\sigma(\sigma_0) = \sigma_0(1-\sigma_0^2) \frac{2a\sigma_0 + (b\sigma_0^2 - a\tau_e)\log\dfrac{1+\sigma_0}{1-\sigma_0}}{2\sigma_0 - (1-\sigma_0^2)\log\dfrac{1+\sigma_0}{1-\sigma_0}} , \tag{4.16}$$

where

$$a = \frac{2\mu\Theta}{r} \qquad \text{and} \qquad b = \frac{\mu}{r}\omega(2m^2-1) . \tag{4.17}$$

It can be seen immediately that

$$\lim_{\sigma_0 \to 0} \sigma_0 \delta_0(\sigma_0) = a(1-\tau_e) , \tag{4.18}$$

i.e.

$$\lim_{\sigma_0 \to 0} \delta\sigma(\sigma_0) = \begin{cases} +\infty, & \text{if} \quad \mu > 0 , \\ -\infty, & \text{if} \quad \mu < 0 . \end{cases} \tag{4.19}$$

Another interesting property follows from (4.16) when σ_0 is approaching its saturation value. The correction term $\delta\sigma$ becomes zero at $\sigma_0 = 1$ but its first derivative with σ_0 goes to infinity unless $b - a\tau_e = 0$. Furthermore, the equation

$$\delta\sigma(\sigma_0) = 0$$

can always be satisfied if $m = 0$ but with $m = 1$ one gets a solution only if $2\Theta\tau_e > \omega$. The characteristics of the temperature dependence of $\delta\sigma$ are listed

Table IV

Characteristics of the temperature dependence of $\delta\sigma$

$m=1$	$\left(\frac{d\delta\sigma}{d\sigma_0}\right)_{\sigma_0=1}$		$\delta\sigma(\sigma_0)=0$		$\delta\sigma(\sigma_0=0)$
	$2\Theta\tau_e>\omega$	$2\Theta\tau_e<\omega$	$2\Theta\tau_e>\omega$	$2\Theta\tau_e<\omega$	
$\mu_1>0$	$+\infty$	$-\infty$	yes	no	$+\infty$
$\mu_1<0$	$-\infty$	$+\infty$	yes	no	$-\infty$

$m=0$	$\left(\frac{d\delta\sigma}{d\sigma_0}\right)_{\sigma_0=1}$	$\delta\sigma(\sigma_0)=0$	$\delta\sigma(\sigma_0=0)$
$\mu_6<0$	$+\infty$	yes	$+\infty$
$\mu_6<0$	$-\infty$	yes	$-\infty$

in Table IV while the $\delta\sigma$ curves versus σ_0 are sketched in Fig. 12 for $\Omega = \gamma = 0$. For completeness the variation of $\delta\sigma$ during the phase transition is also indicated and one can observe that the behaviour is in principle quite similar to that in Fig. 11. The characteristic feature of the variation of $\delta\sigma$ is that an increase of magnetization occurs at both transition temperatures, namely at $\tau = \tau_{\text{sup}}$ and $\tau = \tau_{\text{inf}}$. One has to notice, however, that it is hardly to be expected that the change of magnetization is always positive at both transition

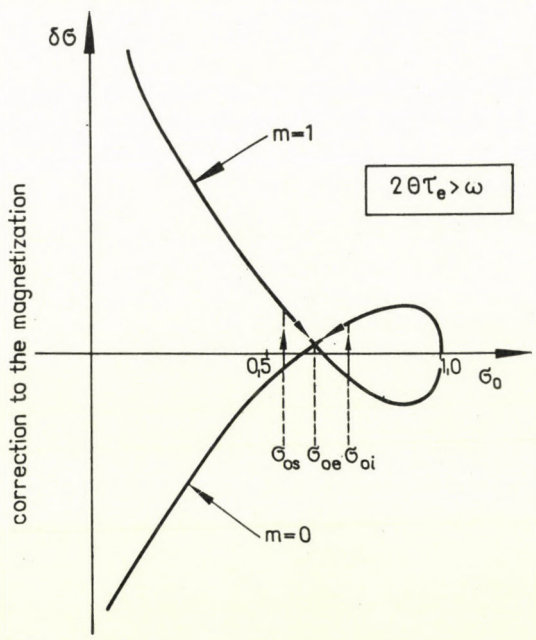

Fig. 12. Correction to average magnetic moment per atom versus σ_0

temperatures. Indeed, it can be easily shown that this is the case only if

$$\mu_0 = \Omega - (1-\gamma)\,\omega < 0\,, \tag{4.20}$$

but

$$\mu_1 = \Omega + (1+\gamma)\,\omega > 0\,. \tag{4.21}$$

Finally, it is important to notice that the temperature variation of $\delta\sigma$ may be rather sharp near absolute zero, i.e. at those temperatures where σ_0 does not vary markedly. Therefore, if the phase transition takes place at very low temperatures ($\tau_{\text{inf}} \sim 0$) one should pay special attention to the temperature variation of $\delta\sigma$.

Let us extend our considerations to the high temperature region near the ordering temperature where the magnetization σ can be regarded as a small parameter. First, let us expand the Gibbs free-energy in power series of σ and neglect all the terms which are smaller than the fourth power of σ. After a short calculation we get

$$G = A_0 M_0^2 \left\{ -\frac{1}{2} r \left(\frac{2\Theta\tau - p}{r} \right)^2 - \left[1 - \tau + \frac{\mu}{r} (2\Theta\tau - r\varepsilon_c - p) \right] \sigma^2 - \right.$$
$$\left. - \frac{1}{2} \left(\frac{\mu^2}{r} - \frac{\tau}{3} \right) \sigma^4 \right\} + 0(\sigma^4)\,. \tag{4.22}$$

As a solution of the equation $dG/d\sigma = 0$ the magnetization can be given by

$$\sigma^2 = 3\, \frac{1 - \tau + \dfrac{\mu}{r}(2\Theta\tau - r\varepsilon_c - p)}{\tau - 3\dfrac{\mu^2}{r}}\,, \tag{4.23}$$

where

$$\tau_c = \frac{1 - \dfrac{\mu}{r}(r\varepsilon_c + p)}{1 - \dfrac{2\mu\Theta}{r}} \tag{4.24}$$

is the ordering (Curie or Néel) temperature. It can be easily shown that $\tau_c(m=1)$ is always higher than $\tau_c(m=0)$ only if

$$2\Theta - r\varepsilon_c - p > 0\,. \tag{4.25}$$

In order to ensure the second-order character of the disappearance of σ one has to require the fulfilment of the condition

$$\frac{d^2 G}{d\sigma^2} \geq 0\,, \tag{4.26}$$

which can be rewritten in the form

$$\tau_c \geq 3 \frac{\mu^2}{r} . \tag{4.27}$$

One has to mention that in many cases the lattice distortion caused by the magneto-elastic interaction is large enough to lead to a first-order transition in σ. In these cases, naturally, an inequality opposite to (4.27) should be satisfied. In BEAN's paper [2] a simplest version of this was discussed.

In the following we shall still suppose the disappearance of σ to be of second-order, and try to find the conditions for the existence of a triple point in the T—P place. To do this we should derive, first of all, the pressure dependence of the coexistence temperature. From

$$G(m = 1) = G(m = 0)$$

we get

$$\left(\tau_e - 3 \frac{\mu_1^2}{r}\right) \sigma_e^2(m = 1) = \left(\tau_e - 3 \frac{\mu_0^2}{r}\right) \sigma_e^2(m = 0) \tag{4.28}$$

which — making use of the expression (4.23) — gives the unknown pressure dependence $\tau_e(p)$. In order to find the "coordinates" of the triple point in the T—P plane it is not necessary to solve the equation (4.28) because it can be seen immediately that

$$\tau_C(m = 1) = \tau_c(m = 0) = \tau_e = 1 , \tag{4.29}$$

when the equation

$$2\Theta - r\varepsilon_c - p = 0 \tag{4.30}$$

is satisfied. In other words, the curves $\tau_c(m = 1, p)$, $\tau_c(m = 0, p)$ and $\tau_e(p)$ have a common point (this is the triple point) at the pressure

$$p_t = 2\Theta - r\varepsilon_c . \tag{4.31}$$

In Fig. 13 the typical phase boundaries and the position of the triple point are shown. There is an interesting possibility for changing the order of phase transition at the triple point. Let us suppose the transition from the state $m = 1$ to the paramagnetic one to be of second-order even very near the triple point. This means that the inequality

$$3 \frac{\mu_1^2}{r} < 1 \tag{4.32}$$

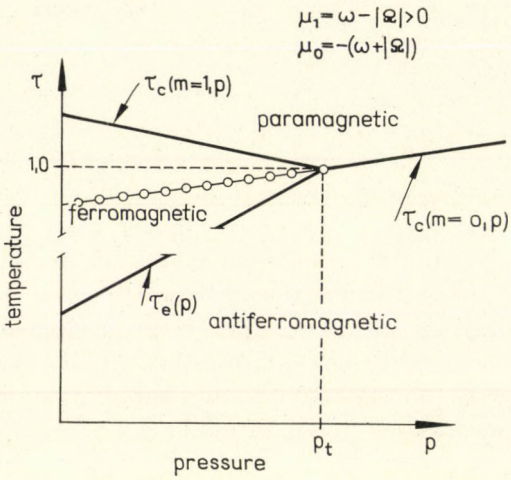

Fig. 13. $T-P$ (i.e. $\tau-p$) phase diagram

has to be satisfied. Further, let us assume that the transition from the state $m = 0$ to the paramagnetic one is of first-order, i.e.

$$3\frac{\mu_0^2}{r} > 1 \tag{4.33}$$

when $\gamma = 0$ and the sign of Ω is different from that of ω, both inequalities can be satisfied if

$$\Omega^2 + \omega^2 = \frac{1}{3} r\,. \tag{4.34}$$

In order to ensure the fulfilment of (4.34) both Ω and ω must be fairly large, nevertheless, μ_1 remains small enough because it is merely the difference between Ω and ω. The possible change in order of the disappearance of σ is of great importance in understanding some recent observations [11].

5. Final remarks

The previous very elementary consideration can be sucessfully applied in many cases listed in Table I. Nevertheless, one should keep in mind that nobody can expect quantitative but only qualitative agreement between the theoretical and experimental results and therefore we do not want to make here any detailed comparison between theory and experiments. However, it seems to be worthwhile to mention one example which has been in the centre of interest for the last five — six years.

This example is the iron-rhodium alloy of equiatomic composition which is ferromagnetic at high and antiferromagnetic at low temperatures. The alloy possesses a body centred cubic lattice in which the chemical order is of CsCl-type and the magnetic structure in the antiferromagnetic state coincides with the structure $AF1$ shown in Fig. 3. This is the so-called G-type structure in which every positive Fe spin in surrounded by six negative Fe spins. The magnetic unit cell edge is thus double that of the chemical cell. The Rh atom, which is located at the body centred position is now surrounded by four positive and four negative Fe spins. Thus the Rh moment may not be ordered. Indeed, according to the neutron diffraction measurements [12] the existence of a non-zero magnetic moment at the Rh sites in the antiferromagnetic state can be excluded.

It is of interest to note that it can be shown on a purely theoretical basis that the average magnetic moment of the Rh atoms must be zero if the iron lattice possesses a collinear antiferromagnetic structure. To do this it is enough to assume the existence of a triple point in the T—P phase diagram similar to that in Fig. 13 and the second-order character of the antiferromagnetic $\rightarrow$ paramagnetic phase transition occurring at pressures higher than the triple point pressure. On the basis of these assumptions making use of the group-theoretical methods one can prove the disappearance of the Rh moment. The proof was done by HARGITAI [13] several years ago and the existence of the triple point in the T—P plane was experimentally shown by WAYNE [11] very recently. One has to mention, however, that the measurements of WAYNE unfortunately indicate the antiferromagnetic $\rightarrow$ paramagnetic phase transition to be of first-order, the possibility of which we discussed in Section 4. This fact alters the situation because the Landau theory cannot be applied in this case. However, the existence of a zero effective exchange field at the Rh sites further suggests the Rh moments must be zero. In the ferromagnetic state the Rh atoms have a fairly large magnetic moment ($\mu_{Rh} \sim 1.0\,\mu_B$) which must play an important role in the phase transition.

The antiferromagnetic $\rightleftarrows$ ferromagnetic phase transition is of first-order and is associated with a relatively large discontinuous change of the lattice parameter. In Fig. 14 the temperature dependence of the lattice parameter measured by ZSOLDOS [14] is shown. The specimen with 49.6 at. per cent rhodium was prepared by melting and was quenched in water after 10 hours annealing at 1000 °C. One can see the hysteresis width to be very small. In order to illustrate the influence of the inhomogeneities on the shape of the hysteresis loop the lattice parameter change in a chemically prepared powdered sample of equiatomic composition was also measured. The results of the measurements are shown in Fig. 15. One has to note that the shape of the hysteresis loop derived from the theory is completely different from that obtained in the experiment.

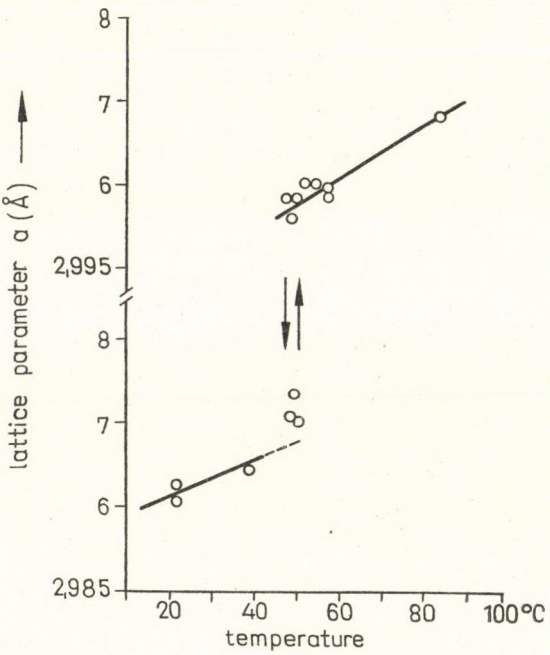

Fig. 14. Lattice parameter versus temperature for FeRh with 49,6 at per cent Rh

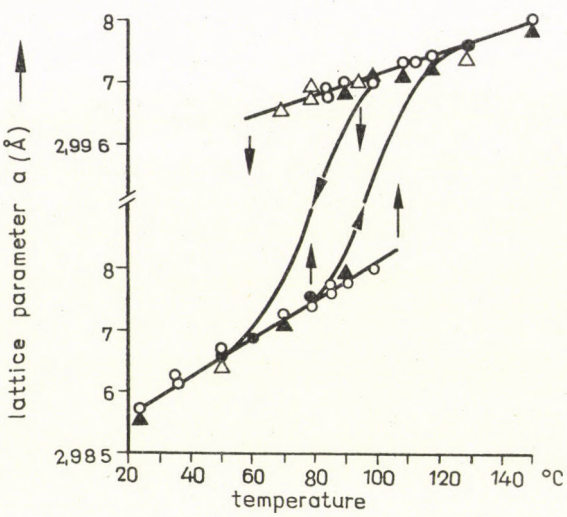

Fig. 15. Lattice parameter versus temperature and hysteresis for chemically prepared FeRh of equiatomic composition

In accordance with the theory, both transition temperatures $T(AF \to F, P) = T_{sup}(P)$ and $T(F \to AF, P) = T_{inf}(P)$increase with increasing pressure and the temperature width of the hysteresis (i.e. the difference T_{sup}—T_{inf}) decreases with increasing pressure if the transition in the triple point is of second-order.

Making use of the results of Section 4 the properties of the magnetic field induced $AF \rightleftarrows F$ transition can be explained very easily. One finds both transition temperatures $T_{sup}(H)$ and $T_{inf}(H)$ as well as the hysteresis width (i.e. T_{sup}—T_{inf}) decreasing with increasing magnetic field. The values of the magnetic field and temperature where the hysteresis disappears can be calculated from the experimental data.

It can also be shown that the transition $AF \to F$ induced by external magnetic field is not reversible above a given temperature. Indeed, we observed that after switching off the external magnetic field the thermodynamically unstable F state does not transform into the stable AF one because of the energy barrier between the minima corresponding to the AF and F phases.

In Section 4 it was shown that the average magnetic moment per atom suffers a discontinuous change at both transition temperatures T_{sup} and T_{inf}. To observe this change by measuring the temperature dependence of the sublattice magnetization with the neutron diffraction technique seems to be very difficult because of the limited sensitivity of this technique. It is well-known, however, that a small change in the atomic magnetic moment may produce a fairly large change in the internal field acting on the nucleus. In the iron-rhodium alloys the temperature dependence of the internal field at the iron nuclei has been measured by several authors [15] and they found a definite jump in it at the transition temperature, in good agreement with the theory.

In the preceding Sections we always neglected the influence of the magnetic behaviour of the rhodium atoms on the phase transition. It would be, however, a serious mistake to think that the onset of the rhodium moment in the ferromagnetic phase does not bring about any substantial influence on the thermodynamics of the phase transition. Now, we do not want to go into the details of the problem here, but we should like to make a few remarks only.

It is obvious that the Rh atoms may have magnetic moment if the antiferromagnetic structure is not collinear. For instance, the presence of an external magnetic field induces a deviation of the moments from their antiparallel orientation and this results in a magnetic moment of the Rh atoms. The onset of the moment on Rh atoms will accelerate the $AF \to F$ transition. Indeed, the calculations show the transition temperature to be lower than in the former case if one takes into account the magnetic properties of the Rh atoms.

Finally, one should not forget that in a collinear antiferromagnet, where the average exchange field is zero at the rhodium sites, the actual value of

this field is never exactly zero but fluctuates about zero. This fluctuating exchange field produces a fluctuating moment on the rhodium atoms, and in turn, this will result in a fluctuating deviation of the iron moments from their antiparallel orientation. If the enhancement of the fluctuations is large enough the stability of the antiferromagnetic state may disappear, i.e. phase transition will take place.

In the stable antiferromagnetic state small fluctuations still exist and if the characteristic decay time of these fluctuations has the same order of magnitude as the period of the Larmor's precession of the iron nuclear moments, a line broadening in the Mössbauer spectrum is to be observed. This line broadening was found by CSER and KESZTHELYI [16] in their very recent measurements. The physical situation is very similar to the Brownian-like motion; the fluctuating rhodium moment as a stochastic driving force induces random deviations of the iron moments from their antiparallel orientation. The details of these calculations will be published elsewhere.

LITERATURE

1. L. D. LANDAU, Sov. Phys., **11**, 545, 1937.
   E. M. LIFSHITZ, JETF, **11**, 255 and 269, 1941.
   L. D. LANDAU and E. M. LIFSHITZ, Statistical Physics, Pergamon Press, London 1958.
2. C. P. BEAN and D. S. RODBELL, Phys. Rev., **126**, 104, 1962.
3. I. E. DZYALOSHINSKY, J. Phys. Chem. Solids, **4**, 241, 1958; Zs. Eksper. Theor. Fiz. (USSR) **46**, 1420, 1964.
4. O. V. KOVALYOV, Fiz. Tverdogo Tela (USSR) **5**, 3156, 1963; **7**, 103, 1965.
5. J. SÓLYOM, Physica, **32**, 1243, 1966.
6. P. W. ANDERSON, Phys. Rev., **79**, 705, 1950.
7. J. S. SMART, Phys. Rev., **90**, 55, 1953.
8. L. NÉEL, Ann. Phys., **8**, 237, 1937.
9. C. KITTEL, Phys. Rev., **120**, 335, 1960.
10. R. W. DE BLOIS and D. S. RODBELL, Phys. Rev., **130**, 1347, 1963
    H. S. JARRETT, Phys. Rev., **134**, A942, 1964.
    R. A. FARRELL and P. H. E. MEIJER, Physica, **31**, 725, 1965.
11. R. G. WAYNE, Phys. Rev., **170**, 523, 1968.
12. F. DE BERGEVIN and L. MULDAWER, Compt. Rend., **252**, 1347, 1961.
    F. BERTAUT, F. DE BERGEVIN and G. ROULT, Compt. Rend., **256**, 1668, 1965; E. KRÉN, L. PÁL and P. SZABÓ, Phys. Letters, **9**, 297, 1964; G. SHIRANE and R. NATHAUS, Phys. Rev., **134**, A1547, 1964.
13. C. HARGITAI, Phys. Letters, **17**, 178, 1965.
14. L. ZSOLDOS, Phys. Stat. Sol., **20**, K25, 1967.
15. G. SHIRANE, C. W. CHEN and P. A. FLINN, Phys. Rev., **131**, 183, 1963; L. CSER, I. DÉZSI and L. KESZTHELYI, Rep. of the Central Research Institute for Physics (Hungary) **12**, 119, 1964.
    F. E. OBENSHAIN, L. D. ROBERTS, D. W. FORESTER, J. O. THOMSON and H. H. F. WEGENER, *ORNL*-**3582**, 18, 1964.
16. L. CSER and L. KESZTHELYI, private communication.

МАГНИТНЫЕ ФАЗОВЫЕ ПЕРЕХОДЫ ПЕРВОГО РОДА

Л. ПАЛ

Резюме

В работе исследованы общие термодинамические свойства магнитных фазовых переходов первого рода. С целью ограничения возможных физических моделей предположено, что причиной фазового превращения является изменение знака выражения, состоящего из констант обменного взаимодействия, чувствительно зависящих от межатомного расстояния. Показано, что фазовому переходу препятствует энергетический барьер упругого происхождения, который разделяет минимумы свободной энергии, связанные с участвующими в переходе фазами. Исследовано влияние внешнего давления и магнитного поля на температуру перехода. В случае антиферромагнитных $\leftrightarrows$ ферромагнитных переходов определена кривая сосуществования в плоскости $T-P$ и рассмотрены условия существования тройной точки на диаграмме $T-P$. Вследствие энергетического барьера возникает гистерезис в переходе. Определены верхняя (T_{sup}) и нижняя (T_{inf}) температуры перехода и их зависимость от внешнего давления. Показано, что при определенных условиях фазовая граница АФ—Ф соединяется с фазовыми границами АФ—П и Ф—П и в плоскости $T-P$ образуется тройная точка.

Исследован характер исчезновения магнитного порядка для обеих магнитных фаз и доказано, что род фазового превращения может быть различным в переходах Ф—П и АФ—П.

Определялась кривая сосуществования плоскости $T-H$ между ферромагнитными и антиферромагнитными фазами. Вычислялась зависимость верхней и нижней температур превращения от внешнего магнитного поля. Найдено, что с возрастанием магнитного поля разница между верхней и нижней температурами превращения (т. е. ширина гистерезиса) уменьшается, а при критическом значении внешнего поля и температуры сливается с кривой сосуществования. При температуре ниже критической, магнитное поле не может вызвать истинного антиферромагнитного → ферромагнитного перехода первого рода, т. к. его действие проявляется только в непрерывном повороте спинов в направлении внешнего поля.

Определена величина скачка параметра решетки и намагниченности при верхней и нижней температурах перехода и также при температуре сосуществования. Показано, что изменение энтропии в переходе вызвано двумя причинами. Одна из них связана с изменением параметра решетки, а другая — с изменением намагниченности. При определенных условиях обе составляющие могут быть по величине одинакового порядка.

Acta Physica Academiae Scientiarum Hungaricae, Tomus 27, pp. 87—110 (1969)

MILLISTRONG C VIOLATION AND η DECAY*

By

A. FRENKEL

CENTRAL RESEARCH INSTITUTE FOR PHYSICS OF THE HUNGARIAN ACADEMY OF SCIENCES, BUDAPEST

and

G. MARX

INSTITUTE FOR THEORETICAL PHYSICS OF THE ROLAND EÖTVÖS UNIVERSITY; BUDAPEST

(Received 13. I. 1969)

The isospin properties of the (assumed) millistrong C violation have been investigated. The consequences of a $\Delta I = 0$ and $\Delta I = 2$ selection rule are discussed for the $\eta \to \pi^+\pi^\circ\pi^-$ and $\eta \to \pi^\circ e^+ e^-$ decays. If the observed charge asymmetry of the $\eta \to \pi^+\pi^\circ\pi^-$ is realistic, the C violating 3 π final state is mainly an $I = 2$ eigenstate, produced by a $\Delta I = 2$ coupling with a constant $g_2 \simeq 10^{-2}$. Since the $I = 0$ eigenstate is here very much suppressed by the centrifugal barrier, the $\Delta I = 0$ coupling may be much stronger, e.g. $g_0 > 10^{-1}$, limited only by the negative results of the $\eta \to \pi^{\circ +} e^-$ experiments. So the $\Delta I = 0$ dominance of the millistrong C violation, suggested by the indication $|\varepsilon| > |\varepsilon'|$ in the K° decays, is by no means in contradiction with the observed $\Delta I = 2$ character of the $\eta \to \pi^+\pi^\circ\pi^-$ asymmetry. The importance of more accurate experiments is emphasized.

1. Possible models of CP violation

The CP violation has been discovered in the decays of the K_L° meson ($K_L^\circ \to \pi^+\pi^-$, $\pi^\circ\pi^\circ$, $e\pi\nu$, $\mu\pi\nu$). Assuming a CPT symmetry, in the case of a complete phenomenological analysis of the K° system two pieces of information may be extracted concerning the nature of the CP violation: the complex parameters ε and ε'. These are defined as follows:

$$2\left[m_L - m_S - \frac{i}{2}\left(\frac{1}{\tau_L} - \frac{1}{\tau_S}\right)\right]\varepsilon = \langle K^\circ | H' + \cdots | \bar{K}^\circ \rangle - \langle \bar{K}^\circ | H' + \cdots | K^\circ \rangle \tag{1}$$

$$\sqrt{2}\,|\varepsilon'| = \left| \mathrm{Im} \frac{\langle \pi\pi, I = 2 | H' + \cdots | K^\circ \rangle}{\langle \pi\pi, I = 0 | H' + \cdots | K^\circ \rangle} \right|.$$

Here H' is the sum of the weak Hamiltonians and of the CP violating Hamiltonians, $m_{L,S}$ and $\tau_{L,S}$ are the masses and life times of the neutral $K_{L,S}^\circ$ mesons. The actual values of ε and ε' are still uncertain, but according to the most popular supposition [1]

$$|\varepsilon| = 2 \cdot 10^{-3} \gg |\varepsilon'|. \tag{2}$$

* Dedicated to Prof. P. GOMBÁS on his 60th birthday.

(The published experimental data [1] still seem to be in conflict with each other, so the possibility $|\varepsilon| \simeq |\varepsilon'|$ is not yet completely excluded.) From Equ. (1) we can deduce the following alternative conclusions:

I. If the CP violating Hamiltonian is characterized by the strangeness selection rule $\Delta S = 2$, then the right-hand side of Equ. (1) may be interpreted as a first order expression; consequently $(f_w \sin\Theta)^2 \varepsilon \simeq g$. (Here g is the coupling constant in the CP violating Hamiltonian, f_w is the weak coupling constant and Θ is the Cabibbo angle.) In this case the CP violation is about 10^4 times weaker than a second order weak interaction. (Superweak CP violation.)

II. If $\Delta S = 1$, one gets $\Delta S = 2$ on the right-hand side of Equ. (1) as the result of an interplay between weak and CP violating interactions; consequently $(f_w \sin\Theta)^2 \varepsilon \simeq g f_w \sin\Theta$. In this case the CP violating coupling may be about 1000 times weaker than the weak interaction. (Milliweak CP violation, according to the nomenclature of L. B. OKUN.)

III. If $\Delta S = 0$ for the C violating Hamiltonian, one reads from Equ. (1) that $(f_w \sin\Theta)^2 \varepsilon \simeq g (f_w \sin\Theta)^2$. The C violating coupling is now of the order of $|\varepsilon| \simeq 2 \cdot 10^{-3}$ (Millistrong C violation.)

IV. If $\Delta S = 0$ but the emission of one photon is associated with the C violating vertex, this photon must be reabsorbed by a conventional electromagnetic interaction, so from Equ. (1) one arrives at the estimate $(f_w \sin\Theta)^2 \varepsilon \simeq e g (f_w \sin\Theta)^2$, which may be solved by writing $g = e$, because $e^2 = 4\pi \cdot 137^{-1}$. (Electromagnetic C violation.)

V. If $\Delta S = 1$, but the CP violation is associated with the emission of one photon, Equ. (1) gives $(f_w \sin\Theta)^2 \varepsilon \simeq e g (f_w \sin\Theta)$, which may be solved by writing $g = e f_w \sin\Theta$. (Weak electromagnetic CP violation.)

The estimation of g is evidently only a very approximate one. The values of ε and ε' are sensitive not only to the S character but also to the I character of the CP violating Hamiltonian. The most interesting possibilities are listed in Table I. In each column we have indicated the most crucial tests of the type of CP violation under consideration. The most important implications are as follows:

a) Very strict restrictions are imposed by the electric dipole moment of the neutron. By dimensional arguments the electromagnetic model of C violation predicts $d_n \simeq |f_w M_n^{-1} = 10^{-19}$ cm. A more detailed calculation suggests 10^{-21} cm in the same model [11]. The millistrong prediction is something like $d_n \simeq |\varepsilon| f_w M_n^{-1} = 10^{-22}$ cm. The most recent experimental value is $d_n = (2 \pm \pm 2) 10^{-23}$ cm [1]. This apparently rules out the possibility of an electromagnetic C violation with $g = e$.

b) The experimental upper limit on the C violating decay $\eta \to \pi^\circ e^+ e^-$ is [13]

$$B(\eta \to \pi^\circ e^+ e^-) = \Gamma(\eta \to \pi^\circ e^+ e^-) : \Gamma(\eta) < 10^{-4}. \tag{4}$$

Table I

ΔS	0			
ΔI	0	1	2	3
CP violating vertex works only among hadrons	$\varepsilon \gg \varepsilon'$ n dipole moment $\eta \to \pi^+\pi^0\pi^-$ nuclear reaction [2, 3, 4]	$\varepsilon \sim \varepsilon'$ n dipole moment $\omega \to \pi^+\pi^0\pi^-$ nuclear reaction	$\varepsilon \sim \varepsilon'$ n dipole moment $\eta \to \pi^+\pi^0\pi^-$ [5, 6]	$\varepsilon \gg \varepsilon'$ $\omega \to \pi^+\pi^0\pi^-$
	millistrong C violation			
CP violating vertex among hadrons plus one photon	$\varepsilon \sim \varepsilon'$ n dipole moment $\eta \to \pi^+\pi^0\pi^-$	$\varepsilon \sim \varepsilon'$ n dipole moment $\eta \to \pi^+\pi^0\pi^-$ $\eta \to \pi^0 e^+ e^-$ $\eta \to \pi^+\pi^-\gamma$ [10, 11]	$\varepsilon \sim \varepsilon'$ n dipole moment $\eta \to \pi^+\pi^0\pi^-$	$\varepsilon \sim \varepsilon'$ $\eta \to \pi^+\pi^0\pi^-$
	electromagnetic C violation			

ΔS	1			2
ΔI	1/2	3/2	5/2	any
CP violating vertex works only among hadrons	$\varepsilon \gg \varepsilon'$	$\varepsilon \sim \varepsilon'$	$\varepsilon \ll \varepsilon'$ [5]	$\varepsilon \gg \varepsilon'$ [9]
	[7, 8]			
	milliweak CP violation			superweak
CP violating vertex among hadrons plus one photon	$\varepsilon \sim \varepsilon'$ $K \to \pi\pi\gamma$	$\varepsilon \sim \varepsilon'$ $K \to \pi\pi\gamma$ [12]	$\varepsilon \sim \varepsilon'$	$\varepsilon \gg \varepsilon'$
	weak electromagnetic C violation			superweak

This is in conflict with the prediction of electromagnetic C violation with $\Delta I = 1$.

c) All the decays $\eta \to 3\pi(I_f = 0,2)$, $\omega \to 3\pi(I_f = 1,3)$, $\varrho \to 3\pi(I_f = 1,3)$ violate the C symmetry. An interference between the C conserving and C violat-

ing amplitudes can produce a charge asymmetry

$$\Delta = \frac{N(E_+ > E_-) - N(E_- > E_+)}{N(E_+ > E_-) + N(E_- > E_+)}, \tag{5}$$

which is of the first order in the ratio of the C violating and C conserving coupling constants (g/G). The most appropriate situation is afforded by the $\eta \to \pi^+\pi^\circ\pi^-$ decay, where the background may be (more or less) eliminated by making use of the small η width,* and where the C violation is competing with a C-symmetric, but I-asymmetric transition. As a matter of fact, from the analysis of 36800 $\eta \to \pi^+\pi^\circ\pi^-$ decays an asymmetry

$$\Delta = (1.52 \pm 0.5)\% \tag{6}$$

has been found [14], which differs from zero by three standard deviations.*

d) The different I and S selection rules predict different inequalities (or approximate equalities) for ε and ε'. If we accept the result [13] as a realistic one, only three possibilities of Table I must be kept in mind:

1) Superweak CP violation $(\Delta S = 2)$,
2) Milliweak CP violation $(\Delta S = 1, \Delta I = {}^1/_2)$,
3) Millistrong C violation $(\Delta S = 0, \Delta I = 0)$.

If we consider the electromagnetic model of C violation as excluded by the experiments, an $\eta \to \pi^+\pi^\circ\pi^-$ charge asymmetry of the order of % or ‰ may be given only by the millistrong models $\Delta I = 0$ or $\Delta I = 2$. The symmetry properties of the $\pi^+\pi^\circ\pi^-$ final state may be visualized on the Dalitz plot (Fig. 1). The N_i denote the numbers of $\eta \to \pi^+\pi^\circ\pi^-$ events in the i-th sextant of the Dalitz domain. The measured values are [14]:

$$\begin{aligned} N_1 &= 1850 & N_4 &= 12419 \\ N_2 &= 4931 & N_5 &= 4723 \\ N_3 &= 12771 & N_6 &= 1824 \end{aligned} \tag{7}$$

The asymmetry Δ is defined according to Equ. (5) as

$$\Delta = \frac{N_1 + N_2 + N_3 - N_4 - N_5 - N_6}{N_1 + N_2 + N_3 + N_4 + N_5 + N_6} \tag{8}$$

and the numbers (7) give the asymmetry value quoted under (6). It has been emphasized by M. NAUENBERG, that in the case of a pure $I = 0$ final state the

* Recently it has been pointed out by H. YUTA and S. OKUBO [15] that in the experiment [14] the asymmetry may be caused by a 10% background effect. This warning must be taken into account in further experimental work. In our paper we arbitrarily suppose that the bulk of the asymmetry is due to the C violation [1].

odd-even "sextant asymmetry"

$$\bar{\Delta} = \frac{N_1 - N_2 + N_3 - N_4 + N_5 - N_6}{N_1 + N_2 + N_3 + N_4 + N_5 + N_6} \tag{9}$$

is three times bigger than the simple "right-left" asymmetry (Fig. 2). The experimental values (7) give, however,

$$\bar{\Delta} = (0.44 \pm 0.5)\% , \tag{10}$$

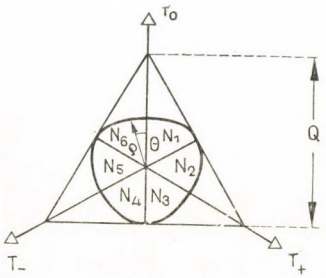

Fig. 1



Fig. 2

which seems to be smaller than Δ given in (6) and is consistent with zero within one standard deviation. The experimental indication $\Delta > \bar{\Delta}$ (instead of $\Delta = \bar{\Delta}/3$) suggests that it is not the $I = 0$, but the $I = 2$ final state that governs the C violating transition.

An apparent contradiction arises: *both the* $K_L^\circ \to \pi\pi$ *decay and the* $\eta \to \pi^+\pi^\circ\pi^-$ *charge asymmetry can be explained by the millistrong model of C violation, but the experimental indication* $|\varepsilon| \gg |\varepsilon'|$ *suggests the* $\Delta I = 0$ *version; the result* $\Delta > \bar{\Delta}$ *suggests the* $\Delta I = 2$ *version of this model.* The aim of the present paper is to present a more detailed discussion of the charge asymmetry in the $\eta \to \pi^+\pi^\circ\pi^-$ decay, in order to clarify this discrepancy.

2. The $\eta \to \pi^+\pi^\circ\pi^-$ decay

In analyzing the $\eta \to \pi^+\pi^\circ\pi^-$ decay we shall write T_+, T_0, T_- for the pion kinetic energies, P_+, P_0, P_- for the pion four momenta. In the rest system of the η meson we evidently have:

$$\mathbf{p}_+ + \mathbf{p}_0 + \mathbf{p}_- = 0 ,$$
$$T_+ + T_0 + T_- = m - 3\mu = Q .$$

(We shall denote the masses of the π, η and ϱ mesons by μ, m and M. For simplicity we shall take $\mu : m : M = 1 : 4 : 5.55$ and we shall disregard electro-

magnetic mass splittings.) We shall also make use of the Mandelstam variables s, t, u which may be expressed in the rest system of the η meason as follows:

$$\begin{aligned} s &= (p_+ + p_-)^2 = (m - \mu)^2 - 2\,mT_0\,, \\ t &= (p_- + p_0)^2 = (m - \mu)^2 - 2\,mT_+\,, \\ u &= (p_+ + p_0)^2 = (m - \mu)^2 - 2\,mT_-\,. \end{aligned} \tag{11}$$

The decay may be analyzed conveniently on the Dalitz diagram (Fig. 1). Let us introduce the Dalitz variables ϱ and Θ according to the formulae

$$\begin{aligned} T_+ &= \frac{Q}{3}\left(1 - \frac{1}{2}\,\varrho\cos\Theta - \frac{\sqrt{3}}{2}\,\varrho\sin\Theta\right), \\ T_0 &= \frac{Q}{3}\,(1 + \varrho\cos\Theta)\,, \\ T_- &= \frac{Q}{3}\left(1 - \frac{1}{2}\,\varrho\cos\Theta + \frac{\sqrt{3}}{2}\,\varrho\sin\Theta\right). \end{aligned} \tag{12}$$

In terms of Dalitz variables the decay probability can be written as follows:

$$\Gamma(\eta \to \pi^+\,\pi^\circ\,\pi^-) = (4\pi)^{-3}\,\frac{Q^2}{6\sqrt{3}\,m}\int_0^{2\pi} d\Theta \int_0^{R(\Theta)} d\varrho\;\varrho\,|A(\varrho,\Theta)|^2. \tag{13}$$

The 30%—100% experimental errors of the measured asymmetries (6) and (10) make very accurate calculation unnecessary. We put simply $R(\Theta) = 1$, allowing an inaccuracy of 20% on the boundary of the Dalitz plot.*

The dominating decay mode is the $\Delta I = 1$ channel, which can be described by the C conserving vertex

$$H_1 = \frac{1}{2}\,G_1\,\eta\pi^\circ(\pi\pi) = G_1\,\eta\left(\pi^+\,\pi^\circ\,\pi^- + \frac{1}{2}\,\pi^\circ\,\pi^\circ\,\pi^\circ\right). \tag{14}$$

If we had only this coupling among η and 3π, the perturbation theory would give $A_1(\varrho,\Theta) = G_1 = \text{const}$ for the invariant amplitude. The observed $\eta \to \pi^+\pi^\circ\pi^-$ width [13]

$$\Gamma(\eta \to \pi^+\,\pi^\circ\,\pi^-) = (0{,}237 \pm 0{,}017)\,\Gamma(\eta) = (0{,}237 \pm 0{,}017)\,(2{,}3 \pm 0{,}5)\,\text{kev} \tag{15}$$

may be obtained if we put

$$|G_1| = 0{,}32 \pm 0{,}04. \tag{16}$$

* We have checked that the conclusions of the present paper remain unchanged if the electromagnetic mass differences and the exact boundary of the Dalitz domain are taken into account. Some figures are of course changed, sometimes by a factor of 2.

The observed value of $\Gamma(\eta \to \pi^0\pi^0\pi^0)$ indicates a small $I = 3$ impurity in the final state, but the corresponding coupling constant is very small and may be taken to zero within three standard deviations. So in our analysis we shall disregard the $\Delta I = 3$ possibility.

The C conserving $\Delta I = 1$ transition amplitude $A_1(\varrho, \Theta)$ is influenced by the final state interactions of the pions. The incomplete knowledge of this modification is perhaps the weakest point in the analysis of the $\eta \to 3\pi$ decay. The observed enhancement in the lower parts of the Dalitz diagram may be simply described by a formula linear in T_0 [17]

$$|A_1(\varrho(\Theta)| = |G_1| \frac{1 + \beta\varrho \cos\Theta}{\left(1 + \frac{1}{4}\beta^2\right)^{1/2}} \tag{17}$$

with

$$\beta = -0{,}55 \pm 0{,}02. \tag{18}$$

The imaginary part of $A_1(\varrho, \Theta)$ can be obtained only from specific assumptions concerning the final state interaction. B. BARRET et al. [18] have suggested the following formula:

$$A_1(\varrho, \Theta) = \frac{a}{1 - ia_0 q(s)} + b\left[\frac{s-u}{D(t)} + \frac{s-t}{D(u)}\right]. \tag{19}$$

This takes into account a $\pi\pi$ interaction in the $I = 0$, $L = 0$ state (described by the scattering length a_0) and a $\pi\pi$ interaction in the $I = 1$, $L = 1$ state (described by the ϱ meson pole). Here $q(s) = 1/2(s—4\mu^2)^{1/2}$ and $D(s)$ comes from the ϱ propagator, being $D(s) = M^2—s—iM^{-1}\Gamma(\varrho)q^3(s)/\sqrt{s}$. The empirical constants a and b are real if the CPT symmetry holds.

The recent analysis [19] suggests a value

$$\mu a_0 = 0{,}2. \tag{20}$$

It is shown in Appendix I that the formula (19) may be well approximated with a linear expression if we make use of the numerical values (18) and (20). So we shall use the following expression for the C conserving amplitude:

$$A_1(\varrho, \Theta) = G_1 e^{i\alpha} \frac{1 + \beta\varrho \cos\Theta}{\left(1 + \frac{1}{4}\beta^2\right)^{1/2}} \tag{21}$$

with

$$\alpha = \arctan\left[a_0\left(\frac{1}{4}m^2 - \frac{2}{3}mQ - \frac{3}{4}\mu^2\right)^{1/2}\right] = 8° 40' \tag{22}$$

coming from fitting (21) to (19). The possible consequences of the nonlinear terms in (21) and of the variation of the scattering length a_0 are discussed in Appendix II.

Let us now turn to the C violating part of the invariant amplitude $A(\varrho, \Theta)$ coming from the $I = 0$ and $I = 2$ final states. B. BARRET et al. [18] have used the following expression:

$$A_0(\varrho, \Theta) + A_2(\varrho, \Theta) = ic\left[\frac{t-u}{D(s)} + \frac{u-s}{D(t)} + \frac{s-t}{D(u)}\right] + id\frac{t-u}{D(s)}. \quad (23)$$

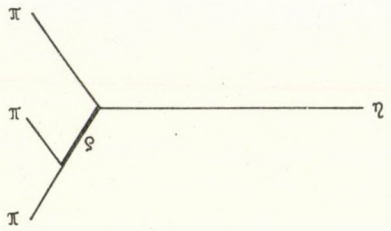

Fig. 3

In the present work we assume that the C violating transitions $\eta \to \pi\pi\pi (I = 0,2)$ are dominated by the ϱ meson (Fig. 3) and the C violation is due to the $\eta\varrho\pi$ vertex [4]:

$$H_0 = g_0\left[\varrho_\mu^+(\pi^-\partial_\mu\eta - \eta\partial_\mu\pi^-) + \varrho_\mu^\circ(\pi^\circ\partial_\mu\eta - \eta\partial_\mu\pi^\circ) + \right. \\ \left. + \varrho_\mu^+(\pi^+\partial_\mu\eta - \eta\partial_\mu\pi^+)\right], \quad (24)$$

$$H_2 = g_2\left[-\varrho_\mu^+(\pi^-\partial_\mu\eta - \eta\partial_\mu\pi^-) + 2\varrho_\mu^\circ(\pi^\circ\partial_\mu\eta - \eta\partial_\mu\pi^\circ) - \right. \\ \left. - \varrho_\mu^-(\pi^-\partial_\mu\eta - \eta\partial_\mu\pi^+)\right]. \quad (25)$$

The C symmetric $\varrho\pi\pi$ vertex is the known strong interaction

$$H_\varrho = G_\varrho\left[\varrho_\mu^+(\pi^\circ\partial_\mu\pi^- - \pi^-\partial_\mu\pi^\circ) + \varrho_\mu^\circ(\pi^-\partial_\mu\pi^+ - \pi^+\partial_\mu\pi^-) + \right. \\ \left. + \varrho_\mu^-(\pi^+\partial_\mu\pi^\circ - \pi^\circ\partial_\mu\pi^+)\right]. \quad (26)$$

The observed ϱ width $\Gamma(\varrho) = 130 \pm 20$ MeV [13] gives

$$G_\varrho = 5{,}6 \pm 0{,}4. \quad (27)$$

The interplay of the couplings (24) and (25) with (26) results in

$$A_0(\varrho, \Theta) + A_1(\varrho, \Theta) = i(g_0 - g_2)G_\varrho\left[\frac{t-u}{M^2-s} - \frac{u-s}{M^2-t} - \right. \\ \left. - \frac{s-t}{M^2-u}\right] + i\,3\,g_2 G_\varrho\frac{t-u}{M^2-s}. \quad (28)$$

(The real part coming from the ϱ width may be neglected compared with the imaginary contribution of $A_1(\varrho, \Theta)$ coming from the final state interactions.) Comparing the expression (28) with the formula (23) one can see that the parameters c and d do not simply describe the $\Delta I = 0$ and $\Delta I = 2$ transitions, but are combinations of g_0 and g_2. In order to avoid any misunderstanding we shall analyze the η asymmetry in terms of the pure isospin constants g_0 and g_2 instead of the usual c and d.

By performing a power expansion according to the new variables $Y_{+,0,-} = 3Q^{-1} T_{+,0,-} - 1$ (see Appendix I) and by introducing the small centrifugal barrier parameter

$$k = \frac{mQ/3}{M^2 - (m-\mu)^2 + \frac{2\,mQ}{3}} = 0{,}054\,, \tag{29}$$

one arrives at the formula

$$A_0(\varrho, \Theta) + A_2(\varrho, \Theta) = i\,6\sqrt{3} G_\varrho \left[g_2 \frac{k\varrho \sin\Theta}{1 + 2\,k\varrho\cos\Theta} + (g_0 - g_2) k^3 \varrho^3 \sin 3\Theta + \ldots \right],$$

which may be written in the more convenient form

$$\begin{aligned} A_0(\varrho, \Theta) + A_2(\varrho, \Theta) = i\,6\sqrt{3}\,G_\varrho\,[g_2(k\varrho + k^3\varrho^3)\sin\Theta - g_2 k^2 \varrho^2 \sin 2\Theta + \\ + g_0 k_0^3 \varrho^3 \sin 3\Theta + 0(k^4)]\,. \end{aligned} \tag{30}$$

We have now everything ready to construct the theoretical distribution on the Dalitz circle. Let us calculate the Θ distribution $f(\Theta)$ up to first powers of g_0/G_1, g_2/G_1 and up to k^3. Evidently,

$$f(\Theta) = \frac{1}{G_1^2 \pi} \int_0^1 |A_1(\varrho, \Theta) + A_0(\varrho, \Theta) + A_2(\varrho, \Theta)|^2 \varrho\, d\varrho\,.$$

By substituting the formulae (21) and (30) one gets the following expression:

$$\begin{aligned} 2\pi f(\Theta) = 1 - \left(1 + \frac{1}{4}\beta^2\right)^{-1} \left\{ -\frac{4}{3}\beta\cos\Theta - \frac{1}{4}\beta^2 \cos 2\Theta \right\} + \\ + \frac{24\sqrt{3}\sin\alpha}{\left(1 + \frac{1}{4}\beta^2\right)^{1/2}} \frac{G_\varrho}{G_1} \left\{ g_2 \left(\frac{k}{3} - \frac{\beta k^2}{10} + \frac{k^3}{5} \right) \sin\Theta - \right. \\ - \left[g_2 \left(-\frac{k\beta}{8} + \frac{k^2}{4} - \frac{k^3\beta}{12} \right) - g_0 \frac{k^3\beta}{12} \right] \sin 2\Theta + \\ \left. + \left[-g_2 \frac{k^2\beta}{10} + g_0 \frac{k^3}{5} \right] \sin 3\Theta + g_0 \frac{k^3\beta}{12} \sin 4\Theta + 0(k^4) \right\} = \\ = 2\pi \left[\sum_n x_n \cos n\Theta + \sum_n y_n \sin n\Theta \right]. \end{aligned} \tag{31}$$

The charge asymmetry is given by the $\sin n\Theta$ terms. The asymmetry parameters, defined in (8) and (9) may be obtained from $f(\Theta)$:

$$\Delta = -\int_0^{\pi} [f(\Theta) - f(-\Theta)]\, d\Theta = -4\left(y_1 + \frac{1}{3} y_3\right),$$

$$\bar{\Delta} = -\int_0^{\pi/3} [f(\Theta) - f(-\Theta)]\, d\Theta + \int_{\pi/3}^{2\pi/3} [f(\Theta) - f(-\Theta)]\, d\Theta -$$

$$- \int_{2\pi/r}^{\pi} [f(\Theta) - f(-\Theta)]\, d\Theta = -4\, y_3$$

i.e.

$$\Delta = -\frac{16\sqrt{3}\sin\alpha}{5\pi\left(1+\frac{1}{4}\beta^2\right)^{1/2}} k^3 \frac{G_\varrho}{G_1}\left[g_0 + g_2\left(\frac{5}{k^2} - \frac{2\beta}{k} + 3\right)\right], \tag{32}$$

$$\bar{\Delta} = -\frac{16\sqrt{3}\sin\alpha}{5\pi\left(1+\frac{1}{4}\beta^2\right)^{1/2}} k^3 \frac{G_\varrho}{G_1}\left[3\, g_0 - g_2 \frac{3}{2} \frac{\beta}{k}\right]. \tag{33}$$

Substituting the numerical values quoted in Equs. (16), (18), (22), (27) and (29), we have, finally,

$$\Delta = 7 \cdot 10^{-4}(g_0 + 1720\, g_2), \tag{34}$$

$$\bar{\Delta} = 7 \cdot 10^{-4}(3\, g_0 + 15\, g_2). \tag{35}$$

For simplicity we take the sign of the product $-G_\varrho G_1^{-1}\sin\alpha$ as positive. If it turns out to be negative, we have to change the sign of g_0 and of g_2.

Remembering that the centrifugal barrier parameter k introduced in Equ. (29) is small, we arrive at the following conclusions:

a) In the case of a pure $\Delta I = 0$ charge asymmetry (i.e. with $g_2 = 0$) one would have $\bar{\Delta} = 3\Delta$. The sextant asymmetry $\bar{\Delta}$ was originally introduced by M. NAUENBERG [16] merely as a good tool to demonstrate the presence of a pure $\Delta I = 0$ asymmetry in the $\eta \to \pi^+\pi^\circ\pi^-$ decay. However, one cannot live with a pure $\Delta I = 0$ C violation: radiative corrections introduce a $\Delta I = 1$ and a $\Delta I = 2$ impurity necessarily, and from Equ. (34) we see that in Δ the contribution of the $\Delta I = 2$ channel will dominate even if $\varrho_2 \simeq \varrho_0/137$. The experimental indication $\Delta > \bar{\Delta}$ then becomes understandable. Let us also remark that to reproduce the observed order of magnitude for the Δ asymmetry with $g_2 = 0$ one has to take $g_0 \simeq 20$. Such a strong C violating $\eta\varrho\pi$ coupling would lead to very large charge asymmetries in many strong and electromagnetic transitions, where the centrifugal barrier effect, specific for the $\eta \to \pi^+\pi^\circ\pi^-$ decay, is absent. Thus we conclude that we are forced to reject the $g_2 = 0$ solution.

b) If $g_2 \neq 0$, the situation becomes more involved. The first thing to note is that the experimental value $\Delta \simeq 10^{-2}$ can be reproduced if $g_2 \simeq 10^{-2}$, which is a reasonable "millistrong" value. At the same time g_0 may be zero, but this is by no means a necessity. Equ. (34) clearly shows that even if $g_0 \simeq 100\ g_2$, the contribution of g_0 will be practically undetectable in Δ. Let us also look at the sextant asymmetry $\bar{\Delta}$. It is important to remark that while in Δ the coefficient of g_2 is almost entirely given by the constant $5k^2 \simeq 1700$; in $\bar{\Delta}$ this coefficient depends also on β, i.e. it is sensitive to the energy dependence of the C conserving matrix element. In Appendix II we show that the value of this coefficient is also influenced by the small quadratic term of the C conserving matrix element, neglected in the formulae given in the text. Thus, the contribution of g_2 to $\bar{\Delta}$ cannot be firmly established, and the calculated value "15" in Equ. (35) can be used only for orientation. It just shows that with $g_2 \simeq 10^{-2}$, $g_0 \leq 100\ g_2$ $\bar{\Delta}$ is expected to be much smaller than Δ, a result which is fully consistent with the measured value $\bar{\Delta} = (0.44 \pm 0.5)\%$.

The basic experimental information $\Delta \simeq 10^{-2}$ and $\Delta > \bar{\Delta}$ given in Equs. (6) and (10) are just at the limit of statistical significance. It would be of great importance to ascertain these experimental results. Indeed, let us suppose that the solution $|\varepsilon| > |\varepsilon'|$ holds for the K_L° decays. Then the CP violation may be superweak ($\Delta S = 2$) or millistrong ($\Delta S = 0$), but in the K_L° decays this can no longer be decided. The experiment crux may then be the $\eta \to \pi^+\pi^\circ\pi^-$ decay. If the value $\Delta \simeq 10^{-2}$ turns out to be realistic,* then the CP violation is millistrong. We have just seen that the results $\Delta \simeq 10^{-2}$, $\Delta > \bar{\Delta}$ are fully compatible with $|\varepsilon| \gg |\varepsilon'|$, since the dominance of the $\Delta I = 2$ channel in the $\eta \to \pi^+\pi^\circ\pi^-$ decay does not necessarily mean that $g_2 \gg g_0$. The possibility $g_0 \gg g_2$ is also open, due to the strong damping of the $\Delta I = 0$ channel by the centrifugal barrier effect.

Let us point out that useful supplementary information on the mechanism of the C violation in the $\eta \to \pi^+\pi^\circ\pi^-$ decay can be extracted from the study of the partial asymmetry parameters Δ_1, Δ_2, Δ_3. These parameters have also been considered by M. NAUENBERG for the pure $\Delta I = 0$ case. They are defined as follows (see Fig. 1):

$$\Delta_1 = \frac{N_1 - N_6}{N_1 + N_6}\ ; \quad \Delta_2 = \frac{N_2 - N_5}{N_2 + N_5}\ ; \quad \Delta_3 = \frac{N_3 - N_4}{N_3 + N_4}\ . \tag{36}$$

Starting from our distribution function $f(\Theta)$ given in Equ. (31), the theoretical expressions for these asymmetry parameters can be easily calculated. The comparison with the experimental values taken from (7) are presented in Table II. We see that the available experimental data on the partial asym-

* See footnote on page 90.

Table II

asymmetry parameter	experiment [17]	THEORY linear approximation		
		$g_0 = 22$, $g_2 = 0$ ($\lvert g_0 + 2g_2 \rvert = 22 > 0.4$)	$g_0 = 0$, $g_2 = 0.0124$ ($\lvert g_0 + 2g_2 \rvert = 0.0248 < 0.4$)	$g_0 = 25g_2 = 0.3075$, $g_2 = 0.0123$ ($\lvert g_0 + 2g_2 \rvert = 0.33 < 0.4$)
$10^3\,\Delta$	15.2 ± 5	15.2	15.2	15.2
$10^3\,\bar{\Delta}$	4.4 ± 5	45.6	0.13	0.82
$10^3\,\Delta_1$	7.06 ± 16	60.8	15.3	16
$10^3\,\Delta_2$	21.6 ± 9	−48	24	22.3
$10^3\,\Delta_3$	13.9 ± 6.4	39.5	9.6	10.1

asymmetry parameter	experiment [17]	THEORY quadratic approximation		
		$g_0 = 35{,}5$, $g_2 = {,}0$ ($\lvert g_0 + 2g_2 \rvert = 35.5 > 0.4$)	$g_0 = 0$, $g_2 = 0.0126$ ($\lvert g_0 + 2g_2 \rvert = 0.0252 < 0.4$)	$g_0 = 25g_2 = 0.3125$, $g_2 = 0.0125$ ($\lvert g_0 + 2g_2 \rvert = 0.34 < 0.4$)
$10^3\,\Delta$	15.2 ± 5	15.2	15.2	15.2
$10^3\,\bar{\Delta}$	4.4 ± 5	64.5	−0.41	0.16
$10^3\,\Delta_1$	7.06 ± 16	56	10.4	10.8
$10^3\,\Delta_2$	21.6 ± 9	−79	23.4	22.4
$10^3\,\Delta_3$	13.9 ± 6.4	52.5	10.2	10.6

metries — with the large statistical errors taken into account — support our conclusions, based on the study of the Δ and $\bar{\Delta}$ parameters alone. The influence of the quadratic energy terms in the C conserving matrix element on the partial asymmetries is discussed in Appendix II.

Let us conclude this discussion with the remark that the data available on the $\eta \to \pi^+\pi^\circ\pi^-$ charge asymmetry do not give an effective upper limit for the coupling constant g_0. As noted above, such a limit may come from C violating effects in strong or electromagnetic processes. It turns out that the working limit is given by the $\eta \to \pi^\circ e^+ e^-$ decay, which we shall discuss shortly.

3. The $\eta \to \pi^\circ e^+ e^-$ decay

It had already been emphasized in 1965 [20], that the millistrong model of the C violation predicted a strict correlation between the branching ratio of the $\eta \to \pi^\circ e^+ e^-$ decay and the charge asymmetry in the $\eta = \pi^+\pi^\circ\pi^-$ decay, if the ϱ pole dominance was assumed in both reactions. In the light of the accurate upper limit (4) it looks worthwhile to reinvestigate this question.

In the ϱ dominance model (Fig. 4) we can express the $\eta \to \pi^\circ e^+ e^-$ decay probability in terms of the coupling constants g_0 and g_2. If the ϱ—γ coupling is given by $f = eG_\varrho^{-1}$, we have [18]:

$$\Gamma(\eta \to \pi^\circ e^+ e^-) = 42\, eV \left(\frac{g_0 + 2g_2}{G_\varrho}\right)^2 \tag{37}$$

i.e.

$$B(\eta \to \pi^\circ e^+ e^-) = \Gamma(\eta \to \pi^\circ e^+ e^-) : \Gamma(\eta) = 2 \cdot 10^{-3} \left(\frac{g_0 + 2g_2}{G_1 G_\varrho}\right)^2. \tag{38}$$

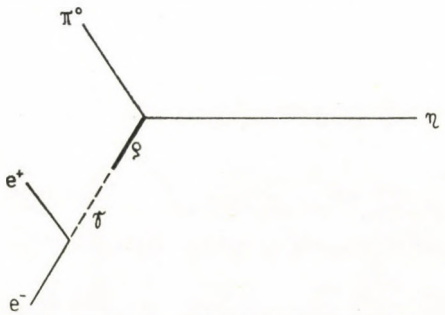

Fig. 4

We can express g_0 and g_2 through A and $\bar{A}$ using the equations (32) and (33). Introducing these expressions into (38) we see that B is independent of G_1. Using the known numerical values of the other parameters, we get

$$B(\eta \to \pi^\circ e^+ e^-) = 132\,(\bar{A} - 0{,}00525\, A)^2. \tag{39}$$

The experimental limit quoted in Equ. (4) puts the restriction

$$|\bar{A} - 0{,}00525 \cdot A| < 10^{-3} \tag{40}$$

on the charge asymmetries A and $\bar{A}$. Consequently (4) and (6) predict $\bar{A}$ to be smaller than 10^{-3}. This is a much more stringent restriction than the experimental limit (10). It must be emphasized that the uncertainty of the "15" value of formula (35) influences only the "0.00525" on the left hand side of Eq. (40), and this uncertainty does not seriously affect the restriction on $\bar{A}$.

If we are ready to use the η width quoted in (15), formula (38) gives

$$|g_0 + 2g_2| = 40\,[B(\eta \to \pi^\circ e^+ e^-)]^{1/2}, \tag{41}$$

and using the limit (4) we get

$$|g_0 + 2g_2| < 0{,}4. \tag{42}$$

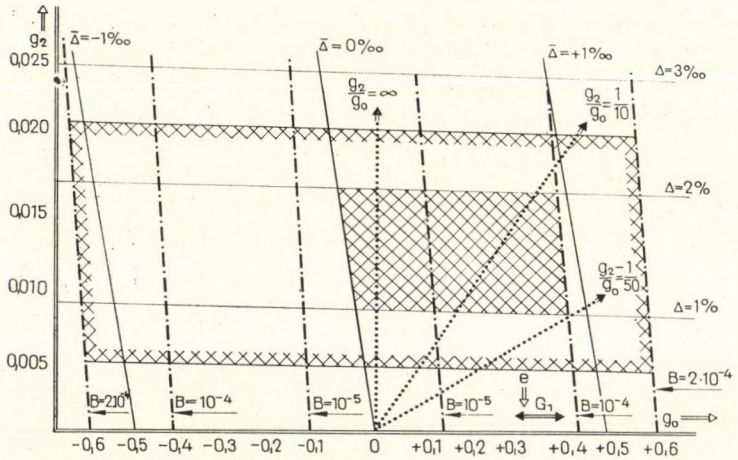

Fig. 5

It can now be seen that g_2 is restricted by the $\eta \to \pi^+\pi^0\pi^-$ result (6) due to formula (34); g_0 on the other hand is restricted by formula (42) much more severely than by the result (10) through formula (35). All these relations are visualized in Fig. 5. It can be seen that the experimental limits $1\% < \Delta < 2\%$ (one standard deviation), $0 < \bar{\Delta} < 1\%$ (one standard deviation) and $B < 10^{-4}$ allow essentially the following possibilities:

$$-0{,}1 < g_0 < +0{,}4\,; \qquad 0{,}008 < g_2 < 0{,}016\,. \tag{43}$$

If we use the more liberal limits $0.5\% < \Delta < 2.5\%$ (two standard deviations), $B < 2 \cdot 10^{-4}$ (the value given by BAZIN et al. [21] with 90% confidence) the possibilities are wider:*

$$-0{,}6 < g_0 < +0{,}6\,; \qquad 0{,}004 < g_2 < 0{,}02\,; \tag{44}$$

the experimental $\bar{\Delta}$ value does not give any further restriction if taken with two standard deviations.

Let us note at this point that in the $\eta \to \pi^0 e^+ e^-$ decay a $\Delta I = 1$ C violating $\eta\omega\pi$ coupling may interfere with the $\Delta I = 0$ and $\Delta I = 2$ couplings. The $\Delta I = 1$ type of C violation is discussed briefly in Appendix III.

We now turn to Table II, where the experimental values of the Δ, $\bar{\Delta}$, Δ_1, Δ_2 and Δ_3 asymmetry parameters are compared with those calculated for some specific choices of the g_0, g_2 coupling constants. For simplicity we have always chosen g_0 and g_2 to reproduce the observed mean value 1.52% of the Δ asymmetry parameter. It can be seen from Table II that the possibility $g_2 = 0$ contradicts both the $\eta \to \pi^0 e^+ e^-$ limit (given in parenthesis at the top of each column), and the measured value of the other asymmetry parameters. On the other hand, the cases $g_2 \neq 0$ are seen to be in agreement with the

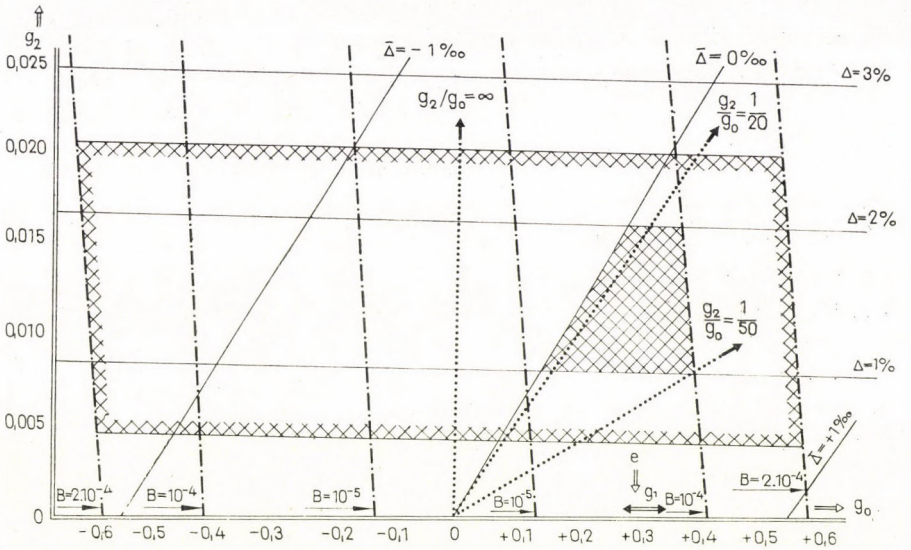

Fig. 6

$\eta \to \pi^+\pi^0\pi^-$ results, and up to $g_0 \simeq 30\ g_2$ also with the $\eta \to \pi^0 e^+ e^-$ limit. We have seen from Fig. 5 that if Δ is also allowed to change, then $g_0 \simeq 50\ g_2$ (one standard deviation for Δ) and even $g_0 \simeq 100\ g_2$ (two standard deviations for Δ) is possible. This means that the measured C violating effects in the $\eta \to \pi^+\pi^0\pi^-$ decays allow a pure $\Delta I = 2$ C violation which is millistrong indeed, being

$$g_2 : G_\varrho \cong 5 \cdot 10^{-3}. \tag{45}$$

In this case an $|\varepsilon| \simeq |\varepsilon'|$ solution would be expected in K_L° decays. A more interesting possibility is offered by the solution $g_0 \gg g_2$. In this case a comparatively strong isosymmetric C violation (g_0) is accompanied by a much weaker isospin asymmetric C violation (g_2). The latter may perhaps be interpreted as an electromagnetic correction to the isosymmetric C violation. In this case the $|\varepsilon| \gg |\varepsilon'|$ property of the K_L° decay can be explained by the dominance of the isosymmetric C violation. In the $\eta \to \pi^+\pi^0\pi^-$ decay the $\Delta I = 0$ transition is very much suppressed by the centrifugal barrier ($\bar{\Delta} \simeq 10^{-3}$ is predicted), and as a radiative correction the $\Delta I = 2$ transition appears in the right-left asymmetry $\Delta \simeq 10^{-2}$.

An interesting possibility (not yet understood) is provided by the following choice:

$$g_0 = G_1 = e = 0{,}3\,; \qquad \frac{2\,g_0}{137} \leqslant g_2 \leqslant \frac{10\,g_0}{137}\,.$$

* Let us mention that in the electromagnetic model of C violation [21] Equ. (4) gives the restriction $g_0 < 0.1e$ from which $\Delta < 0.17\%$ follows, in contradiction with the experimental result (6).

This reproduces the observed values of $\Gamma(\eta \to \pi^+\pi^\circ\pi^-)$ and of the five asymmetry parameters, respects the $\eta \to \pi^0 e^+ e^-$ limit and explains $|\varepsilon| \gg |\varepsilon'|$ at the same time.

The "big g_0" possibility implies come problems. First, one has to find out how $g_0 \simeq 0.1$ leads to $|\varepsilon| = 2 \cdot 10^{-3}$. Second, one has to check whether the big coupling constant is compatible with the restrictive upper limit $4 \cdot 10^{-23}$ cm of the neutron dipole moment or not. Third, one has to look for processes where a $g_0 \gtrsim 0.1$ coupling can manifest itself directly. E.g. $\Gamma(\varrho^+ \to \pi^+\eta)$: $\Gamma(\varrho) \gtrsim 10^{-3}$ is predicted. $N\bar{N}$ annihilation may also be sensitive to a big g_0. Up to now the lowest limit for g_0 is given by the $\eta \to \pi^0 e^+ e^-$ experiment. It would be desirable to improve the accuracy of this experiment, which offers the best method of testing the $\Delta I = 0$ model.

Finally let us formulate the important negative conclusion that the available experimental data on the $\eta \to \pi^+\pi^0\pi^-$ charge asymmetry and on the $\eta \to \pi^0 e^+ e^-$ limit do not contain any serious restriction for the $|\varepsilon| : |\varepsilon'|$ ratio.

Appendix I. The C allowed $\eta \to \pi^+\pi^\circ\pi^-$ decay

We shall now establish the numerical values of the real constants a and b in the C conserving matrix element A_1, which we rewrite from Eq. (19):

$$A_1 = \frac{a}{1 - i a_0 \varrho(s)} + b\left(\frac{s-u}{D(t)} + \frac{s-t}{D(u)}\right),$$
$$\varrho(s) = \frac{1}{2}\sqrt{s - 4\mu^2}, \quad D(s) = M^2 - s - i\frac{\Gamma(\varrho)\, q^3(s)}{M\sqrt{s}}. \tag{I.1}$$

The ratio $b : a$ will be determined by the experimentally established energy dependence of the $\eta \to \pi^+\pi^0\pi^-$ decay [17], and then $|a|$ will be found from the known $\Gamma(\eta \to \pi^+\pi^0\pi^-)$ width. The imaginary part of the $D(s)$ function is less then 3‰ of the real part, and will be neglected. For the $\pi\pi$ scattering length a_0 we shall use the numerical value $a_0\mu = 0.2$ [19]. The influence of the variation of a_0 on the asymmetry formulae will be discussed in Appendix II.

In [17] 7170 $\eta \to \pi^+\pi^0\pi^-$ decays were used to find the energy dependence of a purely phenomenological C conserving $\eta \to \pi^+\pi^0\pi^-$ matrix element M, defined as follows:

$$\overline{M} = 1 + \beta Y_0 + \gamma Y_0^2 + \delta Y_+ Y_-. \tag{I.2}$$

The dimensionless energy variables Y are related to the kinetic energies of the pions in the following manner:

$$Y_{+1,0,-} = \frac{3}{Q} T_{+,0,-} - 1. \tag{I.3}$$

In terms of the polar coordinates ϱ, Θ of the Dalitz plot the Y-s read:

$$Y_0 = \varrho \cos \Theta , \qquad Y_\pm = -\frac{1}{2} \varrho (\cos \Theta \pm \sqrt{3} \sin \Theta). \tag{I.4}$$

These variables are commonly used because it is expected that the non linear terms turn then up with small coefficients in the amplitude M.

The matrix element M is introduced in [17] only for the study of the energy dependence, and its normalization and overall phase are arbitrary. This means that our matrix element A_1 may be written as follows:

$$A_1 = hM , \tag{I.5}$$

where h is a complex number, independent of the energies of the pions. Let us put A_1 into the form (1.5). The second term in A_1 is easily expanded into power series of the Y-s:

$$\begin{aligned} \frac{s-u}{M^2-t} + \frac{s-t}{M^2-u} &= 2k \left(\frac{Y^- - Y^\circ}{1+kY^+} + \frac{Y^+ - Y^\circ}{1+kY^-} \right) = \\ &= -6kY_0 - 4k^2(Y_0^2 + 2Y_+ Y_-) + 0(k^3); \end{aligned} \tag{I.6}$$

[k is the centrifugal barrier parameter, defined in (29)]. In the first term of A_1 the function $q(s)$ cannot be conveniently expanded. A fairly good approximation to it is provided by a parabola, fitted to the points $q_{\max} = 1.12\ \mu$, $q_0 = 0.765\ \mu$ and $q_{\min} = 0$. These values corresponds to $Y_{0\min} = -1$, $Y_0 = 0$ and $Y_{0\max} = 0.875$, respectively. In this approximation we have

$$q(s) = q(Y_0) = (0{,}765 - 0{,}629\, Y_0 - 0{,}274\, Y_0^2)\, \mu . \tag{I.7}$$

Writing now

$$\frac{1}{1 - ia_0 q(s)} = \frac{1}{1 + a_0^2 q^2(s)} \left(1 + ia_0 q(s)\right), \tag{I.8}$$

and expanding the first factor into power series of Y and using (1.7) in the second, we find from (1.6) and (1.8) the desired expression for A_1

$$A_1 = \frac{a}{1 + a_0^2 q_0^2} (1 + ia_0 q_0)(1 + \beta Y_0 + \gamma Y_0^2 + \delta Y_+ Y_-) , \tag{I.9}$$

where

$$\beta = E - Fa_0\mu\,0{,}48 - iF\,0{,}629 - 6\frac{b}{a}k(1 - ia_0 q_0)\,,$$

$$\gamma = E^2 - EFa_0\mu\,0{,}48 - Fa_0\mu\,0{,}189 - \\ - iF(E\,0{,}629 + 0{,}247) - 4\frac{b}{a}k^2(1 - ia_0 q_0)\,,$$

$$\delta = -8\frac{b}{a}k^2(1 - ia_0 q_0)\,; \tag{I.10}$$

$$E \equiv \frac{1}{6}\,\frac{a_0^2 Q\mu}{1 + a_0^2 q_0^2}\,, \qquad F \equiv \frac{a_0\mu}{1 + a_0^2 q_0^2}\,, \\ q_0 \equiv q(Y_0 = 0) = \left(\frac{1}{4}m^2 - \frac{2}{3}mQ - \frac{3}{4}\mu 2\right)^{1/2} = 0{,}765\,\mu\,. \tag{I.11}$$

Let us now remind the reader that in [17] the authors used several working assumptions to find the coefficients β, γ, δ in (1.2). Namely, they tried to fit the experimental energy distribution with: a) $\gamma = \delta = 0$, β arbitrary complex number b) β, γ and δ arbitrary real numbers and c) β, γ and δ arbitrary complex numbers. It turned out that only the real part of $\beta \equiv \beta_1 + i\beta_2$ had a stable value in all cases:

$$\beta_1 = -0{,}55 \pm 0{,}02\,, \tag{I.12}$$

the mean values of all the other coefficients change violently from case to case, and owing to their very large statistical errors are always consistent with zero.

Taking into account this state of affairs, we shall use only the value of β_1 in our calculation. From (1.10) and (1.12) we have

$$E - Fa_0\mu\,0{,}48 - 6k\frac{a}{b} = \beta_1 = -0{,}55\,. \tag{I.13}$$

With $a_0\mu = 0.2$ we find

$$\frac{b}{a} = 1{,}65\,. \tag{I.14}$$

Introducing these values of a_0 and of b/a into (I.10) and then into (I.9), we arrive at the desired result:

$$A_1 = \frac{a}{1{,}023}(1 + i\,0{,}153)\,[1 + (-0{,}55 - i\,0{,}037)\,Y_0 + \\ + (-0{,}028 - i\,0{,}053)\,Y_0^2 + (-0{,}0416 + i\,0{,}0063)\,Y_+\,Y_-]\,. \tag{I.15}$$

We see that $|\beta_1|$ is much bigger than the other coefficients. This result is consistent with, but does not follow from the experimental analysis [17]. If we keep only $\beta = \beta_1 = -0.55$ and introduce the notation

$$\frac{G_1 e^{i\alpha}}{\left(1+\frac{1}{4}\beta^2\right)^{1/2}} = \frac{a}{1+a_0^2 q_0^2}(1+ia_0 q_0), \tag{I.16}$$

we arrive at the matrix element, given in Equ. (21). The value of $|a|$ i.e. the value of $|G_1|$, is then found from the $\Gamma(\eta \to \pi^+\pi^0\pi^-)$ width [see Equ. (16)]:

$$|a| = 0{,}31: \qquad |G_1| = 0{,}32. \tag{I.17}$$

Appendix II

The asymmetry parameters of the $\eta \to \pi^+\pi^\circ\pi^-$ decay in the quadratic approximation

In § 2 we neglected the imaginary part of the Y_0 term and all the quadratic energy terms of the C conserving matrix element (I.9). We have also chosen a value for the $\pi\pi$ scattering length ($a_0 = 0.2\ \mu^{-1}$) which, even if it is correct, may be too low to describe the $I = 0$ final state interaction in the whole physical domain $4\mu^2 \leqslant s \leqslant (m-\mu)^2 = 9\mu^2$ of the $\pi\pi$ system.

Below we shall investigate the effect of the neglected terms and of the variation of a_0 on the charge asymmetry parameters of the $\eta \to \pi^+\pi^0\pi^-$ decay. We shall see that no dramatic changes are produced if those terms are taken into account and if a_0 goes up to $1\mu^{-1}$. This justifies a posteriori the use of the simplified element (21). Admittedly, these results are model dependent. Nevertheless, they illustrate the influence of a possible 10% complexity and non-linearity of the C conserving matrix element on the calculated values of the charge asymmetry parameters.

The full amplitude of the $\eta \to \pi^+\pi^0\pi^-$ decay is given by the expression

$$A_1 + (A_0 + A_2) \equiv A_C + A_{Cv}, \tag{II.1}$$

where $A_1 = A_c$ is the C conserving matrix element (I.1) or (I.9), and $A_0 + A_2 = A_{Cv}$ is the C violating matrix element given in Equ. (30). Let us denote the real and the imaginary part of A by $A^{(1)}$ and $A^{(2)}$, respectively. We also introduce the cumulative notation δ for the asymmetry parameters Δ, $\bar{\Delta}$, Δ_1, Δ_2, Δ_3 defined in Equs. (8) (9) and (36). The general expression for δ is easily seen to be

$$\delta = -2\,\frac{\int_\delta d\Theta \int_0^{R(\Theta)} d\varrho\, \varrho\, A_C^{(2)}(\varrho,\Theta)\, A_{Cv}^{(2)}(\varrho,\Theta)}{\int_{S_\delta} d\Theta \int_0^{R(\Theta)} d\varrho\, \varrho\left(|A_C(\varrho,\Theta)|^2 + |A_{Cv}(\varrho,\Theta)|^2\right)}, \tag{II.2}$$

where the symbols $\int_\delta$ and $\int_{S_\delta}$ mean:

$$\int_\Delta = \int_{S_\Delta} = \int_0^\pi ,$$
$$\int_{\bar{\Delta}} = \int_0^{\pi/3} - \int_{\pi/3}^{2\pi/\tau} \int + \int_{2\pi/3}^{\pi} , \quad \int_{S_{\bar{\Delta}}} = \int_0^\pi , \tag{II.3}$$

and

$$\int_{\Delta_j} = \int_{S_{\Delta_j}} = \int_{\pi/3(j-1)}^{\pi/3(j)} , \quad j = 1, 2, 3 .$$

Let us first discuss the integral

$$\int_0^{R(\Theta)} d\varrho \, A_C^{(2)}(\varrho, \Theta) \, A_{Cv}^{(2)}(\varrho, \Theta) .$$

We again neglect the very small contribution of the ϱ width. Then we find:

$$A_C^{(2)} = \mathrm{Im} \frac{a}{1 - i a_0 q} = a \frac{a_0 q}{1 + a_0^2 q^2} =$$
$$= a \frac{a_0 q_0}{1 + a_0 q_0} (1 + c_1 Y_0 + c_2 Y_0^2 + \ldots), \tag{II.4}$$

where

$$c_1 = E - 0{,}82 ,$$
$$c_2 = E^2 - 0{,}82\, E - 0{,}357 . \tag{II.5}$$

For the definition of E and q_0 see Equ. (I.11).

Let us remark that the dependence of c_1 and c_2 on a_0 is weak. Indeed,

if $a_0\mu = 0.2$, then $c_1 = -0.794$, $c_2 = -0.377$,

if $a_0\mu = 0.6$, then $c_1 = -0.623$, $c_2 = -0.46$,

and if $a_0\mu = 1$, then $c_1 = -0.4$, $c_2 = -0.525$.

Now the ratio of the contribution of the C violating coupling constants g_0 and g_2 to the asymmetry parameters is determined by the product

$$(1 + c_1 Y_0 + c_2 Y_0^2) A_{Cv}^{(2)}, \tag{II.6}$$

and we may expect that the ratio $g_2 : g_0$ is only weakly influenced by a 500% change in a_0.

The coefficients c_1 and c_2 can also be written in the form

$$c_1 = \beta_1 + \frac{\beta_2}{a_0 q_0} , \qquad c_2 = \gamma_1 + \frac{\gamma_2}{a_0 q_0} \tag{II.7}$$

with $\beta = \beta_1 + i\beta_2$, $\gamma = \gamma_1 + i\gamma_2$ defined in Appendix I. The linear approximation used in § 2 with $a_0\mu = 0.2$ corresponds to the substitution of $c_1 = -0.55$ instead of $c_1 = -0.794$ and of $c_2 = 0$ instead of $c_2 = -0.377$.

From (II.4) and (30) we find in the $R(\Theta) = 1$ approximation*

$$\int_0^1 d_{QQ} A_C^{(2)} A_{Cv}^{(2)} = 6\sqrt{3}\, aG_e \frac{a_0 q_0}{1 + a_0 q_0} \sum_{n-1}^{5} u_n \sin n\Theta, \tag{II.8}$$

where

$$\begin{aligned}
u_1 &= g_2\left[\frac{k}{3} + \frac{k^3}{5} - \frac{a_1 k^2}{10}\right] + g_0 \frac{c_2 k^3}{28}, \\
u_2 &= g_2\left[-\frac{k^2}{4} + \frac{1}{2} e_1 \left(\frac{k}{4} + \frac{k^3}{6}\right) - \frac{c_2 k^2}{12}\right] + g_0 \frac{c_1 k^3}{12}, \\
u_3 &= g_2\left[-\frac{c_1 k^2}{10} + \frac{1}{2} c_2 \left(\frac{k}{5} + \frac{k^3}{7}\right)\right] + g_0\left[\frac{k^3}{5} + \frac{c_2 k^3}{14}\right], \\
u_4 &= -g_2 \frac{c_2 k^2}{24} + g_0 \frac{c_1 k^3}{12}, \\
u_5 &= g_0 \frac{c_2 k^3}{28}.
\end{aligned} \tag{II.9}$$

Let us now look at the denominator in Equ. (II.2). The contribution of $|A_{Cv}|^2$ is very small in comparison with that of $|A_C|^2$, and can be neglected. This means that the denominator does not influence the ratio of the contribution of g_0 and g_2 to the asymmetry parameters, but only modifies their common multiplicative factor. This allows us to use the linear approximation for A_C in the integral of the denominator. A straightforward calculation leads to the formulae

$$\begin{aligned}
\Delta &= -12\sqrt{3}\, a_0 q_0 \frac{G_e}{a} \frac{2u_1 + \frac{2}{3}u_3 + \frac{2}{5}u_5}{\frac{\pi}{2}\left(1 + \frac{\beta_1^2}{4}\right)}, \\
\bar{\Delta} &= -12\sqrt{3}\, a_0 q_0 \frac{G_e}{a} \frac{2u_3}{\frac{\pi}{2}\left(1 + \frac{\beta_1^2}{4}\right)}, \\
\Delta_1 &= -12\sqrt{3}\, a_0 q_0 \frac{G_e}{a} \frac{\frac{1}{2}u_1 + \frac{3}{4}u_2 + \frac{2}{3}u_3 - \frac{3}{8}u_4 + \frac{1}{10}u_5}{\frac{\pi}{6}\left(1 + \frac{\beta_1^2}{4}\right) + \frac{\beta_1}{\sqrt{3}} + \frac{\beta_1^2\sqrt{3}}{32}},
\end{aligned} \tag{II.10}$$

* See footnote on page 92.

$$\Delta_2 = -12\sqrt{3}\ a_0 q_0 \frac{G_\varrho}{a} \frac{u_1 - \frac{2}{3}u_3 + \frac{1}{5}u_5}{\frac{\pi}{6}\left(1+\frac{\beta^2}{4}\right) - \frac{\beta_1^2\sqrt{3}}{16}},$$

$$\Delta_3 = -12\sqrt{3}\ a_0 q_0 \frac{G_\varrho}{a} \frac{\frac{1}{2}u_1 - \frac{3}{4}u_2 + \frac{2}{3}u_3 - \frac{3}{8}u_4 + \frac{1}{10}u_5}{\frac{\pi}{6}\left(1+\frac{\beta_1^2}{4}\right) - \frac{\beta_1}{\sqrt{3}} + \frac{\beta_1^2\sqrt{3}}{32}}.$$

Let us denote by $\delta^{(I)}$ an asymmetry parameter in the linear approximation ($c_1 = -0.55$, $c_2 = 0$) and the same parameter in the quadratic approximation by $\delta^{(q)}$. With $a_0\mu = 0.2$ we get the following numerical results (if $a_0 G_\varrho/a < 0$):

$$\begin{aligned}
\Delta^{(l)} &= 7\cdot 10^{-4}[g_0 + 1740\, g_2], & \Delta^{(q)} &= 7\cdot 10^{-4}[0{,}62\, g_0 + 1720\, g_2],\\
\bar{\Delta}^{(l)} &= 7\cdot 10^{-4}[3\, g_0 + 15{,}3\, g_2], & \bar{\Delta}^{(q)} &= 7\cdot 10^{-4}[2{,}6\, g_0 - 47{,}1\, g_2],\\
\Delta_1^{(l)} &= 7\cdot 10^{-4}[4\, g_0 + 1760\, g_2], & \Delta_1^{(q)} &= 7\cdot 10^{-4}[2{,}25\, g_0 + 1180\, g_2],\\
\Delta_2^{(l)} &= 7\cdot 10^{-4}[-3{,}2\, g_0 + 2760\, g_2], & \Delta_2^{(q)} &= 7\cdot 10^{-4}[-3{,}2\, g_0 + 2640\, g_2],\\
\Delta_3^{(l)} &= 7\cdot 10^{-4}[2{,}6\, g_0 + 1100\, g_2], & \Delta_3^{(q)} &= 7\cdot 10^{-4}[2{,}16\, g_0 + 1160\, g_2];
\end{aligned} \tag{II.11}$$

$$\left(7\cdot 10^{-4} = -12\sqrt{3}\ a_0 q_0 \frac{G_\varrho}{a} \frac{4}{\pi\left(1+\frac{\beta_1^2}{4}\right)} \frac{k^3}{15}\right).$$

We see (II.11) and also from Table IV and Fig. 6, that the quadratic approximation — perhaps only fortuitously — makes the agreement with the experiment better and favours the big $g_0 : g_2$ ratio, if we respect the experimental indication sign $\bar{\Delta} = \text{sign}\ \Delta$.

Appendix III
The $\Delta I = 1$ way of C violation

In clarifying the isospin properties of the C violating millistrong Hamiltonian undoubtedly the $\eta \to \pi^+\pi^0\pi^-$ asymmetry is the most convenient tool, because the C violation is competing only with an I forbidden C conserving transition. The C violation is, however, restricted to the $\Delta I = 0$ and $\Delta I = 2$ channels. To learn something about the other isospin possibilities $\Delta I = 1$ and 3 is a much more difficult task. In principle any charge asymmetry in the $\omega \to \pi^+\pi^0\pi^-$ decay would prove a C violation with $\Delta I = 1$ or 3, but the C

violation is competing here with a C conserving strong interaction ($\Delta I = 0$), so the predicted value of the asymmetry is rather small. The centrifugal situation effects are more favourable than in the $\omega \to \pi^+\pi^0\pi^-$ decay, but owing to the high Q value this help is not too effective. The larger ω width makes the elimination of the background more difficult. So one cannot expect any information from ω before we collect statistics about 100 or 1000 times bigger than now available.

The $\Delta I = 3$ way of C violation has already been analyzed in detail [6]. That possibility does not look very interesting because it predicts $|\varepsilon| \ll |\varepsilon'|$, and this is contradicted by the $K_L^\circ \to \pi^\pm l^\mp \nu$ asymmetry experiments. We shall now discuss the $\Delta I = 1$ case to some extent.

CP violation with CPT symmetry means a violation of the time reversal invariance. The upper limit on the violation of the detailed balance is $4 \cdot 10^{-3}$ in the nuclear reactions $^{24}\mathrm{Mg(d, p)}^{25}\mathrm{Mg}$ and $^{24}\mathrm{Mg}(\alpha, \mathrm{p})^{27}\mathrm{Al}$ [22]. This is not enough to prove or exclude the millistrong C violation in the reaction channel $\Delta I=0$, because the C violation is competing here with the isosymmetric strong interaction. A more favourable situation may be expected in those nuclear reactions which are pure $\Delta I=1$ transitions. (The C violation is competing here with a coupling $Z^2/137$). The main difficulty in observing the reversibility of $\Delta I = 1$ transitions is the follwing: the isospin in the ground state of stable $I_3 = 0$ nuclei is always $I = 0$, so it looks difficult to find a $0 \rightleftarrows 1$ transition, which can be observed in both directions with sufficient accuracy. (The nuclear reaction experiments are, on the other hand, sensitive only to long range interactions.)

Possibly the best way to put an upper limit on the C violating vertex with $\Delta I=1$ is just the $\eta = \pi^0 e^+ e^-$ decay. A possible way for this transition is through the ω pole (Fig. 4, with ω instead of the ϱ meson).

By assuming a C violation of the type

$$H_1' = g_1 \omega_\mu (\pi^\circ \partial_\mu \eta - \eta \partial_\mu \pi^\circ),$$

we arrive at the following form of the $\eta \to \pi^0 e^+ e^-$ width:

$$\Gamma(\eta \to \pi^\circ e^+ e^-) = 0{,}47 \text{ keV} [(g_0 + 2 g_2) f_\varrho + g_1 f_\omega]^2. \qquad \text{(III. 1)}$$

Here f_ϱ is the $\varrho - \gamma$ coupling constant, which is usually taken to be $f_\varrho = eG_\varrho = 0.05$. f_ω is the $\omega - \gamma$ coupling, which is about 0.1 [20].

The upper limit (4) now gives the restriction

$$\left| g_0 + 2 g_2 + \frac{f_\omega}{f_\varrho} g_1 \right| < 0{,}4. \qquad \text{(III. 2)}$$

We now have two possibilities: If $g_0 = 0$, g_2 and g_1 may be expected in the "millistrong" range 10^{-2}— 10^{-3} and consequently, (III. 2) is fulfilled. If g_0 is the dominating coupling constant of C violation and g_1, g_2 are only "radiative corrections", (III. 2) is essentially a limitation on g_0, and the g_2, g_1 terms are negligible.

REFERENCES

1. Proceedings of the International Conference on High Energy Physics, Vienna, 1968.
2. J. Prentki and M. Veltman, Physics Letters, **15**, 88, 1965.
3. N. Cabibbo, Phys. Rev. Letters, **14**, 965, 1965.
4. Y. Fujii and G. Marx, Physics Letters, **17**, 75, 1965.
5. M. Veltman, Physics Letters, **24B**, 587, 1967.
6. G. Marx and P. Surányi, Nuovo Cimento, **54**, 856, 1968.
7. S. Glashow, Phys. Letters, **14**, 35, 1964.
8. T. N. Truong, Phys. Rev. Letters, **11**, 358, 1964.
9. L. Wolfenstein, Nuovo Cimento, **42A**, 17, 1966.
10. J. Bernstein, G. Feinberg and T. D. Lee, Phys. Rev., **139B**, 1650, 1965; T. D. Lee, Phys. Rev., **140B**, 959, 1965; **140B**, 967, 1965.
11. G. Feinberg, Phys. Rev., **140B**, 1402, 1965. P. Pabu and M. Suzuki, Phys. Rev., **162**, 1359, 1967.
12. B. A. Abruzov and A. T. Filippov, Physics Letters, **20**, 537, 1966.
13. Review of Particle Properties, UCRL-8030 preprint (August 1968).
14. M. Cormley, E. Hyman, W. Lee, T. Nash, J. Peoples, C. Schultz and S. Stein, Phys. Rev. Letters, **21**, 402, 1968.
15. H. Yuta and S. Okubo, Phys. Rev. Letters, **21**, 781, 1968.
16. M. Nauenberg, Physics Letters, **17**, 329, 1965.
17. A. M. Cnops, G. Finocchiaro, P. Mittner, J. D. Dufey, B. Gobbi, M. A. Pouchon and A. Müller, Physics Letters, **27B**, 113, 1968.
18. B. Barrett, M. Jacob, M. Nauenberg, T. N. Truong, Phys. Rev., **141**, 1342, 196
19. S. Weinberg, review talk in [1].
20. G. Marx, Phys. Rev., **140**, 1068, 1965.
21. M. J. Bazin, A. T. Goshaw, A. R. Zacher and C. R. Sun, Phys. Rev. Letters, **20**, 895, 1968.
22. D. Bodanski et al., Phys. Rev. Letters, **17**, 589, 1966.

МИЛЛИСИЛЬНОЕ НАРУШЕНИЕ С СИММЕТРИИ И РАСПАД η МЕЗОНА

А. ФРЕНКЕЛЬ и Г. МАРКС

Резюме

Рассматриваются изоспиновые свойства (предполагаемого) миллисильного нарушения С чётности. Обсуждаются правила отбора с $\Delta I = 0$ и $\Delta I = 2$ для $\eta \to \pi^+\pi^\circ\pi^-$ и для $\eta \to \pi^\circ e^+ e^-$ распадов. Если наблюдуаемая зарядовая асимметрия в $\eta \to \pi^+\pi^\circ\pi^-$ распаде возникает за счёт нарушения С чётности, то в конечном состоянии 3π, нарушающем С, преобладает компонент с $I = 2$, порожденный переходом $\pi 1 = 2$ с константной связи $g_2 \simeq 10^{-2}$. Так как состояние 3π с $I = 0$ оказывается очень сильно подавленным центрифугальным барьером, связь с $\Delta I = 0$ может быть много сильнее, например $g_0 > 10^{-1}$, ограниченной лишь отрицательным результатом экспериментов по $\pi \to \pi^\circ e^+ e^-$ распаду. Поэтому преобладание перехода с $\Delta I = 0$ в нарушающих С чётность распадах K° мезона, выраженное соотношением $|\varepsilon| \gg |\varepsilon'|$, отнюдь не противоречит наблюдаемому преобладанию перехода с $\Delta I = 2$ в $\eta \to \pi^+\pi^\circ\pi^-$ асимметрии. В работе подчёркивается важность выполнения более точных экспериментов.

Acta Physica Academiae Scientiarum Hungaricae, Tomus 27, pp. 111—129 (1969)

ON THE THEORY OF FERMION DENSITY OPERATORS. I.*

THE DEFINITION OF THE ONE-PARTICLE STATES AND CLUSTER EXPANSIONS OF THE DENSITY OPERATORS

By

J. I. HORVÁTH and I. K. GYÉMÁNT

DEPARTMENT OF THEORETICAL PHYSICS, JÓZSEF ATTILA UNIVERSITY, SZEGED

(Received 13. I. 1969)

After the definitions of density operators (§2), the concept of single particle states is defined via the pure states of the first order reduced density operators (§3). Then the concepts of the NSO's and NSG's, as well as expansions in their terms are treated (§4). Furthermore, KIANG's variational approach is discussed and improved (§5). Finally, cluster expansions of the N-particle density operators are obtained in terms of the first order reduced density operators in various cases.

§ 1. Introduction

The independent particle model is the most familiar approximation for treating many-particle systems. It was originally suggested by its validity for perfect systems with completely separable Hamiltonian. However, for real many-particle systems where owing to the interactions of the particles the collective behaviour of the system is more dominant and characteristic it is clear that the independent particle model loses its validity. Nevertheless it can be accepted if the "bare" particles and the concept of the "bare particle states" are replaced by way of some kind of renormalization processes (such as those of Hartree—Fock or Brueckner) by the so-called "dressed" particles or "dressed particle states". But, in these very familiar cases too, it is a priori not quite evident that (a) individual or single particle states exist at all; (b) how they are related to the classical concept of particles; and (c) in which way the correlation problems of the particles have to be formulated.

Bearing in mind this antagonism between the fundamental ideas of the collective and independent particle models, the remarkable successes of the independent particle models mostly based on the methods of pseudo-potentials — more recently summarized and improved by Professor GOMBÁS in his excellent monograph [1] — suggest once more a reinvestigation of its theoretical background in terms of the new methods that have appeared recently in the theory of many-body (fermion) systems.

The methods mentioned — notably, the methods of density operators and cluster expansions including the most important information about the

* Dedicated to Prof. P. GOMBÁS on his 60th birthday.

collective behaviours of the systems — are, strictly speaking, not new at all, but interest has again focused on them and they have helped in making remarkable progress in this important field.

It can be hoped that they will be of help also in replacing the a posteriori justification of the validity of the independent particle model by a direct one. Thus the aim of the present series of papers is to simplify the conceptual background of the problems investigated, to find a compromise in certain hotly discussed questions and to obtain a clear insight into the ideas involved. Improved mathematical tools are used which are related to simple and natural physical concepts and some relationships are brought out which may be useful in making further improvements.

In this first part after the definitions of the density operators and the brief summary of their fundamental properties needed in the following argumentation (§2), the concept of single particle states is defined via the pure states of the first order reduced density operator (§3). Then, the concepts of the natural spin orbitals and geminals, as well as expansions in their terms are treated (§4), furthermore KIANG's variational approach is discussed and improved (§5). Finally, cluster expansions of the N-particle density operator are obtained in terms of the first order reduced density operators in different cases.

§ 2. The definitions of density operators and their most fundamental properties

It seems that in looking for a consistent method of finding an approximation method in terms of particle states one has to use the method of density operators, where in the case of Hamiltonians with two-body interactions the expectation values of any important observable can be obtained in terms of the so-called one and two particle reduced density operators alone.

The *density* or as it is sometimes also called: *statistical operator* and in a certain representation mostly in co-ordinate representation the *density matrix*, respectively, were introduced by VON NEUMANN [2, 3] and by DIRAC [4] to describe statistical concepts in quantum physics. Their first version is more common in the case of statistical mechanics, i.e., in the case of many, practically infinite degrees of freedom; the second version rather in quantum chemistry, i.e., for atomic and molecular systems with limited degrees of freedom.

The theory of density operators and its applications has been investigated in detail from very different aspects by several authors. The existence of general references [5—8], and of more recent special investigations which have been focused on the problems: (a) how far and under which condition the wave function of the many particle systems can be replaced by the one and two particle density matrices alone [9—12]; (b) what kind of collective problems

of the system's behaviour can be explained [13—19]; (c) in what manner the usual variational method could be reformulated in terms of density matrices [20], etc., makes any extended discussion of the previous results unnecessary and we recall only the salient facts partly in terms of new arguments.

Having in mind atomic and molecular systems with limited degrees of freedom we start with DIRAC's definition of the density operator. Since in this case the number of electrons does not change during the discussion it may be specified implicitly and for a system of N particles in a state with the normalized wave function Ψ, the density matrix $\mathbf{D}$ of the system and the pth order reduced density matrix $\mathbf{D}_p$ — the so-called p-matrix —, respectively, may be regarded as an integral operator with kernels:

$$D(x_1, \ldots, x_N; x'_1, \ldots, x'_N) \equiv \Psi(x_1, \ldots, x_N)\, \Psi^*(x'_1, \ldots, x'_N) \tag{2.1}$$

and

$$D_p(x_1, \ldots, x_p; x'_1, \ldots, x'_p) = \\ = \int dx_{p+1} \ldots dx_N\, \Psi(x_1, \ldots, x_N)\, \Psi^*(x'_1, \ldots, x'_p, x_{p+1}, \ldots, x_N), \tag{2.2}$$

where each co-ordinate x_i of the "configurational space" is a combination of the space co-ordinates $\vec{r}_i$ and spin-coordinate s_i of the particles considered. The integration with respect to the Lebesgue—Stieltjes measure $dx_{p+1} \ldots dx_N$ indicates an integration over the co-ordinates $\vec{r}_{p+1}, \ldots, \vec{r}_N$ and a summation over the dichotomic spin-variables $s_{p+1}, \ldots, s_N$ in the case of spin-half particles (e.g., for systems of electrons).

Independently of any particular representation let us characterize a definite state of the system by the normalized $|\Psi\rangle$ being an element of the abstract Hilbert space $\mathscr{H}$. This means that the state vector in coordinate representation introduced above is an element

$$\Psi(x_1, \ldots, x_N) = \langle x_N, \ldots, x_1 | \Psi \rangle \tag{2.3}$$

of the Hilbert space $\tilde{\mathscr{H}}$ of the square integrable functions over the N-particle configuration space $\{x_1, \ldots, x_N\}$.

In a definite state — i.e., using von Neumann's terms: in a pure state — of the system considered, the density operator $\mathbf{D}$ is the projector of the corresponding subspace $\mathscr{H}^{(N)}$ of the abstract Hilbert space $\mathscr{H}$, i.e.,

$$\mathbf{D} = |\Psi\rangle\langle\Psi| \tag{2.4}$$

being an idempotent operator

$$\mathbf{D}^2 = \mathbf{D}, \tag{2.5}$$

and the expectation value of any dynamical quantity **A** can be obtained as

$$\langle \mathbf{A} \rangle = tr\{\mathbf{AD}\}, \tag{2.6}$$

where $tr\mathbf{M}$ indicates the trace (i.e., the sum of the diagonal elements) of a matrix **M**.

The most important properties of **D** can be summarized as follows:

(1) The condition that $\langle \mathbf{A} \rangle$ has to be real for every Hermitian operator **A**, requires **D** to be Hermitian too,

$$\mathbf{D} = \mathbf{D}^{+}. \tag{2.7}$$

(2) Keeping in mind that the unit operator **1** has the mean value 1, requires

$$tr\{\mathbf{D}\} = 1. \tag{2.8}$$

(3) The condition that every operator with non-negative spectrum has non-negative mean value, requires **D** to be positive definite, i.e., every diagonal element $\langle n|\mathbf{D}|n\rangle$ must be non-negative

$$\langle n|\,\mathbf{D}\,|n\rangle \geqq 0\,. \tag{2.9}$$

(4) Owing to Equs. (2.8) and (2.9) it is easy to prove that

$$tr\{\mathbf{D}^2\} \leqq 1\,, \tag{2.10}$$

which limits the value of every single element of the density matrix. The equality holds only for pure states.

§ 3. The definition of single particle states

In order to find a natural definition of single particle states of an N-particle system we use the concept of pure states which are not only of importance in density matrix theory, but also are adequate to the classical ideas in the background of the independent particle model. We recall the argument which COLEMAN [11] used to prove that it is sufficient to deal with pure states to solve the N-representability problem for a p-matrix.

The set of all N-particle density matrices $\{\mathbf{D}_N\}$ is identical with the set $\mathcal{P}_N$ of positive Hermitian operators of unit trace on the Hilbert space of antisymmetric N-particle functions. The set $\mathcal{P}_N$ is convex and its extreme elements are the pure states in the case of which $\mathbf{D}_N^{(i)}$ is idempotent. The N-particle state introduced above indicated by a single state vector $|\Psi\rangle$ is, of course, a

pure state and the corresponding N-particle density operator $\mathbf{D}$ is idempotent. Therefore, $\mathbf{D}$ is an extreme element of the set $\mathscr{P}_N = \{\mathbf{D}_N\}$.

For fermions, the set $\mathscr{P}_N$ consists of all positive Hermitian operators of unit trace on the space of antisymmetric p-particle functions. Whereas, the set of all $\mathbf{D}_N$ coincides with $\mathscr{P}_N$, the set of $\{\mathbf{D}_p\}$ is a proper subset of $\mathscr{P}_p$ which we denote by $\mathscr{P}_p^{(N)}$. It consists of those positive operators of unit trace on the Hilbert space of the antisymmetric p-particle functions which are p-matrices derived from the N-particle pure state with the state vector $|\Psi\rangle$. Of course, $\mathscr{P}_p^{(N)}$ is a convex subset of $\mathscr{P}_p$, too, and its extreme elements are the p-matrices $\mathbf{D}_p^{(i)}$ being also idempotent and they indicate pure states, as well. In accordance with Krein—Milman's theorem which asserts that a compact convex set is determined by its extreme elements, our p-matrix $\mathbf{D}_p$ can be set up in terms of the pure states p-matrices $\mathbf{D}_p^{(i)}$ in the form

$$\mathbf{D}_p = \sum_i w_i^p \mathbf{D}_p^{(i)}, \qquad \left(\sum_i w_i^p = 1\right) \tag{3.1}$$

where w_i^p-s are again the statistical weights of the pure states. This means that the $\mathbf{D}_p$ is, in general, no longer in a pure state, $||\mathbf{D}_p^2|| \leq ||\mathbf{D}_p||$, but is in a mixed state being a superposition of pure states $\mathbf{D}_{pi}^{(}$.

For if $p = 1$, $\mathbf{D}_1$ means the one-particle reduced density operator which is in a mixed state of the one-particle pure states

$$\mathbf{D}_1 = \sum_i \lambda_i \mathbf{D}_1^{(i)}, \qquad (\Sigma\lambda_i = 1). \tag{3.2}$$

Bearing in mind that $\mathbf{D}_1$ and consequently also $\mathbf{D}_1^{(i)}$ - s corresponding to pure states, are deduced from the N-particle density operator $\mathbf{D}$, they include all the information which follows from the collective behaviour of the system considered. Equ. (3.2) is nothing else but the spectral resolution of the operator $\mathbf{D}_1$ and the operators $\mathbf{D}_1^{(i)}$ are the projectors of its eigenstates which are usually denoted as the *natural spin-orbitals*, NSO's [9].

The NSO's as the eigenstates of the one-particle reduced density matrix are connected, on the one hand, to a single particle degree of freedom of the N-particle systems; on the other, they are uniquely determined by Krein—Milman's theorem. In fact, they can be interpreted as the single particle states of the N-particle system looked for, including all information about the collective behaviour of the real system needed.

§ 4. Natural expansions of the state vector

Suppose that we have an N-particle quantum system in a bound state $|\Psi\rangle$, with norm unity. If the system is imagined to consist of two parts each with p and $N-p$ particles, having respectively $\mathscr{H}_P$ and $\mathscr{H}_Q$ as their complete

state vector spaces, then the original abstract Hilbert space can be formed as a complete tensor product space, $\mathscr{H} = \mathscr{H}_P \otimes \mathscr{H}_Q$. I.e., if $|P\rangle \in \mathscr{H}_P$ and $|Q\rangle \in \mathscr{H}_Q$ are arbitrary unit vectors, and $\{|P_i\rangle\}$ and $\{|Q_j\rangle\}$ are complete orthonormal bases in $\mathscr{H}_P$ and $\mathscr{H}_Q$, respectively, $\{|P_i Q_j\rangle\}$ is a complete orthonormal basis of $\mathscr{H}$ with $|P_i Q_j\rangle \equiv |P_j\rangle|Q_i\rangle = |Q_j\rangle|P_i\rangle$, so that, e.g.,

$$|\Psi\rangle = \sum_{ij} c[P_i;\, Q_j]\,|P_i\,Q_j\rangle \quad (c[P_i;Q_j] = \langle Q_j\,P_i\,|\Psi\rangle), \tag{4.1}$$

where it seems desirable to emphasize by the notation that the coefficients $c[P_i;Q_j]$ are functionals of the state vectors $|P_i\rangle$ and $|Q_j\rangle$, respectively.

Let us consider the mappings $\mathscr{H}_Q \to \mathscr{H}_P$ and $\mathscr{H}_P \to \mathscr{H}_Q$, realized by

$$\begin{aligned} \langle Q_i|\Psi\rangle &= \sum_j a[Q_i;\; P_j]|P_j\rangle, \\ \langle P_j|\Psi\rangle &= \sum_i b[P_j;Q_i]\,|Q_i\rangle, \end{aligned} \tag{4.2}$$

with

$$a[Q_i;P_j] = \langle Q_i\,P_j|\Psi\rangle\,, \quad b[P_j;Q_i] = \langle P_j\,Q_i\,|\Psi\rangle\,. \tag{4.3}$$

It is easy to check the theorems:

Theorem 1. The coefficients $a[Q_i;\, P_j]$ and $b[P_i;\, Q_j]$ generating the mappings (4.2) $\mathscr{H}_Q$ into $\mathscr{H}_P$ and $\mathscr{H}_P$ into $\mathscr{H}_Q$, respectively, are

(a) symmetrical anti-linear functionals of $|Q_i\rangle$ and $|P_j\rangle$:

$$a[Q_i;P_j] = a[P_j;Q_i]\,; \qquad b[P_j;Q_i] = b[Q_i;P_j]\,, \tag{4.4}$$

(b) they are equivalent and the relation

$$a[Q_i;P_j] = b[P_j;Q_i] \tag{4.5}$$

remains valid for any linear combination of the vectors $|Q_i\rangle$ and $|P_j\rangle$, e.g.,

$$a[\alpha_1|Q_1\rangle + \alpha_2\,|Q_2\rangle;\; \beta_1\,|P_1\rangle + \beta_2\,|P_2\rangle] = b[\beta_1\,|P_1\rangle + \beta_2\,|P_2\rangle;\, \alpha_1\,|Q_1\rangle + \alpha_2\,|Q_2\rangle].$$

Of course, the relations

$$\sum_i |Q_i\rangle\langle Q_i| \equiv \mathbf{I}_Q\,, \qquad \sum_j |P_j\rangle\langle P_j| \equiv \mathbf{I}_P \tag{4.6}$$

are the resolution of the unit operators in $\mathscr{H}_Q$ and $\mathscr{H}_P$, respectively.

Let us introduce the reduced operators

$$\mathbf{D}_P \overset{\text{def}}{=} \sum_i \langle Q_i|\Psi\rangle\langle\Psi|Q_i\rangle = \sum_{jj'} |P_j\rangle\, \Lambda_{jj'}^{(P)}\, \langle P_{j'}| \tag{4.7}$$

with

$$\Lambda_{jj'}^{(P)} \equiv \sum_i a[Q_i; P_j]\, a^*[Q_i; P_{j'}]\,; \tag{4.8}$$

and

$$\mathbf{D}_Q \overset{\text{def}}{\equiv} \sum_j \langle P_j|\Psi\rangle\langle\Psi|P_j\rangle = \sum_{ii'} |Q_i\rangle\, \Lambda_{ii'}^{(Q)}\, \langle Q_{i'}| \tag{4.9}$$

with

$$\Lambda_{ii'}^{(Q)} \equiv \sum_j b[P_j; Q_i]\, b^*[P_j; Q_{i'}] = \sum_j a[Q_i; P_j]\, a^*[Q_{i'}; P_j]\,, \tag{4.10}$$

respectively, where the relations (4.2) and (4.5) were used. On the one hand, owing to the Hermitian character of the matrices $\Lambda_{jj'}^{(P)}$ and $\Lambda_{ii'}^{(Q)}$

$$\Lambda_{jj'}^{(P)*} = \Lambda_{j'j}^{(P)} \quad \text{and} \quad \Lambda_{ii'}^{(Q)*} = \Lambda_{i'i}^{(Q)}, \tag{4.11}$$

i.e., their diagonal elements are real. On the other hand owing to the fact that the norm of the state vector $|\Psi\rangle$ is unity:

$$\langle\Psi|\Psi\rangle = \sum_i \langle\Psi|Q_i\rangle\langle Q_i|\Psi\rangle = \sum_{ij} |a[Q_i; P_j]|^2 = 1\,, \tag{4.12}$$

both Hermitian operators $\mathbf{D}_P$ and $\mathbf{D}_Q$ have unit traces:

$$tr\{\mathbf{D}_P\} = 1 \quad \text{and} \quad tr\{\mathbf{D}_Q\} = 1\,. \tag{4.13}$$

Theorem 2. There exist orthonormal basis systems, $\{|q_i\rangle\}$ in $\mathscr{H}_Q$ and $\{|p_i\rangle\}$ in $\mathscr{H}_P$, respectively, such that

$$a[q_i; p_j] = c_i\, \delta_{ij} \tag{4.14}$$

and the mappings (4.2) may be replaced by

$$\begin{aligned} &\langle q_i|\Psi\rangle = c_i|p_i\rangle\,, \\ &\langle p_i|\Psi\rangle = c_i|q_i\rangle\,, \end{aligned} \qquad \text{with } c_i = \langle q_i\, p_i|\Psi\rangle\,. \tag{4.15}$$

Indeed, for an arbitrary orthonormal basis system $\{|p_i\rangle\} \in \mathscr{H}_p$ the state vector $|\Psi\rangle \in \mathscr{H}$ can be expanded in the form

$$|\Psi\rangle = \sum_{ij} a[p_i; Q_j]|p_i\, Q_j\rangle = \sum_i \Big(\sum_j a[p_i; Q_j]|Q_j\rangle\Big)|p_i\rangle \equiv \sum_i \tilde{c}_i\, |\tilde{q}_i\rangle|p_i\rangle\,.$$

The vectors $|\tilde{q}_i\rangle$ of the set $\{|\tilde{q}_i\rangle\}$ are independent and they can be normalized to unity, but they are not necessarily orthogonal. However, for an adequate

$\{|p_i\rangle\}\in\mathscr{H}_P$ the set $\{|\tilde{q}_i\rangle\}$ can be replaced by means of the Gram—Schmidt procedure by an orthonormal one so that

$$|\Psi\rangle = \sum_i c_i\,|q_i\,p_i\rangle \tag{4.16}$$

and, thus, the statement (4.14) is proved.

The vectors $|q_i\rangle$ are linear expressions of the vectors of the set $\{|\tilde{q}_i\rangle\}$, but, owing to Theorem 1/b., if according to (4.14) $a[q_i; p_j]$ is replaced by $c_i\delta_{ij}$ then $b[p_j; q_i] = c_i\delta_{ij}$, too, for the given orthonormal basis $\{|p_i\rangle\}\in\mathscr{H}_P$. Indeed,

$$\langle p_i|\Psi\rangle = \sum_j |q_j\rangle\langle q_j|\,\langle p_i|\Psi\rangle = \sum_j |q_j\rangle\langle p_i|\,\langle q_j|\Psi\rangle =$$

$$= \sum_j |q_j\rangle\langle p_i|p_j\rangle\,c_j = c_i|q_i\rangle\,.$$

This means that there exist such orthonormal bases $\{|p_i\rangle\}$ in $\mathscr{H}_P$ and $\{|q_i\rangle\}$ in $\mathscr{H}_Q$ that the mappings (4.16) are fulfilled for $i = 1, 2, \ldots$ and, thus, the proof of the theorem is completed.

The orthonormal set of vectors $\{|p_i\rangle\}\in\mathscr{H}_P$ is the set of eigenstates of the operator $\mathbf{D}_P$ i.e., the NSO's in $\mathscr{H}_P$

$$\mathbf{D}_P\,|p_i\rangle = \lambda_i|p_i\rangle \quad \text{with} \quad \lambda_i = |c_i|^2\,. \tag{4.17}$$

Then

Theorem 3. (Carlson and Keller) If the set of vectors $\{|p_i\rangle\}\in\mathscr{H}_P$ are the NSO's of $\mathscr{H}_P$, i.e., the eigenstates of the p-matrix $\mathbf{D}_P$ corresponding to the eigenvalues $\lambda_i = |c_i|^2$ then in $\mathscr{H}_Q$ the eigenvalues of the q-matrix $\mathbf{D}_q$ are also λ_i and the corresponding eigenstates $\{|q_i\rangle\}$ are the NSO's in $\mathscr{H}_Q$.

Indeed, by the definitions (4.7) and (4.9) and from Equs. (4.15)

$$\mathbf{D}_P = \sum_i \langle q_i|\Psi\rangle\langle\Psi|q_i\rangle = \sum_i |p_i\rangle\,\lambda_i\,\langle p_i|\,, \tag{4.18}$$

$$\mathbf{D}_q = \sum_i \langle p_i|\Psi\rangle\langle\Psi|p_i\rangle = \sum_i |q_i\rangle\,\lambda_i\,\langle q_i|\,, \tag{4.19}$$

which are just the spectral resolutions of the operators $\mathbf{D}_P$ and $\mathbf{D}_q$, respectively, with the elementary projectors $|p_i\rangle\langle p_i|$ and $|q_i\rangle\langle q_i|$.

Theorem 4. There exists such a partially isometric operator $\mathbf{S}_{PQ} \equiv \sum_i |p_i\rangle\langle q_i|$ of $\mathscr{H}$ that

$$\mathbf{S}_{PQ}^{+}\,\mathbf{S}_{PQ} = \mathbf{I}_P \quad \text{and} \quad \mathbf{S}_{PQ}\,\mathbf{S}_{PQ}^{+} = \mathbf{I}_Q$$

and, from this point of view, $\mathbf{D}_P$ and D_q are unitarily equivalent:

$$\mathbf{S}_{PQ}^{+}\,\mathbf{D}_P\,\mathbf{S}_{PQ} = \mathbf{D}_q. \tag{4.20}$$

This statement can be proved easily and it is another formulation of Carlson—Keller's theorem mentioned previously by KIANG [20], although he did not go into the precise details.

It is easy to see that the operator $\mathbf{D}_P$ in co-ordinate representation is just the p-matrix $\mathbf{D}(x_1, \ldots, x_p; x_1', \ldots, x_p')$ defined by Equ. (2.2).

In order to simplify the writing let us introduce the notations $x_p \equiv \equiv \{x_1, \ldots, x_p\}$, $x_q \equiv \{x_{p+1}, \ldots, x_N\}$, $\Psi(x_p, x_q) = \langle x_q\, x_p|\Psi\rangle$, $p_i(x_p) = \langle x_p|p_i\rangle$ and $q_i(x_q) = \langle x_q|q_i\rangle$, then

$$\Psi(x_p, x_q) = \sum_i c_i \langle x_q\, x_p|p_i\, q_i\rangle = \sum_i c_i \langle x_p|p_i\rangle \langle x_q|q_i\rangle = \sum_i c_i\, p_i(x_p)\, q_i(x_q)\,. \quad (4.21)$$

As COLEMAN [11] pointed out Carlson—Keller's theorem was previously discovered by Schmidt and formulated in the following way:

Theorem 5. (Schmidt) Given a square integrable function $\psi(x_p, x_q)$ suppose that for $u < v$, $f_i(x_p)$ with $1 \leq i \leq u$ and $g_j(x_q)$with $1 \leq j \leq v$ are linearly independent square integrable functions, then the minimum

$$\|\Psi\|^2 - \sum_{i=1}^{u} |c_i|^2$$

of

$$\Delta \equiv \|\Psi(x_p, x_q) - \sum_{ij} A_{ij} f_i(x_p)\, g_j(x_q)\|^2,$$

where A_{ij} are arbitrary complex numbers, is obtained if we put

$$A_{ij} = \begin{cases} c_i\, \delta_{ij}, & j \leq u \\ 0\ , & j > u \end{cases}$$

and choose

$$f_i(x_p) = p_i(x_p), \quad g_i(x_q) = q_i(x_q)\,,$$

where $p_i(x_p)$ and $q_i(x_q)$ indicate the first u NSO's.

The proof of this important theorem can also be found, e.g., in COLEMAN's paper [11].

In other words, the best least-square approximation as a sum of uv products of the form $f_i(x_p)g_i(x_q)$ is $\sum_i c_i p_i(x_p) q_i(x_q)$.

So far the symmetry properties of $\psi(x_p, x_q)$ have not been used. It is, however, well-known and on the basis of its definition it can be easily checked

that for bosons and fermions there is a unique p-matrix associated with a given system. We shall investigate the fermion case below.

From (4.12) and *Theorem* 5 it follows that, except possibly on a set of measure zero, in accordance with (4.21), setting $p = 1$ and $q = N - 1$, we have

$$\Psi(x_1, x_q) = \sum_i c_i \, p_i^{(1)}(x_1) \, q_i^{(N-1)}(x_q) \tag{4.22}$$

with

$$c_i \, q_i^{(N-1)}(x_q) = \int dx_1 \, p_i^{(1)}(x_1) \, \Psi(x_1, x_q) \, . \tag{4.23}$$

Theorem 6. (Coleman) Any function $\chi(x_1) \not\equiv 0$ belonging to the zero space $\tilde{\mathscr{H}}_0^{(1)}$ of the operator $\mathbf{D}^{(1)}$ on $\tilde{\mathscr{H}}^{(1)}$, i.e., being orthogonal to all the Ψ—NSO's, is orthogonal to $q_i^{(N-1)}(x_q)$, too.

Indeed, by (4.22)

$$\begin{aligned} 0 &= \sum_i c_i \, q_i^{(N-1)}(x_q) \int dx_1 \, \chi^*(x_1) \, p_i^{(1)}(x_1) = \int dx_1 \, \chi^*(x_1) \, \Psi(x_1, x_2, x_3, \ldots, x_N) = \\ &= - \int dx_1 \, \chi^*(x_1) \, \Psi(x_2, x_1, x_3, \ldots . \, x_N) = - \\ &= - \sum_i c_i \, p_i^{(1)}(x_2) \int dx_1 \, \chi^*(x_1) \, q_i^{(N-1)}(x_1, x_3, \ldots, x_N) \end{aligned}$$

for all c_i and $p_i^{(1)}(x_2)$, therefore

$$\int dx_1 \, \chi^*(x_1) \, q_i^{(N-1)}(x_1, x_3, \ldots, x_N) = 0 \, , \tag{4.24}$$

qu. e. d.

Corollary. Since Equ. (4.24) is valid for any fixed $x_3, \ldots, x_N$, $q_i^{(N-1)}(x_2, x_3, \ldots, x_N)$ can be expanded in terms of $p_i^{(1)}(x_2)$, i.e.,

$$c_i \, q_i^{(N-1)}(x_2, \ldots, x_N) = \sum_j c_{ij} \, p_i^{(1)}(x_2) \, q_j^{(N-2)}(x_3, \ldots, x_N) \, .$$

Therefore, by induction it can immediately be obtained that

$$\Psi(x_1, \ldots, x_N) = \sum_{k_1 k_2 \ldots k_N} c_{k_1 k_2 \ldots k_N} \, p_{k_1}^{(1)}(x_1) \, p_{k_2}^{(1)}(x_2) \cdots p_{k_N}^{(1)}(x_N), \tag{4.25}$$

or in the language of the abstract Hilbert space formalism

$$|\Psi\rangle = \sum_{k_1 k_2 \ldots k_N} c_{k_1 k_2 \ldots k_N} \, |p_{k_1}^{(1)} p_{k_2}^{(2)} \cdots p_{k_N}^{(N)}\rangle . \tag{4.26}$$

In the factor-space $\mathscr{H}^{(r)}$ of the rth particle one has to define the one-particle density operator in the form

$$\mathbf{D}^{(r)} \equiv \sum_{k_r} |p_{k_r}^{(r)}\rangle \, \lambda_{k_r} \, \langle p_{k_r}^{(r)}| \tag{4.27}$$

with the NSO's $|p_{k_r}^{(r)}\rangle$ or in co-ordinate representation the first order reduced density matrix

$$D_1(x_r; x_r') = \int dx_1 \ldots dx_{r-1}\, dx_{r+1} \ldots dx_N\, \Psi(x_1, \ldots, x_r, \ldots, x_N)\, \Psi^*(x_1, \ldots, x_r', \ldots, x_N)$$

with its eigenfunctions $p_{k_r}^{(1)}(x_r)$. Owing to the unitary equivalence of the operators $\mathbf{D}^{(r)}$ and $\mathbf{D}^{(s)}$ in respect of the partially isometric operator

$$\mathbf{S}_{(rs)} \equiv \sum_i |p_i^{(r)}\rangle \langle p_i^{(s)}|$$

i.e.,

$$\mathbf{S}_{(rs)}^{+}\, \mathbf{D}^{(r)}\, \mathbf{S}_{(rs)} = \mathbf{D}^{(s)},$$

one does not have to distinguish the eigenvalues of $\mathbf{D}^{(r)}$ for the different $r = 1, 2, \ldots, N$.

It is remarkable that the first-order eigenvalues are non-negative and bounded above by $1/N$, i.e.,

$$0 \leqq \lambda_{k_r} \leqq \frac{1}{N}\,. \tag{4.28}$$

The proof is straightforward and can be found in [9] and in papers dealing with the problem of the N-respresentability (e.g. [10,11]).

The set of the NSO's $\{|p_{k_r}^{(r)}\rangle\}$ is complete orthonormal set in $\mathscr{H}^{(r)} \ominus \mathscr{H}_0^{(r)}$, where $\mathscr{H}_0^{(r)}$is the zero-space of the operator $\mathbf{D}^{(r)}$ defined on $\mathscr{H}^{(r)}$. This means, however, that if the state vector $|\Psi\rangle$ considered is expanded in terms of the NSO's, as in Equ. (4.26), only thesubspace $\bigotimes_{r=1}^{N} \{\mathscr{H}^{(r)} \ominus \mathscr{H}_0^{(r)}\}$ of $\mathscr{H}$ is needed. As a consequence, one has to take into account that, of course, for each state vector $|\Psi\rangle$ of the system a special subspace of $\mathscr{H}$ is given. In fact, one has to be careful if the usual perturbation problems of the system are investigated in terms of the density operator technique.

A selection of N indices $k_1 k_2 \ldots k_N$ will in the following be called a configuration and in order to simplify the writing it will be abbreviated by $K \equiv \{k_1 k_2 \ldots k_N\}$. Similarly, the notation $|p_K\rangle \equiv |p_{k_1}^{(1)} p_{k_2}^{(2)} \ldots p_{k_N}^{(N)}\rangle$ will be introduced for the product of the NSO's. Finally, if the rth index is absent in the configuration it will be denoted by

$$K[r] \equiv \{k_1 \ldots k_{r-1} k_{r+1} \ldots k_N\}\,, \quad |p_{k[r]}\rangle \equiv |p_{k_1}^{(1)} \ldots p_{k_{r-1}}^{(r-1)}\, p_{k_{r+1}}^{(r+1)} \ldots p_{k_N}^{(N)}\rangle$$

and analogously $K[rs] \equiv \{k_1 \ldots k_{r-1} k_{r+1} \ldots k_{s-1} k_{s+1} \ldots k_N\}$ etc. Using this new notation (4.26) can be replaced by

$$|\Psi\rangle = \sum_K c_K\, |p_K\rangle\,. \tag{4.29}$$

The N-particle density operator is thus given by

$$\mathbf{D} = \sum_{MN} |p_M\rangle\, c_M\, c_N^*\, \langle p_N| \,. \tag{4.30}$$

Since, owing to the orthonormality of the $|p_M\rangle$-s

$$\langle p_M|p_N\rangle = \delta_{MN} \equiv \delta_{m_1 n_1}\, \delta_{m_2 n_2} \ldots \delta_{m_N n_N} \,, \tag{4.31}$$

the square of $\mathbf{D}$ can easily be calculated:

$$\mathbf{D}^2 = \sum_{MNRS} |p_M\rangle\, c_M\, c_N^*\, \langle p_N|p_R\rangle\, c_R\, c_S^*\, \langle p_S| = \sum_{MNS} |p_M\rangle\, c_M |c_N|^2\, c_S^*\, \langle p_S| \,.$$

However, owing to the unit norm of $|\Psi\rangle$ it holds that

$$\langle \Psi|\Psi\rangle = \sum_{MN} \langle p_M|c_M^*\, c_N|p_N\rangle = \sum_N |c_N|^2 = 1 \tag{4.32}$$

so, finally,

$$\mathbf{D}^2 = \sum_{MS} |p_M\rangle\, c_M\, c_S^* \langle p_S| = \mathbf{D} \tag{4.33}$$

is obtained as was expected. Similarly

$$tr\{\mathbf{D}\} = \sum_{RMN} \langle p_R|p_M\rangle\, c_M\, c_N^* \langle p_N|p_R\rangle = \sum_R |c_R|^2 = 1 \,. \tag{4.34}$$

Furthermore, having its definition (4.7) in mind,

$$\mathbf{D}^{(r)} \stackrel{\text{def}}{=\!=} tr_{\neq r}\{\mathbf{D}\} \equiv \sum_{K_{\setminus r}} \langle p_{K[r]}|\Psi\rangle\langle\Psi|p_{K[r]}\rangle =$$

$$= \sum_{MNK[\ ]} \langle p_{K[r]}|p_{m_r}^{(r)}\, p_{M[r]}\rangle\, c_{m_r M[r]}\, c_{n_r N[r]}^*\, \langle p_{N[r]}\, p_{n_r}^{(r)}|p_{K[r]} = \sum_{m_r n_r} |p_{m_r}^{(r)}\rangle\, \Lambda_{m_r;n_r}^{(1)}\, \langle p_{n_r}^{(r)}| \tag{4.35}$$

with

$$\Lambda_{m_r;n_r}^{(1)} \equiv \sum_{K[r]} c_{m_r K[r]}\, c_{n_r K[r]}^* = \Lambda_{n_r;m_r}^{(1)*} \,, \tag{4.36}$$

where the abbreviation means $c_{m_r K[r]} \equiv c_{k_1 \ldots k_{r-1} m_r k_{r+1} \ldots k_N}$, etc. However, the set $\{|p_i^{(r)}\rangle\}$ is the set of the eigenvectors of $\mathbf{D}^{(r)}$. Therefore,

$$\mathbf{D}^{(r)}\, |p_i^{(r)}\rangle = \lambda_i\, |p_i^{(r)}\rangle \,;$$

since

$$\mathbf{D}^{(r)}\, |p_i^{(r)}\rangle = \sum_{m_r n_r} |p_{m_r}^{(r)}\rangle\, \Lambda_{m_r;n_r}^{(1)}\, \langle p_{n_r}^{(r)}|p_i^{(r)}\rangle = \sum_{m_r} \Lambda_{m_r;i}^{(1)} |p_{m_r}^{(r)}\rangle = \lambda_i |p_i^{(r)}\rangle$$

and

$$\lambda_i = \sum_{m_r} \Lambda_{m_r;i}^{(1)}\, \langle p_i^{(r)}|p_{m_r}^{(r)}\rangle = \Lambda_{i;i}^{(1)} \equiv \sum_{K[r]} |c_{iK[r]}|^2 \,, \tag{4.37}$$

and by (4.35) we have

$$\Lambda^{(1)}_{i;j} = \langle p^{(r)}_j | \mathbf{D}^{(r)} | p^{(r)}_i \rangle = \lambda_i \langle p^{(r)}_j | p^{(r)}_i \rangle = \lambda_i \delta_{ij}\,; \tag{4.38}$$

the important relation

$$\sum_{K[r]} c_{iK[r]}\, c^*_{jK[r]} = \delta_{ij} \sum_{K[r]} |c_{iK[r]}|^2 \tag{4.39}$$

is obtained.

We observed that, indeed,

$$tr\{\mathbf{D}^{(r)}\} = \sum_i \lambda_i = \sum_K |c_K|^2 = 1\,, \tag{4.40}$$

but

$$tr\{\mathbf{D}^{(r)2}\} = tr\{\sum_{ij} |p^{(r)}_i\rangle \lambda_i \langle p^{(r)}_i | p^{(r)}_j\rangle \lambda_j \langle p^{(r)}_j|\} = \sum_i \lambda_i^2 < 1 \tag{4.41}$$

as was expected. Namely, the one-particle state is a mixed one in the N-particle pure state.

Finally, it seems to be worth-while to set up the structural properties of the two-particle reduced density operator, the 2-operator. It is defined by

$$\mathbf{D}^{(rs)} \overset{\text{def}}{=} tr_{\neq r,s}\{\mathbf{D}\} = \sum_{MNK[rs]} \langle p_{K[rs]} | p_M\rangle\, c_M\, c^*_N \langle p_N | p_{K[rs]}\rangle =$$

$$= \sum_{m_r m_s n_r n_s} |p^{(r)}_{m_r} p^{(s)}_{m_s}\rangle\, \Lambda^{(2)}_{m_r m_s; n_r n_s} \langle p^{(s)}_{n_s} p^{(r)}_{n_r}| \tag{4.42}$$

with

$$\Lambda^{(2)}_{m_r m_s; n_r n_s} \equiv \sum_{K[rs]} c_{m_r m_s K[rs]}\, c^*_{n_r n_s K[rs]} = \Lambda^{(2)*}_{n_r n_s; m_r m_s}\,. \tag{4.43}$$

The eigenstates of the 2-operator are usually called *natural spin-geminals* (in the following NSG's). Let them be denoted by $|g^{(rs)}_\nu\rangle$ and the corresponding eigenvalues of $\mathbf{D}^{(rs)}$ by γ_ν, then the spectral resolution of $\mathbf{D}^{(rs)}$ is given as

$$\mathbf{D}^{(rs)} = \sum_\nu |g^{(rs)}_\nu\rangle\, \gamma_\nu \langle g^{(rs)}_\nu|\,. \tag{4.44}$$

The NSG's $|g^{(rs)}_\nu\rangle$ are defined in the complete tensor-product space $\{\mathscr{H}^{(r)} \ominus \mathscr{H}^{(r)}_0\} \otimes \{\mathscr{H}^{(s)} \ominus \mathscr{H}^{(s)}_0\}$ and they can be expanded in terms of the basis $\{|p^{(r)}_i p^{(s)}_j\rangle\}$ as follows

$$|g^{(rs)}_\nu\rangle = \sum_{ij} g^\nu_{ij}\, |p^{(r)}_i\, p^{(s)}_j\rangle\,. \tag{4.45}$$

By the definitions (4.43) and (4.44), the relation

$$\langle p_l^{(s)} p_k^{(r)} | \mathbf{D}^{(rs)} | p_{k'}^{(r)} p_{l'}^{(s)} \rangle = \sum_{\nu} \langle p_l^{(s)} p_k^{(r)} | g_\nu^{(rs)} \rangle \gamma_\nu \langle g_\nu^{(rs)} | p_{k'}^{(r)} p_{l'}^{(s)} \rangle =$$

$$= \sum_{\nu} g_{kl}^{\nu} \gamma_\nu g_{k'l'}^{\nu} = \Lambda_{kl;k'l'}^{(2)} \tag{4.46}$$

and, owing to Equs. (4.42) and (4.43),

$$\gamma_\nu = \langle g_\nu^{(rs)} | \mathbf{D}^{(rs)} | g_\nu^{(rs)} \rangle = \sum_{klk'l'} \langle {}_\nu^{(rs)} | p_k^{(r)} p_l^{(s)} \rangle \Lambda_{kl;k'l'}^{(2)} \langle p_{l'}^{(s)} p_{k'}^{(r)} | g_\nu^{(rs)} \rangle =$$

$$= \sum_{klk'l'} g_{kl}^{\nu *} \Lambda_{kl;k'l'}^{(2)} g_{k'l'}^{\nu} \tag{4.47}$$

may be obtained, by which the connections between the eigenvalues γ_ν and the eigenmatrix $\Lambda_{k,l;k'l'}^{(2)}$ are explicitly given.

§ 5. Remarks on Kiang's variational approach

Let us consider again our system of equations (4.15) getting a special mapping between $\mathscr{H}_P$ and $\mathscr{H}_Q$. It was proved in *Theorem 2* that orthonormal basis systems $\{|q_i\rangle\} \in \mathscr{H}_Q$ and $\{|p_i\rangle\} \in \mathscr{H}_P$ exist which are solutions of Equs. (4.15). Furthermore, it was shown by means of Carlson and Keller's *Theorem 3* that they are exactly the corresponding eigenstates of $\mathbf{D}_q$ and $\mathbf{D}_p$, respectively.

Essentially, the same system of equations was obtained by KIANG [20] in the form

$$\begin{aligned} \langle q|\Psi\rangle &= c|p\rangle\,, \\ \langle p|\Psi\rangle &= c|q\rangle\,, \end{aligned} \tag{5.1}$$

based on the requirement that the functional

$$\langle qp|\Psi\rangle \langle\Psi|pq\rangle = |\langle qp|\Psi\rangle|^2 \tag{5.2}$$

has to be stationary.

This stationary condition may be denoted as the "principle of maximum overlap". Apparently, KIANG did not observe that these principles are solely a special case of Schmidt's *Theorem 5* for $u = 1$. Indeed, the condition $\langle qp|\Psi\rangle|^2 =$ maximum is equivalent to the condition $||\Psi - c|pq\rangle||^2 =$ minimum.

In order to determine the eigenstates of $\mathbf{D}_q$ and $\mathbf{D}_p$ based on this variational principle KIANG assumed the existence of the solutions c_i, $|q_i\rangle$ and $|p_i\rangle$ for $i = 1, 2, \ldots$ As a corollary of *Theorem 2* the existence of such solutions is proved, as mentioned above.

In reverse: due to *Theorems 2, 3* and *5* the solutions of Equs. (4.15) make the functional (5.2) stationary.

Another point should be emphasized, too. KIANG has not observed that the solutions $\{|q_i\rangle\}\in\mathscr{H}_Q$ and $\{|p_i\rangle\}\in\mathscr{H}_P$ are complete orthonormal basis systems only in the subspaces $\mathscr{H}_Q\ominus\mathscr{H}_Q^{(0)}$ and $\mathscr{H}_P\ominus\mathscr{H}_P^{(0)}$, respectively. As a matter of fact, just this is the reason while the variational approach and the iteration method proposed by KIANG is only adequate to determine the highest NSO's in the case of a given $|\Psi\rangle$. However, this resolution of the system state vector in terms of the maximal NSO's is a very interesting and remarkable result obtained by KIANG.

In order to improve the above statements to a certain extent let us consider again the expansion (4.29) of the state vector in terms of NSO's:

$$|\Psi\rangle=\sum_K c_K|p_K\rangle\,. \tag{5.3}$$

In fact, in our case $|\Psi\rangle$ is antisymmetric. This means that $c_k$is antisymmetric in its indices $K=(k_1,\ldots,k_N\}$. If one introduces the ordered configuration $\varkappa=\{k_1,\ldots,k_N\}$ with $k_1<k_2<\ldots<k_N$ instead of K, Equ. (5.3) can be written in the form [9]

$$|\Psi\rangle=\sum_\varkappa c_\varkappa\sqrt{N!}\,\mathbf{A}_N\,|p_{k_1}^{(1)}\cdots p_{k_N}^{(N)}\rangle\,, \tag{5.4}$$

where the operator $\mathbf{A}_N$ denotes the antisymmetrizer

$$\mathbf{A}_N=\frac{1}{N!}\sum_P(-1)^P \tag{5·5}$$

with summation over all permutations of the particle indices bearing in mind the convention that odd permutations have to be taken with negative and even ones with positive sign. This means that Equ. (5.4) is the expansion of $|\Psi\rangle$ in terms of the Slater determinants of the NSO's, and

$$c_\varkappa=\langle p_{k_N}^{(N)}\cdots p_{k_1}^{(1)}|\mathbf{A}_N\sqrt{N!}\,|\Psi\rangle\,. \tag{5.6}$$

PRIMAS [21] pointed out that, owing to the theorem of SCHMIDT—GOLOMB [23], if $|c_\varkappa|^2=$ maximum and the orbitals fulfil the relations

$$\langle p_{k_N}^{(N)}\cdots p_{k_{r+1}}^{(r+1)}\,p_{k_{r-1}}^{(r-1)}\cdots p_{k_1}^{(1)}\,|\Psi\rangle=c_\varkappa\sqrt{N!}\,|p_{k_r}^{(r)}\rangle\,, \tag{5.7}$$

then

$$|\Phi\rangle=\sqrt{N!}\,\mathbf{A}_N|p_{k_1}^{(1)}\cdots p_{k_N}^{(N)}\rangle \tag{5.8}$$

is a uniquely determined optimal Slater-determinant, the so-called Brueckner determinant. It will be proved in the next paragraph that the first highest NSO's fulfil condition (5.7), i.e., they are exactly the Brueckner orbitals.

§ 6. Cluster expansions of the density operator

Now, let us investigate the resolution of **D** in terms of the one-particle density operators, essentially, using the method of the cluster expansion suggested by PRIMAS [21].

Consider the idempotent operator

$$\mathbf{I} \equiv \sum_{KL} \mathbf{P}_{KL} \equiv \sum_{KL} |p_K\rangle\langle p_L| = \sum_{K} |p_K\rangle\langle p_L| + \sum_{K\neq L} |p_K\rangle\langle p_L| \equiv$$

$$\equiv \sum_{K} \mathbf{P}_K + \sum_{KL} \mathbf{P}_{K\neq L} \equiv \mathbf{I}_d + \mathbf{I}_{nd}\,, \tag{6.1}$$

which is a unit super-operator* in respect to **D**. Indeed,

$$\hat{\mathbf{I}}\{\mathbf{D}\} \overset{\text{def}}{=} \sum_{KL} \hat{\mathbf{P}}_{KL}\{\mathbf{D}\} \equiv \sum_{KL} tr\,\{\mathbf{P}_{KL}^{+}\,\mathbf{D}\}\,\mathbf{P}_{KL} = \mathbf{D}\,, \tag{6.2}$$

owing to the fact that

$$tr\{|p_L\rangle\langle p_K|\mathbf{D}\} = \sum_{RMN} \langle p_R|p_M\rangle\, c_M\, c_N^{*}\, \langle p_N|p_R\rangle = c_K\, c_L^{*}\,. \tag{6.3}$$

If we introduce the notation

$$\mathbf{D} = \sum_{M} |p_M\rangle|c_M|^2\langle p_M| + \sum_{M\neq N} |p_M\rangle\, c_M\, c_N^{*}\, \langle p_N| \equiv \mathbf{D}_d + \mathbf{D}_{nd}\,, \tag{6.4}$$

it can be checked easily that

$$tr\,\{\mathbf{P}_{K\neq L}^{+}\,\mathbf{D}\} = 0 \quad \text{and} \quad tr\,\{\mathbf{P}_K\,\mathbf{D}_{nd}\} = 0. \quad (\mathbf{P}_K = \mathbf{P}_K^{+}) \tag{6.5}$$

Since, by (6.2) for

$$\mathbf{I}\{\mathbf{D}_d\} = \sum_{K} \mathbf{P}_K^{+}\,\{\mathbf{D}_d\} = \sum_{K} tr\{\mathbf{P}_K\,\mathbf{D}\}\,\mathbf{P}_K = \sum_{K} |c_K|^2\,\mathbf{P}_K = \mathbf{D}_d \tag{6.6}$$

* A super-operator is a function with the operator algebra of all operators as its domain and range. Any one-electron super-operator can be represented by $\hat{\mathbf{P}}\{\mathbf{X}\} = \mathrm{tr}\,\{\mathbf{P}^{+}\mathbf{X}\}\,\mathbf{P}$ for all operators **X** where **P** is a certain Hermitian one-electron operator of the dynamical system considered.

and, also, the identity

$$\mathbf{P}_K \equiv |p_K\rangle\langle p_K| \equiv \prod_{r=1}^{N} |p_{kr}^{(r)}\rangle\langle p_{kr}^{(r)}| \equiv \prod_{r=1}^{N} \left[\mathbf{D}^{(r)} + \left(|p_{kr}^{(r)}\rangle\langle p_{kr}^{(r)}| - \mathbf{D}^{(r)}\right)\right] \quad (6.7)$$

holds, the remarkable resolution of $\mathbf{D}_d$

$$\mathbf{D}_d = \sum_K |c_K|^2 \left\{ \prod_{r=1}^{N} \mathbf{D}^{(r)} + \sum_{n=1}^{N} \left(|p_{kn}^{(n)}\rangle\langle p_{kn}^{(n)}| - \mathbf{D}^{(n)}\right) \prod_{r\neq n} \mathbf{D}^{(r)} + \right.$$

$$\left. + \frac{1}{2!} \sum_{n\neq m} \left(|p_{kn}^{(n)}\rangle\langle p_{kn}^{(n)}| - \mathbf{D}^{(n)}\right)\left(|p_{km}^{(m)}\rangle\langle p_{km}^{(m)}| - \mathbf{D}^{(m)}\right) \prod_{r\neq n,m} \mathbf{D}^{(r)} + \ldots \right\} \quad (6.8)$$

can be obtained. But owing to the definitions (4.29) and (4.42) and to Equ. (4.40), we have the resolution of $\mathbf{D}_d$ as follows:

$$\mathbf{D}_d = \prod_{r=1}^{N} \mathbf{D}^{(r)} + \frac{1}{2!} \sum_{n\neq m} \left(\mathbf{D}_d^{(nm)} - \mathbf{D}^{(n)}\mathbf{D}^{(m)}\right) \prod_{r\neq n,m} \mathbf{D}^{(r)} + \ldots . \quad (6.9)$$

It is straightforward, even if it is to a certain extent tedious, to prove that the super-operator $\hat{\mathbf{P}}_{K\neq L}\{\mathbf{D}_{nd}\}$ obtains the terms $\mathbf{D}_{nd}^{(nm)}$, etc. at the resolution of $\mathbf{D}$.

Owing to the Pauli principle the density operator has to be antisymmetric in the sense:

$$\mathbf{D} = \hat{\mathbf{A}}_N\{\mathbf{D}\} = \mathbf{A}_N \mathbf{D} \mathbf{A}_N , \quad (6.10)$$

where $\mathbf{A}_N$ is the antisymmetrizer in Equ. (5.5).

Thus, the resolution of $\mathbf{D}$ in terms of the one-particle density operators can be obtained as follows

$$\mathbf{D} = \hat{\mathbf{A}}_N \left\{ \prod_{r=1}^{N} \mathbf{D}^{(r)} + \frac{1}{2!} \sum_{n\neq m} \mathbf{C}^{(nm)} \prod_{r\neq n,m} \mathbf{D}^{(r)} + \frac{1}{3!} \sum_{n\neq m\neq l} \mathbf{C}^{(nml)} \prod_{r\neq n,m,l} \mathbf{D}^{(r)} + \ldots \right\} \quad (6.11)$$

with the cluster operators

$$\mathbf{C}^{(nm)} \stackrel{\text{def}}{=} \mathbf{D}^{(nm)} - \mathbf{D}^{(n)}\mathbf{D}^{(m)} , \quad (6.12)$$

where, e.g., $\hat{\mathbf{A}}_2\{\mathbf{C}^{(nm)}\}$ is related to the two-particle correlation operator of the electrons, which will be discussed in the next part of this investigation.

We can get another useful way of expanding the density operator in terms of one-particle density operators. Let us consider the first N highest eigenstates of the one- and two-particle density operators etc., and introduce

the set of truncated operators

$$\tilde{\mathbf{D}}^{(r)} = \sum_{\mu=1}^{N} |p_\mu^{(r)}\rangle \lambda_\mu \langle p_\mu^{(r)}|, \quad \tilde{\mathbf{D}}^{(rs)} = \sum_{\nu=1}^{N} |g_\nu^{(rs)}\rangle \gamma_\nu \langle g_\nu^{(rs)}| . \tag{6.13}$$

Then, taking into account that the summation over the configuration $K = \{k_1, k_2, \ldots, k_N\}$ is not truncated, we have, e.g.,

$$\begin{aligned} \mathbf{D}_d &= \sum_K |c_K|^2 \prod_{r=1}^{N} \{\tilde{\mathbf{D}}^{(r)} + (|p_{k_r}^{(r)}\rangle \langle p_{k_r}^{(r)}| - \tilde{\mathbf{D}}^{(r)})\} = \\ &= \prod_{r=1}^{N} \tilde{\mathbf{D}}^{(r)} + \sum_{n=1}^{N} (\mathbf{D}^{(n)} - \tilde{\mathbf{D}}^{(n)}) \prod_{r\neq n} \tilde{\mathbf{D}}^{(r)} + \end{aligned} \tag{6.14}$$

$$+ \frac{1}{2!} \sum_{m\neq m} \mathbf{D}^{(nm)} - \mathbf{D}^{(n)} \tilde{\mathbf{D}}^{(m)} - \tilde{\mathbf{D}}^{(n)} \mathbf{D}^{(m)} - \tilde{\mathbf{D}}^{(n)} \tilde{\mathbf{D}}^{(m)}) \cdot \prod_{r\neq n,m} \mathbf{D}^{(r)} + \ldots .$$

If the notations

$$\mathbf{D}^{(n)} = \tilde{\mathbf{D}}^{(n)} + \mathbf{v}^{(n)}, \quad \mathbf{D}^{(nm)} = \tilde{\mathbf{D}}^{(nm)} + \mathbf{v}^{(nm)} \tag{6.15}$$

are introduced, one obtains easily that

$$\mathbf{D} = \hat{\mathbf{A}}_N \left\{ \prod_{r=1}^{N} \tilde{\mathbf{D}}^{(r)} + \frac{1}{2!} \sum_{n\neq m} \{\tilde{\mathbf{C}}^{(nm)} + \mathbf{v}^{(nm)}\} \prod_{r\neq n,m} \mathbf{D}^{(r)} + \ldots \right\} \tag{6.16}$$

where the cluster operators

$$\tilde{\mathbf{C}}^{(nm)} \equiv \tilde{\mathbf{D}}^{(nm)} - \tilde{\mathbf{D}}^{(n)} \tilde{\mathbf{D}}^{(m)} \tag{6.17}$$

are related to the correlation electrons in the ground states corresponding to the first highest NSO's and $\mathbf{v}^{(nm)}$ determines the correlations via excited states.

It is remarkable that the first order cluster operators corresponding to the single particle excitations are absent in both cluster expansions (6.11) and (6.16); i.e.

$$tr_{\neq r} \{\mathbf{P}_{k_r} \mathbf{D}\} = \lambda_{k_r} \mathbf{P}_{k_r} \quad (\mathbf{P}_{k_r} = |p_{k_r}^{(r)}\rangle \langle p_{k_r}^{(r)}|). \tag{6.18}$$

In this way the statment at the end of §5 that the NSO's are just the Brueckner orbitals is proved. This problem, as well as the problems connected with the correlation between the electrons in terms of the cluster operators will also be discussed in the next part of this investigation in more detail.

Finally, let us still mention that if the higher order cluster terms $\mathbf{C}^{(nm)}$, $\mathbf{C}^{(nmk)}$, ... are absent, i.e., if the system of the N electrons is a perfect one, the well known result [9]:

$$\langle x_N \ldots x_1 | \mathbf{D} | x'_1 \ldots x'_N \rangle = \begin{vmatrix} D(x_1; x'_1) \ldots D(x_1; x'_N) \\ \vdots \\ D(x_N; x'_1) \ldots D(x_N; x'_N) \end{vmatrix} \tag{6.19}$$

and a similar expression in the case of the truncated first order reduced density operators are obtained.

REFERENCES

1. P. Gombás, Pseudopotentiale, Springer, Wien, 1967.
2. J. von Neumann, Göttinger Nachr. 245, 1927; 273, 1927.
3. J. von Neumann, Mathematische Grundlagen der Quanten-Mechanik. Springer, Berlin, 1932.
4. P. A. M. Dirac, Cambridge Phil. Soc., **27**, 240, 1930.
5. U. Fano, Rev. Mod. Phys., **29**, 74, 1957.
6. R. McWeeny, Rev. Mod. Phys., **32**, 335, 1960.
7. D. Ter Haar, Rept. Progr. Phys., **24**, 304, 1961.
8. J. I. Horváth, MTESZ Évkönyv, Szeged, 1964.
9. P. O. Löwdin, Phys. Rev., **97**, 1474, 1955; **97**, 1490, 1955; **97**, 1509, 1955.
10. C. N. Yang, Rev. Mod. Phys., **34**, 694, 1962.
11. A. J. Coleman, Rev. Mod. Phys., **35**, 668, 1963.
12. T. Ando, Rev. Mod. Phys., **35**, 690, 1963.
13. K. Kumar, Nucl. Phys., **21**, 99, 1960.
14. A. J. Coleman and S. Pruski, Canadian Journ. Phys., **43**, 2142, 1965.
15. A. J. Coleman, Canadian Journ. Phys., **45**, 1271, 1967.
16. W. Kutzelnigg, Zs. f. Naturforsch., **18**, 1058, 1963.
17. R. McWeeny, Proc. Roy. Soc. London, **A253**, 242, 1959; **A259**, 554, 1960.
18. R. McWeeny and W. Kutzelnigg, Intern. Journ. Quant. Chem., **2**, 187, 1968.
19. M. M. Metechkin, Intern. Journ. Quant. Chem., **1**, 675, 1967.
20. H. S. Kiang, The natural expansion and reduced density operators (Thesis, Indiana University, 1966.); Journ. Math. Phys., **8**, 450, 1967.
21. H. Primas, Modern Quantum Chemistry, ed. by O. Sinanoğlu; Academic Press, New York, 1965, p. 45.
23. M. Golomb, On Numerical Approximation, ed. by R. E. Langer; Wisconsin Univ. Press, Madison, 1959.

О ТЕОРИИ ОПЕРАТОРОВ ПЛОТНОСТИ ФЕРМИОНОВ I.

ОПРЕДЕЛЕНИЕ ОДНОЧАСТИЧНЫХ СОСТОЯНИЙ И КЛАСТЕРНОЕ РАЗЛОЖЕНИЕ ОПЕРАТОРОВ ПЛОТНОСТИ

Я. И. ХОРВАТ и И. К. ДЬЕМАНТ

Резюме

После определения операторов плотности (§ 2) вырабатывается понятие простых частичных состояний на основе чистых состояний приведенных операторов плотности первого порядка (§ 3). Далее рассматривается понятие NSO и NSG и разложения по ним (§ 4). Дискутируется и развивается дальше вариационное приближение Кианга (5 §). Наконец в различных случаях даются кластерные разложения операторов плотности N-частиц по приведенным операторам плотности первого порядка.

Acta Physica Academiae Scientiarum Hungaricae, Tomus 27, pp. 131—149 (1969)

BERECHNUNGEN DER ZUSTÄNDE $1sns\,{}^1\Sigma_g^+$ DES WASSERSTOFFMOLEKÜLS AUF GRUND DER METHODE DER KORRELATIONSMÄSSIGEN MOLEKÜLBAHNEN*

Von

F. BERENCZ

INSTITUT FÜR THEORETISCHE PHYSIK, JÓZSEF ATTILA UNIVERSITÄT, SZEGED

(Eingegangen: 13. I. 1969)

Es wurde die Elektronenenergie des Zustandes $1s2s\,{}^1\Sigma_g^+$ des Wasserstoffmoleküls auf Grund der Methode der korrelationsmässigen Molekülbahnen berechnet. Es wurde weiterhin festgestellt, dass durch die Erweiterung der Eigenfunktion durch den Korrelationsfaktor, nur dann eine wesentliche Energiekorrektion entsteht, wenn dort gar keine Korrelation der Elektronen vorhanden war.

Einleitung

Aus den physikalischen Experimenten ist es wohlbekannt, dass das Wasserstoffmolekül zweierlei angeregte Zustände hat. Im ersten Zustand ist das eine Elektron im Grundzustand und das andere in angeregtem Zustand; dann gibt es auch solche angeregten Zustände, in welchen sich beide Elektronen in angeregtem Zustande befinden.

Im Falle des Wasserstoffmoleküls wurden über die Energie der angeregten Zustände viele Berechnungen durchgeführt. Schon ganz früh, einige Jahre danach, dass die Schrödinger'sche Gleichung angegeben wurde, konnte man über Untersuchungen der angeregten Zustände des Wasserstoffmoleküls bei GUILLEMIN und ZENER [1], bei PRESENT [2] und bei JAMES, COOLIDGE und PRESENT [3] lesen.

Der erste Teil der genauen Berechnungen der angeregten Zustände des Wasserstoffmoleküls wurde mit Funktionen, dargestellt in elliptischen Koordinaten, durchgeführt. Auf Grund solcher Funktionen wurde die Energie des niedrigsten angeregten Zustandes $^3\Sigma_g^+$ des Wasserstoffmoleküls von COOLIDGE und JAMES [4], die Energien der niedrigsten angeregten Zustände $^1\Sigma_g^+$, $^1\Sigma_u^+$ und $^3\Sigma_u^+$ von KOŁOS und ROOTHAAN [5], die Energie des angeregten Zustandes $^1\Sigma_g^+$ von DAVIDSON [6], und die Energien der angeregten Zustände $X\,^1\Sigma_g^+$, $b^3\Sigma_u^+$, $C\,^1\Pi_u^+$ und $B\,^1\Sigma_u^+$ von KOŁOS und WOLNIEWICZ [7] berechnet.

Der zweite Teil der genauen Berechnungen der angeregten Zustände des Wasserstoffmoleküls wurden mit einfachen Bahn-Funktionen durchgeführt. PHILLIPSON und MULLIKEN [8] berechneten auf Grund solcher Funktionen

* Herrn Prof. Dr. P. GOMBÁS zum 60. Geburtstag gewidmet.

die niedrigsten angeregten Zustände $^1\Sigma_u^+$ und $^3\Sigma_u^+$, BERENCZ [9] den angeregten Zustand $^1\Sigma_g^+$ und BROWNE [10] die angeregten Zustände $^1\Pi_u$, $^3\Pi_g$, $^1\Pi_g$, $^3\Pi_g$, $^1\Delta_u$, $^3\Delta_u$, $^1\Delta_g$, $^3\Delta_g$.

Der dritte Teil der genauen Berechnungen der angeregten Zustände des Wasserstoffmoleküls wurde mit solchen Wellenfunktionen durchgeführt, die durch Bildung der Linearkombinationen solcher Atomfunktionen entstehen, die auf den Mittelpunkt der Kernverbindungslinie zentriert sind. Auf Grund solcher Wellenfunktionen wurden die angeregten Zustände des Wasserstoffmoleküls von HUZINAGE [11], TAMÁSSY-LENTEI [12], TAYLOR [13] und KATO, HAYES und DUNCAN [14] berechnet.

ZUNG und DUNCAN [15] veröffentlichten auch Berechnungen des angeregten Zustandes des Wasserstoffmoleküls, die denen von PHILLIPSON und MULLIKEN ähnlich sind, aber diese Verfasser verwendeten ortho-normierten Molekülbahnen.

Zum Schluss müssen noch die Verfasser ROTHENBERG und DAVIDSON [16] erwähnt werden, die die natürlichen Bahnen der angeregten Zustände $^1\Sigma_g^+$, $^1\Sigma_u^+$, $^1\Pi_g$, $^1\Pi_u$, $^1\Delta_g$, $^3\Sigma_g^+$, $^3\Sigma_u^+$, $^3\Pi_u$, $^3\Pi_g$, $^3\Delta_g$ des Wasserstoffmoleküls angegeben haben.

In einer früheren Arbeit des Verfassers [17] wurde untersucht, wie die Berücksichtigung des Korrelationsfaktors $(1 + pr_{12})$ die Berechnungen des Grundzustandes des Wasserstoffmoleküls beeinflusst. In dieser Arbeit werden die früheren Untersuchungen auf die Berechnungen der Zustände $1sns^1\Sigma_g^+$ ausgedehnt. Mit diesen Berechnungen vermehrt sich die Zahl der bekannten Molekülintegrale zwischen 1*s*- und *ns*-Elektronen in grossem Masse.

Die Rechenmethode

Zur Bestimmung von Zustandsfunktionen für die Zustände $1sns^1\Sigma_g^+$ $(n \geq 2)$ des Wasserstoffmoleküls wird es angenommen, dass sie ihren Ursprung aus einer Bahn-Konfiguration nehmen, in welcher sich das erste Elektron im Grundzustand und das zweite Elektron in angeregtem Zustand befindet. Im Falle $n = 2$ haben die Molekülbahnen der einzelnen Elektronen die folgende Gestalt:

$$1\sigma_g = (1S_A + 1S_B)/\sqrt{2(1+S_1)}, \tag{1}$$

$$2\sigma_g = (2S_A + 2S_B)/\sqrt{2(1+S_2)}, \tag{2}$$

wo

$$S_i = \langle iS_A | iS_B \rangle, \qquad i = 1,2. \tag{3}$$

Die Wasserstoffeigenfunktionen der *ns*-Zustände werden durch den folgenden Zusammenhang geliefert:

$$ns(r) = \frac{1}{n^{3/2}\sqrt{\pi}} \exp\left(-\frac{R}{n}\right) R_n(r), \tag{4}$$

wo

$$R_n(r) = 1 - \frac{n-1}{1!\,2!}\left(\frac{2r}{n}\right) + \frac{(n-1)(n-2)}{2!\,3!}\left(\frac{2r}{n}\right)^2 - \ldots . \tag{5}$$

Die Zustandsfunktion ist das antisymmetrische Produkt der einzelnen $1\sigma_g$ und $2\sigma_g$ Molekülbahnen, durch den Korrelationsfaktor $(1 + pr_{12})$ erweitert.

$$\Psi_{1s2s} = 1\,\sigma_g(1)\,2\,\sigma_g(2)\,(1+pr_{12})\,\frac{1}{\sqrt{2}}\,(\alpha_1\beta_2 - \alpha_2\beta_1). \tag{6}$$

Die Elektronenenergie wird dann auf Grund des folgenden Zusammenhanges berechnet:

$$E_{1s2s} = \frac{\int \Psi_{1s2s}\,\mathbf{H}\,\Psi_{1s2s}\,d\tau}{\int \Psi_{1s2s}^2\,d\tau}\,, \tag{7}$$

wo

$$\mathbf{H} = -\frac{1}{2}\Delta_1 - \frac{1}{2}\Delta_2 - \frac{1}{r_{a1}} - \frac{1}{r_{b1}} - \frac{1}{r_{a2}} - \frac{1}{r_{b2}} + \frac{1}{r_{12}} + \frac{1}{R}\,. \tag{8}$$

Die Resultate der Berechnungen

Mit der korrelationsmässigen Molekülbahn (6) ergab sich bei $R = 1.95$ a.u. Kernabstand für die Elektronenenergie des angeregten Zustandes $1s2s\,^1\Sigma_g^+$ des Wasserstoffmoleküls der Wert 0,70221 a.u. In einer früheren Arbeit des Verfassers [9] wurde dieselbe Energie auf Grund der (6) ähnlichen Molekülbahn mit einem Resultat von 0,68086 a.u. für die Elektronenenergie berechnet. Die Erweiterung der Molekülbahn durch den Korrelationsfaktor $(1 + pr_{12})$ gibt also eine Energiekorrektion mit dem Wert von 0,02135 a.u.. Dieselbe Korrektion hat bei der Berechnung der Elektronenenergie des Grundzustandes des Wasserstoffmoleküls den Wert 0,02352 a.u., wie man sich davon aus der Arbeit von FROST und BRAUNSTEIN [18] überzeugen kann. Da die zwei Energiekorrektionen grössenordnungsmässig gleich sind, kann es auch bei den Berechnungen der angeregten Zustände festgestellt werden, dass mit der Erweiterung der Eigenfunktion durch den Korrelationsfaktor $(1 + pr_{12})$ nur dann eine wesentliche Energiekorrektion entsteht, wenn dort gar keine Korrelation der Elektronen vorhanden war.

Ich danke auch an dieser Stelle Fräulein A. BOLDIZSÁR für die Hilfe, die sie mir mit der Vornahme der numerischen Rechnungen geboten hat.

Anhang

Bei der Berechnung der Elektronenergie mussten mehrere Molekül-Integrale bestimmt werden, die in der Literatur bisher noch nicht vorgekommen sind. Diese seien folgendermassen bezeichnet:

$$I(\alpha, \beta, \gamma, \delta, i, j, k, m, n) = \frac{1}{\pi^2} \iint \exp(-\alpha r_{a1} - \beta r_{b1}) \times$$
$$\times \exp(-\gamma r_{a2} - \delta r_{b2})\, r_{a1}^i\, r_{b1}^j\, r_{a2}^k\, r_{b2}^m\, r_{12}^n\, d\tau_1\, d\tau_2 .$$

Bei der Berechnung der Integrale wird die Methode von KOTANI [19] und seiner Mitarbeiter benutzt. Unsere Integrale wurden mit Hilfe der folgenden Hilfsintegrale ausgedrückt:

$$A_n(\alpha) = \int_1^\infty e^{-\alpha\mu}\, \mu^n\, d\mu ,$$

$$B_n(\beta) = \int_{-1}^{+1} e^{-\beta\nu}\, \nu^n\, d\nu ,$$

$$G_\tau^\nu(l, \beta) = \int_{-1}^{+1} P_\tau^\nu(\nu_i)\, e^{-\beta\nu_i}\, \nu_i^l (1 - \nu_i^2)^{\nu/2}\, d\nu_i ,$$

$$H_\tau^\nu(i, \alpha; k, \beta) = \int_1^\infty \int_1^\infty e^{-\alpha\mu_1}\, e^{-\beta\mu_2}\, \mu_1^i\, \mu_2^i\, Q_\tau^\nu(\mu_+)\, P_\tau^\nu(\mu_-) \times$$
$$\times (\mu_1^2 - 1)^{\nu/2}\, (\mu_2^2 - 1)^{\nu/2}\, d\mu_1\, d\mu_2 .$$

Die neuen Integrale können in vier Gruppen davon abhängend eingeteilt werden, dass die Exponentialfunktionen die folgenden Gestalten haben:

$$\exp(-2_{a1}) \exp(-r_{a2}) ,$$
$$\exp(-r_{a1} - r_{b1}) \exp(-r_{a2}) ,$$
$$\exp(-2\, r_{a1}) \exp\left(-\frac{1}{2} r_{a2} - \frac{1}{2} r_{b2}\right) ,$$
$$\exp(-r_{a1} - r_{b1}) \exp\left(-\frac{1}{2} r_{a2} - \frac{1}{2} r_{b1}\right) .$$

Wegen der grossen Zahl der Molekülintegrale werden aus jeder Gruppe nur einige mitgeteilt:

$$I(2, 0, 1, 0, 0, 0, 0, 0, 1) =$$

$$= \frac{R^7}{32} \left\{ H_0^0\left(4, R; 2, \frac{R}{2}\right) G_0^0(0, R)\, G_0^0\left(0, \frac{R}{2}\right) + 3\binom{0}{1} + 5\binom{0}{2} + 7\binom{0}{3} + 9\binom{0}{4} + \right.$$

$$+ H_0^0\left(2, R; 4, \frac{R}{2}\right) G_0^0(0, R)\, G_0^0\left(0, \frac{R}{2}\right) + 3\binom{0}{1} + 3\binom{0}{2} - 7\binom{0}{3} + 9\binom{0}{4} +$$

$$+ H_0^0\left(2, R; 2, \frac{R}{2}\right) G_0^0(2, R)\, G_0^0\left(0, \frac{R}{2}\right) + 3\binom{0}{1} + 5\binom{0}{2} + 7\binom{0}{3} + 9\binom{0}{4} +$$

$$+ H_0^0\left(2, R; 2, \frac{R}{2}\right) G_0^0(0, R) G_0^0\left(2, \frac{R}{2}\right) + 3\binom{0}{1} + 5\binom{0}{2} + 7\binom{0}{3} + 9\binom{0}{4} -$$

$$- 2\, H_0^0\left(3, R; 3, \frac{R}{2}\right) G_0^0(1, R)\, G_0^0\left(1, \frac{R}{2}\right) - 6\binom{0}{1} - 10\binom{0}{2} - 14\binom{0}{3} - 18\binom{0}{4} -$$

$$- 2 H_0^0\left(2, R; 2, \frac{R}{2}\right) G_0^0(0, R)\, G_0^0\left(0, \frac{R}{2}\right) - 10\binom{0}{1} - 10\binom{0}{2} - 14\binom{0}{3} - 18\binom{0}{4} +$$

$$+ \frac{3}{2} H_1^1\left(2, R; 2, \frac{R}{2}\right) G_1^1(0, R)\, G_1^1\left(0, \frac{R}{2}\right) + \frac{5}{18}\binom{1}{2} + \frac{7}{22}\binom{1}{3} + \frac{9}{200}\binom{1}{4} +$$

$$- H_0^0\left(4, R; 0, \frac{R}{2}\right) G_0^0(0, R)\, G_0^0\left(2, \frac{R}{2}\right) - 3\binom{0}{1} - 5\binom{0}{2} - 7\binom{0}{3} - 9\binom{0}{4} -$$

$$- H_0^0\left(2, R; 2, \frac{R}{2}\right) G_0^0(0, R,)\, G_0^0\left(2, \frac{R}{2}\right) - 3\binom{0}{1} - 5\binom{0}{2} - 7\binom{0}{3} - 9\binom{0}{4} -$$

$$- H_0^0\left(2, R; 0, \frac{R}{2}\right) G_0^0(2, R)\, G_0^0\left(2, \frac{R}{2}\right) - 3\binom{0}{1} - 5\binom{0}{2} - 7\binom{0}{3} - 9\binom{0}{4} -$$

$$- H_0^0\left(2, R; 0, \frac{R}{2}\right) G_0^0(0, R)\, G_0^0\left(4, \frac{R}{2}\right) - 3\binom{0}{1} - 5\binom{0}{2} - 7\binom{0}{3} - 9\binom{0}{4} +$$

$$+ 2\, H_0^0\left(3, R; 1, \frac{R}{2}\right) G_0^0(1, R)\left(3, \frac{R}{2}\right) + 6\binom{0}{1} + 10\binom{0}{2} + 14\binom{0}{3} + 18\binom{0}{4} +$$

$$+ 2\, H_0^0\left(2, R; 0, \frac{R}{2}\right) G_0^0(0, R)\, G_0^0\left(2, \frac{R}{2}\right) + 6\binom{0}{1} + 10\binom{0}{2} + 14\binom{0}{3} + 18\binom{0}{4} -$$

$$- \frac{3}{2} H_1^1\left(2, R: 0, \frac{R}{2}\right) G_1^1(0, R)\, Q_1^1\left(2, \frac{R}{2}\right) - \frac{5}{18}\binom{1}{2} - \frac{7}{72}\binom{1}{3} - \frac{9}{200}\binom{1}{4} -$$

$$- H_0^0\left(2, R; 2, \frac{R}{2}\right) G_0^0(2, R)\, G_0^0\left(0, \frac{R}{2}\right) - 3\binom{0}{1} - 5\binom{0}{2} - 7\binom{0}{3} - 9\binom{0}{4} -$$

$$- H_0^0\left(0, R; 4, \frac{R}{2}\right) G_0^0(2, R)\, G_0^0\left(0, \frac{R}{2}\right) - 3\binom{0}{1} - 5\binom{0}{2} - 7\binom{0}{3} - 9\binom{0}{4} -$$

$$- H_0^0\left(0, R; 2, \frac{R}{2}\right) G_0^0(4, R)\, G_0^0\left(0, \frac{R}{2}\right) - 3\binom{0}{1} - 5\binom{0}{2} - 7\binom{0}{3} - 9\binom{0}{4} -$$

$$- H_0^0\left(0, R; 2, \frac{R}{2}\right) G_0^0(2, R)\, G_0^0\left(2, \frac{R}{2}\right) - 3\binom{0}{1} - 5\binom{0}{2} - 7\binom{0}{3} - 9\binom{0}{4} +$$

$$+2H_0^0\left(1,R;3,\frac{R}{2}\right)G_0^0(3,R)\,G_0^0\left(1,\frac{R}{2}\right)+6\binom{0}{1}+10\binom{0}{2}+14\binom{0}{3}+18\binom{0}{4}+$$

$$+2H_0^0\left(0,R;2,\frac{R}{2}\right)G_0^0(2,R)\,G_0^0\left(0,\frac{R}{2}\right)+6\binom{0}{1}+10\binom{0}{2}+14\binom{0}{3}+18\binom{0}{4}-$$

$$-\frac{3}{2}H_1^1\left(0,R;2,\frac{R}{2}\right)G_1^1(2,R)\,G_1^1\left(0,\frac{R}{2}\right)-\frac{5}{18}\binom{1}{2}-\frac{7}{72}\binom{1}{3}-\frac{9}{200}\binom{1}{4}+$$

$$+H_0^0\left(2,R;0,\frac{R}{2}\right)G_0^0(2,R)\,G_0^0\left(2,\frac{R}{2}\right)+3\binom{0}{1}+5\binom{0}{2}+7\binom{0}{3}+9\binom{0}{4}+$$

$$+H_0^0\left(0,R;2,\frac{R}{2}\right)G_0^0(2,R)\,G_0^0\left(2,\frac{R}{2}\right)+3\binom{0}{1}+5\binom{0}{2}+7\binom{0}{3}+9\binom{0}{4}+$$

$$+H_0^0\left(0,R;0,\frac{R}{2}\right)G_0^0(4,R)\,G_0^0\left(2,\frac{R}{2}\right)+3\binom{0}{1}+5\binom{0}{2}+7\binom{0}{3}+9\binom{0}{4}+$$

$$+H_0^0\left(0,R;0,\frac{R}{2}\right)G_0^0(2,R)\,G_0^0\left(4,\frac{R}{2}\right)+3\binom{0}{1}+5\binom{0}{2}+7\binom{0}{3}+9\binom{0}{4}-$$

$$-2H_0^0\left(1,R;1,\frac{R}{2}\right)G_0^0(3,R)\,G_0^0\left(3,\frac{R}{2}\right)-6\binom{0}{1}-10\binom{0}{2}-14\binom{0}{3}-18\binom{0}{4}-$$

$$-2H_0^0\left(0,R;0,\frac{R}{2}\right)G_0^0(2,R)\,G_0^0\left(2,\frac{R}{2}\right)-6\binom{0}{1}-10\binom{0}{2}-14\binom{0}{3}-18\binom{0}{4}+$$

$$+\frac{3}{2}H_1^1\left(0,R;0,\frac{R}{2}\right)G_1^1(2,R)\,G_1^1\left(2,\frac{R}{2}\right)+\frac{5}{18}\binom{1}{2}+\frac{7}{38}\binom{1}{3}+\frac{9}{200}\binom{1}{4}\Bigg\}.$$

$$I(2,0,1,0,0,0,1,0,1)=$$

$$=\frac{R^8}{64}\Bigg\{H_0^0\left(4,R;3,\frac{R}{2}\right)G_0^0(0,R)\,G_0^0\left(0,\frac{R}{2}\right)+3\binom{0}{1}+5\binom{0}{2}+7\binom{0}{3}+9\binom{0}{4}+$$

$$+H_0^0\left(2,R;5,\frac{R}{2}\right)G_0^0(0,R)\,G_0^0\left(0,\frac{R}{2}\right)+3\binom{0}{1}+5\binom{0}{2}+7\binom{0}{3}+9\binom{0}{4}+$$

$$+H_0^0\left(2,R;3,\frac{R}{2}\right)G_2^0(2,R)\,G_0^0\left(0,\frac{R}{2}\right)+3\binom{0}{1}+5\binom{0}{2}+7\binom{0}{3}+9\binom{0}{4}+$$

$$+H_0^0\left(2,R;3,\frac{R}{2}\right)G_0^0(0,R)\,G_0^0\left(2,\frac{R}{2}\right)+3\binom{0}{1}+5\binom{0}{2}+7\binom{0}{3}+9\binom{0}{4}-$$

$$-2H_0^0\left(3,R;4,\frac{R}{2}\right)G_0^0(1,R)\,G_0^0\left(1,\frac{R}{2}\right)-6\binom{0}{1}-10\binom{0}{2}-14\binom{0}{3}-18\binom{0}{4}$$

$$-2H_0^0\left(2,R;3,\frac{R}{2}\right)G_0^0(0,R)\,G_0^0\left(0,\frac{R}{2}\right)-6\binom{0}{1}-10\binom{0}{2}-14\binom{0}{3}-18\binom{0}{4}$$

$$+\frac{3}{2}H_1^1\left(2,R;3,\frac{R}{2}\right)G_1^1(0,R)\,G_1^1\left(0,\frac{R}{2}\right)+\frac{5}{18}\binom{1}{2}+\frac{7}{72}\binom{1}{3}+\frac{9}{200}\binom{1}{4}+$$

$$+H_0^0\left(4,R;2,\frac{R}{2}\right)G_0^0(0,R)\,G_0^0\left(1,\frac{R}{2}\right)+3\binom{0}{1}+5\binom{0}{2}+7\binom{0}{3}+9\binom{0}{4}+$$

$$+H_0^0\left(2,R;4,\frac{R}{2}\right)G_0^0(0,R)\,G_0^0\left(1,\frac{R}{2}\right)+3\binom{0}{1}+5\binom{0}{2}+7\binom{0}{3}+9\binom{0}{4}+$$

$$+H_0^0\left(2,R;2,\frac{R}{2}\right)G_0^0(2,R)\,G_0^0\left(1,\frac{R}{2}\right)+3\binom{0}{1}+5\binom{0}{2}+7\binom{0}{3}+9\binom{0}{4}+$$

$$+H_0^0\left(2,R;2,\frac{R}{2}\right)G_0^0(0,R)\,G_0^0\left(3,\frac{R}{2}\right)+3\binom{0}{1}+5\binom{0}{2}+7\binom{0}{3}+9\binom{0}{4}-$$

$$-2H_0^0\left(3,R;3,\frac{R}{2}\right)G_0^0(1,R)\,G_0^0\left(2,\frac{R}{2}\right)-6\binom{0}{1}-10\binom{0}{2}-14\binom{0}{3}-18\binom{0}{4}-$$

$$-2H_0^0\left(2,R;2,\frac{R}{2}\right)G_0^0(0,R)\,G_0^0\left(1,\frac{R}{2}\right)-6\binom{0}{1}-10\binom{0}{2}-14\binom{0}{3}-18\binom{0}{4}+$$

$$+\frac{3}{2}H_1^1\left(2,R;2,\frac{R}{2}\right)G_1^1(0,R)\,G_1^1\left(1,\frac{R}{2}\right)+\frac{5}{18}\binom{1}{2}+\frac{7}{72}\binom{1}{3}+\frac{9}{200}\binom{1}{4}-$$

$$-H_0^0\left(4,R;1,\frac{R}{2}\right)G_0^0(0,R)\,G_0^0\left(2,\frac{R}{2}\right)-3\binom{0}{1}-5\binom{0}{2}-7\binom{0}{3}-9\binom{0}{4}-$$

$$-H_0^0\left(2,R;3,\frac{R}{2}\right)G_0^0(0,R)\,G_0^0\left(2,\frac{R}{2}\right)-3\binom{0}{1}-5\binom{0}{2}-7\binom{0}{3}-9\binom{0}{4}-$$

$$-H_0^0\left(2,R;1,\frac{R}{2}\right)G_0^0(2,R)\,G_0^0\left(2,\frac{R}{2}\right)-3\binom{0}{1}-5\binom{0}{2}-7\binom{0}{3}-9\binom{0}{4}-$$

$$-H_0^0\left(2,R;1,\frac{R}{2}\right)G_0^0(0,R)\,G_0^0\left(4,\frac{R}{2}\right)-3\binom{0}{1}-5\binom{0}{2}-7\binom{0}{3}-9\binom{0}{4}+$$

$$+2H_0^0\left(3,R;2,\frac{R}{2}\right)G_0^0(1,R)\,G_0^0\left(3,\frac{R}{2}\right)+6\binom{0}{1}+10\binom{0}{2}+14\binom{0}{3}+18\binom{0}{4}+$$

$$+2H_0^0\left(2,R;1,\frac{R}{2}\right)G_0^0(0,R)\,G_0^0\left(2,\frac{R}{2}\right)+6\binom{0}{1}+10\binom{0}{2}+14\binom{0}{3}+18\binom{0}{4}-$$

$$-\frac{3}{2}H_1^1\left(2,R;1,\frac{R}{2}\right)G_1^1(0,R)\,G_1^1\left(2,\frac{R}{2}\right)-\frac{5}{18}\binom{1}{2}-\frac{7}{72}\binom{1}{3}-\frac{9}{200}\binom{1}{4}-$$

$$-H_0^0\left(4,R;0,\frac{R}{2}\right)G_0^0(0,R)\,G_0^0\left(3,\frac{R}{2}\right)-3\binom{0}{1}-5\binom{0}{2}-7\binom{0}{3}-9\binom{0}{4}-$$

$$-H_0^0\left(2,R;2,\frac{R}{2}\right)G_0^0(0,R)\,G_0^0\left(3,\frac{R}{2}\right)-3\binom{0}{1}-5\binom{0}{2}-7\binom{0}{3}-9\binom{0}{4}-$$

$$- H_0^0\left(2, R; 0, \frac{R}{2}\right) G_0^0(2, R)\, G_0^0\left(3, \frac{R}{2}\right) - 3\binom{0}{1} - 5\binom{0}{2} - 7\binom{0}{3} - 9\binom{0}{4} -$$

$$- H_0^0\left(2, R; 0, \frac{R}{2}\right) G_0^0(0, R)\, G_0^0\left(5, \frac{R}{2}\right) - 3\binom{0}{1} - 5\binom{0}{2} - 7\binom{0}{3} - 9\binom{0}{4} -$$

$$+ 2 H_0^0\left(3, R; 1, \frac{R}{2}\right) G_0^0(1, R)\, G_0^0\left(4, \frac{R}{2}\right) + 6\binom{0}{1} + 10\binom{0}{2} + 14\binom{0}{3} + 18\binom{0}{4} -$$

$$+ 2 H_0^0\left(2, R; 0, \frac{R}{2}\right) G_0^0(0, R)\, G_0^0\left(3, \frac{R}{2}\right) + 6\binom{0}{1} + 10\binom{0}{2} + 14\binom{0}{3} + 18\binom{0}{4} -$$

$$- \frac{3}{2} H_1^1\left(2, R; 0, \frac{R}{2}\right) G_1^1(0, R)\, G_1^1\left(3, \frac{R}{2}\right) - \frac{5}{18}\binom{1}{2} - \frac{7}{72}\binom{1}{3} - \frac{9}{200}\binom{0}{4} -$$

$$- H_0^0\left(2, R; 3, \frac{R}{2}\right) G_0^0(2, R)\, G_0^0\left(0, \frac{R}{2}\right) - 3\binom{0}{1} - 5\binom{0}{2} - 7\binom{0}{3} - 9\binom{0}{4} -$$

$$- H_0^0\left(0, R; 3, \frac{R}{2}\right) G_0^0(2, R)\, G_0^0\left(0, \frac{R}{2}\right) - 3\binom{0}{1} - 5\binom{0}{2} - 7\binom{0}{3} - 9\binom{0}{4} -$$

$$- H_0^0\left(0, R; 3, \frac{R}{2}\right) G_0^0(4, R)\, G_0^0\left(0, \frac{R}{2}\right) - 3\binom{0}{1} - 5\binom{0}{2} - 7\binom{0}{3} - 9\binom{0}{4} -$$

$$- H_0^0\left(0, R; 3, \frac{R}{2}\right) G_0^0(2, R)\, G_0^0\left(2, \frac{R}{2}\right) - 3\binom{0}{1} - 5\binom{0}{2} - 7\binom{0}{3} - 9\binom{0}{3} +$$

$$+ 2 H_0^0\left(1, R; 4, \frac{R}{2}\right) G_0^0(3, R)\, G_0^0\left(1, \frac{R}{2}\right) + 6\binom{0}{1} + 10\binom{0}{2} + 14\binom{0}{3} + 18\binom{0}{3} -$$

$$+ 2 H_0^0\left(0, R; 3, \frac{R}{2}\right) G_0^0(2, R)\, G_0^0\left(0, \frac{R}{2}\right) + 6\binom{0}{1} + 10\binom{0}{2} + 14\binom{0}{3} + 18\binom{0}{4} -$$

$$- \frac{3}{2} H_1^1\left(0, R; 3, \frac{R}{2}\right) G_1^1(2, R)\, G_1^1\left(0, \frac{R}{2}\right) - \frac{5}{18}\binom{1}{2} - \frac{7}{72}\binom{1}{3} - \frac{9}{200}\binom{1}{3} -$$

$$- H_0^0\left(2, R; 2, \frac{R}{2}\right) G_0^0(2, R)\, G_0^0\left(1, \frac{R}{2}\right) - 3\binom{0}{1} - 5\binom{0}{2} - 7\binom{0}{3} - 9\binom{0}{4} -$$

$$- H_0^0\left(0, R; 4, \frac{R}{2}\right) G_0^0(2, R)\, G_0^0\left(1, \frac{R}{2}\right) - 3\binom{0}{1} - 5\binom{0}{2} - 7\binom{0}{3} - 9\binom{0}{4} -$$

$$- H_0^0\left(0, R; 2, \frac{R}{2}\right) G_0^0(4, R)\, G_0^0\left(1, \frac{R}{2}\right) - 3\binom{0}{1} - 1\binom{0}{2} - 7\binom{0}{3} - 9\binom{0}{4} -$$

$$- H_0^0\left(0, R; 2, \frac{R}{2}\right) G_0^0(2, R)\, G_0^0\left(3, \frac{R}{2}\right) - 3\binom{0}{1} - 5\binom{0}{2} - 7\binom{0}{3} - 9\binom{0}{4} +$$

$$+ 2 H_0^0\left(1, R; 3, \frac{R}{2}\right) G_0^0(3, R)\, G_0^0\left(2, \frac{R}{2}\right) + 6\binom{0}{1} + 10\binom{0}{2} + 14\binom{0}{3} + 18\binom{0}{4} -$$

$$+2H_0^0\left(0,R;2,\frac{R}{2}\right)G_0^0(2,R)\,G_0^0\left(1,\frac{R}{2}\right)+6\binom{0}{1}+10\binom{0}{2}+14\binom{0}{3}+18\binom{0}{4}-$$

$$-\frac{3}{2}H_1^1\left(0,R;2,\frac{R}{2}\right)G_0^0(2,R)\,G_1^1\left(1,\frac{R}{2}\right)-\frac{5}{18}\binom{1}{2}-\frac{7}{72}\binom{1}{3}-\frac{9}{200}\binom{1}{4}+$$

$$+H_0^0\left(2,R;1,\frac{R}{2}\right)G_0^0(2,R)\,G_0^0\left(2,\frac{R}{2}\right)+3\binom{0}{1}+5\binom{0}{2}+7\binom{0}{3}+9\binom{0}{4}+$$

$$+H_0^0\left(0,R;3,\frac{R}{2}\right)G_0^0(2,R)\,G_0^0\left(2,\frac{R}{2}\right)+3\binom{0}{1}+5\binom{0}{2}+7\binom{0}{3}+9\binom{0}{4}+$$

$$+H_0^0\left(0,R;1,\frac{R}{2}\right)G_0^0(4,R)\,G_0^0\left(2,\frac{R}{2}\right)+3\binom{0}{1}+5\binom{0}{2}+7\binom{0}{3}+9\binom{0}{4}+$$

$$+H_0^0\left(0,R;1,\frac{R}{2}\right)G_0^0(2,R)\,G_0^0\left(4,\frac{R}{2}\right)+3\binom{0}{1}+5\binom{0}{2}+7\binom{0}{3}+9\binom{0}{4}-$$

$$-2H_0^0\left(1,R;2,\frac{R}{2}\right)G_0^0(3,R)\,G_0^0\left(3,\frac{R}{2}\right)-6\binom{0}{1}-10\binom{0}{2}-14\binom{0}{3}-18\binom{0}{4}-$$

$$-2H_0^0\left(0,R;1,\frac{R}{2}\right)G_0^0(2,R)\,G_0^0\left(2,\frac{R}{2}\right)-6\binom{0}{1}-10\binom{0}{2}-14\binom{0}{3}-18\binom{0}{4}+$$

$$+\frac{3}{2}H_1^1\left(0,R;1,\frac{R}{2}\right)G_1^1(2,R)\,G_1^1\left(2,\frac{R}{2}\right)+\frac{5}{18}\binom{1}{2}-\frac{7}{72}\binom{1}{3}-\frac{9}{200}\binom{1}{4}+$$

$$+H_0^0\left(2,R;0,\frac{R}{2}\right)G_0^0(2,R)\,G_0^0\left(3,\frac{R}{2}\right)+3\binom{0}{1}+5\binom{0}{2}+7\binom{0}{3}+9\binom{0}{4}+$$

$$+H_0^0\left(0,R;2,\frac{R}{2}\right)G_0^0(2,R)\,G_0^0\left(3,\frac{R}{2}\right)+3\binom{0}{1}+5\binom{0}{2}+7\binom{0}{3}+9\binom{0}{4}+$$

$$+H_0^0\left(0,R;0,\frac{R}{2}\right)G_0^0(4,R)\,G_0^0\left(3,\frac{R}{2}\right)+3\binom{0}{1}+5\binom{0}{2}+7\binom{0}{3}+9\binom{0}{4}+$$

$$+H_0^0\left(0,R,0,\frac{R}{2}\right)G_0^0(2,R)\,G_0^0\left(5,\frac{R}{2}\right)+3\binom{0}{1}+5\binom{3}{2}+7\binom{0}{3}+9\binom{0}{4}=$$

$$-2H_0^0\left(1,R;1,\frac{R}{2}\right)G_0^0(3,R)\,G_0^0\left(4,\frac{R}{2}\right)-6\binom{0}{1}-10\binom{0}{2}-14\binom{0}{3}-18\binom{0}{4}-$$

$$-2H_0^0\left(0,R;0,\frac{R}{2}\right)G_0^0(2,R)\,G_0^0\left(3,\frac{R}{2}\right)-6\binom{0}{1}-10\binom{0}{2}-14\binom{0}{3}-18\binom{0}{4}-$$

$$+\frac{3}{2}H_1^1\left(0,R;0,\frac{R}{2}\right)G_1^1(2,R)\,G_1^1\left(3,\frac{R}{2}\right)+\frac{5}{13}\binom{1}{2}+\frac{7}{72}\binom{1}{3}+\frac{9}{200}\binom{1}{4}\Bigg\}.$$

$$I(2,0,1,0,0,0,0,0,2) =$$

$$= \frac{R^2}{64}\left\{\left[A_4(R)A_2\left(\frac{R}{2}\right)+A_2(R)A_4\left(\frac{R}{2}\right)-2A_2(R)A_2\left(\frac{R}{2}\right)\right]B_0(R)B_0\left(\frac{R}{2}\right)+\right.$$

$$+A_2(R)A_2\left(\frac{R}{2}\right)\left[B_2(R)B_0\left(\frac{R}{2}\right)+B_0(R)B_2\left(\frac{R}{2}\right)\right]-$$

$$-2A_3(R)A_3\left(\frac{R}{2}\right)B_1(R)B_1\left(\frac{R}{2}\right)-$$

$$-\left[A_4(R)A_0\left(\frac{R}{2}\right)+A_2(R)A_2\left(\frac{R}{2}\right)-2A_2(R)A_0\left(\frac{R}{2}\right)\right]B_0(R)B_2\left(\frac{R}{2}\right)-$$

$$-A_0(R)A_0\left(\frac{R}{2}\right)\left[B_2(R)B_2\left(\frac{R}{2}\right)+B_0(R)B_4\left(\frac{R}{2}\right)\right]+$$

$$+2A_3(R)A_1\left(\frac{R}{2}\right)B_1(R)B_3\left(\frac{R}{2}\right)-$$

$$-\left[A_2(R)A_2\left(\frac{R}{2}\right)+A_0(R)A_4\left(\frac{R}{2}\right)-2A_0(R)A_2\left(\frac{R}{2}\right)\right]B_2(R)B_0\left(\frac{R}{2}\right)-$$

$$-A_0(R)A_2\left(\frac{R}{2}\right)\left[B_4(R)B_0\left(\frac{R}{2}\right)+B_2(R)B_2\left(\frac{R}{2}\right)\right]+$$

$$+2A_1(R)A_3\left(\frac{R}{2}\right)B_3(R)B_1\left(\frac{R}{2}\right)+$$

$$+\left[A_2(R)A_0\left(\frac{R}{2}\right)+A_0(R)A_2\left(\frac{R}{2}\right)-2A_0(R)A_0\left(\frac{R}{2}\right)\right]B_2(R)B_2\left(\frac{R}{2}\right)+$$

$$+A_0(R)A_0\left(\frac{R}{2}\right)\left[B_4(R)B_2\left(\frac{R}{2}\right)+B_2(R)B_4\left(\frac{R}{2}\right)\right]-$$

$$\left.-2A_1(R)A_1\left(\frac{R}{2}\right)B_3(R)B_4\left(\frac{R}{2}\right)\right\}.$$

$$I(1,1,1,0,0,0,0,0,1) =$$

$$= \frac{R^7}{16}\left\{\left[H_0^0\left(4,R;2,\frac{R}{2}\right)+H_0^0\left(2,R;4,\frac{R}{2}\right)-\right.\right.$$

$$\left.-\frac{5}{3}H_0^0\left(2,R;2,\frac{R}{2}\right)\right]G_0^0\left(0,\frac{R}{2}\right)+$$

$$+H_0^0\left(2,R;2,\frac{R}{2}\right)G_0^0\left(2,\frac{R}{2}\right)-2H_1^0\left(3,R;3,\frac{R}{2}\right)G_1^0\left(1,\frac{R}{2}\right)+$$

$$+\frac{2}{3}\left(2,R;2,\frac{R}{2}\right)G_2^0\left(0,\frac{R}{2}\right)+H_1^1\left(2,R;2,\frac{R}{2}\right)G_1^1\left(0,\frac{R}{2}\right)-$$

$$
\begin{aligned}
&- \left[H_0^0\left(4, R; 0, \frac{R}{2}\right) + H_0^0\left(2, R; 2, \frac{R}{2}\right) - \right. \\
&\left. - \frac{5}{3} H_0^0\left(2, R; 0, \frac{R}{2}\right) \right] G_0^0\left(2, \frac{R}{2}\right) - \\
&- H_0^0\left(2, R; 0, \frac{R}{2}\right) G_0^0\left(4, \frac{R}{2}\right) + 2 H_1^0\left(3, R; 1, \frac{R}{2}\right) G_1^0\left(3, \frac{R}{2}\right) - \\
&- \frac{2}{3} H_2^0\left(2, R; 0, \frac{R}{2}\right) G_2^0\left(2, \frac{R}{2}\right) - H_1^1\left(2, R; 0, \frac{R}{2}\right) G_1^1\left(2, \frac{R}{2}\right) - \\
&- \frac{1}{3} \left[H_0^0\left(2, R; 2, \frac{R}{2}\right) + H_0^0\left(0, R; 4, \frac{R}{2}\right) - \right. \\
&\left. - \frac{7}{5} H_0^0\left(0, R; 2, \frac{R}{2}\right) \right] G_0^0\left(0, \frac{R}{2}\right) - \\
&- \frac{1}{3} H_0^0\left(0, R; 2, \frac{R}{2}\right) G_0^0\left(2, \frac{R}{2}\right) + \frac{6}{5} H_1^0\left(1, R; 3, \frac{R}{2}\right) G_1^0\left(1, \frac{R}{2}\right) - \\
&- \frac{2}{3} \left[H_2^0\left(2, R; 2, \frac{R}{2}\right) + H_2^0\left(0, R; 4, \frac{R}{2}\right) - \right. \\
&\left. - \frac{8}{7} H_2^0\left(0, R; 2, \frac{R}{2}\right) \right] G_2^0\left(0, \frac{R}{2}\right) - \\
&- \frac{2}{3} H_2^0\left(0, R; 2, \frac{R}{2}\right) G_2^0\left(2, \frac{R}{2}\right) + H_3^0\left(1, R; 3, \frac{R}{2}\right) G_3^0\left(1, \frac{R}{2}\right) - \\
&- \frac{8}{35} H_4^0\left(0, R; 2, \frac{R}{2}\right) G_4^0\left(0, \frac{R}{2}\right) - \frac{1}{5} H_1^1\left(0, R; 2, \frac{R}{2}\right) G_1^1\left(0, \frac{R}{2}\right) - \\
&- \frac{1}{45} H_3^1\left(0, R; 2, \frac{R}{2}\right) G_3^1\left(0, \frac{R}{2}\right) + \\
&+ \frac{1}{3} \left[H_0^0\left(2, R; 0, \frac{R}{2}\right) + H_0^0\left(0, R; 2, \frac{R}{2}\right) - \right. \\
&\left. - \frac{7}{5} H_0^0\left(0, R; 0, \frac{R}{2}\right) \right] G_0^0\left(2, \frac{R}{2}\right) + \\
&+ \frac{1}{3} H_0^0\left(0, R; 0, \frac{R}{2}\right) G_0^0\left(4, \frac{R}{2}\right) - \frac{6}{5} H_1^0\left(1, R; 1, \frac{R}{2}\right) G_1^0\left(3, \frac{R}{2}\right) + \\
&+ \frac{2}{3} \left[H_2^0\left(2, R; 0, \frac{R}{2}\right) + H_2^0\left(0, R; 2, \frac{R}{2}\right) - \right. \\
&\left. - \frac{8}{7} H_2^0\left(0, R; 0, \frac{R}{2}\right) \right] G_2^0\left(2, \frac{R}{2}\right) +
\end{aligned}
$$

$$+\frac{2}{3}H_2^0\left(0,R;0,\frac{R}{2}\right)G_2^0\left(4,\frac{R}{2}\right)-\frac{4}{5}H_3^0\left(1,R;1,\frac{R}{2}\right)G_3^0\left(3,\frac{R}{2}\right)+$$

$$+\frac{8}{35}H_4^0\left(0,R,0,\frac{R}{2}\right)G_4^0\left(2,\frac{R}{2}\right)+\frac{1}{5}H_1^1\left(0,R;0,\frac{R}{2}\right)G_1^1\left(2,\frac{R}{2}\right)+$$

$$+\frac{1}{45}H_3^1\left(0,R;0,\frac{R}{2}\right)G_3^1\left(2,\frac{R}{2}\right)\Bigg\}.$$

$$I(1,1,1,0,-1,0,0,0,1)=$$

$$=\frac{R^2}{16}\Bigg\{\Bigg[H_0^0\left(3,R;2,\frac{R}{2}\right)+H_0^0\left(1,R;4,\frac{R}{2}\right)-$$

$$-\frac{5}{3}H_0^0\left(1,R;2,\frac{R}{2}\right)\Bigg]G_0^0\left(0,\frac{R}{2}\right)+$$

$$+H_0^0\left(1,R;2,\frac{R}{2}\right)G_0^0\left(2,\frac{R}{2}\right)-2H_1^0\left(2,R;3,\frac{R}{2}\right)G_1^0\left(1,\frac{R}{2}\right)+$$

$$+\frac{2}{3}H_2^0\left(1,R;2,\frac{R}{2}\right)G_2^0\left(0,\frac{R}{2}\right)+H_1^1\left(1,R;2,\frac{R}{2}\right)G_1^1\left(0,\frac{R}{2}\right)-$$

$$-\Bigg[H_0^0\left(3,R;0,\frac{R}{2}\right)+H_0^0\left(1,R;2,\frac{R}{2}\right)-$$

$$-\frac{5}{3}H_0^0\left(1,R;0,\frac{R}{2}\right)\Bigg]G_0^0\left(2,\frac{R}{2}\right)-$$

$$-H_0^0\left(1,R;0,\frac{R}{2}\right)G_0^0\left(4,\frac{R}{2}\right)+2H_1^0\left(2,R;1,\frac{R}{2}\right)G_1^0\left(3,\frac{R}{2}\right)-$$

$$-\frac{2}{3}H_2^0\left(1,R;0,\frac{R}{2}\right)G_2^0\left(2,\frac{R}{2}\right)-H_1^1\left(1,R;0,\frac{R}{2}\right)G_1^1\left(2,\frac{R}{2}\right)-$$

$$-\Bigg[H_1^0\left(2,R;2,\frac{R}{2}\right)+H_1^0\left(0,R;4,\frac{R}{2}\right)-$$

$$-\frac{7}{5}H_1^0\left(0,R;2,\frac{R}{2}\right)\Bigg]G_1^0\left(0,\frac{R}{2}\right)+$$

$$+\frac{2}{3}H_0^0\left(1,R;3,\frac{R}{2}\right)G_0^0\left(1,\frac{R}{2}\right)-H_1^0\left(0,R;2,\frac{R}{2}\right)G_1^0\left(2,\frac{R}{2}\right)+$$

$$+\frac{4}{3}H_2^0\left(1,R;3,\frac{R}{2}\right)G_2^0\left(1,\frac{R}{2}\right)-\frac{2}{5}H_3^0\left(0,R;2,\frac{R}{2}\right)G_3^0\left(0,\frac{R}{2}\right)-$$

$$-\frac{3}{5}H_2^1\left(0,R;2,\frac{R}{2}\right)G_2^1\left(0,\frac{R}{2}\right)+$$

$$+\left[H_1^0\left(2, R; 0, \frac{R}{2}\right) + H_1^0\left(0, R; 2, \frac{R}{2}\right) -\right.$$

$$\left. -\frac{7}{5} H_1^0\left(0, R; 0, \frac{R}{2}\right)\right] G_1^0\left(2, \frac{R}{2}\right) -$$

$$-\frac{2}{3} H_0^0\left(1, R; 1, \frac{R}{2}\right) G_0^0\left(3, \frac{R}{2}\right) + H_1^0\left(0, R; 0, \frac{R}{2}\right) G_1^0\left(4, \frac{R}{2}\right) -$$

$$-\frac{4}{3} H_2^0\left(1, R; 1, \frac{R}{2}\right) G_2^0\left(3, \frac{R}{2}\right) + \frac{2}{5} H_3^0\left(0, R; 0, \frac{R}{2}\right) G_3^0\left(2, \frac{R}{2}\right) +$$

$$+\frac{3}{5} H_2^1\left(0, R; 0, \frac{R}{2}\right) G_2^1\left(2, \frac{R}{2}\right)\Big\}.$$

$$I(1, 1, 1, 0, 0, 0, 0, 0, 2) =$$

$$= \frac{R^8}{32}\left\{\left[A_4(R) A_2\left(\frac{R}{2}\right) + A_2(R) A_4\left(\frac{R}{2}\right) - 2 A_2(R) A_2\left(\frac{R}{2}\right)\right] B_0\left(\frac{R}{2}\right) +\right.$$

$$\left. + A_2(R) A_2\left(\frac{R}{2}\right)\left[\frac{1}{3} B_0\left(\frac{R}{2}\right) + B_2\left(\frac{R}{2}\right)\right] -\right.$$

$$-\left[A_4(R) A_0\left(\frac{R}{2}\right) + A_2(R) A_2\left(\frac{R}{2}\right) - 2 A_2(R) A_0\left(\frac{R}{2}\right)\right] B_2\left(\frac{R}{2}\right) -$$

$$- A_2(R) A_2\left(\frac{R}{2}\right)\left[\frac{1}{3} B_2\left(\frac{R}{2}\right) + B_4\left(\frac{R}{2}\right)\right] -$$

$$-\frac{1}{3}\left[A_2(R) A_2\left(\frac{R}{2}\right) + A_0(R) A_4\left(\frac{R}{2}\right) - 2 A_0(R) A_2\left(\frac{R}{2}\right)\right] B_0\left(\frac{R}{2}\right) -$$

$$- A_0(R) A_2\left(\frac{R}{2}\right)\left[\frac{1}{5} B_0\left(\frac{R}{2}\right) + \frac{1}{3} B_2\left(\frac{R}{2}\right)\right] +$$

$$+\frac{1}{3}\left[A_2(R) A_0\left(\frac{R}{2}\right) + A_0(R) A_2\left(\frac{R}{2}\right) - 2 A_0(R) A_0\left(\frac{R}{2}\right)\right] B_2\left(\frac{R}{2}\right) +$$

$$\left. + A_0(R) A_0\left(\frac{R}{2}\right)\left[\frac{1}{5} B_2(R) + \frac{1}{3} B_4\left(\frac{R}{2}\right)\right]\right\}.$$

$$I\left(2, 0, \frac{1}{2}, \frac{1}{2}, 0, 0, 0, 0, 1\right) =$$

$$= \frac{R^7}{16}\left\{\left[H_0^0\left(4, R; 2, \frac{R}{2}\right) + H_0^0\left(2, R; 4, \frac{R}{2}\right) -\right.\right.$$

$$\left.\left. -\frac{5}{3} H_0^0\left(2, R; 2, \frac{R}{2}\right)\right] G_0^0(0, R) +\right.$$

$$+ H_0^0\left(2, R; 2, \frac{R}{2}\right) G_0^0(2, R) - 2 H_1^0\left(3, R; 3, \frac{R}{2}\right) G_1^0(1, R) +$$

$$+ \frac{2}{3} H_2^0\left(2, R; 2, \frac{R}{2}\right) G_2^0(0, R) + H_1^1\left(2, R; 2, \frac{R}{2}\right) G_1^1(0, R) -$$

$$- \frac{1}{3}\left[H_0^0\left(4, R; 0, \frac{R}{2}\right) + H_0^0\left(2, R; 2, \frac{R}{2}\right) -\right.$$

$$\left. - \frac{7}{5} H_0^0\left(2, R; 0, \frac{R}{2}\right)\right] G_0^0(0, R) -$$

$$- \frac{1}{3} H_0^0\left(2, R; 0, \frac{R}{2}\right) G_0^0(2, R) + \frac{6}{5} H_1^0\left(3, R; 1, \frac{R}{2}\right) G_1^0(1, R) -$$

$$- \frac{2}{3}\left[H_2^0\left(4, R; 0, \frac{R}{2}\right) + H_2^0\left(2, R; 2, \frac{R}{2}\right) -\right.$$

$$\left. - \frac{8}{7} H_2^0\left(2, R; 0, \frac{R}{2}\right)\right] G_1^0(0, R) -$$

$$- \frac{2}{3} H_2^0\left(2, R; 0, \frac{R}{2}\right) G_2^0(2, R) + \frac{4}{5} H_3^0\left(3, R; 1, \frac{R}{2}\right) G_3^0(1, R) -$$

$$- \frac{8}{35} H_4^0\left(2, R; 0, \frac{R}{2}\right) G_4^0(0, R) - \frac{1}{5} H_1^1\left(2, R; 0, \frac{R}{2}\right) G_3^0(0, R) -$$

$$- \frac{1}{45} H_3^1\left(2, R; 0, \frac{R}{2}\right) G_3^1(0, R) -$$

$$- \left[H_0^0\left(2, R; 2, \frac{R}{2}\right) + H_0^0\left(0, R; 4, \frac{R}{2}\right) -\right.$$

$$\left. - \frac{5}{3} H_0^0\left(0, R; 2, \frac{R}{2}\right)\right] G_0^0(2, R) -$$

$$- H_0^0\left(0, R; 2, \frac{R}{2}\right) G_0^0(4, R) + 2 H_1^0\left(1, R; 3, \frac{R}{2}\right) G_1^0(3, R) -$$

$$- \frac{2}{3} H_2^0\left(0, R; 2, \frac{R}{2}\right) G_2^0(2, R) - H_1^1\left(0, R; 2, \frac{R}{2}\right) G_1^1(2, R) +$$

$$+ \frac{1}{3}\left[H_0^0\left(2, R; 0, \frac{R}{2}\right) + H_0^0\left(0, R; 2, \frac{R}{2}\right) -\right.$$

$$\left. - \frac{7}{5} H_0^0\left(0, R; 0, \frac{R}{2}\right)\right] G_0^0(2, R) +$$

$$+ \frac{1}{3} H_0^0\left(0, R; 0, \frac{R}{2}\right) G_0^0(4, R) - \frac{6}{5} H_1^0\left(1, R; 1, \frac{R}{2}\right) G_1^0(3, R) +$$

$$+\frac{2}{3}\left[H_2^0\left(2, R; 0, \frac{R}{2}\right)+H_2^0\left(0, R; 2, \frac{R}{2}\right)-\right.$$

$$\left.-\frac{8}{7}H_2^0\left(0, R; 0, \frac{R}{2}\right)\right]G_2^0(2, R)+$$

$$+\frac{2}{3}H_2^0\left(0, R; 0, \frac{R}{2}\right)G_2^0(4, R)-\frac{4}{5}H_3^0\left(1, R; 1, \frac{R}{2}\right)G_2^0(3, R)+$$

$$+\frac{8}{35}H_4^0\left(0, R; 0, \frac{R}{2}\right)G_4^0(2, R)+\frac{1}{4}H_1^1\left(0, R; 0, \frac{R}{2}\right)G_1^1(2, R)+$$

$$\left.+\frac{1}{45}H_3^1\left(0, R; 0, \frac{R}{2}\right)G_3^1(2, R)\right\}.$$

$$I\left(2, 0, \frac{1}{2}, \frac{1}{2}, 0, -1, 0, 0, 1\right)=$$

$$=\frac{R^6}{8}\left\{\left[H_0^0\left(3, R; 2, \frac{R}{2}\right)+H_0^0\left(1, R; 4, \frac{R}{2}\right)-\right.\right.$$

$$\left.-\frac{5}{3}H_0^0\left(1, R; 2, \frac{R}{2}\right)\right]G_0^0(0, R)+$$

$$+H_0^0\left(1, R; 2, \frac{R}{2}\right)G_0^0(2, R)-2H_1^0\left(2, R; 3, \frac{R}{2}\right)G_1^0(1, R)+$$

$$+\frac{2}{3}H_2^0\left(1, R; 2, \frac{R}{2}\right)G_2^0(0, R)+H_1^1\left(1, R; 2, \frac{R}{2}\right)G_1^0(0, R)-$$

$$-\frac{1}{3}\left[H_0^0\left(3, R; 0, \frac{R}{2}\right)+H_0^0\left(1, R; 2, \frac{R}{2}\right)-\right.$$

$$\left.-\frac{7}{5}H_0^0\left(1, R; 0, \frac{R}{2}\right)\right]G_0^0(0, R)-$$

$$-\frac{1}{3}H_0^0\left(1, R; 0, \frac{R}{2}\right)G_0^0(2, R)+\frac{6}{5}H_1^0\left(2, R; 1, \frac{R}{2}\right)G_1^0(1, R)-$$

$$-\frac{2}{3}\left[H_2^0\left(3, R; 0, \frac{R}{2}\right)+H_2^0\left(1, R; 2, \frac{R}{2}\right)-\right.$$

$$\left.-\frac{8}{7}H_2^0\left(1, R; 0, \frac{R}{2}\right)\right]G_2^0(0, R)-$$

$$-\frac{2}{3}H_2^0\left(1, R; 0, \frac{R}{2}\right)G_2^0(2, R)+\frac{4}{5}H_3^0\left(2, R; 1, \frac{R}{2}\right)G_3^0(1, R)-$$

$$-\frac{8}{35}H_4^0\left(1, R; 0, \frac{R}{2}\right)G_4^0(0, R)-\frac{1}{5}H_1^1\left(1, R; 0, \frac{R}{2}\right)G_1^0(0, R)-$$

$$-\frac{1}{45}H_3^1\left(1,R;0,\frac{R}{2}\right)G_3^1(0,R)+$$

$$+\left[H_0^0\left(2,R;2,\frac{R}{2}\right)+H_0^0\left(0,R;4,\frac{R}{2}\right)-\right.$$

$$\left.-\frac{5}{3}H_0^0\left(0,R;2,\frac{R}{2}\right)\right]G_0^0(1,R)+$$

$$+H_0^0\left(2,R;2,\frac{R}{2}\right)G_0^0(3,R)-2H_1^0\left(1,R;3,\frac{R}{2}\right)G_1^0(2,R)+$$

$$+\frac{2}{3}H_2^0\left(0,R;2,\frac{R}{2}\right)G_2^0(1,R)+H_1^1\left(0,R;2,\frac{R}{2}\right)G_1^1(1,R)-$$

$$-\frac{1}{3}\left[H_0^0\left(2,R;0,\frac{R}{2}\right)+H_0^0\left(0,R;2,\frac{R}{2}\right)-\right.$$

$$\left.-\frac{7}{5}H_0^0\left(0,R;0,\frac{R}{2}\right)\right]G_0^0(1,R)-$$

$$-\frac{1}{3}H_0^0\left(0,R;0,\frac{R}{2}\right)G_0^0(3,R)+\frac{6}{5}H_1^0\left(1,R;1,\frac{R}{2}\right)G_2^0(2,R)-$$

$$-\frac{2}{3}\left[H_2^0\left(2,R;0,\frac{R}{2}\right)+H_2^0\left(0,R;2,\frac{R}{2}\right)-\right.$$

$$\left.-\frac{8}{7}H_2^0\left(0,R;0,\frac{R}{2}\right)\right]G_2^0(1,R)-$$

$$-\frac{2}{3}H_2^0\left(0,R;0,\frac{R}{2}\right)G_0^0(3,R)+\frac{4}{5}\left(1,R;1,\frac{R}{2}\right)G_3^0(2,R)-$$

$$-\frac{8}{35}H_4^0\left(0,R;0,\frac{R}{2}\right)G_4^0(1,R)-\frac{1}{5}H_1^1\left(0,R;0,\frac{R}{2}\right)G_1^1(1,R)-$$

$$\left.-\frac{1}{45}H_3^1\left(0,R;0,\frac{R}{2}\right)G_3^1(1,R)\right\}.$$

$$I\left(2,0,\frac{1}{2},\frac{1}{2},0,0,0,0,2\right)=$$

$$=\frac{R^8}{32}\left\{\left[A_4(R)A_2\left(\frac{R}{2}\right)+A_2(R)A_4\left(\frac{R}{2}\right)-2A_2(R)A_2\left(\frac{R}{2}\right)\right]B_0(R)+\right.$$

$$+A_2(R)A_2\left(\frac{R}{2}\right)\left[\frac{1}{3}B_0(R)+B_2(R)\right]-$$

$$-\frac{1}{3}\left[A_4(R)A_0\left(\frac{R}{2}\right)+A_2(R)A_2\left(\frac{R}{2}\right)-2A_2(R)A_0\left(\frac{R}{2}\right)\right]B_0(R)-$$

$$- A_2(R) A_0\left(\frac{R}{2}\right)\left[\frac{1}{5} B_0(R) + \frac{1}{3} B_2(R)\right] -$$

$$- \left[A_2(R) A_2\left(\frac{R}{2}\right) + A_0(R) A_4\left(\frac{R}{2}\right) - 2A_0(R) A_2\left(\frac{R}{2}\right)\right] B_2(R) -$$

$$- A_0(R) A_2\left(\frac{R}{2}\right)\left[\frac{1}{3} B_2(R) + B_4(R)\right] -$$

$$+ \frac{1}{3}\left[A_2(R) A_0\left(\frac{R}{2}\right) + A_0(R) A_0\left(\frac{R}{2}\right) - 2A_0(R) A_0\left(\frac{R}{2}\right)\right] B_2(R) +$$

$$+ A_0(R) A_0\left(\frac{R}{2}\right)\left[\frac{1}{5} B_2(R) + \frac{1}{3} B_4(R)\right]\Bigg\} .$$

$$I\left(1, 1, \frac{1}{2}, \frac{1}{2}, 0, 0, 0, 0, 1\right) =$$

$$= \frac{R^7}{8}\Bigg\{ H_0^0\left(4, R; 2, \frac{R}{2}\right) + H_0^0\left(2, R; 4, \frac{R}{2}\right) - \frac{4}{3} H_0^0\left(2, R; 2, \frac{R}{2}\right) -$$

$$- \frac{2}{3} H_1^0\left(3, R; 3, \frac{R}{2}\right) + \frac{2}{3} H_1^1\left(2, R; 2, \frac{R}{2}\right) -$$

$$- \frac{1}{3}\left[H_0^0\left(4, R; 0, \frac{R}{2}\right) + H_0^0\left(2, R; 2, \frac{R}{2}\right) - \frac{16}{15} H_0^0\left(2, R; 0, \frac{R}{2}\right)\right] +$$

$$+ \frac{2}{5} H_1^0\left(3, R; 1, \frac{R}{2}\right) - \frac{4}{45} H_2^0\left(2, R; 0, \frac{R}{2}\right) - \frac{2}{15} H_1^1\left(2, R; 0, \frac{R}{2}\right) -$$

$$- \frac{1}{3}\left[H_0^0\left(2, R; 2, \frac{R}{2}\right) + H_0^0\left(0, R; 4, \frac{R}{2}\right) - \frac{16}{15} H_0^0\left(0, R; 2, \frac{R}{2}\right)\right] +$$

$$+ \frac{2}{5} H_1^0\left(1, R; 3, \frac{R}{2}\right) - \frac{4}{45} H_2^0\left(0, R; 2, \frac{R}{2}\right) - \frac{2}{15} H_1^1\left(0, R; 2, \frac{R}{2}\right)\right] +$$

$$+ \frac{1}{9}\left[H_0^0\left(2, R; 0, \frac{R}{2}\right) + H_0^0\left(0, R; 2, \frac{R}{2}\right) - \frac{4}{5} H_0^0\left(0, R; 0, \frac{R}{2}\right)\right] +$$

$$+ \frac{4}{45}\left[H_0^0\left(2, R; 0, \frac{R}{2}\right) + H_2^0\left(0, R; 2, \frac{R}{2}\right) - \frac{2}{7} H_2^0\left(0, R; 0, \frac{R}{2}\right)\right] -$$

$$- \frac{6}{25} H_1^0\left(1, R; 1, \frac{R}{2}\right) - \frac{8}{175} H_3^0\left(1, R; 1, \frac{R}{2}\right) +$$

$$+ \frac{2}{75} H_1^1\left(0, R; 0, \frac{R}{2}\right) + \frac{8}{1575} H_3^1\left(0, R; 0, \frac{R}{2}\right)\Bigg\} .$$

$$I\left(1, 1, \frac{1}{2}, \frac{1}{2}, 0, 0, 0, 1, 1\right) =$$

$$= \frac{R^8}{16}\left\{H_0^0\left(4, R; 3, \frac{R}{2}\right) + H_0^0\left(2, R; 5, \frac{R}{2}\right) - \frac{4}{3}H_0^0\left(2, R; 3, \frac{R}{2}\right) -\right.$$

$$- \frac{2}{3}H_1^0\left(3, R; 4, \frac{R}{2}\right) + \frac{2}{3}H_1^1\left(2, R; 3, \frac{R}{2}\right) -$$

$$- \frac{1}{3}\left[H_0^0\left(4, R; 1, \frac{R}{2}\right) + H_0^0\left(2, R; 3, \frac{R}{2}\right) - \frac{16}{15}H_0^0\left(2, R; 1, \frac{R}{2}\right)\right] +$$

$$+ \frac{2}{5}H_1^0\left(3, R; 2, \frac{R}{2}\right) - \frac{4}{45}H_2^0\left(2, R; 1, \frac{R}{2}\right) - \frac{2}{15}H_1^1\left(2, R; 1, \frac{R}{2}\right) -$$

$$- \frac{1}{3}\left[H_0^0\left(2, R; 3, \frac{R}{2}\right) + H_0^0\left(0, R; 5, \frac{R}{2}\right) - \frac{16}{15}H_0^0\left(0, R; 3, \frac{R}{2}\right)\right] -$$

$$+ \frac{2}{5}H_1^0\left(1, R; 4, \frac{R}{2}\right) - \frac{4}{45}H_2^0\left(0, R; 3, \frac{R}{2}\right) - \frac{4}{45}H_1^1\left(0, R; 3, \frac{R}{2}\right) +$$

$$+ \frac{2}{9}\left[H_0^0\left(2, R; 1, \frac{R}{2}\right) + H_0^0\left(0, R; 3, \frac{R}{2}\right) - \frac{4}{5}H_0^0\left(0, R; 1, \frac{R}{2}\right)\right] +$$

$$+ \frac{4}{45}\left[H_3^0\left(2, R; 1, \frac{R}{2}\right) + H_2^0\left(0, R; 3, \frac{R}{2}\right) - \frac{2}{7}H_2^0\left(0, R; 1, \frac{R}{2}\right) -\right.$$

$$- \frac{6}{25}H_2^0\left(1, R; 2, \frac{R}{2}\right) - \frac{8}{175}H_3^0\left(1, R; 2, \frac{R}{2}\right) +$$

$$\left.+ \frac{2}{75}H_1^1\left(0, R; 1, \frac{R}{2}\right) + \frac{3}{1575}H_3^1\left(0, R; 1, \frac{R}{2}\right)\right\}.$$

$$I\left(1, 1, \frac{1}{2}, \frac{1}{2}, 0, 0, 0, 0, 2\right) =$$

$$= \frac{R^8}{16}\left\{A_4(R)A_2\left(\frac{R}{2}\right) + A_2(R)A_4\left(\frac{R}{2}\right) - \frac{4}{3}A_2(R)A_2\left(\frac{R}{2}\right) +\right.$$

$$+ \frac{1}{3}\left[A_4(R)A_0\left(\frac{R}{2}\right) + A_2(R)A_2\left(\frac{R}{2}\right) - \frac{16}{15}A_2(R)A_0\left(\frac{R}{2}\right)\right] +$$

$$+ \frac{1}{3}\left[A_2(R)A_2\left(\frac{R}{2}\right) + A_0(R)A_4\left(\frac{R}{2}\right) - \frac{16}{25}A_0(R)A_2\left(\frac{R}{R}\right)\right] +$$

$$\left.+ \frac{1}{9}\left[A_2(R)A_0\left(\frac{R}{2}\right) + A_0(R)A_2\left(\frac{R}{2}\right) - \frac{4}{5}A_0(R)A_0\left(\frac{R}{2}\right)\right]\right\}.$$

$\binom{i}{k} = H_k^i G_k^i G_k^i$ mit den Argumenten in den betreffenden Reihen.

LITERATUR

1. V. Guillemin and C. Zener, Phys. Rev., **34**, 999, 1929.
2. R. Present, J. Chem. Phys., **3**, 122, 1936.
3. H. M. James, A. S. Coolidge and R. D. Present, J. Chem. Phys., **4**, 187, 1936.
4. A. S. Coolidge and H. M. James, J. Chem. Phys., **6**, 730, 1938.
5. W. Kołos and C. C. J. Roothaan, Revs. Modern Phys., **32**, 219, 1960.
6. E. R. Davidson, J. Chem. Phys., **33**, 1577, 1960.
7. W. Kołos and L. Wolniewicz, J. Chem. Phys., **43**, 2429, 1965; **45**, 509, 1966.
8. P. E. Phillipson and R. S. Mulliken, J. Chem. Phys., **28**, 1248, 1958.
9. F. Berencz, Acta Phys. Hung., **16**, 49, 1963; **18**, 307, 1965.
10. J. C. Browne, J. Chem. Phys., **40**, 43, 1964; **41**, 1583, 1964; Phys. Rev., **138**, A9, 1965
11. S. Huzinage, Progr. Theoret. Phys., **15**, 162, 1956; **17**, 169, 1957.
12. I. Tamássy-Lentei, Acta Phys. Hung., **12**, 119, 1960.
13. H. S. Taylor, J. Chem. Phys., **39**, 3375, 1963.
14. Y. Kato, E. Hayes, and A. B. F. Duncan, J. Chem. Phys., **41**, 986, 1964.
15. J. T. Zung and A. B. F. Duncan, J. Chem. Phys., **36**, 2140, 1962.
16. S. Rothenberg and E. Davidson, J. Chem. Phys., **45**, 2560, 1966.
17. F. Berencz, Acta Phys. Hung., **6**, 149, 1956.
18. A. A. Frost und J. Braunstein, J. Chem. Phys., **19**, 1133, 1951.
19. M. Kotani, A. Amemiya und T. T. Simose, Proc. Phys. Mat. Soc. Japan, 20, **extra No 1**, 1938; 22. extra No 2, 1940.

ВЫЧИСЛЕНИЕ СОСТОЯНИЯ $1sns\ ^1\Sigma_g^+$ МОЛЕКУЛЫ ВОДОРОДА НА ОСНОВЕ МЕТОДА КОРРЕЛЯЦИОННО-УМЕРЕННЫХ МОЛЕКУЛЯРНЫХ ОРБИТ

Ф. БЕРЕНЦ

Резюме

Определяется электронная энергия состояния $1s2s\ ^1\Sigma_g^+$ молекулы водорода на основе метода корреляционно-умеренных молекулярных орбит. Далее показывается, что расширением собственной функции с корреляционным фактором достигается значительное улучшение в энергии только в случае, если там не имеет место корреляция электронов.

Acta Physica Academiae Scientiarum Hungaricae, Tomus 27, pp. 151—160 (1969)

ON THE STRUCTURE AND SPECTRA OF σ-ELECTRON SYSTEMS*

By

C. SÁNDORFY

DÉPARTEMENT DE CHIMIE, UNIVERSITÉ DE MONTRÉAL, MONTRÉAL, QUÉBEC, CANADA

(Received 13. I. 1969)

Recent advances in the theories of saturated hydrocarbons are briefly reviewed. The problem of the non-additivity of certain ground state properties of these molecules is discussed as well as their electronic absorption spectra.

Introduction

The interest of quantum chemists in the properties of larger saturated organic molecules is relatively recent. The approximate additivity of certain physico-chemical quantities in the case of paraffins seemed to render calculations on these of no great interest. First attempts to treat σ-electron systems by approximative wave mechanical methods were based on group — or bond orbitals. These have been reviewed [1,2] and we shall refrain from doing this again. We prefer to take the attitude that localizability or additivity relationships, if these apply, should be a result of the calculations and not their starting point.

There are at least two properties of saturated molecules which exhibit a clear departure of additivity or localizability.

1) The heats of formation show a slight but well established default of additivity (Table I).

2) The first ionization potentials of normal-paraffins show an outspoken diminishing trend with increasing chain length (Table II). They drop from 13.17 ev for methane to 10.19 for n-decane.

Table I

Observed heats of formation of paraffins in units of resonance integral $\beta = -38.866$ kcal-M after subtracting the contributions of the C—H bonds. After KLOPMAN [6]

Methane	0
Ethane	2
Propane	4.06
Isobutane	6.20
Neopentane	8.34
Cyclohexane	12.43

* Dedicated to Prof. P. GOMBÁS on his 60th birthday. The author wishes to express his deep appreciation of the lifetime scientific work of Professor P. GOMBÁS from whom he received his first training in theoretical physics in the early forties.

Table II

Observed ionization potentials of paraffins in ev. After FUKUI, KATO and YONEZAWA [5] and KLOPMAN [6]

Methane	13.17
Ethane	11.76
Propane	11.21
n-Butane	10.80
n-Pentane	10.55
n-Hexane	10.43
n-Heptane	10.35
n-Octane	10.24
n-Decane	10.19
Isobutane	10.40
Neopentane	10.30
Cyclohexane	10.40

Any theory concerned with single bonded systems should be able to interpret these facts.

The first "individual electron" calculations on saturated hydrocarbons were made in 1954 by SÁNDORFY and DAUDEL [3] and by SANDORFY [4]. These works explored the possibility of applying the simple Hückel molecular orbital method in all-valence electron calculations.

Hückel-type methods similar to the above mentioned were extensively used and improved by FUKUI, KATO and YONEZAWA [5] and by KLOPMAN [6] with the main purpose of explaining the behavior of the ionization potentials and heats of formation in series of normal and branched paraffins. This was successfully achieved by these authors with a suitable choice of parameters. A number of problems relating to chemical reactivity have also been treated [7]. Then HOFFMAN [8] introduced the very simple WOLFSBERG—HELMHOLTZ [9] parametrization into σ-Hückel calculations thus providing them with the flexibility necessary to treat stereochemical problems. POPLE and SANTRY [10], in a more elaborate treatment, examined the causes of delocalization and non-additivity in paraffins.

The next stage in the evolution started in 1964 when the Pariser – Parr – Pople method was adapted to σ-electron problems. This has been done by several authors at almost the same time: KLOPMAN [11], POHL, REIN and APPEL [12], POPLE, SANTRY and SEGAL [13], KAUFMAN [14], KATAGIRI and SÁNDORFY [15], SKANCKE [16], YONEZAWA, YAMAGUCHI and KATO [17].

These methods use either the zero differential overlap approximation or MULLIKEN's approximation and differ mainly in the way of handling the interactions between electrons in orbitals on the same atom and by the extent in which atomic spectral data are used for obtaining parameters.

In the writer's opinion,the Hückel and Pariser—Parr – Pople methods have now attained the same degree of usefulness in σ-electron problems as they have in π-electron problems.

Delocalization and ground state properties

In the empirical methods, if hybrid orbitals are used, the interaction between electrons on the same atom but in different orbitals is represented by the resonance integral $m\beta$ where m is a number chosen to be much less than unity and β is the resonance integral for a C—C bond. It is immediately clear (Fig. 1) that the degree of delocalization depends on the value of m and that for $m = 0$ we obtain completely localized bonds.

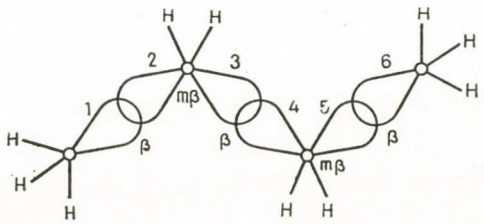

Fig. 1. Carbon hybridized sp^3 orbitals in n-butane

It is interesting in this respect to compare a chain of C—C bonds linked by sp^3 hybrid orbitals and a conjugated chain in which we consider the π—π bonds only.

If all the β were equal in the π calculation every π orbital would have two equivalent neighbors and it is this situation which we call "conjugation", (benzene, for example). In an open chain conjugated molecule like butadiene large β alternate with small ones. In saturated molecules the m value determined by YOSHIZUMI [18] is about 0.35.

Thus we can see that the difference between saturated and conjugated chains is less fundamental than it might appear at first sight. Propane, for example, becomes similar to butadiene. (SIMPSON [19] [20] was able to treat the electronic spectra of both by an excitonic approach that is, supposing localization in individual bonds in the ground state and forming combinations of wave functions excited in anyone bond for the excited states).

KLOPMAN has shown [21] by examining the secular determinants that the introducing of the 2—3 interaction in the Hückel type treatment is equivalent to introducing the nonneighbor 1—4 interaction (Fig. 1). This can be exploited in the treatment of stereochemical problems [22].

If we use pure atomic orbitals instead of hybridized ones in the σ-bond problem (like HOFFMANN [8] or POPLE and SANTRY [10] the relation between delocalization and interactions between orbitals on the same atom is no more evident.

POPLE and SANTRY who used perturbation calculations to establish the causes of delocalization in saturated hydrocarbons found that there are three

of these: the energy difference between $2s$ and $2p$ orbitals; the resonance integrals between chemically non-bonded atoms and the interactions between the $2p_z$ ($\equiv \pi$) orbitals. It is interesting to note that if the axes of the latter are parallel — as in the all-trans isomers — every π electron has two equivalent neighbors although, naturally, the distances between neighbors are now about 1.54 Å.

These considerations may help in the understanding of the behavior of ionization potentials and heats of formation in the paraffin series (cf. Tables I and II).

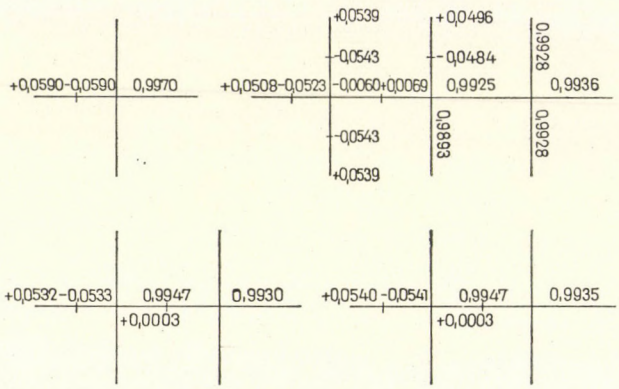

Fig. 2. Effective orbital charges and bond charges in methane, staggered and eclipsed ethane and in propane

The following diagrams (Fig. 2) represent the distribution of electronic charge densities in methane, ethane and propane computed by the PPP-type approximation of KATAGIRI and SÁNDORFY [15]. The hydrogen atoms are seen to loose negative charges amounting to about 0.05 electronic charges. These are picked up essentially by the Csp^3 orbitals linked directly to the hydrogens. Hydrogens on secondary carbons loose slightly less charge than those on primary ones. Bond orders in both C—C and C—H bonds are close to 0.99. This distribution as well as the C—H bond dipole are seen to be in conformity with general chemical knowledge.

It is interesting to note that while delocalization causes an appreciable amount of non-additivity in ionization potentials and heats of formation it affects charge distribution only slightly.

The electronic spectra of σ-electron systems

The electronic spectra of saturated hydrocarbons are located in the far ultraviolet and this is probably the reason why, until recently, they received so little attention. Methane seems to be the only exception. The most complete

works relating to this molecule are those of DITCHBURN [23] and SUN and WEISSLER [24], who also summarized the previous literature. More general works on aliphatic hydrocarbons started appearing four or five years ago. Among these we have to mention those of OKABE and BECKER [25], PARTRIDGE [26], SCHOEN [27] and RAYMONDA and SIMPSON [20]. The absorption spectra of a number of gaseous normal and branched paraffins were measured in the author's laboratory on a McPherson model 225 vacuum ultraviolet monochromator under approximately 0.2 Å resolution from 2000 to 1150 Å using a double beam attachment, a hydrogen light-source and photoelectric recording. Our discussion will be based on these spectra [28] [29].

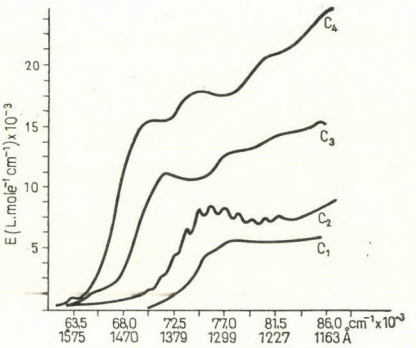

Fig. 3. Far ultraviolet absorption spectra of methane, ethane, propane and n-butane. Molecular extinction coefficients — against wavenumbers

Although a number of theoretical works are now available on ground state properties of saturated hydrocarbons we know only four concerning their electronic spectra. These are: MULLIKEN's united atom treatment [30] [31], the Pariser—Parr—Pople type calculations of KATAGIRI and SÁNDORFY [15] and of BROWN and KRISHNA [32] and the excitonic approach of RAYMONDA and SIMPSON [20].

The following observations can be made.

a) The bands are usually diffuse and no vibrational structure is observed. Ethane is a significant exception to this.

b) There seem to be one or two weak bands, or at least a pronounced inflection between 1630 and 1575 Å, in all the spectra except that of methane. These shift gradually to longer wavelengths.

c) At shorter wavelengths strong bands follow with molecular extinction coefficients in the 10^3—10^4 range. The bands exhibit much larger shifts toward lower frequencies, amounting to 4200 cm^{-1} from ethane to propane for the first strong band, then becoming gradually less and reaching an approximate limit of about 1420 Å for n-pentane. At the same time the intensities increase gradually (Table III), (Fig. 3).

Table III

The wavelengths and molecular extinction coefficients of the first two strong bands of normal paraffins

Compound	I		II	
	λ (Å)	ε(l. mole^{-1}cm^{-1})	λ (Å)	ε(l. mole^{-1}cm^{-1})
Methane	1277	5 839		
Ethane	1318	8 751		
Propane	1395	11 240	1285	13 010
n-Butane	1410	15 420	1335	17 950
n-Pentane	1415	17 330	1345	20 360
n-Hexane	1425	19 560	1335	24 080
n-Heptane	1430	20 950	1340	25 980
n-Octane	1415	24 550	1340	28 960

According to MULLIKEN, the united atom configuration of CH_4 is, omitting carbon 1s orbitals:

$$[sa_1]^2[pf_2]^6\ {}^1A_1\,,$$

where a_1 and f_2 are the usual group theoretical symbols under T_d symmetry. The lowest excited orbitals then would be Rydberg-type, large atomic orbitals 3s, 3p, 3d . . . with 3s lowest. MULLIKEN pointed out, however, that anti-bonding localized C—H orbitals are qualitatively very similar to those of 3s and 3p orbitals of an atom. Thus in this united atom approach the first excited state of methane would have configuration $[sa_1]^2\ [pf_2]^5\ [3sa_1]^1F_2$ and the corresponding transition would be of type

$${}^1F_2 \longleftarrow {}^1A_1 \text{ and allowed}\,.$$

The observed intensity ($\varepsilon = 5800$, oscillator strength $f = 0.26$) seems to justify this assignment although the possibility that the band is a forbidden one borrowing intensity from a stronger transition at higher frequencies is not ruled out. In fact we know from SCHOEN's [27] work that the 1277 Å band of methane is followed by even stronger bands.

In KATAGIRI and SÁNDORFY's scheme (Fig. 4) which is based on the C2s, C2p and H1s orbitals only, the molecular orbitals are, in order of increasing energy, a_1, f_2, a_1, f_2 so that the transition of lowest energy is $a_1 \leftarrow f_2$, that is again ${}^1F_2 \leftarrow {}^1A_1$. The sequence of the excited orbitals, however, depends in a delicate way on the choice of certain parameters. If the order was a_1, f_2, f_2, a_1 the first transition would be $f_2 \leftarrow f_2$ yielding $F_2 \times F_2 = A_1 + E + F_1 + F_2$ the transition to F_2 being allowed and the others forbidden. The latter could be made allowed by vibronic interactions and the band we observed may be

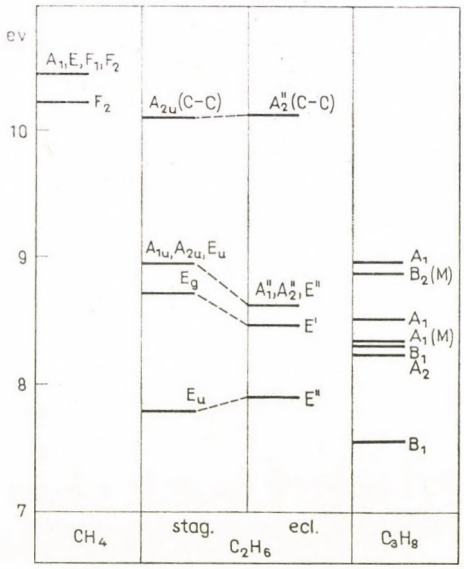

Fig. 4. Energies of the lower singlet—singlet electronic levels of methane, ethane and propane. C—C means that the orbital from which the transition departs (in absorption) has a high population in the C–C bonds; M (mixed) that it has a fairly large population in the C–C bonds. If the state is unmarked then all the charge is in C—H bonds in the orbital of departure. After KATAGIRI and SÁNDORFY[15]

due to these. It is also possible that the shoulder at 1425 Å represents a separate electronic band due to one of these forbidden transitions. We have no means of checking upon these tentative assignments, however.

The ground state of ethane in MULLIKEN's united atom treatment had the following configuration:

$$[sa_1]^2\,[sa_1]^2\,[\pi e]^4\,[\pi e]^4\,[\sigma+\sigma]^2\,{}^1A_1$$
$$CH_3\ \ CH_3\ \ CH_3\ \ CH_3\ \ C-C$$

Here the two methyl groups are treated as two separate united atoms except that a C—C molecular orbital is formed for the two $2p\sigma$ electrons forming that bond. This yields $[\sigma\pm\sigma]$ the plus sign applying to the orbital of lower energy. For the lowest excited state an electron would go to an orbital formed by the two carbon $3s$ atomic orbitals, $[3s+3s]$. Then we obtain the configuration $[sa_1]^2\,[sa_1]^2\,[\pi e]^4\,[\pi e]^4\,[\sigma+\sigma]\,[3s+3s]\,{}^1A_1$ if the electron is taken from the C—C bond. The transition to this state would be ${}^1A_1 \leftarrow {}^1A_1$ and forbidden. From considerations based on ionization potentials MULLIKEN predicted that the corresponding band should be at about 1600 Å. No such band was known at the time but we are now making the tentative suggestion that the weak band we find in the spectrum of ethane corresponds to this transition.

The first strong band would then be due to the transition of an electron in a C—H bond to the same excited orbital:

$$[sa_1]^2\,[sa_1]^2\,[\pi e]^4\,[\pi e]^3\,[\sigma + \sigma]^2\,[3s + 3s]\,{}^1E.$$

The ${}^1E \leftarrow {}^1A$ transition is allowed.

In KATAGIRI and SÁNDORFY's Pariser and Parr type calculations the first transition is of the ${}^1E \leftarrow {}^1A$ type but we find no equivalent for MULLIKEN's low lying ${}^1A_1 \leftarrow {}^1A_1$ transition.

More extended $3s + 3s + 3s + \ldots$ type orbitals may account for the bathochromic shift which is observed when the number of carbon atoms increases.

More elaborate calculations using a basis of atomic orbitals including excited ones will probably be needed before we can pass the speculative stage in the interpretation of these spectra.

It is a matter of some interest to know if the first ionization leaves the "hole" in the C—C bonds or in the C—H bonds or if it is distributed over both. In MULLIKEN's united atom scheme the highest orbital filled in the ground state is of C—C character in ethane. The Hückel-type calculations of FUKUI, KATO and YONEZAWA [7], KLOPMAN [6] [21] and HOFFMANN [8] all seem to favor the C—C.

RAYMONDA and SIMPSON [20] assume that, in first approximation, the C—C electrons can be treated separately (like the π electrons in conjugated systems but with less justification) so that the first ionization is again C—C in their method. However, the Pariser—Parr—Pople type calculations of KATAGIRI and SÁNDORFY [15] yield electron densities mainly concentrated in the C—H bonds in the uppermost occupied orbitals, for at least ethane and propane.

From their photoelectron spectra AL-JOBOURY and TURNER [33] also concluded to the involvement of C—H rather than C—C bonds. Their bands were broad, however, and they have allowed for the possibility that they result from ionization from more than one close-lying orbital.

The matter does not seem to be definitely settled. Changes from C—H to C—C might occur in going from one paraffin molecule to the other and, in particular, between isomers with different degrees of branching.

The diffuse character of the bands in the spectra of the saturated hydrocarbons is usually attributed to dissociation or predissociation in the excited states which are indeed very probable in view of the high excitation energies which are involved. In relatively small molecules where the states are not very crowded the chances for predissociation are expected to be lower and this may be the reason why ethane [6] exhibits some vibrational fine structure.

Despite of the important role plaid by dissociation we should be cautious in attributing all the diffuseness what is observed to these phenomena. We have

to remember in this respect that because of rotational isomerism our spectra are actually spectra of mixtures and that the number of rotational isomers as well as the number of totally symmetrical vibrations increase rapidly with the increase in the number of atoms in the molecules.

There are some significant differences between the spectra of the branched chain paraffins, especially those of the highly branched ones, and those of the normal paraffins.

A typical example is shown in Fig. 5. The first bands are much stronger than in the spectra of the normal paraffin and they are followed by a fairly

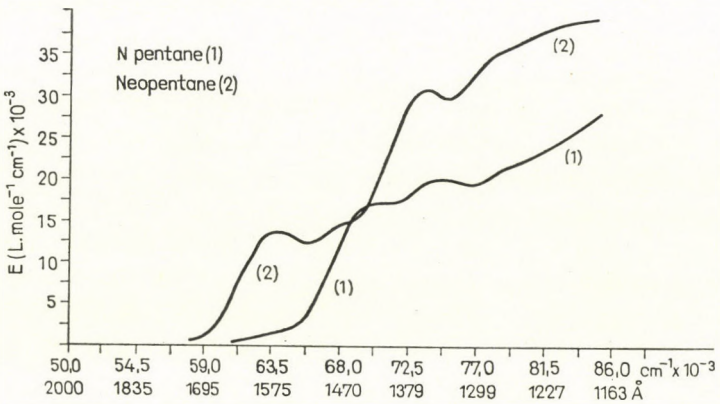

Fig. 5. Far ultraviolet absorption spectra of n-pentane and neopentane. Molecular extinction coefficients against wavenumbers

deep minimum toward higher frequencies. We have no quantum chemical calculations available to help in the interpretation of these spectra. It is possible that in this case the first bands correlate to the first *strong* bands of the normal paraffins. This would again mean that there has been a change in the order of the highest occupied molecular orbitals in the ground state.

All electronic transitions mentioned in this communication were singlet—singlet. The first singlet—triplet transitions were predicted by KATAGIRI and SÁNDORFY [15] to lie by about 1ev to lower frequencies from the first singlet—singlet bands. None of them has been found up to the present time.

We conclude by saying that much remains to be done. The solid theoretical basis for the discussion of σ-electron spectra is yet to be created.

REFERENCES

1. R. DAUDEL, Structure électronique des molécules, pp. 115—140. Paris, Gauthier-Villars 1962.
2. G. KLOPMAN, Tetrahedron, **19**, Suppl. 2, 111, 1963.
3. C. SÁNDORFY and R. DAUDEL, Comptes Rendus Acad. Sci., **238**, 93, 1954.

4. C. SÁNDORFY, Can. J. Chem., **33**, 1337, 1955.
5. K. FUKUI, H. KATO and T. YONEZAWA, Bull. Chem. Soc. Japan, **33**, 1197, 1201, 1960.
6. G. KLOPMAN, Helv. Chim. Acta. **45**, 711, 1962.
7. K. FUKUI, H. KATO and T. YONEZAWA, Bull. Chem. Soc. Japan, **34**, 442, 1111, 1961.
8. R. HOFFMANN, J. Chem. Phys., **39**, 1397, 1963.
9. M. WOLFSBERG and L. HELMHOLTZ, J. Chem. Phys., **20**, 857, 1952.
10. J. A. POPLE and D. P. SANTRY, Mol. Physics, **7**, 269, 1963—1964.
11. G. KLOPMAN, J. Am. Chem. Soc., **86**, 1463, 4550, 1964.
12. H. A. POHL, R. REIN and K. APPEL, J. Chem. Phys., **41**, 3385, 1964.
13. J. A. POPLE, D. P. SANTRY and G. A. SEGAL, J. Chem. Phys., **43**, S 129, 1965.
14. J. J. KAUFMAN, J. Chem. Phys., **43**, S 152, 1965.
15. S. KATAGIRI and C. SÁNDORFY, Theoret. Chim. Acta, **4**, 203, 1966.
16. P. N. SKANCKE, Arkiv För Fysik, **29**, 573, 1965; **30**, 449, 1966.
17. T. YONEZAWA, K. YAMAGUCHI and H. KATO, Bull. Chem. Soc. Japan, **40**, 536, 1967.
18. H. YOSHIZUMI, Trans. Faraday Soc., **53**, 125, 1957.
19. W. T. SIMPSON, J. Am. Chem. Soc., **77**, 6164, 1955.
20. J. W. RAYMONDA and W. T. SIMPSON, J. Chem. Phys., **47**, 430, 1967.
21. G. KLOPMAN, Helv. Chim. Acta, **46**, 220, 1963.
22. H. CAMBRON-BRUDERLEIN and C. SÁNDORFY, Theoret. Chim. Acta, **4**, 224, 1966.
23. R. W. DITCHBURN, Proc. Roy. Soc. London, **A229**, 44, 1955.
24. H. SUN and G. L. WEISSLER, J. Chem. Phys., **23**, 1372, 1955.
25. H. OKABE and D. A. BECKER, J. Chem. Phys., **39**, 2549, 1963.
26. R. H. PARTRIDGE, J. Chem. Phys., **45**, 1685, 1966.
27. R. I. SCHOEN, J. Chem. Phys., **37**, 2032, 1962.
28. B. A. LOMBOS, P. SAUVAGEAU and C. SÁNDORFY, J. Mol. Spectry, **24**, 253, 1967.
29. B. A. LOMBOS, P. SAUVAGEAU and C. SÁNDORFY, Chem. Phys. Letters, **1**, 221, 1967.
30. R. S. MULLIKEN, J. Chem. Phys., **3**, 517, 1935.
31. R. S. MULLIKEN, J. Am. Chem. Soc., **86**, 3183, 1964.
32. R. D. BROWN and V. G. KRISHNA, J. Chem. Phys., **45**, 1482, 1966.
33. M. I. AL-JOBOURY and D. W. TURNER, J. Chem. Soc., B1967, 373.

О СТРУКТУРЕ И СПЕКТРЕ σ-ЭЛЕКТРОННЫХ СИСТЕМ

Ц. ШАНДОРФИ

Р е з ю м е

В первой части работы дается краткий обзор новейших исследований по теоретической химии, касающихся насыщенных углеводородов. Во второй части рассматриваются расхождение некоторых относящиеся к основному состоянию физико-химических свойств от аддитивности и переходы σ-электронов (далекий ультрафиолетовый спектр).

Acta Physica Academiae Scientiarum Hungaricae, Tomus 27, pp. 161—168 (1969)

QUANTUM AND CORRELATION CORRECTIONS TO THE THOMAS–FERMI POTENTIAL*

By

T. TIETZ and S. KRZEMIŃSKI

DEPARTMENT OF THEORETICAL PHYSICS, UNIVERSITY OF ŁÓDZ, ŁÓDZ, POLAND

(Received 13. I. 1969)

This paper studies the correction to the Thomas—Fermi potential arising from the exichange inhomogeneity and correlation effects. Using the BARAFF equation and the approximate solution of the Thomas—Fermi equation for free neutral atoms, given by one of the authors there has been considered the low and high density approximation. It is found that the main contribution to the solution of the BARAFF equation arises from the inhomogeneity, screening and exchange terms.

Lastly the study of correlation effects in many-body systems has attracted the attention of a number of scientific workers [1]. This paper studies the correction of the Thomas—Fermi potential for free neutral atoms from the exchange, inhomogeneity and correlation effects by using the differential equation of BARAFF and a simple analytic expression of the Thomas—Fermi potential with a correct asymptotic behaviour for large distances.

It has been shown by BARAFF [2] that the first nonzero correction Φ_2 to the Thomas—Fermi potential [3] Φ_0 is given by the solution of the differential equation

$$\nabla^2 \Phi_2 - \left(\frac{4me^2}{\pi\hbar^3}\right) p_F \Phi_2 = \frac{4_m e^2}{\pi\hbar^3} p_F (E_{\text{ex}} + E_{\text{corr}}) + \frac{me^2}{12\pi\hbar^3 p_F} \cdot \cdot \left[4\nabla^2 \Phi_0 + \frac{2m}{(p_F)^2}\left(\frac{d\Phi_0}{dr}\right)^2\right], \tag{1}$$

where p_F denotes the Thomas—Fermi momentum, $E_{\text{ex}} = -e^2 p_F/\pi\hbar$ and E_{corr} denote the exchange and correlation energies of the system, respectively. The first term on the right-hand side of Equ. (1) represents the contribution arising from exchange and correlation effects and the second term gives the inhomogeneity correction. The second term on the left-hand side introduces the screening effect, which is one of the important consequences of the long-range Coulomb interaction of electrons. The right-hand side of Equ. (1) depends on Φ_0, the Thomas—Fermi potential, and in solving the differential Equ. (1)

* Dedicated to Prof. P. GOMBÁS on his 60th birthday.

we shall use the simple analytic solution of the Thomas—Fermi equation given by one of the authors [4]

$$\Phi_0(r) = -\frac{Ze^2}{r(1+Ax)^2(1+Bx)}, \tag{2}$$

where $x=r/\mu$ and $\mu=0.88534a_0/Z^{1/3}$. Z is the atomic number and a_0 is the first radius of the hydrogen atom. The numerical values of the constants A, B appearing in Equ. (2) are given by: $A = 0.05367\ Z^{1/3}$, $C = 0.035\,Z^{1/3}$. In the following we use atomic units and so put $e = \hbar = m = a_0 = 1$. The correlation energy of an electron gas has been investigated by several authors and it depends on the density of the system.

Let r_s denote the mean spacing between two electrons measured in units of Bohr radii in the system. We then say that the system has high or low density according to $r_s \lesssim 1$ or $r_s \gg 1$. According to GELLMAN and BRUECKNER [5] the correlation energy of a high density gas is given by

$$E_{\text{corr}} = G - E\ln p_F, \quad \text{where} \quad G = -0.05546 \text{ and } E = 0.0622. \tag{3}$$

For an electron gas for low density the correlation energy in atomic units is given by the WIGNER [6] formula

$$E_{\text{corr}} = -(0.89\,\bar{\alpha}\,\pi - 1)\frac{p_F}{\pi}, \quad \text{where} \quad \bar{\alpha} = \left(\frac{4}{9\pi}\right)^{1/3}. \tag{4}$$

First we shall solve the BARAFF equation for Φ_0 given by Equ. (2) in the case of high density; this means we use E_{corr} given by Equ. (3). Then we solve the BARAFF equation for Φ_0 in the case of low density when E_{corr} is given by the last formula.

Solution of Baraff equation for high density

In the high density limit the BARAFF equation according to Equ. (3) in atomic units is

$$\nabla^2\Phi_2 - \left(\frac{4}{\pi}\right)\sqrt{-2\Phi_0\Phi_2} = \left\{\frac{4\sqrt{-2\Phi_0}}{\pi} + A - B\ln\sqrt{-2\Phi_0}\right\} + \\ + \frac{1}{12\pi\sqrt{(-2\Phi_0)}}\left\{4\nabla^2\Phi_0 - \frac{1}{\Phi_0}\left(\frac{d\Phi_0}{dr}\right)^2\right\}, \tag{5}$$

where Φ_0 is given in atomic units by Equ. (2). The general solution of Φ_2 given by the last differential equation is the sum of the solution of the homogeneous equation and the particular integral. Denoting the solution of the homogeneous equation by Φ and putting a series of the form

$$\Phi = \frac{1}{r} \sum_{k=1}^{\infty} \alpha_k t^{k+s}, \quad \text{where} \quad t = r^{1/2} \tag{6}$$

for Φ we obtain after respecting the initial equation $s = 0$, when $\alpha_0 \neq 0$ and $\alpha_1 = \alpha_2 = 0$ for the expansion coefficient α_k the following recurrence formula:

$$n(n-2)\,\alpha_n - \frac{16}{\pi}\sqrt{2Z} \sum_{j=0}^{l} (-1)^j D_j \alpha_{n-3-2j}, \tag{7}$$

where

$$D_j = A^j + \sum_{k=1}^{j} \frac{(2k-1)!!}{2k!!} A^{j-k} C^k, \quad D_0 = 1. \tag{8}$$

The number l takes the following values: $l=n-1/2$ for even n and $l=n-3/2$ for odd n, where $n = 3, 4, 5, \ldots$ Setting $\Phi_2 = \Phi + \psi$, where ψ is the particular solution of Equ. (5) we see that the particular solution ψ after some simplification satisfies the following differential equation

$$\frac{d^2\Psi}{dr^2} + \frac{2}{r}\frac{d\Psi}{dr} - \frac{4\sqrt{2Z}}{r^{1/2}(1+Ar)(1+Cr)^{1/2}\pi}\Psi = f(r), \tag{9}$$

where

$$\Psi = \Phi_2 + G - E\ln\sqrt{2Z} + \frac{1}{2}E\ln r + E\ln(1+Ar) - \frac{1}{2}E\ln(1+Cr) +$$
$$+ \frac{1}{96}\left[\frac{1}{r^2} + \frac{4A}{r(1+Ar)} + \frac{2C}{r(1+Cr)} - \frac{20A^2}{(1+Ar)^2} - \right.$$
$$\left. - \frac{7C^2}{(1+Cr)^2} - \frac{12AC}{(1+Ar)(1+Cr)}\right] \tag{10}$$

and $f(r)$ can be expanded in ascending powers of r, and one has

$$f(r) = \sum_{n=-4}^{\infty} \beta_{2n} r^n, \tag{11}$$

where the expansion coefficients β_{2n} are given by the following recurrence relations

$$\beta_{-8} = \frac{1}{48}, \qquad \beta_{-6} = 0, \qquad \beta_{-4} = \frac{E}{2},$$

$$\beta_{-2} = 2EA + EC - \frac{8Z}{\pi^2} + \frac{11}{12}A^3 + \frac{1}{4}A^2C + \frac{1}{4}AC^2 + \frac{1}{3}C^3$$

$$\beta_{2n} = (-1)^{n+1}\Bigg\{(n+3)EA^{n+2} + \frac{n+3}{2}EC^{n+2} - \frac{8Z}{\pi^2}\sum_{k=0}^{n+1}(k+1)C^{n\pm1-k}A^k$$

$$\frac{1}{4}A^2C^2\sum_{k=0}^{n}(n-k+1)(k+1)A^{n-k}C^k + \frac{1}{4}AC$$

$$\left[A^2\sum_{k=0}^{n}\frac{(k+1)(k+2)}{2}C^{n-k}A^k + C^2\sum_{k=1}^{n}\cdot\frac{(k+1)(k+l)}{2}A^{n-k}C^k\right]$$

$$+\frac{1}{4}AC\left[A\sum_{k=0}^{n+1}\cdot(k+1)C^{n+1-k}A^k + C\sum_{k=0}^{n+1}(k+1)A^{n+1-k}C^k + \right]$$

$$+\frac{(n+2)(n+3)}{2\cdot3}C^{n-4} + \frac{7}{16}\frac{(n+1)(n+2)(n+3)}{1\cdot2\cdot3}C^{n+4}$$

$$+\frac{15}{12}\frac{(n+1)(n+2)(n+3)}{1\cdot2\cdot3}A^{n+4} + \frac{11}{12}\frac{(n+2)(n+3)}{2}A^{n+4}\Bigg\}$$

and $n = 0, 1, 2, 3, \ldots$.

Equ. (9) cannot be satisfied by a power series alone, and a complete solution of it should also contain a term involving *lnt*. Therefore in order to solve Equ. (9) we put ψ in the form

$$\psi = \sum_{k=-4}^{\infty} a_k t^k + \sum_{s=0}^{\infty} b_s t^s \cdot lnt,$$

where $t = r^{1/2}$. Substituting this in Equ. (9) and comparing different powers of t^k and $t^s lnt$ on both sides of the differential equation we obtain for the expansion coefficients a_k and b_s the following recurrence formulae

$$a_{-4} = \frac{1}{2}\beta_{-8}, \qquad a_{-3} = a_{-2} = a_0 = 0, \qquad a_{-1} = -\frac{16\sqrt{2Z}}{\pi}a_{-4}$$

$$b_0 = 2\beta_{-4}, \qquad b_1 = b_2 = b_4 = 0, \tag{12}$$

$$n(n+2)b_n - \frac{16\sqrt{2Z}}{\pi}\sum_{j=0}^{l}(-1)^j D_j b_{n-3-2j} = 0,$$

where $l = \dfrac{n-4}{2}$ for even n, $l = \dfrac{n-3}{2}$ for odd n, and $n = 3, 4, 5, \ldots$

also

$$n(n+2)\,a_n + 2(n+1)\,b_n - \frac{16\sqrt{2Z}}{\pi} \sum_{j=0}^{l} (-1)^j D_j\, a_{n-3-2j} = 4\beta_{n-4}, \qquad (13)$$

where $l = \dfrac{n}{2}$ for even n, $l = \dfrac{n+1}{2}$ for odd n,

$$\beta_{2n+1} \equiv 0 \text{ and } n = 1, 2, 3, \ldots .$$

The symbols D_j appearing in formulae (12) and (13) are given by Equ. (8). The solution of Equ. (9) still contains one arbitrary constant α_0. This can be

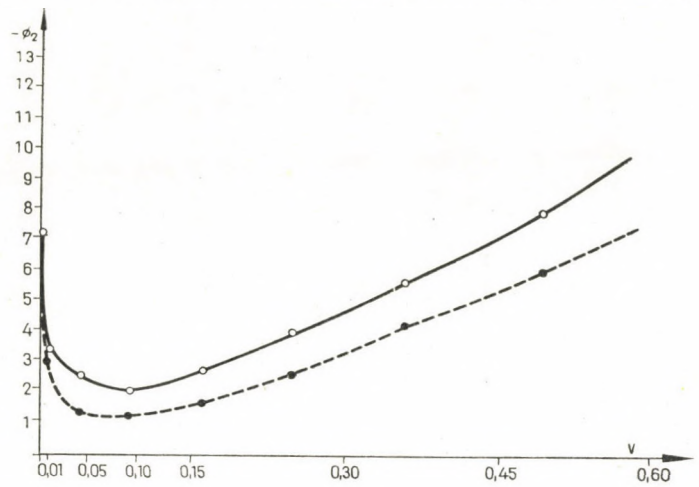

Fig. 1. Graph of $-\Phi_2$ against r for $Z = 28$. —— the results of P. VENKATARANGAN; ---- the results of the authors

evaluated from the boundary condition at the origin. For any neutral atom the potential near the origin is dominated by the nuclear attraction and this is equal to $-Ze^2/r$. Since the Thomas—Fermi potential Φ_0 also tends to $-Ze^2/r$ as $r \to 0$, it is clear that the correlation to the Thomas– Fermi potential contains any $1/t^2$, so that $\alpha_0 = 2A + C/48$. When $\alpha_0 = 2A + C/48$ is substituted in Equ. (8) we get the correction Φ_2 to the Thomas– Fermi potential.

We have studied the nature of variation of Φ_2 with r for the atoms silicon and nickel which have atomic numbers $Z = 14$ and $Z = 28$, respectively. Figs. 1 and 2 give the graphs of Φ_2 as a function of r. Our results have been compared with those of VENKATARANGAN [7], which are based on another approximate solution of the Thomas—Fermi potential given by the author [8].

From the graphs it follows that Φ_2 starts from infinity for very small values of r, decreases to a minimum value and again increases.

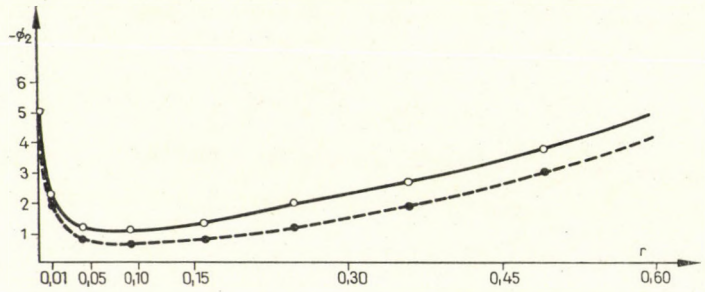

Fig. 2. Graph of $-\Phi_2$ against r for $Z = 14$. —— the results of P. VENKATARANGAN, ---- the results of the authors

Solution of the Baraff equation for low density

For an electron gas of low density the correlation energy is given by the WIGNER formula, i.e. by Equ. (4). The only difference in the differential equation (1) now arises from the term $(E_s - p_F^2/2m)$ which in this case is equal to $-0.89\,\bar{\alpha}\pi(e^2 p_F/\pi\hbar)$.

After some calculation it can be shown that in this case the correction Φ_2 to the Thomas—Fermi potential can be written as

$$\Phi_2 = r^{-2.676} \sum_{k=0}^{\infty} \gamma_k r^{-k} - \frac{1}{96}\left[\frac{1}{r^2} + \frac{4A}{r(1+Ar)} + \frac{2C}{r(1+Cr)} - \right.$$

$$\left. - \frac{20A^2}{(1+Ar)^2} - \frac{7C^2}{(1+Cr)^2} - \frac{12AC}{(1+AC)(1+Cr)}\right] + \sum_{p=0}^{\infty} d_{2p}\, r^{-\frac{2p+4}{2}},$$

where the expansion coefficients d_{2p} are given by

$$d_0 = \frac{\delta_y}{2 - \frac{4}{\pi A}\sqrt{\frac{2Z}{C}}} \qquad d_1 = 0\,,$$

$$\left[(n+2)(n+4) - \frac{16}{\pi A}\sqrt{\frac{2Z}{C}}\right] d_n - \frac{16}{\pi A}\sqrt{\frac{2Z}{C}} \sum_{j=1}^{l} (-1)^j D_j' d_{n-2j} = 4\delta_{n\,\frac{2}{2}+4} \quad (15)$$

for even n, and zero for odd n, where $l = n/2$ for even n, and $l = n - 1/2$ for odd n, and $n = 2, 3, 4, \ldots$, the expansion coefficient γ_k satisfies the following formulae:

$$s = \frac{1}{2} + \frac{1}{2}\sqrt{1 + \frac{4}{\pi A}\sqrt{\frac{2Z}{C}}} \approx 2.676\,, \quad \text{when} \quad \gamma_0 \neq 0\,, \qquad (16)$$

$$\left[(s+n-1)(s+n) - \frac{4}{\pi A}\sqrt{\frac{2Z}{C}}\right]\gamma_n - \frac{4}{\pi A}\sqrt{\frac{2Z}{C}} \sum_{j=0}^{n} (-1)^j D_j' \gamma_{n-j} = 0\,.$$

The symbols D'_j and δ_n appearing in the last formula are:

$$D'_j = A^{-j} + \sum_{k=0}^{j} \frac{(2k-1)!!}{2k!!} A^{k-j} C^{-k} \tag{17}$$

and

$$\delta_4 = \left(\frac{5}{16} - \frac{8Z}{\pi A^2 C} \cdot 0.89 \bar{\alpha} \right)$$

$$\delta_n = (-1)^{n-4} \left[\frac{11}{12} \frac{(n-3)(n-2)}{2} A^{-n+4} + \frac{1}{3} \frac{(n-3)(n-2)}{2} C^{-n+4} + \right.$$

$$+ \frac{1}{4} \sum_{k=0}^{n-4} (k+1) C^{k-n+4} A^{-k} + \frac{1}{4} \sum_{k=0}^{n-4} (k+1) A^{k-n+4} C^{-k} -$$

$$+ \frac{1}{4} \sum_{k=0}^{n-4} \frac{(k+1)(k+2)}{2} A^{k-n+4} - C^{-k} -$$

$$- \frac{1}{4} \sum_{k=0}^{k-4} \frac{(k+1)(k+2)}{2} C^{k-n+4} A^{-k} - \frac{1}{4} \sum_{k=0}^{k-4} (n-k-3)(k+1) \cdot$$

$$\cdot A^{k-n+4} C^{-k} - \frac{15}{12} \frac{(n-3)(n-2)(n-1)}{1 \cdot 2 \cdot 3} A^{-n+4} -$$

$$- \frac{7}{16} \frac{(n-3)(n-2)(n-1)}{1 \cdot 2 \cdot 3} C^{-n+4} -$$

$$\left. - \frac{8Z}{\pi A^2 C} 0.89 \bar{\alpha} \sum_{k=0}^{n-4} (k+1) C^{k-n+4} A^{-k} \right].$$

for $n = 5, 6, 7, \ldots$.

From Equ. (18) it follows that Φ_2 asymptotically tends to zero as r^{-2}. This is an unsatisfactory feature of the BARAFF equation since one would expect the correction to converge more rapidly than the Thomas—Fermi potential

REFERENCES

1. For reference see P. VENKATARANGAN, Can. J. Phys., **43**, 1157, 1965 and K. S. VISWANATHAN and B. N. NARAHARI, Achar, Can. J. Phys., **42**, 2332, 1964.
2. G. A. BARAFF, Phys. Rev., **123**, 2287, 1961.
3. P. GOMBÁS, Encyclopedia of Physics, Vol. 36, Springer Verlag, Berlin—Göttingen—Heidelberg, 1956.
4. T. TIETZ, Il N. Cim., **4**, 1192, 1956.
5. M. GELL-MANN and K. BRIECKNER, Phys. Rev., **106**, 364, 1957.
6. E. WIGNER, Phys. Rev., **46**, 1002, 1934.
7. For reference see [1].
8. T. TIETZ, J. Chem. Phys., **2**, 2094, 1954.

КВАНТОВЫЕ И КОРРЕЛЯЦИОННЫЕ ПОПРАВКИ К ПОТЕНЦИАЛУ ТОМАСА—ФЕРМИ

Т. ТИТЦ и С. КРЗЕМИНСКИЙ

Резюме

В данной работе изучается корреляция к потенциалу Томаса—Ферми, обусловленная неоднородностью обмена и корреляционными эффектами. Применяя уравнение Бараффа и приближенное решение уравнения Томаса—Ферми для свободных нейтральных атомов, данное одним из авторов, рассматривается приближение малой и высокой плотности. Найдено, что основной вклад в решение уравнения Бараффа вносят неоднократные, экранирующие и обменные члены.

Acta Physica Academiae Scientiarum Hungaricae, Tomus 27, pp. 169—177 (1969)

REMARKS CONCERNING THE THEORETICAL EXPLANATION OF HUND'S RULE* **

By

A. LEMBERGER and R. PAUNCZ

DEPARTMENT OF CHEMISTRY, ISRAEL INSTITUTE OF TECHNOLOGY, HAIFA, ISRAEL

(Received 13. I. 1969)

According to the accepted theoretical explanation of HUND's rule the electronic interaction energy is smallest in the ground state which is of the highest multiplicity. A breakdown of the total energy into one- and two-electron contributions in the case of carbon atom based on self-consistent field calculations and configuration interaction treatment shows that this assumption is not valid. According to our results the main differences in the energies of different terms arising from the same electronic configuration are due to differences in the one-electron energies.

1. Introduction

The simplest treatment of atomic spectra is based on the assumption that a single electronic configuration can be attributed to each atomic energy level. The positions of the different terms arising from a given electronic configuration, are determined theoretically by diagonalizing the matrices of electrostatic and spin-orbit interaction [1, 2, 3]. For light atoms the spin-orbit interaction is weak and can be treated as a perturbation, so that the different terms can still be characterized by their *LS* values and parity.

According to HUND's empirical rule [4], of all terms arising from a certain electronic configuration, the term with highest multiplicity has the lowest energy. This rule predicts correctly the ground state of most atoms, but it usually does not hold for excited states.

The accepted theoretical explanation for this rule is based on the phenomenon of the "Fermi hole". It is well known that antisymmetrization of the wave function introduces strong correlation between electrons with parallel spins. LÖWDIN [5] has shown that the diagonal element of the second order density matrix, $\Gamma(x_1x_2|x_1x_2)$ is zero for $x_1 = x_2$, at least up to the second order; that is, the probability of finding two electrons with parallel spins at the same point in space is zero, whereas the probability of finding two electrons with antiparallel spins at the same point can be different from zero. This can be viewed as if each electron is surrounded by a "hole" — the "Fermi hole" — which cannot be penetrated by electrons with spins parallel to its own. In these

* Dedicated to Prof. P. GOMBÁS on his 60th birthday. One of the authors (R. P.) would like to express his gratitude for the stimulus and advice that he received at the beginning of his research work from Professor P. GOMBÁS.

** Part of a thesis (A. L.) submitted to the Senate of the Israel Institute of Tec hnology in partial fulfilment of the requirements for the M. Sc. degree.

circumstances, it may be expected that the electron repulsion energy will be lowest in the term with the highest multiplicity as the latter has the greatest number of electrons with parallel spins.

If we now assume that the one-electron energy is equal, or only slightly different, for the different terms arising from the same electronic configuration, then the energy differences between terms are mainly due to differences in the electron repulsion energy. As the latter is expected to be lowest in the term with highest multiplicity, this term must have the lowest total energy.

When this explanation is examined more carefully, it is worthwhile to pay attention to the following point: The existence of the Fermi hole is a direct result of the antisymmetry of the wave function and does not depend on any approximation method used to calculate the wave function. However the assumption that the one electron energy is equal for the different terms, arising from the same electronic configuration, is based on the accepted approximation method used in atomic spectroscopy, that is, the attribution of a single configuration to each atomic energy level and the use of the same atomic orbitals for the construction of the wave function of each term. (The way by which the "best" orbitals are found is unimportant to this discussion). This method of approximation has the advantages of being simpler than the usual HF method and it can easily be extended for the perturbation calculation of the magnetic interactions (LS-coupling). SINANOĞLU [6] used this approximation as a convenient starting point for his calculations of the correlation energy.

Nevertheless, we have no reason to assume a priori that a similar result for the one-electron energy of the terms will be obtained when a more exact calculation of the wave function is made, that is, when the variational calculation is performed separately for each term, within the framework of the single configuration approximation, or when the more exact method of superposition of configurations is used to calculate the wave function. Moreover, it is known that a separate variational calculation for each term may give appreciably different orbitals for different terms [7]. The influence of superposition of configurations can have even more drastic effects on the energy differences between terms [8], especially in the case of Z-degeneracy.

The object of this study was to examine the various contributions to the energy differences between terms, when a variational calculation is carried out separately for each term, and thus to check the validity of the accepted explanation for HUND's rule.

2. Breakdown of the energy for light atoms from SCF calculations

The first step in the investigation consisted in the calculation of the different components of the energy (kinetic energy, nuclear attraction energy and electron interaction energy) for the low lying terms of the atoms from the first

Table I

Energy components for the three lowest terms of the carbon atom as calculated from CLEMENTI's[1] SCF-functions*

Term	Kinetic energy	Nuclear attraction energy	Electronic repulsion energy	Total energy
^3P	37.689	—88.137	12.760	—37.689
^1D	37.632	—87.992	12.728	—37.631
^1S	37.550	—87.769	12.669	—37.550

* Energy values in this and the following tables are given in atomic units.
[1] See [9].

two rows of the periodic table. The calculations were based on self-consistent wave functions obtained by CLEMENTI [9] using the ROOTHAAN — SCF method [10]. These functions were chosen for two reasons: 1. The variational calculation was made separately for each term, thus omitting the usual simplification. 2. The orbitals are of analytic form so they are easy to deal with and still are very close to the Hartree—Fock functions.

The expressions for the energy as a linear combination of radial integrals are tabulated for each term [11]. All the integrals can be calculated exactly by analytic formulas.

Results for the different energy components exhibited the same behaviour in all cases. In the following tables we shall present data for the case of carbon atom as an illustration of the general trend. Table I contains the different components of the energy for the three lowest terms of carbon arising from the electronic configuration $1s^2 2s^2 2p^2$.

The energy sequence of terms is $^3P < {}^1D < {}^1S$ in accordance with experiment and HUND's rule, but the electron repulsion energy is greatest in the ^3P term, in complete contradiction to the accepted explanation for this rule. The factor which determines the energy-sequence of terms turns out to be the different nuclear attraction energy and not the difference in electron repulsion energy.

Closer examination of the results (Tables II, III) shows that the factor responsible for this behaviour is a concentration of the electronic charge of the $2p$ orbital, closer to the nucleus, in the term with highest multiplicity. This causes an appreciable decrease in the nuclear attraction energy, as compared with the other terms, and at the same time, an increase in the repulsion energy of the charge in the $2p$ orbital with the charge in the closed shell, although to a lesser degree. Comparison of the radial charge distribution in the $2p$ orbital for the three terms (Fig. 1) verifies this finding.

The difference in the energies and charge distributions between the closed shell orbitals, $1s$, $2s$, of the three terms are smaller and have smaller influence

Table II

Components of one-electron energy (kinetic energy and nuclear attraction energy) for the three lowest terms of the carbon atom calculated from CLEMENTI's[1] SCF-functions

Term	Kinetic energy + nuclear attraction energy			
	(1s)	(2s)	(2p)	Total
^3P	−35.869	−7.684	−6.895	−50.448
^1D	−35.870	−7.704	−6.786	−50.360
^1S	−35.871	−7.732	−6.616	−50.219

[1] See [9].

Table III

Components of electronic repulsion energy for the three lowest terms of the carbon atom calculated from CLEMENTI's[1] SCF-functions

Term	Closed-shell repulsion energy	Inter-shell repulsion energy	Open shell repulsion energy	Total repulsion energy
^3P	7.222	5.048	0.490	12.760
^1D	7.237	4.959	0.532	12.728
^1S	7.260	4.822	0.587	12.669

[1] See [9].

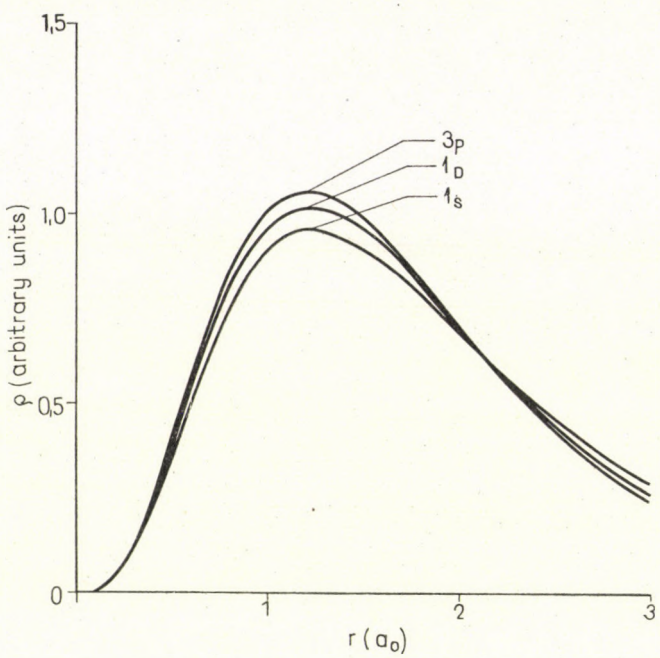

Fig. 1. Mean charge distribution in the 2*p*-orbital for the three lowest terms of carbon atom calculated from CLEMENTI's SCF functions

on the energy differences between the terms. This result could be expected since the inner shell of the atom is known to be influenced only slightly by changes in the outer shell.

Another interesting point which is observed in Table III is that the repulsion energy in the open shell only is in the order $^3P < {}^1D < {}^1S$. That is although there are differences in the $2p$ orbitals of the three terms, it can still be observed that antisymmetrization of the wave function introduces a measure of correlation between electrons with parallel spins. However, this correlation has a slight influence on the energy differences between terms and the main factor is, as was mentioned above, the difference in nuclear attraction energy of the $2p$ orbital.

Exactly analogous results were obtained for the other atoms examined — N($^4S^0$, $^2D^0$, $^2P^0$), O(^3P, ^1D, ^1S) and their counterparts in the second row of the periodic table — Si, P, S.

3. Configuration interaction calculations

In order to ascertain whether the above results are not limited to the single configuration approximation (it is well known that SCF-functions do not yield a good description of two electron observables) the different components of the total energy were calculated for the three lowest terms of carbon, using CI functions.

These functions were calculated by us following a previous calculation made by BOYS [12]. The first step consisted in recalculating BOYS' results and in the second — other configurations were added to the function in view of improving the energy. Computer programs have been written for the calculation of matrix elements between the atomic configurations involved and for the solution of the secular equation. For the latter we used the partitioning technique of LÖWDIN [13], which was found to be very convenient for such calculations.

Results for the wave functions and energies are listed in Table IV. Comparison of the energy values obtained in the different approximations is given in Table V. The fourth column presents the best values known in literature for the carbon atom, published recently by WEISS [14]. Another comparison to experiment is obtained by the interval-ratio ^1S—$^1D/^1D$—^3P for carbon (Table VI).

Superposition of configurations appreciably improves the quantitative agreement of the interval-ratio with experiment, so that it can be expected that these functions will give a better description of the energy-differences between the various terms of the carbon atom. Results for the different components of the energy as calculated from these functions are given in Table VII

Table IV

CI functions and energies for the three lowest terms of the carbon atom (present work)

Configuration	coefficient		
	^3P	^1D	^1S
$(sA^2)(sB^2)pA^2$	1.0	1.0	1.0
$(sAsC)(sB^2)pA^2$	0.00931	0.00925	0.00907
$(sC^2)(sB^2)pA^2$	−0.01511	−0.01510	−0.01505
$(pC^2)(sB^2)pA^2$	0.01604	0.01604	0.01602
$(sA^2)pA^4$	0.12462	−0.12361	−0.24778
$(sA^2)(sBsC)pA^2$	0.00797	0.00905	0.01469
$(sA^2)(sBsD)pA^2$	−0.07872	−0.08039	−0.09033
$(sA^2)(sB^2)pApB$	0.04275	0.07925	0.13294
$(sA^2)(sBdA)^3\ D(pA^2)^3p$	0.09996	0.14982	—
$(sA^2)(sBdA)^3\ D(pA^2)^1D$	0.12085	—	—
$(sA^2)(sBsC)pApB$	0.03357	0.03387	0.03473
$(sA^2)(sBsD)pApB$	−0.05449	−0.05736	−0.06209
$(sA^2)(sB^2)pB^2$	−0.04089	−0.05698	−0.07736
$(sA^2)(sB^2)dA^2$	0.03614	0.04780	0.09714
$(sA^2)(sB^2)pApD'$*	0.13952	0.17279	0.22358
$(sA^2)(sB^2)pApC$	0.03912	0.04454	0.05233
$(sA^2)(dA^2)pA^2$	−0.03496	−0.03482	−0.00544
$(sA^2)(pB^2)pA^2$	0.01861	0.01893	0.00278
$(sAsB)(sC^2)pA^2$	−0.00542	−0.00543	−0.00549
$(sB^2)(sCsD)pA^2$	−0.00375	−0.00376	−0.00380
E(a.u.)	−37.7600	−37.7030	−37.6416

* The orbital pD' is not the one used by BOYS — it is rather a linear combination of BOYS' pD and pC, which is orthogonal to pC.

Table V

Comparison of energies for different calculations for the carbon atom

Term	SCF (CLEMENTI[1])	CI (BOYS[2])	CI (present work)	CI (WEISS[3])	Exp.[2]
^3P	−37.689	−37.747	−37.760	−37.779	−37.841
^1D	−37.631	−37.689	−37.703	−37.731	−37.795
^1S	−37.550	−37.633	−37.642	−37.679	−37.742

[1] See [9].
[2] See [12].
[3] See [14].

Table VI

Comparison of the interval ratio $(^1S-{}^1D)/(^1D-{}^3P)$ for the different calculations

SLATER[1]	SCF (CLEMENTI[2])	CI (present work)	CI (WEISS[3])	Exp.[4]
1.50	1.43	1.08	1.09	1.13

[1] See [2]
[2] See [9]
[3] See [14]
[4] See [2]

Table VII

Energy components for the three lowest terms of the carbon atom, calculated from the CI functions of Table IV

Term	Kinetic energy	Nuclear attraction energy	Electronic repulsion energy	Total energy
^3P	37.635	−87.958	12.563	−37.760
^1D	37.583	−87.821	12.535	−37.703
^1S	37.553	−87.677	12.483	−37.642

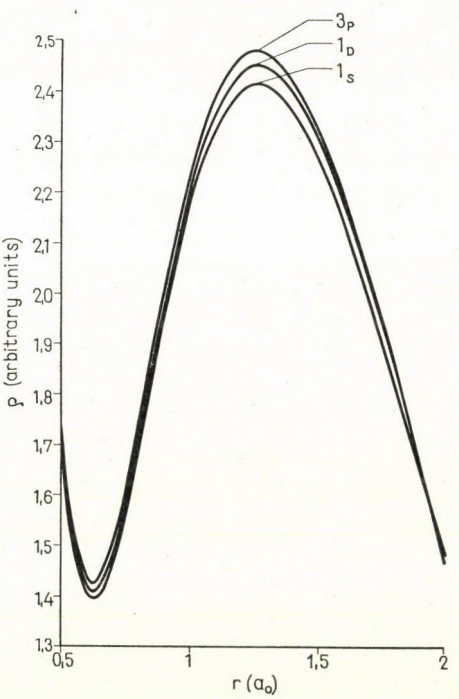

Fig. 2. Mean charge distribution in the *L*-shell for the three lowest terms of carbon atom as calculated from the CI functions given in Table IV

These results indicate exactly the same behaviour as the one observed using SCF functions: The electron repulsion energy is highest in the term with highest multiplicity and the factor responsible for the order $^3P < {}^1D < {}^1S$ is the difference in nuclear attraction energy.

Comparison of the mean radial charge distribution of the three terms indicates that the differences in the inner shell (K shell) are very small but there are differences in the outer shell (L shell). The radial charge distribution in the L shell of carbon for the three lowest terms is given in Fig. 2.

The charge in the ^3P-term is concentrated closer to the nucleus than in the other terms, and this seems to be the reason for the decrease in nuclear attraction energy and for the increase in the electron repulsion energy.

4. Summary

Results of the calculations indicate that the accepted explanation for HUND's rule is based on an approximation and it does not remain valid if more elaborate methods are used for the determination of the atomic wave function. It seems that at least for the three lowest terms of the carbon atom the differences in term energies are due to changes in spatial charge distribution, so that the main factor responsible for the order of energies is the difference in nuclear attraction energy, not in the electron repulsion energy.

Although we cannot conclude that this result is characteristic of all atoms (it is probably not the case with positive ions), the above results still emphasize the fact that the differences in one-electron energy between various terms are of the same order of magnitude as the differences in electron repulsion energy and their neglection is, therefore, unjustified.

REFERENCES

1. E. U. CONDON and G. H. SHORTLEY, The Theory of Atomic Spectra, Cambridge University Press, New York, 1959.
2. J. C. SLATER, Quantum Theory of Atomic Structure, Vol. I., McGraw Hill Book Co. Inc., New York, 1960.
3. P. GOMBÁS, Theorie und Lösungsmethoden des Mehrteilchenproblems der Wellenmechanik, Birkhäuser, Basel, 1950.
4. F. HUND, Linienspektren und periodisches System der Elemente, Springer, Berlin, 1927.
5. P.-O. LÖWDIN, Advances in Chemical Physics, ed. I. Prigogine, Vol. II, Interscience Publishers, New York, 1959.
6. O. SINANOĞLU, Advances in Chemical Physics, ed. I. Prigogine, Vol. VI, Interscience Publishers, New York, 1964.
7. D. R. HARTREE and W. HARTREE, Proc. Roy. Soc. London, **A 154**, 588, 1936.
8. R. N. ZARE, J. Chem. Phys., **45**, 1966, 1966.
9. a. E. CLEMENTI, IBM Journal of Research and Development, **9**, 2, 1965.
   b. E. CLEMENTI, Tables of Atomic Functions, a supplement to (a), table 01.
10. C. C. J. ROOTHAAN and P. BAGUS, Methods of Computational Physics, ed. B. Alder, Vol. 2, Academic Press Inc., New York, 1963.

11. J. C. SLATER, Quantum Theory of Atomic Structure, Vol. II, McGraw Hill Book Co. Inc., New York, 1960, appendix 21.
12. S. F. BOYS, Proc. Roy. Soc. London, **A 217**, 235, 1953.
13. P.-O. LÖWDIN, Technical note from the Uppsala Quantum Chemistry Group, April 23, 1958.
14. A. W. WEISS, Phys. Rev., **162**, 71, 1967.

ПРИМЕЧАНИЯ ОТНОСИТЕЛЬНО ТЕОРЕТИЧЕСКОГО ТОЛКОВАНИЯ ПРАВИЛА ГУНДА

А. ЛЕМБЕРГЕР и Р. ПАУНЦ

Р е з ю м е

Согласно принятому теоретическому толкованию правила Гунда энергия электронного взаимодействия наиболее низка в основном состоянии, что обусловливается высокой мультиплетностью. Распад полной энергии в одно- и двухэлектронный вклады в случае атома углерода, определенный на базе метода самосогласованного поля и конфигурационного взаимодействия, говорит о недействительности данного предположения. Наши результаты показывают, что главное различие в энергиях различных термов, происходящих от одной и той же электронной конфигурации, обусловливается различием в одноэлектронных энергиях.

Acta Physica Academiae Scientiarum Hungaricae, Tomus 27, pp. 179—189 (1969)

DEVELOPMENTS IN THE SEPARATED PAIR THEORY*

By

E. KAPUY

RESEARCH GROUP FOR THEORETICAL PHYSICS OF THE HUNGARIAN ACADEMY OF SCIENCES
BUDAPEST

(Received 28. I. 1969)

In recent years, it has become possible to compute strongly orthogonal geminals for several smaller systems and to investigate the effectiveness of the conventional separated pair theory. The results are compared with those obtained by other many-electron theories and the sources of the main deficiencies are pointed out. Extensions of the separated pair theory using the optimized orbitals of the single antisymmetrized geminal product wave function are also discussed.

Introduction

It was FOCK who first proposed that two-electron functions should be used as building blocks in constructing the total wave function [1]. This method seemed to be the most natural extension of the Hartree—Fock scheme. It was expected that in this way the most important part of the correlation energy could be accounted for and the two-electron functions are transferable at least in certain "localized" systems. The calculation of the energy (and of other physical quantities) is, however, rather cumbersome unless special restrictions are imposed on the two-electron functions [2, 3]. To avoid this difficulty the concept of strong orthogonality was introduced [4]. Given an $2N$-electron system the total wave function Ψ_0 can be written as an antisymmetrized product of N geminals $\psi_K(1, 2)$, $K = 1, 2, \ldots N$. If the geminals are

a) normalized to unity:

$$\int \psi_K^*(1,2)\,\psi_K(1,2)\,d1\,d2 = 1\,, \tag{1}$$

b) antisymmetric in the (space-spin) variables of the electrons:

$$\psi_K(1,2) = -\psi_K(1,2)\,, \tag{2}$$

c) mutually orthogonal in the strong sense:

$$\int \psi_K^*(1,2)\,\psi_L(1,2')\,d1 = 0, \quad \text{if} \quad K \neq L\,, \tag{3}$$

* Dedicated to Prof. P. GOMBÁS on his 60th birthday. The author wishes to express his thanks to Professor P. GOMBÁS for continuously encouraging and supporting research concerning many-electron problems.

the total wave function Ψ_0 normalized to unity has the following form:

$$\Psi_0 = \left[\frac{2^N}{(2N)!}\right]^{1/2} \sum_P (-1)^p P\psi_1(1,2)\,\psi_2(3,4)\ldots\psi_N(2N-1,2N)\,. \tag{4}$$

Here the summation should be extended over only those permutations which interchange the electrons between geminals.

By using (4) and taking into account restrictions (1), (2), (3), the energy expression can be easily calculated [4, 5, 6, 7, 8]

$$E_0 = H(0) + \sum_{K=1}^{N} \int \psi_K^*(1,2)\left[H(1) + H(2) + r_{12}^{-1}\right]\psi_K(1,2)\,d1\,d2 + \tag{5}$$

$$+ 2\sum_K \sum_{L(\neq K)} \int d1\,d2\,d3\,d4\,r_{13}^{-1}\left[1 - P_{13}\right]\psi_K^*(1',2)\,\psi_K(1,2)\,\psi_L^*(3',4)\,\psi_L(3,4)\,.$$

The mean value of an operator O, being the symmetrical sum of one-electron operators

$$O = \sum_{i=1}^{2N} O(i)\,,$$

has the following simple form

$$\bar{O} = 2\sum_{K=1}^{N} \int \psi_K^*(1,2)\,0(1)\,\psi_K(1,2)\,d1\,d2\,.$$

The above formalism has been generalized so that group functions of an arbitrary number of electrons were used as building blocks instead of geminals [7, 8, 9].

By using energy expression (5) and auxiliary conditions (1), (2), (3), a set of coupled integro-differential equations has been derived with the help of the variation theory for determining the best possible geminals [5, 8, 10]. The equations so obtained were inconvenient for practical use owing to the off-diagonal Lagrangian multipliers. To circumvent this difficulty PARKS and PARR suggested that the geminals should be constructed of given one-electron functions ϕ in the following way

$$\psi_K(1,2) = \sum_{\varkappa,\lambda} C_{\varkappa\lambda}^K \phi_\varkappa(1)\,\phi_\lambda(2)\,. \tag{6}$$

The strong orthogonality conditions (3) are satisfied when each of the one-electron functions $\phi_\varkappa$ enters the series (6) of only one geminal. PARKS and PARR also proposed that the coefficients $C_{\varkappa\lambda}^K$ should be calculated self-consistently by minimizing the energy expression of the individual geminals [5, 8].

The meaning of the strong orthogonality condition (SC) was later clarified by ARAI [11], and by LÖWDIN [12]. They proved the following theorem:

Given N strongly orthogonal geminals ψ_K, there always exists at least one complete set of orthonormal one-electron functions $\{\varphi\}$, which can be partitioned into N subsets having no common elements

$$\varphi_{11}, \varphi_{12}, \varphi_{13}, \ldots \varphi_{K1}, \varphi_{K2}, \varphi_{K3}, \ldots \varphi_{N1}, \varphi_{N2}, \varphi_{N3}, \ldots$$

such that each of the geminals can be expanded in terms of its own subset only:

$$\psi_K(1,2) = \sum_{\varkappa,\lambda} a^K_{\varkappa\lambda} \varphi_{K\varkappa}(1) \varphi_{K\lambda}(2) . \tag{7}$$

This means that the representation of the strongly orthogonal geminals by series (7) is completely general provided the coefficients $a^K_{\varkappa\lambda}$ and the one-electron functions $\varphi_{K\varkappa}$ are suitably determined.

This theorem made it possible to work out methods suitable for the practical determination of strongly orthogonal geminals. At the same time the separated pair theory became essentially a particular case of the method of "configuration interaction with optimalized basis functions".

The conventional separated pair theory

Geminals are uniquely defined by the coefficients $a^K_{\varkappa\lambda}$ and the one-electron functions $\varphi_{K\varkappa}$. (The converse is not necessarily true.) Using the variation theory we can derive equations for determining the coefficients $a^K_{\varkappa\lambda}$ and the one-electron functions $\varphi_{K\varkappa}$ [5, 7, 8, 13—15]. Substituting (7) into the energy expression (5) and varying the coefficients subject to the auxiliary conditions

$$\sum_{\varkappa,\lambda} |a^K_{\varkappa\lambda}|^2 = 1, \quad K = 1,2,\ldots N,$$

we obtain N sets of equations

$$\sum_{\mu,\nu} (H^K_{\varkappa\lambda,\mu\nu} - E^K \delta_{\varkappa\mu} \delta_{\lambda\nu}) a^K_{\mu\nu} = 0 , \tag{8}$$

for all $\varkappa$, λ, and K, where

$$H^K = H(1) + H(2) + r_{12}^{-1} +$$

$$+ 2 \sum_{L(\neq K)} \int d3\, d4 \left[r_{13}^{-1} (1 - P_{13}) + r_{23}^{-1} (1 - P_{23}) \right] \varphi^*_L(3',4)\, \psi_L(3,4).$$

Equs. (8) represent N pseudo-eigenvalue equations because the operators H^K depend on the coefficients $a^L_{\varkappa\lambda}$ of all the other geminals.

Varying the energy expression with respect to the one-electron functions $\varphi_{K\varkappa}$ taking into account the following auxiliary conditions

$$\int \varphi^*_{K\varkappa}(1) \varphi_{L\lambda}(1)\, d1 = \delta_{KL} \delta_{\varkappa\lambda} ,$$

we obtain a set of one-electron equations of the form

$$F_{\varkappa}^{K}\varphi_{K\varkappa} = \sum_{L}\sum_{\lambda}\varepsilon_{\varkappa\lambda}^{KL}\varphi_{L\lambda}\,. \tag{9}$$

Here the one-electron operators $F_{\varkappa}^{K}$ depend on all the coefficients $a_{\varkappa\lambda}^{L}$ and all the one-electron functions $\varphi_{L\lambda}$ except $\varphi_{K\varkappa}$.

Equs. (8) define the coefficients $a_{\varkappa\lambda}^{K}$ of the best possible geminals with fixed $\varphi_{K\varkappa}$'s, and Equs. (9) define the one-electron functions $\varphi_{K\varkappa}$ of the best possible geminals with fixed $a_{\varkappa\lambda}^{K}$'s. The $a_{\varkappa\lambda}^{K}$'s and the $\varphi_{K\varkappa}$'s are, however, not independent because any unitary transformation of the $\varphi_{K\varkappa}$'s (and the simultaneous transformation of the $a_{\varkappa\lambda}^{K}$'s with the corresponding adjoint) leaves ψ_K invariant. Instead of adding further auxiliary conditions it is more practical to use the natural spin-orbital expansion of the geminals. Assuming that the $\varphi_{K\varkappa}$ are the natural spin-orbitals of the corresponding geminal, for real ψ_K, only those coefficients $a_{\varkappa\lambda}^{K}$ differ from zero in the series (7) for which $\varphi_{K\lambda} = \varphi_{K\varkappa}^{*}$. As a consequence, Equs. (8) and (9) simplify to some extent [14, 15]. To obtain the best possible geminals these equations should be solved simultaneously [15]. The natural spin-orbitals of the geminals are automatically natural spin-orbitals of the total wave function.

All methods hitherto applied to obtain the best possible geminals are essentially equivalent to some approximate solution of Equs. (8) and (9) with a basis $\varphi_{K\varkappa}$ truncated to finite size.

A) If a set of orthonormal one-electron functions $\phi_{K\varkappa}$ is known which is presumably close to the optimal one, only the pseudo-eigenvalue equations (8) have to be solved. The solution can be carried out by iteration similarly to the Hartree—Fock—Roothaan equations [16, 17].

B) The above procedure can be combined with that of mixing the $\varphi_{K\varkappa}$'s by unitary transformation. The unitary transformation is determined by minimizing the total energy. The two procedures have to be continued alternately until self-consistency is achieved [18, 19].

C) An iterative procedure for solving Equs. (8) and (9) was proposed by KUTZELNIGG [15, 20]. As a first step he simplified Equs. (8) and (9) by decoupling those corresponding to coefficients $a_{\varkappa\lambda}^{K}$ and one-electron functions $\phi_{K\varkappa}$ of different geminals. The first natural orbital in each of the geminals was identified with a suitable "localized" unitary transform of the occupied Hartree—Fock orbitals. By using these decoupled equs. he determined the "excited" natural orbitals, which were required to be orthogonal to all occupied Hartree—Fock orbitals and to all "excited" natural orbitals of the same geminal but not to the "excited" natural orbitals of the other geminals. In the case of Be and LiH the correction owing to the nonorthogonality of the "excited"

natural orbitals was found to be small as the "excited" natural orbitals of different geminals are localized in different spatial regions. Nevertheless this method of approximation does not belong rigorously to the separated pair theory but is closely related to the independent pair model of SINANOĞLU [21, 22] and of NESBET [23].

Similar simplified equations were applied for determining the natural orbitals of geminals by EDMISTON and KRAUSS [24].

D) The method of "optimized valence configurations" is also a special case of the separated pair approximation [25]. Only the bonding pair was correlated but all the one-electron functions were optimized. The Equs. (9) were solved by expanding the $\varphi_{K\varkappa}$ in terms of a fixed set and the off-diagonal Lagrangian multipliers were absorbed in the operators $F_{\varkappa}^{K}$.

Method *B)* was applied to LiH [18] and to beryllium-like systems [26]. In the latter case 15 different Slater orbitals were used as basis functions and the exponents ζ were also varied. In the case of the Be atom 89.8% of the total correlation energy was recovered. Similar results were obtained for other systems.

Method *C)* was applied to Be, LiH [20] and to BeH_2, BH_3, CH_4 [26]. For Be and LiH the results are similar to those obtained by method *B)*. The correlation energy per equivalent geminal corresponding to the bond X—H was found to decrease continuously from LiH to CH_4. A comparison with the empirical correlation energies indicated that the sum of the intrageminal correlation energies comprises a continuously decreasing fraction of the total correlation energy. This means that the intergeminal correlation energies should also be taken into account and that the correlation energy of the X—H bonds is not transferable.

We can easily recognize the shortcomings of the conventional separated pair theory by comparing it with other theories of the correlation energy.

The most developed methods are the "many-electron theory" of SINANOĞLU [21, 22] and the "theory of n-th order Bethe—Goldstone equations" of NESBET [23]. They are closely related but the latter is more convenient for comparison because it applies one-electron function expansions. The exact wave function of a $2N$-electron system is determined by the successive variational solution of effective Schrödinger equations for clusters of one, two, three etc., electrons. Slater determinants Φ_k of $2N$-th order are used as basis functions, which are constructed out of a set of orthogonal one-electron functions $\{\underline{\phi}\}$:

$$\Phi_k = [(2N)!]^{-1/2} \det |\phi_{\varkappa_1} \phi_{\varkappa_2} \ldots \phi_{\varkappa_{2N}}| .$$

The set $\{\phi\}$ is divided into two sets $\phi_{\varkappa}$, $\varkappa = 1, 2, \ldots 2N$, and ϕ_{ϱ}, $\varrho = 2N + 1$, $2N+2, \ldots$, the first of which is usually identified with the occupied Hartree—Fock spin-orbitals. The Slater determinant containing only the functions of the

first set is denoted by Φ_0 and Slater determinants in which the occupied $\phi_\varkappa$, ϕ_λ, ϕ_μ, etc., are replaced by $\phi_\varrho, \phi_\sigma, \phi_\tau$, etc., are denoted by $\Phi^{\varrho\sigma\tau}_{\varkappa\lambda\mu} \ldots$. The first order corrections $e_\varkappa$ to the Hartree—Fock energy E_{HF} are calculated by minimizing separately the expressions

$$e_\varkappa = \frac{\langle f_\varkappa | H | f_\varkappa \rangle}{\langle f_\varkappa | f_\varkappa \rangle} - E_{HF} \tag{10}$$

with respect to the coefficients of trial functions

$$f_\varkappa = \Phi_0 + \sum_\varrho b^\varrho_\varkappa \Phi^\varrho_\varkappa . \tag{11}$$

The second order corrections $e_{\varkappa\lambda}$ are calculated by minimizing separately the expressions

$$e_{\varkappa\lambda} = \frac{\langle f_{\varkappa\lambda} | H | f_{\varkappa\lambda} \rangle}{\langle f_{\varkappa\lambda} | f_{\varkappa\lambda} \rangle} - E_{HF} - e_\varkappa - e_\lambda \tag{12}$$

with respect to the coefficients of trial functions

$$f_{\varkappa\lambda} = \Phi_0 + \sum_\varrho b^\varrho_\varkappa \Phi^\varrho_\varkappa + \sum_\sigma b^\sigma_\lambda \Phi^\sigma_\lambda + \sum_{\varrho,\sigma} b^{\varrho\sigma}_{\varkappa\lambda} \Phi^{\varrho\sigma}_{\varkappa\lambda} . \tag{13}$$

The procedure can be continued by calculating higher order corrections.

The total correlation energy up to second order equals

$$E_C = \sum_{\varkappa=1}^{2N} e_\varkappa + \sum_{\varkappa>\lambda=1}^{2N} e_{\varkappa\lambda} .$$

As the first sum in closed shell systems (Be, Ne) was found to be zero, the total correlation energy in this approximation consists of the sum of the independent pair correlation energies $e_{\varkappa\lambda}$. Calculations carried out on simpler systems indicated that in this approximation 97—98% of the total correlation energy could be recovered using a fairly large basis.

The lowering of the energy is brought about by terms

$$\int d1\, d2\, r_{12}^{-1} (1 - P_{12})\, \phi^*_\varkappa (1')\, \phi^*_\lambda (2')\, \phi_\varrho (1)\, \phi_\sigma (2) \tag{14}$$

in the expression (12) of $e_{\varkappa\lambda}$ where they are multiplied by appropriate coefficients $b^{\varrho\sigma}_{\varkappa\lambda}$. As the matrix elements (14) represent exchange-like interactions their value is significant only when ϕ_ϱ and ϕ_σ are localized in the same regi-

ons of space where the corresponding $\phi_\varkappa$ and ϕ_λ are appreciably different from zero [28]. The electrons in $\phi_\varkappa$ and ϕ_λ can be excited to any ϕ_ϱ and ϕ_σ.

The correlation energy obtained by the separated pair theory can be written approximately in the following form [19, 20]

$$\sum_K \tilde{e}_K ,$$

where $\tilde{e}_K$ denotes that part of the correlation energy which comes from the geminal ψ_K.

This means that the separated pair theory has two main deficiencies:

a) It takes into account only N pair correlations (the so called intrageminal correlations) instead of $\binom{2N}{2}$.

b) Even the pair correlations included are restricted to some extent because the electrons in $\phi_\varkappa$ and ϕ_λ cannot be excited to any ϕ_ϱ and ϕ_σ but only to a subgroup of them as a consequence of the SC's.

These defects are not serious if the system consists of N completely isolated pairs because then

$$\psi_K(1,2)\,\psi_L(1,2') = 0, \quad \text{if} \quad K \neq L ,$$

automatically. This case is, however, an exceptional one. For strongly localized systems as e.g. for the Be atom, the error in the correlation energy caused by deficiency *b)* is not significant (2%). For weakly localized systems even this error may be more serious [29]. The neglect of intergeminal correlations (deficiency *a)*) is inadmissible, even for strongly localized systems. The importance of the interpair correlation energy was stressed by McKoy and Sinanoğlu [30]. If accurate results are needed the conventional separated pair theory should be corrected.

Extension of the separated pair theory

Part of the intergeminal correlation energy within the framework of the separated pair theory can be taken into account as follows [7, 9, 31].

Each set of the equations (8) with fixed H^K has $\binom{n_K}{2}$ linearly independent solutions ψ_{Kk} one of which, ψ_{K1}, is identical with the best possible geminal; the others represent "excited" geminals. (n_K is the number of one-electron functions $\varphi_{K\varkappa}$ in the subspace K.) They obey the following orthogonality relations

$$\int \psi^*_{Kk}(1,2)\,\psi_{Kl}(1,2)\,d1\,d2 = \delta_{kl} ,$$

$$\int \psi^*_{Kk}(1,2)\,\psi_{Ll}(1,2')\,d1 = 0, \quad \text{if} \quad K \neq L .$$

The most general $2N$-electron function of the separated pair theory can be written in the form

$$\Psi_{SP} = \sum_{i,j,\ldots,l} A^{ij\ldots l} \Psi^{ij\ldots l}, \tag{15}$$

where the antisymmetrized products

$$\Psi^{ij\ldots l} = \left[\frac{2^N}{(2N)!}\right]^{1/2} \sum_P (-1)^p P \psi_{1i}(1,2)\,\psi_{2j}(3,4)\ldots\psi_{Nl}(2N-1,2N) \tag{16}$$

contain one geminal of each of the N subspaces. (The function $i = j = \ldots = l = 1$ corresponds to Ψ_0.)

Instead of solving the secular equation corresponding to (15) it is more practical to use the Rayleigh - Schrödinger perturbation theory based on partitioning techniques [7, 31, 32]. We have for the correction to the separated pair ground state energy (5) up to third order

$$\sum_{r>0} \frac{|H_{0r}|^2}{E_0 - H_{rr}} + \sum_{\substack{r>0 \\ s>0}} \frac{H_{0r} H_{rs} H_{s0}}{(E_0 - H_{rr})(E_0 - H_{ss})}, \tag{17}$$

where

$$H_{rs} = \int \Psi_r^* H \Psi_s \, d\tau, \quad \int \Psi_r^* \Psi_s \, d\tau = \delta_{rs}.$$

The matrix element H_{0r} is different from zero only when the configuration Ψ_r contains two "excited" geminals.

It can easily be shown that the first sum of (16) includes the intergeminal correlations consistent with the SC's. If the Hartree–Fock approximation is a fairly good one the natural orbitals in the leading term of the best possible geminals are nearly identical with some unitary transforms of the doubly occupied Hartree–Fock orbitals. In this case we find among the "excited" geminals those the leading term of which is nearly identical with one of the possible singly-excited configurations within the corresponding subspace. These "singly-excited" geminals in the first sum of (17) account for all double excitations which conform to the SC's. Three- and four-particle excitations are also included.

It can be shown that configurations (16) above do not exhaust all the $2N$-electron states which can be constructed out of the known one-electron functions $\varphi_{K\varkappa}$. As a consequence of the SC's the number of electrons N_K in each of the subspaces are conserved and equal to 2 [31]. To get all linearly independent $2N$-electron functions $\Psi^{ij\ldots l}_{N_1 N_2 \ldots N_N}$ which can be derived from the $\varphi_{K\varkappa}$'s we have to construct also the functions corresponding to all possible partitions of the set $N_1, N_2, \ldots N_N$, $\Sigma N_K = 2N$, except for those where $N_1 = N_2 = \ldots = N_N = 2$.

The functions $\Psi^{ij\ldots l}_{N_1 N_2 \ldots N_N}$ are expressed as antisymmetrized products containing one group function $\bar{\psi}_{N_K k}$ of each of the N subspaces [31]:

$$\Psi^{ij\ldots l}_{N_1 N_2 \ldots N_N} = \left[\frac{N_1!\, N_2! \ldots N_N!}{(2N)!}\right]^{1/2} \sum_P (-1)^p P \bar{\psi}_{N_1 i}\, \bar{\psi}_{N_2 j} \ldots \bar{\psi}_{N_N l}\,,$$

where

$$\bar{\psi}_{N_K k} \equiv 1, \quad \text{if} \quad N_K = 0\,,$$
$$\bar{\psi}_{N_K k} \equiv \varphi_{K\varkappa}, \quad \text{if} \quad N_K = 1\,,$$
$$\bar{\psi}_{N_K k} \equiv \psi_{Kk}, \quad \text{if} \quad N_K = 2\,,$$

and for $N_K > 2$

$$\bar{\psi}_{N_K k} \equiv (N_K!)^{-1/2} \det |\varphi_{K\varkappa}(1)\, \varphi_{K\lambda}(2) \ldots \varphi_{K\nu}(N_K)|\,.$$

Every $\Psi^{ij\ldots l}_{N_1 N_2 \ldots N_N}$ can be derived by "exciting" electrons out of the Ψ_0 by elementary excitations of two kinds

—simple excitation: replaces one group function by another belonging to the same subspace and occupation number

$$\bar{\psi}_{N_K k} \rightarrow \bar{\psi}_{N_K l}\,. \quad k \neq l\,,$$

—electron transfer excitation: transfer one electron from one subspace to another, altering two group functions simultaneously

$$\bar{\psi}_{N_K k}\, \bar{\psi}_{N_L l} \rightarrow \bar{\psi}_{N_K - 1 i}\, \bar{\psi}_{N_L + 1 j}\,.$$

The minimum number of simple excitations necessary to transfer a given state into another is always unique. This means that all states having nonzero matrix element with Ψ_0 can be derived from Ψ_0 by two elementary excitations. It is exactly these states which should be taken into account in calculating the correction up to third order (17). The corresponding functions $\Psi^{ij\ldots l}_{N_1 N_2 \ldots N_N}$ can be grouped according to the minimum number of necessary elementary excitations to connect them with Ψ_0:

I) two simple excitations. The corresponding configurations describe the correlations conforming to the SC's.

II) one electron transfer excitations.

III) one simple excitation + one electron transfer excitation,

IV) two electron transfer excitations.

It can be shown that they include all possible two-electron excitations and in addition some of the many-electron excitations.

This procedure was applied to the π-electrons of trans-butadiene in the GOEPPERT—MAYER—SKLAR approximation [33, 34]. The separated pair ground state was calculated using equivalent orbitals constructed from the SCF orbitals of PARR and MULLIKEN [35], and all second order corrections were evaluat-

ed. It was found that the intrageminal correlation energy accounted for is 93% of the standard value which was identified with that obtained by the "full" CI. About 75% of the intergeminal correlation energy came from one electron transfer configurations of type II) and III). The contribution from configurations of type I) which conform to the SC's was less, 25%, and practically the whole came from configurations containing two "singly-excited" geminals. The contribution from two electron transfer configurations was found to be negligible. The result was superior to those obtained by other variants of the Rayleigh—Schrödinger perturbation theory.

The above procedure is convenient especially when perturbation theory is used.

MILLER and RUEDENBERG worked out a different method to obtain all $2N$-electron functions which can be constructed from the $\varphi_{K\varkappa}$'s [26]. Using 28 configurations about 94% of the empirical correlation energy was recovered for beryllium-like systems. The natural orbitals obtained from the separated pair wave functions were very similar to those calculated from the 28 configuration wave function.

Conclusions

The conventional separated pair theory has not completely fulfilled all earlier expectations. The single antisymmetrized product of strongly orthogonal geminals accounts for only a fraction of the total correlation energy. Even for strongly localized systems (Be, CH_4) this fraction is about 90—50%. The transferability of the geminals seems to depend strongly on the environment of the corresponding pairs.

To achieve "chemical accuracy" it is necessary to go beyond the conventional separated pair theory. The extensions up to the present have used the one-electron functions optimized in the conventional theory and for small strongly localized systems have given promising results. The applicability depends mainly on the convergence of the expansion used in the extensions. If the natural orbitals of the separated pair wave function are very close to the natural orbitals of the exact wave function then the rate of convergence is nearly optimal and the second and third order correction of perturbation theory may be sufficient. The evaluation of the higher order corrections seems to be very clumsy. The practicability of the theory can be decided only when the results of further numerical calculations on various systems is available.

REFERENCES

1. V. A. FOCK, Doklady Acad. Nauk SSSR, **73,** 735, 1950.
2. F. BOPP, Z. Physik, **156,** 348, 1959.
E. KRŐNER, Z. Naturforsch., **15***a*, 260, 1960.

3. T. SCHÄFER, Dissertation, Ludwig-Maximilians-Universität, München, 1968.
4. A. C. HURLEY, J. E. LENNARD-JONES and J. A. POPLE, Proc. Roy. Soc., **A220**, 496, 1953.
5. J. M. PARKS and R. G. PARR, J. Chem. Phys., **28**, 335, 1958.
6. E. KAPUY, Acta Phys. Hung., **9**, 237, 1958.
7. R. MCWEENY, Proc. Roy. Soc., **A253**, 242, 1959; Rev. Mod. Phys., **32**, 335, 1960.
8. R. G. PARR, Quantum Theory of Molecular Electronic Structure, New York, W. A. Benjamin Inc. 1963.
9. R. G. PARR, F. O. ELLISON and P. G. LYKOS, J. Chem. Phys., **24**, 1106, 1956.
10. E. KAPUY, Acta Phys, Hung., **12**, 185, 351, 1960.
11. T. ARAI, J. Chem. Phys., **33**, 95, 1960.
12. P.-O. LÖWDIN, J. Chem. Phys., **35**, 68, 1961.
13. E. KAPUY, Acta Phys. Hung., **13**, 461, 1961.
14. W. KUTZELNIGG, Theoret. Chim. Acta (Berl.) **1**, 327, 1963.
15. W. KUTZELNIGG, J. Chem. Phys., **40**, 3640, 1964.
16. R. MCWEENY and K. OHNO, Proc. Roy. Soc., **A255**, 367, 1960.
17. M. KLESSINGER and R. MCWEENY, J. Chem. Phys., **42**, 3343, 1965.
18. D. D. EBBING and R. C. HENDERSON, J. Chem. Phys., **42**, 2225, 1965.
19. K. J. MILLER and K. RUEDENBERG, J. Chem. Phys., **43**, 588, 1965; **48**, 3414, 1968.
20. R. AHLRICHS and W. KUTZELNIGG, J. Chem. Phys., **48**, 1819, 1968.
21. O. SINANOĞLU, J. Chem. Phys., **36**, 706, 3198, 1962.
22. O. SINANOĞLU, Advan. Chem. Phys., **6**, 315, 1964.
23. R. K. NESBET, Phys. Rev., **115**, 51, 56, 1967.
24. C. EDMISTON and M. KRAUSS, J. Chem. Phys., **45**, 1833, 1966; **49**, 192, 1968.
25. G. DAS and A. C. WAHL, J. Chem. Phys., **44**, 87, 1966.
26. K. J. MILLER and K. RUEDENBERG, J. Chem. Phys., **48**, 3444, 3450, 1968.
27. R. AHLRICHS and W. KUTZELNIGG, Chem. Phys. Letters, **1**, 651, 1968.
28. E. KAPUY, J. Chem. Phys., **44**, 956, 1966.
29. E. KAPUY and N. H. MARCH, J. Math. Phys., **8**, 1915, 1967.
30. V. MCKOY and O. SINANOĞLU, J. Chem. Phys., **41**, 2689, 1964.
31. E. KAPUY, Theoret. Chim. Acta (Berl.), **6**, 281, 1966.
32. P.-O. LÖWDIN, Advan. Chem. Phys., **2**, 270, 1959.
33. E. KAPUY, Chem. Phys. Letters, **3**, 43, 1969.
34. E. KAPUY, Theoret. Chim. Acta (Berl.), **12**, 397, 1968.
35. R. G. PARR and R. S. MULLIKEN, J. Chem. Phys., **18**, 1338, 1950.

РАЗВИТИЯ В РАЗДЕЛЕННОЙ ПАРНОЙ ТЕОРИИ

Э. КАПУИ

Резюме

В последние годы стало возможным определить строго ортогональные геминалы для некоторых малых систем и исследовать эффективность конвенциональной разделенной парной теории. Результаты сравниваются с полученными путем применения других многоэлектронных теорий. Обращается внимание на источники главных недостатков. Рассматривается дальнейшее расширение разделенной парной теории, применяющей оптимизированные орбитали волновой функции просто антисимметризированного геминального произведения.

Acta Physica Academiae Scientiarum Hungaricae, Tomus 27, pp. 191—217 (1969)

EINIGE BEMERKUNGEN ZUM KOMBINIERTEN NÄHERUNGSVERFAHREN UND ZUM EFFEKTIVEN POTENTIAL* **

Von

H. PREUSS

MAX-PLANCK-INSTITUT FÜR PHYSIK UND ASTROPHYSIK, 8000 MÜNCHEN 23, BRD

(Eingegangen 3. II. 1969)

Nach einer kurzen Einführung in das kombinierte Näherungsverfahren werden dami die Bindungsenergien und Abstände der Alkalimolekülionen berechnet und die Frage nach der Existenz von Alkalihydridmolekülionen aufgeworfen. Bezüglich einer Verbesserung des Verfahrens wird ein Atomfunktionenansatz benutzt, der sich nur aus Exponentialausdrücken aufbaut. Weitere Verbesserungsmöglichkeiten werden diskutiert.

Ausgehend von diesen Untersuchungen wird die Rolle des effektiven Potentials im Rahmen von Mehrzentrenproblemen untersucht und ganz allgemein gezeigt, dass sich im Rahmen einer naiven Einteilchennäherung kein effektives Potential definieren lässt, sondern die sinnvolle Einführung eines solchen nur dann möglich ist, wenn gewisse Züge des Einteilchenbildes fallen gelassen werden. Dabei wird eine Definition des Zusatzpotentials angegeben, die auf einem Variationsprinzip basiert und Möglichkeiten aufzeigt, wie das effektive Potential bestimmt werden kann. Ferner wird eine vor einiger Zeit vom Verfasser angegebene Gütedefinition der Näherungslösungen der Schrödingergleichung mit einem schon bekannten Variationsverfahren in Zusammenhang gebracht, wobei der Begriff des effektiven Potentials notwendig ist.

1. Einführung

Das für die Valenzelektronen eines Atoms geltende Besetzungsverbot für die von den Rumpfelektronen voll besetzten Quantenzustände bewirkt, dass diese in höhere Zustände gedrängt werden. Mit Hilfe statistischer Betrachtungen lässt sich dieses Besetzungsverbot für den aus abgeschlossenen Schalen bestehenden Rumpf als eine nicht klassische Abstossungskraft formulieren, die zwischen Rumpf- und Valenzelektronen wirkt und die ein Zusatzpotential für die Valenzelektronen liefert, das die Erfüllung des Pauliprinzips zwischen Rumpf- und Valenzelektronen automatisch regelt [1]. Dieses Zusatzpotential ist, entsprechend unserer Voraussetzung abgeschlossener Schalen, kugelsymmetrisch und enthebt uns der Mühe, die Eigenfunktionen der einzelnen Valenzelektronen auf die der einzelnen Rumpfelektronen zu orthogonalisieren. Der dafür nötige Rechenaufwand ist bei grösseren Rümpfen sehr beträchtlich.

* Herrn Prof. P. Gombás in Verehrung zum 60. Geburtstag gewidmet.

** Die vorliegende Arbeit stellt eine Zusammenfassung der vom Verfasser in den letzten Jahren zu diesem Thema vorliegenden Publikationen und Diskussionen dar.

Man führt daher für das i-te Valenzelektron ein modifiziertes Potential φ ein, welches aus einem elektrostatischen Anteil und aus dem Zusatzpotential besteht

$$\Phi(i) = V(i) + V_z(i)\,, \tag{1}$$

und hat im Ansatz für die Valenzelektronen die einzelnen Einelektronenfunktionen voneinander orthogonal zu machen und braucht bei der Berechnung der Energiewerte keine Rücksicht auf die Rumpfelektronen zu nehmen.

Das Vielelektronenproblem durch eine kombinierte Methode zu lösen, indem die Rumpfelektronen statistisch und die Valenzelektronen nach der Wellengleichung behandelt werden, hat zuerst HELLMANN [2] durchgeführt. Eine analytische Form des Zusatzpotentials wurde dann von GOMBÁS [1] [3] und FÉNYES [4] auf verschiedene Weise hergeleitet.

Für die praktische Anwendung setzte HELLMANN das Zusatzpotential analytisch an

$$V_z(r) = \frac{A}{r} e^{-2\mathscr{K}r} \tag{2}$$

und bestimmte $\mathscr{K}$ und A dadurch, dass die tiefsten Terme des freien Atoms möglichst gut übereinstimmen. Dieses Vorgehen ist oft mit Recht kritisiert worden, da das Zusatzpotential, wie GOMBÁS gezeigt hat [1], davon abhängt, in welchem Zustand sich das jeweilige Valenzelektron befindet. Mit anderen Worten, das Zusatzpotential, welches auf ein herausgegriffenes Valenzelektron wirkt, ist gleichzeitig auch eine Funktion des Quantenzustandes des Elektrons. Man muss daher dem Ansatz (2) diei Bedeutung eines Mittelwertes beimessen und darf dann erwarten, dass auch de Ergebnisse nur in diesem Sinne verstanden werden können.

Andererseits geht dieses halbtheoretische Verfahren im Prinzip über die statistische Methode hinaus, da es auch der Polarisation des Rumpfes durch das Valenzelektron und der Austauschwechselwirkung des Valenzelektrons mit den Rumpfelektronen Rechnunlg trägt. Man muss daher das kombinierte Näherungsverfahren als eine Modelrechnung ansehen, bei der man freilich schon ungefähr die gemachten Vernachlässigungen übersieht und darf diesen Rechnungen daher mehr orientierenden Charakter zumessen. Die Ergebnisse, auf die wir noch näher zu sprechen kommen werden, zeigen aber, dass in vielen Fällen auch eine quantitative Diskussion noch möglich ist.

Bei der Berechnung von Molekülproblemen treten weitere Schwierigkeiten auf, die besonders den Einsatz des Zusatzpotentials als Funktion der Elektronenzustände mit einem grossen rechnerischen Aufwand belasten. Zwar könnte man in erster Näherung die Wechselwirkungen der Rümpfe untereinander vernachlässigen, da es ohne weiteres möglich wäre, diese zum Beispiel nach der Störungsrechnung von LENZ [5] und JENSEN [6] ausreichend genau

zu berücksichtigen, doch treten Schwierigkeiten auf, Zusatzpotentiale der verschiedenen Zentren so aufeinander abzustimmen, dass sich die Valenzelektronen eines Moleküls noch in einem sinnvollen effektiven Potential befinden.

2. Bisherige Anwendungen

Nach Separation der Wellengleichung ergibt sich für den Radialanteil $R(r)$ der ψ-Funktion die Differentialgleichung (Z bedeutet Z-fach geladener Rumpf) des Atomproblems zu

$$-\frac{1}{2}R''(r)-\frac{1}{r}R'(r)+\left[\frac{A}{r}e^{-2\mathscr{H}r}+\frac{1}{2}l(l+1)\frac{1}{r^2}-\frac{z}{r}\right]R(r)=ER(r)\,. \quad (3)$$

Die Bestimmung der $\mathscr{H}$ und A (2) wurde mit Hilfe eines Variationsverfahrens durchgeführt [2] [7], in dem man für die ersten drei tiefsten Zustände des Atoms die Funktionen

$$R(1s)=e^{-\varepsilon r}\,,\quad R(2p)=re^{-\omega r}\,,$$
$$R(2s)=\left(1-\frac{\varepsilon+\eta}{\varepsilon}r\right)e^{-\eta r} \quad (4)$$

ansetzte und die Energien (5) bei festem A und $\mathscr{H}$ zum Minimum machte:

$$E(1s)=\frac{1}{2}\varepsilon^2-Z\varepsilon+A\varepsilon\left(\frac{\varepsilon}{\varepsilon+\mathscr{H}}\right)^2,$$
$$E(2p)=\frac{1}{2}\,\omega^2-\frac{Z\omega}{2}+A\frac{\omega}{2}\left(\frac{\omega}{\omega+\mathscr{H}}\right)^4, \quad (5)$$
$$E(2s)=\eta^2\left(\frac{1}{6}+\frac{1}{1-(\varepsilon/\eta)+(\varepsilon/\eta)^2}\right)-$$
$$-\frac{Z\eta}{2}\left(1+\frac{2-(\varepsilon/\eta)}{1-(\varepsilon/\eta)+(\varepsilon/\eta)^2}\right)+$$
$$+A\eta\,\frac{3-2\dfrac{1+\varepsilon/\eta}{1+\mathscr{H}/\eta}+\dfrac{1}{2}\left(\dfrac{1+\mathscr{H}/\eta}{1+\varepsilon/\eta}\right)^2}{(1+\mathscr{H}/\eta)^2\left(1-(\varepsilon/\eta)+(\delta/\eta)^2\right)}.$$

Dann wurden $\mathscr{H}$ und A so gewählt, dass $E(1s)$ mit dem empirischen tiefsten Term völlig übereinstimmte. Die folgende Tabelle I gibt die $\mathscr{H}$ und A-Werte wieder sowie einen Vergleich der Energiewerte, wobei die höheren Terme möglichst gut zur Übereinstimmung mit den Experimentalwerten gebracht wurden.

Tabelle I

Die Konstanten $\mathscr{H}$ und A sowie Energiewerte in eV für Alkaliatome und einige Erdalkali-Ionen

Atom	Konstanten		s-Grundterm		s-Term angeregt		p-Grundterm	
	$\varkappa$	A	theor.	exp.	theor.	exp.	theor.	exp.
Na	0,536	1,826	5,12	5,12	1,85	1,94	2,92	3,02
K	0,449	1,989	4,32	4,32	1,63	1,73	2,73	2,71
Rb	0,358	1,640	4,16	4,16	1,69	1,68	2,56	2,58
Cs	0,333	1,672	3,87	3,87	1,53	1,59	2,45	2,46
Mg^+	0,844	4,656	14,96	14,96	5,75	6,35	10,48	10,55
Ca^+	0,506	3,653	11,81	11,81	4,91	5,37	8,80	8.69

Mit diesen justierten Zusatzpotentialen wurde u. a. in die Berechnung des metallischen Zustands eingegangen [7].

Für das K_2-Molekül im Grundzustand wurden von HELLMANN [2] mit dem Heitler—Londonschen Funktionsansatz in einer groben und orientierenden Rechnung eine Bindungsenergie (BE) von —0,19 eV bei einem Kernabstand (R) von 4,0 Å erhalten. (Experimentelle Werte: R = 3,9 Å, BE = —0,51 eV.) Für die Eigenfunktionen der Valenzelektronen waren nur Exponentialfunktionen verwendet worden.

Ebenso wurde von HELLMANN [2] das KH-Molekül behandelt, wobei zum Heitler—Londonschen Ansatz ein Ionenterm hinzuaddiert wurde. Die prozentuale Beteiligung des Ionenzustandes wurde aus der Minimumsforderung der Energie gewonnen. Die Ergebnisse lauten: R = 2,1 Å (Experiment 2,2 Å) und BE = —0,8 eV (—2.06 eV). Die zu kleinen Energien bei K_2 und KH beruhen auf der vernachlässigten Elektronenwechselwirkung, was HELLMANN durch eine Überlegung am K—H zeigen konnte.

Einen sehr ermutigenden Beweis für die Güte des kN-Verfahrens lieferte die Behandlung des Grundzustandes des Mg-Atoms. Mit den Werten von $\mathscr{H}$ und A nach Tabelle I wurde das Mg-Atom als Zweielektronenproblem behandelt [2] und mit einem von HYLLERAAS [8] am He mit Erfolg benutzten Variationsansatz

$$\psi(1, 2) = e^{-\alpha(r_1+r_2)}(1 + \beta r_{12})$$

der die Elektronenwechselwirkung berücksichtigt, berechnet. Es ergab sich eine Energie von 22,21 eV, die vom experimentellen Wert um 0,39 eV nach oben abweicht.

Diese erwähnten Rechnungen gehören zu den frühesten dieser Art. In den letzten Jahren hat GOMBÁS mit seinen Mitarbeitern zahlreiche Rechnungen durchgeführt [1], besonders mit dem analytischen Zusatzpotential im Rahmen der statistischen Theorie, so dass wir heute die Möglichkeit solcher Verfahrenswege gut übersehen können. Danach kann festgestellt werden, dass

für Atomrechnungen die Anwendung des Zusatzpotentials nach der statistischen Theorie einem analytischen Ansatz nach HELLMANN vorgezogen werden muss, wenn es darum geht, die Diskussionen quantitativ zu führen. Es hat sich darüber hinaus gezeigt, dass sich mit Hilfe der statistischen Theorie eine grosse Anzahl von atomaren Eigenschaften in guter Übereinstimmung mit dem Experiment ergeben und auch in vielen Fällen Voraussagen möglich sind [1].

Andererseits stösst, wie oben schon bemerkt, die Anwendung der statistischen Theorie auf Molekülprobleme auf eine Reihe von Schwierigkeiten, die heute noch nicht zufriedenstellend gelöst sind. Es empfiehlt sich daher, vorerst im Sinne des kombinierten Näherungsverfahrens wie oben besprochen die Werte A und $\mathscr{H}$ an freien Atomen zu justieren und dann mit diesem Potential in die Molekülrechnungen einzugehen. Dabei beachtend, dass man auf diese Weise ein Näherungsverfahren vor sich hat, welches bestenfalls nur die wesentlichsten Züge der chemischen Bindung zu diskutieren gestattet. Dennoch bleiben auch in diesem Rahmen eine Reihe von Fragen offen, so dass es nützlich erscheint, an Hand einiger kleiner Rechnungen weitere Einblicke in die Möglichkeiten des kombinierten Verfahrens (kN-Verfahren) zu erhalten.

Dazu halten wir die Berechnung der Einelektronenbindung für besonders geeignet, weil die Berücksichtigung der Elektronenwechselwirkung wegfällt und somit der rechnerische Aufwand beschränkt bleibt.

Für die Alkalimolekülionen ergibt sich somit nach (1) und (2) der Hamiltonoperator zu (in atomaren Einheiten)

$$\mathscr{H} = \frac{1}{2}\Delta - \left(\frac{1}{r_a} + \frac{1}{r_b}\right) + A\left(\frac{1}{r_a}\, e^{-2\mathscr{H} r_a} + \frac{1}{r_b}\, e^{-2\mathscr{H} r_b}\right) + \frac{1}{R} \tag{6}$$

mit den Werten von A und $\mathscr{H}$ nach Tabelle I, und es ist die Energie

$$\varepsilon = \int \psi^+ \mathscr{H}\psi \, d\tau \Big/ \int \psi^+ \psi \, d\tau \tag{7}$$

mit dem Variationsansatz ψ zum Minimum zu machen. Bezüglich des letzteren entscheiden wir uns für die Form (α, β Variationsparameter)

$$\psi = e^{-\alpha(r_a + r_b)} \{1 + \gamma^2 (r_a - r_b)^2\}, \tag{8}$$

die im Falle des H_2^+-Ions (A = 0 in (6)) praktisch die experimentellen Werte für R und BE ergab (BE-Abweichung etwa 7‰). Der Grund liegt zum Teil darin, dass (8) mit $\gamma = 0$ schon kein schlechter Variationsansatz ist, denn der sich für diesen Fall ergebende Energieausdruck (7) nach R-Variation

$$\varepsilon = \left(-\frac{10}{3}x^2 + x - \frac{1}{2}\right)^2 \Big/ \left[2x^2(2x+1)\left(1 + 2x + \frac{4}{5}x^2\right)\right] \tag{9}$$

mit

$$R = 2x^2(1+2x)\Big/\left(\frac{10}{3}x^2 + x\frac{1}{2}\right),$$

hat sein Minimum von $\varepsilon = 0{,}58135$ at.E. für $x = \alpha R = 1{,}275$ und damit $R = 0{,}98$ Å, was einer BE von 2,20 eV entspricht. Die experimentellen Werte sind $R = 1{,}06$ Å (2,00 at.E.) und BE = 2,79 eV.

In diesem Zusammenhang sei erwähnt, dass der naheliegende Ansatz (10), der nicht so einfache Integrale ergibt wie der Ansatz (8)

$$\psi = e^{-\alpha r_a} + e^{-\alpha r_b} \tag{10}$$

im Minimum $R = 1{,}06$ Å und eine BE von 2,25 eV lieferte. Nach Einführen von elliptischen Koordinaten,

$$r_a + r_b = R\mu, \qquad r_a - r_b = R\nu,$$

$$1 \leqslant \mu < -\infty, \quad -1 \leqslant \nu \leqslant +1, \quad \varphi \quad \text{um} \quad R,$$

erhält (8) die Form

$$e^{-\alpha R\mu}(1 + \gamma^2 R^2 \nu^2), \tag{11}$$

und man kann das Ergebnis von (9) so interpretieren, dass die Annahme einer ellipsoidischen Ladungsverteilung (μ = const sind Ellipsoide um die Kerne als Zentren) eine gute Näherung darstellt.

Mit (8) ergibt sich also für Alkalimolekülionen

$$\varepsilon = (-H_A - H_1 + 2AH_A)/N + \frac{1}{R} \tag{12}$$

mit

$$H_A = \frac{R}{4}\left\{-2\alpha A_1 + \left[\frac{4}{3}A_0(0{,}5+a)\right]c - \left[\frac{2}{15}A_0(9{,}5+a)\right]c^2\right\},$$

$$H_1 = \frac{R^2}{2}\left\{2A_1 + \frac{4}{3}A_1 c + \frac{2}{5}A_1 c_2\right\},$$

$$N = \frac{R^3}{8}\left\{2A_2 - \frac{2}{3}A_0 + 2c\left(\frac{2}{3}A_2 - \frac{2}{5}A_0\right) + \right.$$

$$\left. + 2c^2\left(\frac{1}{5}A_2 - \frac{1}{7}A_0\right)\right\},$$

wobei A_n das Integral

$$A_n(1, 2a) = \int_1^\infty x^n e^{-2ax} dx \tag{13}$$

darstellt und $a = \alpha R$ und $c = \gamma^2 R^2$ bedeuten.

Für H_A erhält man dann

$$H_A = \frac{R^2}{4} \{(A_1 B_0 - A_0 B_1) + 2c (A_1 B_2 - A_0 B_3) + c^2 (A_1 B_4 - A_0 B_5)\}$$

mit

$$A_n = A_n(1, 2a + \mathscr{H}R) \tag{14}$$

und

$$B_n = B_n(\mathscr{H}R) = \int_{-1}^{+1} n^n e^{-2\mathscr{H}Rx} dx \,.$$

Ein grosser Vorteil des kN-Verfahrens ergibt sich daraus, dass sich der Übergang zu einem anderen Molekül der Alkalireihe nur in einer geringfügigen numerischen Änderung in (12) zeigt. Denn um das Energieminimum zu erhalten, müssen für einige a-, c- und R-Werte die Integrale H_Δ, H_1, H_A und N berechnet werden, die auch, mit Ausnahme von H_A, für die anderen Moleküle verwendet werden können, da nach (12) und (14) $\mathscr{H}$ nur in H_A eingeht und A als Faktor vor H_A steht.

Tabelle II gibt die im Minimum der Energie (für $c = 0$) mit den Werten von A und $\mathscr{H}$ nach Tabelle I erhaltenen Bindungsenergien (BE) an, sowie die in diesem Fall erhaltenen Kernabstände (R) und a-Werte.

Tabelle II

Bindungsenergien von Alkaliionen und -molekülen

	BE [eV]	R [at. E.]	a		BE [eV]	R [at.E.]
Na_2^+	—1,06	6,82	1,88	Na_2	—0,77	5,80
K_2^+	—0,93	8,47	2,08	K_2	—0,51	7,39
Rb_2^+	—0,80	8,60	2,20	Rb_2	—0,49	8,00
Cs_2^+	—0,80	9,17	2,22	Cs_2	—0,45	8,60

Zum Vergleich sind in Tabelle II ebenfalls die entsprechenden Werte für die Alkalimoleküle aufgenommen worden [9]. Die Variation in c ergibt keinen wesentlichen Energiegewinn mehr; so erhält man für Na eine BE von —1,13 eV, für $c = -0{,}35$, $R = 6{,}53$ at.E. und $a = 2{,}0$. Die Verhältnisse für K, Rb und Cs liegen ähnlich. Der relativ geringe Energiegewinn für $c \neq 0$ legt, unter der Annahme, dass die Verhältnisse ähnlich wie beim H_2^+ liegen, die Vermutung

nahe, dass mit dem Ansatz (8) eine gute Näherung für die Einelektronenfunktionen gefunden worden ist und die erhaltenen BE-Werte nicht viel von den wirklichen Energiewerten von (7) und (7) abweichen können.

Da die Bestimmung der A-und $\mathscr{H}$-Werte noch sehr grob ist, ist von einer Variation von c für K, Rb und Cs abgesehen worden, zumal die Ergebnisse (Tabelle II) wie gesagt nur orientierenden Charakter haben sollen.

Leider liegen keine experimentellen Werte für die Alkalimolekülionen vor, doch wird man auf Grund der Rechnungen sagen können, dass die Bindungsenergien, im Gegensatz zum Verhältnis bei H_2 und H_2^+, wo sich für BE $(H_2) = -4{,}72$ eV $(R = 1{,}42)$ und BE $(H_2^+) = 2{,}79$ eV $(R = 2{,}00)$ ergibt, bei den Alkalimolekülionen grösser (höchstens gleich) als die der entsprechenden Alkalimoleküle sein werden. Dagegen ist die Vergrösserung des Kernabstandes bei den Einelektronenbindungen durchgehend vorhanden, der wohl darauf beruht, dass sich im Falle der Zweielektronenbindung zwei neutrale Atome entgegenkommen, die ihre Elektronen austauschen, während bei Vorhandensein eines Valenzelektrons dieses schon bei grösseren Kernabständen ungestört von den »Potentialmulden« der beiden Kerne Gebrauch machen kann.

Das unterschiedliche Verhältnis der Bindungsenergien für Zwei- und Einelektronenbindung beim Wasserstoff und den Alkalien scheint seine Ursache in den verschiedenen Potentialen zu haben, in denen sich die Elektronen befinden. Während für H_2 (H_2^+) das Coulomb-Potential $(V_Z = 0)$ vorliegt, ist bei Na, K, Rb, Cs $\Phi(r) = -1/r + V_Z(r)$[(1), (2)] für $r = 0$ positiv unendlich $(A > 1{,}0)$ und besitzt zwischen $1{,}0 \leqq r \leqq 3{,}0$ ein endliches Minimum. Aus diesem Grunde kann der Energiegewinn bei Hinzukommen eines zweiten Elektrons geringer sein als beim Coulomb-Potential und die dann erhaltene Gesamtenergie nur wenig unter der zweifachen Ionisierungsenergie $(R = \infty)$ liegen.

Ganz ähnlich gestaltet sich die Behandlung der Alkalihydridionen. Statt (12) ergibt sich

$$\varepsilon = (-H_A - H_1 + AH_A)/N + 1/R\,, \tag{15}$$

wobei der Variationsansatz (8) wegen der fehlenden Symmetrie des Gebildes in der Form

$$\psi = e^{-(\alpha r_a + \beta r_b)}\{1 + \gamma^2 (r_a - r_b)^2\} \tag{16}$$

angesetzt wurde. Damit ergab sich für die einzelnen Integrale in (15)

$$N = \frac{R^3}{8}\left[(A_2 B_0 - A_0 B_2) + 2c\,(A_2 B_2 - A_0 B_4) + c^2 (A_2 B_4 - A_0 B_0)\right],$$

$$H_1 = \frac{R^2}{4}\left[A_1 B_0 + 2cA_1 B_2 + c^2 A_1 B_4\right],$$

$$H_A = \frac{R}{4}\left[(bA_0 B_1 - aA_1 B_0) + A_0(2cB_0 - 4bcB_1 + \right.$$
$$+ B_2\{2b^2 c + 2c^2 - 6c\} + 4bc\{2 - c\}B_3 + \qquad (17)$$
$$+ \{b^2 c^2 - 2b^2 c - 6c^2\}B_4 + 6bc^2 B_5 - b^2 c^2 B_6) -$$
$$\left. - aA_1\{2cB_2 + c^2 B_4\}\right]$$

mit

$$A_n = A_n(1, 2a), \quad B_n = B_n(2b)$$

und

$$a = \frac{R}{2}(\alpha + \beta), \quad b = \frac{R}{2}(\alpha - \beta), \quad c = (\gamma B)^2$$

sowie

$$H_A = \frac{R^2}{4}\left[(A_1 B_0 - A_0 B_1) + 2c(A_1 B_2 - A_0 B_3) + c^2(A_1 B_4 - A_0 B_5)\right]$$

mit

$$A_n = A_n(1, 2a + \mathscr{H}R), \quad B_n = B_n(2b + \mathscr{H}R).$$

Die Gleichungen (17) gehen für $\alpha = \beta$ ($b = 0$) in die von (12) über. Nach abwechselnder Variation von a und b bis zum absoluten Minimum der Energie bei vorgegebenen Kernabständen ergab sich mit den A- und $\mathscr{H}$-Werten des Natriums keine Bindungsenergie. Allerdings war bei $R \geq 5$ at.E. (2.65 Å) schon die Ionisierungsenergie (—13,54 eV) des H-Atoms erreicht [$\varepsilon(\infty) = -13{,}54$ eV], wobei sich $\alpha \approx 1$ und $\beta \approx 0$ ergab (1s-Funktionen). Für $R \leq 5$ at.E. stieg dann die $E(R)$-Kurve an.

Bemerkenswerterweise ergab die c-Variation keine wesentliche Verbesserung. Für $R \geq 5$ at.E. würde für $c = 0{,}00$ das Energieminimum gefunden, während sich z. B. bei $R = 4{,}2$ at.E. für $c = -0{,}1$ eine geringfügige Erniedrigung von —13,40 eV auf —13,42 eV für ε ergab.

Für die übrigen Alkalien wurden ähnliche Ergebnisse erhalten. Man wird auch hier vermuten können, dass (16) mit $\gamma = 0$ schon ein befriedigender Variationsansatz ist. Dass keine Bindung auftritt, liegt ebenfalls an den Potentialverläufen der Alkalien und des Wasserstoffs, indem das Elektron des H-Atoms ($\alpha \approx 1$, $\beta \approx 0$) zwar von der gebotenen endlichen tiefen Potentialmulde des Bindungspartners Gebrauch macht, aber der Energiegewinn ist gering, um gegen die bei Nähern des Alkaliions anwachsende Coulomb-Abstossung aufzukommen. Dagegen kann jetzt ein zweites Elektron neben dem ausgeprägten 1s-Zustand des H-Atoms, wo es sich bevorzugt aufhält (heteropolarer Anteil), auch von der fast freien Potentialmulde des Alkaliions Gebrauch machen, so dass die Energie entgegen den Verhältnissen bei den Alkalimolekülen noch sehr abfallen kann. Man beobachtet auch dementsprechend bei den Alkalihydriden BE-Werte zwischen 1,0 und 2,0 eV [9].

Die Ergebnisse bezüglich der Bindungsenergien von Zwei- und Einelektronenbindungen lassen sich noch durch ein grobes quantitatives Verfahren herleiten, welches die vorliegenden Verhältnisse näher erläutern soll.

Befindet sich ein Elektron (1) im Potentialfeld $V(1)$ der beiden gleichen Atomrümpfe a und b, so ergibt sich der Hamiltonoperator für das Molekül $2\tilde{n}$

$$H^+(1) = -\frac{1}{2}\Delta_1 - V_a(1) - V_b(1), \tag{18}$$

während er sich für den Fall zweier Elektronen in der Form

$$H(1.2) = H^+(1) + H^+(2) + \frac{1}{r_{12}} \tag{19}$$

schreiben lässt. Mit diesen Ausdrücken berechnen wir unter vereinfachenden Annahmen die Gesamtenergien E^+ und E, indem wir den $1/r_{12}$-Term in (19) vernachlässigen und die ψ-Funktionen (ψ^+, ψ) in der üblichen Weise aus Atomfunktionen φ bestehend ansetzen:

$$\begin{aligned} \psi^+ &= \varphi_a(1) + \varphi_b(1) \\ \psi &= \varphi_a(1)\,\varphi_b(2) + \varphi_a(2)\,\varphi_b(1) \end{aligned} \tag{20}$$

(Heitler—London-Ansatz).

Wir erhalten unter Berücksichtigung der Coulomb-Abstossung der Kerne die Ausdrücke

$$E^+ = (H_{aa} + H_{ab})/(1 + S) + 1/R, \tag{21}$$

$$E = 2(H_{aa} + SH_{ab})/(1 + S^2) + 1/R \tag{22}$$

mit

$$\begin{aligned} H_{aa} = H_{bb} &= \int \varphi_a^*(1)\, H^+(1)\, \varphi_a(1)\, d\tau_1 \\ &= \int \varphi_b^*(1)\, H^+(1)\, \varphi_b(1)\, d\tau_1, \\ H_{ab} = H_{ba} &= \int \varphi_a^1(1)\, H^+(1)\, \varphi_b(1)\, d\tau_1 \\ &= \int \varphi_b^+(1)\, H^+(1)\, \varphi_a(1)\, d\tau_1 \end{aligned} \tag{23}$$

und

$$\begin{aligned} S &= \int \varphi_a^+(1)\, \varphi_b(1)\, d\tau_1, \\ \int |\varphi_a|^2(1)\, d\tau_1 &= 1, \quad \int |\varphi_b|^2(1)\, d\tau_1 = 1. \end{aligned}$$

Nachdem (21) und (22) durch Variation von R zum Minimum gemacht worden sind, erhält man die Bindungsenergien (BE^+, BE) bekanntlich dadurch, dass man die ersten Ionisierungsenergien ($-I_a = -I_b$) der freien Atome abzieht,*

* Dies gilt nur dann, wenn keine Anregungen in den Valenzzustand vorliegen und es sich um reine Zwei- oder Einelektronenbindungen handelt, wie dies hier der Fall ist.

und erhält somit, wenn die Werte von R und der Integrale (23) im Minimum für (21) und (22) mit den Zeichen + und 0 unterschieden werden, die Gleichungen

$$\mathrm{BE}^{+} = \frac{(H^{+}_{aa} + H^{+}_{ab})}{(1 + S^{+})} + \frac{1}{R^{+}} + I_a , \tag{24}$$

$$\mathrm{BE}^{0} = \frac{2(H^{0}_{aa} + S^{0} H^{0}_{ab})}{(1 + S^{02}) + 1} R^{0} + 2I_a . \tag{25}$$

Unter Berücksichtigung der Tatsache, dass die φ-Funktionen (20) Lösungen eines Atomproblems sind,

$$\left[-\frac{1}{2} \Delta_1 - V_a(1) \right] \varphi_a(1) = -I_a \varphi_a \tag{26}$$

(entsprechend für φ_b),

ergibt sich für die Integrale (23)

$$\begin{aligned} H_{aa} &= -I_a - \int \varphi_a^{*} V_b \varphi_a \, d\tau = -I_a - V_{aa} , \\ H_{ab} &= -SI_a = \int \varphi_a^{+} V_b \varphi_b \, d\tau = -SI_a - V_{ab} , \end{aligned} \tag{27}$$

so dass sich die BE-Ausdrücke (24), (25) vereinfachen:

$$\mathrm{BE}^{+} = -(V^{+}_{aa} + V^{+}_{ab})/(1 + S^{+}) + 1/R^{+} , \tag{28}$$

$$\mathrm{BE}^{0} = -2(V^{0}_{aa} + S V^{0}_{ab})/(1 + S^{02}) + 1/R^{0} . \tag{29}$$

Zu weiteren Diskussionen bilden wir die Differenz der BE-Werte (δ) von Ein- und Zweielektronenbindung und erhalten

$$\begin{aligned} \delta = |\mathrm{BE}^{+}| - |\mathrm{BE}^{0}| = \\ = \frac{V^{+}_{aa} + V^{+}_{ab}}{(1 + S^{+})} - \frac{2(V^{0}_{aa} + S^{0} V^{0}_{ab})}{1 + S^{02}} + \left(\frac{1}{R^{0}} - \frac{1}{R^{+}} \right) . \end{aligned} \tag{30}$$

Im Falle des H_2 und H_2^{+} lässt sich (30) streng durchrechnen und ergibt das bekannte Ergebnis. Man kann aber ganz grob schon einsehen, dass für Wasserstoff $\delta < 0$ gilt, weil der grossen Verschiedenheit von R^0 und R^+ ($1/R^0 — 1/R^+ = 0{,}2$) wegen in guter Näherung $S^{+} = S^{02}$ gilt und somit auch V^{+}_{aa} und V^{+}_{ab} viel kleiner als die Integrale V^{0}_{aa} und V^{0}_{ab} sein müssen.

Bei den Alkalien dagegen können wir in einer für unsere Zwecke ausreichenden Näherung $S^0 = S^+$ annehmen** ($1/R^0 — 1/R^+ = 0{,}02$ für K_2,

** Für Na ergibt sich z.B. mit 3*s*-Slater-Funktionen $S^{+} = 0.54$, $S^{0} = 0.59$. Für die anderen Alkalimoleküle wird die prozentuale Änderung von R^0, R^+ noch geringer (s. Tabelle II).

K_2^+), so dass auch $V_{aa}^+ = V_{aa}^0$ und $V_{ab}^0 = V_{ab}^+$ erfüllt sein wird. Führen wir noch das Verhältnis $V_{ab}/V_{aa} = \omega$ ein, so erhält (30) die Form

$$(1 - S^2)\frac{\omega - 1}{\omega + 1} - 2S + \frac{R^+ - R^0}{(\omega + 1)\,R^+ R^0}(1 + S + S^2 + S^3) =$$

$$= (1 + S^2)(1 + S)\,\delta\,. \tag{31}$$

Zur Berechnung von ω wurde für V_b das Potential

$$\frac{1}{r_b} - \frac{A}{r_b}\,e^{-2\mathscr{H} r_b}$$

nach (1), (2) benutzt und φ als Exponentialfunktion angenommen. Es ergibt sich damit für ω ein Wert zwischen 1,0 und 2,0, mit dem aus (31) tatsächlich folgt, dass für kleine S ($S \leqq 0{,}2$) δ positiv ist.

Die erhaltenen Zahlenwerte haben nur orientierende Bedeutung, doch ist es bemerkenswert, dass in dieser groben Näherung die Verhältnisse qualitativ richtig wiedergegeben werden.

3. Verbesserung der Variationsansätze

Die bisherigen Ergebnisse ermutigen dazu, das kN-Verfahren zu verschärfen. Dies lässt sich nur in der Weise durchführen, dass die Parameter $\mathscr{H}$, A im analytischen Ansatz für das Zusatzpotential V_z genauer bestimmt werden. Erst wenn dies möglich ist, könnte erwogen werden, einen verbesserten Ansatz für V_z zu verwenden, wofür wir beispielsweise

$$V_Z = (A/r + B)\,e^{-2\mathscr{H} r}\,;\quad V = -1/r + V_Z \tag{32}$$

vorschlagen. Prinzipiell wäre es damit möglich, A, B und $\mathscr{H}$ so zu bestimmen, dass die ersten drei Energiezustände des Atoms mit den empirischen übereinstimmen. Man geht kaum fehl in der Annahme, dass die weiteren Terme automatisch gut herauskommen werden, da dann, wo die höheren Atomfunktionen wesentlich von Null verschieden sind, nur noch das Coulomb-Potential vorliegt.

Bei allen Verbesserungen, die wir hier diskutieren, dürfen wir aber nicht vergessen, dass es sich doch nur um eine grobe Rechnung handelt und dass hier des guten nicht zuviel getan werden darf, zumal ja der analytische Ansatz für das Zusatzpotential eine Mittelwertbildung, wie oben besprochen, darstellt. Wir wollen uns daher vorerst nur auf zwei Parameter $\mathscr{H}$ und A beschränken und uns die Frage vorlegen, wie gut die bisher berechneten $\mathscr{H}$-und

A-Werte (Tabelle I) sind. Ohne Zweifel liegen die wirklichen Energiewerte für die $\mathscr{H}$-und A-Werte der Tabelle I tiefer, denn diese sind mittels des Ritzschen Verfahrens gewonnen worden, wobei wir die verwendeten Variationsfunktionen (4) noch einmal aufschreiben wollen:

$$s\text{-Grundterm:}\quad \psi = e^{-\varepsilon r}\,, \tag{33}$$

$$p\text{-Grundterm:}\quad \psi = re^{-\omega r}\,, \tag{34}$$

$$s\text{-Term angeregt:}\quad \psi = \left(1 - \frac{1}{3}(\varepsilon + \eta)\, r\right) e^{-\eta r}\,. \tag{35}$$

Um diese zu verbessern, könnte daran gedacht werden, mit den von MORSE, YOUNG und HAURWITZ [10] angegebenen Funktionen

$$\psi(1s) = Ae^{-\alpha r}\,, \tag{36}$$

$$\psi(2p) = Bre^{-\beta r}\,, \tag{37}$$

$$\psi(2s) = C(re^{-\gamma r} - \varrho e^{-\delta r}) \tag{38}$$

mit

$$A = 2\sqrt{\alpha^3}\,, \quad B = 2\sqrt{\beta^5/3}\,,$$

$$C = \frac{1}{\sqrt{\dfrac{3}{4\gamma^5} - \dfrac{12\varrho}{(\gamma+\delta)4} + \dfrac{\varrho^2}{4\delta^3}}} \quad \text{und} \quad \varrho = 3\,\frac{(\alpha+\delta)^3}{(\alpha+\gamma)^4}$$

die Energie zu berechnen. Man muss aber bedenken dass im kN-Verfahren kein reines Coulomb-Potential vorliegt und dass zur Bestimmung von $\mathscr{H}$ und A besonders die genaue Berechnung des Grundzustandes erforderlich ist. Aus diesem Grunde haben wir uns, entgegen den bisher verwendeten Funktionstypen, zu einer anderen Form des Variationsansatzes entschlossen, der ganz allgemein (normiert) als

$$\psi = (e^{-\alpha r} + \gamma e^{-\beta r})\, A(\alpha, \beta, \gamma)\,,$$

$$A(\alpha, \beta, \gamma) = \frac{2}{\sqrt{\dfrac{1}{\alpha^3} + \dfrac{2\gamma}{(\alpha+\beta)^{3/8}} + \dfrac{\gamma^2}{\beta^3}}} \tag{39}$$

geschrieben werden kann [11]. Dieser Ansatz leistet ebenfalls alles, was man schon von vornherein analytisch von s- und p-Funktionen verlangt, und bietet darüber hinaus, neben einer Reihe noch später zu diskutierender Vor-

teile, die Möglichkeit, mehr Parameter zu variieren. Für die wasserstoffähnlichen Funktionsansätze ergibt sich aus (39):

$$\psi(1s) = e^{-\alpha_1 r} A(\alpha_1, 0, 0) \tag{40}$$

$$\psi(2p) = (e^{-\alpha_2 r} - e^{-\beta_2 r}) A(\alpha_2, \beta_2, -1), \tag{41}$$

$$\psi(2s) = (e^{-\alpha_3 r} - \gamma_3 e^{-\beta_3 r}) A(\alpha_3, \beta_3, -\gamma_3), \tag{42}$$

wobei die Orthogonalität von $\psi(2s)$ auf $\psi(1s)$

$$\gamma_3 = [(\alpha_1 + \beta_3)/(\alpha_1 + \alpha_3)]^3$$

ergibt. Wie gefordert, verschwindet $\psi(2p)$ für $r \to 0$ linear in r. Um ein Mass für die Güte dieser Funktionsansätze zu erhalten, sind mit (40), (41) und (42) zur Kontrolle die Energiewerte des H-Atoms berechnet worden. Die folgende Tabelle III gibt die Ergebnisse wieder.

Tabelle III

Energieterme des H-Atoms

Zustand	Wirkliche Energie (at.E.)	$\alpha\beta$-Werte im Energieminimum			Berechnete Energie in at. E.
		α	β	γ	
1*s*	−0,5	1,0	0	0	−0,5
2*s*	−0,125	0,460	0,545	−1,185	−0,124998
2*p*	−0,125	0,414	0,618	−1,0	−0,124998

Die Energien zeigen völlige Übereinstimmung. Die Nullstelle von $\psi(2s)$, $r_0 = ln|\gamma_3|/(\beta_3 - \alpha_3)$ ergibt sich ebenfalls zu $r_0 = 2{,}0$ (at.E.), wie dies auch für die strenge Lösung gilt.

Für die Rechnungen des kN-Verfahrens soll daher die Verwendung der Ansätze (43), (44), (45)

$$s\text{-Grundterm: } \psi = (e^{-\alpha_1 r} - \gamma_1 e^{-\beta_1 r}) A(\alpha_1, \beta_1, -\gamma_1), \tag{43}$$

$$p\text{-Grundterm: } \psi = (e^{-\alpha_2 r} - e^{-\beta_2 r}) A(\alpha_2, \beta_2, -1), \tag{44}$$

$$s\text{-Term angeregt: } \psi = (e^{-\alpha_3 r} - \gamma_3 e^{-\beta_3 r}) A(\alpha_3, \beta_3, -\gamma_3), \tag{45}$$

mit

$$\gamma_3 = \frac{1/(\alpha_1 + \alpha_3)^3 - \gamma_1/(\alpha_3 + \beta_1)^3}{1/(\alpha_1 + \beta_3)^2 - \gamma_1/(\beta_1 + \beta_3)^3} \tag{46}$$

vorgeschlagen werden. Die Anwendung dieser Funktionstypen empfiehlt sich noch aus einem anderen Grunde: da sie nur aus Exponentialfunktionen

bestehen, sind die mit ihnen berechneten Wechselwirkungsintegrale einfacher. Auf die in diesem Zusammenhang wichtigen Probleme der Integralberechnung ist in einer anderen Arbeit ausführlicher eingegangen worden [11]. Nur soviel soll gesagt werden, dass die Menge der erforderlichen Hilfsfunktionen zur Berechnung der Zweizentrenwechselwirkungsintegrale der K- und L-Schale gegenüber der Verwendung von Slater-Funktionen stark reduziert werden kann, und der allen Funktionen gleiche analytische Aufbau (39) eine Vereinfachung in der angewendeten Formel für die Energie bietet, indem diese für verschiedene Zustände nur in den Parametern geändert zu werden braucht. Ein Vorteil, der sich besonders bei den hier zugrunde liegenden elektronisch durchgeführten Rechnungen sehr bemerkbar gemacht hat.

Nachdem wir die Ansätze (43), (44), (45) am H-Atom geprüft haben, sollen diese zur Bestimmung der ersten drei Zustände am Na-Atom herangezogen werden, wenn für A und $\mathscr{H}$ die Werte der Tabelle I gelten ($A = 1{,}826$; $\mathscr{H} = 0{,}536$). Diese Rechnungen werden zeigen, auf welche Weise die A- und $\mathscr{H}$-Werte abzuändern sind. Mit

$$\mathscr{H} = -\frac{1}{2}\Delta - \frac{1}{r} + \frac{A}{r}e^{-2\mathscr{H}R} \tag{47}$$

und dem Ansatz

$$\psi = \left[\frac{(2l+1)\,(l-|\,m\,|)\,!}{4\pi(l+|\,m\,|\,!}\right]^{1/2} A(\alpha,\beta,\gamma)\{e^{-\alpha r} + \gamma e^{-\beta r}\}P_e^{|m|}(w\vartheta)e^{im\varphi} \tag{48}$$

ergibt sich

$$E = (Z_0 + Z_1\gamma + \gamma^2)/(1 + N_1\gamma + N_2\gamma^2) \tag{49}$$

mit

$$\begin{aligned} Z_0 &= \frac{\alpha^2}{2} - \alpha + A\alpha\left(\frac{\alpha}{\alpha+\mathscr{H}}\right)^2 + l(l+1)\,\alpha^2\,, \\ Z_1 &= \left(\frac{\alpha}{\frac{\alpha+\beta}{2}}\right)^3[\alpha\beta - \alpha - \beta] + 2A\alpha\left(\frac{\alpha}{\frac{\alpha+\beta}{2}+\mathscr{H}}\right)^2 \\ &\qquad + 2l(l+1)\frac{2\alpha^3}{\alpha+\beta}\,, \\ Z_2 &= \left(\frac{\alpha}{\beta}\right)^3\left\{\frac{\beta^2}{2} - \beta + A\beta\left(\frac{\beta}{\beta+\mathscr{H}}\right)^2 + \beta^2 l(l+1)\right\}, \\ N_1 &= 2\left(\frac{2\alpha}{\alpha+\beta}\right)^3; \qquad N_2 = \left(\frac{\alpha}{\beta}\right)^3. \end{aligned} \tag{50}$$

Die Energie (49) wurde dann für $l = 0$ (s-Grundterm) in α, β und zum Minimum gemacht, dann wurde $l = 1$ und $\gamma = -1$ gesetzt und in α und β variiert (p-Grundterm) und schliesslich für $l = 0$ der angeregte s-Term berechnet, indem γ nach (46) eingesetzt wurde und wiederum in α und β die Energie minimal gemacht wurde. Tabelle IV enthält die Ergebnisse im Vergleich zu den wirklichen Energiewerten sowie die im Minimum enthaltenen Parameterwerte.

Tabelle IV

Energieterme des Na-Atoms

Zustand	α	β	γ	E_{ber} [eV]	E_{emp} [eV]
s-Grundterm	0,491	1,093	−0,848	−5,55 (5,12)	−5,12
p-Grundterm	0,424	0,380	−1,0	−2,93 (2,92)	−3,02
s-Term angeregt	0,271	0,197	−0,734	−1,86 (1,85)	−1,94

Die in Klammern gesetzten Energiewerte wurden mit den wasserstoffähnlichen Funktionsansätzen (4) erhalten. Wie man sieht, liegt der jetzt sich ergebende Grundzustand wesentlich tiefer, während die höheren Terme keine grossen Abweichungen gegenüber den Energiewerten mit wasserstoffähnlichen Funktionen zeigen, da das Maximum der ψ-Funktionen der höheren Terme an Stellen liegen, wo das Coulomb-Potential schon stark überwiegt.

Auf Grund dieser Ergebnisse unter Hinzunahme der empirischen Werte und der Annahme, dass der Grundzustand besonders wesentlich in die Berechnung von A und $\mathscr{H}$ eingeht, kann man, wie schon oben vermerkt, annehmen, dass die erhaltenen BE-Werte der Alkalimolekülionen und die Energiewerte der Systeme Alkaliion und Wasserstoff nach den A- und $\mathscr{H}$-Werten von Tabelle I untere Grenzen darstellen.

Darüber hinaus hat sich ergeben, dass die Funktionsansätze (43), (44), (45) für das kombinierte Näherungsverfahren geeigneter sind. Zusammen mit dem erweiterten Ansatz für das Zusatzpotential (32) können prinzipiell die Parameter A, B und $\mathscr{H}$ so bestimmt werden, dass die ersten drei Energieterme mit den empirischen übereinstimmen, was für die praktische Anwendung völlig ausreichen sollte.

Verzichtet man auf die Verwendung des Parameters B, so können jedenfalls mit Hilfe der verbesserten Funktionsansätze A und $\mathscr{H}$ genauer als bisher bestimmt werden.

Ein weiteres Problem wirft die Verwendung neuer Funktionsbasen auf. In den letzten Jahren sind in verstärktem Masse Gaussfunktionen bei Molekülrechnungen verwendet worden [12], die folgendes Aussehen haben

$$\varphi_p = \left(\frac{2\eta}{\pi}\right)^{3/\psi} e^{-\eta(\mathfrak{r}-\mathfrak{r}_p)^2}. \tag{51}$$

Diese Funktionen wurden auch zur Beschreibung von Atomzuständen herangezogen und haben sich ganz besonders bei allen wellenmechanischen Verfahren der Quantenchemie bewährt [13]. In diesem Falle wäre zu überlegen, ob auch der Ansatz für das Zusatzpotential entsprechend modifiziert werden sollte, damit die Integrationen so einfach bleiben, wie dies bei den Gaussfunktionen der Fall ist. Es könnte daher daran gedacht werden, in Abänderung von (32) den folgenden Ansatz für das Zusatzpotential

$$V_z = \left(\frac{A}{r} + B\right) e^{-2\mathscr{K}r^2} \tag{52}$$

zu verwenden. In diesem Falle sind bei der Energieberechnung keinerlei neue Integrale zu erwarten.

4. Allgemeine Fragen in der Quantenchemie

In einer Reihe von Verfahren der quantentheoretischen Chemie wird ebenfalls mit dem Begriff des effektiven Potentials (Zusatzpotential) operiert, so z. B. in der Methode von Göppert—Mayer—Sklar, im kombinierten Näherungsverfahren, oder besonders im Hückel-Verfahren mit seinen Erweiterungen und Varianten. Schliesslich geht auch die Elektronengasmethode von einem effektiven Potential aus, in welchem sich die Elektronen befinden. Die Vorstellung des Zusatzpotentials, welche in irgendeiner Form die Elektronenwechselwirkung auf einfache Weise berücksichtigen helfen soll, ist also ganz verschiedenartigen Methoden gemeinsam. Aus diesem Grunde ist es notwendig, sich darüber klar zu werden, ob auch hier eine solche Konzeption überhaupt sinnvoll ist, oder ob diese nur mit gewissen Einschränkungen aufrecht erhalten werden kann.

Es ist bemerkenswert, dass solche Überlegungen bisher noch nicht durchgeführt worden sind, und z. B. die Meinung vorherrscht, dass ein effektives Potential durch kein Variationsprinzip erhalten werden kann, obwohl gerade das Hückel-Verfahren und die Elektronengasmethode ganz wesentlich von der Tatsache eines effektiven Potentials ausgehen. Der Grundgedanke ist dabei der, dass die Wirkungen der übrigen Elektronen auf ein herausgegriffenes durch ein Potential V dargestellt werden können, so dass es möglich ist, die Bewegungen eines jeden Elektrons in Form einer Einteilchen-Schrödingergleichung zu behandeln.

$$H'\Phi_j = \varepsilon'_j \Phi_j, \tag{53}$$

$$H' = -\frac{1}{2}\Delta + U(\mathfrak{r}) \qquad (H' \text{ in at. E.}). \tag{54}$$

Da das Potential U auch noch die Wechselwirkungen mit den Kernen enthält, so ist der Zusammenhang mit V, wenn N Zentren (Atome) der Ladungen Z_λ ($\lambda = 1 \ldots N$) vorliegen, in der folgenden Form gegeben

$$U = -\sum_{\lambda-1}^{N} \frac{z_\lambda}{r_\lambda} + V(\mathfrak{r}) . \tag{55}$$

$V(\mathfrak{r})$ steht also repräsentativ für die Wirkungen von n—1 Elektronen auf das betrachtete. Dementsprechend ergibt sich die Gesamtenergie $\tilde{\varepsilon}$ des aus n Elektronen bestehenden Systems zu

$$\tilde{\varepsilon}_s = \sum_j \varepsilon'_i , \tag{56}$$

wenn entsprechend dem Pauliprinzip die Zustände Φ_j besetzt werden, wobei sich die Gesamtwellenfunktion als Determinante der Φ_j schreibt

$$\tilde{\psi}_s = \det \{\Phi_j(i)\} \qquad (\alpha, \beta : \text{Spinfunktionen}) . \tag{57}$$

Gegebenenfalls treten Summen von Determinanten auf, wenn keine abgeschlossenen Schalen (im Sinne des Einteilchensbildes) vorliegen. Der Index s an $\tilde{\varepsilon}$ in (56) weist auf die verschiedenen Zustände des Gesamtsystems hin, die durch verschiedene Summierungen erhalten werden können (angeregte Zustände).

In Wirklichkeit wäre für ein solches System die Schrödingergleichung

$$\mathscr{H} \psi_s = \varepsilon_s \psi_s ; \qquad \int \psi_x \psi \, d\tau = 1 \tag{58}$$

zu behandeln, mit

$$\mathscr{H} = -\frac{1}{2} \sum_{i=1}^{n} \Delta_i - \sum_{i=1}^{n} \sum_{\lambda=1}^{N} \frac{z_\lambda}{r_{\lambda i}} + \sum_{i=1}^{n-1} \sum_{j=i-1}^{n} \frac{r}{r_{ij}} = \sum_{i=1}^{n} H(i) + \sum_{i=1}^{n-1} \sum_{j=i+1}^{n} \frac{1}{r_{ij}} , \tag{59}$$

wobei

$$H(i) = -\frac{1}{2} \Delta_i - \sum_{\lambda=1}^{N} \frac{z_\lambda}{r_{\lambda i}} . \tag{60}$$

Würde keine Elektronenwechselwirkung vorliegen, so ist $V(\mathfrak{r}) = 0$ und

$$H \equiv H' , \tag{61}$$

so dass auch

$$\tilde{\psi}_s = \psi_s \tag{62}$$

und

$$\tilde{\varepsilon}_s = \varepsilon_s \tag{63}$$

gilt. In diesem Falle zerfällt $\mathscr{H}$ in eine Summe von Einelektronenoperatoren $H(i)$.

Die primitive Vorstellung von einem Zusatzpotential besteht also darin,

$$\mathscr{H} = \sum_{i=1}^{n} H'(i) \tag{64}$$

zu setzen, obwohl Elektronenwechselwirkung vorliegt. Damit wäre dann der Ausgangspunkt für Gl. (53) und die folgenden bis (57) gefunden. Gibt es nun ein H' (bzw. V) von der Art, dass (58) mit (64) in Übereinstimmung gebracht werden kann? Offensichtlich nicht, denn die Besetzungsvorschrift, die sich in (56) zeigt, mit den Energien aus (53), macht keinen Unterschied in den verschiedenen Spinstellungen der Elektronen, so dass im Einklang mit dem Pauliprinzip für Zustände mit verschiedener Spinmultiplizität die gleiche Energie erhalten wird, obwohl in Wirklichkeit die Elektronenwechselwirkung zu einer Aufspaltung der Energie geführt hat. Man ersieht das z. B. aus der Form (39) von H, wenn man im Rahmen einer Störungsrechnung mit

$$H'^{(0)} = \sum_{i=1}^{n} H(i)] \tag{65}$$

als nullte Näherung beginnt und dann die Rechnung mit dem »Störoperator«

$$H'^{(0)} = \sum_{i=1}^{n-1} \sum_{j=i+1}^{n} \frac{1}{r_{ij}} \tag{66}$$

verbessert, der dann eine Aufspaltung der Energie nullter Näherung liefert, wenn diese ursprünglich für verschiedene Spinzustände gleich war. Man pflegt das bildlich etwa so darzustellen (Fig. 1, 2):

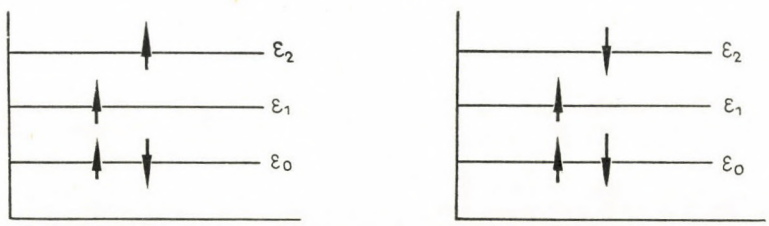

Fig. 1, 2

Im Einteilchenbild nach (53) können z.B. nach Fig. 1 und 2 Triplett- und Singulett-Zustände entsprechend der Vorschrift (56) nicht unterschieden werden, obwohl die $\tilde{\psi}_S$ nach (57) verschieden sind.

Wir können daher vorerst die noch ziemlich triviale Feststellung treffen, dass ein effektives Potential nach (53) und (55) nicht in aller Strenge gefunden werden kann. Die primitive Darstellung (64) für $\mathscr{H}$ lässt sich nicht exakt begründen. Mit anderen Worten: Zerlegt man $\mathscr{H}$ in der Form [14]

$$\mathscr{H} = \sum_{i=1}^{n} H'(i) + \left\{ \sum_{i=1}^{n-1} \sum_{j=i+1}^{n} \frac{1}{r_{ij}} + \sum_{i=1}^{n} [H(i) - H'(i)] \right\} = \mathscr{H}^{(0)} + \mathscr{H}^{(1)}, \tag{67}$$

so lässt sich mit keinem Potential V der Operator $\mathscr{H}^{(1)}$ annullieren, denn es gilt, wegen (54), (55), (59) und (60)

$$\mathscr{H}^{(1)} = \sum_{i=1}^{n-1} \sum_{j=i+1}^{n} \frac{1}{r_{ij}} - \sum_{i=1}^{n} V(i). \tag{68}$$

Man sieht leicht, dass

$$\sum_{i=1}^{n-1} \sum_{j=i+1}^{n} \frac{1}{r_{ij}} = \sum_{i-1}^{n} V(i) \tag{69}$$

nicht gelten kann, wenn man z. B. $\mathfrak{r}_i = \mathfrak{r}_j$ setzt. Oder auch anders ausgedrückt: Es lassen sich mit keinem Potential $V(i)$ die Gleichungen

$$\int \tilde{\psi}_s^* \, \mathscr{H}^{(1)} \, \tilde{\psi}_l \, d\tau \equiv 0 ; \qquad (s, l = 0, 1, 2 \ldots) \tag{70}$$

befriedigen, wenn alle Lösungen ψ_s nach (57) und (53) berücksichtigt werden. Wie kann man nun zu einer sinnvollen Definition eines Zusatzpotentials gelangen?

Offenbar ist die Forderung (70) zu weitgehend. Man wird daher als nächste Erleichterung an die Forderungen

$$\int \tilde{\psi}_s^* \, \mathscr{H}^{(1)} \, \tilde{\psi}_l \, d\tau = 0 ; \qquad (s, l = 0, 1, 2 \ldots) \quad (s \neq l) \tag{71}$$

denken, so dass die Näherungen erster Ordnung

$$\int \tilde{\psi}_s^* \, \mathscr{H}^{(1)} \, \tilde{\psi}_s \, d\tau \neq 0 \tag{72}$$

der Störungsrechnung noch übrig bleiben und somit z. B. die in Fig. 1 und 2 gezeigte energetische Gleichheit aufgehoben werden kann. Leider ist auch diese Forderung zu stark, denn sie bedeutet, dass (62) noch erhalten bleibt, wie man aus der Störungsrechnung erkennt. Auch mit (71) kann daher kein Zusatzpotential definiert werden, was diesmal sogar schon nicht mehr in der primitivsten Form (63) enthalten ist, denn $\mathscr{H}^{(1)}$ nach (68) braucht nach (72) nicht mehr zu verschwinden.

Wenn (72) beibehalten werden soll, so könnte ein Zusatzpotential noch durch

$$\int \tilde{\psi}_s^* \, \mathscr{H}^{(1)} \, \tilde{\psi}_l \, d\tau = \min ; \qquad (s, l = 0, 1, 2 \ldots) \quad (s \neq l) \tag{73}$$

definiert werden. Wir fassen eine Reihe von Bedingungen (73) zusammen und erhalten daraus die schwächeren Forderungen (gegebenenfalls Summierung in s)

$$\sum_{\substack{l \\ l \neq s}} [\int \tilde{\psi}_s^* \, \mathscr{H}^{(1)} \, \tilde{\psi}_l]^2 \, d\tau = \min ; \qquad (s = 0, 1, 2 \ldots). \tag{74}$$

Diese sollen als Definitionsgleichungen für ein Zusatzpotential V verwendet werden. Sie sind in vielerlei Hinsicht sinnvoll. Entwickeln wir im Rahmen der Störungsrechnung die exakte Lösung der Schrödingergleichung (mit $\mathscr{H}$) nach den Lösungen des ungestörten Systems ($\mathscr{H}^{(0)}$)

$$\psi_s = \tilde{\psi}_s + \sum_l \frac{\int \tilde{\psi}_s^* \, \mathscr{H}^{(1)} \, \tilde{\psi}_l \, d\tau}{\tilde{\varepsilon}_s - \tilde{\varepsilon}_l} \, \tilde{\psi}_l + \ldots \qquad (l \neq s), \tag{75}$$

so sehen wir, dass die Forderungen (73) auf ein Minimisieren der einzelnen Terme der rechts stehenden Summen hinausläufen, so dass auf diese Weise die Variationsgleichungen (73) mit den Forderungen

$$\int (\psi_s - \tilde{\psi}_s)^2 \, d\tau = \min ; \qquad (s = 0, 1 \ldots) \tag{76}$$

zusammenhängen, wenn ψ_S nach (57) zu verstehen ist. Die Variation in (76) wird mit Hilfe des effektiven Potentials V durchgeführt, so dass (immer im Sinne der Forderungen (73) und schwächer nach (74)) die beste Determinantendarstellung nach (57) gesucht wird. Diese dürfte kaum mit der Hartree—Fock-Lösung identisch sein, da diese bekanntlich durch die Forderungen [15]

$$\int \tilde{\psi}_s^* \, \mathscr{H}^{(1)} \, \tilde{\psi}_s \, d\tau = 0 ; \qquad (s = 0, 1 \ldots) \tag{77}$$

festgelegt wird und als effektives Potential das Hartree—Fock-Potential liefert. Man wird daher erwarten dürfen, dass die aus (76) sowie aus (73) bzw. (74) erhaltenen $\tilde{\psi}$-Funktionen zwar nicht die Gesamtenergie im Sinne der Energievariation minimisieren, aber dafür Näherungen darstellen, die gegebenenfalls bezüglich gewisser Erwartungswerte und Übergangselemente zu besseren Ergebnissen führen können [16]. Hier wären noch weitere Untersuchungen notwendig, besonders über den Zusammenhang von (73), (74) mit (76) und den daraus resultierenden Fragen nach der Güte von Näherungslösungen. Vorläufig lässt sich aus (74) mit Hilfe des Überganges

$$\sum_{\substack{l \\ l \neq s}} \left[\int \tilde{\psi}_s^* \, \mathscr{H}^{(1)} \, \tilde{\psi}_l \, d\tau \right]^2 = \int \tilde{\psi}_s^* \, \mathscr{H}^{(1)2} \, \tilde{\psi}_s \, d\tau - \left(\int \tilde{\psi}_s^* \, \mathscr{H}^{(1)} \, \tilde{\psi}_s \, d\tau \right)^2 = \min \tag{78}$$

bei dem die Definitionsbereiche von $\mathscr{H}^{(1)}$und $(\mathscr{H}^{(1)})^2$ beachtet werden müssen, zeigen, dass (74) in die Forderungen

$$\int \left[\left(\mathscr{H} - \int \tilde{\psi}_s^+ \, \mathscr{H} \tilde{\psi}_s \, d\tau \right) \tilde{\psi}_s \right]^2 d\tau = \min \, (s = 0, 1 \ldots) \tag{79}$$

übergeführt werden kann.

Dabei ist verwendet worden, dass die $\tilde{\psi}_S$ Eigenfunktionen von $\mathscr{H}^{(0)}$ sind. Das Variationsprinzip (79), und eine Erweiterung davon, sind in der Literatur schon bekannt [17, 18, 19].

Bezüglich einer praktischen Durchführung der Variation (78) könnte etwa daran gedacht werden,

$$V = \sum_{\alpha} C_\alpha V_\alpha(\mathfrak{r}) \tag{80}$$

für das Einteilchenpotential zu setzen (mit festgewählten V_α) und die Rechnungen mit einem bestimmten Satz von C_α zu beginnen. Mit den dazugehörenden $\tilde{\psi}_S$-Funktionen (gegebenenfalls näherungsweise als Linearkombinationen angesetzt), wird dann in (78) oder (79) eingegangen und die C_α variiert. Damit ist ein iteratives Verfahren gewonnen, in welchem nur solche V_α verwendet werden dürfen, die die Existenz der Integrale in (78) garantieren. Auch hier müssen weitere Untersuchungen angeschlossen werden.

Die Überlegungen dieses Abschnitts unterscheiden sich in der Interpretation wesentlich von denjenigen der vorhergehenden Abschnitte. Während im Falle der Atome die Zusatzpotentiale so gewählt worden sind, dass Austausch und Pauliprinzip berücksichtigt wurden, ging es hier darum, ein Potential aufzubauen, welches in gewisser Weise so gut wie möglich einen Teil des Hamiltonoperators, nämlich die Elektronenwechselwirkung durch eine Summe von Einteilchenpotentialen ersetzt. Damit ist die Schwierigkeit eines jeweils vom Elektronenzustand abhängigen Zusatzpotentials beseitigt. Andererseits ist mit der Variation (78) ein Weg beschritten worden, der zu einer anderen Auffassung des Zusatzpotentials geführt hat. Man darf nicht vergessen, dass auch hier wieder die Tatsache zu beachten ist, dass sich in der GOMBÁS'schen Fassung des Zusatzpotentials völlig richtig eine Abhängigkeit von den Elektronenzuständen ergeben muss. Die Mittelwertbildung im kN-Verfahren dagegen zeigt Zusammenhänge mit der hier angegebenen Definition des effektiven Potentials, wobei in jedem Falle jedes Elektron unabhängig sich im gleichen effektiven Potential befindet.

5. Zusammenhänge zur Güte der Wellenfunktion

In einer früheren Arbeit des Verfassers [20] wurde auf die Möglichkeiten von Gütedefinitionen der Näherungslösungen $\tilde{\psi}$ der Schrödingergleichung

$$(\mathscr{H} - \varepsilon)\,\psi_s = 0\,; \qquad \int \varphi_s^*\,\psi_s\,d\tau = 1 \tag{81}$$

eingegangen und vorgeschlagen, diese in der Form

$$\int [f(\psi_s - \tilde{\psi}_s)]^2\,d\tau = \eta^2(f, \tilde{\psi}_s) \tag{82}$$

einzuführen, indem die Grösse von $\eta^2(f,\tilde{\psi}_s)$ ein Mass dafür ist, wie gut die mit $\tilde{\psi}_s$ ($s = 0,1\ldots$) zu bildenden Erwartungswerte und Übergangselemente von

f zu erwarten sind. Dabei ergab sich unter anderem, dass $\eta^2(1, \tilde{\psi}_s)$ kein Mass für Integrale der Form $\int \tilde{\psi}_g^* f \tilde{\psi}_s, \, d\tau$ ist.

Es wäre daher grundsätzlich möglich, ein Variationsverfahren

$$\eta^2 (f, \tilde{\psi}_s) = \min \tag{83}$$

einzuführen, in welchem $\tilde{\psi}_s$ variiert wird. Leider ist dies in dieser Form nicht ohne weiteres möglich, da in (82) auch die exakte Lösung ψ auftritt. Die Forderung (83) lässt sich aber, wenn man in ähnlicher Weise wie in einer früheren Arbeit des Verfassers [21] vorgeht, nur in schwächerer Fassung auf ein brauchbares Variationsprinzip zurückführen.

Zerlegen wir $\mathscr{H}$ in (81) in der Form

$$\mathscr{H} = \tilde{\mathscr{H}} + \mathscr{H}^{(1)} \tag{84}$$

wobei $\tilde{\mathscr{H}}$ so definiert sein soll, dass

$$\tilde{\mathscr{H}} \tilde{\psi}_s = \tilde{\varepsilon}_s \tilde{\psi}_s ; \qquad \int \tilde{\psi}_s^* \tilde{\psi}_{s'} \, d\tau = \delta_{ss'} \tag{85}$$

gilt, so liefert die Störungsrechnung die Darstellung

$$\psi_s = \tilde{\psi}_s + \sum_{s'}{}' \frac{\int \tilde{\psi}_s^* \mathscr{H}^{(1)} \tilde{\psi}_{s'} \, d\tau}{\tilde{\varepsilon}_s - \tilde{\varepsilon}_{s'}} \psi_{s'} + \ldots \quad (s \neq s') . \tag{86}$$

Wie oben gezeigt, kann in diesem Zusammenhang durch

$$\sum_{\substack{s' \\ s \neq s'}} \left[\int \tilde{\psi}_s^* \mathscr{H}^{(1)} \tilde{\psi}_{s'} \, d\tau \right]^2 = \int \tilde{\psi}_s^+ \mathscr{H}^{(1)2} \tilde{\psi}_s \, d\tau - \left(\int \tilde{\psi}_s^+ \mathscr{H}^{(1)} \tilde{\psi}_s \, d\tau \right)^2 = \min \tag{87}$$

ein effektives Potential definiert werden, wenn $\tilde{\mathscr{H}}$ aus einer Summe von Einelektronenoperatoren besteht, wobei $\tilde{\psi}$ aus einer Reihe von Determinanten (bestehend aus Einelektronenfunktionen) aufgebaut werden muss. Gl. (87) kann dann umgeformt werden in

$$\delta^2 (1, \tilde{\psi}_s) = \int \left[\left(\mathscr{H} - \int \tilde{\psi}_s^* \mathscr{H} \tilde{\psi}_s \, d\tau \right) \tilde{\psi}_s \right]^2 d\tau = \min , \tag{88}$$

wenn von (85) Gebrauch gemacht wird.

Bei der ersten Ordnung der Störungsrechnung nach (86) sind auch in der Summe, wenn vorhanden, die Zustände des Kontinuums zu berücksichtigen. Dies ist praktisch undurchführbar. Aus diesem Grunde hat man versucht, die erste Näherung in (86) dadurch zu erfassen, dass man einen Mittelwert den »Energienenner« vor die Summe zog

$$\psi_s \cong \tilde{\psi}_s + \frac{1}{E'} \sum_{s'} \left(\int \tilde{\psi}_s^* \mathscr{H}^{(1)} \tilde{\psi}_{s'} \, d\tau \right) \tilde{\psi}_{s'} \quad (s \neq s') . \tag{89}$$

Diese Approximation ist, wie die Erfahrung gezeigt hat, recht gut [22], und kann unter Umständen noch einen Teil der zweiten Näherung mit erfassen [23]. Im Rahmen dieses Näherungsstandpunktes kann $\eta^2\,(1, \tilde{\psi})$ mit (88) in Zusammenhang gebracht werden, denn aus (89) folgt.

$$\eta^2(1, \tilde{\psi}_s) = \int (\psi_s - \tilde{\psi}_s)^2\, d\tau \approx \frac{1}{E'^2}\left[\sum_{s'}\left(\int \tilde{\psi}_s^+ \mathscr{H}^{(1)} \tilde{\psi}_{s'}\, d\tau\right)\tilde{\psi}_{s'} + \ldots\right]^2 d\tau\,. \tag{90}$$

Unter der Annahme, dass die $\tilde{\psi}_s$, ein orthonormiertes System darstellen, folgt bei alleiniger Berücksichtigung der ersten Näherung

$$\begin{aligned}\eta^2\,(1, \tilde{\psi}_s) &\approx \frac{1}{E'^2} \sum_{s'\,(s'\neq s)} \left(\int \tilde{\psi}_s^* \mathscr{H}^{(1)} \tilde{\psi}_{s'}\, d\tau\right)^2 = \\ &= \frac{1}{E'^2}\left[\int \tilde{\psi}_s^+ \mathscr{H}^{(1)2} \tilde{\psi}_s\, d\tau - \left(\int \tilde{\psi}_s^* \mathscr{H}^{(1)} \tilde{\psi}_s\, d\tau\right)^2\right],\end{aligned} \tag{91}$$

wenn (87) beachtet wird. Die rechte Seite von (91) ist dann mit (88) identisch, wobei für jedes $\tilde{\psi}_s$ der Hamiltonoperator $\mathscr{H}$ nach (84) und (85) zerlegt gedacht wird. Die Approximation, die in (91) durch die beiden äusseren Seiten dargestellt wird, hat die bemerkenswerte Eigenschaft, dass (88), welches immer positiv ist, für die exakte Lösung von $\mathscr{H}$ verschwindet, ebenso wie $\eta^2(1, \tilde{\psi}_s)$. Man wird daher daraus den Schluss ziehen können, dass man durch das Variationsverfahren (88) ein $\tilde{\psi}_s$ erhält, was im wesentlichen durch einen kleinen Wert von $\eta^2(1, \tilde{\psi}_s)$ charakterisiert ist. Anders ausgedrückt: Beim Ansetzen eines bestimmten $\tilde{\psi}_s$ als Variationsansatz (mit bestimmten freien Parametern) wird das aus der Energievariation

$$\int \tilde{\psi}_s^* \mathscr{H} \tilde{\psi}_s\, d\tau = \min \tag{92}$$

resultierende $\tilde{\psi}_s$ andere Parameterwerte enthalten, als das gleiche analytische $\tilde{\psi}_s$, welche aus (88) folgt. Einfache Testrechnungen bestätigen diesen Zusammenhang [24, 20]. Erst wenn $\tilde{\psi}_s$ sehr gut in fast allen Raumbereichen mit ψ_S übereinstimmt, dürfte der Unterschied in den Parameterwerten nicht mehr gross sein. Für die exakte Lösung gilt $\delta^2(1, \psi_s) = 0$, danach verschwinden nach (91) alle Glieder in der mittleren Summe, es gilt also

$$\left(\int \psi_s \middle| \mathscr{H}^{(1)} \tilde{\psi}_{s'}\, d\tau\right)^2 = 0, \quad (s' = 0, 1 \ldots). \tag{93}$$

Der Operator $\mathscr{H}^{(1)}$ ist bezüglich ψ_s zu einem Nulloperator geworden. Es ist nach (84)

$$\mathscr{H} = \tilde{\mathscr{H}}\,. \tag{94}$$

Diese Beziehungen können prinzipiell nur erfüllt werden, wenn vom Einteilchenbild abgegangen wird. Andernfalls kann durch

$$(\int \tilde{\psi}_s^* \mathscr{H}^{(1)} \tilde{\psi}_{s'} d\tau)^2 = \min ; \quad \begin{matrix}(s' = 0, 1 \ldots) \\ (s' \neq s)\end{matrix} \tag{95}$$

mit $\tilde{\mathscr{H}}$ nach (84) ein effektives Einteilchenpotential (effektives Potential) eingeführt werden, wie oben gezeigt. Die bisherigen Überlegungen können nun auch für den Ausdruck $\eta^2(f,\tilde{\psi}_s)$ angewendet werden. Hier erhält man mit Hilfe von (89) die Beziehung

$$\eta^2(f, \tilde{\psi}_s) = \int f^2(\psi_s - \tilde{\psi}_s)^2 d\tau \simeq \frac{1}{E'^2} \int [\sum_{s'} (\int \tilde{\psi}_s^+ \mathscr{H}^{(1)} \tilde{\psi}_{s'} d\tau) f \tilde{\psi}_{s'} + \ldots]^2 d\tau \tag{96}$$

aus der weiter folgt

$$\eta^2(f, \tilde{\psi}_s) \approx \frac{1}{E'^2} \sum_{s'} \sum_{s''} (\int \tilde{\psi}_s^* \mathscr{H}^{(1)} \tilde{\psi}_{s'} d\tau)(\int \tilde{\psi}_s^* \mathscr{H}^{(1)} \tilde{\psi}_{s''} d\tau)(\int \tilde{\psi}_s^* f^2 \psi_{s''} d\tau) . \tag{97}$$

Analog des Überganges von (87) ist die rechte Seite von (97) mit

$$\delta^2(f, \tilde{\psi}_s) = \int f^2 [(\mathscr{H} - \int \tilde{\psi}_s^* \mathscr{H} \tilde{\psi}_s d\tau) \tilde{\psi}_s]^2 d\tau \tag{98}$$

identisch, wobei zwischendurch bei der Herleitung ein $\tilde{\mathscr{H}}$ nach (84) und (85) eingeführt wird. Dabei ist noch zu beachten, dass in der Regel

$$\int f^2 \mathscr{H} \tilde{\psi}_s^* \mathscr{H} \tilde{\psi}_s d\tau \neq \int \tilde{\psi}_s^* f^2 \mathscr{H}^2 \tilde{\psi}_s d\tau \tag{99}$$

gilt. Der Zusammenhang zwischen (97) und (98) kann daher mit Hilfe von $\tilde{\mathscr{H}}$ nach (84) und (85) erkannt werden. Das Potential in $\tilde{\mathscr{H}}$ spielt hier die Rolle des bekannten Fehlerpotentials [25], welches im Falle der Einteilchennäherung, wenn damit die Forderungen $\delta^2(f,\tilde{\psi}_s) = \min$ verknüpft werden, in das effektive Potential übergeht. Dieses kann somit als Funktion von f definiert werden. Wir wollen aber die in Abschnitt 4 angegebene Definition bevorzugen, weil damit auch in der Bestimmung der Energie die bekannten Gleichungen der Störungsrechnung 1. Ordnung erhalten bleiben, die zur Aufspaltung der ursprünglich entarteten Zustände führen können. Dagegen ist (98), im Hinblick auf die ψ-Berechnung, ein brauchbares Variationsverfahren, welches gerade im Hinblick auf die später zu berechnenden Erwartungswerte und Übergangselemente von f bessere Ergebnisse zu erwarten gestattet [20], da es mit (82) zusammenhängt. Die vor einigen Jahren gemachten Versuche, die Handhabung des Variationsverfahrens nach (98) und verwandter Formen (»gesteuerte Verbesserung«) zu erleichtern, zeigen schon hoffnungsvolle Ansätze [28].

Weiter zu untersuchen wäre noch der Einfluss der positiven Grösse E^{12} in (90). Erst dann ist es möglich, gegebenenfalls den vollen Zusammenhang zwischen η^2 und δ^2 aufzuklären.

6. Ausblicke

Die Problematik des effektiven Potentials hat sich in einer umfangreichen Literatur niedergeschlagen, und solange man im Rahmen der Wellenmechanik versucht hat, möglichst alle Elektronen eines Systems zu berücksichtigen (ab-initio-Verfahren), ist auch parallel dazu immer die Frage aufgeworfen worden, ob diese Rechnungen nicht vereinfacht werden könnten, indem die Wirkungen einiger bestimmter Elektronenteilsysteme durch Potentiale ersetzt werden können, obwohl man sich immer darüber klar war, dass diese ein Näherungsstandpunkt ist, der zu einer Reihe recht diffiziler Fragen führen muss. Heute, nachdem die ab-initio-Verfahren so grosse Erfolge aufzuweisen haben, ist das Problem des Zusatzpotentials von gleicher Aktualität. Man kann nämlich aus den Absolutrechnungen ersehen, dass auch in den Molekülen ein grosser Teil der kernnahen Elektronen weitgehendst die gleiche Dichteverteilung haben wie in den freien Atomen, obwohl die Einteilchenergien des SCF-Verfahrens von der chemischen Bindung abhängig sind. Mit anderen Worten, die ab-initio-Verfahren implizieren noch einmal die Berechtigung, näherungsweise die Anzahl der zu behandelnden Elektronen zu reduzieren, indem effektive Potentiale eingeführt werden. In diesem Zusammenhang sei auch an die Versionen des SCF-Verfahrens erinnert, die nur einen Teil der Elektronendichten iterativ behandeln [27].

In diesem Zusammenhang sollte abschliessend noch daran erinnert werden, dass es in der Quantenchemie zwei Aspekte gibt. Einmal kann versucht werden, die Resultate möglichst genau zu halten, wobei heute besonders die Fragen der Korrelationsenergie eine grosse Rolle spielen, zum andern genügt es manchmal nur, qualitative Ergebnisse zu haben, die für die Chemie (besonders was die Reaktivität betrifft) von grossem Nutzen sein können. Die Methoden, die mit effektiven Potentialen arbeiten, werden wohl immer auf seiten der qualitativen Diskussionen stehen, und sie werden sich immer dann behaupten können, wenn ihre Handhabung einfach und der Weg zu ihren Ergebnissen leicht zu übersehen ist. Ohne Zweifel aber wird man in den meisten Fällen wohl doch den Verfahren den Vorzug geben, die alle Elektronen berücksichtigen, wobei die Verwendung von Zusatzpotentialen eine Orientierung ermöglichen kann, bevor der Rechenaufwand aus diesen oder jenen Gründen vergrössert werden muss.

Für die hierzu durchgeführten Rechnungen sei besonders Frau I. FUNKE herzlich gedankt. Herrn Prof. W. A. BINGEL danke ich für Diskussionen zu einigen Punkten dieses Themas.

LITERATUR

1. In diesem Zusammenhang sei auf das sehr lesenswerte Buch »Pseudo-Potentiale« von P. GOMBÁS hingewiesen (Springer-Verlag, 1967), welches eine Zusammenfassung aller damit verbundenen Fragen darstellt.
2. H. HELLMANN, C. R. Acad. Sci. URSS, **3,** 444, 1934; J. Chem. Phys., **3,** 61, 1935; Acta Physicochimica URSS, **1,** 913, 1935; **4,** 225, 1936; **4,** 324, 1936.
3. P. GOMBÁS, Z. Phys., **94,** 473, 1935.
4. I. FÉNYES, Csillagászati Lapok (Budapest), **6,** 49, 1943.
5. W. LENZ, Z. Phys., **77,** 713, 1932.
6. H. JENSEN, Z. Phys., **77,** 722, 1932.
7. H. HELLMANN und W. KASSATOTSCHKIN, Acta Physicochimica URSS, **5,** 23, 1936.
8. A. HYLLERAAS, Z. Phys., **48,** 469, 1928; **51,** 150, 1928; **54,** 347, 1929; **65,** 209, 1930; **60,** 624, 1930; **63,** 291, 1930.
9. LANDOLT-BÖRNSTEIN, Bd. 1, »Moleküle« (1951).
10. P. M. MORSE, L. A. YOUNG und E. S. HAURWITZ, Phys. Rev., **48,** 948, 1935.
11. H. PREUSS, Z. Naturforsch., **10***a*, 365, 1955; **10***a*, 267, 1955.
12. H. PREUSS, Z. Naturforsch., **11***a*, 823, 1956.
13. Man vgl. z. B. preprint No. 199 der Quantum Chemistry Group, University of Uppsala (1967) oder Fortschritte d. Chemischen Forschung Bd. 9/3, 325 (1967).
14. Man vgl. etwa H. HARTMANN: »Theorie der chemischen Bindung auf quantentheoretischer Grundlage«, S. 88, Berlin—Göttingen—Heidelberg, Spinger-Verlag, 1954.
15. W. T. SIMPSON, Theory of electrons in molecules, p. 8, Prentice Hall, 1962.
16. H. PREUSS, Z. Naturforsch. **13***a*, 439, 1958; **169,** 598, 1961; Fortschritte d. Physik, **10,** 271, 1962.
    T. SZONDY, Z. Naturforsch., **17***a*, 552, 1962.
17. J. W. BARTLETT, Phys. Rev., **78,** 1067, 1955.
18. H. M. JAMES und A. S. COOLIDGE, Phys. Rev., **51,** 860, 1957.
19. R. E. WILLIAMSON, Phys. Rev., **62,** 538, 1942.
20. H. PREUSS, Z. Naturforsch., **16***a*, 598, 1961; **13***a*, 439, 1958.
21. H. PREUSS, Fortschritte d. Physik, **10,** 271, 1962.
22. P. GOMBÁS, Theorie und Lösungsmethoden des Mehrteilchenproblems der Wellenmechanik, S. 209, Birkhäuser, 1950.
23. W. HELLMANN, Einführung in die Quantenchemie, S. 70, Deuticke, 1936.
24. H. PREUSS und E. TREFFTZ, Phys. Rev., **107,** 1282, 1957.
25. A. LAFORGUE, C. R. Acad. Sci. Paris, **238,** 1033, 1954.
26. T. SZONDY, Z. Naturforsch., **17***a*, 552, 1962;
    T. SZONDY und I. VAGLO, Z. Naturforsch., **18***a*, 263, 1963; preprint 1963.
27. Man vgl. z. B. R. DAUDEL, R. LEFEBVRE, C. MOSER, Quantum Chemistry, Interscience Publishers, Inc., New York, S. 554, 1959.

НЕКОТОРЫЕ ЗАМЕЧАНИЯ К КОМБИНИРОВАННЫМ ПРИБЛИЖЕННЫМ МЕТОДАМ И ЭФФЕКТИВНЫМ ПОТЕНЦИАЛАМ

Г. ПРАЙС

Резюме

После короткого введения в комбинационные приближенные методы вычисляются энергии связи и равновесные расстояния ионов щелочных молекул и рассматривается вопрос существования ионов щелочно-гидридных молекул. По отношению усовершенствования методов предлагается одна исходящая атомная функция, состоящая только из экспоненциальных членов. Дискутируются дальнейшие возможности усовершенствования методов.

Исходя из данного исследования, рассматривается роль эффективных потенциалов в рамках проблемы многих центров и в самом общем случае показывается, что в рамках наивного одночастичного приближения нельзя определять эффективного потенциала, однако, имеется возможность для умного введения данного потенциала при отказе от определенной, характерной для одной частицы, картины. Далее дается одно определение добавочного потенциала, основанное на вариационном принципе, и показывается возможность определения эффективного потенциала. Наконец, приводится недавно сформулированное автором определение доброты приближенного решения уравнения Шредингера в связи с уже известным вариационным приемом, причем понятие эффективного потенциала оказалось лишним.

Acta Physica Academiae Scientiarum Hungaricae, Tomus 27, pp. 219—224 (1969)

ON THE CANONICAL TRANSFORMATION IN CLASSICAL AND QUANTUM MECHANICS* **

By

V. Fock

INSTITUTE OF PHYSICS, LENINGRAD UNIVERSITY, LENINGRAD, USSR

(Received 3. II. 1969)

A more exact formulation for Dirac's proposition on the analogy between the unitary transformations in quantum theory and the contact transformations in classical theory is given. It is shown that approximate expressions for the matrix elements of the unitary operator defining the transformation can be constructed in terms of classical quantities. One can thus speak not only of an analogy between unitary and contact transformations, but also of an approximate equality between the quantum mechanical and semi-classical expressions for the corresponding quantities.

In his famous book on the principles of quantum mechanics Dirac formulates (in § 26) the following proposition: "for a quantum dynamical system that has a classical analogue, unitary transformations in the quantum theory are the analogue of contact transformations in the classical theory". No detailed description of this analogy is, however, given in Dirac's book. In the following we intend to investigate this analogy in some more detail.

Let $q_1, q_2, \ldots q_n; p_1, p_2, \ldots p_n$ be the original and $Q_1, Q_2, \ldots Q_n; P_1, P_2, \ldots P_n$ the transformed coordinates and momenta of a dynamical system with n degrees of freedom. We consider the case when the transformation function S depends on the old and on the new coordinates:

$$S = S(q_1, \ldots q_n; Q_1, \ldots Q_n). \tag{1}$$

The contact transformation is defined by the relation between the differentials

$$\sum_{r=1}^{n} p_r \, dq_r - \sum_{r=1}^{n} P_r \, dQ_r = dS \tag{2}$$

from which it follows

$$p_r = \frac{\partial S}{\partial q_r}; \quad P_r = -\frac{\partial S}{\partial Q_r}. \tag{3}$$

* Dedicated to Prof. P. Gombás on his 60th birthday.

** First published in Russian in the Bulletin (Viestnik) of the Leningrad University, N° 16, p. 67, 1959. See also Appendix to the Russian edition of Dirac's book "The Principles of Quantum Mechanics", Moscow, 1960. The present English text prepared for Acta Physica Hungarica has been partly revised by the author.

The expressions for the quantities q, p in terms of Q, P and the inverse expressions are obtained by solving Equs. (3). The solution is always possible, since the determinant

$$D = Det \frac{\partial^2 S}{\partial q_r \partial Q_s} \neq 0 \tag{4}$$

is assumed to be different from zero.

The contact transformation thus defined corresponds in quantum mechanics to a unitary transformation from the representation in which the quantities q are "diagonal" to the representation in which the quantities Q are "diagonal".*

This unitary transformation has the following form. Let $\psi_Q(q)$ be a complete set of simultaneous eigenfunctions of the operators $Q_1, \ldots Q_n$ expressed in the variables $q_1, \ldots q_n$. Let F be the operator undergoing the transformation. Then the kernel (or the matrix) of the transformed operator will have the form

$$(Q'|F^*|Q) = \int \overline{\psi}_{Q'}(q)\, F \psi_Q(q)\, dq\,, \tag{5}$$

where dq denotes the product of the differentials

$$dq = dq_1 \ldots dq_n\,. \tag{6}$$

In DIRAC's notation

$$\psi_Q(q) = \langle q|Q\rangle \tag{7}$$

and formula (5) takes the form

$$(Q'|F^*|Q) = \int \langle Q'|q\rangle\, F\, \langle q|Q\rangle\, dq. \tag{8}$$

The eigenfunction $\psi_Q(q)$ can be considered as the kernel $(q|\overline{U}|Q)$ of a unitary operator $\overline{U} = U^{-1}$ and formula (8) can be written as

$$F^* = UFU^{-1}. \tag{8*}$$

In the case $F = 1$, formula (5) reduces to the orthogonality condition, and the kernel of the unit operator expressed in variables Q must appear on its left-hand side, i.e. the expression

$$(Q'|1|Q) = \delta_0(Q - Q') \equiv \delta(Q_1 - Q_1') \ldots \delta(Q_n - Q_n')\,, \tag{9}$$

* The set of variables $q_1, \ldots q_n$ will often be denoted by a single letter q; a similar meaning will be assigned to the symbol Q and also to p and P.

where δ is DIRAC's delta function.

In semi-classical approximation we may take as $\psi_Q(q)$ the quantity

$$\psi_Q(q) = c \sqrt{\left| \frac{\partial^2 S}{\partial q \, \partial Q} \right|} \, e^{(i/h)S}. \tag{10}$$

We have put for brevity

$$\frac{\partial^2 S}{\partial q \, \partial Q} = Det \frac{\partial^2 S}{\partial q_r \, \partial Q_s} = D \tag{11}$$

and under the square-root sign in (10) stands the absolute value of the determinant. The constant c equals

$$c = (2\pi h)^{-n/2}. \tag{12}$$

Let us verify that the semi-classical functions (10) approximately satisfy the orthogonality relations. Inserting expressions (10) in the integral and taking $F = 1$, we obtain under the integral sign a rapidly varying exponential factor $\exp\left[\left(\frac{i}{h}\right)(S—S')\right]$, where S' is the value of S with Q replaced by Q'. This factor ceases to be rapidly varying only if Q' is near Q; this is the condition that the integral should noticeably differ from zero. Consequently, the difference $S—S'$ in the exponent may be replaced by the expression

$$S - S' = -\sum_{r=1}^{n} (Q'_r - Q_r) \frac{\partial S}{\partial Q_r} \tag{13}$$

or

$$S - S' = \sum_{r=1}^{n} (Q'_r - Q_r) P_r, \tag{14}$$

where P_r has the value (3). Formula (14) may be briefly written as

$$S - S' = (Q' - Q) P. \tag{15}$$

In all factors of the exponential we may put $Q' = Q$. We then have

$$\int \overline{\psi}_{Q'}(q) \, \psi_Q(q) \, dq = c^2 \int e^{\frac{i}{h}(Q'-Q)P} \left| \frac{\partial^2 S}{\partial Q \, \partial q} \right| dq. \tag{16}$$

Now, if P_r has the value (3), the determinant under the integral sign in (16) is the Jacobian for the transformation from P to q, so that

$$\left| \frac{\partial^2 S}{\partial Q \, \partial q} \right| dq = dP_1 \ldots dP_n = dP. \tag{17}$$

Thus, formula (16) may be written as

$$\int \overline{\psi}_{Q'}(q)\,\psi_Q(q)\,dq = c^2 \int e^{\frac{i}{h}(Q'-Q)P}\,dP. \tag{18}$$

But the remaining integral (multiplied by c^2) is simply the product (9) of the delta functions. We obtain finally

$$\int \overline{\psi}_{Q'}(q)\,\psi_Q(q)\,dq = \delta_0(Q-Q') \tag{19}$$

and the orthogonality condition (as well as the normalization condition) is thus satisfied.

We now consider the matrix for an arbitrary operator F expressed in terms of q_r and of $p_r = -ih\,\partial/\partial q_r$.

Let

$$F = F(q,p) = F\left(q, -ih\frac{\partial}{\partial q}\right). \tag{20}$$

When applied to the exponential function $\exp\left(\frac{i}{h}S\right)$, the operator F yields approximately this function multiplied by $F(q, \partial S/\partial q)$. Thus

$$F\left(q, -ih\frac{\partial}{\partial q}\right) e^{\frac{i}{h}S} \cong e^{\frac{i}{h}S}\,F\left(q, \frac{\partial S}{\partial q}\right). \tag{21}$$

A similar relation holds if we replace the exponential in (21) by the function $\psi_Q(q)$ which is approximately equal to (10). Accordingly, we may mean by F in formula (5) not the differential operator on the left-hand side of (21), but the function on the right-hand side of this equation. Putting, as before, $Q' = Q$ in all factors of the exponential, we obtain

$$(Q'|F^*|Q) = c^2 \int F\left(q, \frac{\partial S}{\partial q}\right) e^{\frac{i}{h}(S-S')} \left|\frac{\partial^2 S}{\partial Q\,\partial q}\right| dq. \tag{22}$$

As in formula (18), we take in (22) the quantities P as integration variables. Transforming to the said variables the function F, we shall have

$$F(q,p) = F\,(q\,(Q,P), p(Q,P)) = F^*(Q,P), \tag{23}$$

where p and P are the classical expressions (3). Using the approximate expression (15) for the quantity in the exponent, we may write

$$(Q'|F^*|Q) = c^2 \int F^*(Q,P)\,e^{\frac{i}{h}(Q'-Q)P}\,dP. \tag{24}$$

To evaluate this integral we note that the multiplication of the exponential in the integrand by P is equivalent to the application of the operator $-ih\,\partial/\partial Q'$.

We also use our previous statement (which led us to (16)) that in the factors of the exponential we may put $Q' = Q$. We may then write

$$\int F^*(Q, P)\, e^{\frac{i}{\hbar}(Q'-Q)P}\, dP = \int F^*\left(Q', -ih\frac{\partial}{\partial Q'}\right) e^{\frac{i}{\hbar}(Q'-Q)P}\, dP. \qquad (25)$$

Taking the operator F^* out of the integral sign and using (18) and (19) we obtain

$$(Q'|F|Q) = F^*\left(Q', -ih\frac{\partial}{\partial Q'}\right)\delta_0(Q - Q') \qquad (26)$$

and interchanging Q' and Q

$$(Q|F|Q') = F^*\left(Q, -ih\frac{\partial}{\partial Q}\right)\delta_0(Q - Q'). \qquad (26^*)$$

Now, the result of applying the operator F^* to a given function $\Psi(Q)$ is by definition,

$$F^*\Psi(Q) = \int (Q|F^*|Q')\,\Psi(Q')\,dQ'. \qquad (27)$$

Using (26*) we obtain

$$F^*\Psi(Q) = F^*\left(Q, -ih\frac{\partial}{\partial Q}\right)\Psi(Q). \qquad (28)$$

This equation gives (apart from terms depending on the order of factors in $F^*(Q, P)$) the form of the transformed operator as applied to the function $\Psi(Q)$.

Our calculations can be summarized as follows. The approximate equation (21) has been used twice. First, we made a transition from the operator $F(q, -ih\,\partial/\partial q)$ to the function $F(q, p)$; this function was expressed by means of classical formulae in terms of new canonical variables Q, P. Second, we made the inverse transition from the resulting function $F = F^*(Q, P)$ to the operator $F^*(Q, -ih\,\partial/\partial Q)$. This transition presented itself naturally when we applied the method of differentiation with respect to a parameter to the calculation of the integral for the matrix element of the operator considered.

The results of our calculations can be stated as follows. Let the operator

$$F = F(q, p); \quad p = -ih\frac{\partial}{\partial q}, \qquad (29)$$

first expressed in variables q, be then transformed, by means of a unitary transformation, to new variables Q. When expressed like (29), the resulting operator F^* will have the form

$$F^* = F^*(Q, P); \quad P = -ih\frac{\partial}{\partial Q}. \tag{30}$$

Suppose that the unitary transformation is performed by means of eigenfunctions having in classical approximation the form (10) (so that their phase is $\frac{1}{h}S(q,Q)$). Then the form of F^* can be obtained from that of F (if one disregards the order of the factors) by means of a purely algebraic transformation expressed by the formulae

$$F(q, p) = F^*(Q, P), \tag{31}$$

$$p = \frac{\partial S}{\partial q}; \quad P = -\frac{\partial S}{\partial Q}, \tag{32}$$

where S is the function involved in the phase of the unitary transformation. These formulae represent a contact transformation of classical mechanics.

We see that one can speak not only of an analogy between unitary and contact transformations but also on an approximate equality between the corresponding quantum mechanical and classical expressions.

О КАНОНИЧЕСКОМ ПРЕОБРАЗОВАНИИ В КЛАССИЧЕСКОЙ И КВАНТОВОЙ МЕХАНИКЕ

В. ФОК

Резюме

Уточнено утверждение Дирака об аналогии между унитарными преобразовани. ями квантовой механики и касательными преобразованиями классической механики. Показано, что для матричных элементов оператора унитарного преобразования могут быть построены приближенные выражения через классические величины. Таким образом можно говорить не только об аналогии между унитарными и касательными преобразованиями, но и о приближенном равенстве между квантово-механическими и полу-классическими выражениями для соответствующих величин.

Acta Physica Academiae Scientiarum Hungaricae, Tomus 27, pp. 225—229 (1969)

VERGLEICH EINER LCAO-MO- UND EINER VB-ZUSTANDSFUNKTION DES Li_2-MOLEKÜLS*

Von

N. GRÜN und B. KOCKEL

INSTITUT FÜR THEORETISCHE PHYSIK DER UNIVERSITÄT, GIESSEN, BRD

(Eingegangen, 3. II. 1969)

Eine neu berechnete VB-Zustandsfunktion des Li_2-Grundzustands wird verglichen mit einer von B. J. RANSIL angegebenen LCAO-MO ohne CJ-Zustandsfunktion.

Eine einfache, nicht mit Konfigurationsüberlagerung arbeitende von RANSIL[1] angegebene LCAO-MO-Zustandsfunktion des Li_2-Grundzustands soll verglichen werden mit einer aus der VB-Vorstellung entwickelten Zustandsfunktion. Beide gehen aus von Slaterfunktionen $s_0, s_0', s, s', z, z', x, x', y', y$.

$$s_0 = \sqrt{\frac{k_0^3}{\pi}}\, e^{-k_0 r}\,, \quad s = \sqrt{\frac{k^5}{3\pi}}\, r e^{-kr}\,, \qquad x, y, z = \sqrt{\frac{k^5}{\pi}}\, e^{-kr}\ (x, y, z),$$

$$s_0' = \sqrt{\frac{k_0^3}{\pi}}\, e^{-k_0 r'}\,, \quad s' = \sqrt{\frac{k^5}{3\pi}}\, r' e^{-kr'}\,, \quad x', y'. z' = \sqrt{\frac{k^5}{\pi}}\, e^{-kr'}\,(x', y', z').$$

r, r' = Abstände von den beiden Kernen; Richtung der x', y', z'-Achsen entgegengesetzt zur Richtung der x, y, z-Achsen.

RANSIL setzt seine Zustandsfunktion an als

$$\psi = |1\sigma_g\, 1\sigma_u\, 2\sigma_g \cdot 1\sigma_g\, 1\sigma_u\, 2\sigma_g|\,,$$

wobei $1\sigma_g$, $2\sigma_g$ Linearkombinationen von $s_0 + s_0'$, $s + s'$, $z + z'$ sind, $1\sigma_u$ eine Linearkombination von s_0—s_0', s—s', z—z' ist. Die VB-Zustandsfunktion belässt beiden Li-Atomen ihre K-Schalen-Elektronen s_0 und s_0' mit beiden Spins (die deshalb in den folgenden Slaterdeterminanten nicht mit aufgeschrieben werden) und überlagert alle mit zwei L-Schalen-Elektronen möglichen $^1\Sigma_g^+$-Konfigurationen. So entsteht entweder bei Verwendung von nur σ-Elektronen der Ansatz a und bei Mitberücksichtigung der π-Elektronen der Ansatz b

$$\psi_a = \sum_{i=1}^{6} c_{ia}\, \psi_i\,, \qquad \psi_b = \sum_{i=1}^{8} c_{ib}\, \psi_i\,,$$

* Herrn Prof. Dr. P. GOMBÁS zum 60. Geburtstag gewidmet.

[1] B. J. RANSIL, Rev. Mod. Phys., **32**, 245, 1960.

mit

$$\psi_1 = \frac{1}{\sqrt{2}}\{|s\cdot s'|+|s'\cdot s|\}^2,$$

$$\psi_2 = \frac{1}{\sqrt{2}}\{|s\cdot s|+|s'\cdot s'|\},$$

$$\psi_3 = \frac{1}{\sqrt{4}}\{|s\cdot z'|+|z'\cdot s|+|s'\cdot z|+|z\cdot s'|\},$$

$$\psi_4 = \frac{1}{\sqrt{4}}\{|s\cdot z|+|z\cdot s|+|s'\cdot z'|+|z'\cdot s'|\},$$

$$\psi_5 = \frac{1}{\sqrt{2}}\{|z\cdot z'|+|z'\cdot z|\},$$

$$\psi_6 = \frac{1}{\sqrt{2}}\{|z\cdot z|+|z'\cdot z'|\},$$

$$\psi_7 = \frac{1}{\sqrt{4}}\{|x\cdot x'|+|x'\cdot x|+|y'\cdot y|+|y\cdot y'|\},$$

$$\psi_8 = \frac{1}{\sqrt{4}}\{|x\cdot x|+|y\cdot y|+|x'\cdot x'|+|y'\cdot y'|\}.$$

Die Parameterwerte k_0 und k, der Kernabstand, die Gesamtenergie und die Bindungsenergie sind[3]

	bei RANSILS Funktion I	bei Ansatz a	bei Ansatz b
k_0	2,70	2,68	2,68
k	0,65	0,67	0,67
kR		3,5	3,5[5]
R	5,051[4]	5,224	5,224
E	— 14,840 75	— 14,851 48	— 14,863 66
E_B	0,151 eV	0,462 eV	0,794 eV

Die Bindungsenergie wurde jeweils berechnet als Differenz der mit denselben Parameterwerten berechneten Atomenergien und der Molekülenergie. Bevor die beiden Zustandsfunktionen näher miteinander verglichen werden, sei noch

[2] Die Nenner $\sqrt{2}$ und $\sqrt{4}$ bewirken natürlich Normierung nur bei Trennung der Atome, sind aber günstig für die Berechnung und die anschauliche Ausdeutung. Auch die Faktoren $1/\sqrt{6}$! sind unterdrückt.

[3] In atomaren Einheiten, Bindungsenergie in eV.

[4] 5.051 ist der experimentelle Abstand.

[5] Ansatz *b* führte bei Variation von R zu einem Energieminimum in unmittelbarer Nähe von $kR = 3.5$

einmal daran erinnert, dass beide Methoden (LCAO-MO und VB) nach Verwendung bestimmter Anzahlen von Konfigurationen immer wieder einmal zu identischer, nur verschieden geschriebenen Zustandsfunktionen führen müssen. Beim H_2-Grundzustand tritt das zum ersten Mal bei zwei Konfigurationen auf

$$|(s_0+s_0')\cdot(s_0+s_0')| \quad \text{und} \quad |(s_0+s_0')\cdot(s_0-s_0')|$$

bzw.

$$|s_0\cdot s_0'|+|s_0'\cdot s_0| \quad \text{und} \quad |s_0\cdot s_0|+|s_0'\cdot s_0'| \,.$$

Bei der grösseren Elektronenzahl des Li_2-Moleküls tritt das für den Grundzustand aber erst bei einer viel höheren Anzahl von Konfigurationen auf, nämlich bei Verwendung von 92 Konfigurationen, wenn nur die zwölf σ-Funktionen $s_0\alpha$ bis $z'\beta$, und erst bei 412 Konfigurationen, wenn auch die acht π-Funktionen $x\alpha$ bis $y'\beta$ verwendet werden. Die Überlagerung einer so grossen Zahl von Konfigurationen wäre aber wenig sinnvoll, weil dann viele von ihnen mit extrem kleinen Koeffizienten auftreten und nur geringe Verbesserungen bei allen aus der Zustandsfunktion berechneten Moleküleigenschaften bringen würden.

Vergleicht man eine LCAO-MO- und eine VB-Zustandsfunktion geringerer Konfigurationszahl miteinander, indem man eine Funktion der einen Art als Linearkombination der Funktionen der anderen Art schreibt, so erhält man im Falle des Li_2-Grundzustands ebenfalls sofort 92 bzw. 412 Anteile in der Linearkombination. Die von RANSIL angegebene, von ihm mit I bezeichnete Funktion wird bei Zusammensetzung aus VB-Funktionen zu

$$\begin{aligned} |1\sigma_g\,1\sigma_u\,2\sigma_g\cdot 1\sigma_g\,1\sigma_u\,2\sigma_g| = \quad & 0{,}38924(\psi_1+\psi_2) \\ & +0.12432(\psi_3+\psi_4) \\ & +0{,}01985(\psi_5+\psi_6) \end{aligned}$$

+ 86 weitere Summanden, in denen die K-Schalen aufgebrochen sind, also nur 3, 2, 1 oder kein Elektron enthalten.

Der wichtigste Teil dieses Restes ist —0,02584 $(\psi_9+\psi_{10})$ mit

$$\psi_9 = \frac{1}{2}\{|s_v\,s_0'\,s'\cdot s_0\,ss'|+|s_0\,s_0'\,s\cdot s_0'\,ss'|+|s_0ss'\cdot s_0\,s_0'\,s'|+|s_0'\,ss'\cdot s_0\,s_0'\,s|\}$$

$$\psi_{10} = \frac{1}{2}\{|s_0\,s_0'\,s\cdot s_0\,ss'|+|s_0\,s_0'\,s'\cdot s_0'\,ss'|+|s_0\,ss'\cdot s_0\,s_0'\,s|+|s_0'\,ss'\cdot s_0\,s_0'\,s'|\}\,.$$

Alle weiteren Glieder haben wesentlich kleinere Koeffizienten. Die nach der VB-Vorstellung aufgebauten Zustandsfunktionen heissen

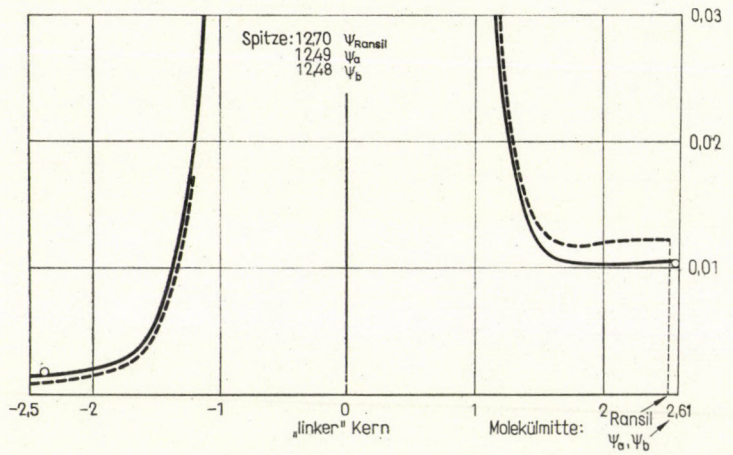

Fig. 1. Dichte auf der Kernverbindungslinie. ····· für ψ_{Ransil}; ——— für ψ_b; ○ für ψ_a

bei Ansatz a

$$\begin{aligned}\psi_a = {} & 0{,}900\ 03\psi_1 - 0{,}084\ 04\psi_2 \\ & + 0{,}266\ 14\psi_3 - 0{,}021\ 02\psi_4 \\ & - 0{,}026\ 70\psi_5 - 0{,}095\ 31\psi_6\end{aligned}$$

bei Ansatz b

$$\begin{aligned}\psi_b = {} & 0{,}772\ 91\psi_1 + 0{,}011\ 37\psi_2 \\ & + 0{,}255\ 12\psi_3 + 0{,}004\ 35\psi_4 \\ & - 0{,}017\ 02\psi_5 - 0{,}077\ 39\psi_6 \\ & + 0{,}120\ 13\psi_7 - 0{,}129\ 03\psi_8\end{aligned}$$

Bei dem direkten Vergleich der beiden VB-Funktionen mit der MO-Funktion ist also wenig Ähnlichkeit zu erkennen. Allenfalls kann man darauf verweisen, dass die bei der RANSIL-Funktion zwangsweise gleichen Koeffizienten von ψ_1 und ψ_2 bzw. ψ_3 und ψ_4 ungefähr das arithmetische Mittel der entsprechenden Koeffizienten in den beiden VB-Funktionen sind. Vergleicht man dagegen bei den nach den beiden Methoden bestimmten Zustandsfunktionen die Elektronendichte im 3-dimensionalen Raum, so findet man nur geringfügige Unterschiede. Als Beleg dafür sind in den Fig. 1 und 2 die Elektronendichte längs der Kernverbindungslinie und längs einer in der Molekülmitte errichteten Senkrechten zur Verbindungslinie gezeichnet, und zwar in gestrichelten Kurven für die Ransilfunktion, in ausgezogenen Kurven für ψ_b und nur durch einige Kreise angedeutet für ψ_a. Obgleich nun die Abbildungen für das Dichte »plateau« um die Molekülmitte deutlich einen höheren Wert bei der RANSIL-funktion zeigen, ist doch die Folgerung zu ziehen, dass die drei Funktionen ψ_{Ransil}, ψ_a, ψ_b in diesem Gebiet zu fast gleicher Dichte führen würden, wenn die Kernabstände gleich wären; denn bei der Verkürzung des Abstands von 5,224 auf 5,051 ist natürlich eine Erhöhung der Dichte um den Faktor $\left(\frac{5{,}224}{5{,}051}\right)^3$, d.h. um 11% zu erwarten. Nur der über diese 11% hinausgehende Unterschied zwischen den Dichten ist also als echter Unterschied anzusehen. Er ist sehr

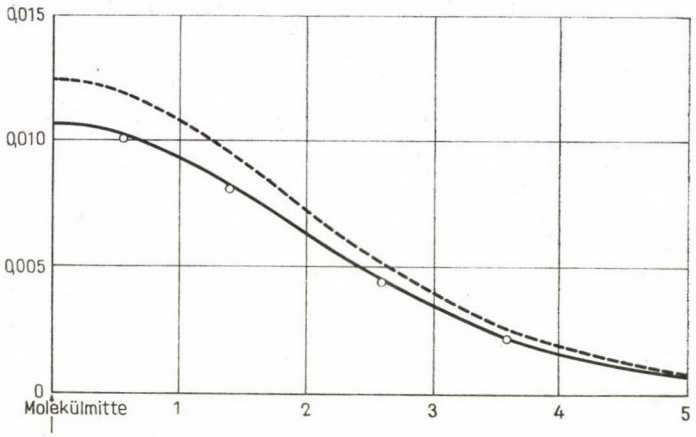

Fig. 2. Dichte längs einer Senkrechten zur Verbindungslinie, errichtet in der Molekülmitte. --------- für ψ_{Ransil}; ——— für ψ_b; ○ für ψ_a

klein und rührt her von der Gleichheit der Koeffizienten für homöopolare und ionische Anteile und dem Aufbrechen der *K*-Schale bei der RANSILschen Zustandsfunktion.

СРАВНЕНИЕ ФУНКЦИЙ СОСТОЯНИЯ LCAO-MO И VB

Н. ГРЮН и Б. КОКЕЛЬ

Резюме

Вновь определенная функция состояния VB основного состояния Li_2 сравнивается с функцией состояния LCAO-MO (без CJ), данной Б. И. Ранзилом.

Acta Physica Academiae Scientiarum Hungaricae, Tomus 27, pp. 231—235 (1969)

COSMIC RAYS AND THE ORIGIN OF THE SOLAR SYSTEM*

By

A. J. R. PRENTICE and D. TER HAAR

DEPARTMENT OF THEORETICAL PHYSICS, OXFORD UNIVERSITY, OXFORD OX1 3PQ, GREAT BRITAIN

(Received 3. II. 1969)

It is shown that cosmic rays may have caused sufficient ionisation in a solar disc in a KANT—VON WEIZSÄCKER type of theory about the origin of the solar system to produce a conductivity high enough for magnetohydrodynamic effects to be important.

It is well known that all theories produced so far to explain the formation of our solar system with its planets moving in regular orbits and falling into two families — the inner or terrestrial and the outer or major planets — have run into difficulties of one kind or another. The theory which seems to introduce fewest special ad-hoc assumptions is the KANT—VON WEIZSÄCKER theory [1] in which the sun more or less in its present state is surrounded by a gaseous disc in which the planets are formed by condensation. This kind of theory is able to explain quite satisfactorily the differences between the two families of planets [2], but it runs into serious difficulties because the life time of such a disc against turbulent dissipation is much shorter than the time needed to form the planets [3, 4]. Although VON WEIZSÄCKER's regular pattern of vortices [1] may increase the life time, perhaps by as much as an order of magnitude, this will not be sufficient and it seems that the only possible way to save this kind of theory would be to invoke electromagnetic phenomena. This kind of approach has been used by ALFVÉN [5] and HOYLE [6] has shown how electromagnetic effects may lead to a slowly rotating sun (compare also [7]).

At first sight it seems unlikely that electromagnetic effects can have played a significant role in the evolution of the solar disc in a KANT—VON WEIZSÄCKER theory. The relative importance of hydromagnetic effects as compared to hydrodynamic effects is measured by the so-called Hartmann number M which in Gaussian units is given by the equation [8, 9, 10]

$$M = \frac{HL}{c}\sqrt{\frac{\sigma}{\eta}}, \tag{1}$$

where H is a characteristic magnetic field, L a characteristic length, σ the electrical conductivity, η the viscosity, and c the velocity of light. If $M \gg 1$, hydromagnetic effects will be important.

* Dedicated to Prof. P. GOMBÁS on his 60th birthday.

In order to get a safe lower limit for M, we shall assume that in the solar disc $H > 10^{-6}$ gauss, $L \sim 1$ AU $= 1.5.10^{13}$ cm, $\eta \sim 10^{-4}$ poise, and we shall use for σ the gas-kinetic formula

$$\sigma = n_e e^2 \lambda / mv , \tag{2}$$

where n_e is the electron density, v the average electron velocity, λ the electron mean free path, and e and m the electron charge and mass. As we shall see later on, only a fraction of the solar disc will be ionised so that λ is governed by collisions between electrons and neutral hydrogen atoms. It has been calculated by TEMPKIN and LAMKIN [11] who find

$$\lambda \sim 3 \cdot 10^{14} n_H^{-1} \tag{3}$$

where n_H is the neutral hydrogen density. Expressing v in terms of the temperature T and using the various formulae and estimates which we have just given, we find for the Hartmann number M (T in °K):

$$M \gtrsim 2 \cdot 10^7 \left(\frac{n_e}{n_H} \right)^{1/2} T^{-1/4} . \tag{4}$$

If we take for n_H and T the values characteristic for a distance of about 1 AU from the sun [2, 3] — L, n_H, and T will all depend on the distance from the sun — we have $T \sim 300$ °K, $n_H \sim 10^{14}$ cm^{-3}, and thus

$$M \gtrsim n_e^{1/2} . \tag{5}$$

One can easily show that ionisation by solar radiation is totally absent [2], and for the ionisation by thermal motion, we get from the usual thermodynamic argument (see [2], p. 32)

$$n_e \lesssim 10^{-40} \text{ cm}^{-3} , \tag{6}$$

showing practically total neutrality, and $M \ll 1$.

However, it is well known (i) that cosmic rays produce ionisation in the earth's atmosphere and (ii) that the cosmic ray intensity has probably not varied greatly during the lifetime of our sun. It is therefore of interest to see whether they may produce sufficient ionisation in a solar disc to bring about a large Hartmann number. We also remind ourselves that in a different connection POTTASCH [12] recently has considered the ionisation properties of cosmic rays.

The degree of ionisation produced by cosmic rays can be estimated in two different, but equivalent ways. We can either use the data about ionisa-

tion produced in the terrestrial atmosphere or we can try to sketch a theoretical treatment of the problem.

If d is the mass path traversed by the cosmic rays, entering the atmosphere (ϱ: mass density),

$$d = \int_0^l \varrho dl\,, \tag{7}$$

it was found by MILLIKAN, NEHER, and PICKERING [13] that the number of ion pairs $W_i(d, \text{air})$ created per unit volume of air per unit time at depth d is given by the expression

$$W_i(d, \text{air}) \sim 750\, e^{-d/160}, \tag{8}$$

where d is in g cm^{-2}. The exponential factor derives from the attenuation of the cosmic ray intensity due to cascade and ionisation processes. It will differ slightly between air and the hydrogen atmosphere in the solar disc. Roughly speaking we expect a factor exp $(-d/\Lambda)$ where

$$\frac{\Lambda(H)}{\Lambda(\text{air})} \sim \frac{\sigma(\text{air})}{\sigma_H\, A(\text{air})}\,, \tag{9}$$

where the σ are the relevant nuclear cross-sections and A the mass number. We find then

$$\Lambda(H) \sim \frac{8}{9}\,\Lambda(\text{air}). \tag{10}$$

Correcting also for the difference in density in the terrestrial atmosphere and in the solar disc, we find

$$W_i(d,\text{H}) \sim W_i(0, \text{air})\, \frac{n(\text{H},d)}{n(\text{air})_{1\,\text{atm},\,20\,^\circ\text{C}}}\, e^{-d/\Lambda(\text{H})}, \tag{11}$$

or

$$W_i(d,\text{H}) \sim 2 \cdot 10^{-18}\, n_{\text{H}}\, e^{-d/140}. \tag{12}$$

A similar expression is obtained by using GINZBURG and SYROVATSKII's expression [14] for the rate of ionisation, GLOECKLER and JOKIPII's estimate [15] for the proton flux in the cosmic rays, and DALGARNO's discussion [16] of ionisation processes.

As d for the solar disc will be of the order of 100 (compare the data in [2]) we can safely put the exponential in (12) equal to unity, so that throughout the solar disc we can use

$$W_i(d, \text{H}) \sim 2 \cdot 10^{-18}\, n_{\text{H}} \text{ ion pairs/cm}^3 \text{ sec}. \tag{13}$$

From ALLEN's data [17] it follows that the rate of recombination R will be given by the equation

$$R = 10^{-9} T^{-3/4} n_e^2 \,\mathrm{cm}^{-3} \,\mathrm{sec}^{-1}\,, \tag{14}$$

and from (13) and (14) and the balance equation $W_i = R$ it follows that

$$n_e \sim 4 \cdot 10^{-5} n_{\mathrm{H}}^{1/2} T^{3/8} \,\mathrm{cm}^{-3}\,, \tag{15}$$

which for $n_H \sim 10^{14}$ cm^{-3}, $T \sim 300$ °K, leads to

$$n_e \sim 3 \cdot 10^3 \,\mathrm{cm}^{-3}. \tag{16}$$

Combining this with (5) we get

$$M \gtrsim 10^2\,, \tag{17}$$

showing that, indeed, hydromagnetic effects must be taken into account, especially since the value obtained is certainly a conservative lower limit.

Acknowledgements

We should like to express our gratitude to the Royal Commission for the Exhibition of 1851 for awarding a Research Scholarship and to Wolfson College, Oxford, for awarding a Junior Research Fellowship to one of us (A. J. R. P.).

REFERENCES

1. C. F. VON WEIZSÄCKER, Zs. Astrophys., **22,** 319, 1944.
2. D. TER HAAR, Proc. Dan. Acad. Sci., **25,** No. 3, 1948.
3. D. TER HAAR, Astrophys. J., **111,** 179, 1950.
4. D. TER HAAR, Ann. Rev. Astron. Astrophys., **5,** 267, 1967.
5. H. ALFVÉN, On the Origin of the Solar System, Oxford University Press, 1954.
6. F. HOYLE, Quart. J. Roy. Astron. Soc., **1,** 28, 1960.
7. D. TER HAAR, Ap. J., **110,** 321, 1949.
8. N. G. VAN KAMPEN and B. U. FELDERHOF, Theoretical Methods in Plasma Physics, North Holland Publishing Company, 1967.
9. P. H. ROBERTS, An Introduction to Magnetohydrodynamics, Longmans, 1967.
10. T. G. COWLING, Magnetohydrodynamics, Interscience, 1957.
11. A. TEMPKIN and J. C. LAMKIN, Phys. Rev., **121,** 788, 1961.
12. S. R. POTTASCH, Bull. Astron. Inst. Netherl., **19,** 469, 1968.
13. R. A. MILLIKAN, H. V. NEHER, and W. H. PICKERING, Phys. Rev., **66,** 295, 1944.
14. V. L. GINZBURG and S. I. SYROVATSKII, The Origin of Cosmic Rays, Pergamon, 1964.
15. G. GLOECKLER and J. R. JOKIPII, Ap. J., **148,** L41, 1967.
16. A. DALGARNO, Atomic and Molecular Processes (Ed. D. R. Bates), Academic Press, 1962, p. 637.
17. C. W. ALLEN, Astrophysical Quantities, Athlone Press, 1963. p. 259.

КОСМИЧЕСКИЕ ЛУЧИ И НАЧАЛО СОЛНЕЧНОЙ СИСТЕМЫ

А. Й. Р. ПРЕНТИС и Д. ТЕР ХААР

Р е з ю м е

Показывается, что космические лучи смогли обеспечить достаточную ионизацию в солнечном диске, соответствующем теории типа Канта—фон Вайцзеккера о начале солнечной системы, для создания вполне достаточной проводности, необходимой при протекании важных магнетогидродинамических эффектов.

Acta Physica Academiae Scientiarum Hungaricae, Tomus 27, pp. 237—239 (1969)

POLYNOMIAL WAVE FUNCTIONS IN ELLIPTICAL COORDINATES FOR MOLECULES*

By

R. GÁSPÁR and I. TAMÁSSY-LENTEI

INSTITUTE OF THEORETICAL PHYSICS, KOSSUTH LAJOS UNIVERSITY, DEBRECEN

(Received 3. II. 1969)

Polynomial wave functions in elliptical coordinates are suggested for molecules. Calculations have been made in the case of H_2^+. A three-terms function approximates the ground state energy with high accuracy.

In molecular calculations Slater type orbitals are the functions most used as radial factors in molecular orbitals [1]. For small molecules, orbitals in elliptical coordinates are used for very precise calculations [2]. Gaussian orbitals are also used for theoretical predictions [3]. In all of these calculations a common fact is that they use exponential factors to achieve convergence of the integrals in unbound space, so that normalization can be assured. Under such conditions some of the integrals can be calculated exactly; others with fair approximation.

There is an other way to achieve convergence. Theoretically the possibility of box normalization has been frequently mentioned. If a sufficiently large box is selected the correction caused by the shape of the box will be unimportant. Recently, GIMARC [4] has demonstrated that polynomial functions of the form

$$R(r) = \begin{cases} b(1 - r/a)^l r^k & 0 \leq r \leq a \\ 0 & r > a \end{cases} \tag{1}$$

are suitable as radial parts in the theory of atoms. In (1) a, k and l are positive variational parameters and for technical reasons k and l must be selected as integers; b is a normalization factor. The selection of the wave function (1) is equivalent to enclosing the electron in a spherical box. For the hydrogen atom, one obviously gets back to the exact ground state wave function by choosing for the parameters the values

$$k = 0\,, \qquad 1/a = 1/l\,, \qquad l \to \infty\,.$$

* Dedicated to Prof. P. GOMBÁS on his 60th birthday.

For the H_2^+-molecular ion one easily selects

$$\psi_i = b_i(1-\mu/a_i)^{l_i}\nu^{k_i}e^{i\lambda_i\varphi}, \qquad \begin{matrix} 0 \leq \mu \leq a_i, \\ -1 \leq \nu \leq 1, \\ 0 \leq \varphi \leq 2\pi, \end{matrix} \tag{2}$$

as a one-electron trial function, where

$$\mu = \frac{1}{R}(r_a + r_b), \qquad \nu = \frac{1}{R}(r_a - r_b) \quad \text{and} \quad \varphi \tag{3}$$

are elliptical coordinates, a and b, its reference centres coincide with the site of the protons. R is the distance of the protons. a_i, l_i, k_i and λ_i are variational parameters with the restrictions $k_i = 0, 2, 4, \ldots$; $l_i = 1, 2, 3, \ldots$; $a_i > 0$; b_i is the normalization factor. ψ_i is zero with $V \to \infty$ if $a_i < \mu \leq \infty$ corresponding to an orbital enclosed within an ellipsoid. If one takes a suitable linear combination of the orbitals with the form (2) like

$$\psi_{(n)} = \sum_{i=1}^{n} c_i \psi_i \tag{4}$$

one expects it to be possible to approximate the exact orbital as closely as possible.

For the H_2^+-molecular ion the ground state is $^2\Sigma_g^+$, which means that $\lambda_i = 0$ must be selected. One gets the matrix elements of the Hamiltonian and the overlap matrix easily without any approximation. We have solved the secular equation of the linear combination method. Table I gives the parameters and the calculated and experimental energy values. We have restricted the variation of the parameters by the conditions $l_i = l$ and $a_i = a$ for all values of i.

Evidently one can get

$$\psi_{(1)} = \psi_1 = b_1(1-\mu/a)^l \xrightarrow[(l=ac\to\infty)]{} N_{\mathrm{I}}\, e^{-c\mu} = \psi_{\mathrm{I}}$$

and

$$\psi_{(2)} = c_1\psi_1 + c_2\psi_2 = c_1 b_1(1-\mu/a)^l + c_2 b_2(1-\mu/a)^l\nu^2 \xrightarrow[(l=ac\to\infty)]{} N_{\mathrm{II}}\, e^{-c\mu}(1+b\nu^2) = \psi_{\mathrm{II}}$$

where N_{I} and N_{II} are normalization factors and b is a linear variational parameter. ψ_{II} is the trial function of JAMES [5] giving the surprisingly good result quoted in Table I.

The trial functions $\psi_{(1)}$ and $\psi_{(2)}$ give better energy values than the corresponding exponential forms and in spite of its simplicity $\psi_{(3)}$ gives a value for the energy which approximates the exact calculated one with high accuracy.

Table I

Energy values for the H_2^+-molecular ion calculated with different polynomial wave functions in atomic units (in e^2/a_0) at the internuclear distance $R = 2a_0$

n	i	k_i	l	a	E (present work)	E
1	1	0	44	34.86	—0.579933	—0.57975[a]
2	1, 2	0, 2	47	36.56	—0.602553	—0.60238[b]
3	1, 2, 3	0, 2, 4	47	36.56	—0.602620	—0.602634[c]

[a] calculated with ψ_{I}
[b] calculated with ψ_{II} (JAMES type wave function [5])
[c] E_{exact} [6]

In the above mentioned calculations the value of l was fairly high, differing little in the various cases. Furthermore, the value of l after variation coincides for $\psi_{(2)}$ and $\psi_{(3)}$. The situation with a is similar, which means that the size of the enclosing ellipsoid is nearly the same for all the trial functions.

Because of the high value of l we had to use double precision sub-routines on the electronic calculating machines.

We do not see any problem in the future application of this method for other poly-electronic systems and we plan to extend the calculations for them.

LITERATURE

1. See e. g. P. GOMBÁS, Theorie und Lösungsmethoden des Mehrteilchenproblems der Wellenmechanik, Verlag Birkhäuser, Basel, 1950.
2. See e. g. W. KOŁOS and C. C. J. ROOTHAAN, Rev. Mod. Phys., **32,** 219, 1960.
3. See e. g. H. PREUSS, Integraltafeln zur Quantenchemie, Vierter Band, Springer-Verlag, Berlin, 1960.
4. B. M. GIMARC, J. Chem. Phys., **44,** 373, 1966.
5. H. M. JAMES, J. Chem. Phys., **3,** 9, 1935.
6. D. R. BATES, K. LEDSHAM and A. L. STEWART, Phil. Trans. Roy. Soc., **A246,** 215, 1953; H. WIND, J. Chem. Phys., **42,** 2371, 1965; J. M. PEEK, J. Chem. Phys., **43,** 3004, 1965.

ПОЛИНОМИАЛЬНЫЕ ВОЛНОВЫЕ ФУНКЦИИ В ЭЛЛИПТИЧЕСКИХ КООРДИНАТАХ ДЛЯ МОЛЕКУЛ

Р. ГАШПАР и И. ТАМАШИ-ЛЕНТЕИ

Резюме

Предлагаются полиномиальные волновые функции в эллиптических координатах для молекул. Вычисления проведены в случае H_2^+. Функцией в три члена энергия основного состояния определяется с высокой точностью.

Acta Physica Academiae Scientiarum Hungaricae, Tomus 27, pp. 241—252 (1969)

SOME ACCURATE RESULTS FOR THREE-PARTICLE SYSTEMS*

By

W. KOŁOS

DEPARTMENT OF THEORETICAL CHEMISTRY, UNIVERSITY OF WARSAW, WARSAW, POLAND

(Received 3. II. 1969)

Results of a variational calculation of the nonadiabatic ground state energy of H_2^+ are presented. Diagonal corrections for nuclear motion have also been calculated for the electronic ground state of H_2^+. The adiabatic potential energy curve has been employed to calculate the rotational and vibrational levels for the H_2^+ ion and for muonic molecules. Nonadiabatic energy corrections are discussed. For $pp\mu d$ the adiabatic wave function is compared with the corresponding nonadiabatic result.

I. Introduction

Three-particle molecular systems, such as H_2^+, are sufficiently simple to make accurate calculations of their properties feasible. Results of these calculations may give an insight into some fundamental approximations which are unavoidable when dealing with more complex molecules. In particular, this applies to the adiabatic approximation which plays a fundamental role in the theory of molecular structure.

In the present article new results are presented obtained for the H_2^+ ion, and for muonic molecules. They are used to discuss some problems of the adiabatic approximation and of its accuracy.

II. The adiabatic approximation

Let us express [1] the exact Hamiltonian of a diatomic molecule in the centre of mass system as

$$H = H^\circ + H', \tag{1}$$

where H° is the "electronic" Hamiltonian which is independent of the nuclear masses M_a and M_b, and H' represents the kinetic energy of the relative motion of the nuclei and the coupling between electronic and nuclear motion. Explicitly, H' has the form

$$H' = H_1 + H_2 + H_3, \tag{2}$$

* Dedicated to Prof. P. GOMBÁS on his 60th birthday.

where

$$H_1 = -\frac{1}{2\mu} \Delta_R,$$

$$H_2 = -\frac{1}{8\mu} \left(\sum_i \nabla_i\right)^2, \tag{3}$$

$$H_3 = -\frac{1}{2\mu_a} \nabla_R \sum_i \nabla_i,$$

and the symbols used in (3) have the following meaning: $\mathbf{R} = \mathbf{R}_a - \mathbf{R}_b$ where $\mathbf{R}_a$ and $\mathbf{R}_b$ denote the radius vector for the nuclei a and b, respectively; the index i labels the electrons; $\mathbf{r}_i$ are measured from the geometrical centre of the molecule; $\mu^{-1} = M_a^{-1} + M_b^{-1}$ and $\mu_a^{-1} = -M_a^{-1} + M_b^{-1}$.

Let us also assume [2] the complete wave function in the form

$$\Psi = \sum_n \Psi_n(r, R)\, \chi_n(\mathbf{R}), \tag{4}$$

where r denotes the coordinates of all the electrons and Ψ_n is the solution of

$$H^\circ \Psi_n(r, R) = U_n(R)\, \Psi_n(r, R). \tag{5}$$

Using (1) and (4) in the complete Schrödinger equation

$$H\Psi = E\Psi \tag{6}$$

one gets the following set of coupled differential equations for the functions χ_n

$$\left[-\frac{1}{2\mu} \Delta_R + U_n(R) + H'_{nn}(R) - E\right] \chi_n(\mathbf{R}) = -\sum_{m \neq n} (H'_{nm} + B_{nm} \nabla_R)\, \chi_m(\mathbf{R}), \tag{7}$$

where

$$H'_{nm} = \int \Psi_n H' \Psi_m \, d\tau_r, \tag{8}$$

$$B_{nm} = -\int \Psi_n \left(\frac{1}{\mu} \nabla_R + \frac{1}{2\mu_a} \sum_i \nabla_i\right) \Psi_m \, d\tau_r. \tag{9}$$

The adiabatic approximation [2] is obtained by neglecting the right-hand side of Equs. (7). In contrast to the Born—Oppenheimer (clamped nuclei) appro-

ximation it includes the diagonal corrections for nuclear motion, H'_{nn}, in the adiabatic potential

$$U_n^{ad}(R) = U_n(R) + H'_{nn}(R) \tag{10}$$

which governs the nuclear motion.

III. Nonadiabatic energy for H_2^+

Nonadiabatic calculations for a diatomic molecule can be carried out in two different ways: (a) One can solve the set of Equs. (7); (b) One can employ the Ritz variational method using the complete Hamiltonian (1) and assuming the trial function in the form

$$\Psi = \sum_{n=1}^{N} c_n \Phi_n(\mathbf{r}, \mathbf{R}), \tag{11}$$

where $\Phi_n(\mathbf{r}, \mathbf{R})$ is some set of functions in the space of $\mathbf{r}$, $\mathbf{R}$. For H_2^+ both approaches are feasible.

Calculations based essentially on the set of Equs. (7) have been carried out by HUNTER and PRITCHARD [3], and with only a few terms in the expansion (4) accurate energies have been obtained. This approach, however, does not seem to be practical for more complex systems and, therefore, in the present work the second approach has been tested. This method has already been used by several authors [4, 5, 6], but the wave functions employed were not flexible enough to yield accurate results.

For a non-rotational state the wave function does not depend on the orientation of $\mathbf{R}$, and in the present calculation the following basis set was employed

$$\Phi_n = \exp(-\alpha\xi)\cosh(\beta\eta)\,\xi^{r_n}\eta^{s_n}\exp(-x^2/2)\,\mathscr{H}_{k_n}(x)R^{-3/2}. \tag{12}$$

The symbols used in (12) have the following meanings: ξ and η denote the elliptic coordinates; $\mathscr{H}_k$ is the k-th Hermitian polynomial; $x = \gamma\ (R—R_e)$; and α, β, γ, R_e are treated as variational parameters, in addition to the linear parameters c_i in the expansion (11).

Convergence of the energy resulting from the wave function (11) with the basis set (12) is displayed in Table I for the ground state of H_2^+. N denotes the number of terms in the expansion (11), $(r + s)_{\max}$ the maximum value of the sum of powers of ξ and η included in the expansion, and $k_{\max}$ the maximum degree of the Hermitian polynomials. All energies given in Table I were obtained with one set of the nonlinear parameters which were optimized for the maximum number of terms. The proton mass used was $M_p = 1836.12$. For the second lowest vibrational state a still larger number of terms was needed to get the final value of the energy.

Table I

Convergence of the nonadiabatic energy, E, and of the binding energy, D, for the ground state of H_2^+

N	$(r+s)_{max}$	k_{max}	E (a. u.)	D (cm^{-1})
24	3	3	−0.5971166	21 374.3
30	3	4	−0.5971356	21 378.5
40	4	4	−0.5971367	21 378.8
44	4	5	−0.5971380	$21\,379.0_6$
51	5	5	−0.5971381	$21\,379.0_8$
55	5	6	−0.5971385	$21\,379.1_7$
57	5	7	−0.5971387	$21\,379.2_1$

IV. Adiabatic energy for H_2^+

The adiabatic energy is obtained by solving Equ. (7) with the right-hand side equal to zero. Assuming $\chi(R) = f_{vk}(R) Y_K^M(\Theta,\varphi) R^{-1}$ the appropriate equation for the vibrational wave function reads

$$\left[-\frac{1}{2\mu}\frac{d^2}{dR^2} + U_n(R) + H'_{nn}(R) + \frac{J(J+1)}{2\mu R^2} - E\right] f_{vk}(R) = 0\,, \qquad (13)$$

where v and J denote the vibrational and rotational quantum numbers, respectively.

Very accurate clamped nuclei potential has recently been published [7, 8], and adiabatic energies have also been computed [7]. However, in the latter calculation relatively poor values [9] of H'_{nn} were used. To get reliable non-adiabatic effects, which are very small and which are represented by the differences between the non-adiabatic and adiabatic values, highly accurate results are indispensable. Therefore the diagonal nuclear motion corrections (3) have been computed using for the wave function an expansion in terms of 10 basis functions of the form

$$\Phi_n = \exp(-\alpha\xi)\cosh(\beta\eta)\,\xi^{r_n}\eta^{s_n} \qquad (14)$$

and the results are listed in Table II. ΔD given in the last column (in cm^{-1}) is defined as $\langle H'(\infty)\rangle - \langle H'(R)\rangle$ and represents the correction to the binding energy due to the diagonal nuclear motion corrections.

Using the calculated values of H'_{nn}, and accurate clamped nuclei potential U_n, the vibrational equation (13) has been solved for several vibrational

Table II

Clamped nuclei energy, E, and diagonal corrections for nuclear motion (2) for H_2^+ calculated for various internuclear distances R

R	E	$H_1\times10^3$	$H_2\times10^3$	ΔD
0			0.54463	—59.766
0.3	1.4666385	0.07470	0.45537	—56.571
0.4	0.6992462	0.08327	0.41811	—50.275
0.5	0.2650120	0.09104	0.38414	—44.526
0.6	—0.0048180	0.09556	0.35388	—38.875
0.7	—0.1826248	0.09794	0.32718	—33.537
0.8	—0.3044800	0.09899	0.30371	—28.617
0.9	—0.3902705	0.09925	0.28307	—24.144
1.0	—0.4517863	0.09905	0.26489	—20.109
1.1	—0.4964118	0.09859	0.24884	—16.486
1.2	—0.5289745	0.09803	0.23462	—13.241
1.3	—0.5527406	0.09743	0.22199	—10.338
1.4	—0.5699835	0.09686	0.21074	—7.744
1.5	—0.5823232	0.09635	0.20069	—5.426
1.6	—0.5909372	0.09592	0.19169	—3.358
1.7	—0.5966963	0.09559	0.18362	—1.513
1.8	—0.6002536	0.09536	0.17636	0.131
1.9	—0.6021058	0.09522	0.16983	1.593
2.0	—0.6026342	0.09519	0.16395	2.891
2.1	—0.6021349	0.09527	0.15864	4.039
2.2	—0.6008396	0.09544	0.15386	5.052
2.3	—0.5989309	0.09570	0.14954	5.941
2.4	—0.5965536	0.09606	0.14565	6.718
2.5	—0.5938235	0.09650	0.14214	7.391
2.6	—0.5908332	0.09702	0.13898	7.968
2.7	—0.5876573	0.09762	0.13615	8.459
2.8	—0.5843560	0.09830	0.13361	8.868
2.9	—0.5809780	0.09904	0.13134	9.204
3.0	—0.5775628	0.09984	0.12932	9.471
3.1	—0.5741424	0.10070	0.12753	9.676
3.2	—0.5707425	0.10161	0.12595	9.822
3.3	—0.5673841	0.10257	0.12457	9.915
3.4	—0.5640840	0.10357	0.12337	9.959
3.5	—0.5608555	0.10461	0.12233	9.958
3.6	—0.5577092	0.10567	0.12146	9.917
3.7	—0.5546535	0.10676	0.12073	9.838

Table II (continued)

R	E	$H_1\times10^3$	$H_2\times10^3$	ΔD
3.8	−0.5516947	0.10787	0.12013	9.725
3.9	−0.5488373	0.10899	0.11966	9.582
4.0	−0.5460848	0.11012	0.11930	9.412
4.1	−0.5434394	0.11126	0.11905	9.219
4.2	−0.5409022	0.11239	0.11890	9.005
4.3	−0.5384735	0.11351	0.11883	8.772
4.4	−0.5361531	0.11463	0.11884	8.525
4.5	−0.5339400	0.11572	0.11893	8.265
4.6	−0.5318328	0.11680	0.11908	7.996
4.7	−0.5298295	0.11785	0.11930	7.718
4.8	−0.5279281	0.11888	0.11956	7.435
4.9	−0.5261259	0.11987	0.11987	7.148
5.0	−0.5244202	0.12084	0.12022	6.859
5.1	−0.5228082	0.12176	0.12061	6.571
5.2	−0.5212866	0.12265	0.12103	6.284
5.3	−0.5198521	0.12350	0.12147	6.000
5.4	−0.5185016	0.12432	0.12193	5.720
5.5	−0.5172315	0.12509	0.12241	5.446
5.6	−0.5160385	0.12582	0.12290	5.177
5.7	−0.5149192	0.12652	0.12340	4.916
5.8	−0.5138701	0.12718	0.12390	4.661
5.9	−0.5128878	0.12779	0.12440	4.415
6.0	−0.5119690	0.12838	0.12490	4.178
6.1	−0.5111105	0.12892	0.12540	3.949
6.2	−0.5103089	0.12943	0.12589	3.729
6.3	−0.5095612	0.12991	0.12638	3.518
6.4	−0.5088644	0.13035	0.12685	3.317
6.5	−0.5082155	0.13077	0.12731	3.124
6.6	−0.5076116	0.13115	0.12776	2.940
6.7	−0.5070501	0.13151	0.12820	2.766
6.8	−0.5065282	0.13185	0.12862	2.600
6.9	−0.5060437	0.13216	0.12903	2.442
7.0	−0.5055940	0.13245	0.12942	2.292
7.1	−0.5051769	0.13271	0.12980	2.151
7.2	−0.5047902	0.13296	0.13016	2.017
7.3	−0.5044319	0.13319	0.13051	1.891
7.4	−0.5041001	0.13340	0.13084	1.772
7.5	−0.5037929	0.13360	0.13115	1.660

Table II (continued)

R	E	$H_1\times10^3$	$H_2\times10^3$	ΔD
7.6	−0.5035087	0.13378	0.13145	1.554
7.7	−0.5032458	0.13395	0.13174	1.454
7.8	−0.5030027	0.13411	0.13201	1.361
7.9	−0.5027780	0.13425	0.13226	1.273
8.0	−0.5025704	0.13438	0.13251	1.190
8.2	−0.5022013	0.13462	0.13295	1.040
8.4	−0.5018866	0.13483	0.13335	0.908
8.6	−0.5016184	0.13500	0.13370	0.792
8.8	−0.5013900	0.13516	0.13401	0.691
9.0	−0.5011954	0.13529	0.13428	0.603
9.2	−0.5010298	0.13540	0.13452	0.526
9.4	−0.5008887	0.13549	0.13473	0.458
9.6	−0.5007685	0.13558	0.13492	0.400
9.8	−0.5006661	0.13565	0.13508	0.349
10.0	−0.5005787	0.13571	0.13522	0.305
10.5	−0.5004121	0.13583	0.13549	0.218
11.0	−0.5002992	0.13591	0.13568	0.158
11.5	−0.5002221	0.13597	0.13582	0.115
12.0	−0.5001683	0.13601	0.13591	0.085
13.0	−0.5001035	0.13607	0.13602	0.049
14.0	−0.5000689	0.13610	0.13608	0.030
15.0	−0.5000490	0.13611	0.13611	0.020
17.5	−0.5000247	0.13614	0.13613	0.009
20.0	−0.5000143	0.13615	0.13614	0.005
∞	−0.5000000	0.13616	0.13616	0.000

All results in a. u. only ΔD in cm^{-1}.

and rotational states. The resulting adiabatic energies for the ground electronic state of H_2^+ are shown in Table III.

By comparing the adiabatic energies for $K = 0$ and $v = 0$, 1, 2 with the corresponding nonadiabatic results [3] one gets the nonadiabatic energy correction $\Delta E = E_{\text{nonad}} - E_{\text{ad}} = 0.12$, 0.21 and 0.35 cm^{-1} for the three lowest vibrational states, respectively. The correction is very small and is seen to be roughly a linear function of the vibrational excitation. The differences between the adiabatic and clamped nuclei [10] dissociation energies (for $J = 0$) are shown in Table IV. Their maximum for $v = 8$ results from the shape of the H'_{nn} versus R curve which has a minimum at $R = 3.4$ a.u., and the expectation value of the internuclear distance for $v = 8$ is just $\langle R\rangle = 3.362$ a.u.

Acta Physica Academiae Scientiarum Hungaricae 27, 1969

Table III

Adiabatic energies (in a.u.) for various vibrational (v) and rotational (J) levels in the ground electronic state of H_2^+

v \ J	0	1	2	3	4	5	6
0	−0.5971382	−0.5968729	−0.5963443	−0.5955567	−0.5945162	−0.5932307	−0.5917097
1	−0.5871538	−0.5869025	−0.5864018	−0.5856557	−0.5846702	−0.5834528	−0.5820126
2	−0.5777492	−0.5775113	−0.5770375	−0.5763316	−0.5753992	−0.5742476	−0.5728856
3	−0.5689050	−0.5686802	−0.5682324	−0.5675654	−0.5666846	−0.5655969	−0.5643107
4	−0.5606050	−0.5603929	−0.5599706	−0.5593415	−0.5585109	−0.5574855	−0.5562733
5	−0.5528359	−0.5526363	−0.5522388	−0.5516469	−0.5508655	−0.5499012	−0.5487615
6	−0.5455872	−0.5453999	−0.5450269	−0.5444716	−0.5437387	−0.5428344	−0.5417663
7	−0.5388515	−0.5386763	−0.5383276	−0.5378085	−0.5371235	−0.5362789	−0.5352817
8	−0.5326241	−0.5324611	−0.5321365	−0.5316534	−0.5310164	−0.5302311	−0.5293048
9	−0.5269037	−0.5267527	−0.5264523	−0.5260055	−0.5254165	−0.5246910	−0.5238358
10	−0.5216918	−0.5215531	−0.5212772	−0.5208670	−0.5203266	−0.5196617	−0.5188788
11	−0.5169938	−0.5168676	−0.5166167	−0.5162438	−0.5157531	−0.5151500	−0.5144411
12	−0.5128188	−0.5127055	−0.5124802	−0.5121459	−0.5117064	−0.5111673	−0.5105349
13	−0.5091802	−0.5090803	−0.5088818	−0.5085875	−0.5082015	−0.5077292	−0.5071770
14	−0.5060962	−0.5060104	−0.5058401	−0.5055881	−0.5052587	−0.5048572	−0.5043904
15	−0.5035904	−0.5035197	−0.5033796	−0.5031730	−0.5029044	−0.5025794	−0.5022052
16	−0.5016922	−0.5016379	−0.5015307	−0.5013740	−0.5011722	−0.5009319	−0.5006612
17	−0.5004349	−0.5003989	−0.5003287				

Table IV

Differences between the adiabatic and clamped nuclei dissociation energies (in cm^{-1}) for various vibrational levels of H_2^+

v	$D_{ad.} - D_{cl.n.}$	v	$D_{ad.} - D_{cl.n.}$
0	3.23	9	6.13
1	3.96	10	5.95
2	4.60	11	5.66
3	5.12	12	5.27
4	5.54	13	4.76
5	5.86	14	4.15
6	6.08	15	3.43
7	6.19	16	2.57
8	6.22	17	1.59

V. Adiabatic results for muonic molecules

The clamped nuclei potential energy curve with diagonal corrections for nuclear motion, computed for the H_2^+ ion, can be directly employed, by changing only the mass ratio, to calculate the adiabatic energies for muonic molecules. These consist of two singly-charged nuclei (proton, p, deuteron, d, triton, t) bound by a muon μ. The results are listed in Table V where, in addition to the energy, the expectation values of R and R^{-2} are also given. In the same Table we give the nonadiabatic energies calculated recently by CARTER [11] using the Ritz variational method. Convergence of the energy becomes slower with decreasing ratio of the muon mass, m, to the reduced mass of the two nuclei. Inspection of CARTER's results shows that they have converged to roughly 4 figures except for the excited state of $d\mu d$ where the accuracy is significantly lower and therefore this energy is not given in Table V. The previous nonadiabatic results (see e.g. [12]) also seem to be of a lower accuracy and are not included in the Table. For comparison the results for the H_2^+ ion are listed in the last column. The corresponding nonadiabatic results are those of HUNTER and PRITCHARD [3].

The ΔE values given in Table V represent the nonadiabatic energy correction, i.e., $\Delta E = E_{nonad} - E_{ad}$. They are seen to be of the expected order of magnitude, i.e., of the order of $(m/\mu)^2$. They are also seen to be larger for the excited vibrational states than for the ground states. For the states under consideration the nonadiabatic effects are due to interaction with higher states of the same Λ, where Λ is the quantum number for the component of the angular momentum along the internuclear axis. The energy differences between these upper states and the state under consideration are smaller when the

Table V
Energies and other properties of the muonic molecules

Molecule $m(M_a+M_b)/M_aM_b$		$p\mu p$ 4.4400	$p\mu d$ 5.9185	$p\mu t$ 6.65648	$d\mu d$ 8.87324	$d\mu t$ 10.64216	$t\mu t$ 13.29192	H_2^+ 917.06
	E_{ad}	−0.4885066	−0.5080172	−0.5148851	−0.5294507	−0.5372619	−0.5455846	−0.5971382
	E_{nonad}	−0.49437	−0.51266		−0.53097	−0.53840		−0.5971387
$v=0$	ΔE	−0.00586	−0.00464		−0.00152	−0.00114		−0.0000005
	$\langle R \rangle$	3.303708	3.081971	3.003851	2.838290	2.749622	2.655254	2.063922
	$\langle R^{-2} \rangle$	0.1492881	0.1618795	0.1667037	0.1776637	0.1839713	0.1910392	0.2439225
	E_{ad}				−0.4777144	−0.4860214	−0.4957138	−0.5871537
	E_{nonad}					−0.48773		−0.5871548
$v=1$	ΔE					−0.00171		−0.0000011
	$\langle R \rangle$				5.743900	5.067744	4.481494	2.199147
	$\langle R^{-2} \rangle$				0.0720091	0.0870771	0.1036442	0.2310860

All results in "natural units", i.e. assuming $m = 1$, where for the muonic molecules and for the H_2^+ ion m denotes the muon and electron mass, respectively.

latter is an excited vibrational state. Therefore, by a common argument of the perturbation theory one may conclude that the nonadiabatic effects should increase with increasing vibrational excitation. Table V proves that this is indeed the case, and the results given in the previous Section show that the conclusion is also valid for higher vibrational states of H_2^+.

VI. Adiabatic and nonadiabatic vibrational wave functions

It may be also of some interest to compare the adiabatic and nonadiabatic vibrational wave functions. A comparison of this type has already been made [13] for the ground state of the hydrogen molecule. However, in that

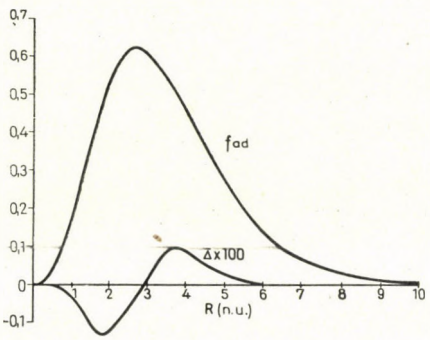

Fig. 1

case the nonadiabatic calculations [14] were not sufficiently accurate to make such a fine comparison of the wave functions meaningful. Similar and more accurate calculations have recently been carried out for the $p\mu d$ system [15]. In this case one may expect that the nonadiabatic effect in the wave function is sufficiently large to be reliably detectable in a fairly accurate calculation. The 128-term nonadiabatic wavefunction calculated [15] for $p\mu d$ has been used in the present work to calculate the vibrational pseudo-wave function defined as

$$f_{\text{nonad}}(R) = R\left[\int |\Psi(\mathbf{r}, R)|^2 \, d\tau_\mu\right]^{1/2}, \tag{15}$$

where Ψ denotes the complete wave function for $p\mu d$ and the integration is to be carried out only over the coordinates of the muon. The calculated pseudo-wave function can be compared with the adiabatic vibrational wave function $f_{vK}(\equiv f_{\text{ad}})$ discussed in Section IV.

The calculated difference $f_{\text{nonad}} - f_{\text{ad}}$ does not vanish with increasing internuclear distance (for $R \leqslant 10$ n.u.) which is probably due to a relatively large error in the wave function for large R. Therefore, it seems that a weighted difference, i.e.,

$$\Delta = (f_{\text{nonad}} - f_{\text{ad}}) f_{\text{ad}}^2 \tag{16}$$

has more physical meaning, and this difference is presented in Fig. 1 where the adiabatic vibrational wave function is also shown. Thus the nonadiabatic effects seem to increase the mean value of the internuclear distance in spite of the fact that they increase the binding of the two nuclei. This is supported by the results of TIPPING and HERMAN [16] who concluded that the nonadiabatic effects decrease the rotational constant of H_2. The binding is more directly related to the piling up of negative charge between the two nuclei. For H_2 it has been found [13, 14] that the nonadiabatic value of $\langle z^2 \rangle$ is smaller than the adiabatic one, where z denotes the sum of the electronic coordinates in the direction of the molecular axis. This is consistent with the increase of binding by the nonadiabatic effects.

Acknowledgment

The author is indebted to Dr. L. WOLNIEWICZ for interesting and helpful discussions.

REFERENCES

1. W. KOŁOS and L. WOLNIEWICZ, Rev. Mod. Phys., **35**, 473, 1964.
2. M. BORN and R. OPPENHEIMER, Ann. Phys., **84**, 457, 1927; M. BORN, Nachr. Akad. Wiss. Göttingen, 1, 1951; M. BORN and K. HUANG, Dynamical Theory of Crystal Lattices, Oxford University Press, New York, 1956.
3. G. HUNTER and H. O. PRITCHARD, J. Chem. Phys., **46**, 2153, 1967.
4. W. KOŁOS, C. C. J. ROOTHAAN and R. A. SACK, Rev. Mod. Phys., **32**, 178 1960.
5. H. DIEHL and S. FLÜGGE, Z. Physik, **162**, 21, 1961.
6. A. FRÖMAN and J. L. KINSEY, Phys. Rev., **123**, 2077, 1961.
7. H. WIND, Thesis, University of Utrecht, 1965; J. Chem. Phys., **42**, 2371, 1965.
8. J. M. PEEK, Sandia Corporation Report No. SC—RR—65—77, 1965.
9. S. COHEN, D. L. JUDD and R. J. RIDDELL, Univ. of California, Lawrence Radiation Lab. Report No. UCRL—8802, 1959.
10. J. M. PEEK, private communication, 1968.
11. B. P. CARTER, Phys. Rev., **165**, 139, 1968.
12. B. P. CARTER, Phys. Rev., **141**, 863, 1966.
13. L. WOLNIEWICZ, J. Chem. Phys., **45**, 515, 1966.
14. W. KOŁOS and L. WOLNIEWICZ, J. Chem. Phys., **41**, 3674, 1964.
15. W. KOŁOS, Phys. Rev., **165**, 165, 1968.
16. R. TIPPING and R. M. HERMAN, J. Chem. Phys., **44**, 3112, 1966.

НЕСКОЛЬКО ТОЧНЫХ РЕЗУЛЬТАТОВ ДЛЯ СИСТЕМ ТРЕХ ЧАСТИЦ

В. КОЛОС

Резюме

Сообщается о результатах вариационного вычисления неадиабатической энергии основного состояния H_2^+. Для электронного основного состояния H_2^+ определялись и диагональные поправки для ядерного движения. Кривая адиабатической потенциальной энергии используется для вычисления ротационных и вибрационных уровней молекулярного иона H_2^+ и для мюонных молекул. Дискутируются поправки к неадиабатической энергии. Адиабатическая волновая функция для $p\mu d$ сравнивается с соответствующим неадиабатическим результатом.

Acta Physica Academiae Scientiarum Hungaricae, Tomus 27, pp. 253—260 (1969)

LEE MODEL AS A Z LIMIT*

By

K. L. NAGY

INSTITUTE FOR THEORETICAL PHYSICS, ROLAND EÖTVÖS UNIVERSITY, BUDAPEST

(Received 3. II. 1969)

Limits are investigated in a generalized Lee model without cut off which reproduce the elementary + composite particle case found in the original model.

1. One of the most interesting problems in particle physics is to find some answer to the question as to which particles among the vast number of stable or instable particles are elementary and which are composed somehow from others. Different lines of attack offer certain types of criteria which might be especially useful in bootstrap calculations. In a Lagrangian field theory e.g. $Z \to 0$ limits are assumed to turn an elementary particle into a composite one. Detailed references concerning these problems can be found in [1].

Former investigations of the Lee model without cut-off (i.e. when a ghost is present) have shown that there the typical elementary + composite particle case arises [2], with the consequence that one of the particles is elementary and the other composite, but one cannot say which belongs to either type.

Here we deal with the question of the kind of limit which produces this situation. The model which we have chosen is the generalized model with two V-particles [3], which with a cut-off, has been investigated already from the point of view of a Z limit [4], where, of course, it gives a different result.

In the Lee model all information arises [5] from a function $h(z)$ having the form

$$h(z) = a + bz + z^2 G(z)$$

a, b finite

$$G(z) = \int \frac{k^2\, dk}{2\omega^3(\omega - z)} \,.$$

Thus, reproducing the results of the Lee model means just reproducing the above form for the corresponding function of the generalized theory.

* De dicated to Prof. P. GOMBÁS on his 60th birthday.

2. The generalized model we are discussing is described by the Hamiltonian

$$H = H_0 + H_1$$

$$H_0 = \sum_{i=1}^{2} m_i \delta_i \psi_{v_i}^* \psi_{v_i} + \int \omega(k)\, a^*(k)\, a(k)\, \mathrm{d}k\,,$$

$$H_1 = -\sum_{i=1}^{2} \frac{g_i}{\sqrt{4\pi}} \int \frac{1}{\sqrt{2\omega}} \left[\psi_N^* \psi_{v_i}\, a^*(k) + \delta_i \psi_{v_i}^* \psi_N\, a(k)\right] \mathrm{d}k\,, \tag{1}$$

$$\omega = \sqrt{m_0^2 + k^2}.$$

We have taken two V-particles, and fixed the energy scale by setting $m_N = 0$. The commutation relations are the conventional ones except for the V-particles, for which

$$\{\psi_{v_i}, \psi_{v_i}^*\} = \delta_i \tag{2}$$

is prescribed. $\delta_i = +1$ for a normal particle, $\delta_i = -1$ for a particle quantized with indefinite metric. m_i and g_i are the bare masses and coupling constants. We have taken the convenient form (1) in order to retain the maximal possible symmetries in the following equations [5]. H is Hermitian if g_i is real with $\delta_i = +1$, and pure imaginary for $\delta_i = -1$. Now we wish to solve the problem of the N—Θ sector. Here a general state possesses the form

$$|E> = \left(\Sigma \alpha_i \delta_i\, \psi_{v_i}^* + \psi_N^* \int \varphi(k)\, a^*(k)\, \mathrm{d}k\right)|0>, \tag{3}$$

$$\psi_{v_i}|0> = \psi_N|0> = a(k)\,|0> = 0\,, \qquad <0|0> = 1\,,$$

with the norm

$$<E|E> = \Sigma\, \delta_i\, \alpha_i^*\, \alpha_i + \int \varphi^*(k)\, \varphi(k)\, \mathrm{d}k. \tag{4}$$

The eigenvalue equation

$$H|E> = E|E>$$

gives

$$(m_i - E)\, \alpha_i = \frac{g_i}{\sqrt{4\pi}} \int \frac{\mathrm{d}k}{2\omega}\, \varphi(k)\,,$$

$$(\omega - E)\, \varphi(k) = \frac{\Sigma\, \alpha_i\, g_i}{\sqrt{4\pi}\sqrt{2\omega}}\,. \tag{5}$$

Thus, for real particle states

$$\varphi(k) = -\frac{\Sigma\, \alpha_i\, g_i}{\sqrt{4\pi}\sqrt{2\omega}\,(E - \omega + i\varepsilon)}, \tag{6}$$

in the continuous spectrum (S wave)

$$\varphi(k) = \frac{1}{k_0}\delta(k - k_0) - \frac{\Sigma \alpha_i g_i}{\sqrt{4\pi}\sqrt{2\omega}\,(E-\omega+i\varepsilon)} \tag{7}$$

(outgoing waves). Substituting (6) and (7) into (5) one gets

$$\begin{aligned} A_1\alpha_1 + B\alpha_2 &= 0\,, \\ B\alpha_1 + A_2\alpha_2 &= 0\,, \end{aligned} \tag{8}$$

or

$$\begin{aligned} A_1\alpha_1 + B\alpha_2 &= E_1\,, \\ B\alpha_1 + A_2\alpha_2 &= E_2\,. \end{aligned} \tag{9}$$

Here

$$A_i = m_i - E + g_{i(i)}^2 \int \frac{k^2\,dk}{2\omega(E-\omega+i\varepsilon)}\,,$$

$$B = g_1 g_2 \int \frac{k^2\,dk}{2\omega(E-\omega+i\varepsilon)}\,,$$

$$E_i = g_i \frac{k_0}{\sqrt{2E}}\,, \qquad E = \sqrt{m_0^2 + k_0^2}\,.$$

From (8) the necessary condition for finding real particle states is

$$A_1 A_2 - B^2 = 0\,. \tag{10}$$

For continuum states from (9)

$$\Sigma \alpha_i g_i = \frac{k_0}{\sqrt{2E}}\left[g_1^2(m_2 - E) + g_2^2(m_1 - E)\right](A_1 A_2 - B^2)^{-1}\,. \tag{11}$$

Next we distinguish four special cases:

i.) $m_1 = m_2 = m$.	ii.) $m_1 \neq m_2$.
a) $g_1^2 = -g_2^2$,	a) $g_1^2 = -g_2^2$,
b) $g_1^2 \neq -g_2^2$,	b) $g_1^2 \neq -g_2^2$.

In cases a) one of the particles is normal; the other is abnormal by prescription.

For the case i. a) (10) gives

$$(m - E)^2 = 0\,.$$

From (6) and (8) $\varphi = 0$, namely

$$\Sigma \alpha_i g_i = \alpha_1 g_1 - \left.\frac{A_1}{B}\right|_{E=m} \cdot \alpha_2 g_2 = 0 .$$

Actually, the eigenstate with (for the sake of definiteness)—$\delta_1 = \delta_2 = 1$

$$|E> = -\alpha \left(\psi^*_{v_1} + \frac{g_1}{g_2} \psi^*_{v_2}\right) |0> \tag{12}$$

possesses zero norm

$$<E|E> = 0 .$$

Then from general principles it follows that a dipole ghost satisfying

$$(H - E)|D> = E|E>$$

must exist. Indeed, replacing

$$|D> = \left(\Sigma \beta_i \delta_i \psi^*_{v_i} + \psi^*_N \int \Phi(k)\, a^*(k)\, \mathrm{d}k\right) |0>$$

and (12), by $E = m$, one gets

$$-\frac{g_i}{\sqrt{4\pi}} \int \frac{\mathrm{d}k}{\sqrt{2\omega}} \Phi(k) = m\alpha_i ,$$

$$(\omega - m)\, \Phi(k) = \frac{\Sigma \beta_i \alpha_i}{\sqrt{4\pi}\sqrt{2\omega}} .$$

From these

$$\Phi(k) = -\frac{\alpha m}{g_1 \int \dfrac{k^2\, \mathrm{d}k}{2\omega\,(m - \omega)}} \frac{1}{\sqrt{4\pi}\sqrt{2\omega}\,(m - \omega)}$$

and the state

$$|D> = \left[-\beta \psi^*_{v_1} + \left(\frac{\alpha m}{g_1 g_2 \int \dfrac{k^2\, \mathrm{d}k}{2\,\omega(m - \omega)}} - \frac{g_1}{g_2}\beta\right) \psi^*_{v_2} + \psi^*_N \int \Phi(k) a^*(k)\, \mathrm{d}k\right] |0> .$$

Obviously $\langle E|D\rangle \neq 0$. Choosing β and

$$\gamma = \frac{\alpha}{g_1 \int \dfrac{k^2\, \mathrm{d}k}{2\,\omega(m - \omega)}}$$

one can appropriately prescribe

$$<D|D> = 0, \quad <E|D> = 1.$$

Similarly from (11) one can see that there is no scattering $S = 1$. These two interactions of equal strength distort the two bare eigenvectors into a complete dipole ghost situation. It is interesting that only the dipole ghost is surrounded by a meson cloud, otherwise a compensation has occurred which is, of course, trivial.

For the other cases it is most convenient to introduce the function of the complex variable

$$h(z) = -\frac{(m_1 - z)(m_2 - z)}{g_1^2(m_2 - z) + g_2^2(m_1 - z)} + \int \frac{k^2\,\mathrm{d}k}{2\,\omega(\omega - z)}. \tag{13}$$

From (8), (9), (10) and (11) by standard methods one can see that the dressed particle eigenvalues are given by

$$h(E) = 0, \tag{14}$$

and the N—Θ scattering S matrix is

$$S = 1 - \frac{i\pi k_0}{h(E + i\varepsilon)} = \frac{h(E - i\varepsilon)}{h(E + i\varepsilon)}. \tag{15}$$

Furthermore, the norms of the dressed particle eigenvectors are (for E real)

$$<E|E> = \frac{\delta_i|\alpha_i|^2\,[g_1^2(m_2 - E) + g_2^2(m_1 - E)]}{m_j - E + g_j^2 \int \frac{k^2\,\mathrm{d}k}{2\omega(E - \omega)}} \cdot h'(z)|_{z=E}, \tag{16}$$

$$i \neq j, \qquad \text{i.e.} \quad i = 1, j = 2 \quad \text{or} \quad i = 2, j = 1.$$

Now, without cut off, $h(z)$ with

$$G(z) = \int \frac{k^2\,\mathrm{d}k}{2\,\omega^3(\omega - z)}$$

i.b) $$h(z) = a + bz + z^2\,G(z),$$

$$a = -\frac{m}{g_1^2 + g_2^2} + \int \frac{k^2\,\mathrm{d}k}{2\,\omega^2}, \tag{17}$$

$$b = \frac{1}{g_1^2 + g_2^2} + \int \frac{k^2\,\mathrm{d}k}{2\,\omega^3},$$

ii.a)
$$h(z) = a + bz + cz^2 + z^2 G(z)\,,$$
$$a = \frac{m_1 m_2}{g_1^2(m_1 - m_2)} + \int \frac{k^2\,\mathrm{d}k}{2\,\omega^2}\,,$$
$$b = \frac{m_1 + m_2}{g_1^2(m_2 - m_1)} + \int \frac{k^2\,\mathrm{d}k}{2\,\omega^3}\,, \tag{18}$$
$$c = \frac{1}{g_1^2(m_1 - m_2)}\,.$$

ii.b)
$$h(z) = \frac{A}{E_0 - z} + a + bz + z^2 G(z)\,,$$
$$a = -\frac{g_1^2 m_1 + g_2^2 m_2}{(g_1^2 + g_2^2)^2} + \int \frac{k^2\,\mathrm{d}k}{2\,\omega^2}\,, \quad b = \frac{1}{g_1^2 + g_2^2} + \int \frac{k^2\,\mathrm{d}k}{2\,\omega^3}\,,$$
$$A = \frac{(g_1 g_2(m_1 - m_2))^2}{(g_1^2 + g_2^2)^3}\,, \quad E_0 = \frac{g_1^2 m_2 + g_2^2 m_1}{g_1^2 + g_2^2}\,. \tag{19}$$

All (real) constants a, b, c, A, E_0 are kept finite. After fixing them a model theory is defined. From the forms of b we see also that in cases i, ii, b) one or both of the V particles must be quantized with indefinite metric. $h(z)$ in the case of i.b) corresponds completely to that of the Lee model implying the same results, except, of course, that the two real states are produced now by two bare fields. The real particle state structure of ii.a) is the same as that of the Lee model; the structure of ii.b) corresponds to the model described in [6] implying three real V particle states.

3. Let us now turn to the problem of what type of limits reproduce the results of the original Lee model. From case i.a.) there is no transition, of course. (17) corresponds to the Lee model as it stands, (18) requires $c = 0$, (19) $A = 0$. On the other hand, the elementary composite particle case can be attributed to $|\alpha_i(\mathrm{E})|^2 = 0$, $i = 1$ or 2 with $h(E) = 0$. The connection and difference between this condition and $\det Z = 0$ can be found in [1,4]. Therefore let us study the behaviour of α_i. Since $\langle E|E\rangle$, $h'(E)$ are finite $|\alpha_i|^2$ is essentially determined from (16) by the factor

$$B_j = \frac{m_j - E + g_j^2 \int \dfrac{k^2\,\mathrm{d}k}{2\,\omega(E - \omega)}}{g_1^2(m_2 - E) + g_2^2(m_1 - E)}\,, \qquad \text{with} \qquad h(E) = 0\,.$$

Since in all cases we are discussing here a field theory with indefinite metric, $|\alpha_i|^2$ is not restricted to $0 \leqslant |\alpha_i|^2 \leqslant 1$. Actually, in general, it diverges. Anyway $|\alpha_i|^2$ vanishes if and only if $B_j = 0$. Using (13)

$$B_j = \frac{g_i^2 (m_j - E)^2}{[g_1^2 (m_2 - E) + g_2^2 (m_1 - E)]^2} \,. \tag{20}$$

Here we are dealing with divergent quantities. Therefore, double care is necessary. These are the same as in the original model; the constants in equations (17), (18), (19) are kept finite, also the divergent integrals by cut off at ω; finally $\omega \to + \infty$. But then one has to treat the cases separately.

In case i.b)

$$B_j = \frac{g_i^2}{(g_1^2 + g_2^2)^2} = g_i^2 \left(b - \int \frac{k^2 \, \mathrm{d}k}{2 \omega^3} \right).$$

Therefore, $|\alpha_i|^2$ vanishes if $g_i^2 = 0$; i.e. from the beginning there is no interaction at all with one of the particles. For case ii.a)

$$B_j = \frac{g_i^2 (m_j - E)^2}{g_1^4 (m_2 - m_1)^2} = c^2 g_i^2 (m_j - E)^2 .$$

From (18)

$$m_i = \frac{1}{2c} \left(- b + \frac{1}{g_i^2} + \int \frac{k^2 \, \mathrm{d}k}{2 \omega^3} \right),$$

$$\frac{1}{g_1^4} = \frac{1}{g_2^4} = \left(- b + \int \frac{k^2 \, \mathrm{d}k}{2 \omega^3} \right) - 4c \left(a - \int \frac{k^2 \, \mathrm{d}k}{2 \omega^2} \right),$$

therefore from $c = 0$, $|\alpha_i|^2$ vanishes for the particle with $g_i^2 \geq 0$. That is, the remaining one has to be quantized with indefinite metric.

For the last case, from (19)

$$g_1^2 = \frac{1 \pm \sqrt{1 - AD}}{2G} , \quad g_2^2 = \frac{1 \mp \sqrt{1 - AD}}{2G} ,$$

$$m_1 - m_2 = \frac{1}{G} \left(a - \int \frac{k^2 \, \mathrm{d}k}{2 \omega^2} \right) - E_0 ,$$

$$D = \frac{4}{(m_1 - m_2)^2 \, G} , \quad G = b - \int \frac{k^2 \, \mathrm{d}k}{2 \omega^3} .$$

Then $A = 0$ leads to a particular g_i, let us say g_2, equal to zero, $|\alpha_2|^2 = 0$ as in the first case.

4. We have seen that the original Lee model without cut off can be generalized to the case of two V particles. The theory requires quantization with indefinite metric. Case i.a) is quite different from the Lee model; $m_1 = m_2$,

$g_1^2 \neq -g_2^2$ reproduces the results of the original model without requiring the condition

$$|\alpha_i(E_j)|^2 = |<0|\psi_{v_i}|E_j>|^2 = 0, \qquad j = 1, 2. \tag{21}$$

When (21) is required g_i must be zero. $m_1 \neq m_2$, $g_1^2 = -g_2^2$, $c = 0$ and $m_1 \neq m_2$, $g_1^2 \neq -g_2^2$, $A = 0$ correspond to the Lee model. In the first case $g_i^2 \neq 0$ at the beginning, in the second case one of the g_i is equal to zero giving $|\alpha_i(E_j)|^2 = 0$ for one i and all j in both cases.

It is interesting to notice the various behaviours of the different variants of the extended model. It can also be seen that the most general case (19) with its three real particle states can be produced from an appropriate model with three free V fields.

REFERENCES

1. K. KANG, Nuovo Cimento, **49A**, 415, 1967.
   K. HAYASHY et al., Fortsch. d. Phys., **15**, 625, 1967
   K. HAYASHY et al., Nuovo Cimento, **57A** 746, 1968.
2. K. L. NAGY, Acta Phys. Hung., **24** 433, 1968.
3. P. K. SRIVASTAVA, Phys. Rev., **128**, 2906, 1962.
4. H. YABUKI, Progr. Theor. Phys., **35**, 889, 1966.
5. W. HEISENBERG, Nuclear Physics, **4**, 532, 1957.
6. K. L. NAGY, Nuovo Cimento, **17**, 384, 1960.

МОДЕЛЬ ЛИ КАК Z-ПРЕДЕЛ

К. Л. НАДЬ

Р е з ю м е

Исследуются пределы в общей модели Ли без отреза, которые воспроизведут случай, элементарный + составной частицы, найденный в оригинальной модели.

Acta Physica Academiae Scientiarum Hungaricae, Tomus 27, pp. 261—268 (1969)

IS POINCARÉ INVARIANCE COMPATIBLE WITH GENERAL RELATIVITY?*

By

M. SÜVEGES

RESEARCH GROUP FOR THEORETICAL PHYSICS OF THE HUNGARIAN ACADEMY OF SCIENCES
BUDAPEST

(Received 3. II. 1969)

We have shown previously that an invariance principle is defined in curved space by invariance under the Brandt groupoid consisting of elements given by parallel displacements along all possible curves in space-time. It is argued here that the Brandt groupoid might contain the Poincaré group as a local group in each tangent space but then space-time must have non-vanishing torsion. Such a conclusion might also be implied by recent measurements of SADEH et al. For an Einstein manifold, on the other hand, the Brandt groupoid contains only the homogeneous Lorentz group.

1. Introduction

SADEH, KNOWLES and YAPLEE [1,2] observed an anomalous decrease of frequency in the 21 cm absorbtion line from Taurus A. They also found the effect when a terrestrial source was used and they found the decrease roughly proportional to distance. This decrease cannot be accounted for by general relativity and in a recent paper SZEKERES [3] argues this indicates that space-time is not Einstein—Riemannian (a space with a symmetric metric and symmetric connection). He assumes a linear connection with non-vanishing torsion and calculates the contribution of the torsion part to the shift of frequency and finds it in agreement with the observations of SADEH et al. He therefore concludes that these measurements do suggest a physical space-time of non-vanishing torsion.

In this paper, while we do not argue with his physical interpretation of the torsion tensor, we want to point out that a similar conclusion is already implied by our previous work, though in an indirect way. More precisely, our previous results imply that either the Poincaré group is a good local symmetry group and then space-time has torsion or general relativity holds (no torsion) and then the local invariance group is the homogeneous Lorentz group without translations.

In our earlier papers we made an attempt to introduce an invariance principle in curved space-time. The first thing in such an attempt is to face

* Dedicated to Prof. P. GOMBÁS on his 60th birthday.

the fact that there are only local inertial systems, namely the geodesic systems at each point x. We assumed that these local inertial systems are still physically completely equivalent and then determined the invariance transformations connecting them. Let T_x and T_y denote ennuples of unit vectors in the local inertial systems, the geodesic systems, introduced at space-time points x and y, respectively. Then one of our main results is as follows [4]. The invariance transformations mapping T_x into T_y are defined by Levi-Civita parallel displacement along all possible curves connecting x and y. Different experimental consequences of this invariance have been worked out [4, 5, 6]. For example it has been shown that the three experimental tests of general relativity follow.

Consider now the set $B(x, y)$ of transformations defined by parallel displacement along all possible oriented curves connecting x and y and denote by B the set as x and y run through all points of space-time. There is nothing that would distinguish one space-time point among the others, therefore each element of the set B is an invariance transformation. Therefore the set B defines an invariance principle in curved space and an important problem is then what is the structure of B. Clearly it cannot be a group but one can show [7] that it is a Brandt groupoid.

The fundamental fact in our present argument is that the Lorentz group is contained in the groupoid B as a subset working in each tangent space T_x, it is indeed the holonomy group ψ_x, defined by parallel displacement along all possible closed curves through x of the underlying space-time manifold, discussed extensively [5, 10]. Indeed, the identity component* of the holonomy group (hg) is the six-dimensional homogeneous Lorentz group for a non-vacuum Einstein manifold. However, the Poincaré group P can never be realised as the hg of an Einstein manifold since the hg associated with a symmetric connection is always homogeneous.

Now it is known that the hg associated with a linear, non-symmetric, connection is inhomogeneous and therefore the Poincaré group could be interpreted as a local invariance group in such a space.

However, our invariance principle in curved space is defined by the Brandt groupoid B which is an object more general than a group. To see the intimate relationship between measurements of the red-shift type and local invariance groups, such as the Lorentz, or Poincaré, group we first give in Section 3 a remarkable decomposition theorem for the groupoid B.

* It can be shown [10] that the existence of inversions in ψ_x depends on the topological properties of space-time. Introduce topology by defining space-time to be a differentiable manifold M_n. Let π_1 be the first homotopy group of M_n and ψ_x^0 the identity component of ψ_x. Then one can prove [10] that the homomorphism $\pi_1 \to \psi_x/\psi_x^0$ exists and the problem of the existence of inversions is therefore reduced to the computation of π_1.

2. The Brandt groupoid

A Brandt groupoid [8] (also [9], p. 121) is a set G of elements in which the product exists only for certain pairs and which satisfies the following conditions.

I. If for three elements a, b, c, $\in$, G the relation

$$ab = c$$

holds, then each of them is uniquely determined by the other two.

II. If ab and bc exist then there exist also $(ab)c$ and $a(bc)$, if ab and $(ab)c$ exist, then there exist also bc and $a(bc)$, if bc and $a(bc)$ exist, then there exist also ab and $(ab)c$. In all three cases the equality

$$(ab)c = a(bc)$$

holds.

III. For every element $b \in G$ there exists a uniquely determined element $i(b)$, the right unit, a uniquely determined element $i'(b)$, the left unit, and a uniquely determined inverse element b^{-1} such that

$$bi(b) = i'(b)b = b,$$

$$b^{-1}b = i, \; bb^{-1} = i'.$$

IV. For any two units i and i' there exists at least one element $b \in G$ such that i is the right unit and i' is the left unit of b.

It is easy to see that our set B of invariance transformations defined by parallel displacements satisfies these axioms. Indeed, for any parametrised curve $x^\alpha = x^\alpha(t)$, the equations

$$\frac{du^\alpha}{dt} = \omega^\alpha_\beta(t)\, u^\beta, \tag{1}$$

where $\omega^\alpha_\beta(t) = -\left\{{\alpha \atop \beta\gamma}\right\} \mathrm{d}x^\gamma/\mathrm{d}t$, have a unique set of solutions of the form [7, 11]

$$u^\alpha(t) = b^\alpha_\beta(t, t_0)\, u^\beta(t_0), \tag{2}$$

where the matrices b^α_β are non-singular (at least under the conditions discussed below). This defines a linear homogeneous isometry $u(t_0) \to u(t)$ from the tangent space at $x(t_0)$ to that at $x(t)$. The matrices also satisfy [11]

$$\left.\begin{aligned} b^\alpha_\beta(t, t')\, b^\beta_\gamma(t', t'') &= b^\alpha_\gamma(t, t'') \\ b^\alpha_\beta(t, t')\, b^\beta_\gamma(t', t) &= \delta^\alpha_\gamma. \end{aligned}\right\} \tag{3}$$

Denote now by $b(t_y,t_x)$ any curve with parameter t connecting x and y and denote the matrix (2) defined by the curve also by the same symbol $b(t_y,t_x)$.

Elements of the groupoid B are of the form $b(t_y,t_x)$ (we use matrix notation) for the oriented curves from x to y, in this order, as x and y run through all points. Define multiplication in B as: Two elements $b(t_x, t_z)$ and $b(t_\omega, t_y)$ can be multiplied, in this order, if $z = \omega$ and only in this case and the product is then given by the appropriate form of Equs.(3). The set B with this multiplication is clearly a Brandt groupoid.

Indeed, consider first Condition IV. Our transformations (2) defined by Equs. (1) are determined by the Christoffel symbols, which in turn are functions of the metric tensor and its derivatives. IV thus implies that a continuous metric tensor must exist everywhere. It was pointed out [10] that topological properties must be introduced into the definition of space-time. One way to do this is to suppose [10] space-time to be a differentiable manifold M_n. Now a differentiable manifold always admits a positive definite metric tensor, but admits a continuous metric tensor of signature (3,1) if and only if the Euler—Poincaré characteristic $\chi = \sum_k (-1)^k v_k$, where v_k is the *kth* Betti number, vanishes ([12],p. 18). In this case then the matrix in Equ. (2) is non-singular.

Condition II is trivially satisfied and the non-singular nature of $[b(t_y,t_x)]$ ensures I. III is also satisfied: For any element $b(t_x,t_y)$ the left and right units $b(t_x,t_x)$ and $b(t_y,t_y)$, the (unit) matrices associated with the points x and y, respectively, and the inverse $b^{-1}(t_x,t_y) = b(t_y,t_x)$ associated with the inversely oriented curve, clearly exist. This proves the groupoid nature of B under the above restriction.

3. Direct product decomposition of the groupoid

We now construct two subsets of B and then show that B is the direct product of these.

It is clear from axioms I to IV that the condition for B to be a group is that it should contain a single unit element. Therefore B can never be group in curved space, nevertheless it contains groups.

Consider indeed the subset of all those elements b for which the left and right units coincide $i(b) = i'(b) = i_x$. It is clear from the axioms that this set is a group consisting of the elements defined by transformations along all closed curves through the point x. It is indeed the holonomy group $\psi_x(M_n)$ at x discussed extensively [5,10].

We now construct another subset of B as follows. Take the right and left unit elements $i(x)$ and $i'(y)$ at two arbitrary but fixed points x and y, in this

order, and connect x and y by a single, but arbitrarily chosen, curve $b(y,x)$. Denote the transformation along the curve also by the same symbol $b(y,x) \in B$. When x and y run through all points of M_n we obtain a subset S_b of B which is also a groupoid. Since S_b has the same set of units as B it is a subgroupoid of B and it is also clear from the construction that this is the minimal subgroupoid which has the same set of units as B.

If we connect x and y with any different but well defined curve $c(y,x)$ we get another subgroupoid S_c which is isomorphic with S_b since they have the same set of units.

Let us now fix S_b and let $x \in M_n$ be any arbitrary but fixed point. We want to prove that $B = S_b \otimes \psi_x(M_n)$ where $\otimes$ is direct product.

To this end we first remark that any arbitrary element $t(z, y)$ of B can be written as the product $b(z,x)a(x)b(x,y)$, where $a(x) \in \psi_x$ and $b(z,x)$, $b(x,y) \in S_b$, in a unique way. To see that this is so one has only to choose $a(x) = b^{-1}(z,x)t(z,y)b^{-1}(x,y)$ which is clearly a transformation defined by the closed loop $b^{-1}(z,x)t(z,y)b^{-1}(x,y)$ through x.

Let now $t(v,\omega) = b(v,x)a'(x)b(x,\omega)$, where $a'(x) \in \psi_x$ and $b(v,x)$, $b(x,\omega) \in S_b$, be the above product decomposition of any other arbitrary element $t(v, \omega)$ of B. Then the product $t(v, \omega)t(z,y)$ exists only if $\omega = z$ and it is in this case $t(v,y) = b(v,x)\ a'(x)a(x)\ b(x,y)$.

This shows that in the product of arbitrary elements $t(v,\omega)$ and $t(z,y)$ of B, elements of S_b and elements of ψ_x are multiplied separately. In other words we have

$$B = S_b \otimes \psi_x(M_n)\,. \tag{4}$$

4. Local groups

We are now able to discuss the problem put forward in the Introduction. In our effort to introduce an invariance principle in curved space the starting point was [4] the problem of how to compare physical quantities in the (inertial) tangent spaces at different space-time points. We have seen that we can compare physical quantities by means of the transformations contained in the groupoid B.

Obviously, the decomposition (4) classifies physical measurements into two classes:

a) local measurements, in which quantities in the same tangent space T_x are compared, can be evaluated by the local invariance group ψ_x,

b) measurements, in which quantities in the tangent spaces at different space-time points are compared, can be evaluated by elements of the minimal sub-groupoid S_b.

Supposing now general relativity, the three crucial tests fall into class b). Red shift between any x and y has been shown [4,6] to follow from invarianc under parallel displacement along any curve connecting x and y, i.e. from invariance under an element of S_b. Also, if one chooses geodesics for elements of S_b then the geodesic axioms follow.

As to class a) it is well known that the holonomy group ψ_x is subgroup of the homogeneous Lorentz group for an Einstein manifold and the Lie-algebra of ψ_x, which defines local invariance in the tangent space T_x, is spanned [13] by the $\overset{\varkappa}{\lambda}$-domains of the curvature tensor and its covariant derivatives

$$p^\alpha q^\beta R^\varkappa_{\alpha\beta\lambda}, q^\omega \nabla_\omega p^\alpha q^\beta R^\varkappa_{\alpha\beta\lambda}, \ldots, (q^\omega \nabla_\omega)^k p^\alpha q^\beta R^\varkappa_{\alpha\beta\lambda}, \tag{5}$$

where the arbitrary vectors p,q and the curvature tensor R and its covariant derivatives are to be understood at x.

It is seen from expression (5) that ψ_x is reduced to the identity for a flat manifold. We have on the other hand the important theorem of BEIGLBÖCH [14], which says that the Lie-algebra of ψ_x is always six-dimensional for a non-vacuum Einstein manifold. Therefore the restricted Lorentz group $L^\uparrow_+$ (for inversions see [10] and also the footnote on p. 262) can be interpreted as a local property of a non-vacuum Einstein manifold. However, the local invariance group $\psi_x(M_n)$ is always homogeneous for an Einstein manifold. This follows from the fact that the hg associated with a symmetric connection is homogeneous. This is an unpleasant feature of local invariance since translation invariance has deep physical consequences and there is therefore interest in more general spaces for which the hg is non-homogeneous.

Maybe the simplest such generalization is in which the Chistoffel symbols are replaced by a non-symmetric connection $\Gamma^\varrho_{\mu\nu}$. It is indeed well known that the hg associated with such a connection is non-homogeneous and the infinitesimal translations at x are generated by expressions of the form ([13] p. 362)

$$- T^k_{\mu\nu} df^{\mu\nu}, \tag{6}$$

where $df^{\mu\nu}$ is an infinitesimal facet at x and $T^k_{\mu\nu} = \Gamma^k_{\mu\nu} - \left\{{k \atop \mu\nu}\right\}$ is the torsion tensor.

Consider now the set B' (Section 2) of invariance transformations defined by parallel displacement associated with this new connection. B' is again a Brandt groupoid and the decomposition of Section 3 also holds. In this way the Poincaré group might be obtained, just as $L^\uparrow_+$ has been in the case of an Einstein manifold, as the hg of this generalized space.

Suppose now that the Poincaré group is a local invariance group. Then if our invariance principle, i.e. invariance under the Brandt groupoid, is valid, then invariance, in measurements of class b), under S'_b must also hold as can be seen from the decomposition (4). But this is just the interpretation of SZEKERES of the anomalous frequency shift found by SADEH et al.

Clearly, the measurements of SADEH et al. belong to class b) and what SZEKERES calculates is just the contribution to parallel displacement of the non-symmetric part of the connection when S'_b is constructed from geodesics.

We do not want here to argue about the physical interpretation of the torsion tensor, only want to point out that, if the Poincaré group is to be interpreted as a local invariance group in a curved space, then a non-vanishing torsion tensor must be involved.

5. Discussion

Recent cosmological observations seem to confirm that physical space-time is curved. The Lorentz, or the Poincaré group cannot then be interpreted as the motion group of that space. In a curved space we have only local inertial systems and in this case the considerations of this, and previous papers (see the Introduction) are relevant. We want here to emphasise that our basic assumption is that these local systems are still physically equivalent. At the basis of this assumption is really the Eötvös experiment. The choice of the connection, which defines the invariance transformations connecting these systems, is a matter of experiment.

Once, however, a particular connection is selected then the structure of, for example, the local invariance group is determined. In particular the argument presented here suggests that either general relativity holds and then the local invariance group is only the homogeneous Lorentz group in each tangent space, or the Poincaré group is good and then the underlying space-time manifold has non-vanishing torsion.

In conclusion it must be emphasized that our full invariance principle is defined not by a group but a Brandt groupoid which is a more general object.

REFERENCES

1. D. SADEH, S. H. KNOWLES and B. S. YAPLEE, Science, **159,** 307, 1968.
2. D. SADEH, S. H. KNOWLES and B. AU, Science, **161,** 567, 1968.
3. G. SZEKERES, Nature, **220,** 1116, 1968.
4. M. SÜVEGES, Acta Phys. Hung., **20,** 41, 1966.
5. M. SÜVEGES, Acta Phys. Hung., **20,** 51 1966.
6. M. SÜVEGES, Phys. Letters, **20,** 265, 1966.
7. M. SÜVEGES, (to be published).
8. H. BRANDT, Math. Ann., **96,** 36, 1926.
9. O. BORUVKA, Grundlagen der Gruppoid und Gruppentheorie, VEB Deutscher Verlag der Wissenschaften, Berlin, 1960.
10. M. SÜVEGES, Acta Phys. Hung., **20,** 273, 1966.
11. O. VEBLEN and J. H. C. WHITEHEAD, The Foundations of Differential Geometry, Chapt. V, The University Press, Cambridge, 1953.
12. A. LICHNEROWICZ, Théorie globales des connections et des groupes d'holonomie, Edizioni Cremonese, Roma, 1962.
13. J. A. SCHOUTEN, Ricci-Calculus Chap. VII., Springer-Verlag, Berlin, Göttingen, Heidelberg, 1954.
14. W. BEIGLBÖCK, Z. Physik, **179,** 148, 1964.

ИНВАРИАНТНОСТЬ ПУАНКАРЕ СОВМЕСТИМА С ОБЩЕЙ ТЕОРИЕЙ ОТНОСИТЕЛЬНОСТИ?

М. ШЮВЕГЕШ

Р е з ю м е

Предварительно показали, что определен инвариантный принцип в искривленном пространстве инвариантностью по отношению группоиде Брандта, состоящего из элементов, данных параллельными смещениями по всем возможным кривым в пространстве времени. Доказывается, что группоид Брандта может содержать группу Пуанкаре как локальную группу в каждом тангенциальном пространстве, но в этом случае пространство-время должно иметь неисчезающую крутизну Такое условие может быть применено и современными измерениями Саде и др. С другой стороны, в случае одного множества Эйнштейна группоид Брандта содержит только однородную группу Лоренца.

Acta Physica Academiae Scientiarum Hungaricae, Tomus 27, pp. 269—276 (1969)

SMALL AMPLITUDE WAVES AND WEAK DISCONTINUITIES IN THE RELATIVISTIC HYDRODYNAMICS OF AN IDEAL FLUID*

By

I. ABONYI

INSTITUTE OF THEORETICAL PHYSICS, ROLAND EÖTVÖS UNIVERSITY, BUDAPEST

(Received 7. II. 1969)

Waves of small amplitude and the propagation of the surfaces of weak discontinuity (jumping derivatives) are studied in relativistic fluid dynamics. It is shown that in analogy with classical fluid dynamics, small amplitude waves and weak discontinuities have similar character. Both small amplitude waves, and surfaces of weak discontinuity are propagated with the velocity of sound, which, however, contains a relativistic correction.

1. Introduction — Basic assumptions

In this paper we consider a relativistic ideal fluid. The equation of state of a simple one component fluid can be written in the form

$$\mu^0 = \mu^0(p, s), \tag{1}$$

where μ^0 is mass of the fluid in unit co-moving volume, p is the pressure, s is the entropy of the fluid in unit co-moving volume.

It is required that the equation of state should be valid following the motion of the volume element

$$u_k \partial_k \mu^0 = \left(\frac{\partial \mu^0}{\partial p}\right)_s u_k \partial_k p + \left(\frac{\partial u^0}{\partial s}\right)_p u_k \partial_k s . \tag{2}$$

Here u_k stands for the four vector velocity of the fluid and ∂_k denotes the four vector gradient. (Summation convention is understood for doubly occurring Latin indices, with $x_4 = ic$.)

As is well known, the energy-momentum tensor T_{ik} of an ideal fluid has the form

$$T_{ik} = \frac{1}{c^2}(\varepsilon + p) u_i u_k + p\delta_{ik}, \tag{3}$$

* Dedicated to Prof. P. GOMBÁS on his 60th birthday.

where ε is the energy of the fluid in unit co-moving volume. We may define the mass density

$$\mu = \frac{1}{c^2}(\varepsilon + p) \tag{4}$$

the mass equivalent of all energies in a unit co-moving volume. This, clearly, differs from μ^0, since ε may be decomposed to give

$$\frac{\varepsilon}{c^2} = \mu^0 + \frac{1}{c^2}\mu^0 \varepsilon^0, \tag{5}$$

where μ^0 stands for the rest mass density, while ε^0 is the specific internal energy of the fluid.

So we shall write

$$\mu = \mu^0\left(1 + \frac{\varepsilon^0}{c^2} + \frac{p}{\mu^0 c^2}\right) = \mu^0 v = \mu^0\left(1 + \frac{1}{c^2}w\right), \tag{6}$$

where the symbol v is the so called "index" of the fluid, and w stands for the specific enthalpy.

Then, the energy momentum tensor is

$$T_{ik} = \mu^0 v u_i u_k + \delta_{ik} p, \tag{7}$$

and the equations of motion of the fluid are

$$\partial_k T_{ik} = 0. \tag{8}$$

We have to assure the interpretation of u_i as a velocity four vector therefore

$$u_k u_k = -c^2 \tag{9}$$

and the conservation of the number of particles

$$\partial_k(\mu^0 u_k) = 0. \tag{10}$$

From equations (8), (9) and (10) it is easy to deduce by means of the thermodynamic relation

$$dw = \frac{1}{\mu^0} dp = T ds, \tag{11}$$

that the motion of the fluid is isentropic, namely

$$u_k \partial_k s = 0. \tag{12}$$

So the equation of state (2) takes the simpler *barotropic* form: $\mu^0 = \mu^0(p)$, i.e.:

$$u_k \partial_k \mu^0 - a^2 u_k \partial_k p = 0 , \tag{13}$$

where

$$a^2 = \left(\frac{\partial u^0}{\partial p} \right) .$$

Then the basic equations of the simple one-component relativistic fluid are:

$$\left.\begin{array}{l} \mu^0 u_k \partial_k (v u_i) + \partial_i p = 0 \\ \partial_k (\mu^0 u_k) = 0 \\ u_k u_k = - c^2 \\ u_k \partial_k \mu^0 - a^2 u_k \partial_k p = 0 \end{array}\right\} . \tag{14}$$

There are seven equations for seven variables (u_k, p, μ^0 and v). We stress that p, μ^0 and v are invariant scalars with respect to Lorentz-transformations.

In this treatment the fluid is assumed to have an infinite extent to avoid, for the time being, boundary condition problems.

2. Small amplitude waves

It can be seen that the basic equations (14) are solved by the system of variables

$$\left\{\begin{array}{c} u_k \\ p \\ \mu^0 \\ v \end{array}\right\} = \text{constants in space and time,}$$

if u_k is chosen so as to obey (9). We then superpose small perturbations of the form

$$\left\{\begin{array}{c} \delta \bar{u}_k \\ \delta \bar{p} \\ \delta \bar{\mu}^0 \\ \delta \bar{v} \end{array}\right\} = \left\{\begin{array}{c} \delta u_k \\ \delta p \\ \delta \mu^0 \\ \delta v \end{array}\right\} \exp \; i k_r x_r , \tag{15}$$

where the amplitudes (δu_k, δp, $\delta \mu^0$, δv) are small quantities of the first order, and any term containing at least two first order factors will be omitted. Then the equations of motion will be

$$\begin{aligned} &\mu^0 u_k \partial_k (v \, \delta \bar{u}_k + u_i \, \delta \bar{v}) + \partial_i \, \delta \bar{p} = 0 , \\ &\partial_k (\mu^0 \, \delta \bar{u}_k + u_k \, \delta \, \bar{\mu}^0) = 0 , \\ &(u_k + \delta \bar{u}_k)(u_k + \delta \bar{u}_k) = - c^2 , \\ &u_k \partial_k \, \delta \bar{\mu}^0 - a^2 u_k \partial_k \, \delta \bar{p} = 0 . \end{aligned}$$

In such a way we arrive at a set of linear algebraic equations, namely:

$$\left.\begin{aligned} &u_i\,\mu^0\,L\,\delta v + \mu^0\,v\,L\,\delta u_i + k_i\,\delta p = 0\,,\\ &L\,\delta\mu^0 + \mu^0\,k_r\,\delta u_r = 0\,,\\ &u_r\,\delta u_r = 0,\\ &L\,\delta\mu^0 - a^2\,L\,\delta p = 0\,. \end{aligned}\right\} \tag{16}$$

Here $L = u_r k_r$. The existence of a nontrivial solution for the amplitudes $(\delta u_k,\ \delta p,\ \delta\mu^0,\ \delta v)$ is guaranteed by the vanishing of the determinant

$$D = \begin{vmatrix} \mu^0 Lv & 0 & 0 & 0 & \mu^0 Lu_1 & 0 & k_1 \\ 0 & \mu^0 Lv & 0 & 0 & \mu^0 Lu_2 & 0 & k_2 \\ 0 & 0 & \mu^0 Lv & 0 & \mu^0 Lu_3 & 0 & k_3 \\ 0 & 0 & 0 & \mu^0 Lv & \mu^0 Lu_4 & 0 & k_4 \\ \mu^0 k_1 & \mu^0 k_2 & \mu^0 k_3 & \mu^0 k_4 & 0 & L & 0 \\ u_1 & u_2 & u_3 & u_4 & 0 & 0 & 0 \\ 0 & 0 & 0 & 0 & 0 & L & -a^2 L \end{vmatrix} = 0. \tag{17}$$

This requirement gives

$$D = \mu^{05}\,v^4\,L^4\left\{L^2\,(a^2\,c^2\,v - 1) - c^2\,k_r\,k_r\right\} = 0\,, \tag{18}$$

which is a relation between k_r and the properties of the fluid. Therefore, it can be envisaged as the dispersion relation of small amplitude waves. The system (15) can be a wave solution to the linearized basic equations (14) if and only if k_r is chosen so as to satisfy (18).

There are two possibilities. The first where $L \neq 0$, is

$$L^2 = (1 - a^2\,c^2\,v)^{-1}\,c^2\,k_r\,k_r\,,$$

i.e.

$$(u_r\,k_r)^2\,(a^2\,c^2\,v - 1) - c^2\,k_r\,k_r = 0 \tag{19}$$

which, for the co-moving system of reference, where

$$u_r = \{0, 0, 0, ic\}\,,\quad k_r = \left\{k_1, k_2, k_3, \frac{i}{c}\,\omega\right\}$$

gives

$$V^2 \equiv \left(\frac{\omega}{k}\right)^2 = a^{-2}\,\frac{1}{v} = a^{-2}\,\frac{\mu^0}{\mu} \tag{20}$$

for the square of the phase velocity V of the wave with respect to the fluid. Since a is the reciprocal of the classical velocity of sound c_s, we have

$$V^2 = c_s \left(1 + \frac{\varepsilon^0}{\mu^0 c^2} + \frac{p}{\mu^0 c^2}\right)^{-1}. \tag{21}$$

This corresponds to the sound wave in the classical limit.

The other possibility is that

$$L = 0$$

which means that in the co-moving frame $\omega = 0$, therefore

$$V^* = \frac{\omega}{k} = 0\,; \tag{22}$$

this perturbation does not propagate with respect to the fluid.

In the first case equations (16) yield

$$\left.\begin{aligned} &k_r\,\delta u_r = -\frac{1}{L}\,\delta\mu^0, \quad \delta u_i = -\frac{a^{-2}}{\mu^0 vL}\left\{k_i + \frac{L}{c^2}\,u_i\right\}\delta\mu^0\,, \\ &\delta v = (\mu^0 c^2 a^2)^{-1}\,\delta\mu^0, \quad \delta p = a^{-2}\,\delta\mu^0\,, \end{aligned}\right\} \tag{23a}$$

the amplitudes of the longitudinal velocity perturbation, the "index" and pressure perturbations can be given in terms of the density perturbation $\delta\mu^0$. Therefore $\delta\mu^0$ must be different from zero, otherwise this type of small amplitude wave cannot exist.

In the second case, because $L = 0$, after some manipulations we obtain from (16)

$$\left.\begin{aligned} &k_r\,\delta u_r = 0, \quad \delta u_i = 0\,, \\ &\delta p = 0, \\ &\delta v = 0\,, \\ &\delta\mu^0 = \text{arbitrary}\,. \end{aligned}\right\} \tag{23b}$$

Because of (22), we may realize this perturbation as a stratification in the fluid which is immobile with respect to the fluid, and since now $\delta\mu^0$ is the only variable of the entropy, the stratification causes an immobile variation of entropy which does not propagate with respect to the fluid (entropy wave). And since the fluid is an ideal one, this stratification of entropy can move only together with the fluid.

3. Weak discontinuities

When the hydrodynamic quantities (u^k, p, μ^0, v) themselves are continuous, but their derivatives have jumps along a surface, we speak of that surface as a surface of weak discontinuity.

Let us denote by

$$f(x_1, x_2, x_3, x_4) = 0$$

the equation of the surface, across which the derivatives of the hydrodynamic quantities are not continuous.

The unit normal to this hypersurface has the components

$$N_k = \frac{\partial_k f}{(\partial_r f \partial_r f)^{1/2}}$$

and following [1, 2] we use $V = cU$ as the velocity of the hypersurface along its normal, with the definition

$$1 - U^2 = \frac{\sum_1^4 g_{rs} \partial_r f \partial_s f}{\sum_1^3 a_{\varrho\sigma} \partial_\varrho f \partial_\sigma f},$$

where g_{rs} is the four dimensional metric tensor, while $a_{\sigma\tau}$ is the three dimensional one. So

$$N_4 = \frac{-iU}{[1 - U^2]^{1/2}}. \tag{24}$$

It is obvious tat einhther the phase velocity of small amplitude waves, nor the velocity of this surface is a covariant notion.

By definition, the discontinuities along the surface in question of the hydrodynamical quantity F can be written in the form

$$[\partial_S F] = N_S \delta F,$$

where the difference

$$[\partial_S F] = \lim_{\rightarrow} \partial_S F - \lim_{\leftarrow} \partial_S F$$

involves the limits taken on the different sides of the hypersurfaces, and δF represents the jump of $\partial_s F$.

Effecting the limiting processes we obtain from the basic equations:

$$\left.\begin{aligned} &\mu^0 u_i \Lambda\delta v + \mu^0 v \Lambda\delta u_i + N_i \delta p = 0 \\ &\mu^0 N_k \delta u_k + \Lambda\delta\mu^0 = 0 \\ &u_k \delta u_k = 0 \\ &\Lambda\delta\mu^0 - a^2 \Lambda \delta p = 0 \end{aligned}\right\}, \tag{25}$$

where

$$\Lambda = u_k N_k .$$

The (25) is a homogeneous linear system of seven algebraic equations for seven unknowns, the condition of the existence of a nontrivial solution is that the determinant

$$\Delta = \begin{vmatrix} \mu^0 \Lambda v & 0 & 0 & 0 & \mu^0 \Lambda u_1 & 0 & N_1 \\ 0 & \mu^0 \Lambda v & 0 & 0 & \mu^0 \Lambda u_2 & 0 & N_2 \\ 0 & 0 & \mu^0 \Lambda v & 0 & \mu^0 \Lambda u_3 & 0 & N_3 \\ 0 & 0 & 0 & \mu^0 \Lambda v & \mu^0 \Lambda u_4 & 0 & N_4 \\ \mu^0 N_1 & \mu^0 N_2 & \mu^0 N_3 & \mu^0 N_4 & 0 & \Lambda & 0 \\ u_1 & u_2 & u_3 & u_4 & 0 & 0 & 0 \\ 0 & 0 & 0 & 0 & 0 & \Lambda & -a^2 \Lambda \end{vmatrix} = 0,$$

which has the same structure as (17). This requirement gives

$$\Delta = \mu^{05} v^4 \Lambda^4 \left\{\Lambda^2 (a^2 c^2 v - 1) - c^2 N_r N_r\right\} = 0 .$$

There are two possibilities again. First let us take $\Lambda \neq 0$, then

$$\Lambda^2 = c^2 (1 - a^2 c^2 v)$$

and we obtain in the co-moving system

$$U^2 = \frac{1}{a^2 v} = c_s^2 \frac{\mu^0}{\mu} = c_s^2 \left(1 + \frac{\varepsilon^0}{\mu^0 c^2} + \frac{p}{\mu^0 c^2}\right)^{-1},$$

stating that this type of the surface of weak discontinuity propagates with the velocity of sound. In this case the jumps are connected by the relations (23a).

In the second case $\Lambda = 0$, which in the co-moving frame means that the surface does not propagate with respect to the fluid, the jumps are then connected by the relations (23b).

4. Conclusions

We have shown that the velocity of propagation of small amplitude waves is modified in the relativistic case by the presence of a factor

$$\left(1 + \frac{\varepsilon^0}{\mu^0 c^2} + \frac{p}{\mu^0 c^2}\right)^{-1/2}.$$

This means that if the specific internal energy and the pressure of the system is comparable to its rest energy density, the corrective factor may be important. The well known modification of sound velocity [3] because of the extreme relativistic equation of state

$$p = \frac{1}{3} e ,$$

where e means the total energy density of the system makes its important contribution particularly to c_s, and not to the correcting factor.

Finally we have shown that, as in classical hydrodynamics, the surfaces of weak discontinuity propagate with the same velocity as do small amplitude waves, and can be classified in an analogous manner.

REFERENCES

1. A. Lichnerowicz, Théories relativistes de la gravitation et de l'électromagnétisme, Masson Paris 1955.
2. A. C. Giere, Journal of Math. Phys., **7**, 1648, 1966.
3. L. D. Landau and E. M. Lifshitz, Fluid Mechanics, Pergamon Press, 1963.

ВОЛНЫ НЕБОЛЬШИХ АМПЛИТУД И СЛАБЫЕ РАЗРЫВЫ В РЕЛЯТИВИСТИЧЕСКОЙ ГИДРОДИНАМИКЕ ИДЕАЛЬНОЙ ЖИДКОСТИ

И. АБОНИ

Р е з ю м е

Изучаются волны небольших амплитуд и распространение поверхностей слабого разрыва (скачок производных) в релятивистской динамике жидкости. Показывается, что в аналоге с классической динамикой жидкости волны небольшой амплитуды и слабые разрывы имеют подобный характер. Как волны небольшой амплитуды, так и поверхности слабого разрыва распространяются со скоростью звука, которая, однако, содержит релятивистическую поправку.

Acta Physica Academiae Scientiarum Hungaricae, Tomus 27, pp. 277—287 (1969)

STUDY OF V-CENTRES STABLE AT ROOM TEMPERATURE IN NaCl(Ca) CRYSTALS*

By

R. VOSZKA and A. WATTERICH

CRYSTAL PHYSICS RESEARCH LABORATORY OF THE HUNGARIAN ACADEMY OF SCIENCES, BUDAPEST

(Received 7. II. 1969)

Following X-irradiation of OH-free NaCl(Ca) crystals at room temperature, the authors observed new absorption bands at 360, 336 and 193 nm wavelengths, in addition to the V_2 band appearing in pure crystals at 223 nm. These new bands were assigned to V_F, V_1^M and V_2^M centres, respectively.

The M superscript refers to the presence of the divalent metal impurity, thus distinguishing the centres from similar centres in the pure crystal. In the case of X-irradiation at —80°C a new band was observed at 330 nm shown to be due to V_K^M centres. The models of the appearing centres are well-known, except in the case of V_1^M centres for which the authors propose a model.

I. Introduction

In previous papers we investigated the V-type centres created by X-irradiation in the KCl(Ca) system and their conversion [1, 2]. The results obtained in this system were comparatively simple and clear-cut since here only one V-type centre which can be considered stable appears at RT, i.e. the V_2^M centre created by the association of V_K^M centres. But in the case of NaCl(Ca), also according to our previous investigations, we are confronted with a more complicated situation. We had shown e.g. the appearance of V_F centres stable at RT [3], and the NaCl(Ca) system also exhibits a different behaviour concerning ionic conduction, since its conductivity, contrary to the KCl(Ca) system, is decreased by irradiation [4].

The paper gives further data concerning the V-type centres stable at RT appearing in the OH-free NaCl(Ca) system.

II. Experimental method

The crystals were grown free from OH by a method which we developed [5] from starting material purified in our laboratory [6]. 0.1 Mole% $CaCl_2$ was added to the melt; then to reduce the concentration of other impurities it was zone-refined several times. During zone-melting the Ca concentration

* Dedicated to Prof. P. GOMBÁS on his 60th birthday.

did not change considerably since the distribution coefficient of Ca in NaCl is approximately 1. At the final zone-melting a single crystal was grown at a speed of 3 mm/hour. In our experiments we have used the lower 2/3 part of the cylindrical crystal block of 200 mm length and 40 mm diameter. In the middle of the part used the Ca concentration, determined afterwards, was found to be 8×10^{-4} Mole/Mole.

In some of our experiments the OH-free crystals were submitted to subsequent annealing, consisting of keeping them in a furnace at 350°C in air for ~ 10 min, then cooling to RT in a few minutes.

We carried out experiments on crystals air-grown by the Kyropoulos method from reagent grade material some months earlier. In these cases the subsequently determined Ca concentration was 3×10^{-3} Mole/Mole.

The specimens for absorption measurements were cleaved to have a surface of 10×20 mm^2 and a thickness of 0.4—5.0 mm. The measurements were made with a UNICAM SP—700 spectrophotometer, placing a metal cryostat in one of its lightbeams when necessary. X-irradiation was carried out with a THX—250 deeptherapy apparatus at 200 kV, 20 mA using a 3.5 mm Al filter. In these conditions the dose rate was about 2500 R/min. The focussed light of a tungsten lamp was used (0.1 W/cm^2) to illuminate the crystals.

III. Experimental results

III. 1. In Figs. 1 and 2 the absorption spectra of NaCl(Ca) crystals grown OH-free and X-irradiated at RT are shown for increasing doses. From the difference-curves the following facts can be established. In the beginning of colouration (irradiation time less than ~ 1 min, Fig. 1) a well-defined maximum in the UV region appears only at 336 nm growing nearly proportionally with the F band. With increasing dose the maximum at 336 nm approaches saturation and a new band with a maximum at 193 nm begins to develop (curves *b* and *c* of Fig. 2). The 193 nm band lies near to the limit of the measuring range of the SP—700. Therefore, its position was determined with a vacuum monochromator as well. In Fig. 3 it can be seen that the 193 nm band is superposed on the tail of the steeply rising β band.

III. 2. Curve *a* of Fig. 4 shows the absorption spectrum of a crystal X-irradiated at RT, exhibiting the 336 and 193 nm bands in the UV region. Curve *b* was obtained after warming the crystal to 80°C. Under the effect of the few minutes warming the F' band disappears as expected and a slight decrease of the F band takes place. In the course of this process the 336 nm band becomes decomposed and the 193 nm band increases. Afterwards, the crystal was illuminated with white light and its absorption spectrum taken after illumination is shown by curve *c*. The changes in the F band can be

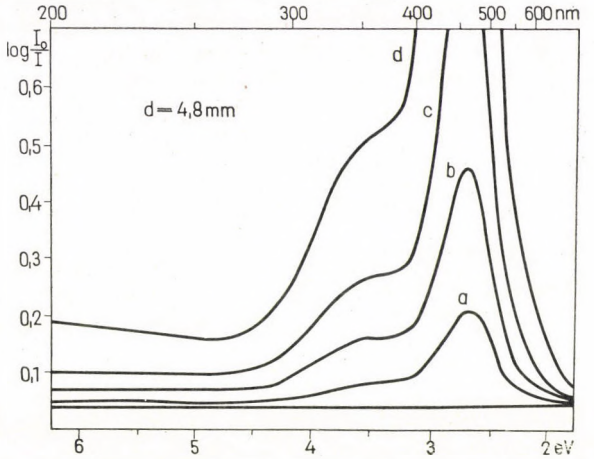

Fig. 1. Absorption spectra of OH-free NaCl(Ca). X-irradiation and measurement at RT. Irradiation times: a) 10 sec b) 30 sec c) 60 sec d) 150 sec

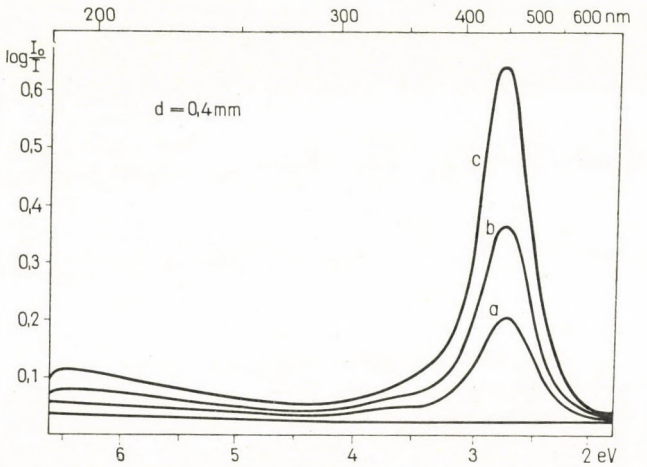

Fig. 2. Absorption spectra of OH-free NaCl(Ca). X-irradiation and measurement at RT. Irradiation times: a) 2 min b) 5 min c) 10 min

explained by bleaching and by $F \rightarrow Z_1$ conversion. Further, the illumination causes a decrease in the 193 nm band and an increase in the 336 nm band.

III. 3. Curve *a* of Fig. 5 was obtained on a crystal grown OH-free and X-irradiated at —80 °C (30 min). Beside the F band (and F') a well-expressed maximum can be seen only at 333 nm. Warming to RT changes the spectrum. Curve *b* was obtained after warming for a few minutes and curve *c* after 40 minutes. A decrease takes place first in the F band maximum and mainly in the vicinity of 330 nm. The maximum of the remaining band lies at 336 nm,

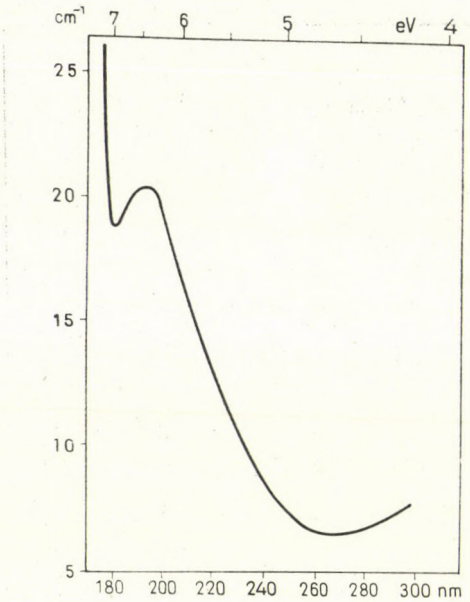

Fig. 3. Absorption spectrum of OH-free NaCl(Ca) in the vacuum UV region. X-irradiation (30 min) at RT, measurement at LNT

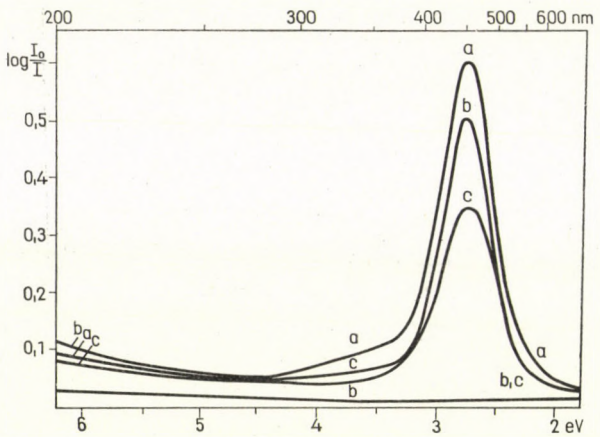

Fig. 4. Absorption spectra of OH-free NaCl(Ca). X-irradiation and measurement at RT. a) immediately after 2 min X-irradiation, b) after a short warming to 80 °C, c) after subsequent illumination with white light

that is, at the wavelength where a maximum also appears in crystals X-irradiated at RT. Keeping the crystal at RT for 40 minutes causes the F' band to disappear and the 336 nm band to decrease. This phenomenon is similar to the previous one observed in crystals X-irradiated at RT and warmed

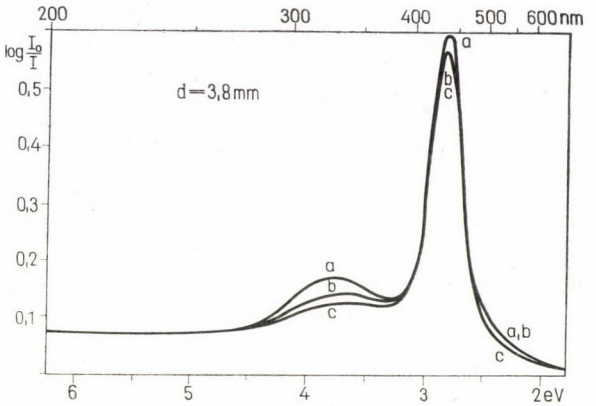

Fig. 5. Absorption spectra of OH-free NaCl(Ca). X-irradiation at —80 °C (30 min.), measurement at LNT, a) immediately after X-irradiation, b) after a short warming to RT, c) after 40 min at RT

to 80 °C. The only difference is that the process takes place faster at 80 °C and after the disappearance of the F' band the conversion of the 336 nm band into the 193 nm band can also be plainly observed.

III. 4. In Fig. 6 the absorption spectrum of a crystal can be seen which was grown OH-free, then annealed and X-irradiated at RT. Evaluation of the curves corresponding to increasing doses reveals that in less colored crystals bands appear at 223 nm and 360 nm and the 193 nm band mentioned above grows considerably only at higher doses. Whether the crystal is kept for a few minutes in air or in an inert atmosphere during annealing does not affect the result. If an annealed crystal is X-irradiated after several days of recovery its behaviour becomes similar to that of an unannealed crystal.

III. 5. Fig. 7 shows the absorption spectra of a NaCl(Ca) crystal grown in the traditional way and X-irradiated at RT for different irradiation doses. First, at a broad maximum, appears 350 nm, then the 193 nm band becomes more and more pronounced. An analysis of the curves shows that the maximum at 350 nm consists of the previously observed 336 nm and 360 bands. According to our result, obtained here too, the 336 nm band decreases at RT mainly together with the F' band, and after the disappearance of the latter the decrease becomes slower.

III. 6. The peak positions and estimated half-widths of the 5 observed bands in the UV region are summarized in Table I. We should like to point out that the exact determination of peak positions in the 300—400 nm range is impossible because of the overlapping of the F band, the comparatively small extinction constants and the great half-widths. The exact data of the 193 nm band, superposed on the tail of the β band similarly cannot be determined. The data are given for LNT but they are not significantly different

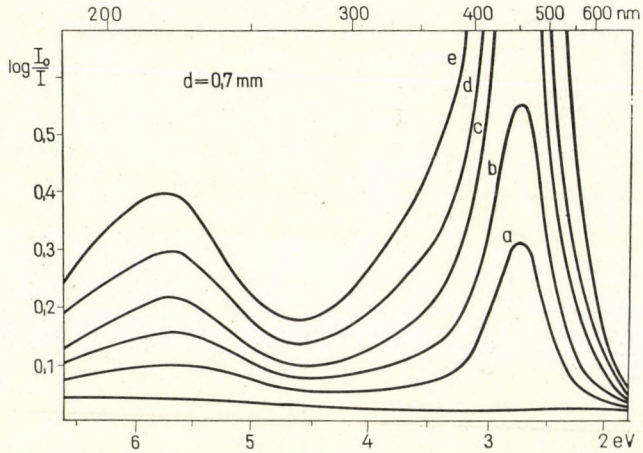

Fig. 6. Absorption spectra of OH-free grown and annealed NaCl(Ca). X-irradiation and measurement at RT. Irradiation times: a) 3 min b) 6 min c) 10 min d) 15 min e) 25 min

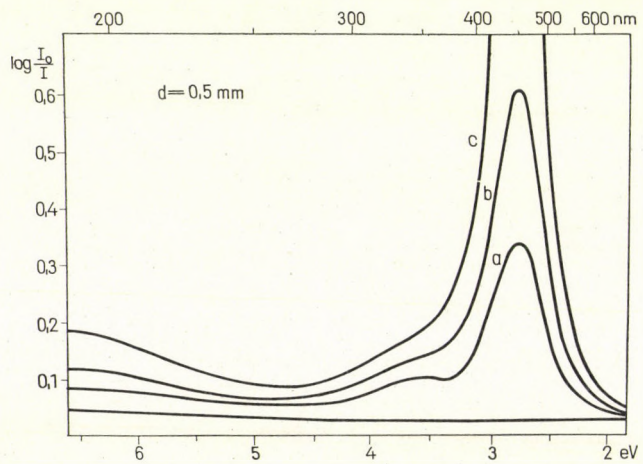

Fig. 7. Absorption spectra of an NaCl(Ca) crystal air-grown by the Kyropoulos method. X irradiation and measurement at RT. Irradiation times: a) 3 min b) 6 min c) 15 min

from RT data which can be explained by the mentioned inaccuracy and by the fact that they change only slightly with temperature.

III. 7. By examining and comparing the absorption and ESR spectra the 330 nm band can be assigned to the V_K^M centres proposed by HAYES and NICHOLS [7] and the 360 nm band to the V_F centres proposed by KÄNZIG [8]. ESR signals were not observed in connection with the other bands.

III. 8. The bands exhibit a measurable decrease at RT due to bleaching or to the conversion of the corresponding centres. From the initial part of the decrease which can be considered to be exponential we obtained data on the

Table I

Band maximum (nm)	Half-width (eV)	Life-time
193	1	$>$ 1200 h
223	1	$\sim$ 5 h
330	0.7	$<$ 0.5 min
336	0.7	$\sim$ 45 min
360	0.7	$\sim$ 22 h

mean life-time of the bands at RT (Table 1). The value given for the 336 nm band refers to the process related to the disappearance of the F' band. After the disappearance of the F' band the life-time reaches 300 hours. The values obtained for the 330 and 360 nm bands agree with those obtained from ESR spectra, that is, in our crystals the mean life-time of V_K^M centres is certainly less than 0.5 min and that of V_F centres is about 22 hours.

IV. Discussion

IV. 1. We attribute all UV bands to V-type centres. In connection with this we should like to show that neither of the bands found between 300 and 400 nm is identical with the Z_3 band due to interstitial Ca^+ ions found by K. KOJIMA in additively coloured NaCl(Ca) crystals [9]. Our arguments are the following:

a) The maximum of the Z_3 band lies at 402 nm at LNT and we did not observe such a maximum.

b) Were the Z_3 band present, the Z_2 band should appear, too. Its maximum is at 474 nm on LNT and it widens the F band on the long wavelength side. We did not observe this either; that is, we found only the F' band on the long wavelength side of the F band.

c) We have shown that the 360 nm band, nearest to the Z_3 band is due to V_F centres and the 330 nm band may be attributed to V_K^M centres. As was mentioned in III. 1 the 336 nm band grows together with the F band in the initial stage of colouration, and since in this stage no other band is observable, it can be considered to be the V-type "partner" of the F band.

d) It is worth mentioning that we did not observe Z_3 and Z_2 bands even in the KCl(Ca) system [1], where the V bands do not overlap the Z_3 band.

IV. 2. In the following we deal with the models for the centres corresponding to the observed bands. To start with, the following can be stated:

a) In the case of the applied irradiation doses the observed bands are due to centres created mainly by the conversion of defects already existing in

the uncoloured crystal (so-called first stage of colouration). Atoms or ions in interstitial positions are not present for any considerable period.

b) Owing to the presence of Ca^{++} ions in the OH-free unannealed crystals the cation vacancy concentration is much higher than the anion vacancy concentration. Some of the Ca^{++} ions and the accompanying cation vacancies are associated to each other, and the other part is in a dissociated state, and in the process of colour centre formation it is mainly the latter which take part [10]. Most anion vacancies are present at RT in vacancy pairs. The OH-free grown and annealed crystal differs from the unannealed one in having a greater number of isolated vacancies. The increase in the number of isolated vacancies is indicated by the higher ionic conductivity of annealed crystals, exceeding the conductivity of unannealed crystals by about one order of magnitude. In crystals grown in the traditional way one part of the calcium forms molecular bonds [11, 12, 13] and in the colouration it is mainly the vacancy pairs which play an active part.

c) We did not observe V bands varying simultaneously proportionally with each other. Therefore, we assume the detected five bands to be due to five different centres.

d) The centres giving rise to the observed bands contain only one or two holes trapped by two or three halide ions.

e) Based on the results of H. N. HERSCH obtained on solutions [14] we assume that bands appearing in the 300—400 nm region are due to two-chlorine molecules or molecule-ions, and bands in the vicinity of 200 nm to three-chlorine ones.

IV. 3. The V_K^M centre giving rise to the 330 nm band and the V_F centre responsible for the 360 nm one satisfy the above conditions. The V_K^M centre is a $\langle 100 \rangle$ oriented Cl_2^- molecule ion situated in a vacancy pair. Its "partner" is an F centre. On the formation of a V_K^M centre and an F centre the number of cation vacancies in the crystal decreases by one. The V_F centre is also a Cl_2^- molecule ion but situated in two anion and one cation vacancy nearly $\langle 110 \rangle$ oriented. Its "partner" is an F centre. On the formation of a V_F centre and an F centre the numbers of cation and anion vacancies both decrease by one.

The centre giving rise to the 336 nm band is diamagnetic and we assume it to contain a Cl_2 molecule. Such a centre may be formed from the V_K^M centre by capturing a second hole. In the following we denote it by V_1^M, where the "1" subscript refers to the relationship with the V_1 centres observed in some pure crystals, which are stable only at quite low temperatures. In our opinion the Cl_2 molecule of the V_1^M centre is situated in a vacancy pair $\langle 100 \rangle$ oriented and locally neutral; it is more stable than the V_K^M centre. Its "partners" are either one F' centre or two F centres. On the formation of a V_1^M centre and an F' centre, only the number of cation vacancies decreases by one, and on the

formation of a V_1^M centre and two F centres the number of anion vacancies decreases, too.

Based on the above results and deductions, the processes shown in Fig. 5 can be explained in the following way. When the crystal is kept at RT for a few minutes (curve *b*) the unstable V_K^M centres are destroyed by recombination with F centres. As a result of further warming (curve *c*) the F' centres are totally annihilated through recombination with V_1^M centres.

Let us note that the creation of V_F and V_1^M centres accompanied by the "partner" F centres equally reduces the number of anion and cation vacancies. Compare now the formation of V_F and V_1^M centres in OH-free grown annealed crystals and in crystals air-grown by the Kyropoulos method. Though the anion and cation vacancy concentrations are high in both types of crystals, yet in the initial stage of colouration V_F centres are created in the former type and V_1^M centres in the latter. In our opinion the difference is related to the fact that in OH-free, annealed crystals immediately after annealing mainly isolated vacancies are present while in a crystal grown in the traditional way the vacancies are associated ones. In the first case conditions are favourable for the formation of V_F centres, and in the second for the formation of V_1^M centres. In OH-free unannealed crystals, too, there are associated vacancies present, therefore V_1^M centres are also created here at the beginning of colouration. But since the number of associated pairs is comparatively small, the concentration of V_1^M centres quickly approaches a saturation value. V_F centres appear in an observable number only at high doses, when we already reach the second stage of colouration.

Accepting the above facts, the concentration of vacancy pairs (anion vacancies) in the uncoloured crystals can be estimated in the given case from Fig. 1. Namely, this is the concentration at the moment when the V_1^M centres are near their saturation value (curve *c*)and no other V-type centres are yet present in a detectable quantity. Calculation gives the concentration of anion vacancies in the given uncoloured crystal to be approximately 9×10^{15} cm^{-3}, i.e. 8×10^{-7} Mole/Mole. This value is high compared with the RT equilibrium concentration. It is possible that the concentration is increased by frozen-in anion vacancies, but neither do we exclude the possibility that anion vacancies are brought into the crystal by some trace impurity. In the case of NaCl even the purity of the starting material is about 8×10^{-7} Mole/Mole.

The centres giving rise to the 193 nm and 223 nm bands are diamagnetic and in our opinion they contain Cl_3^- molecule ions. The first we denote by V_2^M, because we think that they are created similarly to V_2^M centres in the KCl(Ca) system from V_K^M centres [1]. In the V_2^M centres the Cl_3^- ion is situated in 2 cation and 1 anion vacancy in the vicinity of 2 Ca^{++} ions. But we leave open the question, open in the literature, too [7, 10, 15, 16, 17], whether the Ca^{++} is closely bound to the V_K^M and consequently to the V_2^M centres or not. We con-

sider the centres giving rise to the 223 nm band to be similar to the V_2 centres responsible for the 223 nm band observed in pure NaCl crystals. Since V_2 centres in the pure crystal appear at the beginning of colouration, it seems probable to us that they are created from vacancies already existing in the crystal. Therefore we consider the V_2 centre to consist of a Cl_3^- molecule ion situated in a 2 anion and 1 cation vacancy. This model agrees with that suggested previously for V_3 centres [18]. In our opinion the V_3 centre is more probably related to interstitially placed halogen, which assumption is supported by hardening studies [15]. Both the V_2^M and V_2 centres may be ⟨100⟩ oriented but we think that other orientations are also possible.

The model constructed for the V_2^M centre is supported by the experiment mentioned in III. 2 concerning the fact that the V_2^M centres may be formed from V_1^M centres by thermal activation, and under the effect of white light may be transformed back into V_1^M centres. Therefore, in our opinion the following transformations may possibly take place:

$$V_1^M + F \rightarrow V_K^M + \boxminus,$$

$$2\,V_K^M \rightarrow V_2^M$$

and

$$V_2^M + \boxminus \rightarrow V_1^M + \boxplus.$$

In conclusion we summarize the observed V centres in Table II, indicating the positions of band maxima measured at LNT, the possible models and the probable orientation of the centres. A question-mark denotes models requiring further support. For this purpose luminescence and ionic conductivity measurements are under way and the first informative measurements indicate that the decrease of ionic conductivity is caused by V_2^M centres.

Table II

Centre	Abs. max. nm	Orientation	Possible model
V_K^M	330	100	Cl_2^- in vacancy pair ($+Ca^{++}$?)
V_F	360	110	Cl_2^- in 2 anion vacancy + 1 cation vacancy
V_1^M	336	100?	Cl_2 in vacancy pair?
V_2^M	193	100?	Cl_3^- in 1 anion and 2 cation vacancy ($+ 2\,Ca^{++}$)?
V_2	223	100?	Cl_3^- in 2 anion and 1 cation vacancy?

Acknowledgment

The authors express their gratitude to Prof. Dr. I. TARJÁN for helpful discussions, to Mr. K. RAKSÁNYI for performing the chemical analysis and to Dr. Á. SOMLÓ for absorption measurements in the vacuum UV region.

REFERENCES

1. R. Voszka, T. Horváth and A. Watterich, Acta Phys. Hung., **24,** 255, 1968.
2. R. Voszka, T. Horváth and A. Watterich, phys. stat. sol., **23,** K71, 1967.
3. A. Watterich, M. Gécs and R. Voszka, phys. stat. sol., **31,** 571, 1969.
4. I. Tarján, R. Voszka, Á. Siegler and L. Berkes, Journal de Physique, **28,** C4—135, 1967.
5. R. Voszka, I. Tarján, L. Berkes and J. Krajsovszky, Kristall u. Technik, **1,** 423, 1966.
6. K. Raksányi and R. Voszka, Kristall u. Technik, **4,** 227, 1969.
7. W. Hayes and G. M. Nichols, Phys. Rev., **117,** 993, 1960.
8. W. Känzig, J. Phys. Chem. Sol., **17,** 80, 1960.
9. K. Kojima, J. Phys. Soc. Japan, **19,** 868, 1964.
10. M. Ikeya, N. Itoh, T. Okada and T. Suita, J. Phys. Soc. Japan, **21,** 1304, 1966.
11. J. B. Fritz, F. L. Lüty and J. Anger, Z. für Phys., **174,** 240, 1963.
12. N. Jannuzzi, S. Mascarenhas and N. Ferrejra de Souza, Color Center Symposium Rome, **97,** 1968.
13. A. Kessler and E. Mariani, Czech. J. Phys., **B17,** 786, 1967.
14. H. N. Hersch, Color Centers in Alkali Halides Int. Symp. Urbana **81,** 1965.
15. W. A. Sibley and J. R. Russel, J. Appl. Phys., **36,** 810, 1965.
16. M. Beltrami, R. Cappelletti and R. Fieschi, Phys. Letters, **10,** 279, 1964.
17. C. Laj, P. Bergé, M. Dubois and J. Tournon, Color Centers in Alkali Halides Symposium Rome, **121,** 1968.
18. T. P. Zavskiewicz and R. W. Christy, Phys. Rev., **135,** A194, 1964.

ИССЛЕДОВАНИЕ V-ЦЕНТРОВ, СТАБИЛЬНЫХ ПРИ КОМНАТНОЙ ТЕМПЕРАТУРЕ, В КРИСТАЛЛАХ NaCl(Ca)

Р. ВОСКА и А. ВАТТЕРИХ

Резюме

Авторы наблюдали в NaCl(Ca) кристаллах, несодержащих OH, под действием рентгеновского облучения кроме V_2 полосы, находящейся в чистых кристаллах тоже на 223 нм, новые полосы поглощения на длинах волн 360, 336 и 193 нм, причисленные ими к $V_F' = V_1^M$ и V_2^M-центрам. (Буква «M» обозначает наличие двухвалентной металлической примеси, чтобы различать их от соответствующих центров чистого кристалла.) В случае облучения при температуре —80° C наблюдалась новая полоса на 330 нм и было показано, что эта полоса происходит из V_K^M-центров Модели перечисленных центров известны исключая V_1^M центров, для которых авторы предлагают модель.

Acta Physica Academiae Scientiarum Hungaricae, Tomus 27, pp. 289—298 (1969)

A SIMPLIFIED METHOD FOR CALCULATING THE INTERNAL STRUCTURE OF NEUTRON STARS*

By

D. KISDI

RESEARCH GROUP FOR THEORETICAL PHYSICS OF THE HUNGARIAN ACADEMY OF SCIENCES, BUDAPEST

(Received 13. II. 1969)

A very economical method is proposed for solution of the hydrostatic equilibrium equations of neutron stars. As a simple example the model of homogeneous internal distribution is constructed. Utilizing BRUECKNER's equation of state the importance of the effect of correlation can be demonstrated.

I. Introduction

It was suggested by ZWICKY [1] that the suddenness and magnitude of energy generation in supernovae might be explained as a partial gravitational collapse of a star (or a gas cloud) into a neutron core. There has recently been renewed interest in this possibility because observations indicate that some of the remnants of supernovae are sources of X-rays, and it can be stated with reasonable assurance that a neutron star is responsible directly or indirectly for X-radiation [2].

In this paper we shall not deal with the problem of observing such neutron stars. Instead we confine ourselves to the internal structure of cold, degenerate neutron stars. To investigate the static structure of such a star, one needs an equation of state, i.e. an energy—density relation for neutron matter. In consideration of this, there are two great uncertainties. First, the behaviour of nuclear forces in the high-energy region is not well known. In principle, the neutron–neutron forces can be determined from proton–proton phase shift analysis, assuming charge independence and correcting for Coulomb effects. Various models of nuclear forces have been constructed by different authors which fit the phase shifts up to 300 MeV bombarding energy. But the results in the many-body problem (in the case of high density) for these nuclear force models may be seriously different, i.e. the equation of state is sensitive to the choice of nuclear force model.

The second uncertainty arises from the fact that certain terms must be neglected in any calculation method for the many-body problem. In most of

* Dedicated to Prof. P. GOMBÁS on his 60th birthday.

the various equations of state which have been proposed for neutron matter, very crude methods are used for solving the many-body problem. OPPENHEIMER and VOLKOFF [3] assume an equation of state of an ideal Fermi gas, i.e. the neutron—neutron forces are completely neglected. The semi-empirical equation of state due to SKYRME [4] is expected to describe average nuclear properties. SALPETER [5] worked out a more complete equation of state applying the scattering limit theory and used an effective range approximation. To interpret the effect of a hard core of neutrons WHEELER et al. [6] studied the incompressible fluid model of neutron matter. Several very simple forms of equation of state were derived taking into account the nuclear forces by the Hartree—Fock method [7]. In this paper we shall utilize the neutron matter calculation of BRUECKNER et al. [8] for GAMMEL—THALER potential with repulsive core. BRUECKNER's t-matrix approach to the many-body problem takes into account the two particle correlations exactly, and this is the most accurate neutron matter calculation which has been performed up to now.

The various equations of state may be used to construct neutron star models by solving the equations of hydrostatic equilibrium. Such calculations have been carried out by several authors. The OPPENHEIMER—VOLKOFF [3] star model consists of non-interacting neutrons, CAMERON's [9] model is based upon SKYRME's [4] equation of state. The ideal and real gas models constructed by AMBARTSUMYAN and SAAKYAN [10] take into account strange particles in the stellar matter. More recently two neutron star model calculations have been made, using Hartree—Fock equations of state. TSURUTA and CAMERON [11] (henceforth cited as "TC") assumed an equation of state as suggested by LEVINGER and SIMMONS [7], GOMBÁS and KISDI [7] an equation of state based upon GOMBÁS's semi-empirical nuclear force model (which does not fit the two-body data, but the average nuclear binding energies).

The integration of the hydrostatic equations, in principle, can be carried out without any difficulty. Because of the sufficient increase of pressure with increasing density the Schwarzschild singularity does not occur in neutron-star models, and any conventional method for numerical integration can be applied. Nevertheless, the construction of a star model is not a simple problem for it needs a lot of numerical calculations. In Section II of this paper we propose a new numerical method for solving the hydrostatic equations.* This may be more economical than the usual step-by-step methods and makes it possible to discuss the neutron star models without using digital computers. In this work we apply this method in the simplest form which results in a star model of homogeneous internal distribution (Section III). Inspecting the numerical solution of the hydrostatic equations of TC, we can conclude that

* Our method is closely connected with the method of momenta in differential equation theory. See, e.g. L. COLLATZ, Numerische und graphische Methoden. (Handbuch der Physik, Vol. II. Springer, Berlin, 1955.)

this homogeneous model is a reasonable approximation if the density is in the region of 10^{14}—10^{15} gcm^{-3}, which is the region of the heaviest neutron stars. In Section IV, we calculate the gravitational and proper masses and the (constant) density as functions of the radius, assuming the equation of state of BRUECKNER et al. [8]. The results are compared with those of some previous works.

II. The equations of hydrostatic equilibrium

A spherical neutron star in hydrostatic equilibrium is described by the following structure equations:

a) Pressure equation [12]

$$\frac{dP}{dr} = -\frac{G}{c^4} \cdot \frac{(\varepsilon + P)\,(mc^2 + 4\pi r^3 P)}{r^2\left(1 - \dfrac{2Gm}{c^2 r}\right)}\,, \tag{1}$$

where P and ε are the local pressure and energy density at radius r, m is the mass inside the radius r, G and c are the gravity constant and the velocity of light, respectively.

b) Conservation of mass:

$$\frac{dm}{dr} = \frac{4\pi}{c^2} r^2 \varepsilon\,. \tag{2}$$

c) Equation of state:

$$\varepsilon = \varepsilon(\varrho) = \varrho \cdot \left(\mu c^2 + E_b(\varrho)\right), \tag{3}$$

where ϱ is the neutron number density, μ is the neutron mass and E_b is the energy per particle in a neutron gas of density ϱ. The relation between E_b and ϱ must be calculated from a many-body theory. In this Section we do not fix the special form of this $E_b - \varrho$ relation.

The pressure is given by

$$P(\varrho) = \varrho \frac{\partial \varepsilon}{\partial \varrho} - \varepsilon = \varrho^2 \frac{\partial E_b}{\partial \varrho}\,. \tag{4}$$

d) The boundary conditions are

$$m = 0 \quad \text{at} \quad r = 0\,, \tag{5}$$

$$\varrho = 0 \quad \text{at} \quad r = R\,, \tag{6}$$

where R is the radius of the neutron star; the outer edge of the star is assumed to have zero density. From Eqs. (3) and (4) it then follows that both ε and P are also zero at the surface.

It is clear that Eqs. (1)—(6) uniquely determine the internal distribution of the quantities ϱ, ε, P and m. The star model has only one free characteristic quantity, the radius R. After solving the hydrostatic equations (1)—(6), the gravitational and proper masses are obtained from

$$M_g = m(R)\,, \tag{7}$$

$$M_p = \mu \int_0^R \frac{\varrho(r)\, 4\pi r^2\, dr}{\sqrt{1 - \dfrac{2Gm(r)}{c^2 r}}}\,, \tag{8}$$

respectively. The gravitational mass of the star is the mass as perceived by a distant observer and the proper mass is the neutron number of the star, multiplied by the neutron mass μ.

We define the moment of order $\varkappa$, of the neutron distribution to be

$$\int_0^R \varrho(r)\, r^{\varkappa}\, dr\,, \tag{9}$$

where $\varkappa \geqslant 0$. Integrating by parts and taking into account the boundary condition $\varrho(R) = 0$, we get:

$$\begin{aligned} \int_0^R \varrho r^{\varkappa}\, dr &= -\frac{1}{\varkappa + 1} \int_0^R \frac{d\varrho}{dr}\, r^{\varkappa+1}\, dr = \\ &= \frac{G}{(\varkappa+1)\, c^4} \int_0^R \frac{\varepsilon + P}{P'} \cdot \frac{mc^2 + 4\pi r^3 P}{r - \dfrac{2G}{c^2} m}\, r^{\varkappa}\, dr\,, \end{aligned} \tag{10}$$

where

$$P' = \frac{dP}{d\varrho} = \varrho \frac{\partial^2 \varepsilon}{\partial \varrho^2}\,.$$

This means that for every order $\varkappa$, the moment of ϱ is identical with

$$\frac{G}{(\varkappa+1)\, c^4}$$

times the moment of

$$\frac{\varepsilon + P}{P'} \cdot \frac{mc^2 + 4\pi r^3 P}{r - \dfrac{2G}{c^2} m}\,.$$

Now we can introduce a very economical approximation procedure for solving Eqs. (1)—(6). We take a trial function for ϱ which, besides r, depends on a set of parameters $\beta_1, \beta_2, \ldots, \beta_s$.

$$\varrho = \varrho(r; \beta_1, \beta_2, \ldots, \beta_s). \tag{11}$$

We suppose that the boundary condition (6) is satisfied for every value of the β-s. The energy density and the pressure are determined from ϱ by the equation of state (3) and (4):

$$\varepsilon = \varepsilon(r; \beta_1, \beta_2, \ldots, \beta_s), \tag{12}$$

$$P = P(r; \beta_1, \beta_2, \ldots, \beta_s), \tag{13}$$

and m is calculated from (2) and (5):

$$m = \frac{4\pi}{c^2} \int_0^r \varepsilon r^2 \, dr = m(r; \beta_1, \beta_2, \ldots, \beta_s). \tag{14}$$

Instead of (1) we require that the moment equation (10) must be satisfied for S different $\varkappa$ values. This determines the parameters $\beta_1, \beta_2, \ldots, \beta_s$. Putting these β-s into the expressions (11)—(14) we get the solution of our problem.

Naturally, we have drawn our procedure as general as possible. *How* to introduce the parameters $\beta_1, \beta_2, \ldots, \beta_s$, and for *what values of* $\varkappa$ the moment equation is satisfied, is, in principle, arbitrary. But one can imagine that the accuracy of our method depends on the proper choice of the trial function and the values of the $\varkappa$-s.

III. Star model of homogeneous internal distribution

As a simple example of our method we treat a neutron star model in which the internal density distribution is homogeneous.

$$\begin{aligned} \varrho(r) &= \varrho_0, \quad \text{if} \quad r < R, \\ \varrho(r) &= 0, \quad \text{if} \quad r > R. \end{aligned} \tag{15}$$

Here R is the radius of the star and ϱ_0 is the only parameter of the model which is to be determined from a moment equation.

The equation of state then gives the homogeneous distribution for the energy density and pressure:

$$\begin{aligned} \varepsilon(r) &= \varepsilon_0 \quad \text{and} \quad P(r) = P_0, \quad \text{if} \quad r < R, \\ \varepsilon(r) &= 0 \quad \text{and} \quad P(r) = 0, \quad \text{if} \quad r > R, \end{aligned} \tag{16}$$

where $\varepsilon_0 = \varepsilon(\varrho_0)$ and $P_0 = P(\varrho_0)$. The quantity m is determined by (2) and (5):

$$m(r) = \frac{4\pi r^3 \varepsilon_0}{3c^2}, \quad \text{if} \quad r < R,$$
$$m(r) = \frac{4\pi R^3 \varepsilon_0}{3c^2}, \quad \text{if} \quad r > R. \tag{17}$$

Putting the expressions (15), (16) and (17) into the moment equation (10) we obtain a transcendental equation for ϱ_0.

$$\varrho_0 = \frac{4\pi R^2 G}{3c^4} \cdot \frac{(\varepsilon_0 + P_0)(\varepsilon_0 + 3P_0)}{P_0'} \int_0^1 \frac{x^{\varkappa+2}}{1 - \dfrac{8\pi R^2 G \varepsilon_0}{3c^4} x^2} dx, \tag{18}$$

where $x = r/R$ and the abbreviation P_0' stands for

$$P'(\varrho_0) = \left(\frac{\partial P}{\partial \varrho}\right)_{\varrho=\varrho_0}.$$

Introducing the dimensionless quantities

$$\xi = \frac{\varrho_0 \varepsilon_0 P_0'}{(\varepsilon_0 + P_0)(\varepsilon_0 + 3P_0)} \quad \text{and} \quad \eta = \frac{8\pi R^2 G \varepsilon_0}{3c^4}, \tag{19}$$

Eq. (18) takes the very simple form

$$\xi = \frac{1}{2}\eta \int_0^1 \frac{x^{\varkappa+2}}{1 - \eta x^2} dx. \tag{20}$$

As our simple model has only one parameter, ϱ_0, the moment equation (18) or (20) can be satisfied only for one value of the order $\varkappa$. We choose the value $\varkappa = 2$, because then (10) guarantees a good approximation for the integral

$$\int_0^R \varrho\, 4\pi r^2\, dr$$

which is closely connected with the mass of the star. For $\varkappa = 2$ Eq. (20) gives

$$\xi = \frac{1}{2}\left[\frac{1}{2\sqrt{\eta^3}} \ln\left(\frac{1+\sqrt{\eta}}{1-\sqrt{\eta}}\right) - \frac{1}{\eta} - \frac{1}{3}\right]. \tag{21}$$

Summarizing, the construction of the homogeneous model consists of the following steps:

a) Choose a value for ϱ_0. This can be regarded as the free characteristic quantity of the star model.

b) Determine ε_0, P_0 and P_0' from the equation of state and ξ according to (19).

c) Calculate η from (21). For this we need the inverse of the function which stands on the right-hand side of (21). This can be determined numerically.

d) Finally, the radius R can be obtained from (19):

$$R = \left(\frac{3\,c^4}{8\pi G} \cdot \frac{\eta}{\varepsilon_0} \right)^{1/2} . \tag{22}$$

In this way we get a radius — neutron density relation, which is one of the fundamental characteristic relations of the neutron star model.

If we have determined R by the above procedure, then we get the gravitational and proper masses from (7) and (8), respectively. The gravitational mass is

$$M_g = \frac{4\pi R^3 \varepsilon_0}{3\,c^2} = \frac{c^2}{2G}\,\eta R\,, \tag{23}$$

and for the proper mass we have

$$M_p = 4\pi R^3 \mu \varrho_0 \int_0^1 \frac{x^2\,dx}{\sqrt{1-\eta x^2}} = \frac{4\pi R^3 \mu \varrho_0}{3} \cdot \frac{3}{2\eta} \left(\frac{\arcsin \sqrt{\eta}}{\sqrt{\eta}} - \sqrt{1-\eta} \right). \tag{24}$$

From these equations we get M_g and M_p as functions of ϱ_0 (or R). These mass — density and mass — radius relations are also fundamental characteristics of the model.

IV. Results for Brueckner's equation of state

BRUECKNER et al. [8] have calculated the energy per particle, E_b, in neutron matter as a function of neutron density ϱ, solving the integral equations of the BRUECKNER's many-body theory exactly. We reproduce their result in Fig. 1. We have found that a convenient and very accurate analytical fit for BRUECKNER's $E_b = E_b(\varrho)$ is given by the following polytropic expression:

$$E_b = a\varrho^{\lambda}\,, \tag{25}$$

where $\lambda = 0.576$ and $a = 57.9$, if E_b is measured in MeV and ϱ in 10^{39} cm^{-3} units. Assuming (25), the equation of state (3) and (4) is

$$\begin{aligned} \varepsilon &= \varrho(\mu c^2 + a\varrho^{\lambda})\,, \\ P &= \lambda a \varrho^{\lambda+1}. \end{aligned} \tag{26}$$

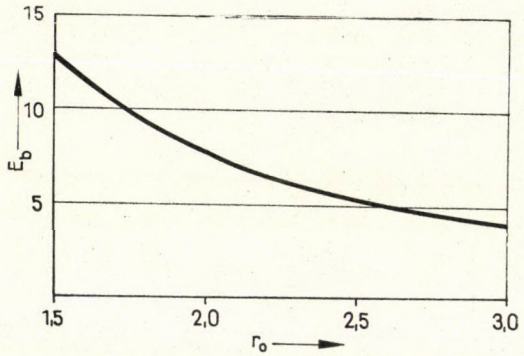

Fig. 1. Total energy per particle in a neutron gas. The distance parameter $r_0 = \left(\frac{3}{4\pi\varrho_0}\right)^{1/3}$ is given in 10^{-13} cm, the energy E_b in MeV units. (From BRUECKNER et al. [8])

In this case the quantity ξ, defined by (19), is the following function of ϱ_0

$$\xi = \frac{\lambda(\lambda+1)\, a\varrho_0^{\lambda}\,[\mu c^2 + a\varrho_0^{\lambda}]}{[\mu c^2 + (\lambda+1)\, a\varrho_0^{\lambda}][\mu c^2 + (3\lambda+1)\, a\varrho_0^{\lambda}]} \,. \tag{27}$$

Utilizing this, the radius R, the gravitational mass M_g and the proper mass M_p can be determined as has been described in Section III. The results are given in Table I.

In Fig. 2 the relation between the energy density ε_0 and the gravitational mass M_g is shown. For comparison the central energy density — gravitational mass relations of TC and of the OPPENHEIMER—VOLKOFF model are also plotted.

We believe the reality of our model lies only in the region II of Fig. 2. In the low density region (marked I) the neutrons are unstable against the decay $n \to p + e + \bar{\nu}$. The models of TC have taken into account this possibility and in this region, are composed of neutrons, electrons and heavy ions. Our simplified model works with stable "neutrons" and therefore cannot be compared, in this region, with the results of TC. On the other hand, the OPPENHEIMER—VOLKOFF model is also composed of stable Fermi particles. The big difference between our and their results shows the importance of the effect of nuclear forces. In the region of superdense neutron stars (marked III in Fig. 2) our homogeneous model is not reliable. According to TC, in this region the matter of the star accumulates near the centre and the deviation from constant density distribution becomes serious. To deal with this effect, our simple trial function must be replaced by a more flexible one.

The remnants of the heaviest supernovae lie around the mass peak in the intermediate density region (marked II in Fig. 2). The drastic deviation among the various results in this region give an indication of the poorness of

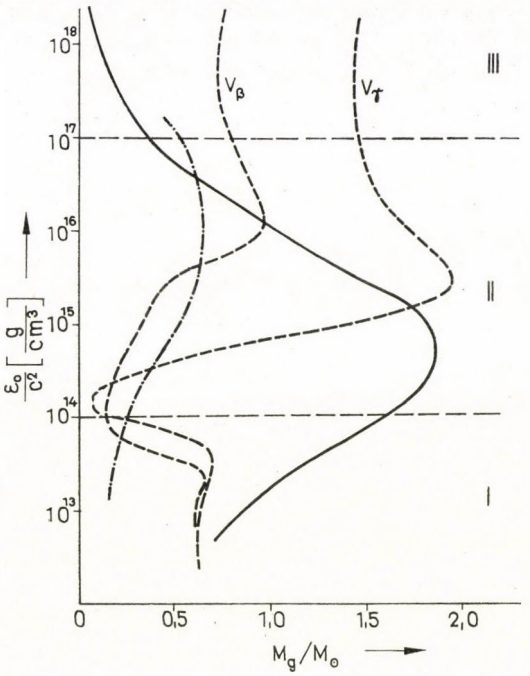

Fig. 2. Gravitational mass — energy density relation: ——— our result, —·—·— result of OPPENHEIMER and VOLKOFF [3] for an ideal Fermi gas, -------- results of TC for their nuclear forces V_β and V_γ, respectively

Table I

Characteristics of the homogeneous neutron star model with BRUECKNER's equation of state. ϱ_0 in $g\ cm^{-3}$, ε and P_0 in erg cm^{-3}, R in km and, M_g, M_p in $M_\odot$ units

ϱ_0	ε_0	P_0	ξ	η	R	M_g	M_p
7.19×10^{12}	6.48×10^{33}	9.94×10^{30}	0.00657	0.0626	37.4	0.792	0.805
1.44×10^{13}	1.30×10^{34}	2.96×10^{31}	0.00976	0.0908	31.8	0.976	0.999
2.88×10^{13}	2.60×10^{34}	8.83×10^{31}	0.0144	0.130	26.8	1.175	1.210
7.19×10^{13}	6.53×10^{34}	3.74×10^{32}	0.0242	0.205	21.3	1.479	1.568
1.44×10^{14}	1.31×10^{35}	1.12×10^{33}	0.0354	0.282	17.6	1.680	1.823
2.88×10^{14}	2.64×10^{35}	3.33×10^{33}	0.0522	0.377	14.4	1.832	2.059
7.19×10^{14}	6.71×10^{35}	1.41×10^{34}	0.0834	0.514	10.5	1.828	2.150
1.44×10^{15}	1.37×10^{36}	4.20×10^{34}	0.118	0.635	8.20	1.761	2.178
2.88×10^{15}	2.80×10^{36}	1.25×10^{35}	0.163	0.720	6.09	1.484	1.893
7.19×10^{15}	7.39×10^{36}	5.30×10^{35}	0.238	0.823	4.01	1.117	1.482
1.44×10^{16}	1.57×10^{37}	1.58×10^{36}	0.303	0.877	2.84	0.843	1.122
2.88×10^{16}	3.40×10^{37}	4.71×10^{36}	0.371	0.913	1.97	0.608	0.785
7.19×10^{16}	9.93×10^{37}	2.00×10^{37}	0.450	0.941	1.17	0.373	0.435
5.39×10^{17}	1.31×10^{39}	4.77×10^{38}	0.201	0.780	0.293	0.077	0.041

neutron star theories. The difference between the two curves of TC shows what uncertainty can arise from the extrapolation of nuclear potentials originally constructed for two body problems. One should not be surprised if our result deviates appreciably from the TC curves, since our model is based on a third nuclear potential (introduced by GAMMEL and THALER).

Furthermore, BRUECKNER's equation of state, which we have used in our model, takes into account the two particle correlations in neutron matter. The correlation has been neglected in previous neutron star models and the deviation of our model from others may be due partially to this. The effect of correlation seems to be very important and requires further investigations.

Acknowledgment

We wish to express our gratitude to Professor P. GOMBÁS for support and interest in this work.

REFERENCES

1. F. ZWICKY, Astrophys. J., **88,** 522, 1938; Phys. Rev., **55,** 726, 1939; Rev. Mod. Phys., **12,** 66, 1940; Observatory, **68,** 121, 1948; Handbuch der Physik (Springer-Verlag,, Berlin), **51,** 766, 1958.
2. H. Y. CHIU, Ann. Phys. N. Y., **26,** 364, 1964,
   D. C. MORTON, Nature, **201,** 1308, 1964.
3. J. R. OPPENHEIMER and G. M. VOLKOFF, Phys. Rev., **55,** 374, 1939.
4. T. H. R. SKYRME, Nucl. Phys., **9,** 615, 1959.
5. E. E. SALPETER, Ann. Phys. N. Y., **11,** 393, 1960.
6. B. K. HARRISON, M. WAKANO and J. A. WHEELER, "La Structure et l'Evolution de l' Universe", Stoops, Brussels, 1958.
7. P. GOMBÁS and D. KISDI, Z. Naturforsch., **21,** 2009, 1966.
   L. GRATTON and G. SZAMOSI, Nuovo Cimento, **33,** 1056, 1964.
   J. S. LEVINGER and L. M. SIMMONS, Phys. Rev., **124,** 916, 1961.
8. K. A. BRUECKNER, J. L. GAMMEL and J. T. KUBIS, Phys. Rev., **118,** 1095, 1960.
9. A. G. W. CAMERON, Astrophys. J., **130,** 884, 1959.
10. V. A. AMBARTSUMYAN and G. S. SAAKYAN, Soviet Astron., **5,** 601, 1962..
11. S. TSURUTA and A. G. W. CAMERON, Can. J. Phys., **44,** 1895, 1966.
12. R. C. TOLMAN "Relativity, Thermodynamics and Cosmology", pp. 239—244, Oxford Univ. Press 1934.

УПРОЩЕННЫЙ МЕТОД ДЛЯ ОПРЕДЕЛЕНИЯ ВНУТРЕННЕЙ СТРУКТУРЫ НЕЙТРОННЫХ ЗВЕЗД

Д. КИШДИ

Резюме

Для определения гидростатического равновесия нейтронных звезд предлагается действительно эффективный метод. В качестве простого примера подробно рассматривается модель с постоянной плотностью. Применением уравнения состояния Брюкнера для нейтронной материи сможем демонтировать важность корреляционных эффектов.

Acta Physica Academiae Scientiarum Hungaricae, Tomus 27, pp. 299—307 (1969)

SUM RULES AND THEIR APPLICATION IN THE THEORY OF SUPERFLUID HELIUM*

By

P. SZÉPFALUSY

INSTITUTE FOR THEORETICAL PHYSICS, ROLAND EÖTVÖS UNIVERSITY, BUDAPEST

(Received 17. II. 1969)

The first part of this paper is devoted to investigating the static response functions of superfluid helium in the hydrodynamic region which results in obtaining a new sum rule. Sum rules are then specialized to zero temperature and exploited to determine matrix elements of the particle creation and annihilation operators between the ground state and the one quasi-particle state in the long wavelength limit. We examine the particle distribution function and besides calculating the leading term, we are able to give a lower limit to the next one in the expansion for small wave numbers.

1. Introduction

We consider liquid helium below its lambda point, where it is characterized by the condensation of a finite fraction of particles into a particular single-particle state. The connection between the microscopic theory based upon the presence of the condensation and the phenomenological two-fluid hydrodynamical equations was first studied by BOGOLIUBOV [1] and by HOHENBERG and MARTIN [2]. In particular, in this way various sum rules in the hydrodynamical region have been obtained. In the first part of the present paper a new sum rule is derived by investigating the disturbance in the condensate and the particle density due to an external potential and particle sources.

Then, we are concerned with liquid helium at zero temperature with a homogeneous condensate. We limit ourselves to the long wavelength behaviour of the system and wish to explore the consequences of the sum rules. PINES [3] has proved that the one quasiparticle states exhaust the f-sum rule and the compressibility sum rule in the long wavelength limit and he has obtained the density fluctuation spectrum and the dynamic form factor in this limit. We extend his method to other sum rules and in this way we are able to calculate the matrix elements of particle creation and annihilation operators between the ground state and the one quasi-particle state in the long wavelength limit, without using perturbation theory and avoiding assumptions about the behaviour of self-energies. With the aid of these matrix elements we

* Dedicated to Prof. P. GOMBÁS on his 60th birthday.

can examine the particle distribution function in the long wavelength limit. The leading term obtained agrees with the result of the detailed microscopic calculation by GAVORET and NOZIÈRES [4] and has also been derived by applying quantum hydrodynamics [5]. Furthermore, we are able to give a lower limit for the next term in the expansion. Finally, we discuss the sum rules and the results in the BOGOLIUBOV approximation.

2. Sum rules

We consider liquid helium at a temperature T below the lambda temperature T_λ, where it is characterized by the condensation of a finite fraction of particles into a particular single-particle state. The condensate wave function is the average value of the particle field operator

$$\langle \psi(r, t) \rangle = \sqrt{n_0(r, t)}\, e^{i\varphi(r,t)}, \tag{1}$$

which is to be regarded as a quasi average [6] being nonzero by virtue of the broken symmetry.

We are interested in the linear response of the system disturbed slightly from equilibrium due to an external potential U and external sources η and η^* coupled to the particle field. Thus, we have a modified Hamiltonian

$$H + \delta H\,,$$

where

$$\delta H = \int U(r)\, n(r)\, d^3 r + \int \left(\eta(r)\, \psi^+(r) + \eta^*(r)\, \psi(r)\right) d^3 r$$

with

$$n(r) = \psi^+(r)\, \psi(r)\,.$$

By taking

$$U(r) = U_k\, e^{ikr} + U_{-k}\, e^{-ikr}$$

with $U_k = U^*_{-k}$ and

$$\eta(r) = \eta_k\, e^{ikr} + \eta_{-k}\, e^{-ikr}$$

and by substituting

$$\psi(r) = \sum_k a_k\, e^{ikr}$$

we get

$$\delta H = U_k\, n_k + U_{-k}\, n_{-k} + \eta_k\, a_k^+ + \eta_{-k}\, a_{-k}^+ + \eta_k^*\, a_k + \eta_{-k}^*\, a_{-k}. \tag{2}$$

By applying the usual procedure, one can write

$$\delta n_0^{1/2}(r) = \delta Re\, \langle \psi(r) \rangle = \delta n_0^{1/2}(k) e^{ikr} + \delta n_0^{1/2}(-k)\, e^{-ikr}\,, \tag{3}$$

where

$$\delta n_0^{1/2}(k) = \frac{1}{2}\left[\chi^s_{aa}(k,-k) + \chi^s_{a^+a}(-k,-k)\right]\eta^*_{-k} + \\ + \frac{1}{2}\left[\chi^s_{aa^+}(k,k) + \chi^s_{a^+a^+}(-k,k)\right]\eta_k + \\ + \frac{1}{2}\left[\chi^s_{an}(k,-k) + \chi^s_{a^+n}(-k,-k)\right]U_{-k} \tag{4}$$

and

$$\delta\langle n(r)\rangle = \delta n(k)\, e^{ikr} + \delta n(-k)\, e^{-ikr}, \tag{5}$$

where

$$\delta n(k) = \chi^s_{na}(k,-k)\,\eta^*_{-k} + \chi^s_{na^+}(k,k)\,\eta_k + \chi^s_{nn}(k,-k)\,U_{-k}. \tag{6}$$

Here $\chi^S_{AB}(k,k')$ denotes the static response function given by

$$\chi^s_{AB}(k,k') = \chi^s_{BA}(k',k) = P\int_{-\infty}^{\infty}\frac{d\omega}{2\pi}\,\frac{\tau_{AB}(k,k',\omega)}{\omega}, \tag{7}$$

where τ_{AB} is defined by

$$\langle[A_k(t), B_{k'}(t')]\rangle = \int_{-\infty}^{\infty}\frac{d\omega}{2\pi}\,\tau_{AB}(k,k';\omega)\,e^{-i\omega(t-t')}. \tag{8}$$

According to the well-known compressibility sum rule [7]

$$\lim_{k\to 0}\chi^s_{nn}(k,k) = -\frac{n}{mc^2}. \tag{9}$$

Here c is the isothermal sound velocity $c^2 = m^{-1}(\partial P/\partial n)$, where P denotes the pressure.

Using invariance under time reversal and space inversion and Equs. (3)—(9) we find the following sum rules

$$\lim_{k\to 0}\chi^s_{an}(k,-k) = -\frac{n^{1/2}}{mc^2}\left(\frac{n}{n_0}\right)^{1/2}\left(\frac{\partial n_0}{\partial n}\right)_\eta \tag{10}$$

and

$$\lim_{k\to 0}\left[\chi^s_{a^+a}(k,k) + \chi^s_{aa}(k,-k)\right] = -\frac{1}{2\,mc^2}\,\frac{n}{n_0}\left(\frac{\partial n_0}{\partial n}\right)_\eta\left(\frac{\partial n_0}{\partial n}\right)_U, \tag{11}$$

where the derivatives are taken at constant temperature. The sum rule (10) is implicitly present in KRASNIKOV's paper [8] devoted to the generalization of BOGOLIUBOV's work to the non-ideal fluid. On the other

hand, by using the two-fluid hydrodynamical equations the expression obtained by KRASNIKOV for $\chi^s_{a+a} + \chi^s_{aa}$ contains as unknown parameter the real part of the coefficient of the source terms in the hydrodynamical equations.

Finally let us quote the following sum rule, derived by BOGOLIUBOV [1] and HOHENBERG and MARTIN [2]

$$\lim_{k\to 0} [\chi^s_{aa^+}(k, k) - \chi^s_{aa}(k, -k)] = -\frac{2n_0}{n_s}\frac{m}{k^2}, \tag{12}$$

where n_s is the superfluid density. The next term on the right hand side of Equ. (12) is a k independent one which could only be determined from microscopic theory or from knowing the parameters of a generalized two-fluid hydrodynamics taking into account derivatives of third order.

In the next Section we consider superfluid helium at zero temperature where the sum rules (9), (10) read

$$\lim_{k\to 0} \sum_{\alpha} \frac{|\langle \alpha|n_k^+|0\rangle|^2}{\omega_{\alpha 0}} = \frac{n}{2mc^2}, \tag{13}$$

$$\lim_{k\to 0} \sum_{\alpha} \frac{\langle 0|a_{-k}|\alpha\rangle\langle\alpha|n_k|0\rangle + \langle 0|n_k|\alpha\rangle\langle\alpha|a_{-k}|0\rangle}{\omega_{\alpha 0}} = \frac{n^{1/2}}{2mc^2}\left(\frac{n}{n_0}\right)^{1/2}\left(\frac{\partial n_0}{\partial n}\right)_\eta, \tag{14}$$

where $\omega_{\alpha 0} = E_\alpha - E_0$ is the excitation energy. Furthermore from the sum of Equs. (11) and (12) we get

$$\lim_{k\to 0} \sum_{\alpha} \frac{|\langle 0|a_k|\alpha\rangle|^2 + |\langle\alpha|a_k|0\rangle|^2}{\omega_{\alpha 0}} = \frac{n_0}{n}\frac{m}{k^2} + \\ + \frac{1}{2mc^2}\left(\frac{\partial n_0}{\partial n}\right)_\eta\left(\frac{\partial n_0}{\partial n}\right)_U + A, \tag{15}$$

where $-A$ denotes the constant term on the right hand side of Equ. (12).

3. Application of the sum rules

Our purpose in this section is to calculate the matrix elements of particle creation and annihilation operators in the long wavelength limit by means of the sum rules (13) (14), (15). For this we need the matrix elements of the density fluctuation, which were determined by PINES [3]. First let us summarize his results. From translational invariance it follows that

$$\lim_{k\to 0} \langle\alpha|\mathbf{J}_k|0\rangle \sim k^a, \qquad a > 0, \tag{16}$$

where $\mathbf{J}_k$ is the current density fluctuation, which is related to the density fluctuation by particle conservation:

$$\omega_{\alpha 0} \langle \alpha | n_k^+ | 0 \rangle = \mathbf{k}\, \mathbf{J}_k \tag{17}$$

Another essential point is that for a multi-particle state $|\alpha\rangle$ the excitation energy $\omega_{\alpha 0}$ tends to a finite value $\bar{\omega}$ in the long wavelength limit. Then, one finds for such a state from Equs. (16) and (17) that

$$\lim_{k \to 0} \langle \alpha | n_k^+ | 0 \rangle \sim \frac{k^{1+a}}{\bar{\omega}}, \qquad a > 0. \tag{18}$$

It follows that the single quasiparticle state exhausts both the f sum rule [7]

$$\sum_{\alpha} \omega_{\alpha 0} |\langle \alpha | n_k^+ | 0 \rangle|^2 = \frac{nk^2}{2m} \tag{19}$$

and the compressibility sum rule (13) in the long wavelength limit, whence

$$\lim_{k \to 0} \omega_k = ck\,, \tag{20}$$

$$\lim_{k \to 0} \langle -k | n_k | 0 \rangle = \lim_{k \to 0} \langle 0 | n_k | k \rangle = \left(\frac{nk}{2\,mc} \right)^{1/2}. \tag{21}$$

Here $|k\rangle$ and ω_k denote the single quasiparticle state of momentum $\mathbf{k}$ and its energy, respectively. Equs. (18), (20) and (21) which are the results obtained by PINES [3] make possible the calculation of the matrix elements $\langle 0 | a_k | k \rangle$ and $\langle -k | a_k | 0 \rangle$ from the sum rules (14), (15) and from the relationship

$$\sum_{\alpha} \left(\langle 0 | a_k | \alpha \rangle \langle \alpha | n_{-k} | 0 \rangle - \langle 0 | n_{-k} | \alpha \rangle \langle \alpha | a_k | 0 \rangle \right) = n_0^{1/2}, \tag{22}$$

which is a direct consequence of the commutation relation

$$a_k\, n_{-k} - n_{-k}\, a_k = a_0\,.$$

One can easily see by inspection of the sum rule (15) that the matrix elements $\langle 0 | a_k | \alpha \rangle$ and $\langle \alpha | a_k | 0 \rangle$ cannot be more singular than k^{-1} in the long wavelength limit. Then, using Equ. (18) it follows that the multi-particle configurations do not contribute to the sum rules (14) and (22) in the long wave-

length limit and we obtain the equations

$$\langle 0|a_k|k\rangle\langle k|n_{-k}|0\rangle - \langle 0|n_{-k}|-k\rangle\langle -k|a_k|0\rangle = n_0^{1/2} + O(k^b) \tag{23}$$

$$\langle 0|a_k|k\rangle\langle k|n_{-k}|0\rangle + \langle 0|n_{-k}|-k\rangle\langle -k|a_k|0\rangle = \\ = n^{1/2}\left(\frac{n}{n_0}\right)^{1/2}\left(\frac{\partial n_0}{\partial n}\right)_\eta \frac{k}{2mc} + O(k^{1+b}), \tag{24}$$

where $b \geqq a$ (this condition will be sharpened in the following).* By using Equs. (20) and (21) we find for the leading term in the small k limit

$$\langle 0|a_k|k\rangle = -\langle -k|a_k|0\rangle = \left(\frac{n_0}{2n}\frac{mc}{k}\right)^{1/2}. \tag{25}$$

We note that to obtain this result it has been necessary only that the right hand side of Equ. (15) is not more singular than k^{-2}. By substituting Equs. (20) and (25) into the sum rule (15) it turns out that the one phonon state alone is responsible for the k^{-2} singular term. As a consequence the matrix elements $\langle 0 \mid a_k \mid \alpha\rangle$ and $\langle \alpha \mid a_k \mid 0\rangle$ for a multi-particle configuration can only be less singular than k^{-1}, which involves $b > a$.

Let us consider now the particle distribution function

$$N_k \equiv \langle 0|a_k^+ a_k|0\rangle = |\langle -k|a_k|0\rangle|^2 + \sum_\alpha{}' |\langle \alpha|a_k|0\rangle|^2, \tag{26}$$

where the primed summation symbol means that the summation is extended over the multi-particle configurations. According to our above results, the leading term of N_k in the small k limit is as follows

$$N_k = \frac{n_0}{n}\frac{mc}{2}\frac{1}{k}. \tag{27}$$

This agrees with the result by GAVORET and NOZIÈRES [4] obtained by analyzing the structure of the perturbation expansion and has also been derived in [5] by means of an application of quantum hydrodynamics. The derivation presented here in our opinion uses the weakest assumptions.

To obtain further results we have to take $a \geqq 1$, the lower limit of which corresponds to assuming that $\langle \alpha|\mathbf{J}_k|0\rangle$ for a multi-particle configuration has

* From now on a is always considered to refer to multi-particle configurations.

a power series expansion in $\mathbf{k}$ [3]. In that case $b > 1$. Furthermore from the f sum rule (19) and Equ. (18) we find*

$$(\langle 0|n_k|k\rangle)^2 = \frac{1}{\omega_k}\left(\frac{nk^2}{2m} + O(k^4)\right) \tag{28}$$

and thus Equs. (23) and (24) give

$$(\langle -k|a_k|0\rangle)^2 + (\langle 0|a_k|k\rangle)^2 = \omega_k\left(\frac{n_0}{n}\,\frac{1}{k^2} + O(k^0)\right).$$

After substituting this into Equ. (15) we arrive at the conclusion that $\langle 0|a_k|\alpha\rangle$ and $\langle \alpha|a_k|0\rangle$ cannot be singular in the small k limit for multi-particle configurations and consequently $b \geqq 2$.

Let us assume the phonon dispersion law in the form

$$\omega_k = ck(1 + O(k^d)), \qquad d > 0.$$

Then according to Equ. (28) we have a term in $\langle 0|n_k|k\rangle$ proportional to $k^{d+1/2}$ and the solution of Equs. (23) and (24) can be written in the following form

$$\langle -k|a_k|0\rangle = -\left(\frac{n_0}{n}\,\frac{mc}{2}\right)^{1/2}\frac{1}{k^{1/2}} + \frac{1}{2}\left(\frac{n}{n_0}\,\frac{1}{2\,mc}\right)^{1/2}\left(\frac{\partial n_0}{\partial n}\right)_\eta k^{1/2} + \\ + O(k^{b-1/2}) + O(k^{d-1/2}) \tag{29}$$

and

$$\langle 0|a_k|k\rangle = \left(\frac{n_0}{n}\,\frac{mc}{2}\right)^{1/2}\frac{1}{k^{1/2}} + \frac{1}{2}\left(\frac{n}{n_0}\,\frac{1}{2\,mc}\right)^{1/2}\left(\frac{\partial n_0}{\partial n}\right)_\eta k^{1/2} + \\ + O(k^{b-1/2}) + O(k^{d-1/2}). \tag{30}$$

We recall that $b \geqq 2$. The last terms do not give contribution to Equs. (29) and (30) to the order $k^{1/2}$ if $d > 1$. (This is fulfilled by the usual expression for the phonon dispersion law, which assumes that ω_k^2 has a power series expansion in k^2 giving $d = 2$.) Then Equs. (26) and (29), together with the result that the contribution of the multi-particle configurations to N_k is not singular, give in the small k limit

$$N_k = \frac{n_0}{n}\,\frac{mc}{2}\,\frac{1}{k} + M \tag{31}$$

with

$$M \geqq -\frac{1}{2}\left(\frac{\partial n_0}{\partial n}\right)_\eta. \tag{32}$$

* We neglect the effects connected with the damping of the phonons, which being proportional to $\mathbf{k}^5$ at zero temperature (see for a review [2]) might not influence the long wavelength properties of the system to the order we are going to calculate them.

For liquid helium presumably $(\partial n_0/\partial n) < 0$, while in the BOGOLIUBOV approximation for the dilute Bose gas (see below) we have $(\partial n_0/\partial n) \approx 1$.

Finally let us examine the sum rule [9], [10]

$$\sum_{\alpha} \omega_{\alpha 0} \left(\langle 0|a_k|\alpha\rangle \langle \alpha|n_k|0\rangle + \langle 0|n_k|\alpha\rangle \langle \alpha|a_k|0\rangle \right) = \frac{n_0^{1/2} k^2}{2m} \tag{33}$$

which is a counterpart of the f sum rule coming from the continuity equation and the presence of the condensate. By inserting the results (21), (29) and (30) we can see that this sum rule is not exhausted by the one phonon mode in the long wavelength limit unless (n_0/n) is equal to $(\partial n_0/\partial n)$.

We conclude this Section with some remarks concerning the BOGOLIUBOV approximation [11]. The ground state $|0\rangle$ is the vacuum state of quasiparticles, i.e.

$$\alpha_k|0\rangle = 0 .$$

The quasiparticle operator α_k is given by the Bogoliubov canonical transformation:

$$\alpha_k = u_k a_k - v_k a_{-k}^{+} ,$$

where

$$\left.\begin{matrix} u_k^2 \\ v_k^2 \end{matrix}\right\} = \frac{1}{2}\left[\pm 1 + \left(1 + \frac{m^2 c^4}{E_k^2}\right)^{1/2} \right], \tag{34}$$

$$u_k v_k = -\frac{mc^2}{2 E_k} .$$

Here E_k is the quasiparticle energy given by

$$E_k = \sqrt{c^2 k^2 + \left(\frac{k^2}{2m}\right)^2} , \tag{35}$$

where the sound velocity c is related to the interparticle potential V, taken to be k — independent in the small k region we are interested in, by

$$c^2 = \frac{n_0 V}{m} . \tag{36}$$

One can easily calculate the matrix elements between the ground state and the one quasiparticle state:

$$\langle 0|n_k|k\rangle = n_0^{1/2}(u_k + v_k) , \tag{37}$$

$$\langle 0|a_{-k}^{+}|k\rangle = v_k , \tag{38}$$

$$\langle 0|a_k|k\rangle = u_k , \tag{39}$$

where we have used as an abbreviation

$$|k\rangle = \alpha_k^+ |0\rangle \, .$$

Furthermore, one can easily check that (38) and (39) are the only non zero matrix elements of particle creation and annihilation operators. By substituting the expressions (34)—(39) into Equs. (22) and (33) we can see that they become identities.

In the long wavelength limit we get from Equs. (34), (35) that

$$\left.\begin{matrix} u_k \\ v_k \end{matrix}\right\} = \pm \frac{1}{\sqrt{2}} \left(\frac{mc}{k}\right)^{1/2} + \frac{1}{\sqrt{8}} \left(\frac{k}{mc}\right)^{1/2} + \ldots \, .$$

It is well known that to the extent that the Bogoliubov approximation is valid, one can take $n_0 \approx n$, and c as given by Equ. (36) agrees with the macroscopic relationship for the sound velocity: $c^2 = (\partial P/\partial \varrho)$. Thus, one can easily tee that the sum rules (14) and (15) are satisfied and $A = 0$ in this approximasion. Furthermore N_k is given by Equ. (31) with $M = -1/2$ in the small k limit.

REFERENCES

1. N. N. Bogoliubov, On the Problem of Hydrodynamics of a Superfluid, Dubna preprint, 1963.
2. P. C. Hohenberg and P. C. Martin, Annals of Physics, **34**, 291, 1965.
3. D. Pines, in 1962 Cargese Lectures in Theoretical Physics, W. A. Benjamin Inc., New York, 1963; See furthermore: D. Pines, in Many-Body Theory, Syokabo, Tokyo and Benjamin, New York, 1966.
4. J. Gavoret and P. Nozières, Annals of Physics, **28**, 349, 1964.
5. R. A. Ferrell, N. Menyhárd, H. Schmidt, F. Schwabl and P. Szépfalusy, Annals of Physics, 565, 1968.
6. N. N. Bogoliubov, Quasi-averages in the Problems of Statistical Mechanics, Dubna Preprint, 1961.
7. See e.g.: D. Pines and P. Nozières, The Theory of Quantum Liquids I, W. A. Benjamin, Inc., New York, 1966.
8. V. A. Krasnikov, DAN, USSR, **174**, 1037, 1967.
9. F. de Pasquale, G. Jona-Lasinio and E. Tabet, Annals of Physics, **33**, 81, 1965.
10. H. Wagner, Z. Physik, **195**, 273, 1966.
11. N. N. Bogoliubov, J. Phys. USSR, **9**, 23, 1947. See furthermore: D. Pines, The Many-Body Problem, W. A. Benjamin, Inc., New York, 1962.

ПРАВИЛА СУММ И ИХ ПРИМЕНЕНИЕ В ТЕОРИИ СВЕРХТЕКУЧЕГО ГЕЛИЯ

П. СЕПФАЛУШИ

Резюме

Первая часть данной работы посвящена исследованию функций статической реакции сверхтекучего гелия в гидродинамической области, которое результирует в выходе новое правило сумм. Правила сумм затем специализированы к нулевой температуре и использованы при определении матричных элементов операторов рождения и уничтожения частиц между основным и одним квазичастичным состоянием в пределе большой длины волны. Проводилось исследование функции распределения частиц и кроме вычисления начального члена, удалось определить низшую границу следующего члена в выражении для маленьких волновых чисел.

Acta Physica Academiae Scientiarum Hungaricae, Tomus 27, pp. 309—322 (1969)

OSCILLATIONS OF A RELATIVISTIC ELECTRON PLASMA IN AN EXTERNAL MAGNETIC FIELD*

By

G. Roth**

INSTITUTE FOR THEORETICAL PHYSICS, ROLAND EÖTVÖS UNIVERSITY, BUDAPEST

(Received 20. II. 1969)

A relativistic treatment of plasma oscillations is presented. The calculations are carried out for the so called low β plasma, where the pressure is negligible as compared to the magnetic energy density. The covariant dispersion relations are derived and their meaning is compared to that of the classical ones.

§ 1. Introduction

The aim of this work is to study the small amplitude waves of an electron plasma on the basis of relativistic dynamics, to deduce the covariant forms of the dispersion relations of the typical modes of oscillations.

In order to motivate the necessity of the relativistic treatment we mention only a theoretical remark. As is well known, the problem of plasma oscillations is studied in classical plasma physics by means of the Newtonian equations of motion and some restricted, approximative forms of Maxwell's equations. The results of this classical treatment are in general well compatible with the experimental data, a discrepancy arises in the fact, that Newtonian equations are Galilei invariant while Maxwell's equations are Lorentz invariant. So it can well happen that this half Galileian half Lorentzian treatment will lead to false results. Therefore it is desirable to investigate this problem in a fully covariant manner. It is generally cited that relativistic effects become important only at high temperatures, which statement is only the half of the truth. Relativistic effects will be important also in the case when the involved energies — e.g. electromagnetic energy, compression energy, etc. — are comparable with the rest energy of the system.

Here for the sake of simplicity we consider an ideal electron plasma and we shall investigate the possible modes in a covariant manner. It is supposed that the electron gas is a classical one, and it is neutralized by a homogeneous positive background which is immobile in the rest frame and does not take part

* Dedicated to Prof. P. Gombás on his 60th birthday.

** Present address: Institute for Theoretical Physics, University of Mainz, BRD.

in the oscillations. Restriction is made to the so called low β plasma case, i.e. it is supposed that the density of electromagnetic energy is much greater than the compression energy, so the latter is omitted for the moment. Since the pressure is neglected, there will be no information concerning the acoustic waves of the electron plasma in this model.

In the treatment we shall consider the oscillations of the electron plasma both without and with external magnetic fields and in the discussion of the results comparison will be made with the classical dispersion relations.

§ 2. Fundamental equations

When the electron gas is not too dense the electromagnetic field can be described by the field tensor

$$F_{ik} = \begin{Vmatrix} 0 & H_z & -H_y & -iE_x \\ -H_z & 0 & H_x & -iE_y \\ H_y & -H_x & 0 & -iE_z \\ iE_x & iE_y & iE_z & 0 \end{Vmatrix}, \tag{1}$$

which satisfies the source free group of Maxwell's equations:

$$\varepsilon_{iklm}\, \partial_k F_{lm} = 0\,. \tag{2}$$

Here $\partial_k = \partial/\partial x_k$, $x_4 = ict$ and ε_{iklm} is the completely antisymmetric Levi-Civita tensor with $\varepsilon_{1234} = +1$. The summation convention is understood for doubly occurring Latin indices.

The electromagnetic field F_{ik} is coupled to its sources by Maxwell's second equation

$$\partial_k F_{ik} = \frac{4\pi}{c} j_i, \tag{3}$$

where the current four vector

$$i_i = env_i\,, \tag{4}$$

e being the electronic charge, the invariant scalar n is the density of electrons (measured in the comoving frame of reference), and v_i is the four velocity of the electrons.

The equations of motion is

$$\partial_k(nv_i\, v_k) = \frac{en}{mc} F_{ik}\, v_k\,, \tag{5}$$

where the pressure term is omitted. This approximation is valid if

$$\beta = \left| \frac{p}{\frac{1}{8\pi} \vec{H}^2} \right| = \left| \frac{p}{\frac{1}{16\pi} F_{rs} F_{rs}} \right| \ll 1,$$

i.e. we consider a low β plasma. Here m is the rest mass of the electron. The velocity four vector must satisfy the equation

$$v_r v_r = - c^2 . \tag{6}$$

The charge conservation

$$\partial_i \partial_k F_{ik} = \frac{4\pi e}{c} \partial_i (n v_i) = 0$$

leads to

$$v_k \partial_k v_i = \frac{e}{mc} F_{ik} v_k \tag{7}$$

the final form of the equation of motion we use.

The extension of the electron plasma is supposed to be infinite, to avoid boundary value problems for the moment.

The system of fundamental equations of the low β plasma is then

$$\left.\begin{aligned} &\varepsilon_{iklm} \partial_k F_{lm} = 0 \\ &\partial_k F_{ik} = \frac{4\pi e}{c} n v_i \\ &\partial_k (n v_k) = 0 \\ &v_r v_r = - c^2 \\ &v_k \partial_k v_i = \frac{e}{mc} F_{ik} v_k \end{aligned}\right\}, \tag{8}$$

which is a coupled system of nonlinear partial differential equations.

In order to linearize (8) we suppose that the electron gas is in a nonperturbed equilibrium state. In this state its charge is completely neutralized by the immobile positive background. There is no charge, no current without external perturbation. In covariant way this reads

$$(N e^+ + N e^-) u_k = 0 ,$$

where u_k is the electron equilibrium four velocity, N the equilibrium particle

density. If F_{ik} denotes the field in the equilibrium system, then in the unperturbed state

$$\mathring{F}_{ik}\, u_k = 0\,.$$

Therefore $(\mathring{F}_{ik},\ u_k,\ N) = (\text{const})$ is a solution to (8), if $u_k u_k = -c^2$ in the unperturbed equilibrium state.

Then we superimpose to this state some small amplitude disturbances $(\delta F_{ik},\ \delta u_k,\ \delta n)$ and retain those terms where only one disturbance occurs. This procedure leads to

$$\left.\begin{aligned}
&\varepsilon_{iklm}\,\partial_k\,\delta F_{lm} = 0\\
&\partial_k\,\delta F_{ik} = \frac{4\pi e}{c}\,(N\delta u_i + u_i\,\delta n)\\
&N\,\partial_r\,\delta u_r + n_r\,\partial_r\,\delta n = 0\\
&u_k\,\partial_k\,\delta u_i = \frac{e}{mc}\,(u_k\,\delta F_{ik} + \mathring{F}_{ik}\,\delta u_k)\\
&u_r\,\delta u_r = 0
\end{aligned}\right\}, \tag{9}$$

which is a coupled system of linear partial differential equations for the disturbances. In order to solve these coupled first order homogeneous linear differential equations we use the trial functions

$$\begin{Bmatrix}\delta n\,(x_r)\\ \delta u_i\,(x_r)\\ \delta F_{ik}\,(x_r)\end{Bmatrix} = \begin{Bmatrix}\delta n\\ \delta u_i\\ \delta F_{ik}\end{Bmatrix} \exp\ ik_r\,x_r \tag{10}$$

stating the validity of the superposition principle. Here δn, δu_i and δF_{ik} will be appropriately chosen constants, the determination of which requires a nontrivial solution of the algebraic system of homogeneous equations

$$\left.\begin{aligned}
&\varepsilon_{iklm}\,k_k\,\delta F_{lm} = 0\\
&k_k\,\delta F_{ik} = \frac{4\pi e}{ic}\,(N\delta u_i + u_i\,\delta n)\\
&Nk_r\,\delta u_r + u_r\,k_r\,\delta n = 0\\
&iu_r\,k_r\,\delta u_i = \frac{e}{mc}\,u_r\,\delta F_{ir} + \frac{e}{mc}\ \mathring{F}_{ik}\,\delta u_k\\
&u_r\,\delta u_r = 0
\end{aligned}\right\}. \tag{11}$$

Before looking for the solutions of (11), some transformations will be useful.

The decomposition of the first equation of (11) gives

$$k_k \delta F_{lm} + k_m \delta F_{kl} + k_l \delta F_{mk} = 0. \tag{12}$$

Then multiplication with u_m and summation over m provides an equation for the quantity

$$\delta \Phi_i = u_k \delta F_{ik}, \tag{13}$$

which gives the perturbation of the electric field in the comoving frame, namely

$$L \delta F_{kl} = k_l \delta \Phi_k - k_k \delta \Phi_l, \tag{14}$$

where

$$L = k_r u_r. \tag{15}$$

This combined with the second equation of (11) gives

$$k_r k_r \delta \Phi_i - k_i k_r \delta \Phi_r = \frac{4\pi e L}{ic} (N \delta u_i + u_i \delta n). \tag{16}$$

Finally we introduce the notation

$$\Omega_{ik} = \frac{e}{mc} \mathring{F}_{ik}. \tag{17}$$

Ω_{ik} is an antisymmetric tensor, built up from the equilibrium values of the electromagnetic fields. Since in equilibrium there is no electric field at all, we have

$$\Omega_{ik} u_k = \frac{e}{mc} \mathring{F}_{ik} u_k \equiv 0.$$

In other words Ω_{ik} contains only the components of the electron cyclotron frequency $\vec{\omega}_c = (e/mc)\vec{H}_0$, or the components of the external magnetic field.

With this we write the fourth equation of (11) in the form

$$iL \delta u_i = \frac{e}{mc} \delta \Phi_i + \Omega_{ik} \delta u_k. \tag{18}$$

§ 3. Oscillations of the relativistic electron plasma when no external magnetic field is present

If there is no external magnetic field, we have $\Omega_{ik} = 0$ and the fundamental algebraic equations are

$$\left.\begin{aligned} &(Q^2 \delta_{ir} - k_i k_r) \delta \Phi_r = \frac{4\pi e L}{ic} (N \delta u_i + u_i \delta n) \\ &L \delta n + N k_r \delta u_r = 0 \\ &iL \delta u_i = \frac{e}{mc} \delta \Phi_i \end{aligned}\right\}, \tag{19}$$

where

$$Q^2 = k_r k_r . \tag{20}$$

It is easy to see that (19) incorporates all the equations of (11), making use of (13) and (14).

The system (19) can be written in the form

$$\delta u_i = \frac{e}{imc\,L} \delta \Phi_i , \tag{21}$$

$$\delta n = - \frac{Ne}{imcL^2} k_r \delta \Phi_r \tag{22}$$

and

$$\left[Q^2 \delta_{ir} - k_i k_r + \frac{\omega_\pi^2}{c^2} \delta_{ir} - \frac{\omega_\pi^2}{c^2} \frac{u_i k_r}{L} \right] \delta \Phi_r = 0 , \tag{23}$$

where

$$\omega_\pi^2 = \frac{4\pi e^2 N}{m} \tag{24}$$

is the electron plasma frequency, an invariant scalar. One has to solve (23) first and then use (21) and (22) to derive the accompanying perturbations of the density and the velocity.

Instead of attacking directly Equ. (23) we decompose it into transverse and longitudinal perturbations.

A transverse oscillation of $\delta \Phi_r$ satisfies

$$k_r \delta \Phi_r = 0 , \tag{25}$$

whereas the longitudinal one obeys

$$(k_r k_r \delta_{is} - k_i k_s) \delta \Phi_s = 0. \tag{26}$$

Therefore the *transverse amplitude* is chosen by the projection tensor

$$\Pi_{ij} = \left(\delta_{ij} - k_i k_j \frac{1}{k_p k_p} \right) . \tag{27}$$

Application of (27) to (23) gives

$$\left(Q^2 + \frac{\omega_\pi^2}{c^2} \right) \Pi_{ir} \delta \Phi_r = 0$$

and a nontrivial transverse oscillation can exist if and only if

$$c^2 k_r k_r + \omega_\pi^2 = 0. \tag{28}$$

This equation is the covariant dispersion relation of a transverse plasma oscillation without external magnetic field. In the rest frame

$$k_r = \left(k_1, k_2, k_3, \frac{i}{c}\Omega\right)$$

and (28) will give

$$\Omega^2 = \omega_\pi^2 + c^2 \vec{k}^2$$

in accordance with the classical results. This transverse perturbation of $\delta\Phi_r$ is accompanied neither by density fluctuation nor longitudinal velocity fluctuation as it is guaranteed by (21) and (22).

In the case of a longitudinal oscillation from (23) we obtain by means of multiplication with u_i, and some manipulation

$$(\omega_\pi^2 - L^2)\, k_r\, \delta\Phi_r = 0\,, \tag{29}$$

where $k_r \delta\Phi_r \neq 0$, therefore

$$(k_r u_r)^2 = \omega_\pi^2$$

is the covariant dispersion relation of a longitudinal plasma oscillation without external magnetic field. In the rest frame this reduces to the classical form:

$$\Omega^2 = \omega_\pi^2\,.$$

This longitudinal perturbation of $\delta\Phi_r$ is accompanied by a longitudinal velocity fluctuation and a density fluctuation, as it can be seen from (21) and (22), but there is no transverse perturbation.

In the absence of external fields, the longitudinal and transverse oscillations decouple, and the covariant dispersion relations reduce to the classical ones in the rest frame.

§ 4. Oscillations of the relativistic electron plasma in the presence of an external magnetic field

a) *Reduction of the equations*

Let us suppose that the electron plasma is subjected to an external magnetic field in the rest frame. Then the basic algebraic equations we have to

solve are the following

$$L\delta n + Nk_r\,\delta u_r = 0\,, \tag{30}$$

$$iL\,\delta u_i = \frac{e}{mc}\,\delta\Phi_i + \Omega_{ik}\,\delta u_k\,, \tag{31}$$

$$(Q^2\,\delta_{ik} - k_i\,k_k)\;\delta\Phi_r = \frac{4\pi eL}{ic}\,(N\delta u_i + u_i\,\delta n)\,. \tag{32}$$

We use (31) to express δu_i in terms of $\delta\Phi_i$. Since

$$\frac{e}{mc}\,\delta\Phi_i = (iL\,\delta_{ik} - \Omega_{ik})\,\delta u_k$$

and

$$\mathrm{Det}\,\{iL\,\delta_{ik} - \Omega_{ik}\} = L^2\left(L^2 + \frac{1}{4}\,\Omega_{rs}\,\Omega_{sr}\right) \neq 0\,,$$

we have

$$\delta u_r = \frac{L^2\,\delta_{ir} - iL\,\Omega_{ri} - \Omega_{rs}\,\Omega_{si} + \dfrac{1}{4}\,\delta_{ri}\,\Omega_{kl}\,\Omega_{lk}}{iL\left(L^2 + \dfrac{1}{4}\,\Omega_{pq}\,\Omega_{qp}\right)}\,\frac{e}{mc}\,\delta\Phi_i\,. \tag{33}$$

Making use of (31)

$$\delta n = -\frac{N}{L}\,k_r\,\delta u_r$$

and (33) we arrive at

$$\left[\left(Q^2 + \frac{\omega_\pi^2}{c^2}\right)\delta_{ir} - k_i\,k_r - \frac{\omega_\pi^2}{c^2}\left\{\frac{1}{L}\,u_i\,k_r + \right.\right.$$
$$\left.\left. + \frac{iL\,\Omega_{ir} + \Omega_{il}\,\Omega_{lr}}{L^2 + \dfrac{1}{4}\,\Omega_{pq}\,\Omega_{qp}} - \frac{u_i\,k_m}{L}\,\frac{iL\,\Omega_{mr} + \Omega_{ml}\,\Omega_{lr}}{L^2 + \dfrac{1}{4}\,\Omega_{pq}\,\Omega_{qp}}\right\}\right]\delta\Phi_r = 0. \tag{34}$$

In this model all information concerning plasma oscillations in the presence of external magnetic field is contained in (34). Before discussing the special modes of oscillation, however, it will be advantageous to simplify (34) by means of the introduction of a convenient four vector in the place of Ω_{pq}, as we have done with the introduction of Φ_i.

Starting from $F_{ik} = -F_{ki}$, and following the idea of A. M. PRATELLI [1], we have defined

$$\Phi_i = F_{ik}\,u_k$$

which in the rest frame has the components

$$\Phi_i = (E_x, E_y, E_z, 0) .$$

If we define the dual tensor of F_{ik} by the relation

$$F^*_{ik} = \frac{1}{2} \varepsilon_{ikrs} F_{rs}$$

we have the opportunity to define a four vector

$$h_i = -\frac{1}{ic} F^*_{ik} u_k$$

which in the rest frame has the components

$$h_i = (H_x, H_y, H_z, 0) .$$

Then it is possible to write F_{ik} in terms of Φ_i and h_i. It is easy to verify

$$F_{mn} = \frac{i}{c} \varepsilon_{ilmn} h_i u_l + \frac{1}{c} (\Phi_n u_m - \Phi_m u_n) .$$

Applying this to the particular $\overset{\circ}{F}_{ik}$, we have

$$\Omega_{mn} = \frac{i}{c} \varepsilon_{ilmn} \omega_i u_l , \tag{35}$$

where in the rest frame

$$\omega_i = \left(\frac{eH_x}{mc}, \frac{eH_y}{mc}, \frac{eH_y}{mc}, 0 \right) \tag{36}$$

and may therefore be called the cyclotron frequency four vector. We need other relations, too, namely

$$-\frac{1}{4} \Omega_{rs} \Omega_{rs} = \omega_l \omega_l \tag{37}$$

and since $\omega_q u_q = 0$ in all inertial frames, we have

$$\Omega_{mt} \Omega_{tr} = \frac{1}{c^2} \left[\omega_p \omega_p (u_m u_r - c^2 \delta_{mr}) + c^2 \omega_r \omega_m \right] . \tag{38}$$

Making use of these notations (34) can be written in the form

$$\left[\left(Q^2+\frac{\omega_\pi^2}{c^2}\right)\delta_{ir}-k_i k_r-\frac{\omega_\pi^2}{c^2}\left\{\frac{u_i k_r}{L}+\frac{L}{c}\,\frac{1}{L^2-\omega_q\omega_q}\,\varepsilon_{plir}\,\omega_p u_l+\right.\right.$$
$$+\frac{1}{L^2-\omega_q\omega_q}(\omega_r\omega_i-\omega_p\omega_p\delta_{ri})-$$
$$-\frac{1}{c}u_i k_m\,\frac{1}{L^2-\omega_q\omega_q}\,\varepsilon_{plmr}\,\omega_p u_l- \tag{39}$$
$$\left.\left.-\frac{1}{L}u_i k_m\,\frac{1}{L^2-\omega_q\omega_q}(\omega_r\omega_m-\omega_p\omega_p\delta_{rm})\right\}\right]\delta\Phi_r=0\,.$$

b) *Discussion of the oscillations*

I. Transverse waves. For transverse oscillations the equation (39) reduces to

$$\left[\left(Q^2+\frac{\omega_\pi^2}{c_2}+\frac{\omega_\infty^2}{c^2}\,\frac{1}{L^2-\omega_q\omega_q}\right)\delta_{ir}-\right.$$
$$-\frac{\omega_\pi^2}{c^2}\left\{\frac{L}{c}\,\frac{1}{L^2-\omega_q\omega_q}\,\varepsilon_{plir}\,\omega_p u_l+\frac{\omega_i\omega_r}{L^2-\omega_q\omega_q}-\right. \tag{40}$$
$$\left.\left.-\frac{\varepsilon_{plmr}\,u_i k_m\,\omega_p u_l}{c(L^2-\omega_q\omega_q)}-\frac{u_i k_m\omega_m\omega_r}{L(L^2-\omega_q\omega_q}\right\}\Pi_{rl}\,\delta\Phi_l=0$$

where $\Pi_{rl}\delta\Phi_l$ is the transverse part of $\delta\Phi_i$.

The transverse oscillations may be decomposed into two cases, polarized perpendicularly

$$\omega_r\,\delta\Phi_r=0 \tag{41}$$

or parallel

$$(\delta_{ir}-(\omega_s\omega_s)^{-1}\omega_i\omega_r)\,\delta\Phi_r=0, \tag{42}$$

to the external field ω_s. In the case (41), Equ. (40) takes the simpler form

$$(T\delta_{ir}+R\varepsilon_{plir}\,\omega_p u_l+S\varepsilon_{plmr}\,\omega_p u_l k_m u_i)\,\Pi_{rt}\,\delta\Phi_t=0\,, \tag{43}$$

where

$$T=Q^2+\frac{\omega_\pi^2}{c^2}\left(1+\frac{\omega_p\omega_p}{L^2-\omega_q\omega_q}\right), \tag{44}$$

$$R=-\frac{\omega_\pi^2}{c^2}\,\frac{L}{c}\,\frac{1}{L^2-\omega_q\omega_q}\,, \tag{45}$$

$$S=\frac{\omega_\pi^2}{c^2}\,\frac{1}{L^2-\omega_q\omega_q}\,. \tag{46}$$

In this (41) case, we may consider *propagation along the external magnetic field*, $k_r = \alpha\omega_r$, with a convenient constant α. So (43) takes the form

$$(T\delta_{ir} + R\varepsilon_{plir}\,\omega_p\,u_l)\,\Pi_{rt}\,\delta\Phi_t = 0\,. \tag{47}$$

The existence of a nontrivial solution to Equ. (47) is expressed by the vanishing of its determinant:

$$\left(\frac{T}{R}\right)^2\left\{\left(\frac{T}{R}\right)^2 - c^2\,\omega_p\,\omega_p\right\} = 0. \tag{48}$$

From $T = 0$ we obtain

$$c^2\,k_r\,k_r\,\{(u_s\,k_s)^2 - \omega_s\,\omega_s\} + \omega_\pi^2\,(u_s\,k_s)^2 = 0. \tag{49}$$

This is the covariant dispersion relation of a transverse plasma oscillation, which propagates along the external magnetic field. In the rest frame (49) gives

$$\Omega^2 = c^2\,\vec{k}^2 + \omega_\pi^2\,\frac{\Omega^2}{\Omega^2 - \omega^2}\,. \tag{50}$$

If $V = \Omega/k$ means phase velocity of the wave (49) in the rest frame of the plasma, then according to the dispersion relation (49)

$$\left(\frac{V}{c}\right)^2 = \frac{1}{1 - \dfrac{\omega_\pi^2}{\Omega^2 - \omega_c^2}}\,. \tag{51}$$

This mode of oscillation cannot propagate in the frequency interval

$$\sqrt{\omega_c^2 + \omega_\pi^2} < \Omega < \omega_c\,. \tag{52}$$

A prototype of this propagating wave in low frequency approximation ($\Omega/\omega_c \ll 1$) is the Alfvén wave, for which (50) yields

$$\Omega^2 = \frac{k^2\,c_A^2}{1 + \dfrac{c_A^2}{c^2}}\,, \tag{53}$$

where

$$c_A^2 = \frac{H_0^2}{4\pi\,mN}$$

is the square of the Alfvén velocity.

This filter type behaviour of the electron plasma for this frequency interval is in connection with the cyclotron resonance.

Always in the case (41) the vanishing of the second factor in (48) yields

$$k_r k_r + \frac{\omega_\pi^2}{c^2} \frac{(k_r u_r)^2 \pm \omega k_r u_r}{(k_p u_p)^2 - \omega^2} = 0, \tag{54}$$

where $\omega = \omega_c = (\omega_s \omega_s)^{1/2}$. In the rest frame we obtain

$$\Omega^2 = c^2 \vec{k}^2 + \omega_\pi^2 \frac{\Omega}{\Omega \pm \omega}, \tag{55}$$

the two signs corresponding to the two different circular polarizations. This type of oscillation will not propagate if

$$\omega < \Omega < \frac{1}{2}\left[-|\omega| + \sqrt{\omega^2 + 4\omega_\pi^2}\right]$$

for the upper sign and

$$\Omega > \frac{1}{2}\left[-|\omega| + \sqrt{\omega^2 + 4\omega_\pi^2}\right]$$

for the lower sign.

The other type of class transverse waves polarized perpendicularly to ω_r contains the ones which *propagate across the external magnetic field*. In this case $k_r \omega_r = 0$, and the relevant equation is:

$$0 = \left[\left(Q^2 + \frac{\omega_\pi^2}{c^2} \frac{L^2}{L^2 - \omega^2}\right) \delta_{ir} - \frac{\omega_\pi^2}{c^3} \frac{1}{L^2 - \omega^2} \{L \varepsilon_{plir} \omega_p u_l - \right.$$

$$\left. - \varepsilon_{plmr} \omega_p u_l u_i k_m\}\right] \delta \Phi_{ir}. \tag{56}$$

Since in this case the covariant dispersion relation would involve the evaluation of the determinant

$$D = \det \{a \delta_{ir} - P_{ir} + u_i R_r\}, \tag{57}$$

where

$$a = \frac{1}{L} \frac{Q^2 + \frac{\omega_\pi^2}{c^2} \frac{L^2}{L^2 - \omega^2}}{\frac{\omega_\pi^2}{c^3} \frac{1}{L^2 - \omega^2}},$$

$$P_i = \varepsilon_{plir} \omega_p u_l, \qquad R_r = \frac{1}{L} k_m P_{mr},$$

we write here only the classical limit of (57):

$$\Omega^2 = c^2 \vec{k}^2 + \omega_\pi^2 \left(\frac{\mu^2}{\Omega^2 - \omega^2} \pm \frac{\omega\Omega}{\Omega^2 - \omega^2} \right), \tag{58}$$

where $\omega = \omega_c = (\omega_s \omega_s)^{1/2}$. The expression (54) is the dispersion relation of the transverse oscillations propagating across and polarized perpendicularly to the external magnetic field.

II. Longitudinal waves. For longitudinal waves k_r and $\delta\Phi_r$ must be parallel, and k_r and ω_r may be either parallel or perpendicular. We can therefore speak of propagation across ($\omega_r k_r = 0$) and along ($\omega_r \| k_r$) the external magnetic field.

In the case of propagation across the magnetic field we have the dispersion relation from (39) (by multiplication with u_i)

$$L^2 = \omega_\pi^2 + c^2 \frac{\omega^2}{L^2 - \omega^2} \tag{59}$$

with $\omega^2 = (\omega_q \omega_q)$. This in covariant form

$$(k_r u_r)^2 = \omega_\pi^2 + c^2 \frac{\omega_q \omega_q}{(k_r u_r)^2 - \omega_q \omega_q}$$

or in the rest frame

$$\Omega^2 (\Omega^2 - \omega^2 - \omega_\pi^2) = 0$$

contains only the classical result.

Finally in the case of propagation along the external magnetic field by multiplication with ω_i we obtain from (39) the dispersion relation

$$c^2 k_r k_r + \omega_\pi^2 = 0 \tag{60}$$

or in the rest frame

$$\Omega^2 = c^2 \vec{k}^2 + \omega_\pi^2$$

being also the classical result.

§ 5. Acknowledgements

These calculations have been carried out during the author's stay at the Institute of Theoretical Physics of the Roland Eötvös University, Budapest. The author is indebted to Prof. TH. NEUGEBAUER and to DR. I. ABONYI for the stimulating discussions, for their encouraging attention and interest in the work.

The author's stay was made possible by a scholarship of the Deutscher Akademischer Austauschdienst, which is gratefully acknowledged.

REFERENCES

1. A. M. Pratelli, Missili, Fasc. 4. August 1961.

КОЛЕБАНИЯ РЕЛЯТИВИСТИЧЕСКОЙ ЭЛЕКТРОННОЙ ПЛАЗМЫ ВО ВНЕШНЕМ МАГНИТНОМ ПОЛЕ

Г. РОТ

Р е з ю м е

Дается релятивистическое рассмотрение колебаний плазмы. Вычисления проведены для так называемой низкой β-плазмы, в случае которой давлением можно пренебречь по сравнению с плотностью магнитной энергии. Выводятся ковариантные дисперсионные соотношения и их смысл сравнивается со значением подобных классических выражений.

Acta Physica Academiae Scientiarum Hungaricae, Tomus 27, pp. 323—344 (1969)

SIMULATION OF THE INFLUENCE OF CORE ELECTRONS BY A PSEUDOPOTENTIAL II*

APPLICATIONS TO SOME MOLECULES WITH TWO AND THREE ATOMS

By

W. A. BINGEL, R.-J. KOCH and W. KUTZELNIGG

THEORETICAL CHEMISTRY GROUP, UNIVERSITY OF GÖTTINGEN. GÖTTINGEN, GERMANY

(Received 20. II. 1969)

Pseudopotential theory is combined with the Hartree—Fock and natural expansion method to calculate the molecular constants D_e, R_e and k_e for Na_2, K_2, NaCs and BeH_2. We treat these molecules as two- or four-electron problems respectively in the pseudopotential field of their cores. We then analyze the energies and wave functions in terms of the contributions of the different natural orbitals to the correlation energy. The calculated equilibrium distances agree well with the experimental ones. The dissociation energies are in better agreement with experiment than those of previous calculations.

1. Introduction

Ab initio calculations are at present possible with rather high accuracy for small molecules and with modest accuracy for large molecules.

On the other hand — since the early days of quantum chemistry — the obvious similarities in the chemical and spectroscopical behaviour of the elements of one column of the periodic system have encouraged people to simplify many-electron theory by dividing the electrons into core and valence electrons [1]. If one limits oneself to a treatment of the valence electrons of an atom or molecule one has to account for a twofold influence of the inner electrons. On one hand they shield part of the nuclear charge for the valence electrons, on the other hand the Pauli principle requires that the valence orbitals are orthogonal to the core orbitals.

The last requirement has already been recognized in 1935 by H. HELLMANN [1] and P. GOMBÁS [2] who independently developed the concept of pseudopotential theory. They started from expressions for the pseudopotential in terms of the electron density ϱ of the core electrons based on the Thomas-Fermi model. Whereas GOMBÁS refined his expressions and replaced the statistical electron density ϱ by its quantummechanical analogue [3] HELLMANN chose an analytic 'ansatz' with adjustable parameters. He started from the observation that the kinetic and potential energies of a valence-electron cancel to a high extent inside the core region. The logical consequence of this argument would have been to use a cut-off Coulomb potential (cf. Equ. (4)).

* Dedicated to Prof P. GOMBÁS on his 60th birthday.

For other reasons HELLMANN preferred the following analytical form of the pseudopotential:

$$W(r) = -\frac{Z'}{r} + A\frac{e^{-\varkappa r}}{r}, \tag{1}$$

where Z', A and $\varkappa$ are parameters which are adjusted such that the lowest states of the atom are well reproduced. This potential (1) is still being applied [4], but during the last few years many other types of pseudopotentials have been discussed in the literature. With the potential

$$\begin{aligned} W(r) &= \frac{-Z_R}{r}, & r > R_c, \\ &= \infty, & r < R_c, \end{aligned} \tag{2}$$

where R_c is the core radius and Z_R the reduced nuclear charge R. PARSONS and V. WEISSKOPF [5] obtained surprisingly good results for the Rydberg series of alkali atoms. An alternative but related potential is that used by B. J. AUSTIN and H. HEINE [6]

$$\begin{aligned} W(r) &= \frac{-Z_R}{r}, & r > R_c, \\ &= 0, & r < R_c, \end{aligned} \tag{3}$$

in a qualitative discussion of atomic properties in relation to the periodic system. As the discontinuity of this potential at R_c does not seem to be very physical the present authors preferred the so-called 'cut-off' potential

$$\begin{aligned} W(r) &= -\frac{Z_R}{r}, & r > R_c, \\ &= -\frac{Z_R}{R_c}, & r < R_c. \end{aligned} \tag{4}$$

In the first part of this series [7] (hereafter referred to as part I) we have used this potential to calculate Rydberg series of alkali-atoms, alkali-like positive ions and ground- and excited states of atomic two-valence electron systems (Be, Mg, Ca).

Rather than to use one of those pseudopotentials that contain adjustable parameters one can also use (as SZASZ and MCGINN [4e] have done for atoms and for molecules) the pseudopotential (Equ. (6)) derived by PHILLIPS and KLEINMANN [8] on the grounds of rigorous quantum mechanics. It turns out

that the behaviour of the pseudopotential inside the core is relatively irrelevant as far as the total energy of the valence electrons in this field is concerned. As A. U. HAZI and S. A. RICE [9] have pointed out, the agreement of the pseudopotential eigenvalues with the correct orbital energies depends more significantly on the proper boundary conditions imposed on the wave function by the pseudopotential than on the behaviour inside the core. This is consistent with the observation (see part I) that pseudopotentials which are very different inside the core lead to quite similar results.

The pseudopotentials just discussed (except the HELLMANN potential*) can be regarded as special cases of the general expression:

$$\begin{aligned} W^n(r) &= \sum_{\nu=0}^{n} a_\nu r^\nu , \qquad r < R_c , \\ &= -\frac{Z_R}{r} , \qquad r > R_c . \end{aligned} \tag{5}$$

By choosing the parameters of this potential appropriately one may hope to combine the advantages of the different types just mentioned. The computation of the necessary matrix elements of this potential with a basis of Gaussian-functions is straightforward (see the Appendix), which is important for the applicability to molecules.

2. General theory

a. *Choice of the pseudopotential*

If, in the atomic case, one wants to take care of the orthogonality of the valence-orbitals to the core orbitals in a quantum-mechanically straightforward way one may use the PHILLIPS—KLEINMANN potential [8]

$$W = U + \sum_{\alpha=1}^{\nu-1} (\epsilon_\nu - \epsilon_\alpha) \, |\Phi_\alpha\rangle\langle\Phi_\alpha| \, . \tag{6}$$

Here U denotes a Coulomb-potential of the atoms, Φ_α are the core orbitals with orbital energies ϵ_α and with valence orbital energy ϵ_ν. Although the derivation of this potential is based on a one-electron model it can also be justified [9], [4b], [4c] in the framework of Hartree—Fock theory. This pseudopotential contains a non-local operator which projects a given function on the core orbitals.

* Note, however, that for $n = 2$ the potential (5) is very close to the HELLMANN potential (1).

The question whether it is justified to replace the correct non-local pseudopotential by a local model potential has been discussed by several authors [4b, 4c, 5, 9]. Actually the model potentials mentioned in the Introduction are either local or just l-dependent, i.e. of the form

$$W = \sum_{l=0} W_l P_l \,, \tag{7}$$

where P is the projection operator on the subspace of orbitals with angular quantum number l. (see also [23]).

Now the question arises how to choose the corresponding pseudopotential for a molecule. As a first approximation one expects it to be a sum of atomic contributions. This question has recently been discussed by SCHWARZ [18] and HAZI and RICE [9c]. (As to earlier work on this question see HARRISON [19] and GOMBÁS [3]). In fact there are only very few practical experiences concerning the relation of the molecular and atomic pseudopotentials and about the role of correction terms [18]. Most practical applications of the pseudopotentials deal with atomic states or solids [21], [9b], [18], except for HELLMANN's early molecular calculations [1]. So far only SZASZ and MCGINN [4e] (see also PREUSS [20]) have contributed to the study of molecular binding, using a pseudopotential approach, namely for the molecules Li_2, Na_2, K_2, LiH, NaH, and KH. The results of these authors encourage one to construct the molecular pseudopotential from those of the constituent atoms. We regard it as sufficiently justified to write our molecular model potential in the form

$$\begin{aligned} W^n(r_{i\alpha}) = \sum_\alpha W_\alpha^n(|\mathbf{r}_i - \mathbf{r}_\alpha|) &= \sum_\alpha \sum_{\nu=0}^{n} a_\nu^\alpha |\mathbf{r}_i - \mathbf{r}_\alpha|^\nu, \quad r_i < R_c^{\alpha,n} \\ &= -\sum_\alpha \frac{Z_R^\alpha}{|\mathbf{r}_i - \mathbf{r}_\alpha|}, \; r_i > R_c^{\alpha,n} \end{aligned} \tag{8}$$

for the i-th electron, where α labels the nuclei, where the a_ν^α are semiempirical parameters and where n, the degree of the polynomial, is fixed in advance. In fact, we only consider the possibilities $n = 0$ and $n = 1$, i.e. we chose either a cut-off Coulomb-potential (W^0) or a potential with a linear repulsive part inside the core region (see Fig. 1).

In part I we have limited ourselves to W^0, i.e. the cutoff Coulomb potential. The results were rather satisfactory for the atomic calculations. However, we found that the second and third s-type Rydberg states were not too well reproduced and that the 'radii' of the ions were somewhat too large. In order to remedy these slight defects we have started investigations with the more general type (8) of pseudopotential which in fact led to still better agreement for the Rydberg series and to smaller 'ionic radii'. Whereas in atoms the nonlocal properties of the pseudopotential can to some extent be accounted for

by the l-dependent form of Equ. (7), for molecules the use of such angular-dependent atomic pseudopotentials in the sum (8) would mean great computational difficulties. Calculation of the matrix elements would imply that every basis orbital has to be expanded in terms of spherical harmonics with respect to any of the present nuclei. In order to avoid these difficulties we have used local (i.e. l-independent) atomic contributions to the potential, namely those that are appropriate for s-orbitals. In the case of Li and Na the p-orbitals (and of course d and higher orbitals) should have a more attractive potential (i.e. a smaller

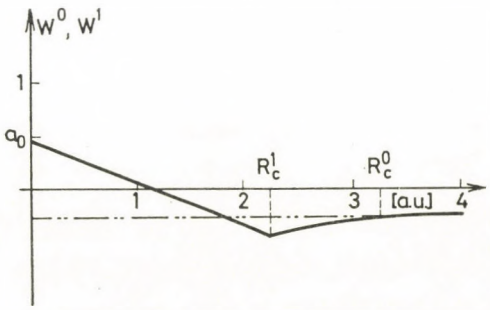

Fig. 1. Pseudopotentials W^0 and W^1 for Na (in correct scale)

cut-off radius). So by using the pseudopotential appropriately for s-orbitals the contribution of the p-orbitals is expected to be underestimated. This should result in an increase of the energy value like that due to the use of a poorer basis. For K, Rb and Cs the cut-off radii corresponding to s- and p-orbitals do not differ much so that a local potential is justified as long as d-contributions to binding are neglegible.

We do not, however, regard the local approximation as completely satisfactory and work is in progress to account for the l-dependence of the atomic pseudopotential in molecular calculations.

In connection with pseudopotential theory the question arises how one should represent the repulsion of the cores. If the cores are rigorously non-overlapping it is justified to replace them by point charges. So far we have not considered effects due to an overlap of the cores. They are supposed to depend exponentially on the distance and to be non-negligible only for very short interatomic distances.

b. *Natural orbital expansions and their combination with the pseudopotential method*

Since by using the pseudopotential method we are left with a rather small number of valence electrons, we can therefore treat this small number by rather sophisticated methods which would not be manageable in a treatment of all

electrons. Let us start with the Hamiltonian for the valence electrons

$$H = -\frac{1}{2}\sum_i \left(\Delta_i - \sum_\alpha W_\alpha^n(r_{i\alpha})\right) + \sum_{i,j}\frac{1}{r_{ij}} \tag{9}$$

in which $\sum_\alpha W_\alpha^n$ stands for the potential of Equ. (8). The HF equations for a valence electron in a closed shell state will then be

$$\left[-\frac{1}{2}\Delta_i - \sum_\alpha W_\alpha^n(r_{i\alpha}) + \sum_j (2J^j - K^j)\right]\Phi_i = \epsilon_i \Phi_i\,, \tag{10}$$

where J^j and K^j are the Coulomb and exchange operators, respectively and Φ_i is a HF pseudo-orbital.

In order to compare the calculated total energies with their experimental counterparts one has to note that the zero of the energy scale corresponds to the sum of the core energies, i.e. the sum of the energies of the ions obtained from the neutral atoms by ionizing off all the valence electrons.

In part I we have obtained good agreement for the orbital energies and the total valence-electron energies between complete Hartree—Fock calculations and HF calculations in the field of a pseudopotential. This agreement turns out to hold in our molecular calculations as well. If we want to get even better agreement with experiment we have, of course, to go beyond the Hartree—Fock approximation. This is why we combined the pseudopotential approach with a CI-calculation in terms of approximate natural orbitals like it has been applied in all electron calculations [13c].

The equations to be solved for a two-valence electron system are those derived previously [13a, b]

$$\begin{aligned}&(h + J')\,\chi_1 = \lambda_{11}\,\chi_1\,,\\ &Q_i\,[n_i(h + K^i) + K^1]\,Q_i\,\chi_i = \lambda_{ii}\,\chi_i\,, \qquad i \neq 1\,.\end{aligned} \tag{11}$$

Here χ_1 is the 'strongly' occupied (spinfree) natural orbital, χ is a 'weakly' occupied one, Q_i a projection operator projecting onto the subspace which is orthogonal to the first (i—1) natural orbitals. h is the one-electron part of the Hamiltonian containing here the pseudopotential, J^i and K^i are Coulomb and exchange operators originating from an electron pair in the space orbital χ_i. $(1k|k1)$ is an exchange integral involving orbital χ_1 and χ_k. The coefficients c_i in the natural expansion of a two-electron function*

$$\Psi(\mathbf{r}_1, \mathbf{r}_2) = \sum_i c_i\,\chi_i(1)\,\chi_i^*(2) \tag{12}$$

* For a generalization to systems with more than two electrons, see [13b].

are finally obtained from the secular equations

$$2c_i h_{ii} + \sum_k c_k (ik|ki) = \mu c_i . \tag{13}$$

The lowest eigenvalue of these equations is the ground-state energy of a two-electron system in the pseudopotential. The equations are solved algebraically, each natural orbital (NO) being represented as a linear combination of a given orthonormal set of one-electron basis functions which are constructed from Gaussian-type orbitals φ. We therefore have to evaluate the matrix elements $(\varphi_a, W_c^n, \varphi_b)$ with respect to the pseudopotential W_c^n.

c. *Calculation of the matrix elements*

The only matrix elements not known from the literature are those involving the pseudo-potential W_α^n. As basis set for the expansion of the pseudo-orbitals χ_i we use Gaussian-type functions of the form

$$\varphi_\mu = \left(\frac{2\alpha_\mu}{\pi}\right)^{3/4} \exp\left[-\alpha_\mu(\mathbf{r}-\mathbf{r}_\mu)^2\right] \quad \mu = a, b, c, \ldots . \tag{14}$$

The following matrix elements have to be calculated

$$W_{ab,c} \overset{\text{def}}{=} (\varphi_a, W_c^n \varphi_b) , \tag{15}$$

where W_c^n stands for the pseudopotential. In this Section we only give the final expression (for a detailed description of the evaluation see Appendix A).

$$\begin{aligned} W_{ab,c} = {} & \sqrt{\frac{\gamma}{\pi}} S_{ab} \left\{ \frac{a_0}{2} \sqrt{\frac{\pi}{\gamma}} \left[\operatorname{erf}\left(\sqrt{\gamma}(r_{cp}+R)\right) - \operatorname{erf}\left(\sqrt{\gamma}(r_{cp}-R)\right)\right] + \right. \\ & + \frac{Z_R}{2\, r_{cp}} \sqrt{\frac{\pi}{\gamma}} \left[\operatorname{erf}\left(\sqrt{\gamma}(r_{cp}+R)\right) + \operatorname{erf}\left(\sqrt{\gamma}(r_{cp}-R)\right)\right] + \\ & + \frac{a_0}{2\gamma r_{cp}} \left[e^{-\gamma(r_{cp}+R)^2} - e^{-\gamma(r_{cp}-R)^2}\right] + \\ & + \sum_{\nu=1}^{n} a_\nu \left[\frac{r_{cp}^\nu}{\sqrt{\gamma}} \left(\int_{-\sqrt{\gamma} r_{cp}}^{\sqrt{\gamma}(R-r_{cp})} e^{-u^2} du + (-1)^\nu \int_{\sqrt{\gamma} r_{cp}}^{\sqrt{\gamma}(R+r_{cp})} e^{-u^2} du \right) + \right. \\ & \left. \left. + \sum_{\lambda=1}^{\nu+1} \binom{\nu+1}{\lambda} r_{cp}^{\nu-\lambda} \gamma^{-\lambda/2+1/2} \left(\int_{\sqrt{\gamma} r_{cp}}^{\sqrt{\gamma}(R-r_{cp})} u^\lambda e^{-u^2} du + (-1)^{\nu-\lambda} \int_{\sqrt{\gamma} r_{cp}}^{\sqrt{\gamma}(R+r_{cp})} u^\lambda e^{-u^2} du \right) \right] \right\} . \end{aligned} \tag{16}$$

In this expression S_{ab} is the overlap integral (φ_a, φ_b)

$$S_{ab} = (\alpha_a \cdot \alpha_b)^{-3/4} A^{3/2} e^{-1/2(r_a - r_b)^2 \cdot A}, \qquad A = -\frac{2\alpha_a \cdot \alpha_b}{\alpha_a + \alpha_b}, \qquad \gamma = \alpha_a + \alpha_b, \tag{17}$$

and

$$\mathbf{r}_{cp} = \mathbf{r}_c - \mathbf{r}_p$$

with

$$\mathbf{r}_p = \frac{1}{\gamma}[\alpha_a A_x + \alpha_b B_x, \alpha_a A_y + \alpha_b B_y, \alpha_a A_z + \alpha_b B_z] \tag{18}$$

which is a point on the line between **a** and **b** where the position vectors of the nuclei are defined by

$$\mathbf{a} = [A_x, A_y, A_z], \quad \mathbf{b} = [B_x, B_y, B_z], \quad \mathbf{c} = [C_x, C_y, C_z]. \tag{19}$$

A further reduction of the integrals in this expression for I is possible if we define $J_\lambda(a, b)$ as

$$J_\lambda(a, b) = \int_a^b u^\lambda e^{-u^2} du.$$

We then obtain the recurrence relation

$$J_\lambda(a, b) = \frac{1}{2}[(\lambda - 2) J_{\lambda-2}(a, b) + a^{\lambda-2} e^{-a^2} - b^{\lambda-2} e^{-b^2}].$$

3. The choice of the parameters for the model potential in the calculations of Na_2, K_2, NaCs and BeH_2

Our method is semiempirical in the sense that the pseudopotential contains at least one parameter to be adjusted using experimental data. Our philosophy is to adjust the pseudopotential from data of the constituent atoms (ionization energy and possibly higher Rydberg levels), but not from data of the molecule that we want to calculate or from any related molecule. For one atom in different molecules the same pseudopotential should be used. The number of parameters should be as small as possible. If we use W^0 then a single parameter describes the particular type of (singly positive) core, in W^1 two parameters are necessary to characterize the core, but it turns out that for different alkali atoms the optimum choice is in good agreement with the relation $a_0 = +Z_R/R_c$ so that we are again left with one parameter. R_c is then fitted to the lowest Rydberg states with the resulting values of Table I.

Table I

Rydberg states of Na, K, Cs resulting from the pseudopotential W^1 (all quantities in a.u.)

Molecule	a_0	a_1	R_c	$-E(1s)$	$-E(2s)$	$-E(3s)$	$-E(4s)$
Na	+ 0.44	— 0.399	2.266	(0.18886)	0.07242	0.0380	0.0233
Na (exp.)				0.18886	0.07158	0.0376	0.0231
K	+ 0.34	— 0.236	2.908	(0.15952)	0.06507	0.0351	0.02189
K (exp.)				0.15952	0.06371	0.0344	0.0216
Cs	+ 0.29	— 0.174	3.394	(0.14310)	0.05864	0.0323	0.0205
Cs (exp.)				0.14310	0.0606	0.0333	0.0208

a_0, a_1, R_c pseudopotential parameters as defined in Equ. (8). To be fitted at $E(1s)$

4. Results of the calculations

One may wonder why in almost all pseudopotential calculations only molecules like Na_2, K_2 etc. have been investigated. Actually they play the same role in pseudopotential theory as does the H_2 molecule in all-electron calculations. In the pseudopotential method these molecules can be treated as pseudo-H_2 problems. Just as in H_2, the 1*s*-pseudo-AO's contribute much more to the binding MO's of the ground state than do any other, in particular *p*-AO's. It is therefore not too crucial to ignore the *l*-dependence of the pseudopotential and to use that local approximation which is justified for *s*-AO's.

NaCs has recently been investigated by W. NEUMANN [22] in molecular beam experiments. This stimulated our interest in a theoretical study of this heteronuclear molecule.

The choice of the orbital basis is suggested by the fact that we are dealing with pseudo-H_2 problems. We actually chose the basis of Gaussians used by HOYLAND [14] in his H_2 calculations omitting, however, the Gaussians with highest α_μ-values which in the genuine H_2 problem take care of the representation of the cusp at the nuclei, but adding some Gaussians with smaller α_μ-values in the binding region as is illustrated in Table II.

Since the pseudopotential does not contain any singularities, the problem of the correct cusp does not matter and a Gaussian basis should be better than in the real H_2 problem. The results of our calculations on diatomics using the two model-potentials W^0 and W^1 can be found in Table III.

The parameters a_0, a_1, R_c are taken from Table I. The dissociation energies D_e are obtained from $D_e = |E_{\mathrm{HF+corr}} + 2I_p|$ where $E_{\mathrm{HF+corr}}$ is the sum of HF- and the correlation energy of the system. The equilibrium distances r_e have been obtained by 4-th degree polynomial fitting, (see Figs. 2—4), from which

Table II

Gaussian basis functions in the calculation of Na_2, K_2, NaCs and BeH_2. The functions are characterized by their 3 group parameters (exponent/group-coefficient/origin relative to the corresponding atoms) (see [23] for further details). The parameters are given for the corresponding atoms, not for the molecules. The groups are not normalized

Na, K, Cs				BeH$_2$			
Group Nr. 1				Group Nr. 1			
type param.				type param.			
(*s*) exp.	4.76	1.24	0.377	(*s*) exp.	30.2	4.76	1.24
coeff.	−0.06275	0.06051	−3.3068	coeff.	0.035598	0.235445	0.804848
orig.	0	0.2	0.08	orig.	0	0	0.12
Group Nr. 2		Nr. 4		Nr. 2		Nr. 5	Nr. 8
(*s*) 0.118		(*s*) 0.03		*H*(*s*) 0.377		(*s*) 2.1847	(*s*) 0.06
1		1		1		1	1
0.19		0.5		0.068		0	0
(*s*) Nr. 3		Nr. 5		Nr. 3		Nr. 6	Nr. 9
0.06		(*s*) 0.01		(*s*) 0.118		(*s*) 0.8590	(*p*) 0.9
1		1		1		1	1
1.0		0.6		0.205		0	0.5
				Be			
				Nr. 4		Nr. 7	Nr. 10
				(*s*) 17.62	5.9326	(*s*) 0.2	(*p*) 0.27
				0.1729	−1.1347	1	1
				0	0	0	1.2

Table III

The computed data for the A_2, AB-type molecules with the pseudopotentials W^1 and W^0. All quantities are in atomic units

	Molecule	1 R_c	2 a_0	3 a_1	4 $-I_p$	5 $-E_{HF}$	6 $-E_{HF+corr.}$
W^1	Na_2	2.266	0.44138	−0.38963	0.3777	0.3759	0.3993
	K_2	2.91	0.3438	−0.2364	0.3190	0.3142	0.3360
	NaCs Na	2.266	0.44138	−0.38963			
	NaCs Cs	3.39	0.2946	−0.1736	0.3319	0.3284	0.3510
W^0	Na_2	3.25	$\frac{-1}{3.25}$	0	0.3777	0.3700	0.3955
	K_2	4.16	$\frac{-1}{4.16}$	0	0.3190	0.3100	0.3320
	Li_2	3.00	$\frac{-1}{3.0}$	0	0.3963	0.3907	0.4147

	Molecule	7[b] $-\varepsilon_{HF}$	8 R_e calc.	9[a] R_e exptl.	10 D_e calc.	11[a] D_e exptl.	12 D_e HF
W^1	Na_2	0.1699	5.78	5.8	0.0216	0.0272	−0.0075
	K_2	0.1401	7.1	7.39	0.0170	0.0192	
	NaCs Na Cs	0.1456	6.9		0.0191		
W^0	Na_2	0.1670	5.8	5.8	0.018	0.0272	−0.0075
	K_2	0.1350	7.1	7.39	0.013	0.0192	
	Li_2	0.182		3.02	0.0184	0.0419	0.006

a) Experimental data from G. HERZBERG, Molecular Spectra and Molecular Structure, I. Spectra of diatomic Molecules (D. Van Nostrand Co., Inc. New York, 1950)

1. core radius
2—3. pseudopotential parameters
4. Sum of ionization potential for the free atoms
5. Total HF energy
6. HF energy plus σ and π correlation energy
7. HF orbital energies [b) for Li_2 the orbital energy is the same in an all-electron calculation]
8. Calculated equilibrium distance
9. Experimental equilibrium distance
10. Calculated dissociation energy (for Li_2 only σ-correlation is included)
11. Experimental dissociation energy
12. HF binding energy of an all-electron calculation according to A. C. WAHL [21] (for Na_2) and G. DAS [25] (for Li_2)

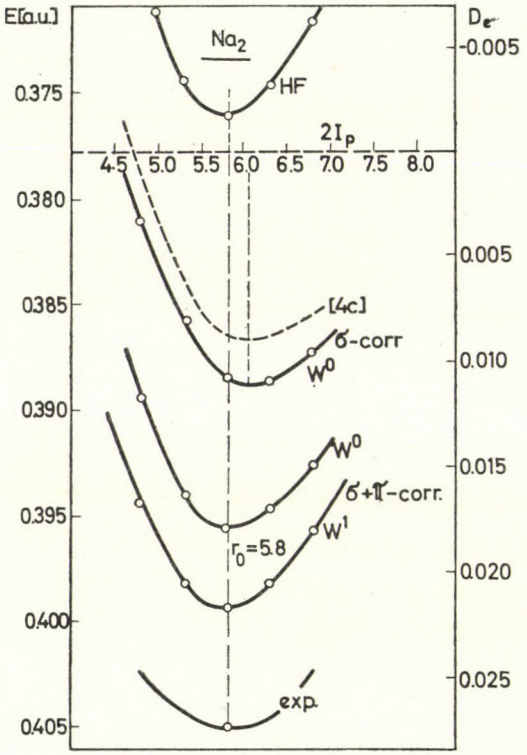
E[a.u.]
D_e
Na_2
HF
$2I_p$
4.5 5.0 5.5 6.0 6.5 7.0 7.5 8.0
0.375
0.380
0.385
0.390
0.395
0.400
0.405
-0.005
0.005
0.010
0.015
0.020
0.025
[4c]
σ-corr
W^0
W^0
σ+π-corr.
W^1
r_0=5.8
exp.

Fig. 2

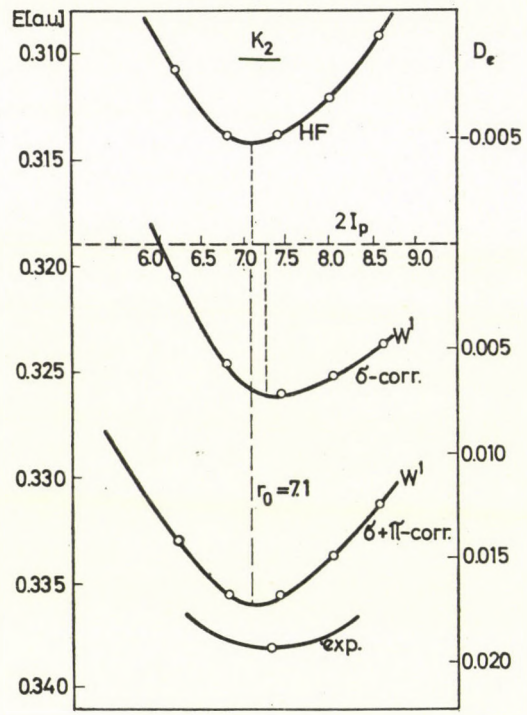
E[a.u.]
D_e
K_2
HF
$2I_p$
6.0 6.5 7.0 7.5 8.0 8.5 9.0
0.310
0.315
0.320
0.325
0.330
0.335
0.340
-0.005
0.005
0.010
0.015
0.020
W^1
σ-corr.
W^1
r_0=7.1
σ+π-corr.
exp.

Fig. 3

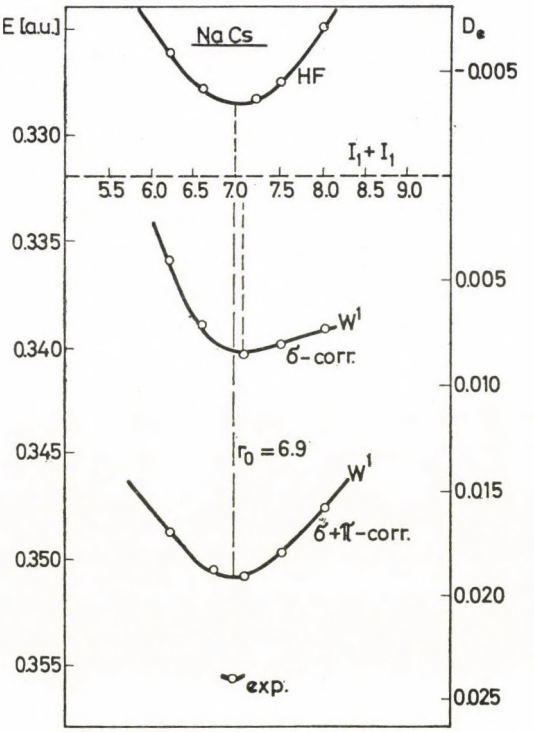

Fig. 4

Figs. 2—4. Energy-potential for Na_2, K_2 and NaCs as calculated by the pseudopotential method with pseudopotentials W^0, W^1

HF = Hartree—Fock approximation. σ-corr. = HF + σ-correlation. $\sigma + \pi$-corr. = HF + + $\sigma + \pi$-correlation. exp. = experimental energy curve which we obtained by subtracting the binding energy D_e (see right hand scale) from the level of the separated atoms (broken line with energy $2I_p$). The curvature corresponds to a quadratic parabola obtained from the experimental force-constant. See [4c]

we obtained the force constants K_e as well. The resulting values are collected in Table IV for different approximations. In comparing the results with their experimental counterparts one sees that the geometry of these systems is already accounted for in the Hartree—Fock approximation like one finds in all-electron HF calculations. The equilibrium distances are increased if one allows for σ-correlation (i.e. by performing CI with configurations constructed from σ-orbitals only) but are decreased again to the correct values if π-correlation is taken into account, too.* (For a more detailed discussion of this problem see [13c]). In fact, the σ-correlation energy contributions increase with distance while the π-correlation decreases with distance, so that the sum of both re-

* A Weinbaum function (Heitler—London function + ionic terms) as used by SZASZ and MCGINN accounts to some extent for σ-correlation (but not for π-correlation). This is the reason for their too large equilibrium distances.

Table IV

Equilibrium distances, force constants and total energies for Na_2, NaCs, K_2

Molecule	approximation	r_0 [a.u.] calc.	r_0 [a.u.] exp.	K_e [a.u.] theor.	K_e [mdyn/Å] theor.	K_e [mdyn/Å] exp.	$-E_0$ [a.u.]
Na_2	SCF	5.8	5.8	0.009	0.14	0.083	0.3759
	SCF + corr.	5.8		0.007	0.11		0.3993
NaCs	SCF	7.0	—	0.0057	0.09	0.051	0.3284
	SCF + corr.	6.9	—	0.0051	0.08		0.3510
K_2	SCF	7.1	7.39	0.0048	0.075	0.048	0.3142
	SCF + corr.	7.1		0.0045	0.07		0.3360

Table V

Correlation analysis of Na_2 for different distances r. All quantities are in atomic units

r	E_{HF}	$-E(1\sigma_u)$	$-E(1\pi_u^y)$	$-E(2\sigma_g)$	$-E(\sigma+\pi)$
4.8	0.3691	0.00944	0.00686	0.00257	0.02526
5.3	0.3744	0.00807	0.00618	0.00325	0.02368
5.8	0.3759	0.00902	0.00544	0.00353	0.02343
6.3	0.3745	0.01030	0.00477	0.00373	0.02358
6.8	0.3715	0.01193	0.00419	0.00383	0.02414

mains approximately constant as can be seen from the correlation-energy analysis for Na_2 in Table V.

The corresponding natural orbitals which contribute to the correlation energy are plotted in Figs. 5—8 for NaCs. Although the accuracy of these NO's (particularly of those with small expansion coefficients) should not be overestimated these plots are quite illustrative. The broken lines indicate the core region of the corresponding atoms. Inside this region the niveau lines have no physical meaning.

In Table VI the results of our calculations on BeH_2 are summarized for the equilibrium distance $r_{Be-H} = 2\,5$ a.u. for the linear symmetric molecule. The results are somewhat poorer, similar to those which have been found for hybrides in general [4e], a phenomenon which is not yet fully understood.

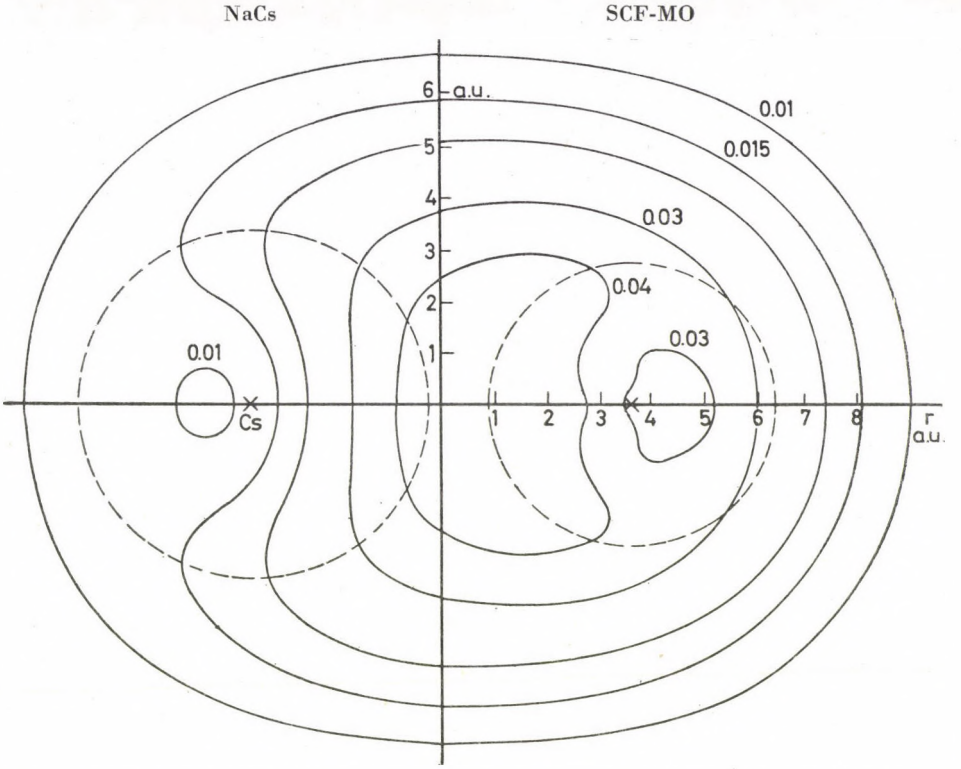

Fig. 5. Ground state SCF—MO for NaCs. The broken line indicates the core region. Insid this region the plots have no physical meaning

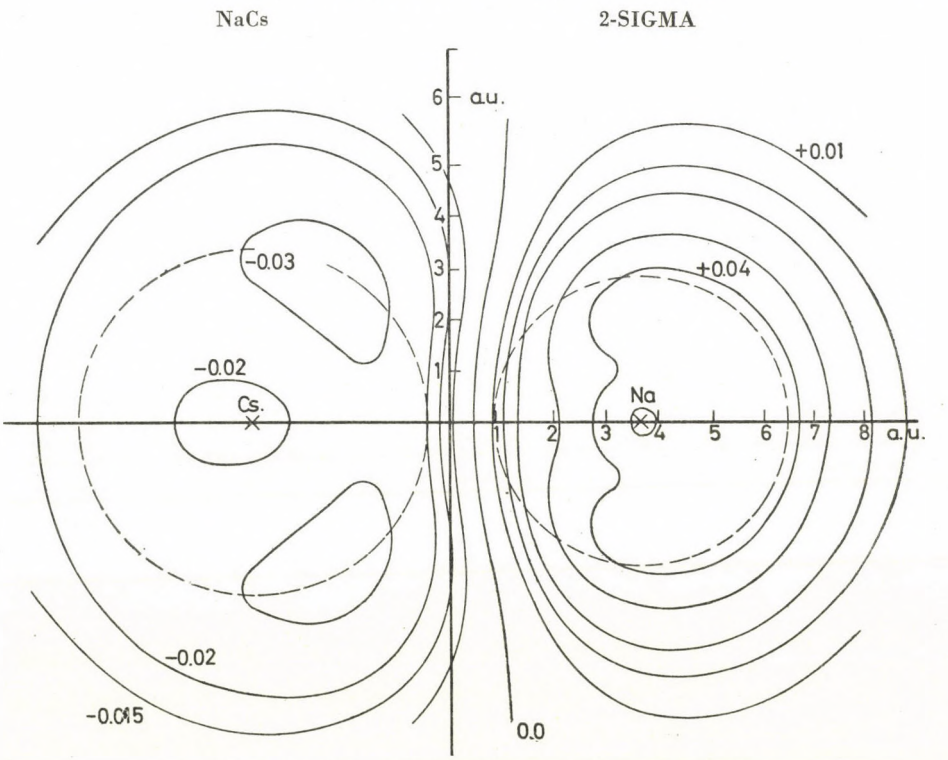

Fig. 6. 2σ—NO of NaCs with one node in the middle

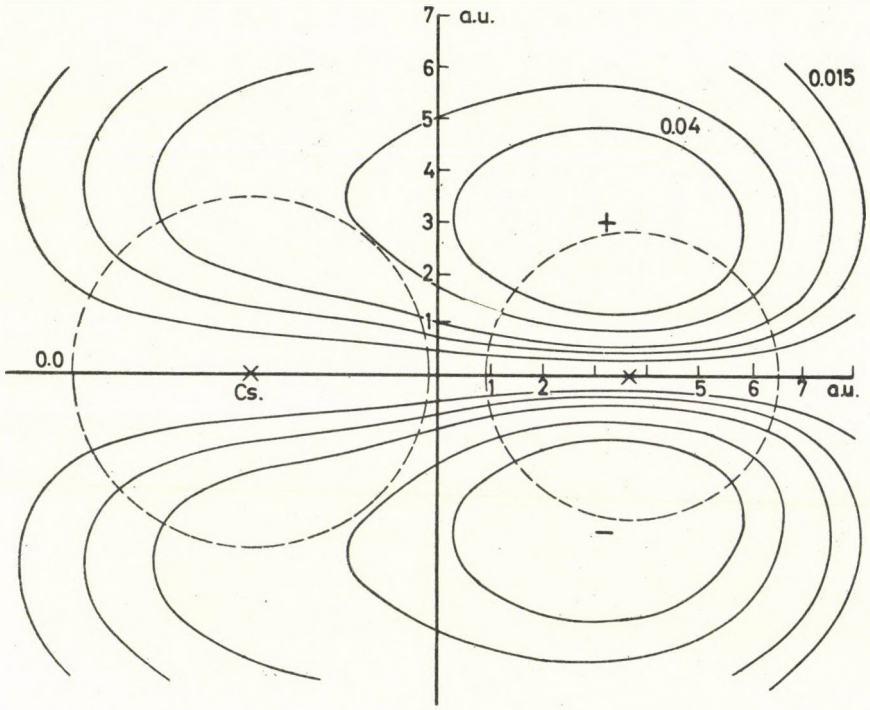

Fig. 7. 1π—NO of NaCs in the x—y-plane

NaCs 3-SIGMA

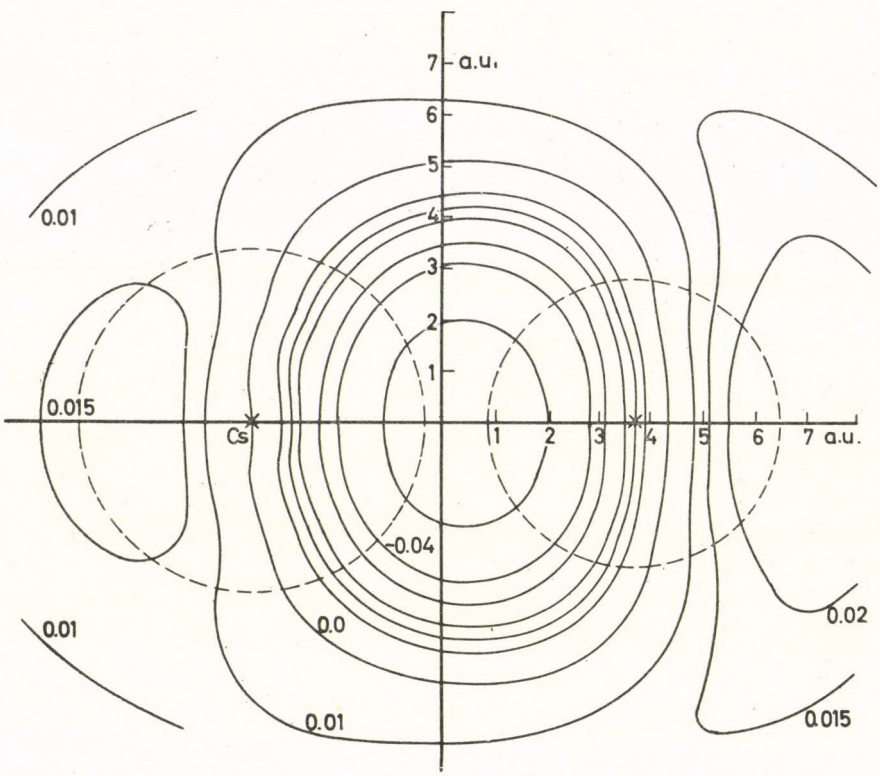

Fig. 8. 3σ—NO of NaCs with one node

Table VI

Comparison of BeH_2 in the pseudopotential scheme and a complete treatment. All quantities are in atomic units

approx.	R_e	a_0	a_1	r_e	$-E_{HF}$	$-\varepsilon_{HF}$
pseudo-potential	1.356	−1.478	2.175	2.5	2.0558	$\varepsilon_1 = 0.5124$ $\varepsilon_2 = 0.4019$
complete SCF—NO				2.5	15.7624	$\varepsilon_1 = 0.4916$ $\varepsilon_2 = 0.4559$

approx.	$-E^{\sigma}_{\mathrm{corr}}$	$-E^{\pi}_{\mathrm{corr}}$	$-E_{\mathrm{Tot.}}$	$-I_p$	D_e calc.	D_e estim.
pseudo-potential	0.0335	0.0230	2.11237	2.01184	0.1005	0.239
complete SCF—NO	0.0322	0.0245	15.8119		0.202	15.906

Conclusions

In performing molecular calculations in a pseudopotential approach one introduces two possible sources of errors. One is due to the approximation inherent in the chosen pseudopotential, the other to the limitations in the ansatz of wave functions. The latter source of error is the same as in all electron calculations and it is these errors which we tried to reduce as much as possible by aiming at a rather accurate treatment of the two and four valence-electron problem in the field of a pseudopotential that has a simple analytic form.

We performed Hartree—Fock calculations in the pseudopotential field and obtained good agreement with all-electron Hartree—Fock calculations (as far as those are available), both with respect to orbital energies and binding energies. Since Hartree—Fock calculations generally lead to good molecular geometries it is not surprising that the bond distances of our pseudopotential Hartree-Fock calculations agree well with the experimental ones.

The binding energies obtained in the Hartree—Fock approximation are as poor in a pseudopotential as in an all-electron treatment. In order to obtain the correct values one has to account for electron correlation. If one does so, by using the natural orbital expansion method one obtains about 60—80% of the experimental binding energies. (Whereas in the Hartree—Fock approach not even the sign of the binding energy is correct). In those cases where we could make the comparison, the correlation energies and the contributions of

the different NO's to it were quite similar in a pseudopotential and in an all-electron calculation. (This is demonstrated by the examples BeH_2 and Li_2. For the larger systems the all-electron calculations would be much too time-consuming).

Two forms of the pseudopotential have been used, which differ appreciably inside the core region but which lead to rather similar results. A more careful inspection shows that the potential W^1 (see Fig. 1) is preferable to W^0 both with respect to Rydberg series and to binding energies.

Our results suggest that the pseudopotential method should be applicable successfully to larger molecules although some problems still remain. In particular we think that a strictly local potential is too poor for systems where the contributions of p-AO's to bonding is as important as that of s-AO's, so that for such systems either an l-dependent potential has to be used or one has to find a local potential that reproduces both s- and p-type Rydberg states if this is possible.

Appendix

If we write the pseudopotential in the form

$$\begin{aligned} -W_c^n(|\mathbf{r}-\mathbf{r}_c|) &= \sum_{\nu=0}^{n} a_\nu |\mathbf{r}-\mathbf{r}_c|^\nu \qquad r<R \\ &= +\frac{Z_R}{|\mathbf{r}-\mathbf{r}_c|} \qquad r>R \end{aligned} \tag{1}$$

the basis functions φ_μ as

$$\varphi_\mu = \left(\frac{2\alpha_\mu}{\pi}\right)^{3/4} e^{-\alpha_\mu(\mathbf{r}-\mathbf{r}_\mu)^2} \qquad \mu = a, b, c, d, \ldots \tag{2}$$

then we get in a first step with $\gamma = \alpha_a + \alpha_b$

$$-J = (\varphi_a, W_c^n \varphi_b) = \left(\frac{\alpha_a+\alpha_b}{\pi}\right)^{3/2} S_{ab} \int e^{-\gamma(\mathbf{r}-\mathbf{r}_p)^2} W_c^n(|\mathbf{r}-\mathbf{r}_c|)\, d\tau\,. \tag{3}$$

In this expression S_{ab} means the overlap integral (φ_a, φ_b) which is given by

$$\begin{aligned} S_{ab} &= (\alpha_a \cdot \alpha_b)^{-3/4} A^{3/2} e^{-1/2(\mathbf{r}_a-\mathbf{r}_b)^2 A}, \\ A &= \frac{2\alpha_a \cdot \alpha_b}{\alpha_a+\alpha_b}\,. \end{aligned} \tag{4}$$

Defining the position vector of the function centers or nucleus c by

$$\begin{aligned} \mathbf{a} &= [A_x;\ A_y;\ A_z]\,, \\ \mathbf{b} &= [B_x;\ B_y;\ B_z]\,, \\ \mathbf{c} &= [C_x;\ C_y;\ C_z] \end{aligned} \tag{5}$$

the point P with position vector $\mathbf{r}_p$ in Equ. (3) is situated on the line between $\mathbf{a}$ and $\mathbf{b}$ with coordinates

$$\mathbf{r}_p = \frac{1}{\gamma}\left[\alpha_a A_x + \alpha_b B_x;\ \alpha_a A_y + \alpha_b B_y;\ \alpha_a A_z + \alpha_b B_z\right]. \tag{6}$$

Now we can transform our coordinates according to $\mathbf{r}' = \mathbf{r}—\mathbf{r}_c$ and get

$$-J = \left(\frac{\gamma}{2}\right)^{3/2} S_{ab} \int e^{-\gamma(\mathbf{r}'-\mathbf{r}_{cp})^2}\, W(|\mathbf{r}'|)\, d\tau' \tag{7}$$

with $\mathbf{r}_{cp} = \mathbf{r}_c—\mathbf{r}_p$.

Now we separate the integrations

$$-J = \left(\frac{\gamma}{\pi}\right)^{3/2} S_{ab}\left[\int_0^{\infty} e^{-\gamma(r^2+r_{cp}^2)}\, W(r)\, r^2\, dr \int_{-1}^{+1} e^{2\gamma r_{cp} r\chi}\, dx \int_0^{2\pi} d\varphi\right] \tag{8}$$

and get after a short calculation

$$-J = \left(\frac{\gamma}{\pi}\right)^{3/2} S_{ab}\, \frac{\pi}{\gamma r_{cp}}\left[\int_0^{\infty} e^{-\gamma(r-r_{cp})^2}\, W(r)\, r dr - \int_0^{\infty} e^{-\gamma(r+r_{cp})^2}\, W(r)\, dr\right]. \tag{9}$$

Up to this point the derivation does not depend on the explicit potential expression from which we make use now.

$$\begin{aligned} J = \left(\frac{\gamma}{\pi}\right)^{3/2} S_{ab}\, \frac{\pi}{\gamma r_{cp}} \Bigg\{ \sum_{\nu=0}^{n} a_\nu \left[\int_0^{R} r^{\nu+1}\, e^{-\gamma(r-r_{cp})^2}\, dr - \int_0^{R} r^{\nu+1}\, e^{-\gamma(r+r_{cp})^2}\, dr\right] + \\ + Z_R \int_R^{\infty} e^{-\gamma(r-r_{cp})^2}\, dr - Z_R \int_R^{\infty} e^{-\gamma(r+r_{ap})^2}\, dr \Bigg\}. \end{aligned} \tag{10}$$

After substitution

$$u = r - r_{cp}\,, \quad v = r + r_{cp}$$

we get for $r^{\nu+1}$ an expression

$$(u + r_{cp})^{\nu+1} = \sum_{\lambda=0}^{\nu+1} \binom{\nu+1}{\lambda} u^\lambda\, r_{cp}^{\nu-\lambda+1} \tag{11}$$

and the corresponding one for $(v—r_{cp})^{\nu+1}$. Therefore we can write for the whole integral

$$J=\left(\frac{\gamma}{\pi}\right)^{3/2} S_{ab}\left\{\frac{\pi}{\gamma}\sum_{\nu=0}^{n} a_\nu \sum_{\lambda=0}^{\nu+1}\binom{\nu+1}{\lambda} r_{cp}^{\nu-\lambda}\left[\int_{-r_{cp}}^{R-r_{cp}} u^\lambda e^{-\gamma u^2}\,du+(-1)^{\nu-\lambda}\int_{r_{cp}}^{R+r_{cp}} v^\lambda e^{-\gamma v^2}\,dv\right]+\right.$$
$$\left.+\frac{Z_R\pi}{\gamma r_{cp}}\left[\int_{R-r_{cp}}^{\infty} e^{-\gamma u^2}\,du-\int_{R+r_{cp}}^{\infty} e^{-\gamma u^2}\,du\right]\right\}. \tag{12}$$

After some simplifications in the last two integrals and a splitting of the first term in the sum over ν we obtain the final form

$$J=\sqrt{\frac{\gamma}{\pi}}\,S_{ab}\left\{\frac{a_0}{2}\sqrt{\frac{\pi}{\gamma}}\left[\operatorname{erf}\left(\sqrt{\gamma}(r_{cp}+R)\right)-\operatorname{erf}\left(\sqrt{\gamma}(r_{cp}-R)\right)\right]+\right.$$
$$+\frac{Z_R}{2\,r_{cp}}\sqrt{\frac{\pi}{\gamma}}\left[\operatorname{erf}\left(\sqrt{\gamma}(r_{cp}+R)\right)+\operatorname{erf}\left(\sqrt{\gamma}(r_{cp}-R)\right)\right]+$$
$$+\frac{a_0}{2\gamma r_{cp}}\left[e^{-\gamma(r_{cp}+R)^2}-e^{-\gamma(r_{cp}-R)^2}\right]+ \tag{13}$$
$$+\sum_{\nu=1}^{n} a_\nu\left[\frac{r_{cp}^\nu}{\sqrt{\gamma}}\left(\int_{-\sqrt{\gamma}r_{cp}}^{\sqrt{\gamma}(R-r_{cp})^2} e^{-u^2}\,du+(-1)^\nu\int_{\sqrt{\gamma}r_{cp}}^{\sqrt{\gamma}(R-r_{cp})^2} e^{-u^2}\,du\right)+\right.$$
$$\left.\left.+\sum_{\lambda=1}^{\nu+1}\binom{\nu+1}{\lambda} r_{cp}^{\nu-\lambda}\sqrt{\gamma}^{-\lambda-1}\left(\int_{-\sqrt{\gamma}r_{cp}}^{\sqrt{\gamma}(R-r_{cp})^\lambda} u^\lambda e^{-u^2}du+(-1)^{\nu-\lambda}\int_{\sqrt{\gamma}r_{cp}}^{\sqrt{\gamma}(R+r_{cp})} u^\lambda e^{-u^2}du\right)\right]\right\}.$$

(II: $\sqrt{\gamma}r_{cp}$ to $\sqrt{\gamma}(R-r_{cp})^2$; I: $-\sqrt{\gamma}r_{cp}$ to $\sqrt{\gamma}(R-r_{cp})^\lambda$)

In this expression the terms with $\nu = 0$ and $\lambda = 0$ are written down separately because they can be reduced to simple analytic expressions. So II can be written as

$$\mathrm{II}=\sqrt{\frac{\pi}{4}}\left[\left(1-(-1)^\nu\right)\operatorname{erf}\left(\sqrt{\gamma}\,r_{cp}\right)+\operatorname{erf}\left(\sqrt{\gamma}(R-r_{cp})\right)+(-1)^\nu\operatorname{erf}\left(\sqrt{\gamma}(R+r_{cp})\right)\right] \tag{14}$$

with

$$\operatorname{erf}(z)=\frac{2}{\sqrt{\gamma}}\int_0^z e^{-u^2}\,du. \tag{15}$$

The remaining integrals which are of the form

$$J_\lambda(a,b)=\int_a^b u^\lambda e^{-u^2}\,du \tag{16}$$

can easily be evaluated by a recurring relation one can derive from (16)

$$J_\lambda(a,b)=\frac{1}{2}\left[(\lambda-2)J_{\lambda-2}(a,b)+a^{\lambda-2}e^{-a^2}-b^{\lambda-2}e^{-b^2}\right] \tag{17}$$

which connects $J_\lambda(a, b)$ with $J_{\lambda-2}(a, b)$.

The initial integrals $J_1(a, b)$ and $J_2(a, b)$ are

$$J_1(a, b) = \frac{1}{2}\sqrt{\pi}\,[\mathrm{erf}\,(b) - \mathrm{erf}\,(a)]\,,$$

$$J_2(a, b) = \frac{1}{2}\,[e^{-a^2} - e^{-b^2}]$$

so that the whole integral $(\varphi_a, W_c\,\varphi_b)$ is reduced to the evaluation of the error-function.

For practical calculations it is useful to introduce some approximations for the limiting case $r_{cp} \ll 1$, to avoid numerical instabilities.

In this case we have approximated the expressions for I and II by

$$\mathrm{I} = \frac{r_{cp}^{\nu-\lambda}}{\sqrt{\gamma}^{\lambda+1}}\left(\int_{-\sqrt{\gamma}\,r_{cp}}^{\sqrt{\gamma}(R-r_{cp})} u^\lambda e^{-u^2}\,du + (-1)^{\nu-\lambda}\int_{\sqrt{\gamma}\,r_{cp}}^{\sqrt{\gamma}(R+r_{cp})} u^\lambda e^{-u^2}\,du\right) \approx$$

$$\approx \frac{1}{\sqrt{\gamma}^{\nu+1}}\left[\left(1+(-1)^{\nu-\lambda}\right)(\sqrt{\gamma}\,r_{cp})^{\nu-\lambda}\int_0^{\sqrt{\gamma}\,R} u^\lambda e^{-u^2}\,du - \right.$$

$$\left. - (\sqrt{\gamma}\,r_{cp})^{\nu+1-\lambda}(\sqrt{\gamma}\,R)^\lambda\, e^{-\gamma R^2}\left(1-(-1)^{\nu-\lambda}\right)\right]$$

$$\mathrm{II} \approx \frac{\sqrt{\pi}}{2}\left(1+(-1)^\nu\right)\mathrm{erf}\,(\sqrt{\gamma}\,R) + \left(1-(-1)^\nu\right)\sqrt{\gamma}\,r_{cp}(1 - e^{\gamma R^2}).$$

Acknowledgement

The research reported here has been sponsored in part by "Deutsche Forschungsgemeinschaft" and "Fond der chemischen Industrie". Several subroutines used are due to Dr. R. AHLRICHS to whom the authors are also indebted for stimulating discussions. Thanks are also due to various colleagues (C. K. JÖRGENSEN and G. KLOPMAN formerly in Geneva, W. H. E. SCHWARZ, formerly in Frankfurt and the audience of the Theoretical Chemistry Symposium 1968 in Elmau) for discussions following talks by two of the authors (R. J. K. and W. K.) on this subject.

REFERENCES

1. J. H. VAN VLECK and A. SHERMAN, Rev. Mod. Phys., **7**, 167, 1935.
2. H. HELLMANN, Acta Physicochim. USSR, **1**, 913, 1935; **4**, 225, 1936; P. GOMBÁS, Z. Physik, **94**, 472, 1935.
3. P. GOMBÁS, Pseudopotentiale, Springer-Verlag, Wien—New York, 1967.
4a. H. PREUSS, Z. Naturforschung, **10a**, 365, 1955.
4b. I. SZASZ and G. MCGINN, J. Chem. Phys., **42**, 2363, 1965.
4c. I. SZASZ and G. MCGINN, J. Chem. Phys., **45**, 2898, 1966.
4d. I. SZASZ and G. MCGINN, J. Chem. Phys., **47**, 3495, 1967.
4e. I. SZASZ and G. MCGINN, J. Chem. Phys., **48**, 2997, 1968.
5. R. G. PARSONS and V. F. WEISSKOPF, Z. Physik, **202**, 492, 1967.
6. AUSTIN and H. HEINE, J. Chem. Phys., **45**, 928, 1966.

7. W. KUTZELNIGG, R.-J. KOCH and W. A. BINGEL, Chem. Phys. Letters, **2**, 197, 1968.
8. J. G. PHILLIPS and L. KLEINMANN, Phys. Rev., **116**, 287, 1959; **118**, 1351, 1960.
9. A. U. HAZI and S. A. RICE, a) J. Chem. Phys., **48**, 495, 1968; b) J. Chem. Phys., **45**, 3004, 1966; c) J. Chem. Phys., **47**, 1125, 1967.
10. I. V. ABARENKOV and V. HEINE, Phil. Mag., **12**, 529, 1965.
11. G. J. IAFRATE, J. Chem. Phys., **45**, 1072, 1966; J. Chem. Phys., **46**, 728, 1967.
12. M. N. COHEN and V. HEINE, Phys. Rev., **122**, 1821, 1961.
13. W. KUTZELNIGG a) Theoret. Chim. Acta, **1**, 327, 1963; b) J. Chem. Phys., **40**, 3640, 1964. c) R. AHLRICHS and W. KUTZELNIGG, J. Chem. Phys., **48**, 1829, 1967.
14. J. R. HOYLAND, J. Chem. Phys., **40**, 3540, 1964.
15. MCGOLDBERG and J. R. RITTER, J. Phys. Chem., **71**, 3111, 1967.
16. S. PEYERIMHOFF, R. F. BUENKER and L. C. ALLEN, J. Chem. Phys., **45**, 734, 1966.
17. R. AHLRICHS and W. KUTZELNIGG, Theoret. chim. Acta, **10**, 377, 1968.
18. W. H. E. SCHWARZ, Theoret. chim. Acta, **11**, 307, 1968; **11**, 377, 1968, Z. Physik, **214**, 149, 1968.
19. W. A. HARRISON, Pseudopotentials in the theory of metals, W. A. Benjamin, Inc. New York, 1966.
20. H. PREUSS, Z. f. Naturforsch., **10***a*, 365, 1955.
21. P. GOMBÁS, Theoret. chim. Acta, **5**, 112, 1966; **5**, 127, 1966;
G. J. IAFRAGE, J. Chem. Phys., **45**, 1072, 1966;
T. C. CHEN, J. Chem. Phys., **29**, 347, 1958.
22a. W. NEUMANN and H. PAULY, Phys. Rev Letters, **20**, 357, 1968.
22b. CH. SCHLIER and E. VIETZKE, Chem. Phys. Letters, **3**, 250, 1969.
23. L. R. KAHN and W. A. GODDARD III., Chem. Phys. Letters, **2**, 667, 1968.
24. A. C. WAHL: private communication.
25. G. DAS, J. chem. Phys., **44**, 87, 1966.

ПОДРАЖЕНИЕ ВЛИЯНИЯ ЭЛЕКТРОНОВ АТОМНОГО ОСТАТКА ПСЕВДОПОТЕНЦИАЛАМ. II.

ПРИМЕНЕНИЯ К НЕКОТОРЫМ МОЛЕКУЛАМ С ДВУМЯ И ТРЕМЯ АТОМАМИ

В. А. БИНГЕЛ, Р. Й. КОХ и В. КУЦЕЛЬНИГ

Резюме

Псевдопотенциальная теория комбинируется с методом Харти—Фока и методом естественного разложения в ряд с целью определения молекулярных постоянных D_e, R_e и k_e для Na_2, K_2, NaCs и BeH_2. Эти молекулы рассматривались как двух- и четырехэлектронные проблемы соответственно в псевдопотенциальном поле своих атомных остатков. Далее были анализированы энергии и волновые функции с точки зрения взноса различных натуральных орбит в корреляционную энергию. Вычисленные расстояния равновесия хорошо согласуются с экспериментальными данными Соответствие диссоциационных энергий с экспериментальными данными лучше, чем в предыдущих вычислениях.

Acta Physica Academiae Scientiarum Hungaricae, Tomus 27, pp. 345—349 (1969)

FURTHER NOTE ON THE SADDLE-POINT CHARACTER OF HARTREE–FOCK WAVE FUNCTIONS*

By

C. A. COULSON

MATHEMATICAL INSTITUTE, OXFORD OX1 3LB, ENGLAND

(Received 20. II. 1969)

A simple argument is provided to show that the energy of a Hartree—Fock wave function is a saddle-point on the energy surface obtained by "opening-out" each pair of electrons from the same orbital w_j into two different orbitals u_j and v_j. A discussion is also given of the best direction in which to move away from the saddle-point in order to lower the energy as rapidly as possible. The argument applies quite generally, to atoms or to molecules, and both when using a finite basis (LCAO type functions) and when using an infinite basis (true Hartree—Fock functions).

1. Introduction

In recent years considerable attention has been given to the nature of the Hartree—Fock (HF) energy and wave function, whether for an atom or a molecule, and whether determined by complete solution of the HF equations or by solution of the Roothaan equations which result when the function space is limited and a finite basis set is used for each constituent orbital. The case of the two-electron atom such as helium was discussed by COULSON [1], by HIBBERT and COULSON [2], and by HIBBERT [3], who showed that the HF energy was indeed a saddle-point, and that by suitable small changes in the HF orbitals it was possible to lower the energy, while still retaining the singlet character of the wave function. More recently HIBBERT and COULSON [4], and FLURRY and COULSON [5] have discussed the more general situation with more than two electrons, and have given very thorough analyses of the situation. [Full references to other work are given in [4]]. However, the following very simple discussion showing the saddle-point character of the HF energy for closed-shell systems, may be worth describing, even though it adds very little to the work in [4] and [5].

* It is a pleasure to dedicate this short paper to my friend Professor Dr. P. GOMBÁS on the occasion of his 60th birthday. Professor GOMBÁS's contributions to the statistical theory of atoms and molecules, as exemplified in his books and research papers, have been an inspiration to many younger workers. These contributions have been made over a period of many years, and have shown him to be one of the most important leaders in this field. On this happy occasion his friends and colleagues, as well as his students, join to congratulate him and to wish him happiness in the future.

2. Open-shell wave functions

We begin with a HF wave function ψ_{HF} corresponding to a closed-shell in which the orbitals $w_1, w_2, \ldots w_n$ are each doubly-occupied.

$$\psi_{\mathrm{HF}} = \mathscr{A}\{w_1(1)\,\bar{w}_1(2)\,w_2(3)\,\bar{w}_2(4)\ldots w_n(2n-1)\,\bar{w}_n(2n)\}\,. \tag{1}$$

In (1) a bar above a symbol denotes β-spin, and $\mathscr{A}$ is the antisymmetrizer

$$\left(\frac{1}{(2n)!}\right)^{1/2} \sum_P (-1)^P P,$$

where P is an odd or even permutation of the electrons. Since we may take the w-functions to be orthonormal, ψ_{HF} is already normalized.

We know that the energy E_{HF} associated with (1) is stationary with respect to small changes in the w_r; we shall be concerned with the ground state for which E_{HF} is a minimum.

Now let us open out the paired orbitals $w_1\bar{w}_1$, replacing them by two new orbitals u_1 and v_1. It will be convenient to put

$$\begin{aligned} u_1 &= w_1 + a_1 + b_1\,, \\ v_1 &= w_1 + a_1 - b_1\,, \end{aligned} \tag{2}$$

where, since $a_1 + b_1$ and $a_1 - b_1$ may be taken orthogonal to w_1, the same is true of a_1 and b_1. But there is no reason why a_1 and b_1 should be orthogonal. The resulting singlet wave function is

$$\mathscr{A}\{[u_1(1)\,v_1(2) + v_1(1)\,u_1(2)]\,\alpha(1)\,\beta(2)\,w_2(3)\ldots/\,\bar{w}_n(2n)\}\,. \tag{3}$$

In what follows we shall be dealing with wave functions close to the HF function (1), so that a_1 and b_1 may be supposed to be of the first order of small quantities. Now substitution of (2) into (3) leads to the expression:

$$\begin{aligned} \mathscr{A}\{&[w_1(1) + a_1(1)]\,[\bar{w}_1(2) + \bar{a}_1(2)]\,w_2(3)\,\bar{w}_2(4)\ldots \\ &- b_1(1)\,\bar{b}_1(2)\,w_2(3)\,\bar{w}_2(4)\ldots\}. \end{aligned} \tag{4}$$

On account of the orthogonality properties of the w, a, and b functions this last expression is actually normalized correct to terms of the second order of small quantities. It can be thought of as a kind of configurational interaction wave function, in which we have terms of zero-, first- and second-order.But on account of Brillouin's theorem there will be no interaction between the zero-order terms (which are simply the HF wave function) and the first-order terms. So the energy of wave function (4) is of the form

$$E = E_{\mathrm{HF}} + \text{second-order terms.}$$

If we now write (4) in the form ψ_{I}—ψ_{II}, the energy will be

$$H_{\mathrm{I\,I}} - 2H_{\mathrm{I\,II}} + H_{\mathrm{II\,II}}.$$

The terms of second order in this expression occur in $H_{\mathrm{I\,I}}$ and $H_{\mathrm{I\,II}}$. So far as $H_{\mathrm{I\,II}}$ is concerned they depend only on the w's and b_1. So for fixed b_1 the energy (to this order) will be least when $H_{\mathrm{I\,I}}$ is least. But if w_1, w_2 ... are the HF functions this will occur when $a_1 = 0$. Thus, independent of b_1, we do best to put $a_1 = 0$ in (2). This means that the pair of orbitals w_1, $\bar{w}_1$ are opened out to

$$\begin{aligned} u_1 &= w_1 + b_1\,, \\ v_1 &= w_1 - b_1\,. \end{aligned} \tag{5}$$

We now repeat this process with all the other pairs w_2, $\bar{w}_2$ etc. To second order the energy terms will be additive, and so (as is shown in more detail in [4]—[5]) we are led to an open-shell wave function

$$\begin{aligned} \psi_{os} = \mathscr{N}\{\mathscr{A}\{w_1\,\bar{w}_1\,w_2\,\bar{w}_2\,w_3\,\ldots\} - \mathscr{A}\{b_1\,\bar{b}_1\,w_2\,\bar{w}_2\,w_3\,\ldots\} - \\ - \mathscr{A}\{w_1\,\bar{w}_1\,b_2\,\bar{b}_2\,w_3\,\ldots\} - \ldots + \mathscr{A}\{b_1\,\bar{b}_1\,b_2\,\bar{b}_2\,w_3\ldots\} + \ldots\}. \end{aligned} \tag{6}$$

The wave function (6) is correct to terms of the third order of small quantities. Moreover it is clear from (6) that we may take b_1 orthogonal to w_2, w_3, ... etc., without loss of generality, to this order.

The normalizing factor $\mathscr{N}$ is easily obtained. Let us put

$$\langle b_1|b_1\rangle = S_1\,, \quad \text{etc.}\,, \tag{7}$$

so that S_1, S_2, ... are of the second order of small quantities. Then, correct to fourth order

$$\mathscr{N}^{-2} = 1 + \sum_1^n S_j^2\,, \qquad \mathscr{N} = 1 - \frac{1}{2}\sum S_j^2. \tag{8}$$

The energy E_{os} associated with ψ_{os} is found by expanding $\langle\psi_{os}|H|\psi_{os}\rangle$. So

$$E_{os} = \mathscr{N}^2\left\{E_{\mathrm{HF}} - 2\left\langle w_1(1)\,w_1(2)\left|\frac{1}{r_{12}}\right|b_1(1)\,b_1(2)\right\rangle - \text{etc.} + \begin{matrix}\text{terms of the}\\ \text{fourth order}\end{matrix}\right\}. \tag{9}$$

Correct to second order

$$E_{os} = E_{\mathrm{HF}} - 2\sum_j\left\langle w_j(1)\,w_j(2)\left|\frac{1}{r_{12}}\right|b_j(1)\,b_j(2)\right\rangle. \tag{10}$$

Each of the electron-repulsion integrals in (10) is positive, as shown first by SLATER [6]. So $E_{os} < E_{\mathrm{HF}}$. But if we keep $u_j = v_j$, we know from the statio-

nary (minimum) character of the HF energy that the total energy must increase. It follows therefore that the energy has a saddle point for the HF wave function. In this way we have generalized the two-electron discussion of [1]—[3]. The argument, of course, is independent of whether we use a finite or infinite basis set.

3. Direction of optimum improvement of HF wave function

Since it may not always be practicable to make complete calculations of the functions a_j and b_j in (2) to determine the absolute minimum of the open-shell wave function (6), it becomes important to know in what direction we can most profitably improve the wave function, starting with ψ_{HF}. This matter was dealt with for the two-electron problem in [2] and [3]. We now extend this argument to wave functions of type (6), retaining always terms of the lowest order for our discussion.

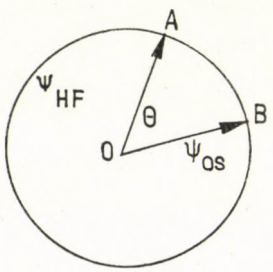

Fig. 1

We can represent ψ_{HF} and ψ_{os} as vectors OA, OB of unit length in an appropriate Hilbert space (Fig. 1). In that case we can define the "distance" AB by the angle Θ, where

$$\cos\Theta = \langle\psi_{\mathrm{HF}}|\psi_{os}\rangle$$

Since ψ_{HF} and ψ_{os} differ by only small terms, it follows from (6) that

$$1 - \frac{1}{2}\Theta^2 = \mathscr{N}.$$

Thus

$$\Theta^2 = 2(1-\mathscr{N}) = \Sigma S_j^2, \quad \text{from (8).} \tag{11}$$

The most profitable direction, therefore, in which to move from the HF point A of Fig. 1 will be the direction which maximizes $|E_{\mathrm{HF}}—E_{os}|$ for fixed

arc length AF, i.e. for fixed Θ. We are therefore to maximize

$$\Sigma \left\langle w_j w_j \left| \frac{1}{r_{12}} \right| b_j b_j \right\rangle \text{ for fixed } \Sigma \langle b_j | b_j \rangle^2 .$$

This process is equivalent to proceeding along the direction of steepest descent away from the saddle-point A in Hilbert space. However, since A is a saddle-point, this is really equivalent to moving away from A in the direction of greatest downward curvature. If we are working with a finite basis each b_j can be expressed as a linear combination of the virtual orbitals complementary to $w_1 \ldots w_n$. The maximization process is then fairly simple. But with an infinite basis it is more troublesome, and some sort of variational approximation would have to be adopted.

This is as far as we can proceed in general terms. Each separate problem will now have to be dealt with on its own, taking into account the nature of the occupied orbitals w_j.

The writer would like to acknowledge the benefit of discussions and correspondence with Prof. R. L. FLURRY and Dr. A. HIBBERT.

REFERENCES

1. C. A. COULSON, "Quantum Theory of Atoms, Molecules and the Solid State", J. C. Slater Commemorative Volume, Ed. P.-O. Löwdin, Academic Press, New York, 1966, p. 97.
2. A. HIBBERT and C. A. COULSON, Proc. Phys. Soc., **92**, 17, 1967.
3. A. HIBBERT, J. Phys. B., **1**, 402, 1968.
4. A. HIBBERT, and C. A. COULSON, J. Phys. B., **2**, 458, 1969.
5. R. L. FLURRY, and C. A. COULSON, in course of publication.
6. J. C. SLATER, "Quantum Theory of Atomic Structure", Vol. 1, McGraw-Hill, New York, 1960, appendix 19.

ДАЛЬНЕЙШИЕ ЗАМЕЧАНИЯ О СЕДЛОВО-ТОЧЕЧНОМ ХАРАКТЕРЕ ВОЛНОВЫХ ФУНКЦИЙ ХАРТРИ—ФОКА

К. А. КУЛЬСОН

Резюме

Приводится простой аргумент для доказательства того, что энергия волновой функции Хартри—Фока есть седловая точка на поверхности энергии, полученной путем «развертывания» каждой пары электронов из одной и той же орбиты w_j в две разные орбиты u_j и v_j Далее дискутируется соответствующее направление, в котором удаляясь от седловой точки, энергия падает с наибольшей скоростью Применение аргумента довольно общее, его можно применять в случае атомов или молекул, используя при этом как конечную базу (функции типа LCAO) так и бесконечную базу (настоящие функции Хартри—Фока).

Acta Physica Academiae Scientiarum Hungaricae, Tomus 27, pp. 351—371 (1969)

ИНТЕРПРЕТАЦИЯ МЕТОДА ХАРТРИ—ФОКА КАК МЕТОДА ЧАСТИЧНОГО СУММИРОВАНИЯ АТОМНЫХ ФЕЙНМАНОВСКИХ ДИАГРАММ*

В. В. ТОЛМАЧЕВ

УНИВЕРСИТЕТ ЧИЛЕ, САНТИАГО, ЧИЛЕ**

(Поступило 20. II. 1969)

На методе Хартри—Фока [1, 2, 3] основываются почти все проводимые в настоящее время атомные и молекулярные расчеты, и поэтому его интерпретация как метода суммирования определенного класса атомных фейнмановских диаграмм [4] является очень важной. Она позволяет глубже понять смысл приближений, заложенных в методе Хартри-Фока, и причины той особой эффективности этого метода, которая проявляется при конкретных расчетах энергий, в частности, основных состояний легких атомов. В результате удается более осмысленно строить на основе метода Хартри—Фока различные теории электронной корреляции.

Кроме того такая интерпретация позволяет с большой легкостью эффективно составлять сами уравнения метода Хартри—Фока в тех или иных достаточно сложных конкретных случаях, скажем с учетом взаимодействия конфигураций. Последнего впрочем мы не будем касаться в этой статье, иллюстрируя все наши рассуждения только на простейших примерах атомных состояний с замкнутыми электронными оболочками и состояний с одной открытой оболочкой конфигурации и терма $(n_a l_a)^q SL$, предполагая, что этот терм конфигурации $(n_a l_a)^q$ единственный и не повторяется.

1. Состояния с замкнутыми электронными оболочками

Гамильтониан многоэлектронного атома, состояние которого с замкнутыми электронными оболочками мы собираемся изучать, в нерелятивистском приближении имеет вид

$$H = H_0 + H_{\text{int}}, \tag{1}$$

$$H_0 = -\frac{1}{2}\sum_{(1\leqslant i\leqslant N)} \Delta_{\vec{r}_i} - \sum_{(1\leqslant i\leqslant N)} \frac{Z}{r_i}, \tag{2}$$

$$H_{\text{int}} = \sum_{(1\leqslant i<j\leqslant N)} \frac{1}{|\vec{r}_i - \vec{r}_j|}. \tag{3}$$

Здесь Z — заряд ядра атома, N — полное число электронов в атоме (предполагается, что в общем случае $N \neq Z$, то есть все рассмотрение относится как к нейтральным атомным состояниям, так и к соответствующим состояниям положительных и отрицательных атомных ионов).

В теории атомных фейнмановских диаграмм варьируемое хартри-фоковское выражение для энергии изучаемого атомного состояния с замкнутыми электронными оболочками можно получить следующим образом.

* Профессору П. Гомбаш на день 60го рождения.

** Постоянный адрес: Московский Государственный Университет, Математико—Механический Факультет, Москва, СССР

Прежде всего возьмем некоторое сферически симметричное добавочнок полю ядра $-Z/r$ внешнее поле $U(r)$, ортонормированные радиальные функции которого определяются из уравнения

$$\left(-\frac{1}{2}\frac{d^2}{dr^2}-\frac{1}{r}\frac{d}{dr}+\frac{l(l+1)}{2r^2}-\frac{Z}{r}+U(r)\right)R_{nl}(r)=\varepsilon_{nl}R_{nl}(r), \quad (4)$$

$$\int_0^{+\infty} r^2\,dr\,R_{nl}(r)\,R_{nl}(r)=1 \quad (5)$$

(предполагаем, что спектр ε_{nl} не имеет случайного вырождения водородопо добного атома, то есть ε_{nl} реально зависят от l, и скажем например $\varepsilon_{2p}\neq\varepsilon_{2s}$) Соответственно мы должны ввести новый нулевой гамильтониан и гамильтониан взаимодействия

$$H_0^U=-\frac{1}{2}\sum_{(1\leqslant i\leqslant N)}\Delta_{\vec{r}_i}-\sum_{(1\leqslant i\leqslant N)}\frac{Z}{r_i}+\sum_{(1\leqslant i\leqslant N)}U(r_i), \quad (6)$$

$$H_{\mathrm{int}}^U=H_{\mathrm{int}}=\sum_{(1\leqslant i\leqslant N)}U(r_i). \quad (7)$$

Возьмем далее некоторое невырожденное состояние гамильтониан- H_0^U, которое характеризуется следующей совокупностью индексов заполненных электронных оболочек $nl\in f_0$. Указанное состояние следует сопоставлять тоже невырожденному состоянию исходного нулевого гамильтониана H_0 с теми же индексами заполненных оболочек $nl\in f_0$ и подобному состоянию полного гамильтониана H. Рассматриваемое состояние имеет энергию

$$E_0=\sum_{n_1l_1\in f_0}2(2l_1+1)\,\varepsilon_{n_1l_1} \quad (8)$$

и соответствующее состояние полного гамильтониана энергию

$$E_0+\Delta E, \quad (9)$$

причем добавок ΔE можно рассчитать как сумму вкладов от всех соответствующих атомных диаграмм.

Правила составления атомных фейнмановских диаграмм и вкладов от них в случае $U\equiv 0$ подробно описаны в [4]. Правила в случае $U\not\equiv 0$, которые нам сейчас нужны, практически не отличаются от этих правил. В частности описывающий межэлектронное взаимодействие четверной вертекс вносит своим вкладом радиальный интеграл

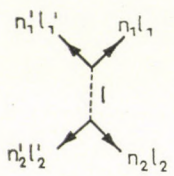

$$-R_l(n_1'l_1', n_2'l_2';\ n_2l_2, n_1l_1);$$

только теперь для этого радиального интеграла мы имеем следующее выражение

$$R_l(n_1' l_2', n_2' l_2';\ n_2 l_2, n_1 l_1) = \\ = \int_0^{+\infty} r_1^2 dr_1 \int_0^{+\infty} r_2^2 dr_2 R_{n_1' l_1'}(r_1) R_{n_2' l_2'}(z_2) U_l(r_1, r_2) R_{n_2 l_2}(r_2) R_{n_1 l_1}(r_1); \tag{10}$$

$$U_l(r_1, r_2) = \begin{cases} \dfrac{r_1^l}{r_1^{l+1}} & r_1 < r_2, \\ \dfrac{r_2^l}{r_1^{l+1}} & r_1 > r_2, \end{cases} \tag{11}$$

в которое входят радиальные функции (4), (5), а не соответствующие водородоподобные функции, получаемые из них, если наложить $U \equiv 0$. Кроме четверного вертекса, теперь появляется описывающий взаимодействие электронов с внешним полем $U(r)$ парный вертекс, который вносит своим вкладом интеграл

$$n_1' l_1' \cdot n_1 l_1 \quad U(n_1' l_1';\ n_1 l_1)\, \delta_{l_1', l_1},$$

причем полное выражение для соответствующего интеграла имеет вид

$$U(n_1' l_1';\ n_1 l_1) = \int_0^{+\infty} r_1^2 dr_1 R_{n_1' l_1'}(z_1) U(r_1) R_{n_1' l_1'}(r_1); \tag{12}$$

опять сюда входят радиальные функции (4), (5).

Обратим внимание, что в силу (4), (5) имеем

$$-\int_0^{+\infty} r_1^2 dr_1 R_{n_1' l_1'}(r_1) U(r_1) R_{n_1' l_1}(r_1) = \\ = \int_0^{+\infty} r_1^2 dr_1 R_{n_1' l_1'}(r_1) \left(-\frac{1}{2} \frac{d^2}{dr_1^2} - \frac{1}{r_1} \frac{d}{dr_1} - \frac{Z}{r_1} - \varepsilon n_1 l_1 \right) R_{n_1' l_1'}(r_1),$$

так что

$$\sum_{n_1 l_1 \in f_0} 2(2l_1 + 1)\, \varepsilon_{n_1 l} - \sum_{n_1 l_1 \in f_0} 2(2l_1 + 1)\, U(n_1 l_1, n_1 l_1) = \sum_{n_1 l_1 \in f_0} 2(2l_1 + 1)\, I(n_1 l_1)_1, \tag{13}$$

где

$$I(n_1 l_1) = -\frac{1}{2} \int_0^{+\infty} r_1^2 dr_1 R_{n_1' l_1'}(r_1) \left(\frac{d^2}{dr_1^2} + \frac{2}{r_1} \frac{d}{dr_1} + \frac{2Z}{r_1} - \right. \\ \left. - \frac{l(l+1)}{r_1^2} \right) R_{n_1' l_1'}(r_1). \tag{14}$$

В хартри-фоковском приближении нам необходимо рассчитать для ΔE вклады атомных диаграмм только первого порядка, так как

$$E_{\mathrm{HF}} \equiv E_0 + \Delta E_1 . \tag{15}$$

Этот расчет очень прост [4], и в результате мы получаем для вкладов атомных диаграмм первого порядка окончательные выражения



$$2 \sum_{n_1 l_1 \in f_0,\ n_2 l_2 \in f_0} (2l_1+1)(2l_2+1)\, R_0(n_1 l_1, n_2 l_2;\ n_2 l_2, n_1 l_1) ,$$

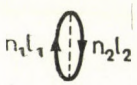

$$- \sum_{n_1 l_1 \in f_0,\ n_2 l_2 \in f_0} (2l_1+1)(2l_2+1) \sum_l [l_1\, l_2\, l]^2\, R_l\,(n_1 l_1, n_2 l_2;\ n_1 l_1, n_2 l_2) ,$$



$$- 2 \sum_{n_1 l_1 \in f_0} (2l_1+1)\, U(n_1 l_1; n_1 l_1) .$$

Таким образом для полной хартри-фоковской энергии мы имеем с учетом (15), (13)

$$\begin{aligned} E_{\mathrm{HF}} = & \sum_{n_1 l_1 \in f_0} 2(2l_1+1)\, I(n_1 l_1) + \\ & + 2 \sum_{n_1 l_1 \in f_0,\ n_2 l_2 \in f_0} (2l_1+1)(2l_2+1)\, R_0\,(n_1 l_1, n_2 l_2;\ n_2 l_2, n_1 l_1) - \\ & - \sum_{n_1 l_1 \in f_0,\ n_2 l_2 \in f_0} (2l_1+1)(2l_2+1) \sum_l [l_1\, l_2\, l]^2\, R_l(n_1 l_1, n_2 l_2; n_1 l_1, n_2 l_2) . \end{aligned} \tag{16}$$

Если ввести обычные обозначения [2] для полного числа состояний в электронной оболочке $g(nl) = 2(l+1)$ и для прямого и обменного радиальных интегралов

$$\begin{aligned} F_l(n_1 l_1, n_2 l_2) &\equiv R_l(n_1 l_1, n_2 l_2;\ n_2 l_2, n_1 l_1) , \\ G_l(n_1 l_1, n_2\ l_2) &\equiv R_l(n_1 l_1, n_1 l_2;\ n_1 l_1, n_2 l_2) , \end{aligned}$$

то выражение (16) можно представить в более привычном виде

$$\begin{aligned} E_{\mathrm{HF}} = & \sum_{n_1 l_1 \in f_0} q(n_1 l_1)\, I(n_1 l_1) + \sum_{n_1 l_1 \in f_0} \frac{1}{2}\, q(n_1 l_1)\,\big(q(n_1 l_1) - 1\big)\, F_0(n_1 l_1, n_1 l_1) + \\ & + \sum_{\substack{n_1 l_1 \in f_0,\ n_2 l_2 \in f_0 \\ (n_1 l_1 > n_2 l_2)}} q(n_1 l_1)\, q(n_2 l_2)\, F_0(n_1 l_1, n_2 l_2) - \sum_{n_1 l_1 \in f_0} \sum_{l \neq 0} A_{l_1 l}\, F_l(n_1 l_1, n_1 l_1) - \\ & - \sum_{\substack{n_1 l_1 \in f_0,\ n_2 l_2 \in f_0 \\ (n_1 l_1 \geq n_2 l_1)}} \sum_l B_{l_1 l_2 l}\, G_l(n_1 l_1, n_2 l_2) , \end{aligned} \tag{17}$$

причем

$$A_{l_1 l} = (2l_1+1)^2 [l_1 l_1 l]^2 \quad \text{при} \quad l \neq 0\,, \tag{18}$$

$$B_{l_1 l_2 l} = 2(2l_1+1)(2l_2+1)[l_1 l_2 l]^2\,, \tag{19}$$

где символ $[l_1 l_2 l]$ означает взятый по модулю соответствующий $3j$ — коэффициент с нулевыми проекциями моментов [4].

Формулы (18), (19) позволяют рассчитывать необходимые значения коэффициентов A, B и, в частности, получить важные таблицы

$A_{l_1 l}$

	$l=2$
s	0
p	$\frac{6}{5}$

$B_{l_1 l_2 l}$

	$l=0$	$l=1$	$l=2$
ss	2	0	0
sp	0	2	0
pp	6	0	$\frac{12}{5}$

Выражение (17) для E_{HF} вместе с соответствующими таблицами значений коэффициентов A, B совпадают с получаемыми обычным способом в теории хартри-фоковского приближения [2]; настоящий способ получения этого приближения позволяет не проводить вычислений в каждом конкретном случае, и сразу дает общие формулы (18), (19) для коэффициентов $A_{l_1 l}$ при $l \neq 0$ и $B_{l_1 l_2 l}$.

Вводя множители Лагранжа и варьируя следующее выражение

$$F_{\mathrm{HF}} = E_{\mathrm{HF}} - \sum_{n_1 l_1 \in f_0} 2(2l_1+1)\,\varepsilon_{n_1 l_1} \int_0^{+\infty} r^2\,dr\,R_{n_1 l_1}(r)\,R_{n_1 l_1}(r)\,, \tag{20}$$

то есть раскрывая вариационное условие

$$\frac{\delta F_{\mathrm{HF}}}{\delta R_{nl}(r)} = 0\,, \tag{21}$$

мы получаем из (16) хартри-фоковские уравнения в случае состояний с заполненными электронными оболочками

$$\begin{aligned}
&\left(\frac{d^2}{dr^2} + \frac{2}{r}\frac{d}{dr} - \frac{l(l+1)}{r^2} + \frac{2Z}{r}\right) R_{nl}(r) - \\
&\quad - 4 \sum_{n_1 l_1 \in f_0} (2l_1+1) \int_0^{+\infty} r_1^2\,dr_1\,R_{n_1 l_1}(r)\,U_0(r,r_1)\,R_{n_1 l_1}(r_1)\,R_{nl}(r) + \\
&\quad + 2 \sum_{n_1 l_1 \in f_0} (2l_1+1) \sum_{l'} [l_1\, l l']^2 \int_0^{+\infty} r_1^2\,dr_1\,R_{n_1 l_1}(r_2)\,U_{l'}(r,r_1)\,R_{nl}(r_1)\,R_{n_1 l_1}(r) + \\
&\quad + 2\,\varepsilon_{nl}\,R_{nl}(r) = 0\,,
\end{aligned} \tag{22}$$

причем, разумеется,

$$\int_0^{+\infty} r^2\, dr\, R_{nl}(r)\, R_{nl}(r) = 1\,. \tag{23}$$

Помножая правую и левую часть (22) на $R_{nl}(r)$ и интегрируя по r от 0 до $+\infty$, с учетом (23) получим условие

$$\begin{aligned} &2\,U(nl\,;\,nl) - 4 \sum_{n_1 l_1 \in f_0} (2l_1+1)\, R_0(n_1 l_1, nl\,;\; nl, n_1 l_1) + \\ &+2 \sum_{n_1 l_1 \in f_0} (2l_1+1) \sum_{l'} [l_1\, ll']^2\, R_{l'}(n_1 l_1, nl; n_1 l_1, nl) = 0\,. \end{aligned} \tag{24}$$

Это важное условие, являющееся непосредственным следствием (21), мы должны интерпретировать на диаграммах: на диаграммном языке оно означает, что

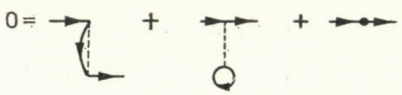

(причем обе внешние линии никак не нужно учитывать, здесь они не дают никакого вклада).

Таким образом условие (24) означает, что среди диаграмм теории возмущений, развиваемой на основе хартри-фоковских уравнений (22), (23), мы должны не рассматривать вовсе диаграммы, содержащие парные вертексы и собственно-энергетические части первого порядка, так как вследствие (24) вклады от всех указанных диаграмм взаимно сокращаются.

Это характерное свойство теории возмущений на основе хартри-фоковского приближения по сравнению с другими теориями возмущений на основе произвольного нулевого гамильтониана H_0^U, и, в частности, теорией возмущения на основе исходного нулевого гамильтониана H_0, делает ее очень удобной в работе. Большое количество диаграмм, виртуально присутствующих в теории возмущений, теперь не нужно рассматривать.

В частности во втором порядке в рассматриваемой теории возмущений остаются только следующие две диаграммы

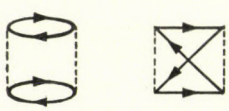

а в третьем порядке только шесть диаграмм, вернее все временные версии этих шести диаграмм,

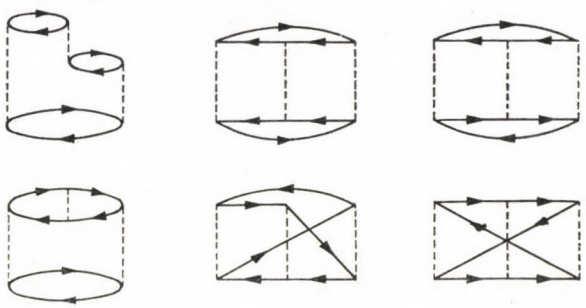

То что это так, в этом легко убедиться, рассматривая в первых порядках решение по теории возмущений уравнений (22), (23) и вычисляя в первых порядках энергию по формуле (16). В представлении водородоподобных функций

$$\left(-\frac{1}{2}\frac{d^2}{dr^2}-\frac{1}{r}\frac{d}{dr}+\frac{l(l+1)}{2r^2}-\frac{z}{r}-E_{nl}\right)R^0_{nl}(r)=0\,, \tag{25}$$

$$\int_0^{+\infty} r^2\,dr\,R^0_{n'l'}(r)\,R^0_{nl}(r)=\delta_{n',n'}\,\delta_{l',l'}\,, \tag{26}$$

мы должны рассмотреть разложение

$$R_{nl}(r)=\sum_{n'} c^l_{n',n}\,R^0_{n'l}(r) \tag{27}$$

причем для коэффициентов этого разложения получим уравнения

$$\begin{aligned}&E_{n_2l}\,c^l_{n,n}+\\&+2\sum_{n_1l_1\in f_0}(2l_1+1)\sum_{n_1',n_1'',n'} c^{l_1}_{n_1'',n_1}\,c^{l_1}_{n_1',n_1}\,c^l_{n'',n}\,R^0_0(n_1'l_1,n_2l;n'l,n_1''l_1)-\\&-\sum_{n_1l_1\in f_0}(2l_1+1)\sum_k[l_1lk]^2\sum_{n_1',n',n_1''} c^{l_1}_{n_1',n_1}\,c^l_{n_1',n}\,c^{l_1}_{n_1'',n_1}R^0_k(n_1'l_1,n_2l;n_1''l_1,n'l)-\\&-\varepsilon_{nl}\,c^l_{n_2,n}=0,\end{aligned} \tag{28}$$

$$\sum_{n'} C^l_{n',n_1}\,C^l_{n',n_2}=\delta_{n_1,n_2}. \tag{29}$$

Здесь предполагается, что в величинах $C^l_{n',n}$ индексы $nl\in f_0$.

Разрешая уравнения (28), (29) разложениями

$$C^l_{n',n}=\delta_{n',n}+c^{l(1)}_{n',n}+\ldots, \tag{30}$$

$$\varepsilon_{nl}=E_{nl}+\varepsilon^{(1)}_{nl}+\ldots, \tag{31}$$

получим, в частности, при $n_2' \neq n_2$

$$C^{l(1)}_{n_2',n_2} = \frac{1}{E_{n_2'l} - E_{n_2l}} \left\{ -2 \sum_{n_1 l_1 \in f_0} (2l_1 + 1)\, R^0_0(n_1 l_1, n_2' l_2; n_2 l, n_1 l_1) + \right.$$
$$\left. + \sum_{n_1 l_1 \in f_0} (2l_1 + 1) \sum_l [l_1 l_2 l]^2 R^0_l(n_1 l_1, n_2' l_2; n_1 l_1, n_2 l) \right\} \tag{32}$$

и при $n_2' = n_2$

$$C^{l(1)}_{n_2,n_2} = 0\,. \tag{33}$$

Подставим разложения (30), (31), (32), (33) в выражение (16). Отметим предварительно, что

$$I(nl) = \sum_{n'}{}' E_{n'l}\, C^l_{n',n}\, C^l_{n',n} =$$
$$= E_{nl} + 2E_{nl}\, C^{l(2)}_{n,n} + \sum_{n'} E_{n'l}\, C^{l(1)}_{n',n}\, C^{l(1)}_{n',n} + \ldots .$$

Но так как в силу условия ортонормировки

$$C^{l(1)}_{n_2,n_1} + C^{l(1)}_{n_1,n_2} + \sum_{n'} C^{l(1)}_{n',n_1}\, C^{l(1)}_{n',n_2} = 0$$

имеем

$$2C^{l(2)}_{n,n} = -\sum_{n'} C^{l(1)}_{n',n}\, C^{l(1)}_{n',n}$$

то приближенно

$$I(nl) = E_{nl} + \sum_{n'}{}' (E_{n'l} - E_{nl})\, C^{l(1)}_{n',n}\, C^{l(1)}_{n',n} + \ldots \tag{34}$$

Во втором порядке получим

$$E^{(2)}_{\mathrm{HF}} = \sum_{n_2 l_2 \in f_0}{}' 2(2l_2 + 1) \sum_{n_2'} (E_{n_2' l_2} - E_{n_2 l_2})\, C^{l_2(1)}_{n_2',n_2}\, C^{l_2(1)}_{n_2',n_2} +$$
$$+ 8 \sum_{n_1 l_1 \in f_0,\, n_2 l_2 \in f_0} (2l_1 + 1)(2l_2 + 1) \sum_{n_2'} C^{l_2(1)}_{n_2',n_2}\, R^0_0(n_1 l_1, n_2' l_2; n_2 l_2, n_1 l_1) -$$
$$- 4 \sum_{n_1 l_1 \in f_0,\, n_2 l_2 \in f_0} (2l_1 + 1)(2l_2 + 1) \sum_l [l_1 l_2 l]^2 \sum_{n_2'} C^{l_2(1)}_{n_2',n_2}\, R^0_l(n_1 l_1, n_2' l_2; n_1 l_1, n_2 l_2)\,. \tag{35}$$

Подставляя (32), (33) в (38), мы получим довольно громоздкое выражение, которое однако можно представить в виде суммы вкладов от трех атомных хартри-фоковских диаграмм второго порядка в естественно возникающей здесь теории возмущений на водородоподобных функциях (см. табл. I).

Таким образом вклады от этих трех диаграмм второго порядка с собственно-энергетическими частями первого порядка уже автоматически включены в хартри-фоковское приближение, и следовательно, они не могут появиться в теории возмущения на хартри-фоковских функциях.

2. Состояния с открытыми электронными оболочками

Ограничимся здесь рассмотрением вырожденного состояния атома с заполненными электронными оболочками $nl \in f_0$ и открытой оболочкой $n_a l_a$; все остальные пустые электронные оболочки этого состояния $nl \in g_0$. Более того, будем рассматривать здесь только простейший случай неповторяющегося терма SL конфигурации l_a^q, где q — число электронов в открытой оболочке.

Опять мы рассматриваем точное состояние гамильтониана H_0^U и соответствующее ему, но неизвестное нам состояние, полного гамильтониана H. Так что рассматриваемое состояние имеет энергию

$$E_0 = \sum_{n_1 l_1 \in f_0} 2(2l_1 + 1)\, \varepsilon_{n_1 l_1} + q\, 2(2l_a + 1)\, \varepsilon_{n_a l_a}\,; \tag{36}$$

соответствующее ему состояние полного гамильтониана имеет энергию

$$E_0 + \Delta E\,, \tag{37}$$

Согласно общей теории [4] величину ΔE нужно представить в виде суммы

$$\Delta E = \Delta E_0 + \Delta E'\,, \tag{38}$$

причем $E\Delta_0$ — это величина для невырожденного состояния остова $n_1 l_1 \in f_0$, в котором открытая оболочка $n_a l_a$ пустая; эта величина дается суммой вкладов от соответствующих атомных фейнмановских диаграмм без внешних линий, см. § 1.

Согласно общей теории [4], чтобы вычислить величину $\Delta E'$, нужно решать секулярные уравнения с матрицей M по индексу α повторяемости терма SL рассматриваемой конфигурации l_a^q. Так как мы рассматриваем случай неповторяющегося терма SL, то, следовательно, нам не нужно решать никаких секулярных уравнений, а нужно просто вычислить соответствующий диагональный матричный элемент матрицы M, ибо в рассматриваемом случае указанные секулярные уравнения сводятся к соотношению

$$\Delta E' = M\big((n_a l_a)^q\, SL, (n_a l_a)^q\, SL; \Delta E'\big)\,. \tag{39}$$

Диагональный элемент (39) матрицы M дается суммой вкладов соответствующих атомных диаграмм с двумя, четырьмя и т. д. внешними электронными линиями; нужно рассматривать только диаграммы с числом электрон-

ных линий меньшим или равным удвоенному числу электронов в открытой оболочке $2q$.

Правила составления вкладов от таких диаграмм с внешними линиями при $U \equiv 0$ подробно разобраны в [4], и здесь нет необходимости их повторять. Единственно, что важно, что в рассматриваемом случае $U \not\equiv 0$ мы имеем в теории кроме четверного, также и парные вертексы, см. § 1.

Диаграммы фактически составляются только для того случая, когда число внешних электронных линий в точности равно удвоенному числу электронов в открытой оболочке [4]. Если оно меньше его, то надо пользоваться формулой редукции, которая в случае рассматриваемого состояния $(n_a l_a)^q SL$ принимает вид для суммы всех диаграмм с $2p$ свободными концами

$$M_p\big((n_a l_a)^q SL; (n_a l_a)^q SL; \Delta E'\big) =$$

$$= \sum_{\alpha\beta S' l'} g(l_a^q SL, l_a^p \alpha S'L'; l_a^p \beta S'L', l_a^q SL) \times$$

$$\times M_p\big((n_a l_a)^p \alpha S'L'; (n_a l_a)^p \beta S'L'; \Delta E'\big). \tag{40}$$

Разумеется

$$M = \sum_{p=1}^{q} M_p. \tag{41}$$

При составлении выражения для хартри-фоковской энергии E_{HF} нам здесь необходимо рассмотреть только диаграммы первого порядка; в этом порядке имеются диаграммы только с двумя и четырьмя внешними электронными линиями. Так что фактически нам нужны величины g из (40) только при $p = 1$ и $p = 2$.

Используя общее условие нормировки величин g, можно сразу определить их для случая $p = 1$. Действительно, согласно этому условию

$$\sum_{\alpha S'L'} g(l_a^q SL, l_a^p \alpha S'L'; l_a^p \alpha S'L', l_a^q SL) = \frac{q!}{p!\,(q-p)!} \tag{42}$$

и отсюда в случае $p = 1$ сразу получаем

$$g(l_a^q SL, l_a) = q. \tag{43}$$

Для $p = 2$ величины g следует специально рассчитывать, используя их выражения через соответствующие генеалогические коэффициенты. Мы приводим здесь таблицы значений соответствующих величин g в важных частных случаях

$g(p^3\,SL,\ p^2\,S'\,L')$

p^3/p^2	^1S	^3P	^1D
^4S	0	3	0
^2P	$\frac{2}{3}$	$\frac{3}{2}$	$\frac{5}{6}$
^2D	0	$\frac{3}{2}$	$\frac{3}{2}$

$g(p^4\,SL,\ p^2\,S'\,L')$

p^4/p^2	^1S	^3p	^1D
^1S	$\frac{4}{3}$	3	$\frac{5}{3}$
^3P	$\frac{1}{3}$	4	$\frac{5}{3}$
^1D	$\frac{1}{3}$	3	$\frac{8}{3}$

$(gp^5\,SL\,;\ p^2\,S'\,L')$

p^5/p^2	^1S	^3P	^1D
^2P	$\frac{5}{2}$	6	$\frac{10}{3}$

Оставляя вклады атомных фейнмановских диаграмм, только первого порядка, мы получим для величины $\Delta E'_{\mathrm{HF}}$ для вкладов диаграмм первого порядка в случае $q = p$.

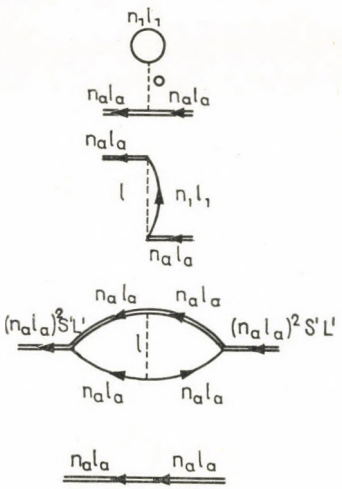

$$2 \sum_{n_1 l_1 \in f_0} (2l_1 + 1)\, R_0(n_1 l_1, n_a l_a; n_a l_a, n_1 l_1)\,,$$

$$- \sum_{n_1 l_1 \in f_0} (2l_1 + 1) \sum_l [l_a l_1 l]^2\, R_l(n_1 l_1, n_a l_a; n_1 l_1, n_a l_a),$$

$$(-1)^{L'} \delta_{S',1/2,1/2} \sum_l R_l(n_a l_a, n_a l_a; n_a l_a, n_a l_a) \times$$

$$\times [l_a l_a l]^2 (2l_a + 1) \begin{Bmatrix} l_a l_a l \\ l_a l_a L' \end{Bmatrix},$$

$$- u(n_a l_a; n_a l_a)\,,$$

и окончательно для полной хартри-фоковской энергии рассматриваемого состояния $(n_a l_a)^q\, SL$

$$E_{\mathrm{HF}} = \sum_{n_1 l_1 \in f_0} 2(2l_1 + 1)\, I(n_1 l_1) +$$

$$+ 2 \sum_{n_1 l_1 \in f_0,\, n_2 l_2 \in f_0} (2l_1 + 1)(2l_2 + 1)\, R_0(n_1 l_1, n_2 l_2; n_2 l_2, n_1 l_1) -$$

$$- \sum_{n_1 l_1 \in f_0,\, n_2 l_2 \in f_0} (2l_1 + 1)(2l_2 + 1) \sum_l [l_1 l_2 l]^2\, R_l(n_1 l_1, n_2 l_2; n_1 l_1, n_2 l_2) +$$

$$+ f \Big\{ 2(2l_a + 1)\, I(n_a l_a) +$$

$$+4\sum_{n_1 l_1 \in f_0}(2l_a+1)(2l_1+1)\,R_0(n_1 l_1, n_a l_a; n_a l_a, n_1 l_1) -$$
$$-2\sum_{n_1 l_1 \in f_0}(2l_a+1)(2l_1+1)\sum_l [l_a l_1 l]^2 R_l(n_a l_a, n_1 l_1; n_a l_a, n_1 l_1)\Big\} +$$
$$+\sum_l \sum_{S'L'} g(l_a^q SL, l_a^2 S'L')\,(-1)^{L'} \begin{Bmatrix} l_a l_a l \\ l_a l_a L' \end{Bmatrix} \times$$
$$\times (2l_a+1)^2 [l_a l_a l]^2 R_l(n_a l_a, n_a l_a; n_a l_a, n_a l_a)\,, \tag{44}$$

где $f=q/2(2l_a+1)$, и эта величина характеризует степень заполнения электронами рассматриваемой открытой оболочки.

В важном случае $l_a = 1$ для состояний $(n_a p)^q SL$ Рутан [3], используя процедуру усреднения энергии по всем состояниям данного терма SL, получил выражение

$$E_{\mathrm{HF}} = 2\sum_k H_k + \sum_{kl}(2I_{kl} - K_{kl}) +$$
$$+f\Big\{2\sum_m H_m + 2\sum_{km}(2I_{km} - K_{km}) +$$
$$+f\sum_{mn}(2aI_{mn} - bK_{mn})\Big\}\,. \tag{45}$$

Здесь индексы k, l относятся к заполненным оболочкам; индексы m, n — k остальным оболочкам. Далее $k \equiv (n_1 l_1 m_1)$, $l \equiv (n_2 l_2 m_2)$ и т. д.

$$H_k \equiv I(n_1 l_1)\,,$$
$$I_{kl} \equiv R_0(n_1 l_1, n_2 l_2; n_2 l_2, n_1 l_1)\,,$$
$$K_{kl} \equiv \sum_l [l_1 l_2 l]^2 R_l(n_1 l_1, n_2 l_2; n_1 l_1, n_2 l_2)$$

и т. д. Выражение Рутана (45) полностью совпадает с нашим (44) при $l_a = 1$, причем мы получаем общие явные выражения для коэффициентов a, b Рутана

$$b = -\frac{36}{q^2}\sum_{S'L'} g(p^q SL; p^2 S'L')\,(-1)^{L'} \begin{Bmatrix} 1 & 1 & 2 \\ 1 & 1 & L' \end{Bmatrix}, \tag{46}$$

$$6a - b = \frac{36}{q^2}\sum_{S'L'} g(p^q SL; p^2 S'L')\,(-1)^{L'} \begin{Bmatrix} 1 & 1 & 0 \\ 1 & 1 & L \end{Bmatrix}. \tag{47}$$

По этим формулам легко составить таблицу значений коэффициентов a, b, полностью совпадающую с приведенной Рутаном [3].

	p^2			^3p			p^4			p^5
	^1S	^3P	^1D	^4S	^2P	^2D	^1S	^3P	^1D	^2P
a	0	$\frac{3}{4}$	$\frac{9}{20}$	1	$\frac{2}{3}$	$\frac{4}{5}$	$\frac{3}{4}$	$\frac{15}{16}$	$\frac{69}{80}$	$\frac{24}{25}$
b	-3	$\frac{3}{2}$	$-\frac{3}{10}$	2	0	$\frac{4}{5}$	0	$\frac{9}{8}$	$\frac{27}{40}$	$\frac{24}{25}$

Выражение (44) можно также сравнить с приводимим Хартри [2], который использовал процедуру усреднения самосогласованного поля по различным направлениям в пространстве. Это выражение имеет следующий вид

$$E_{\mathrm{HF}} = \sum_{n_1 l_1 \in f_0} q(n_1 l_1)\, I(n_1 l_1) + \sum_{n_1 l_1 \in f_0} \frac{1}{2}\, q(n_1 l_1)\,(q(n_1 l_1) - 1)\, F_0(n_1 l_1, n_1 l_1) +$$

$$+ \sum_{\substack{n_1 l_1 \in f_0,\, n_2 l_2 \in f_0 \\ (n_1 l_1 > n_2 l_2)}} q(n_1 l_1)\, q(n_2 l_2)\, F_0(n_1 l_1, n_2 l_2) - \sum_{n_1 l_1 \in f_0} \sum_{l \neq 0} A_{l_1 l}\, F_l(n_1 l_1, n_1 l_1) -$$

$$- \sum_{\substack{n_1 l_1 \in f_0,\, n_2 l_2 \in f_0 \\ (n_1 l_1 \geqslant n_2 l_2)}} \sum_{l} B_{l_1 l_2 l}\, G_l(n_1 l_1, n_2 l_2) +$$

$$+ q(n_a l_a)\, I(n_a l_a) + q(n_a l_a) \sum_{n_1 l_1 \in f_0} q(n_1 l_1)\, F_0(n_a l_a\,; n_1 l_1) +$$

$$+ \frac{1}{2}\, q(n_a l_a)\,(q(n_a l_a) - 1)\, F_0(n_a l_a; n_a l_a) -$$

$$- \frac{q(n_a l_a)}{2(2l_a+1)} \sum_{n_1 l_1 \in f_0} \sum_{l} B_{l_a l_1 l}\, G_l(n_a l_a; n_1 l_1) -$$

$$- \sum_{l} A_{l_a l}\, F_l(n_a l_a; n_a l_a)\,. \tag{48}$$

Сравнивая (48) с (44), получаем явные выражения для коэффициентов Хартри

$$B_{l_a l_1 l} \equiv 2(2l_a + 1)\,(2l_1 + 1)\,[l_a l_1 l]^2\,, \tag{49}$$

$$A_{l_a l} \equiv - \sum_{S'L'} g(l_a^q\, SL;\, l_a^2\, S'L)\,(-1)^{L'} \begin{Bmatrix} l_a l_a l \\ l_a l_a L' \end{Bmatrix} \times$$

$$\times\, (2l_a + 1)^2\,[l_a\, l_a\, l]^2\,. \tag{50}$$

По этим формулам можно составить таблицы значений этих коэффициентов, полностью совпадающие со значениями из таблиц, приводимых в [2].

A_{1l}		
p^2/l	0	2
^1S	-1	$-\frac{2}{5}$
^3P	-1	$\frac{1}{5}$
^1D	-1	$-\frac{1}{25}$

A_{1l}		
p^3/l	0	2
^4S	-3	$\frac{3}{5}$
^2P	-3	0
^2D	-3	$\frac{6}{25}$

A_{1l}		
p^4/l	0	2
^1S	-6	0
^3P	-6	$\frac{3}{5}$
^1D	-6	$\frac{9}{25}$

A_{1l}		
p^5/l	0	2
^2P	-10	$\frac{3}{5}$

Отметим, что ввиду того, что $\left\{ \begin{matrix} l_a\, l_a\, 0 \\ l_a\, l_a L' \end{matrix} \right\} = \frac{(-1)^{L'}}{2l_a+1}\,\delta_{l_a\,,\,l_a\,,\,L'}$ и что $[l_a\, l_a\, 0] = \frac{1}{2l_a+1}$, мы имеем

$$A_{l_a} 0 = -\frac{q(q-1)}{2}\,. \tag{51}$$

Получим теперь хартри-фоковские уравнения. Вводя множители Лагранжа и варьируя выражение

$$\begin{aligned} F_{\mathrm{HF}} = E_{\mathrm{HF}} &- \sum_{n_1 l_1 \in f_0} 2(2l_1+1)\,\varepsilon_{n_1 l_1} \int_0^{+\infty} r^2\,dr\, R_{n_1 l_1}(r)\, R_{n_1 l_1}(r) - \\ &- 2(2l_a+1) f \varepsilon_{n_a l_a} \int_0^{+\infty} r^2\,dr\, R_{n_a l_a}(r)\, R_{n_a l_a}(r) - \\ &- 4f \sum_{n_1 l_1 \in f_0} (2l_a+1)\,(2l_1+1)\,\varepsilon_{n_1 l_1,\, n_a l_a} \int_0^{+\infty} r^2\,dr\, R_{n_1 l_1}(r)\, R_{n_a l_a}(r) - \\ &- 4f \sum_{n_1 l_1 \in f_0} (2l_a+1)\,(2l_1+1)\,\varepsilon_{n_a l_a,\, n_1 l_1} \int_0^{+\infty} r^2\,dr\, R_{n_a l_a}(r)\, R_{n_1 l_1}(r)\,, \end{aligned} \tag{52}$$

то есть раскрывая в явном виде вариационные условия

$$\frac{\delta F_{\mathrm{HF}}}{\delta R_{n_1 l_1}(r)} = 0\,, \qquad \frac{\delta F_{\mathrm{HF}}}{\delta R_{n_a l_a}(r)} = 0\,, \tag{53}$$

получим хартри-фоковские уравнения в случае состояний с одной открытой электронной оболочкой $(n_a l_a)^q SL$ с неповторяющимся термом

$$\begin{aligned} &\left(\frac{d^2}{dr^2} + \frac{2}{r}\,\frac{d}{dr} - \frac{l(l+1)}{r^2} + \frac{2Z}{r} \right) R_{nl}(r) - \\ &- 4 \sum_{n_1 l_1 \in f_0} (2l_1+1) \int_0^{+\infty} r_1^2\,dr_1\, R_{n_1 l_1}(r_1)\, U_0(r, r_1)\, R_{n_1 l_1}(r_1)\, R_{nl}(r) + \\ &+ 2 \sum_{n_1 l_1 \in f_0} (2l_1+1) \sum_{l'} [l_1\, l l']^2 \int_0^{+\infty} r_1^2\,dr_1\, R_{n_1 l_1}(r_1)\, U_{l'}(r, r_1)\, R_{nl}(r_1)\, R_{n_1 l_1}(r) + \\ &+ f[-4(2l_a+1) \int_0^{+\infty} r_1^2\,dr_1\, R_{n_a l_a}(r_1)\, U_0(r, r_1)\, R_{n_a l_a}(r_1)\, R_{nl}(r) + \\ &+ 2(l_a+1) \sum_{l'} [l_a\, l l']^2 \int_0^{+\infty} r_1^2\,dr\, R_{n_a l_a}(r)\, U_{l'}(r, r_1)\, R_{nl}(r_1)\, R_{n_a l_a}(r) \Big) + \\ &+ 2\varepsilon_{nl} R_{nl}(r) + f4(2l_a+1)\,\varepsilon_{nl,\, n_a l_a}\, R_{n_a l_a}(r) = 0\,, \end{aligned} \tag{54}$$

$$f\left(\frac{d^2}{dr^2}+\frac{2}{r}\frac{d}{dr}-\frac{l(l+1)}{r^2}+\frac{2z}{r}\right)R_{n_al_a}(r)-$$

$$-4f\sum_{n_1l_1\in f_0}(2l_1+1)\int_0^{+\infty}r_1^2dr_1\,R_{n_1l_1}(r_1)\,U_{\cdot}(r,r_1)\,R_{n_1l_1}(r_1)\,R_{n_al_a}(r)-$$

$$+2f\sum_{n_1l_1\in f_0}(2l_1+1)\sum_{l'}[l_1\,l_a\,l']^2\int_0^{+\infty}r_1^2dr_1R_{n_1l_1}(r_1)U_{l'}(r,r_1)\,R_{n_al_a}(r_1)\,R_{n_1l_1}(r)=$$

$$-(2l_a+1)\sum_{l'}\sum_{S'L'}g(l_a^0\,SL;\,l_a^2\,S'L')(-1)^{L'}\begin{Bmatrix}l_a\,l_a\,l'\\l_a\,l_a\,L'\end{Bmatrix}[l_a\,l_a\,l']^2\times \tag{55}$$

$$\times\int_0^{+\infty}r_1^2\,dr_1\,R_{n_al_a}(r_1)\,U_{l'}(r,r_1)\,R_{n_al_a}(r_1)\,R_{n_al_a}(r)+$$

$$+2f\,\varepsilon_{n_al_a}R_{n_al_a}(r)+4f\sum_{n_1l_1\in f_0}(2l_1+1)\,\varepsilon_{n_al_a,n_1l_1}R_{n_1l_1}(r)=0\,,$$

причем имеем $\varepsilon_{n_an_a,l_1l_1}\equiv\varepsilon_{n_1n_1,l_al_a}$ разумеется, эту важную величину мы не можем просто положить равной нулю [2].

3. Интерпретация уравнений Хартри-Фока для открытой оболочки $(n_al_a)^qSL$ на атомных фейнмановских диаграммах

Поступим теперь так же, как в конце § 1 в случае замкнутых электронных оболочек. Возьмем хартри-фоковские уравнения (54), (55), прейдем в них в представление водородоподобных функций (25), (26), (27) и разрешим получившиеся уравнения по теории возмущений. Затем подставим эти приближенные решения в выражение для энергии (44) и попытаемся интерпретировать возникающие там различные вклады в хартри-фоковскую энергию на атомных фейнмановских диаграммах. Так мы установим, с какого рода диаграммами связано приближение Хартри—Фока в случае открытых оболочек.

Не будем здесь выписывать исходные точные уравнения для C, полностью аналогичные (28), (29), а сразу приведем уравнения первого приближения

$$c^l_{n',n}=\delta_{n',n}+c^{l(1)}_{n',n}+\ldots\,, \tag{56}$$

$$\varepsilon_{nl}=E_{nl}+\varepsilon^{(1)}_{nl}+\ldots\,, \tag{57}$$

$$\varepsilon_{n_al_a,\,n_1l_1}=\varepsilon^{(1)}_{n_al_a,n_1l_1}+\ldots\,. \tag{58}$$

Имеем для функций замкнутых оболочек

$$
\begin{aligned}
&(E_{n_2 l} - E_{nl})\, c^{l(1)}_{n_2,n} + \\
&\quad + 2 \sum_{n_1 l_1 \in f_0} (2l_1+1)\, R^0_0 (n_1 l_1, n_2 l;\ nl, n_1 l_1) - \\
&\quad - \sum_{n_1 l_1 \in f_0} (2l_1+1) \sum_k [l_1 lk]^2\, R^0_k (n_1 l_1, n_2 l;\ n_1 l_1, nl) + \\
&\quad + f \{2(2l_a+1)\, R^0_0 (n_a l_a, n_2 l;\ nl, n_a l_a) - \\
&\quad - (2l_a+1) \sum_k [l_a lk]^2\, R^0_k (n_a l_a, n_2 l;\ n_a l_a, nl)\} - \\
&\quad - \varepsilon^{(1)}_{kl}\, \delta_{n_2,n} - f\, 2\,(2l_a+1)\, \varepsilon^{(1)}_{nl,n_a l_a}\, \delta_{n_2,n_a}\, \delta_{l,l_a} = 0
\end{aligned}
\tag{59}
$$

и для функции открытой оболочки

$$
\begin{aligned}
&f\,(E_{n_2 l_a} - E_{n_a l_a})\, c^{l_a(1)}_{n_2,n_a} + \\
&\quad + 2f \sum_{k_1 l_1 \in f_0} (2l_1+1)\, R^0_0 (n_1 l_1.\ n_2 l_a;\ n_a l_a, n_1 l_1) - \\
&\quad - f \sum_{n_1 l_1 \in f_0} [l, l_a k]^2\, R^0_k (n_1 l_1, n_2 l_a;\ n_1 l_1, n_a l_a) + \\
&\quad + (2\,l_a+1) \sum_k \sum_{S'L'} g(l^q_a SL; l^2_a S'L')(-1)^{L'} \begin{Bmatrix} l_a & l_a & k \\ l_a & l_a & L' \end{Bmatrix} \times \\
&\quad \times [l_a l_a k]^2\, R^0_k (n_a l_a, n_2 l_a;\ n_a l_a, n_a l_a) - \\
&\quad - f\, \varepsilon^{(1)}_{n_a l_a}\, \delta_{n_2,n_a} - 2f \sum_{n_1 l_1 \in f_0} (2l_1+1)\, \varepsilon^{(1)}_{n_a l_a, n_1 l_1}\, \delta_{n_2 l_1}\, \delta_{l_a,l_1} = 0\,.
\end{aligned}
\tag{60}
$$

Кроме того, из условий нормировки имеем

$$
c^{l(1)}_{n_2,n_1} + c^{l(1)}_{n_1,n_2} = 0 \qquad \text{при} \qquad n_1 l \in f_0,\ n_2 l \in f_0\,, \tag{61}
$$

$$
c^{l_a(1)}_{n_a,n_1} + c^{l_a(1)}_{n_1,n_a} = 0 \qquad \text{при} \qquad n_1 l_a \in f_0,\ c^{l_a(1)}_{n_a,n_a} = 0\,. \tag{62}
$$

В результате вычислений мы получаем следующий результат. Энергия первого порядка $E^{(1)}_{\mathrm{HF}}$ включает в себя вклады от всех соответствующих диаграмм первого порядка, и поэтому ее не надо рассматривать. Энергия второго порядка $E^{(2)}_{\mathrm{HF}}$, напротив, не включает в себя вклады всех диаграмм второго порядка.

Прежде всего, существует большое количество диаграмм, содержащих собственно-энергетические части первого порядка, вклады которых полностью включены в $E^{(2)}_{\mathrm{HF}}$. Эти диаграммы изображены ниже, кроме очевидных вакуумных диаграмм, отличающихся от приведенных в табл. I для

Таблица I

Вклады вакуумных Хартри—фоковских диаграмм второго порядка

2 A) 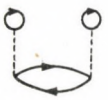	$$-8\sum_{n_2l_2\in f_0}(2l_2+1)\sum_{n_2'l_2\in g_0}\frac{1}{E_{n_2'l_2}-E_{n_2l_2}}\times\left(\sum_{n_1l_1\in f_0}(2l_1+1)\,R_0^0(n_1l_1,n_2'l_2;\;n_2l_2,n_1l_1)\right)^2$$
2 B_1) 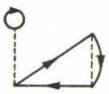 2 B_2) 	$$8\sum_{n_2l_2\in f_0}(2l_2+1)\sum_{n_2'l_2\in g_0}\frac{1}{E_{n_2'l_2}-E_{n_2l_2}}\times\left(\sum_{n_1l_1\in f_0}(2\,l_1+1)\,R_0^0\,(n_1\,l_1,n_2'\,l_2;\;\;n_2\;l_2,n_1\,l_1)\right)^2\times$$ $$\times\left(\sum_{n_1l_1\in f_0}(2l_1+1)\sum_l[l_1l_2l]^2\,R_l^0(n_1l_1,n_2'l_2;\,n_1l_1,n_2l_2)\right)$$
2 C) 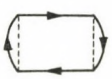	$$-2\sum_{n_2l_2\in f_0}(2l_2+1)\sum_{n_2'l_2\in g_0}\frac{1}{E_{n_2'l_2}-H_{n_2l_2}}\times\left(\sum_{n_1l_1\in f_0}(2l_1+1)\sum_l[l_1l_2l]^2R_l^0(n_1l_1,n_2'l_2;\,n_1l_1,n_2l_2)\right)^2$$

замкнутых оболочек только тем, что вместо g_0 надо поставить теперь $g_0+n_al_a$; приводятся также вклады этих диаграмм, составленные по обычным правилам составления атомных фейнмановских диагра мм(см. табл. IIа, IIб, III).

Кроме вкладов от указанных диаграмм с собственно-энергетическими частями первого порядка величина $E_{\mathrm{HF}}^{(2)}$ содержит также другие вклады, диаграммная интерпретация которых затруднительна или даже невозможна.

Эти недиаграммные вклады мы тем не менее можем как-то осмыслить и проверить правильность вычисленных коэффициентов перед ними, если рассмотрим очень частный случай, когда рассматриваемая открытая оболочка полностью занята электронами, то есть когда имеются только вакуумные диаграммы без внешних концов. Все эти вклады оказываются очень важными.

Таблица II

Вклады Хартри-фоковских диаграмм с двумя внешними линиями второго порядка

2G$_1$) 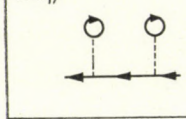	$$-8f(2l_a+1)\sum_{n_2l_a\in g_0}\frac{1}{E_{n_2l_a}-E_{n_al_a}}\times\left(\sum_{n_1l_1\in f_0}(2l_1+1)\,R^0_0(n_1l_1,n_2l_a;n_al_a,n_1l_1)\right)^2$$
2G$_2$) 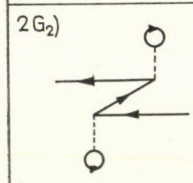	$$8f(2l_a+1)\sum_{n_2l_a\in f_0}\frac{1}{E_{n_al_a}-E_{n_2l_a}}\times\left(\sum_{n_1l_1\in f_0}(2l_1+1)R^0_0(n_1l_1,n_2l_a;n_al_a,n_1l_1)\right)^2$$
2H$_1$) 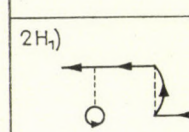 2H$_2$) 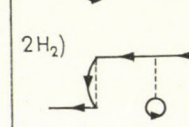	$$8f(2l_a+1)\sum_{n_2l_a\in g_0}\frac{1}{E_{n_2l_a}-E_{n_al_a}}\times\left(\sum_{n_1l_1\in f_0}(2l_1+1)\,R^0_0(n_1l_1,n_2l_a;n_al_a,n_1l_1)\right)\times\left(\sum_{n_1l_1\in f_0}(2l_1+1)\sum_l[l_1l_al]^2R^0_l(n_1l_1,n_2l_a;n_1l_1,n_al_a)\right)$$
2I$_1$) 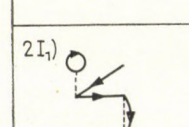 2I$_2$) 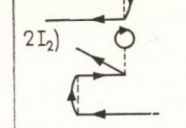	$$-8f(2l_a+1)\sum_{n_2l_a\in f_0}\frac{1}{E_{n_al_a}-E_{n_2l_a}}\times\left(\sum_{n_1l_1\in f_0}(2l_1+1)\,R^0_0(n_1l_1,n_2l_a;n_al_a,n_1l_1)\right)\times\left(\sum_{n_1l_1\in f_0}(2l_1+1)\sum_l[l_1l_al]^2\,R^0_l(n_1l_1,n_2l_a;n_1l_1,n_al_a)\right)$$
2J$_1$) 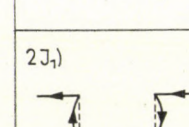	$$-2f(2l_a+1)\sum_{n_2l_a\in g_0}\frac{1}{E_{n_2l_a}-E_{n_al_a}}\times\left(\sum_{n_1l_1\in f_0}(2l_1+1)\sum_l[l_1l_al]^2\,R^0_l(n_1l_1,n_2l_a;n_1l_1,n_al_a)\right)^2$$
2J$_2$) 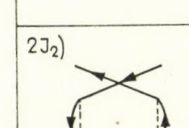	$$2f(2l_a+1)\sum_{n_2l_a\in f_0}\frac{1}{E_{n_al_a}-E_{n_2l_a}}\times\left(\sum_{n_1l_1\in f_0}(2l_1+1)\sum_l[l_1l_2l]^2\,R^0_l(n_1l_1,n_2l_a;n_1l_1,n_al_a)\right)^2$$

Таблица II б

Вклады Хартри-фоковских диаграмм с двумя внешними линиями второго порядка

2 K$_1$) 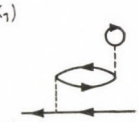 2 K$_2$) 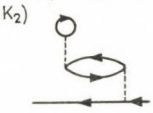	$$-16f(2l_a+1)\sum_{n_2l_2\in f_0}(2l_2+1)\sum_{n_2'l_2\in g_0+n_al_a}\frac{1}{E_{n_2'l_2}-E_{n_2l_2}}\times$$ $$\times R_0^0(n_al_a, n_2'l_2; n_2l_2, n_al_a)\times$$ $$\times\left(\sum_{n_1l_1\in f_0}(2l_1+1)R_0^0(n_1l_1, n_2'l_2; n_2l_2, n_1l_1)\right)$$
2 L$_1$) 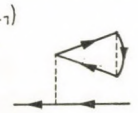 2 L$_2$) 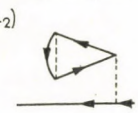	$$8f(2l_a+1)\sum_{n_2l_2\in\ _0}(2l_2+1)\sum_{n_2'l_2\in g_0+n_al_a}\frac{1}{E_{n_2'l_a}-E_{n_2l_2}}\times$$ $$\times R_0^0(n_al_a, n_2'l_2; n_2l_2, n_2l_a)\times$$ $$\times\left(\sum_{n_1l_1\in\ _0}(2l_1+1)\sum_l[l_1l_2l]^2R_l^0(n_1l_1, n_2'l_2; n_1l_1, n_2l_2)\right)$$
2 M$_1$) 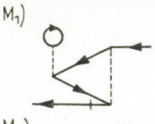 2 M$_2$) 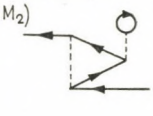	$$8f(2l_a+1)\sum_{n_2l_2\in f_0}(2l_2+1)\sum_{n_2'l_2\in g_0+n_al_a}\frac{1}{E_{n_2'l_2}-E_{n_2l_2}}\times$$ $$\times\left(\sum_l[l_al_2l]^2R_l^0(n_al_a, n_2'l_2; n_al_a, n_2l_2)\times\right.$$ $$\times\left.\left(\sum_{n_1l_1\in f_0}(2l_1+1)R_0^0(n_1l_1, n_2'l_2; n_2l_2, n_1l_1)\right)\right.$$
2 N$_1$) 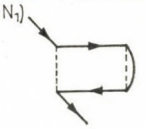 2 N$_2$) 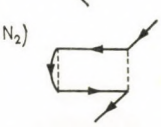	$$-4f(2l_a+1)\sum_{n_2l_2\in f_0}(2l_2+1)\sum_{n_2'l_2\in g_0+n_al_a}\frac{1}{E_{n'l_2}-E_{n_2l_2}}\times$$ $$\times\left.\sum_l[l_al_2l]^2R_l^0(n_al_a, n_2'l_2; n_al_a, n_2l_2)\right)\times$$ $$\times\left(\sum_{n_1l_1\in f_0}(2l_1+1)\sum_l[l_1l_2l]^2R_l^0(n_1l_1, n_2'l_2; n_1l_1, n_2l_2)\right)$$

Таблица III

Вклады Хартри-фоковских диаграмм с четырьмя внешними линиями второго порядка

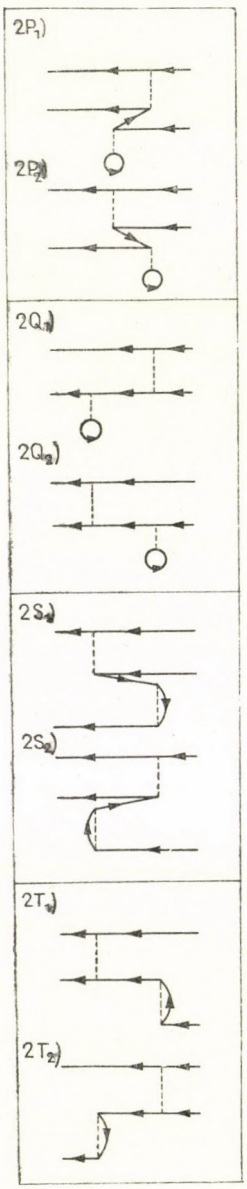

$$8 \sum_{n_2 l_a \in f_0} \frac{(2l_a+1)^2}{E_{n_a l_a} - E_{n_2 l_a}} \times$$

$$\times \left(\sum_{n_2 l_2 \in f_0} (2l_1+1)\, R_0^0 (n_1 l_1, n_2 l_a; n_a l_a, n_1 l_1) \right) \times$$

$$\times \left(\sum_{l} \sum_{S' L'} g(l_a^q SL; l_a^2 S'L')\, (-1)^{L'} \begin{Bmatrix} l_a l_a l \\ l_a l_a L' \end{Bmatrix} \times \right.$$

$$\left. \times [l_a l_a l]^2\, R_l^0 (n_a l_a, n_2 l_a; n_a l_a, n_a l_a) \right)$$

$$-8 \sum_{n_2 l_a \in f_0} \frac{(2l_a+1)^2}{E_{n_2 l_a} - E_{n_a l_a}} \times$$

$$\times \left(\sum_{n_2 l_2 \in f_0} (2l_1+1)\, R_0^0 (n_1 l_1, n_2 l_a; n_a l_a, n_1 l_1) \right) \times$$

$$\times \left(\sum_{l} \sum_{S' L'} g(l^a SL; l_a^2 S'L')\, (-1)^{L'} \begin{Bmatrix} l_a l_a l \\ l_a l_a L' \end{Bmatrix} \times \right.$$

$$\left. \times [l_a l_a l]^2\, R_l^0 (n_a l_a, n_2 l_a; n_a l_a, n_a l_a) \right)$$

$$-4 \sum_{n_2 l_a \in f_0} \frac{(2l_a+1)^2}{E_{n_a l_a} - E_{n_a l_2}} \times$$

$$\times \left(\sum_{n_2 l_2 \in f_0} (2l_1+1) \sum_{l} [l_1 l_a l]^2\, R_l^0 (n_1 l_1, n_2 l_a; n_1 l_1, n_a l_a) \right) \times$$

$$\times \left(\sum_{l} \sum_{S' L'} g(l_a^q SL; l_a^2 S'L')(-1)^{L'} \begin{Bmatrix} l_a l_a l \\ l_a l_a L' \end{Bmatrix} \times \right.$$

$$\left. \times [l_a l_a l]^2\, R_l^0 (n_a l_a, n_2 l_a; n_a l_a, n_a l_a) \right)$$

$$4 \sum_{n_2 l_a \in g_0} \frac{(2l_a+1)^2}{E_{n_2 l_a} - E_{n_a l_a}} \times$$

$$\times \left(\sum_{n_2 l_2 \in f_0} (2l_1+1) \sum_{l} [l_1 l_a l]^2\, R_l^0 (n_1 l_1, n_2 l_a; n_1 l_1, n_a l_a) \right) \times$$

$$\times \left(\sum_{l} \sum_{S' L'} g(l_a^q SL; l_a^2 S'L')\, (-1)^{L'} \begin{Bmatrix} l_a l_a l \\ l_a l_a L' \end{Bmatrix} \times \right.$$

$$\left. \times [l_a l_a l]^2\, R_l^0 (n_a l_a, n_2 l_a; n_a l_a, n_a l_a) \right)$$

4. Заключение

Исследование, проведенное в настоящей статье, показывает, что несмотря на то, что метод Хартри—Фока в случае состояний с заполненными электронными оболочками допускает простую наглядную диаграммную интерпретацию и связан с частичным суммированием диаграмм, построенных из собственно-энергетических частей первого порядка, в случае состояний с открытыми оболочками мы не имеем чего-либо подобного.

Приближение Хартри—Фока в случае открытых оболочек не имеет простой интерпретации на языке атомных фейнмановских диаграмм.

Это связано возможно с тем, что эти уравнения не получены в существующей теории математически последовательным образом. С одной стороны, используя на разных основаниях орбитали замкнутых открытых оболочек при составлении отдельных детерминантов, мы как бы хотим учесть полностью тождественность электронов открытой оболочки с электронами замкнутых оболочек. С другой стороны, открытая оболочка в излагаемой теории существенно отличается от остальных тем, что она всегда незаполнена. Возможно более правильно, чтобы восстановить полностью симметрию между электронами замкнутых оболочек и открытой оболочки, мы должны рассматривать при составлении линейной комбинации детерминантов также такие, в которых электроны из заполненных оболочек могут переходить в открытую оболочку и даже вообще полностью ее заполнить. Тем самым заполненные оболочки в некоторых детерминантах тоже становятся открытыми, а открытая оболочка может быть заполненной.

ЦИТИРОВАННАЯ ЛИТЕРАТУРА

1. П. Гомбаш, Проблема многих частиц в квантовой механике, ИЛ, Москва, 1952.
2. D. R. Hartree, The Calculation of Atomic Stuctures, John Wiley, N. Y.—London, 1957.
3. C. C. J. Roothaan, Rev. Mod. Phys., **32**, 178, 1860.
4. V. V. Tolmachev, Adv. Phys. Chem., ed. I. R. Prigogine, v. 14, 1969.

INTERPRETATION OF THE HARTREE—FOCK METHOD AS THE METHOD OF PARTIAL SUMMATION OF ATOMIC FEYNMAN DIAGRAMS

V. V. TOLMACHEV

Summary

The Hartree—Fock method is now the basis for almost all numerical calculations of characteristics of atomic and molecular states. So its interpretation as the method of partial summation of some class of atomic Feynman diagrams is very important. This interpretation permits us to understand deeply the sense of approximation inherent in the Hartree—Fock method and also the reasons of its peculiar effectiveness which we realize for example in calculations of ground states of light atoms. As a result we will be able to construct on the basis of the Hartree-Fock method the different theories of electronic correlations more thoughtfully.

Acta Physica Academiae Scientiarum Hungaricae, Tomus 27, pp. 373—376 (1969)

WELLENMECHANISCHE STRUKTURUNTERSUCHUNG AM Li_4*

Von

R. JANOSCHEK

MAX-PLANCK-INSTITUT FÜR PHYSIK UND ASTROPHYSIK, 8000 MÜNCHEN 23, BRD

(Eingegangen 20. II. 1969)

Das Atomsystem Li_4 wurde mit Hilfe des SCF-MO-LCGO-Verfahrens für verschiedene Kernkonfigurationen berechnet. Li_4 erweist sich als nicht stabil. Anhand der dargestellten Potentialflächen werden Anordnung und Eigenschaften des Lithium-Metallgitters diskutiert.

Einleitung

Das Atomsystem Li_4, das bis jetzt experimentell nicht beobachtet wurde, lässt sich weder dem Molekülbegriff unterordnen noch kann es als Elementarbaustein des Metallgitters betrachtet werden. Seine Existenz ist jedoch entscheidend dafür, ob sich Lithium-Metall in der Gasphase bilden kann aus Li_2. Auch im Falle der Instabilität des Li_4-Gebildes lassen sich aus den Potentialflächen für die Reaktionen $2 \cdot Li_2 \rightleftharpoons Li_4$ und $4 \cdot Li \rightleftharpoons Li_4$ für tetraedrische oder quadratische Anordnung der vier Lithiumatome Tendenzen für das Metallgitter zeigen.

Methode

Die Berechnungen wurden mit dem SCF-MO-LCGO-Verfahren durchgeführt. Bei dem verwendeten Funktionensatz zur Beschreibung der Elektronendichte wurden jeweils vier Gaussfunktionen in jedes Atomzentrum gesetzt zur Darstellung der *s*-Funktionen [1]. Zur besseren Beschreibung der Elektronendichte zwischen den Atomen wurde bei rechteckiger Atomanordnung je eine Gaussfunktion in die Mitte zwischen zwei Li-Atome gesetzt. Die exponentiellen Parameter dieser Gaussfunktionen wurden für jede Kernkonfiguration erneut variiert. Bei der tetraedrischen Atomanordnung wurde je eine Gaussfunktion in die Verbindungslinie Tetraederzentrum — Atomzentrum gesetzt.

* Herrn Prof. Dr. P. GOMBÁS zum 60. Geburtstag gewidmet

Ergebnisse

Die Energieflächen für die Bildung von Li_4 aus $2 \cdot Li_2$ oder $4 \cdot Li$ sind qualitativ in Abb. 1 dargestellt. Das obere Feld gilt für die pyramidale Atomanordnung, das untere Feld für die rechteckige Atomanordnung. Verfolgt man die Energie entlang der Winkelhalbierenden ($R_1 = R_2$), so erhält man die beiden Potentialkurven für den tetraedrischen (T) und quadratischen Fall (Q) in Abb. 2. Das relative Energieminimum für das quadratische Li_4 liegt bei einem Atomabstand von 5,484 at. E. (2,902 Å). Die Gesamtenergie beträgt —29,63435

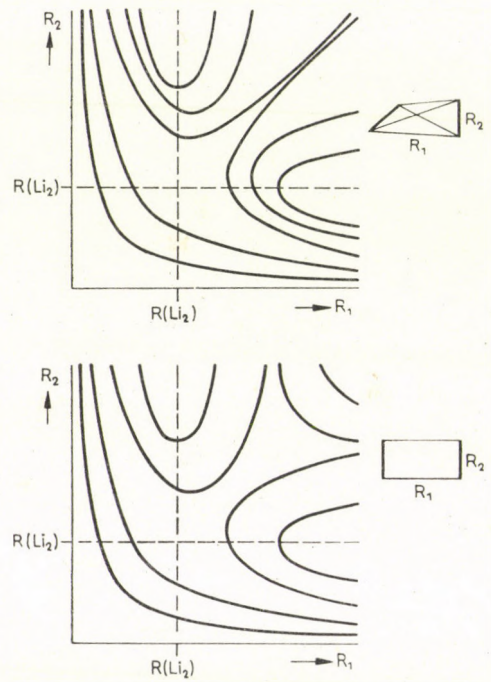

Abb. 1. Potentialflächen für Li_4

at. E. Diese Energie liegt um 0.79 eV höher als die von zwei getrennten Li_2-Molekülen und um 0,52 eV tiefer als die von vier getrennten Li-Atomen.

Die errechneten Moleküldaten von Li_2 sind in Tabelle I aufgeführt, wobei die experimentellen Werte in Klammern stehen.

Tabelle I

Errechnete Moleküldaten von Li_2; (experimentelle Werte in Klammern)

Gleichgewichtsabstand	2.728 Å	(2.672)	[2]
Gesamtenergie	—14.83163 at. E.		
Ionisierungsenergie	4.51 eV	(4.96)	[3]
Schwingungsfrequenz	374 cm^{-1}	(351)	[4]
Dissoziationsenergie	0.65 eV	(1.1)	[4]

In Tabelle II ist die Abstossungskurve zweier ein Rechteck bildender Li_2-Moleküle aufgeführt.

Tabelle II

Li_2—Li_2-Abstossungskurve

Li_2—Li_2-Abstand [at. E.]	Gesamtenergie [at. E.]
6,0	—29,64069
8,0	—29,65566
10,0	—29,65974
12,0	—29,66189
∞	—29,66326

Diskussion

Vergleicht man die beiden Potentialkurven der Abb. 2, so bemerkt man, dass die Gesamtenergie des quadratischen Li_4 geringer als die des tetraedrischen Li_4 ist. Darüber hinaus weist das quadratische Li_4 ein Energiemini-

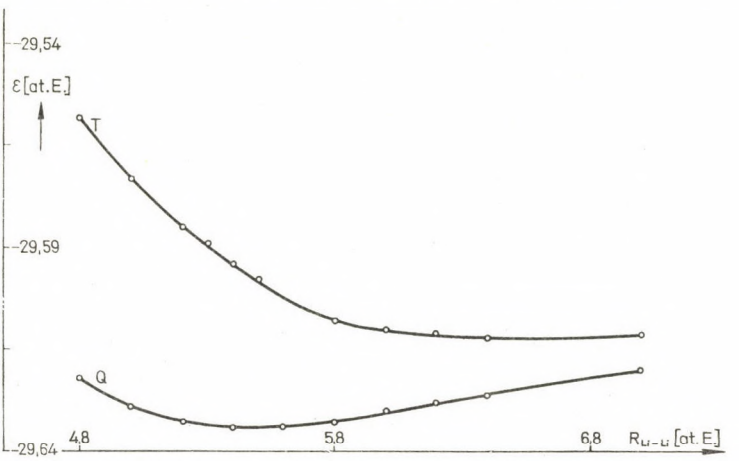

Abb. 2. Potentialkurven für Li_4, tetraedrische Anordnung (T), quadratische Anordnung (Q)

mum auf, das sich nach Abb. 1 zwar nur als Sattelpunkt herausstellt, aber deutlich die quadratische Struktur gegenüber der tetraedrischen energetisch bevorzugt.

Diese Tatsache könnte schon entscheidend sein bei der Anordnung des Metallgitters. Li_4 ist energetisch günstiger in einer Form mit zwei äquivalenten Nachbaratomen (Quadrat) als in einer Form mit drei äquivalenten Nachbaratomen (Tetraeder). Auf das Metallgitter übertragen kann man sagen, dass Lithium nicht in einer dichtesten Kugelpackung vorliegt sondern in einer kubischen mit geringerer Koordinationszahl. Die Ergebnisse des quadratischen Li_4

in Tabelle II zeigen, dass die Energiefläche des instabilen Atomsystems den Metallcharakter bereits andeutet, nämlich Erniedrigung der Ionisierungsenergie und Vergrösserung des Atomabstandes durch Delokalisierung der äusseren Elektronen.

Tabelle III

Atomabstand und Ionisierungsenergie von Li_n; (experimentelle Werte in Klammern)

	Atomabstand [Å]		Ionisierungsenergie [eV]	
Li	—		4,98	(5,39)
Li_2	2,73	(2,67)	4,51	(4,96)
Li_4	2,90		3,31	
Li-Metall	(3,04)		(2,46)	

Die numerischen Rechnungen wurden auf der Rechenmaschine G3 ausgeführt. Ich danke Frau I. FUNKE für die Programmierung des SCF-Verfahrens.

LITERATUR

1. H. PREUSS, Z. f. Naturforschg., **20a**, 1290, 1965.
2. Tables of Interatomic Distances and Configurations in Molecules and Ions. The Chemical Society, London, 1965.
3. R. W. KISER, Tables of Ionization Potentials, United States Atomic Energy Commission, 1960.
4. Compendium of ab initio Calculations of Molecular Energies and Properties. U. S. Department of Commerce, National Bureau of Standards, Washington, 1967.

ВОЛНОВОМЕХАНИЧЕСКОЕ ИССЛЕДОВАНИЕ СТРУКТУРЫ Li_4

Р. ЯНОШЕК

Резюме

С помощью метода SCF-MO-LCGO вычисляется атомная система Li_4 для различных ядерных конфигураций. Результаты говорят о нестабильности Li_4. На основе представленных потенциальных поверхностей дискутируются расположение и свойства металлической решетки лития.

Acta Physica Academiae Scientiarum Hungaricae, Tomus 27, pp. 377—390 (1969)

VIBRATIONAL ANALYSIS OF AB INITIO POTENTIAL ENERGY SURFACES FOR NITRYL FLUORIDE*

By

M. SCHOENBORN and I. G. CSIZMADIA

DEPARTMENT OF CHEMISTRY, UNIVERSITY OF TORONTO
TORONTO 5, ONTARIO, CANADA

(Received 20. II. 1969)

A series of self-consistent molecular orbital (SCF-MO) calculations using the method of linear combination of Gaussian type functions (GTF), were performed on nitryl fluoride, using variable geometry, in order to obtain an *ab initio* potential hypersurface. This hypersurface was used to obtain harmonic force constants for an FG matrix calculation, from which he fundamental frequencies associated with the normal modes were calculated. The calculations reported here found hypersurfaces for two different basis sets, containing 24 and 44 GTF, espectively. It was found that using the larger basis set, the values of the fundamental frequencies agreed very well with experimental values, even if the interaction force constants were scaled from the smaller calculations using 24 GTF.

Introduction

To perform a single near-Hartree—Fock calculation on the 32 electron molecule nitryl fluoride (NO_2F) requires a basis set of 112 uncontracted GTF [1]. On the other hand a single calculation using the most recent technique, in which a basis set of 136 primitive GTF is contracted to 40 basis functions [2], requires about 18 hours on the present generation of computing machinery. It follows that to study the general properties of *ab initio* surfaces, where many such calculations would be required, it is necessary to use a much smaller basis set so that enough points may be calculated. Then, if accurate results are needed, it may be possible to make generalizations that permit the calculation of more accurate surfaces with larger basis sets, without having to calculate a prohibitively large number of individual points.

In this work, uncontracted basis sets [3] of 24 GTF were used for the preliminary calculation of a complete hypersurface. This basis set consisted of 3*s*-type and 1*p*-type Gaussians on each atom [abbreviated as: $(3^s, 1^p)$]. For the more accurate calculations, cross-sections were taken using 44 GTF $(5^s, 2^p)$.

All energy values are given in Hartree atomic units. The computations were carried out using a modified POLYATOM system [4] on an IBM-7094-II computer.

* Dedicated to Prof. P. GOMBÁS on his 60th birthday.

The FG matrix calculation

(i) *Fitting analytical function to ab initio surfaces*

It was found that the nature of the surfaces made least squares fitting of a general quadratic potential impossible, even in regions very near the minima. The cross-sections of the surfaces contained an inherent and consistent asymmetry in the vicinity of the minima, and a "weighted" parabola

$$E(X) = E_0 + a(X - X_0)^2 e^{-b(X-X_0)} \tag{1}$$

provided an excellent fit to points on such cross-sections. This curve could have been used to provide anharmonic corrections to the fundamental frequencies, but within the accuracy of the present calculations, no attempt was made to include such corrections. Changing the coordinate system in such a way that $x = X - X_0$ then (1) may be written as (1a)

$$E(x) = E_0 + ax^2 e^{-bx}. \tag{1a}$$

Diagonal force constants can then be obtained directly from (1a).

$$F_{xx} = \left(\frac{d^2 E(x)}{dx^2}\right)_{x=0}$$

$$= (2ae^{-bx} - 4abxe^{-bx} + ab^2 x^2 e^{-bx})_{x=0}$$

$$= 2a\,, \tag{2}$$

i. e.

$$a = 1/2\, F_{xx}\,. \tag{2a}$$

If a two-dimensional surface is now considered, a study of interaction force constants is possible. An analogous relative coordinate system is chosen for which $x = y = 0$ at E_{00}, the absolute minimum of the surface.

$$E(x, y) = E_{00} + 1/2\, F_{xx} x^2 e^{-bx} + 1/2\, F_{xy} xy + 1/2\, F_{yy} y^2 e^{-cy}\,. \tag{3}$$

If the behaviour of (3) is studied near the minima, for fixed values of y, the exponential terms become approximately equal to 1. Then, if successive cross-sections of (3) are taken at $y = 0$ and $y = \delta y$, (3) becomes (4) and (5) respectively.

$$E(x, 0) = E_{00} + 1/2\, F_{xx} x^2, \tag{4}$$

$$E(x, \delta y) = (E_{00} + 1/2\, F_{yy} \delta y^2) + 1/2\, F_{xx} x^2 + 1/2\, F_{xy} x\delta y\,. \tag{5}$$

Of these, it can be seen that (5) is a parabola with respect to x with a minimum not exactly at $x = 0$, but rather at some non-zero value of x, say $x = \delta x_0$, which can be obtained graphically, or from a least squares curve fit.

From geometrical consideration, the equation of such a parabola with minimum at δx_0 is

$$E(x, \delta y) = E_0 + 1/2\, F_{xx}\, x^2 - F_{xx}\, x \delta x_0 . \tag{6}$$

Comparing terms in (5) and (6), and taking the limit as $\delta y \to 0$,

$$1/2\, F_{xy}\, x \delta y = - F_{xx}\, x \delta x_0 , \tag{7}$$

$$F_{xy} = -2\, F_{xx} \left(\frac{dx_0}{dy} \right)_{y=0} . \tag{7a}$$

Thus, at least in principle, the way is open for a rigorous theoretical study of the normal modes of vibration of a polyatomic molecule like NO_2F. This method can be extended to include anharmonic interaction force constants if the functional variation of the minima is considered, rather than just the slope at $y = 0$.

(iii) *Calculation of F-matrix elements (Small Basis Set)*

It was found that unnormalized symmetry coordinates could be used, so that simple bond stretching and bending could be represented by them, since the constant introduced by the degree of unnormalization was inversely accounted for in the calculation of G-matrix elements. The symmetry coordinates used are shown in Fig. 1.

Calculations with a small basis set provided results which were only qualitatively useful, as was expected from a basis set of this size. Four surfaces were studied — the three pairwise combinations of the three A_1 symmetry coordinates (S_1, S_2 and S_3), and the pair of B_1 symmetry coordinates (S_4 and S_4).

It should be noted that for bending modes in which the asymmetry was small, parabola fits were used, rather than the anharmonic potential previously chosen in Equ. (1). The subscripts of the F-matrix elements refer to the symmetry coordinates defined in Fig. 1.

(iii) *Scaling of interaction force constants (Medium Basis Set)*

Though the force constants obtained by calculations using small (24 GTF) basis sets were quantitatively very poor, it is seen that qualitatively they fall in the right sequence. (A trial FG-matrix calculation using the force con-

stants from Table VII would give frequencies uniformly too high by a factor of 3, so the force constants are too high by an order of magnitude.) As the basis set sizes for the MO calculations were increased to 44 GTF the improvements in the diagonal force constants were very encouraging, and these new force constants were found to remain proportional to those determined using the smaller basis set. It was also found in the calculation with the small basis set that even

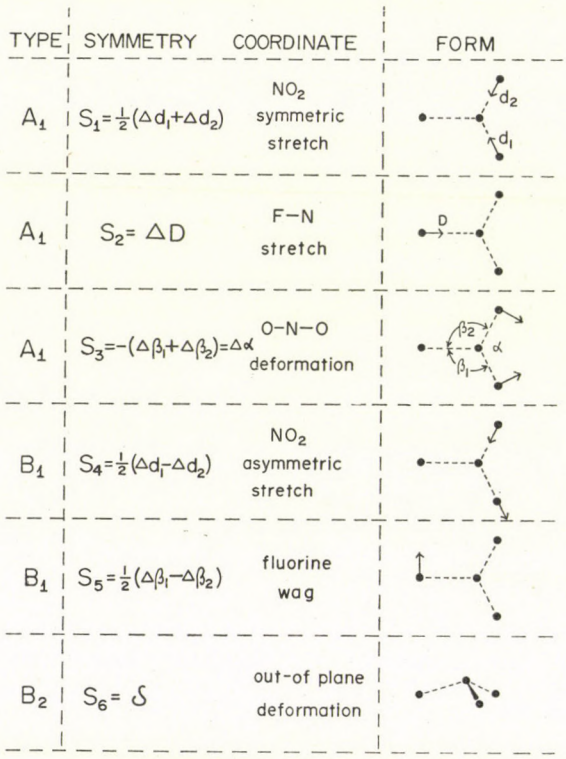

Fig. 1. Symmetry coordinates for NO_2F (unnormalized)

fairly large changes in the interaction force constants did not greatly affect predicted frequencies. Thus it might be assumed that the inaccuracy introduced using interaction force constants scaled from those found with the smallest basis set should be much less than the inaccuracy arising from the use of a single determinant wave function considerably above the Hartree—Fock limit. Since using a very large basis set, calculation of many points on a potential surface becomes economically infeasible, it was decided that scaled interaction force constants should be studied in some detail. The formula adopted for this purpose was

$$F'_{xy} = F_{xy}\left(\frac{F'_{xx}\,F'_{yy}}{F_{xx}\,F_{yy}}\right)^{1/2}, \tag{8}$$

Table I

Elements of the *G*-matrix*

$$G_{11} = \frac{1}{2}(\mu_1(1+\cos\alpha) + \mu_3) \qquad G_{12} = \mu_1 \cos\beta \qquad G_{13} = -\mu_1 \frac{\sin\alpha}{d}$$

A_1 type

$$G_{22} = \mu_1 + \mu_2 \qquad G_{23} = 2\mu_1 \frac{\sin\beta}{d}$$

$$G_{33} = \frac{2}{d^2}(\mu_1(1-\cos\alpha) + \mu_3)$$

$$G_{44} = \frac{1}{2}(\mu_1(1-\cos\alpha) + \mu_3) \qquad G_{45} = \mu_1 \frac{\sin\beta\,(D\cos\beta - d)}{Dd}$$

B_1 type

$$G_{55} = \mu_1\left(\frac{D\cos\beta - d)}{Dd}\right)^2 + \frac{\mu_2}{D^2} + \frac{\mu_3}{2d^2}$$

$$G_{66} = \frac{\mu_1}{2d^2\cos\alpha/2} + \frac{\mu_2}{D^2} + \mu_3 \cdot \frac{(D + d\cos\alpha)^2}{D^2 d^2 \cos^2\alpha/2}$$

B_2 type

* The numbering for the reciprocal masses, μ_i, is as follows: 1 : N, 2 : F, 3 : O. All other ymbols are defined in Fig. 1.

where the prime represents the new set of force constants associated with the larger basis set. If only the diagonal elements of the F matrix (i e. F'_{xx}, F'_{yy}, etc. were computed in an *a priori* manner with the large basis set (44 GTF) then the interaction force constant for the basis set, F'_{xy}, is to be scaled. Since the coordinates x and y used in this description are merely one of the symmetry coordinates $S_i (i = 1, \ldots, 6)$, the force constants are henceforth specified using the subscripts of the relevant symmetry coordinates. (8) can conveniently be written as (8a).

$$F'_{ij} = F_{ij}\left(\frac{F'_{ii}\,F'_{jj}}{F_{ii}\,F_{jj}}\right)^{1/2}. \tag{8a}$$

A comparison of results using scaled and computed interaction force constants for the larger basis set is included in the reported frequencies and force constants.

(iv) *The FG matrix formalism*

Once the numerical values for the elements of the F-matrix are known the elements of the G-matrix have to be calculated. These are given in Table I, using the labels from 1 to 6 of the unnormalized symmetry coordinates $(S_1, \ldots, S_6)$ from Fig. 1. Due to symmetry, the 6×6 matrix was blocked to a 3×3

(A_1), a 2×2 (B_1) and a 1×1 (B_2), block. The fundamental frequencies, ν_i, can be obtained using WILSON's method [5], by solving the secular equation

$$|FG - \lambda| = 0\,, \tag{9}$$

which is normally done by diagonalization of the FG matrix product. The solutions, λ_i, of (9) are related to the ν_i by the equation

$$\lambda_i = 4\pi^2 c^2 \nu_i^2\,, \tag{10}$$

i.e.

$$\nu_i = \frac{(\lambda_i)^{1/2}}{2\pi c}\,. \tag{11}$$

Equ. (11), however, obtains λ_i from an FG matrix in c.g.s. units. If λ_i is obtained using the usual units for such calculations, viz., masses in a.m.u., lengths in angstroms, angles in radians, stretching force constants in mdyne/Å, bending force constants in mdyne Å/rad.^{2} and stretch-bend interactions in mdyne/rad., then (11) becomes

$$\nu_i = 1{,}302\cdot 9\sqrt{\lambda_i}\,. \tag{11a}$$

Results and discussion

The calculations which used only 24 GTF gave energies of the order of —284 hartrees, or only about 90% of the Hartree–Fock limit. Previous calculations [6] have also indicated that the force constants found with the minimal basis sets have been rather inconsistent with those computed with more functions. The calculations using 44 GTF gave considerably better energies, about 99% of the Hartree—Fock limit, and the force constants were expected to be much better. The energies for the various cross-sections calculated using 44 GTF, are given in Tables II to VI. The set of A_1 cross-sections at the experimental conformation was used together with interaction force constants scaled from the minimum basis set using (8a), while the second set of A_1 cross-sections was taken at the absolute minimum of the hypersurface, and was used to calculate interaction force constants. The B_1 cross-sections were used with a scaled interaction constant only.

The diagonal force constants given in Table VII are in good general agreement with experimental values, except that the value of the FN stretching constant (F_{22}) is considerably higher. This result could arise from the way in which fluorine is represented in the present molecular orbital calculations or from the method by which experimental force constants are found. Since the determination of experimental force constants is made by reconstructing the

Table II
Energies for N—O symmetric bond stretching (S_1)

r_{NO} (Å)	experimental configuration*	$r_{NF} = 1.413$Å, $\sphericalangle$ ONO = 132°
1.13	—300.16445	—
1.18	—300.23121	—
1.23	—300.27335	—300.28293
1.28	—300.29566	—300.30310
1.21	—300.30113	—
1.33	—300.30211	—300.30784
1.36	—300.29953	—300.30467
1.39	—	—300.29780

* Taken to be [7]: $r_{NF} = 1.35$Å, ONO = 125°, apart from r_{NO} which is varied here but which at equilibrium is 1.23Å.

Table III
Energies for N—F bond stretching (S_2)

r_{NF} (Å)	experimental conformation	$r_{NO} = 1.33$ Å, $\sphericalangle$ ONO = 132°*
1.25	—300.24245	—
1.30	—300.26201	—
1.333	—	—300.29926
1.35	—300.27335	—
1.373	—	—300.30448
1.40	—300.27793	—
1.413	—	—300.30586
1.443	—	—300.30484
1.45	—300.27725	—
1.473	—	—300.30230

* First s exponent on nitrogen taken as 0.42 instead of 0.425 results in slight energy discrepancy.

Table IV
Energies for ONO bending (S_3)

$\sphericalangle$ ONO	experimental configuration	$r_{NO} = 1.33$ Å, $r_{NF} = 1.413$ Å
120°	—300.26667	—
125°	—300.27335	—
127°	—	—300.30727
130°	—300.27526	—
132°	—	—300.30784
135°	—300.27459	—
137°	—	—300.30566

Table V

Cross-sections of B_1 surface*

S_5/S_4	0	±0.05 Å	±0.10 Å
0°	−300.30701	−300.30180	−300.28893
±5°	−300.30472	—	—
±10°	−300.29815	—	—

* $\sphericalangle$ ONO = 132°, r_{NF} = 1.418 Å, $\frac{r_{NO_1} + r_{NO_2}}{2}$ = 1.329 Å

FG matrix from the observed frequencies (and hence the known eigenvalues), some suitable way of estimating the signs and magnitudes of the off-diagonal force constants must be determined. Although it is possible then to reconstruct the observed frequencies, if these off-diagonal force constants are substantially inaccurate, the numerical value of the resulting diagonal force constants will also be greatly changed.

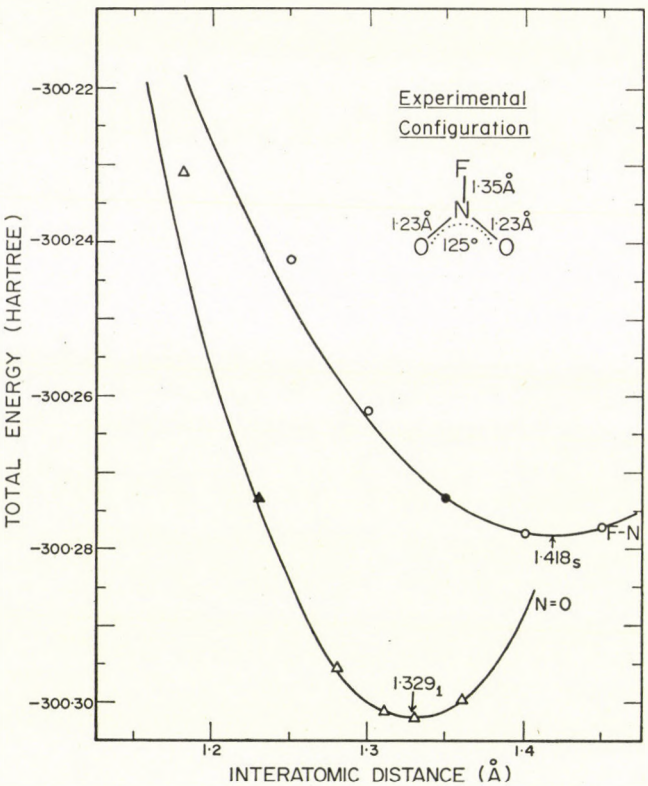

Fig. 2. Parabola fit to S_1 and S_2 potential curves

Table VI

Total energy for out-of-plane bending (S_6)

S_6	total energy
0°	−300.27289
±5°	−300.27213
±10°	−300.27059
±20°	−300.26488
±30°	−300.25491

For example, the off-diagonal force constant for the interaction between the asymmetric stretch (S_4) and the asymmetric bend (S_5), was taken [8] to be +1.24 mdyne/rad., giving as the diagonal stretching and bending constants 21.9 mdyne/Å and 2.81 mdyne Å/rad.^{2}, respectively. This result is rather unusual in the sense that normally, a lower force constant is expected for an asymmetric stretching mode than for the corresponding symmetric one. The

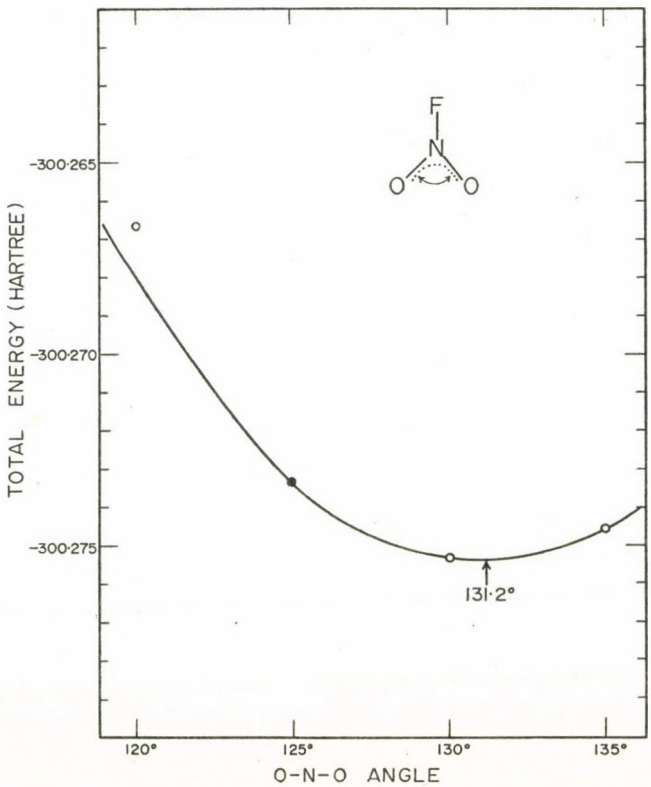

Fig. 3. Potential curve for variation of S_3

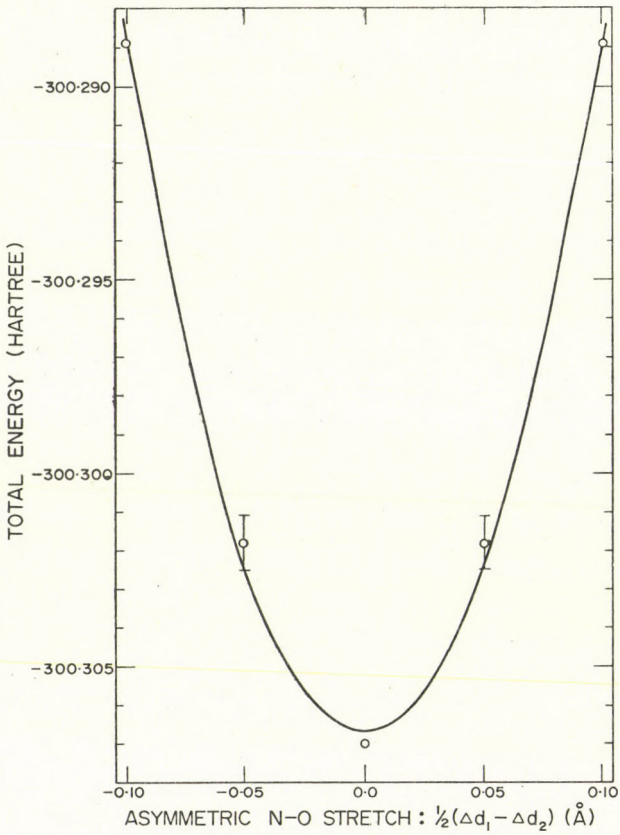

Fig. 4. Potential curve for asymmetric NO stretch (S_4)

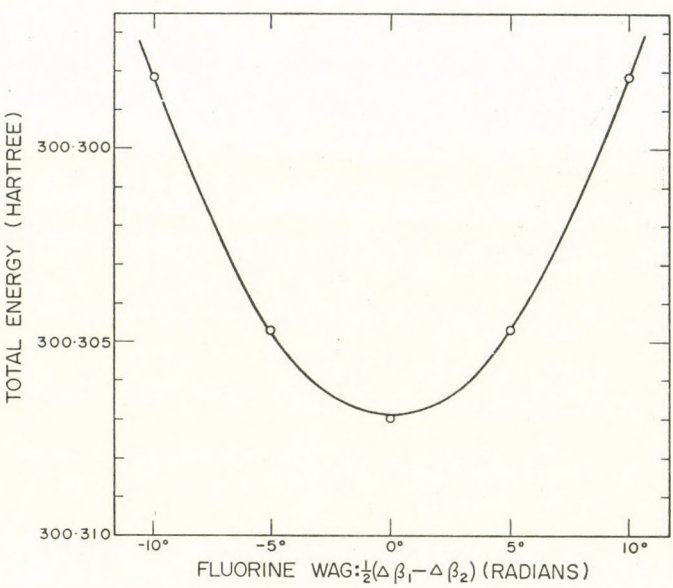

Fig. 5. Potential curve for variations of S_5

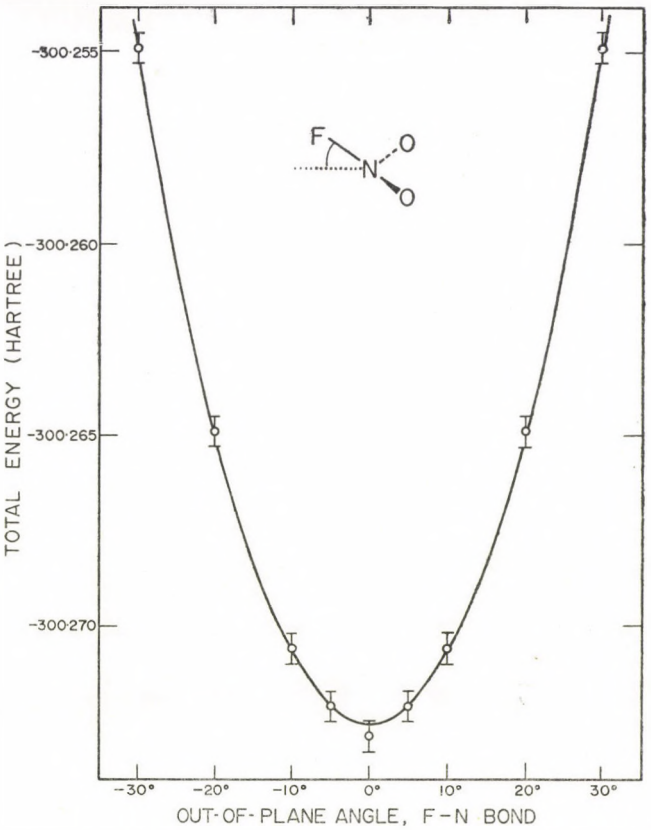

Fig. 6. Potential curve for out-of-plane deformation (S_6)

Table VII

Force constants for nitryl fluoride*

F_{ij}	24 GTF calculated	44 GTF scaled	44 GTF calculated	reported [8]**	reported [9]**
F_{11}	81.69	22.26	22.26	18.8	25.5
F_{12}	3.61	1.05	1.6	1.49	0.0
F_{13}	1.94	0.572	1.0	−1.57	1.82
F_{22}	27.25	8.478	8.478	4.57	2.66
F_{23}	−2.38	−0.75	−0.73	−0.583	−0.808
F_{33}	3.60	1.149	1.149	1.36	2.235
F_{44}	78.12	15.432	—	21.9	19.36
F_{45}	−5.41	−1.649	—	+1.24	0.0
F_{55}	5.366	2.524	—	2.82	2.63
F_{66}	—	(0.859)	—	—	0.501

* Units are mdyne/Å for stretch, mdyne Å/rad.^{2} for bend and mdyne/rad for stretch-bend interaction. Subscripts refer to the symmetry coordinates given in Fig. 1.

** Values converted from valence force constants with appropriate charges of normalization for the symmetry coordinates used (Fig. 1).

Table VIII

Calculated fundamental frequencies (cm^{-1}) for nitryl fluoride

	scaled	calculated	reported [10]	reported [9]
$\nu_1 (A_1)$	1480	1415	1312	1310
$\nu_2 (A_1)$	1030	1060	822	822
$\nu_3 (A_1)$	510	510	460	568
$\nu_4 (B_1)$	1740	—	1793	1792
$\nu_5 (B_1)$	465	—	570	560
$\nu_6 (B_2)$	(880)	—	742	742

Table IX

Summary of normal coordinate analysis*

		Q_1	Q_2	Q_3	Q_4	Q_5
	λ_k	1.2889	0.6300	0.1549	1.7869	0.1271
	ν_k	1480	1030	510	1740	465
N	Δx_1	0.0	0.0	0.0	−0.2293	−0.0569
	Δy_1	−0.2097	−0.0514	0.0972	0.0	0.0
	Δz_1	0.0	0.0	0.0	0.0	0.0
F	Δx_2	0.0	0.0	0.0	0.0238	0.1392
	Δy_2	0.0847	0.1420	0.0995	0.0	0.0
	Δz_2	0.0	0.0	0.0	0.0	0.0
O_1	Δx_3	0.0777	−0.1195	0.1045	0.0862	−0.0578
	Δy_3	0.0415	−0.0619	−0.1016	0.0220	−0.1224
	Δz_3	0.0	0.0	0.0	0.0	0.0
O_2	Δx_4	−0.0777	0.1195	−0.1045	0.0862	−0.0578
	Δy_4	0.0415	−0.0619	−0.1016	−0.0220	0.1224
	Δz_4	0.0	0.0	0.0	0.0	0.0

* In this notation, the relative values of the cartesian displacement coordinates are given in such a way that the molecule is lying in the xy plane, with N at the origin and F on the positive y-axis.

calculated surface suggests that this interaction force constant is actually negative, and if the calculations are repeated assuming —1.24 mdyne/rad. for this constant, it is found that greatly changed values of the diagonal force constants (see Table VII), are obtained; viz. $F_{44} = 16.5$ mdyne Å and $F_{55} = 3.58$ mdyne Å/rad.^{2}. It might be assumed that similar changes would occur if the symmetric stretch-bend interaction constant (F_{13}) had been taken [8] as positive instead of negative.

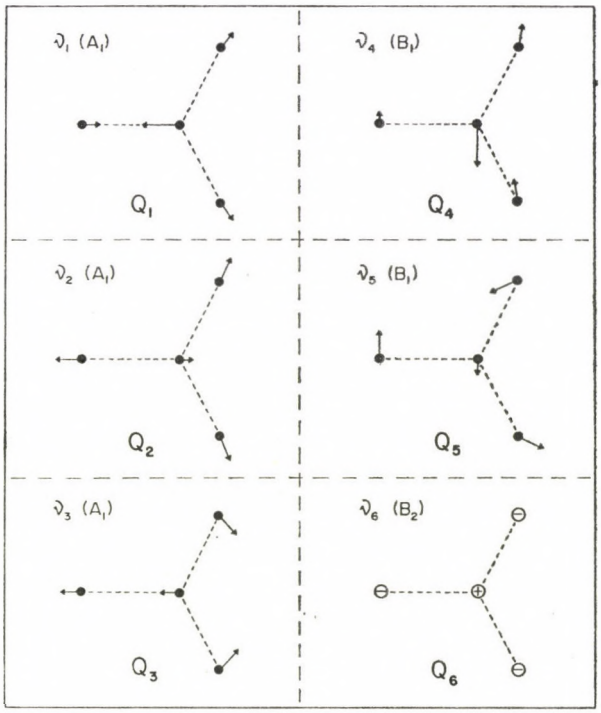

Fig. 7. Normal coordinates for NO_2F

A computer program was used to calculate numeric values of *G*-matrix elements and the *FG* matrix. The *FG* matrix was diagonalized, yielding the eigenvalues and eigenvectors. The results of this calculation are given in Tables VIII and IX and shown in Fig 7.

Conclusion

It can be seen that although theoretical surfaces using the smallest basis sets give force constants which are too high by an order of magnitude, surfaces found even with the next larger basis set provide a very reasonable quantitative estimate of force constants and fundamental frequencies. In particular, the calculated interaction force constants could be used together with experimental frequencies and *FG* calculations to give a more unique set of experimental force constants, while the theoretically predicted frequencies might occasionally be helpful in clarifying assignments of the fundamental frequencies. It is hoped that further calculations using larger basis sets would give even more accurate predictions.

Acknowledgements

A research grant provided by the Defence Research Board of Canada and the continuous financial support of the National Research Council of Canada are gratefully acknowledged. One of us (M.S.) would like to thank the Province of Ontario for a graduate fellowship (1966—1968) and the National Research Council of Canada for a graduate studentship (1968—1969). The authors wish to express their appreciation to the Institute of Computer Science at the University of Toronto for making their computing facilities available for this work.

REFERENCES

1. S. Huzinaga, J. Chem. Phys., **42**, 1293, 1965.
2. S. Huzinaga and Y. Sakai, Gaussian-Type Functions for Polyatomic System. II. J. Chem. Phys. (in press).
3. I. G. Csizmadia, M. C. Harrison, J. W. Moskowitz and B. T. Sutcliffe, Theoret. chim. Acta. (Berl.), **6**, 191, 1966.
4. I. G. Csizmadia, M. C. Harrison, J. W. Moskowitz, S. S. Seung, B. T. Sutcliffe and M. P. Barnett, "The POLYATOM System". Tech. Notes No. 36 and 40, Co-operative Computing Laboratory, M. I. T. (unpublished) Submitted to Quantum Chemistry Program Exchange, Chemistry Department, Indiana University, Bloomington, Indiana 47405, U. S. A.
5. E. B. Wilson, J. Chem. Phys., **7**, 1047, 1939.
6. I. G. Csizmadia, M. C. Harrison and B. T. Sutcliffe, Theoret. Chim. Acta (Berl.), **6**, 217, 1966.
7. D. F. Smith and D. W. Magnuson, Phys. Rev., **87**, 226, 1952.
8. K. Venkateswarlu, P. Thirugnanasambandam, and C. Balasubramanian, Z. Physik. Chem., **218**, 7, 1961.
9. D. L. Bernitt, R. H. Miller and I. C. Hiatsune, Spectrochim. Acta, **23A**, 237, 1967.
10. R. E. Dodd, J. A. Rolfe and L. A. Woodward, Trans. Faraday Soc., **52**, 145,1956.

ВИБРАЦИОННЫЙ АНАЛИЗ ПОВЕРХНОСТЕЙ AB INITIO ПОТЕНЦИАЛЬНОЙ ЭНЕРГИИ ДЛЯ НИТРИЛОФЛУОРИДА

М. ШЭНБОРН и И. Г. ЧИЗМАДИЯ

Резюме

Проведена серия вычислений самосогласованных молекулярных орбит (SCF—MO) для нитрилофлуорида, применяя метод линейной комбинации функций типа Гаусса (GTF). Для получения гиперповерхности ab initio потенциала применяется варьируемая геометрия. Данная гиперповерхность использована для получения гармонических силовых констант для FG матричного вычисления, из которого определяются основные частоты, связанные с нормальными частотами. Представленные в данной работе вычисления результируют гиперповерхности для двух различных базисных сетей, содержащих 24 и 44 GTF соответственно. Найдено, что применяя широкую базисную сеть, значения основных частот очень хорошо согласуются с экспериментальными данными, даже в том случае, если силовые константы взаимодействия определены приемом, использующим 24 GTF.

Acta Physica Academiae Scientiarum Hungaricae, Tomus 27, pp. 391—403 (1969)

DAS KOMBINIERTE NÄHERUNGSVERFAHREN*

II. UNTERSUCHUNGEN ZU EINER GEEIGNETEN WAHL DES EFFEKTIVEN POTENTIALS UND ZUR BERÜCKSICHTIGUNG DER RUMPF—RUMPF-WECHSELWIRKUNG

Von

W. H. EUGEN SCHWARZ**

INSTITUT FÜR PHYSIKALISCHE CHEMIE DER UNIVERSITÄT FRANKFURT AM MAIN, DEUTSCHLAND

(Eingegangen 30. VIII. 1968)***

Die Valenzelektronenniveaus von Alkalimetall- und Kupfer-Atomen werden mittels der Pseudopotentialmethode berechnet. Von den verschiedenen Näherungsformeln liefert das kürzlich von GOMBÁS hergeleitete statistische G^{korr}-Besetzungsverbotpotential die besten Ergebnisse. Von empirischen effektiven Potentialen ist ein solches mit ausgeprägter Mulde am geeignetsten. Die Wechselwirkungsenergie der Atomrümpfe eines Moleküls wird unter Verwendung statistischer Methoden abgeschätzt.

1. Einleitung

Fast alle bisherigen quantenchemischen *ab initio*-Rechnungen wurden für Moleküle aus leichten Elementen durchgeführt. Insbesondere fehlt es an Untersuchungen der den Chemiker besonders interessierenden Unterschiede der Eigenschaften einer Reihe von Verbindungen aus verschiedenen Elementen einer Gruppe oder Familie des Periodensystems. Weiterhin lässt eine exakte Theorie die wesentliche chemische Erfahrung der Homologie der Elemente einer Familie unberücksichtigt: Der Hamiltonoperator eines Li- und eines Cs-Atoms etwa weisen nicht die geringste Ähnlichkeit auf, das gleiche gilt für die entsprechenden Valenzorbitale.

Um diesem Mangel abzuhelfen, haben schon 1935 sowohl GOMBÁS [1] als auch HELLMANN [2] vorgeschlagen, die Rumpfelektronen der Atome näherungsweise zu behandeln und ihren Einfluss auf die Valenzorbitale durch sogenannte Pseudopotentiale [3] zu beschreiben. Obwohl in der Zwischenzeit, nicht zuletzt von GOMBÁS (vergl. [3]), eine grosse Anzahl von Arbeiten auf dem Gebiet der Atom- und Festkörperphysik nach diesem von HELLMANN sogenannten Kombinierten Näherungsverfahren (KN) erschienen sind, hat diese Idee in der Quantenchemie erst in neuester Zeit wieder Interesse gefunden.

Nach [4] lautet der Hamiltonoperator für ein molekulares System in der Näherung des KN

$$\mathscr{H} = \sum_i \left(-\frac{\Delta_i}{2} + \sum_A \mathscr{W}^A(i) \right) + \frac{1}{2} \sum_{i \neq j} \frac{1}{r_{ij}} + \frac{1}{2} \sum_{A \neq B} E_{AB}. \qquad (1)$$

* Herrn Prof. Dr. P. GOMBÁS zum 60. Geburtstag in Verehrung gewidmet.

** Jetzige Adresse: Lehrstuhl für Theoretische Chemie der Universität Bonn.

*** In das Sekretariat der Redaktion aus technischen Gründen leider erst am 20. II. 1969 eingelangt.

i, j sind die Valenzelektronen, A, B die Atomrümpfe und die $\mathscr{W}^A$ die effektiven Atomrumpf-Potentialoperatoren

$$\mathscr{W}^A = \sum_{l,m} W_l^A(r)\, \mathscr{P}_{lm}^A \tag{2}$$

mit

$$\mathscr{P}_{lm}^A = \sum_n g_n(r) \cdot Y_{lm}(\varphi, \vartheta) \cdot \int d\tau \cdot g_n(r) \cdot Y_{lm}(\varphi, \vartheta)\,, \tag{3}$$

wobei n über eine vollständige Funktionenbasis $g_n(r)$ läuft. Die W_l^A sind von der Nebenquantenzahl abhängige zentrosymmetrische Potentiale, die im wesentlichen die Summe aus dem elektrostatischen und dem Besetzungsverbotpotential darstellen; die E_{AB} sind die Wechselwirkungsenergien der Atomrümpfe A, B.

Im folgenden sollen einige Rechnungen und Bemerkungen zur näherungsweisen theoretischen (Abschnitt 2) und zur empirischen Bestimmung (Abschnitt 3) der Potentialfunktionen W_l^A und zur Abschätzung der Rumpf—Rumpf-Wechselwirkungsenergien (Abschnitt 4) mitgeteilt werden.

2. Vergleich näherungsweise berechneter effektiver Potentiale

Die $W_l^A(r)$-Funktionen können entweder in einem vollständigen Hartree—Fock-Verfahren (Szasz [5]) oder einfacher aus den Elektronendichten der Rümpfe nach verschiedenen statistischen oder wellenmechanischen Näherungsformeln berechnet werden. Hier sollen diese Näherungen anhand der damit berechneten Termenergien der Atome Li, Na, K, Rb, Cu miteinander verglichen werden.

Rechenmethoden

Folgende Ausdrücke für die Besetzungsverbotpotentiale wurden herangezogen:

1) Das rein statistische F_l^0-Potential von Gombás ([3], Formel (12, 11))[1]:

$$F_l^0 = \sqrt[3]{\frac{9\pi^2}{128}} \cdot (D^{2/3} - D_l^{*2/3})/r^{4/3}. \tag{4}$$

2) Die halbstatistischen G_l^0- und G_l-Potentiale (ibid., Formeln (11,9)

[1] Die Bedeutung der Symbole ist folgende: D — radiale Rumpfelektronendichte $4\pi r^2 \varrho$, D_l — entsprechend für Rumpfelektronen mit der Nebenquantenzahl 1, D_l^* — entsprechend für Rumpfelektronen in Schalen, die tiefer als die $(n = l + 1, l)$-Schale liegen; P — Dichte des zu berechnenden Valenzelektronenzustands (da P nur zu kleinen Korrekturen führt, wurde in allen Fällen die SCF-Valenzdichte des Grundzustands eingesetzt); N — Zahl der Rumpfelektronen.

Tabelle I

Negative Valenzelektronenenergien nach der Besetzungsverbotpotentialmethode in eV

Besetzungsverbotpotential	Li				Na			
	2*s*	3*s*	2*p*	3*p*	3*s*	4*s*	3*p*	4*p*
$U^{(1)}$	5,87	2,16	3,59	1,52	5,86	2,18	3,12	1,42
$U^{(2)}$	5,18	2,02	3,59	1,52	5,28	2,16	2,95	1,37
F^0	6,91	2,37	3,59	1,52	5,09	1,96	3,17	1,44
G^0	6,25	2,20	3,59	1,52	6,08	2,15	3,17	1,44
G	6,10	2,18	3,59	1,52	5,91	2,12	3,14	1,44
G^{korr}	5,36	2,01	3,59	1,52	5,19	1,96	2,98	1,38
experimentell [14]	5,39	2,02	3,54	1,57	5,14	1,95	3,04	1,39
SCF-Wert [13]	5,34				4,95			

Besetzungsverbotpotential	K				Cu			
	4*s*	5*s*	4*p*	5*p*	4*s*	5*s*	4*p*	5*p*
$U^{(1)}$	4,63	1,80	2,75	1,31	8,53	2,70	3,74	1,61
$U^{(2)}$	4,24	1,81	2,59	1,25	7,39	2,52	3,44	1,52
F^0	4,33	1,79	2,78	1,30	4,33	1,80	2,79	1,33
G^0	5,01	1,90	2,93	1,35	9,44	2,54	4,05	1,68
G	4,82	1,86	2,88	1,33	9,16	2,49	3,96	1,65
G^{korr}	4,22	1,71	2,68	1,27	7,51	2,35	3,52	1,53
experimentell [14]	4,34	1,73	2,73	1,28	7,73	2,38	3,92	1,60
SCF-Wert [13]	4,01				6,44			

und (11,8)):

$$G_l^0 = \frac{1}{8}\left[\left(\frac{\pi^2}{2l+1}\right)^2 D_l^2 + \frac{1}{r^2}\right]. \tag{5}$$

$$G_l = \frac{1}{8}\left[\left(\frac{\pi^2}{2l+1}\right)^2 (D_l^2 + 2D_l P) + \frac{1}{r^2}\right]. \tag{6}$$

3) Die mit diesen Potentialen erhaltenen Ergebnisse waren unbefriedigend (s. Tabelle I), was offenbar darauf beruht, dass zu ihrer Ableitung die statistische Theorie des *homogenen* Elektronengases verwendet wurde. GOMBÁS hat daraufhin kürzlich unter Verwendung eines einfachen Modells dem Inhomogenitätseffekt in einem korrigierten G-Potential Rechnung getragen [6]:

$$G_l^{\text{korr}} = \frac{1}{8}\left[\left(\frac{\pi^2}{2l+1}\right)^2 (\gamma^2 D_l^2 + 2\gamma D_l P) + \frac{1}{r^2}\right], \tag{7}$$

wobei der Korrekturfaktor $\gamma = 1 + (n_l - l + 1)/4(n_l - l)$ ist und n_l die Haupt-

quantenzahl der höchsten besetzten Schale mit der Nebenquantenzahl l bedeutet.

4) Ein exakter Ausdruck für den Besetzungsverbotoperator lautet nach HEINE [7]

$$\mathcal{U}_v = -\sum_r \langle \varphi_r | V_e | \varphi_v \rangle \cdot \frac{\varphi_r}{\varphi_v}, \tag{8}$$

wobei φ_r die Rumpforbitale, V_e das elektrostatische Potential und φ_v das zu berechnende Valenzpseudoorbital sind. Um für $\mathcal{U}_v$ einen Näherungsausdruck in Form eines lokalen Potentials zu erhalten, muss man für φ_v eine Funktion einsetzen, die das Pseudoorbital im Rumpfbereich einigermassen wiedergibt. HEINE hatte $\varphi_v \cong r^l Y_{lm}$ vorgeschlagen ($U_l^{(1)}$). Wie numerische Rechnungen zeigten, ist diese Approximation zu roh (s. Tabelle I). Nur in Kernnähe wird nämlich der Verlauf der Pseudoorbitale durch r^l gut beschrieben, nicht dagegen in den für das Potential besonders wichtigen Randgebieten des Atomrumpfes. Es wurde daher auch die Näherung $\varphi_v \cong r^l \cdot \exp(-\alpha r) \cdot Y_{lm}$ untersucht ($U_l^{(2)}$), wobei α so gewählt wurde, dass φ_v mit dem nach den SLATERschen Regeln [8] gebildeten Valenzorbital maximal überlappt.

Aus den nach dem Hartree–Fock–Slater-Verfahren (nach HERMAN und SKILLMAN [9]) erhaltenen Dichten der Atomrümpfe wurden die elektrostatischen und Besetzungsverbotpotentiale in numerischer Form berechnet und dann die Valenzelektronenzustände in einer STO-Basis bestimmt. Um die Ergebnisse mit exakten Hartree–Fock-Daten vergleichen zu können, muss noch der Rumpf–Valenz-Austauscheffekt berücksichtigt werden. Dazu wurde das kürzlich von GOMBÁS korrigierte [11] DIRACsche Austauschpotential [10]

$$V_a^{\text{korr}} = \sqrt[3]{\frac{3}{\pi}\varrho} \cdot \max\left[0;\, 1-(\varrho_0/\varrho)^{4/3}\right] \tag{10}$$

mit $\varrho_0 = 125/192\pi^5$ verwendet. Und zwar wurde die Austauschenergie nachträglich als Störungsenergie erster Ordnung berechnet, was sich auch an anderer Stelle [12] für Valenzelektronen als günstiger erwiesen hat als die Erweiterung des effektiven Potentials durch V_a.

Ergebnisse

In Tabelle I finden sich einige der berechneten Valenzelektronenenergien. Es zeigt sich (im Gegensatz zu [3]), dass bei Verwendung der unkorrigierten G-Potentiale die Energien speziell der tiefsten Niveaus beträchtlich unter die experimentellen Werte absinken, wenn man den Austausch berücksichtigt und mit einer genügend flexiblen Funktionenbasis[2] arbeitet, obwohl die be-

[2] Beschreibt man die Valenzorbitale mit nur einem STO, erhält man um bis zu einige % höhere Energien (vergl. auch Tabelle III).

rechneten Werte um die Interschalenkorrelation über den experimentellen liegen sollten. Ebenso sind die Ergebnisse mit dem HEINEschen $U_l^{(1)}$-Potential unbefriedigend. Viel besser sind schon die Resultate mit dem Potential $U_l^{(2)}$ und bemerkenswerterweise auch mit dem einfachen statistischen F-Potential, ausser bei Lithium (Anwendung der Statistik auf einen 2-Elektronen-Rumpf) und Kupfer (die einfache Statistik lässt die Drehimpulsquantelung und damit die anormale Dichteverteilung der d-Elektronen bei den Nebengruppenelementen unberücksichtigt).

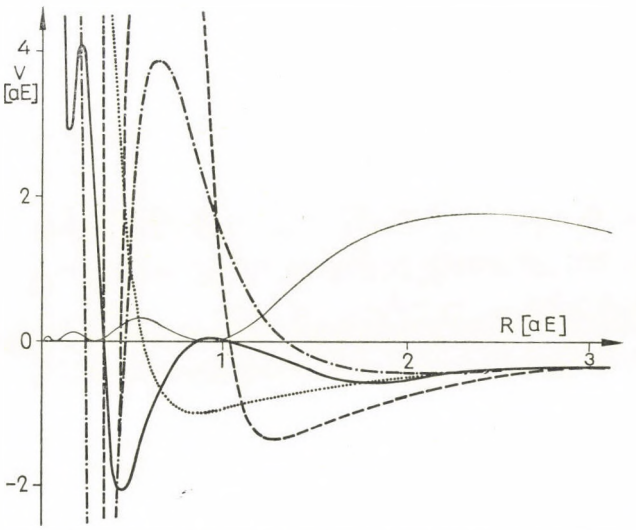

Fig. 1. Effektive Potentiale (elektrostatisches + Austausch + Besetzungsverbotpotential) von Kupfer für s-Elektronen: berechnet mit G^{korr} — — —, mit F^0 ·—·—·—, mit numerischem SCF-Verfahren ——— (radiale Valenzelektronendichte ———); adjustiertes Modellpotential nach HELLMANN.....

Die besten Ergebnisse aber werden mit dem G-Potential erhalten, wenn man den Inhomogenitätseffekten nach GOMBÁS [6] Rechnung trägt: Die Besetzungsverbotpotentiale steigen an, und die berechneten Valenzelektronenenergien sind i.a. nicht mehr tiefer als die experimentellen Werte, wenn sie auch immer noch um einige $^0/_{00}$ bis $^0/_0$ unter den entsprechenden Hartree—Fock-Werten liegen. Dies gilt besonders für Cu, wo man unter Berücksichtigung der Korrelationsenergie im Gegensatz zur Vermutung von GOMBÁS [6] eine (um fast 1 eV) zu tiefe Energie erhält.

Eine ähnliche Verbesserung sollte auch beim F-Potential möglich sein, wenn man entsprechend einem Vorschlag von HELLMANN [15] der Inhomogenität der Elektronendichte durch Mitnahme wenigstens des niedrigsten nichtverschwindenden Terms der Fermienergie in $\nabla\varrho$ Rechnung trägt, etwa nach Art der WEIZSÄCKERschen Korrektur [16].

In Fig. 1 sind einige effektive Potentiale für Cu-s-Elektronen der Anschaulichkeit halber abgebildet.

Tabelle II

Vergleich empirischer Pseudopotentiale[a)]

Mittlere Fehler der ersten zwei angeregten Einvalenzelektronenterme in %, berechnet mit verschiedenen einparametrigen Modellpotentialen. Der Parameter wurde so adjustiert, dass der entsprechende Grund-Term so gut wie möglich reproduziert wird. Negatives Vorzeichen bedeutet, dass die Pseudopotentialmethode zu zu tiefen Energien führt

	Potentialform (*s*-Potential von Na)	I	II	III	IV
		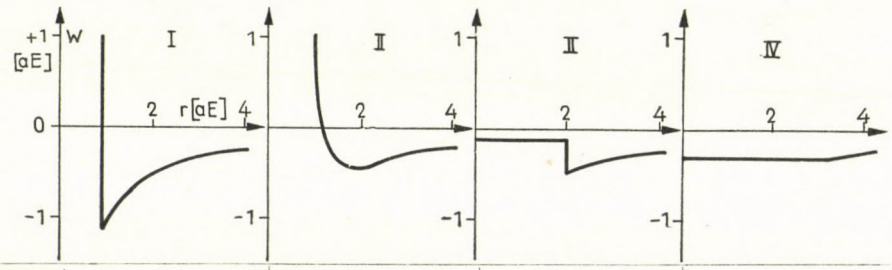			
s-Terme	Li	0,4	−0,3	−0,9	−2,5
	Na	−0,1	−0,7	−1,2	−3,3
	K	−0,7	−1,6	−1,2	−5,2
	Rb	−1,3	−2,0	−1,8	−6,0
	Cs	−1,8	—	−2,1	−7,3
	Cu	—	−4,6	−5,2	—
p-Terme[c)]	Li[b)]	3	0,0	0,0	3
	Na	−0,2	−0,1	−0,1	0,8
	K	−0,1	−0,7	−0,3	−0,2
	Rb	0,1	−0,6	−0,1	—

I. "Hard core"-Potential, $W = -Z^R/r$ für $r > R_c$, $= \infty$ für $r < R_c$. Parameter ist $R_c \cdot Z^R$ ist die Rumpfladung. Ergebnisse nach PARSON und WEISSKOPF [17].

II. HELLMANN-Potential, $W = -(Z^R - A \cdot e^{-\alpha r})/r$; Parameter ist α. Eigene Rechenergebnisse, vergl. Tabelle III.

III. Potential von ABARENKOV und HEINE [18], $W = Z^R/r$ für $r > R_c$, $= V$ für $r < R_c$. Parameter ist V. R_c wurde für alle Potentiale gleich 2 a E. gesetzt[d)]. Die Termenergien wurden aus den Potentialtabellen von ABARENKOV [19] berechnet.

IV. "Cut off"-Potential, $W = -Z^R/r$ für $r > R_c$, $= -Z^R/R_c$, für $r < R_c$. Parameter ist R_c. Ergebnisse nach KOCH und KUTZELNIGG [20]. Dies Potential lässt sich aus dem einfachen Fermischen Atommodell herleiten.

a) Bei Elementen mit höherer Rumpfladung Z^R ist der prozentuale Fehler geringer.

b) Im Falle, dass das Besetzungsverbotpotential Null ist, wie bei Li-*p*-Orbitalen, können natürlich die Potentiale I und IV schon den Grundterm nicht richtig wiedergeben und führen zu beträchtlich zu hohen Energien.

c) Die Fehler bei den *d*-Termen sind noch geringer.

d) Durch zusätzliche Variation von R_c lässt sich der Fehler z.T. ganz erheblich verringern. So führt beispielsweise bei Cu ein Potential untenstehender Form mit $R_c = 3.5$ a.E. nur zu Abweichungen von 0.0 bzw. −0,5% beim ersten bzw. zweiten angeregten *s*-Term.

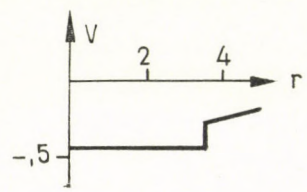

3. Empirische effektive Potentiale

Der Hauptnachteil dieser wie auch der von SZASZ [5] exakt berechneten Besetzungsverbotpotentiale ist, dass man für sie komplizierte analytische Ausdrücke erhält, die noch um die Austausch- und Korrelationspotentiale erweitert werden müssten, und die bei Molekülrechnungen zu einer Vielzahl von Zwei- und Dreizentrenintegralen führen. Daher scheint für quantenchemische Rechnungen noch immer der HELLMANNsche Vorschlag [2] der beste Kompromiss zu sein, die effektiven Potentiale W_l^A durch an experimentellen Atomenergien adjustierte einfache analytische Ausdrücke zu beschreiben.

In Tabelle II sind mit einigen einfachen Modellpotentialen erhaltene Ergebnisse zusammengestellt. Es zeigt sich zweierlei.

1) Wie in [4] vermutet, erhält man für angeregte Terme etwas zu tiefe Energien.

2) Die Ergebnisse sind i.a. für das Potential I mit der tiefsten Mulde am besten und für das Potential IV mit der flachsten Mulde am schlechtesten.

Die theoretisch berechneten effektiven Potentiale weisen wegen des elektrostatischen, Austausch- und Korrelationspotentialanteils ein Potentialminimum auf, das besonders bei schweren Elementen, speziell solchen der Nebengruppen, merklich unter dem Coulomb-Potential eines punktförmigen Atomrumpfes liegt (s. auch Abb. 1 und [31]). Daher sollte ein Modellpotential mit ausgeprägter Mulde, das das exakte effektive Potential in dem besonders wichtigen Bereich mittlerer r besser beschreiben kann, gewählt werden, was übrigens schon LADÁNYI [21] bei einigen Nebengruppenelementen getan hatte.

4. Die Rumpf—Rumpf-Wechselwirkung[3]

Der Hauptanteil der Wechselwirkungsenergie der Atomrümpfe [22] in einem Molekül wird durch die *Abstossung* entsprechender *punktförmiger Ionen* erfasst:

$$E_{AB}^{\text{Ion}} = Z_A^{\text{Rumpf}} \cdot Z_B^{\text{Rumpf}} / R_{AB} . \tag{11}$$

Wegen der Überlappung der Rumpfelektronenwolken, die beim Gleichgewichtsabstand R_0 in der Regel bei etwa 10^{-3} liegt, verringert sich die *elektrostatische Abstossung* gegenüber der von Punktladungen um einen kleinen Betrag $E^{\text{korrig.}}$. Da dieser auch noch bei Abständen von $2/3\ R_0$ i.a. unter 10^{-2} eV liegt, kann er vernachlässigt werden.

Um eine Grössenordnung grösser ist der durch die Überlappung hervorgerufene *Anstieg der kinetischen Energie*, E^{Fermi}. Zur Abschätzung dieses Effekts

[3] Alle Rechnungen wurden mit den HFS-Rumpf-Dichten der neutralen Atome von HERMAN und SKILLMAN [9] durchgeführt.

Tabelle III

Einelektronenterme (in —eV) im HELLMANN-Potential

$W_l = -(Z^R - A_l \cdot e^{-\alpha_l r})/r$; Z^R ist die Ladung des Atomrumpfes; α_l wurde so gewählt, dass die experimentelle Ionisierungsenergie des Grundzustands richtig erhalten wird; A_l wurde willkürlich gewählt, aber so gross, dass sich der Fehler der angeregten Termenergien bei Variation von A_l kaum noch verändert (es gibt anscheinend kein A, bei dem auch der erste angeregte Term exakt erhalten wird). Die Wellenfunktionen wurden durch Variationsrechnung in einer Funktionenbasis von 4 STOs mit optimierten Exponenten bestimmt. Daneben finden sich Ergebnisse für einfache Orbitale vom SLATER-Typ $r^{n-1}e^{-\zeta r}Y_{lm}$ (die angeregten s-Zustände wurden durch Linearkombination mit den Grundzustands-STOs auf diesen orthogonalisiert mit optimalen ζ, n.)

Die hier optimierten Parameter A α sind viel grösser als die von HELLMANN und anderen angegebenen. Alle diese hatten nämlich die sehr ungünstigen $1s$ (und $2p$) STOs als Variationsfunktionen verwendet.

s-Terme

Atom	A_0	α_0	Grundzustand				1. anger. Zustand					2. anger. Zustand	
			E	SLATERorbital			E_{exp}	E_{ber}	SLATERorbital			E_{exp}	E_{ber}
				E	n	ζ			E	n	ζ		
Li	10	2,202	5,391	5,27	2	0,616	2,019	2,028	1,98	3	0,357	1,051	1,052
Na	14	2,267	5,139	5,10	3	0,901	1,948	1,965	1,97	4	0,447	1,023	1,027
K	18	1,866	4,340	4,32	3	0,730	1,734	1,763	1,76	4	0,405	0,937	0,950
Rb	26	1,940	4,177	4,12	3	0,684	1,681	1,716	1,70	4	0,392	0,915	0,931
Cu	30	6,134	7,726	7,62	2	0,942	2,378	2,499	2,13	3	0,442	1,174	1,222
Be	20	3,362	18,210	17,40	2	0,994	7,271	7,302	6,97	3	0,621	3,895	3,902
Mg	30	2,855	15,034	14,90	3	1,234	6,380	6,430	6,38	4	0,741	3,531	3,555
Ca	50	2,336	11,870	11,80	4	1,262	5,391	5,466	5,44	5	0,764	3,108	3,139
Sr	60	2,205	11,029	10,95	5	1,472	5,111	5,190	5,18	6	0,840	2,975	3,017
Zn	60	4,505	17,963	17,75	3	1,492	6,999	7,189	7,13	4	0,820	3,768	3,848

p-Terme

Atom	A_1	α_1	Grundzustand				1. anger. Zustand		2. anger. Zustand	
			E	SLATERorbital			E_{exp}	E_{ber}	E_{exp}	E_{ber}
				E	n	ζ				
Li	—2	2,330	3,544	3,52	2	0,537	1,557	1,557	0,870	0,869
Na	14	2,231	3,035	3,02	3	0,616	1,386	1,388	0,794	0,794
K	18	1,635	2,726	2,71	3	0,514	1,276	1,284	0,744	0,749
Rb	26	1,568	2,598	2,55	3	0,470	1,230	1,239	0,725	0,728
Cu	—10	3,600	3,920	3,59	2	0,566	1,604	1,629	0,913	0,890
Be	—2	3,347	14,251	14,21	2	1,083	6,246	6,247	3,486	3,485
Mg	30	2,895	10,605	10,52	3	0,990	5,037	5,042	2,951	2,952

Tabelle III (Fortsetzung)

d-Terme

Atom	A_2	α_2	Grundzustand				1. anger. Zustand		2. anger. Zustand	
			E	SLATERorbital			E_{exp}	E_{ber}	E_{exp}	E_{ber}
				E	n	ζ				
Li	−2	1,855	1,513	1,51	3	0,334	0,841	0,851	0,545	0,545
Na	−10	1,953	1,522	1,52	3	0,339	0,856	0,856	0,547	0,547
K	−18	1,973	1,671	1,66	3	0,356	0,944	0,939	0,598	0,599
Rb	−6	0,984	1,777	1,63	3	0,407	0,990	0,992	0,620	0,619
Cu	−10	1,709	1,535	1,53	3	0,343	0,859	0,863	0,548	0,550
Be	−2	3,031	6,054	6,05	3	0,669	3,404	3,405	2,178	2,179
Mg	−10	2,604	6,171	6,15	3	0,701	3,466	3,470	2,213	2,213

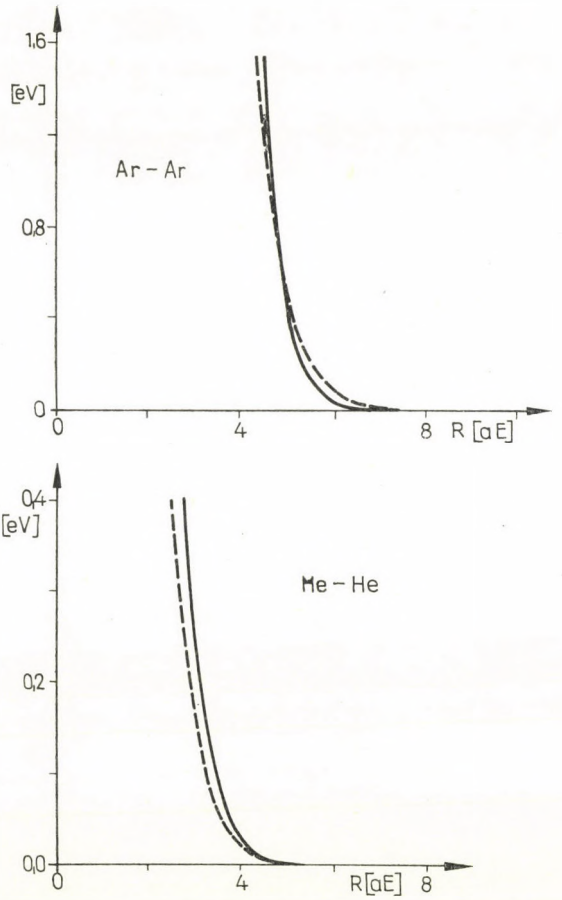

Fig. 2. Wechselwirkungspotentiale zweier Edelgasatome: experimentell ———, berechnet — — —

wurde der statistische Ausdruck [22]

$$E_{AB}^{\text{Fermi}} = \varkappa^* \cdot \int \left[(\varrho_A + \varrho_B)^{5/3} - \varrho^{5/3} - \varrho^{5/3} \right] d\tau \tag{12}$$

mit

$$\varkappa^* = \left(1 - \frac{2}{N_A + N_B} \right) \frac{9\pi}{10} \sqrt[3]{\frac{\pi}{3}} \tag{13}$$

herangezogen, wobei ϱ_A und N_A Elektronendichte und -zahl des Atomrumpfes A sind. Zwar ist E^{Fermi} danach beim Gleichgewichtszustand i. a. noch vernachlässigbar; doch steigt es mit Verringerung von R stark an. Z. B. erhält man bei Na_2 und $R = 0{,}6\, R_0$ $E^{\text{Fermi}} = 0.1$ eV. Die statistische *Austauschenergie-Korrektur*, die man nach [22] aus (12) erhält, wenn man jeweils $\varrho^{5/3}$ durch $5/6\pi\,(3/\pi)^{2/3}\,\varrho^{4/3}$ ersetzt, ist gegen E^{Fermi} vernachlässigbar, da sie sich um eine bis zwei Zehnerpotenzen kleiner ergibt.

Um die Genauigkeit von Formel (12) zu prüfen, wurden unter Berücksichtigung auch der weiter unten besprochenen Korrekturen die Edelgaspotentiale berechnet, bei denen E^{Fermi} den Hauptanteil ausmacht und die recht genau bekannt sind (s. [23] und die dort zitierte Literatur). Aus Fig. 2, die die He—He- und Ar—Ar-Potentiale zeigt, ersieht man, dass Gleichung (12) den Effekt in der Tat recht befriedigend beschreibt. (Gleichung (12) kann man durch die Bornsche Abstossungsformel [24, 25] approximieren.)

Als Effekte zweiter Ordnung sind nun noch die *Rumpf—Rumpf-Korrelation* und die Rumpf-Polarisation zu berücksichtigen. Da sich die Rümpfe im Molekül so wenig überlappen, sollte zur Abschätzung von $E^{\text{korrel.}}$ ein Van der Waalssches c/r^6-Potential hinreichend sein. Nach einer sehr einfachen Theorie von KIRKWOOD [26] lassen sich die Koeffizienten c nach der Formel

$$c = \frac{2}{9N} \langle r^2 \rangle^3 \tag{14}$$

oder aus den Polarisierbarkeiten nach LONDON [25, 27] bestimmen. Die direkte Anwendung von Gleichung (14) ist zwar zu ungenau; da aber die entsprechenden Koeffizienten zumindest für alle Edelgase, c_E, experimentell bekannt sind [28], kann man von der Beziehung

$$c = c_E \cdot \langle r^2 \rangle^3 / \langle r^2 \rangle_E^3 \tag{15}$$

ausgehen, wobei der Index E das mit dem betrachteten Atomrumpf-Kation isoelektronische Edelgasatom bezeichnet. So berechnete Rumpf—Rumpf-Korrelationsenergien übersteigen nur bei schweren Elementen sowie bei kleinen Abständen 10^{-2} eV und können daher häufig vernachlässigt werden.

Schliesslich bleibt noch die Energieänderung aufgrund der Deformation der Rumpfelektronenwolken im Feld der Umgebung, die *Polarisationsenergie* $E^{\text{Pol.}}$, zu untersuchen. Die Variationsstörungsrechnung nach KIRKWOOD [26] kann hier nicht angewendet werden, da wegen der Singularität des elektrosta-

tischen Potentials am Kernort $\langle \mathrm{grad}^2 V_e \rangle$ keinen endlichen Wert besitzt. Es wurde daher die Näherungsformel von NEUGEBAUER und GOMBÁS [29] herangezogen:

$$E_A^{\mathrm{Pol.}} = -\frac{\langle \Phi^A | V_e^2 | \Phi^A \rangle}{\langle \Phi^A | z^2 | \Phi^A \rangle} \cdot \frac{\alpha_A}{2}, \quad \left(z = \sum_i z_i\right). \tag{16}$$

(Dabei ist der Nullpunkt von V_e so zu wählen, dass $\langle \Phi^A | V_e | \Phi^A \rangle$ verschwindet.) Werte für die Rumpf-Dipolpolarisierbarkeiten α_A finden sich z. B. in [30] und der dort zitierten Literatur. Über eine andere Methode vergl. [25].)

NEUGEBAUER hatte vorgeschlagen, in Gleichung (16) für Φ^A eine einfache Produktfunktion einzusetzen, und angenommen, dass sich die Fehler in Zähler und Nenner kompensieren würden.

Berechnet man $\langle z^2 \rangle$ für eine Determinantenfunktion und für eine entsprechende Produktfunktion, so zeigt sich, dass (ausser bei K-Schalen) der letztere Wert um über die Hälfte zu gross ist. Beispielsweise wurde für $\langle z^2 \rangle_{\mathrm{Prod.}} / \langle z^2 \rangle_{\mathrm{Det.}}$ bei Na^+ 1.61, bei Ar 1.58 erhalten. Es ist nun zu untersuchen, ob auch für inhomogene Felder $\langle V_e^2 \rangle_{\mathrm{Prod.}}$ mit dem gleichen relativen Fehler behaftet ist. Betrachtet man etwa statt $V \sim z = r \cdot Y_{10}$ ein Potential $V \sim r \cdot Y_{20}$ und ein Atom ohne d-Orbitale, so verändert sich $\langle V^2 \rangle$ beim Übergang von einer Determinanten- zu einer Produktfunktion überhaupt nicht. Ebenso wird der Fehler geringer, wenn V höhere Potenzen von r enthält. Es ergibt sich also qualitativ, dass sich $\langle V^2 \rangle_{\mathrm{Prod.}}$ um so weniger von $\langle V^2 \rangle_{\mathrm{Det.}}$ unterscheidet, je inhomogener das Feld ist, d.h. für inhomogene Felder ist $[\langle V^2 \rangle / \langle z^2 \rangle]_{\mathrm{Prod.}} / [\langle V^2 \rangle / \langle z^2 \rangle]_{\mathrm{Det.}} < 1$. Z. B. erhält man bei Na_2^{2+} für diesen Quotienten bei $R = 6$ aE 0.99, bei $R = 4$ aE 0.91 (Gleichgewichtsabstand von Na_2 ist $R = 5$ aE). Die NEUGEBAUERsche Vereinfachung von Gleichung (16) sollte daher nicht kritiklos zur Berechnung der Rumpf-Polarisation bei kleinen Abständen oder gar der Kristallfeldpolarisation verwendet werden.

Zu einer vollständigen Vernachlässigung von Feldinhomogenitätseffekten und zu noch kleineren Werten führt die sehr einfache Formel

$$\tilde{E}_A^{\mathrm{Pol.}} = \frac{1}{2} \alpha_A F_A^2, \tag{17}$$

wobei F_A die mittlere elektrische Feldstärke der umgebenden Atome im Rumpf von A sein soll. F_A ist nur bei ionisierten Molekülen und bei kleineren Abständen, wo die Rumpfladung durch die Valenzelektronen nicht vollständig abgeschirmt wird, und α_A nur bei den schwach geladenen Rümpfen nicht vernachlässigbar klein. Betrachten wir als Beispiel wieder Na_2^{2+}; die Polarisationsenergien in eV sind

R	Gleichung (16) Determinante	Gleichung (16) Produktfunktion	Gleichung (17)
4 aE	0,17	0,16	0,13
6 aE	0,03	0,03	0,03

Der auf Gleichung (17) zurückgehende Fehler und $E^{\mathrm{Korrel.}}$ sind nun in vielen Fällen von ähnlicher Grösse wie $-E^{\mathrm{Fermi}}$ und kompensieren letzteres weit-

gehend. Zur Bestimmung der Rumpf—Rumpf-Energie ist daher ($E^{\text{Ion}} + E^{\text{Pol.}}$) häufig ausreichend, wie sich am Beispiel Na^+—Na^+ zeigt:

R	E^{Ion} (eV)	$E^{\text{Ion}} + E^{\text{Pol.}}$ (eV)	alle Korrekturglieder (eV)
4 aE	6,80	6,67	6,65
6 aE	4,53	4,51	4,50
8 aE	3,40	3,39	3,39

Bei Elementen mit hochliegenden *d*-Elektronen wie z. B. Cu sind allerdings alle diese Näherungen nur dann erlaubt, wenn die *d*-Elektronen nicht mehr zum Rumpf gezählt werden (vergl. auch GOMBÁS [32], LADÁNYI [21] und HARE et al. [33]). Anderenfalls ist die Überlappung der »Rümpfe« so gross, dass die erwähnten Energiebeiträge, besonders E^{Fermi}, schon im Gleichgewichtsabstand von der Grössenordnung 1 eV sind und auf diese Weise kaum noch genau genug bestimmt werden können. Beispielsweise erhält man so bei Cu_2 im Gleichgewichtsabstand (4.2 a. E.) für E^{Fermi} 1.1 eV und für die gesamte Korrektur der Rumpf—Rumpf-Wechselwirkung 0.4 eV.

Dank. Ich danke Herrn Professor Dr. H. HARTMANN für die Ermöglichung dieser Arbeit, der Deutschen Forschungsgemeinschaft für finanzielle Unterstützung und dem Deutschen Rechenzentrum Darmstadt für Rechenzeit.

LITERATUR

1. P. GOMBÁS, Z. Physik, **94**, 473, 1935.
2. H. HELLMANN, J. chem. Physics, **3**, 495, 1935.
3. P. GOMBÁS, Pseudopotentiale, Springer, Wien—New York, 1967.
   A. HARRISON, Pseudopotentials in the Theory of Metals, Benjamin, New York, 1966.
4. W. H. E. SCHWARZ, Theoret. chim. Acta (Berlin), **11**, 307, 1968.
5. L. SZASZ and G. MCGINN, J. chem. Physics, **47**, 3495, 1967; Vergl. auch W. A. GODDARD, Phys. Rev., **174**, 659, 1968.
6. P. GOMBÁS, Theoret. chim. Acta (Berlin), **11**, 210, 1968.
7. M. H. COHEN and V. HEINE, Phys. Rev., **122**, 1821, 1961.
8. J. C. SLATER, Phys. Rev., **36**, 57, 1930.
9. F. HERMAN and S. SKILLMAN, Atomic Structure Calculations, Prentice Hall, Englewood Cliffs (New Jersey), 1963.
10. P. A. M. DIRAC, Proc. Cambridge Phil. Soc., **26**, 376, 1930.
11. P. GOMBÁS, Theoret. chim. Acta (Berlin), **8**, 157, 1967.
12. W. H. E. SCHWARZ, Z. Physik, **214**, 149, 1968.
13. E. CLEMENTI, Tables of Atomic Functions, Supplement to IBM J. Research Develop., **9**, 2, 1965.
14. C. E. MOORE, Atomic Energy Levels, National Bureau of Standards, Circular 467, Washington D. C. 1949, 1952, 1958.
15. H. HELLMANN, Acta physicochim. URSS, **4**, 225, 1936.
16. C.-F. v. WEIZSÄCKER, Z. Physik, **96**, 431, 1935.
17. R. G. PARSON and V. F. WEISSKOPF, Z. Physik, **202**, 492, 1967.
18. I. V. ABARENKOV and V. HEINE, Phil. Mag. (Ser. 8), **12**, 529, 1965.
19. Technical Reports No. 1 und 2 der Solid State Theory Group, Cavendish Laboratory, Cambridge, 1965.

20. R. J. Koch, Diplomarbeit, Lehrstuhl für Theoretische Chemie der Universität Göttingen 1967.
W. Kutzelnigg, R. Koch and W. A. Bingel, Chem. Physics Letters, **2**, 197, 1968.
21. K. Ladányi, Acta Phys. Hung., **5**, 361, 1956.
22. P. Gombás, in Handbuch der Physik, ed. S. Flügge, Bd. 36/2, S. 108, Springer, Berlin—Göttingen—Heidelberg, 1956; Die statistische Theorie des Atoms und ihre Anwendungen, bes. S. 143, Springer, Wien, 1949.
23. T. L. Gilbert and A. C. Wahl, J. Chem. Phys., **47**, 3425, 1967.
24. M. Born und J. E. Mayer, Z. Physik, **75**, 1, 1932.
25. E. S. Rittner, J. Chem. Phys, **19**, 1030, 1951.
26. J. C. Kirkwood, Physik. Z., **33**, 57, 1932.
T. Neugebauer, Z. Physik, **107**, 785, 1937.
27. F. London, Z. Physik, **63**, 245, 1930.
28. R. B. Bernstein and J. T. Muckerman, Adv. chem. Physics, **12**, 389, 1967; R. G. Gordon, J. Chem. Phys., **48**, 3929, 1968.
29. T. Neugebauer und P. Gombás, Z. Physik, **89**, 480, 1934; Z. Physik, **95**, 717, 1935; Acta Phys. Hung., **12**, 279, 1960.
30. H. Hartmann und G. Kohlmaier, Theoret. chim. Acta (Berlin), **7**, 189, 1967.
J. Thorhallsson, C. Fisk and S. Fraga, Theoret. chim. Acta (Berlin), **10**, 388, 1968.
31. B. J. Austin and V. Heine, J. Chem. Phys., **45**, 928, 1966.
32. P. Gombás, Acta Phys. Hung., **1**, 301, 1952.
33. C. R. Hare, T. P. Sleight, W. Cooper and G. A. Clarke, Inorg. Chem., **7**, 669, 1968.

КОМБИНИРОВАННОЕ ПРИБЛИЖЕНИЕ

II. ИССЛЕДОВАНИЯ С ЦЕЛЬЮ ПОДХОДЯЩЕГО ВЫБОРА ЭФФЕКТИВНОГО ПОТЕНЦИАЛА И ОПИСАНИЯ ВЗАИМОДЕЙСТВИЯ МЕЖДУ АТОМНЫМИ ОСТАТКАМИ

В. Г. ЭУГЕН ШВАРЦ

Р е з ю м е

Применением метода псевдопотенциалов определяются уровни валентных электронов атомов щелочных металлов и меди. Среди различных приближенных методов наилучшие результаты получены запретным потенциалом заполнения $G^{\text{korr.}}$ выведенным в последнее время Гомбашом. Из эмпирических эффективных потенциалов сформирован подобный с определенным корытом. В качестве примера статистическим методом оценивается энергия взаимодействия атомных остатков одной молекулы.

Acta Physica Academiae Scientiarum Hungaricae, Tomus 27, pp. 405—419 (1969)

ÜBER DIE PHYSIKALISCHE REALITÄT DES LENNARD-JONESSCHEN POTENTIALS*

Von

TH. NEUGEBAUER

INSTITUT FÜR THEORETISCHE PHYSIK DER ROLAND EÖTVÖS UNIVERSITÄT, BUDAPEST

(Eingegangen 20. II. 1969)

Die Frage, ob das LENNARD-JONESsche Potential tatsächlich ein Naturgesetz darstellt, oder ob es nur eine allerdings in der Praxis sich sehr gut bewährende rein empirische Formel ist, wird besprochen. Von dem zweiten Gliede lässt es sich leicht zeigen, dass dieses von der infolge der Fermistatistik auftretenden Abstossung der sich überlappenden Elektronenwolken herrührt, gegen die Deutung des ersten Gliedes als van der Waalssche Energie hat man dagegen oft die Bedenken geäussert, dass dieser Ausdruck nur das erste Glied der Reihe dieser Energie ist und die weiteren Glieder bei der Wechselwirkung von elektronenreichen Atomen und in kondensierter Materie so gross sind, dass sogar die Konvergenz dieser Reihe oft fraglich zu sein scheint. In der vorliegenden Arbeit wird gezeigt, dass diese Glieder garnicht die physikalische Realität besitzen, die man ihnen nach der einfachen Theorie zugesprochen hat. Auf die Bedeutung dieses Umstandes in der Festkörperphysik und in neuester Zeit in der Molekularbiologie wird verwiesen.

1. Einleitung

Bekannterweise hat sich in sehr vielen Fällen (in denen es sich weder um elektrostatische noch um quantenmechanische Valenzwechselwirkungen handelt) das empirische LENNARD-JONESsche Potential, das man ganz allgemein in der Form

$$V = -AR^{-m} + BR^{-n} \tag{1}$$

schreiben kann, bestens bewährt [1]. In (1) bedeutet R die Entfernung der fraglichen in Wechselwirkung stehenden Teilchen, A und B sind empirische Konstanten und n und m relativ grosse ganze Zahlen. Am vorzüglichsten hat sich der Ansatz $m = 6$ und $9 \leqq n \leqq 12$ bewährt. Den zweiten Virialkoeffizienten erhält man z. B. mit $n = 12$ am besten.

Setzt man diese Werte in (1) ein, schreibt also

$$V = -AR^{-6} + BR^{-12} \tag{2}$$

und führt ausserdem die Gleichgewichtsentfernung R_0 der fraglichen Teilchen ein, so kann man damit die eine der zwei Konstanten A oder B eliminieren, da ja

$$\frac{dV}{dR} = 6AR_0^{-7} - 12BR_0^{-13} = 0 \tag{3}$$

* Herrn Prof. Dr. P. GOMBÁS zum 60. Geburtstag gewidmet.

sein muss. Aus (3) folgt

$$B = \frac{1}{2} A R_0^6 . \tag{4}$$

Das alles bezieht sich auf die Wechselwirkung von zwei Atomen oder Molekülen. Handelt es sich dagegen um eine kristallgitterartige Anordnung von Teilchen, so können wir dann ähnlich zu (2)

$$V = - C_m A R^{-6} + C_n B R^{-12} \tag{5}$$

schreiben. C_m und C_n sind hier die Analoga der Madelungschen Konstante in der elektrostatischen Theorie der Ionengitter. Allerdings haben in diesem Fall, wegen den grossen negativen Potenzen, die weiteren als die unmittelbaren Nachbaren, eine viel untergeordnetere Bedeutung.

Aus (5) folgt analog zu (4)

$$C_n B = \frac{1}{2} C_m A R_0^6 . \tag{6}$$

Abgesehen von den in die reine Physik gehörenden Erscheinungen die in Gasen und kondensierter Materie auftreten, hat in neuester Zeit dieser Potentialansatz eine sehr grosse Bedeutung in der Molekularbiologie erlangt, da es sich ja bei der Entstehung von Eiweissmolekülen und Viren nach einer DNS- bzw. RNS-Schablone, dann in der Vererbungslehre usw. bei den dort auftretenden feinen biophysikalischen Prozessen ausser Wasserstoffbindungen grösstenteils um solche Wechselwirkungen handeln wird. Es ist deshalb eine sehr wichtige Frage, dass was für einen physikalischen Sinn man dem Ansatz (1) bzw. (2) geben kann. Die Besprechung dieses Problems ist das Ziel der vorliegenden Arbeit. Von der sehr umfangreichen Literatur über das LENNARD-JONESsche Potential wollen wir nur die neuesten Arbeiten [2] zitieren. Die ältere Literatur ist in diesen zu finden.

2.

Sieht man sich den Ansatz (2) an, so scheint auf dem ersten Blick die plausibelste physikalische Deutung von dem zu sein, dass das erste Glied auf der rechten Seite die van der Waalssche Energie, das zweite dagegen die infolge der Fermistatistik auftretende Abstossung der Ladungswolken der in Wechselwirkung stehenden Atome oder Moleküle ist. Für dieses zweite Glied ist das tatsächlich im Wesentlichen richtig, gegen die erwähnte Deutung des ersten Gliedes hat man jedoch oft den Einwand erhoben, dass dieses nur das erste Glied der die van der Waalssche Wechselwirkung darstellenden Reihe ist. Die angenäherte Berechnung der weiteren Glieder bei elektronenreichen Atomen liefert dagegen so grosse Werte, das besonders im Falle von konden-

sierter Materie sogar die Konvergenz der Reihe in einigen Fällen fraglich zu sein scheint und es deshalb garnicht selbstverständlich ist, dass man sich nur mit dem ersten Gliede begnügen kann. Auf diese Frage kommen wir noch zurück, jetzt wollen aber zuerst den viel einfacheren Fall des Abstossungsgliedes besprechen.

3.

Ein ähnliches Abstossungsglied tritt auch in der Born—Landéschen Theorie der Ionengitter auf. Dort hat sich der Exponent $n = 9$ oder 10 am besten bewährt. (Noch vor der Entdeckung der Quantenmechanik hat man angenommen, dass dieses Glied von abstossenden elektrostatischen Multipolkräften herrührt.) Jetzt wissen wir schon, dass dieser Teil von der Fermiabstossung der sich überdeckenden Landungswolken verursacht wird, (doch spielen dabei allerdings in einem viel geringeren Masse auch die von der Überdeckung der Ladungswolken herrührenden elektrostatischen Kräfte eine Rolle) Eigentlich würde dann die Annahme einer exponentiellen Funktion die auftretenden Verhältnisse besser beschreiben, eben wegen der exponentiellen Abnahme der Eigenfunktionen in grösseren Entfernungen von den Atomkernen. Doch da in diesem Fall die ganze Abstossungsenergie bloss ca. 10% der elektrostatischen Energie ausmacht, so genügt schon eine grössere negative Potenz zur angenäherten Beschreibung der auftretenden Verhältnisse. Tatsächlich haben aber nach der Entdeckung der Quantenmechanik BORN und MAYER [3] die erwähnte Abstossungsfunktion durch einen halbempirischen exponentiellen Ausdruck mit negativem Exponenten ersetzt und erhielten so zur Erfahrung noch etwas näherstehende Resultate. Man könnte sich deshalb denken, dass es auch in (1) bzw. (2) zweckmässig wäre, das zweite Glied durch eine Exponentialfunktion zu ersetzen. Dazu ist jedoch zu bemerken, dass hier, da es sich um viel schwächere Anziehungskräfte handelt, die Überdeckung der Ladungswolken noch viel geringer sein wird und man deshalb noch viel eher eine annähernde Funktion, (die mathematisch viel bequemer ist). benützen darf Der hier zweckmässige grössere negative Exponent rührt übrigens vom selben Umstand der schwächeren Überdeckung her; der exponentielle Abfall der Eigenfunktionen ist dort schon viel steiler. Es ist noch interessant zu bemerken, dass SLATER und KIRKWOOD [4] schon in 1931 eine Formel für die Wechselwirkung von zwei He-Atomen angegeben haben, die ebenfalls ein exponentielles Glied enthält, das jedoch nach den Verfassern den Umstand berücksichtigt, dass wegen der Überdeckung der Ladungswolken die van der Waalsschen Kräfte geringer werden. Die genannten Autoren erhielten

$$E = -\frac{3{,}18}{(R/a_H)^6} + 35{,}3 \exp\left(-2{,}43\,\frac{R}{a_H}\right) \tag{7}$$

in Rydbergschen Einheiten ($e^2/2a_H$).

4.

Nach der Besprechung des relativ einfachen Problems der Abstossungskräfte, wollen wir jetzt die Anziehungskräfte bzw. die dieser zufolge auftretende negative Energie betrachten. Aus der sehr umfangreichen Literatur der van der Waalsschen Energie wollen wir hier ebenfalls nur die neuesten Arbeiten [5] zitieren, die ältere Literatur ist in diesen zu finden. Tatsächlich beginnt die Reihe der van der Waalsschen Energie bei der Wechselwirkung von Atomen, Ionen oder Molekülen, also Gebilden die aus Atomkernen und umkreisenden Elektronen bestehen, mit einem zu R^{-6} proportionalen Gliede. Bei der Wechselwirkung von Elementarteilchen ist jedoch dieses erste Glied R^{-7} proportional. Bezüglich dieser Frage, die uns hier nicht weiter interessiert, erwähnen wir nur die neueste Arbeit von SOFFER und SUCHER [6], in der die ganze Literatur von diesem Problem zusammengestellt ist.

Bekannterweise erhält man aus der Quantenmechanik die van der Waalssche Energie auf dem Wege, dass man die in der Heitler—Londonschen Theorie der chemischen Valenz auftretenden Störglieder in die zweite Näherung für die Energie in der Schrödingerschen Störungstheorie einsetzt [7]. In den gewohnten Bezeichnungen erhält man bei der Wechselwirkung von zwei Wasserstoffatomen für diese Glieder

$$H_1 = -\frac{e^2}{r_{1b}} - \frac{e^2}{r_{2a}} + \frac{e^2}{r_{12}} + \frac{e^2}{R}\,. \tag{8}$$

Bezeichnen wir die Koordinaten der einzelnen Elektronen bezogen auf dem Kern zu dem sie gehören mit x_1, y_1, z_1 und x_2, y_2, z_2, so folgt für den in diesen Koordinaten linearen Teil von H_1

$$H_1 = \frac{e^2}{R^3}(x_1 x_2 + y_1 y_2 - 2 z_1 z_2)\,. \tag{9}$$

Setzt man dieses Störglied in die zweite Näherung der Formel für die Energie tatsächlich ein, so folgt endlich für die van der Waalssche Energie in erster Näherung

$$W_w = -\frac{6e^4}{R^6} \sum_{m,n}{}' \frac{|z_1(om)|^2 \cdot |z_2(on)|^2}{h[\nu(mo) + \nu(no)]}\,, \tag{10}$$

wo jetzt die $z_1(om)$ und $z_2(on)$ Matrizenelemente sind welche z. B. die Formel $z_1(om) = \int \psi_0 z_1 \bar{\psi}_m \, d\tau$ definiert. Die ν bedeuten die Bohrschen Frequenzen. Im Falle von zwei Wasserstoffatomen kann (10) tatsächlich exakt berechnet werden wie das zuerst EISENSCHITZ und LONDON [8] getan haben. Sie erhielten

$$W = -\frac{6{,}47}{R^6} \tag{11}$$

in Hartreeschen atomaren Einheiten (e^2/a_H). Eine neue sehr genaue Berechnung von O'CAROLL und SUCHER (loc. cit.) lieferte für die in (11) stehende Konstante 6,4990267.

Weitere Glieder der Reihe für die van der Waalssche Energie für Wasserstoffatome hat zuerst MARGENAU [9] berechnet. Nach ihm muss (9), wenn man noch Quadrupolglieder berücksichtigt, mit den Ausdrücken

$$+\frac{3\,e^2}{2\,R^4}\left[-r_1^2 z_2 - r_2^2 z_1 + (2\,x_1 x_2 + 2\,y_1 y_2 - 3\,z_1 z_2)(z_1 - z_2)\right]$$
$$+\frac{3\,e^2}{4\,R^5}\left[r_1^2 r_2^2 - 5\,z_1^2 r_2^2 - 5\,z_2^2 r_1^2 - 15\,z_1^2 z_2^2 + 2\,(4\,z_1 z_2 + x_1 x_2 + y_1 y_2)^2\right] \tag{12}$$

ergänzt werden. Addiert man also solche Glieder zu (9) noch hinzu und setzt dann diese ganze Reihe in die Formel für die zweite Näherung der Störungsenergie ein, so folgt

$$W_w = -\frac{e^4}{R^6}\left\{\frac{2}{3}\sum_{m,n}{}' \frac{|r_1(om)|^2 \cdot |r_2(on)|^2}{h[\nu(mo) + \nu(no)]}\right.$$
$$+\frac{1}{R^2}\sum_{m,n}{}' \frac{|r_1^2(om)|^2 \cdot |r_2(on)|^2 + |r_2^2(on)|^2 \cdot |r_1(om)|^2}{h[\nu(mo) + \nu(no)]} \tag{13}$$
$$\left.+\frac{14}{5\,R^4}\sum_{m,n}{}' \frac{|r_1^2(om)|^2 \cdot |r_2^2(on)|^2}{h[\nu(mo) + \nu(no)]}\right\}.$$

Die in (13) stehenden Matrizenelemente haben z. B. die folgende Bedeutung

$$r_i(om) = \int \psi_0\, r_i\, \bar{\psi}_m\, d\tau\,, \qquad \text{wo} \qquad r_i^2 = x_i^2 + y_i^2 + z_i^2$$

ist. Das erste Glied auf der rechten Seite von (13) entspricht der Formel (10), was man gleich erkennt, wenn man berücksichtigt, dass

$$\overline{x_i^2} = \overline{y_i^2} = \overline{z_i^2} = \frac{1}{3}\,\overline{r_i^2}$$

usw. sein muss.

Im Falle der Wechselwirkung von zwei Wasserstoffatomen kann man auch (13) exakt auswerten. Diese sehr mühsame Berechnung vollführten zuerst PAULING und BEACH [10] und zwar mit Hilfe einer gestörten Eigenfunktion, deren Koeffizienten sie variiert haben, um die Energie zu minimalisieren. Sie erhielten

$$W_w = -\frac{12{,}99806}{(R/a_H)^6} - \frac{248{,}798}{(R/a_H)^8} - \frac{2270{,}42}{(R/a_H)^{10}} \tag{14}$$

in Rydberg-Einheiten ($e^2/2a_H$). Um (14) mit (11) vergleichen zu können, müssen wir also die erstere Formel noch mit 2 dividieren. HIRSCHFELDER und LINNETT [11] haben eine ähnliche Berechnung durchgeführt, wobei sie jedoch auch die Überlappung der Ladungswolken berücksichtigten.

Beim analogen He-Problem verfügt man wenigstens noch über vorzügliche angenäherte Eigenfunktionen. Tatsächlich hat MOORE [12] eine zu der Methode von HIRSCHFELDER und LINNETT analoge Berechnung für diesen Fall vollführt. Ausserdem behandelten dieses Problem auch noch SLATER und KIRKWOOD (loc. cit.)

5.

Alle diese Berechnungen haben jedoch ein nur mehr oder weniger theoretisches Interesse. Freie Wasserstoffatome gibt es ja weder in Gasen noch in kondensierter Materie, He-Atome sind zwar in beiden Fällen tatsächlich vorhanden, die van der Waalssche Wechselwirkung von denen ist jedoch, wegen der geringen Zahl ihrer Elektronen, sehr klein. Das Wasserstoffatom hat ausserdem eine so ausgedehnte Elektronenwolke, dass die für dieses Atom erhaltenen Resultate für das Verhalten von Atomen höherer Ordnungszahl in dieser Hinsicht auch qualitativ wenig aufschlussreich sind.

Theoretisch steht zwar dem garnichts im Wege, die für Wasserstoffatome erhaltenen Resultate auf elektronenreiche Atome, Ionen oder Moleküle zu verallgemeinern. Zu diesem Zwecke muss man ja nur unsere Formeln (8), (9) und (12) über alle Elektronenpaare, die zwischen den in Wechselwirkung stehenden Atomen oder Molekülen vorhanden sind, summieren. Die Schwierigkeit der tatsächlichen numerischen Berechnung liegt nur darin, (abgesehen von der sehr mühsamen Auswertung) dass die Eigenfunktionen dieser Atome nicht genügend bekannt sind. Man trachtete deshalb wenigstens einfach berechenbare Näherungsformeln für die van der Waalssche Energie herzuleiten. Besonders zwei solche Formeln wurden allgemeiner bekannt, die eine rührt von LONDON [13] her, die andere von SLATER und KIRKWOOD [14] und diese letztere wurde dann noch von KIRKWOOD [15] weiter vervollkommnet. Wir können hier auf die Besprechung dieser Formeln nicht eingehen und verweisen deshalb auf die zusammenfassende Arbeit von MARGENAU [16]. Hier sei nur so viel erwähnt, dass die LONDONsche Formel die unmittelbar messbaren Polarisierbarkeiten der Atome und Ionen ausnützt, die KIRKWOODsche dagegen den Umstand, dass die Schrödingersche Ladungsverteilung von elektronenreichen Atomen wenigstens im Grundzustande nach verschiedenen bekannten Methoden angenähert berechenbar ist. Es ist jedoch möglich die Kenntnis von beiden physikalischen Daten auszunützen und auf diesem Wege eine noch viel bessere Annäherungsformel herzuleiten [17].

Summieren wir nämlich bei der Berechnung der Wechselwirkung von elektronenreichen Atomen oder Ionen Ausdrücke vom Typ (9) über alle auftretenden Elektronenpaare, so erhalten wir ein Resultat, das man wieder ganz so, wie unsere Formel (10) schreiben kann, doch haben jetzt die auf der rechten Seite stehenden Matrizenelemente die folgende Bedeutung

$$z_1(om) = \int \varphi_0 \sum_{(1)} z\, \bar{\varphi}_m \, d\tau \tag{15}$$

und

$$z_2(on) = \int \chi_0 \sum_{(2)} z\, \bar{\chi}_m \, d\tau, \tag{16}$$

wo jetzt φ und χ die ganzen Eigenfunktionen des ersten und zweiten in van der Waalsscher Wechselwirkung stehenden Atoms sind und die Summen sind über alle Elektronen des ersten bzw. zweiten Atoms zu erstrecken. In (10) führen wir jetzt statt den im Nenner stehenden Bohrschen Frequenzen Mittelwerte von diesen Grössen ein, die wir mit $\bar{\nu}_1$ und $\bar{\nu}_2$ bezeichnen, dann folgt aus (10)

$$W_w = -\frac{6e^4}{R^6} \frac{\sum_{m,n}' |z_1(om)|^2 \cdot |z_2(on)|^2}{h(\bar{\nu}_1 + \bar{\nu}_2)}. \tag{17}$$

Da jetzt die Summierung hier sich nur mehr auf den Zähler bezieht, so können wir einen bekannten matrizentheoretischen Satz anwenden, nach dem

$$\sum_m z(om)\, z(mo) = z^2(00) \tag{18}$$

ist. In (17) fehlt zwar das erste Glied der Reihe, das auf der linken Seite von (18) steht, dieses Matrizenelement verschwindet jedoch wegen den Auswahlregeln Wir erhalten also für (17)

$$W_w = -\frac{6\, e^4}{R^6} \frac{z_1^2(00)\, z_2^2(00)}{h(\bar{\nu}_1 + \bar{\nu}_2)}, \tag{19}$$

wo jetzt z. B.

$$z_1^2(00) = \int \varphi_0 \Big(\sum_{(1)} z\Big)^2 \bar{\varphi}_0 \, d\tau$$

ist. Weiter können wir noch, da es sich bei der Berechnung dieser Matrizenelemente um die nullte Näherung handelt und deshalb die drei Raumrichtungen einander vollständig äquivalent sind,

$$z_1^2(00) = \frac{1}{3} r_1^2(00) \quad \text{und} \quad z_2^2(00) = \frac{1}{3} r_2^2(00)$$

setzen, dann folgt

$$W_w = -\frac{2\,e^4}{3R^6}\,\frac{r_1^2(00)\,r_2^2(00)}{h\,(\bar{\nu}_1+\bar{\nu}_2)}\,. \tag{20}$$

Ganz analog können wir auch die quantenmechanischen Formeln für die Polarisierbarkeiten der zwei in Wechselwirkung stehenden Atome umformen. Wir erhalten z. B.

$$\alpha_1 = 2\,e^2 \sum_m{}' \frac{|z_1(om)|^2}{h\nu(mo)} = \frac{2e^2}{3}\,\frac{r_1^2(00)}{h\bar{\nu}_1} \tag{21}$$

und eine analoge Formel für α_2.

Benützen wir zuerst für die Eigenfunktionen der Atome einfache Produkteigenfunktionen, (auf die Korrektionen die anzubringen sind, wenn wir uns der antisymmetrischen Determinanteneigenfunktion bedienen, kommen wir noch zurück) so bedeuten die Ausdrücke $r_1^2(00)$ und $r_2^2(00)$ einfach eine Mittelung von r^2 über die Ladungsverteilung des ersten und zweiten Atoms. Also sind diese Grössen z. B. aus den mit Hilfe der Hartree—Fockschen Methode gewonnenen Tabellen berechenbar. Da man aber andererseits die Polarisierbarkeiten empirisch kennt, so kann man auf dem Wege aus (21) den Mittelwert $h\bar{\nu}_1$ bzw. $h\bar{\nu}_2$ berechnen. Es liegt auf der Hand anzunehmen, dass diese Mittelwerte ungefähr die selben, wie die in (17) eingeführten sein werden. Damit ist aber auch schon (20) vollständig berechenbar geworden. Ausgenützt haben wir also um (17) angenähert auswertbar zu machen, auch die empirische Kenntnis der Polarisierbarkeiten und auch die Berechenbarkeit der Ladungsverteilung im Grundzustande.

Ganz analog, wie wir unsere Formel (10) auf Mehrelektronenprobleme erweitert und dann umgeformt haben, um sie berechenbar zu gestalten, können wir das auch mit dem Ausdruck (13) tun, der noch zwei weitere Glieder der Reihenentwicklung enthält. Summieren wir nämlich bei der Berechnung der Wechselwirkung von elektronenreichen Atomen oder Ionen Ausdrücke vom Typ (8) über alle auftretenden Elektronenpaare, und setzen dann die Reihenentwicklung dieser ganzen Summe in die Formel für die Energie zweiter Näherung der Störungstheorie ein, so sehen wir gleich, dass wir wieder eine Formel vom Typ (13) erhalten, in der jedoch die auf der rechten Seite stehenden Matrizenelemente jetzt die Bedeutung

$$|\,r_1(om)|^2 = |\int \varphi_0 \sum_{(1)} r\bar{\varphi}_m\,d\tau_1\,|^2, \tag{22}$$

$$|\,r_2(on)|^2 = |\int \chi_0 \sum_{(2)} r\bar{\chi}_n\,d\tau_2\,|^2, \tag{23}$$

$$|(r_1^2)\,(om)|^2 = |\int \varphi_0 \sum_{(1)} r^2\,\bar{\varphi}_m\,d\tau_1\,|^2, \tag{24}$$

und

$$|(r_2^2)\,(on)|^2 = |\int \chi_0 \sum_{(2)} r^2\, \bar{\chi}_n\, d\tau_2\,|^2 \tag{25}$$

haben. Zu summieren ist wieder über alle Elektronen der fraglichen Atome. Führen wir wieder auch die erwähnten Frequenzmittelwerte $\bar{\nu}_1$ und $\bar{\nu}_2$ ein und berücksichtigen wieder den erwähnten matrizentheoretischen Satz (18), so erhalten wir jetzt statt (13), wenn wir auch noch berücksichtigen, dass bei der Berechnung von $\sum_m{}' |(\sum_{(1)} r^2)(om)|^2$ das nullte Glied in (18) also $|(\sum_{(1)} r^2)(00)|^2$ nicht verschwindet

$$W_w = -\frac{e^4}{R^6}\,\frac{2}{3}\,\frac{r_1^2(00)\,r_2^2(00)}{h(\bar{\nu}_1+\bar{\nu}_2)} - \frac{e^4}{R^8}\,\frac{r_1^2(00)\,r_2'^4(00)+r_2^2(00)\,r_1'^4(00)}{h\,(\bar{\nu}_1+\bar{\nu}_2)} - \frac{e^4}{R^{10}}\,\frac{14}{5}\,\frac{r_1'^4(00)\,r_2'^4(00)}{h\,(\bar{\nu}_1+\bar{\nu}_2)}\,, \tag{26}$$

wo jetzt

$$r_1^2(00) = 3\int \varphi_0 \Big(\sum_{(1)} z^2\Big)\,\bar{\varphi}_0\, d\tau_1 \tag{27}$$

und

$$r_1'^4(00) = \int \varphi_0 \Big(\sum_{(1)} r^2\Big)^2\,\bar{\varphi}_0 d\tau_1 - |\int \varphi_0 \sum_{(1)} r^2\,\bar{\varphi}_0\, d\tau_1|^2 \tag{28}$$

bzw.

$$r^4(00) = \int \varphi_0 \Big(\sum_{(1)} r^2\Big)^2\,\bar{\varphi}_0\, d\tau_1 \tag{28a}$$

ist, und $r_2^2(00)$ und $r_2'^4(00)$ analoge Bedeutungen haben. Das erste Glied auf der rechten Seite von (26) ist selbstverständlich das selbe wie (20), aber auch die weiteren zwei Glieder sind jetzt wegen der Berechenbarkeit von $\bar{\nu}_1$ und $\bar{\nu}_2$ und der Kenntnis der Ladungsverteilung der zwei Atome im Grundzustande ohne jede Schwierigkeit auswertbar.

6.

Wir wollen jetzt erstens noch sehen, dass inwiefern unsere erhaltenen Resultate abzuändern sind, wenn wir für die in Wechselwirkung stehenden Atome statt einfache Produkteigenfunktionen, die theoretisch streng richtigen antisymmetrischen Determinanteneigenfunktionen benützen und zweitens was wir über die physikalische Realität der weiteren zwei auf der rechten Seite von (26) stehenden Glieder erfahren können, wenn wir die in denen stehenden Matrizenelemente mit Hilfe dieser Eigenfunktionen tatsächlich numerisch berechnen.

Betrachten wir zuerst z. B. das Matrizenelement (27). Die einfache Produkteigenfunktion des ersten Atoms haben wir dort mit einem kleinen φ bezeichnet, benützen wir jetzt für die antisymmetrische Determinanteneigenfunktion ein grosses Φ. Setzen also

$$\Phi = \frac{1}{\sqrt{N!}} \begin{vmatrix} \varphi_1(1) & \dots & \varphi_1(N) \\ \vdots & & \\ \varphi_N(1) & \dots & \varphi_N(N) \end{vmatrix}, \tag{29}$$

wo jetzt N die Zahl der Elektronen des ersten Atoms bedeutet und die φ_i die Eigenfunktionen der einzelnen Elektronen sind. Analog zu (27) haben wir dann

$$r_1^2(00) = 3 \int \Phi \Big(\sum_{(1)} z\Big)^2 \bar{\Phi}\, d\tau \tag{30}$$

und weiter

$$\int \Phi \Big(\sum_{(1)} z\Big)^2 \bar{\Phi}\, d\tau = \int \Phi \sum_{i=1}^{N} z_i^2\, \bar{\Phi}\, d\tau + \int \Phi \sum_{\substack{i,k \\ i\neq k}}^{N} z_i z_k\, \bar{\Phi}\, d\tau . \tag{31}$$

Das erste Glied auf der rechten Seite bedeutet einfach eine Mittelung von z^2 bzw. $\frac{1}{3} r^2$ über die Schrödingersche Ladungsdichte, entspricht also der Benützung der einfachen Produkteigenfunktion. Das zweite Glied hat dagegen einen »Austauschcharakter«. Setzen wir in dem jetzt Φ aus (29) tatsächlich ein, so folgt

$$\begin{aligned} \int \Phi \sum_{\substack{i,k \\ i\neq k}}^{N} z_i z_k \bar{\Phi}\, d\tau = {} & \frac{1}{N!} \sum_{\substack{i,k=1 \\ i\neq k}}^{N} \sum_{\substack{\mu,\nu=1 \\ \mu\neq\nu}}^{N} \int \varphi_\mu(i)\, z_i\, \bar{\varphi}_\mu(i)\, d\tau_i \cdot \int \varphi_\nu(k)\, z_k\, \bar{\varphi}_\nu(k)\, d\tau_k \\ & - \frac{1}{N!} \sum_{\substack{i,k=1 \\ i\neq k}}^{N} \sum_{\substack{\mu,\nu=1 \\ \mu\neq\nu}}^{N} \int \varphi_\mu(i)\, z_i\, \bar{\varphi}_\nu(i)\, d\tau_i \cdot \int \varphi_\nu(k)\, z_k\, \bar{\varphi}_\mu(k)\, d\tau_k . \end{aligned} \tag{32}$$

Das erste Glied verschwindet wegen den Auswahlregeln. Zur Berechnung des zweiten führen wir die Summierung nach i und k durch. Zu jedem festgehaltenen Wertepaar von μ und ν wird es $N!$ solche Glieder geben, die nur in der Benennung der Veränderlichen voneinander verschieden sind und deshalb zu demselben numerischen Resultat führen. Wir haben also

$$\int \Phi \sum_{\substack{i,k \\ i\neq k}}^{N} z_i z_k \bar{\Phi}\, d\tau = - \sum_{\mu,\nu} |\varphi_\mu\, z \bar{\varphi}_\nu\, d\tau|^2 = - \sum_{\substack{n,l,m,s \\ n',l',m',s'}} |\varphi_{nlms}\, z \bar{\varphi}_{n'l'm's'}\, d\tau|^2 . \tag{33}$$

Nach einer bekannten Summenregel [18] folgt weiter

$$\sum_m \left| z \begin{pmatrix} n & l-1 & m \\ n' & l & m \end{pmatrix} \right|^2 = \frac{1}{3} l \left| r \begin{pmatrix} n' & l-1 \\ n & l \end{pmatrix} \right|^2 \tag{34}$$

und aus der erhalten wir für (33)

$$-\frac{2}{3}\sum_{nn'}\sum_{l}\left\{l\left|r\begin{pmatrix}n' & l-1\\ n & l\end{pmatrix}\right|^2+(l+1)\left|r\begin{pmatrix}n' & l+1\\ n & l\end{pmatrix}\right|^2\right\}. \tag{35}$$

Der Zweier-Faktor rührt von Spin her. Also folgt endlich aus (30), (31), (32), (33), (34) und (35)

$$r_1^2(00)=\sum_{i=1}^{N}\overline{r_i^2}-2\sum_{nn'}\sum_{l}\left\{l\left|r\begin{pmatrix}n' & l-1\\ n & l\end{pmatrix}\right|^2+(l+1)\left|r\begin{pmatrix}n' & l+1\\ n & l\end{pmatrix}\right|^2\right\}. \tag{36}$$

Selbstverständlich können wir auch ganz analog $r_2^2(00)$ berechnen. Zur Auswertung von $r_1^4(00)$ setzen wir analog zu (30) und (31)

$$r_1^4(00)=\int\Phi\Big(\sum_{(1)}r^2\Big)^2\bar{\Phi}\,d\tau=\int\Phi\sum_{(1)}r^4\,\bar{\Phi}\,d\tau+\int\Phi\sum_{\substack{i,k\\ i\neq k}}^{N}r_i^2\,r_k^2\,\bar{\Phi}\,d\tau\,. \tag{37}$$

Das erste Glied auf der rechten Seite von (37) bedeutet einfach eine Mittelung von r^4 über die ganze Schrödingersche Ladungsverteilung, entspricht aber jetzt noch nicht der Benützung einer einfachen Produkteigenfunktion. Das zweite Glied hat dagegen wieder wenigstens teilweise einen »Austauschcharakter«. Setzen wir in dieses jetzt (29) tatsächlich ein, so folgt analog zu (32)

$$\begin{aligned}\int\Phi\sum_{\substack{i,k\\ i\neq k}}^{N}r_i^2\,r_k^2\,\bar{\Phi}\,d\tau=&\frac{1}{N!}\sum_{\substack{i,k=1\\ i\neq k}}^{N}\sum_{\substack{\mu,\nu=1\\ \mu\neq\nu}}^{N}\int\varphi_\mu(i)\,r_i^2\,\bar{\varphi}_\mu(i)\,d\tau_i\cdot\int\varphi_\nu(k)\,r_k^2\,\bar{\varphi}_\nu(k)\,d\tau_k\\ &-\frac{1}{N!}\sum_{\substack{i,k=1\\ i\neq k}}^{N}\sum_{\substack{\mu,\nu=1\\ \mu\neq\nu}}^{N}\int\varphi_\mu(i)\,r_i^2\,\bar{\varphi}_\nu(i)\,d\tau_i\cdot\int\varphi_\nu(k)\,r_k^2\,\bar{\varphi}_\mu(k)\,d\tau_k\,.\end{aligned} \tag{38}$$

Das erste Glied auf der rechten Seite von (38) verschwindet aber jetzt nicht, weil ja jedes Integral die Mittelung von r^2 über die Ladungsverteilung von einem Elektron bedeutet. Zu jedem festgehaltenen Wertepaar von μ und ν wird es $N!$ solche Glieder geben, die wieder nur in der Benennung der Veränderlichen voneinander verschieden sind und deshalb zu dem selben numerischen Ergebnis führen. Das erste Glied von (37) und dieser erste Teil von dem zweiten Gliede in dieser Formel liefern also das selbe Ergebnis, welches die Benützung einer einfachen Produkteigenfunktion geben würde. Ganz ähnlich können wir auch das zweite Glied in (38) umformen und erhalten dann endlich für das ganze zweite Glied in (37)

$$\int\Phi\sum_{\substack{i,k\\ i\neq k}}^{N}r_i^2\,r_k^2\,\bar{\Phi}\,d\tau=\sum_{\substack{\mu,\nu\\ \mu\neq 1}}^{N}r^2(\mu\mu)\,r^2(\nu\nu)-\sum_{\substack{\mu,\nu\\ \mu\neq\nu}}^{N}|r^2(\mu\nu)|^2. \tag{39}$$

Ganz nach der selben Methode, die wir hier angewandt haben, können wir auch das auf der rechten Seite von (28) stehende zweite Glied (bzw. das hier auftretende Analogon von dem) umformen. Wir erhalten

$$\left|\int \Phi_0 \sum_{(1)} r^2 \bar{\Phi}_0 \, d\tau\right|^2 = \sum_{\mu=1}^{N} [r^2(\mu\mu)]^2 + \sum_{\substack{\mu,\nu \\ \mu \neq \nu}}^{N} r^2(\mu\mu)\, r^2(\nu\nu). \tag{40}$$

Das zweite Glied auf der rechten Seite von (40) ist jedoch das selbe, wie das erste Glied in (39) und vernichtet deshalb dieses, so dass wir aus (28), (37), (39) und (40) endlich

$$r_1'^4(00) = \int \Phi \sum_{(1)} r^4 \bar{\Phi} \, d\tau - \sum_{\mu=1}^{N} [r^2(\mu\mu)]^2 - \sum_{\substack{\mu,\nu \\ \mu \neq \nu}}^{N} |r^2(\mu\nu)|^2 \tag{41}$$

erhalten. Die zwei negativen Glieder in (41) schwächen also den Wert von $\int \Phi \sum_{(1)} r^4 \bar{\Phi} d\tau$, den wir einfach als $\overline{r^4}$ schreiben können, (der ist einfach der über die Schrödingersche Ladungsverteilung gemittelte Wert von r_1^4) noch etwas ab.

7. Besprechung der erhaltenen Ergebnisse

Wie wir das in dem vorangehenden Abschnitt gesehen haben, kann man auch die in der Formel (26) stehenden höheren Glieder für elektronenreiche Atompaare in guter Näherung berechnen. Doch müssen wir noch einen Umstand berücksichtigen, der sehr dafür spricht, dass man auf diesem Wege die physikalische Realität der erwähnten Glieder überschätzt.

Mittelt man nämlich gerade Potenzen von r über die Schrödingersche Ladungsverteilung eines Atoms (oder Ions), so liegt zwar das Gebiet, welches den grössten Beitrag zu den Integralen liefert, bei der Mittelung von r^2 noch ziemlich gut innerhalb der experimentellen Atom- oder Ionenradien, bei der Mittelung von r^4 aber schon fast ganz ausserhalb und diese Verhältnisse werden selbstverständlich noch viel krasser, wenn man noch höhere Potenzen von r über die Ladungsverteilung integriert.

Beim einfachen Wasserstoffproblem kann man diese Verhältnisse prompt rechnerisch erfassen: Benützen wir wieder Hartreesche atomare Einheiten, so haben wir für die Eigenfunktion des Grundzustandes des H-Atoms $\psi = 2e^{-r}$. Die fraglichen Integrale sind also von der Form

$$\frac{1}{4\pi}\overline{r^n} = 4\int_0^{\infty} e^{-2r} r^n r^2 \, dr. \tag{42}$$

Uns interessiert jetzt, wo die Maxima der Intergranden liegen, die wir aus

$$\frac{d}{dr}(e^{-2r} r^{n+2}) = 0 \tag{43}$$

erhalten. Schon für $n = 2$ erhalten wir $r_{max} = 2$, für $n = 4$ folgt $r_{max} = 3$ und ganz allgemein $r_{max} = (n + 2)/2$. Also schon bei der Mittelung von r^2 liegt beim Wasserstoff das Maximum bei zwei Bohrschen Halbmesser und bei der von r^4 bei drei, also schon ganz ausserhalb des Atomradius. Es ist schon wahr, dass eben das Wasserstoffatom eine sehr ausgedehnte Elektronenwolke besitzt, doch kann man diese erwähnten Integrale auch bei elektronenreichen Atomen oder Ionen z. B. aus den HARTREE—FOCKschen Tabellen numerisch berechnen und findet dann ähnliche Verhältnisse. Als Beispiel wollen wir das Cl^--Ion erwähnen, da für dieses schon seit langer Zeit HARTREE-FOCKsche Tabellen [19] vorliegen. Nach den Berechnungen des Verfassers liegt das Maximum bei der Integration von r^2 über die Elektronendichte bei ungefähr $2{,}2a_H$, bei der von r^4 dagegen bei $4{,}3a_H$. Der empirische Ionenradius vom Cl^--Ion beträgt dagegen nach GOLDSCHMIDT $3{,}42a_H$. Wir sehen also, dass in kondensierter Materie, in der sich die Atome oder Ionen infolge der Fermiabstossung der Ladungswolken gegenseitig stark zusammendrücken, der für $\overline{r^2}$ berechnete Wert noch eine ziemliche Realität besitzt, der für $\overline{r^4}$ erhaltene dagegen nur mehr wenig. Innerhalb des Ionenradius liefert die numerische Integration für $\overline{r^4}$ nur einen wenig bedeutenden Wert. Es sei nur noch erwähnt, dass auch das Cl^- als negatives Ion eine sehr ausgedehnte Elektronenwolke besitzt. Für $\overline{r^2}$ liefert die numerische Integration bei diesem Ion 38,55 in Hartreeschen atomaren Einheiten. Die Berechnung der in (36) stehenden Austauschglieder liefert dagegen 12,84, so dass demzufolge der numerische Wert von $r_1^2(00)$ ungefähr 2/3 von dem von $\sum_i \overline{r_i^2}$ sein wird. Wahrscheinlich werden diesbezüglich auch bei anderen Atomen oder Ionen ähnliche Verhältnisse auftreten. Die Auswertung von $\overline{r^4}$ liefert einen Betrag von etwas über 400. Die in (41) stehenden Korrektionsglieder, die noch zu $\Sigma\overline{r^4}$ hinzutreten, werden diesen Wert etwas herabsetzen. Zu dem erwähnten Betrag von $\overline{r^4}$ gibt der innerhalb des empirischen Ionenradius liegende Teil der Elektronenwolke nur ungefähr 27%.

Ausserdem müssen wir noch einen Umstand berücksichtigen. Die HARTREE—FOCKschen Eigenfunktionen sind tatsächlich die besten die man erhalten kann, jedoch unter der Annahme, dass die Eigenfunktion immer ein Produkt von solchen Funktionen bleibt, die nur die Koordinaten von einem Elektron enthalten. Es ist jedoch garnicht sicher, dass solch eine Eigenfunktion die eigentliche Lösung der Schrödingerschen Differentialgleichung ist und es ist sehr wahrscheinlich, dass eine wirkliche Lösung, welche dieser Einschränkung nicht unterworfen ist, eine noch stärker zusammengezogene Ladungsverteilung geben würde.

Wir kommen also zu dem Schluss, dass die in (13) bzw. (26) auf der rechten Seite stehenden zwei höheren Glieder (Dipol—Quadrupol und Quadrupol—Quadrupolglied) in kondensierter Materie relativ wenig physikalische Realität besitzen und man deshalb den zwei Gliedern im LENNARD-JONESschen Poten-

tialansatz tatsächlich eine ziemlich genaue physikalische Deutung geben kann. Da in diesem Potential mit negativem Vorzeichen ein R^{-6} enthaltendes Glied und mit positivem ein zu R^{-12} proportionales steht, so kann man weitere recht kleine Korrektionen, die zu R^{-8} bzw. R^{-10} proportional sind, durch kleine Abänderungen der Faktoren der erwähnten Glieder berücksichtigen.

In Gasen sind die Verhältnisse von den in diesem Abschnitt beschriebenen ganz verschieden, aber auch dort werden die erwähnten höheren Glieder bei grösseren Entfernungen, wegen der schnellen Abnahme dieser Glieder mit zunehmendem R eine untergeordnete Bedeutung haben. Die Bemerkung bezüglich der noch stärkeren Zusammengezogenheit der Ladungswolken, als die der HARTREE—FOCKschen Theorie entsprechende, bezieht sich übrigens auch auf diesen Fall.

Weiter könnte man noch fragen, dass wenn man die in (13) stehenden höheren Glieder berücksichtigt, man nicht auch gleichzeitig weitere Glieder in der Störungstheorie mitberücksichtigen müsste. Doch entsteht dann auch das Problem über die physikalische Realität dieser Glieder. H. A. WILSON [20] konnte zeigen, dass die zeitabhängige quantenmechanische Störungstheorie wenn auch nicht konvergent, so doch wenigstens asymptotisch ist, ganz ebenso wie das nach H. POINCARÉ bei der astronomischen Störungstheorie der Fall ist.

Ausserdem könnten noch besonders bei kristallgitterartigen Anordnungen auch Dreikörperkräfte eine gewisse Rolle spielen. Wir erwähnen hierauf bezüglich nur die neuen Arbeiten von CHAN und DALGARNO [21] und JANSEN [22].

LITERATUR

1. R. H. FOWLER, Statistical Mechanics 2. ed., Cambridge, University Press 1955. S. 292—337. Kap. X. Interatomic Forces. Verfasst von J. E. LENNARD-JONES. Weiter z. B. I. PRIGOGINE. The Molecular Theory of Solutions, Amsterdam, North-Holland Publishing Comp. 1957.
2. A. SARAN und A. K. BARNA, Canad. J. of Phys., **42**, 2026, 1964; S. CARRA und D. D. KONOWALOW, Nuovo Cim., **34**, 205, 1964; S. C. SAXENA und B. P. MATHUR, Rev. Mod. Phys., **37**, 316, 1965; J. S. ROWLINSON, Mol. Phys., **9**, 197, 1965; P. G. MIKOLAJ und C. J. PINGS, Phys. Rev. Letters, **15**, 849, 1965 und **16**, 4, 1966; J. L. FINNEY und J. D. BERNAL, Nature, **213**, 1079, 1967; U. BUCK und H. PAULY, Z. f. Phys., **208**, 390, 1968; J. MEHRA, Physica, **37**, 145, 1967; G. K. HORTON, Am. J. of Phys., **36**, 93, 1968; J. L. LEBOWITZ, Phys. Letters, **28 A**, 596, 1969; S. KIM, D. HENDERSON und J. A. BARKER, Canad. J. of Phys., **47**, 99, 1969; J. P. WESLEY und A. E. S. GREEN, Amer. J. of Phys., **36**, 1093, 1969 (Anwendung auf Atomkerne); G. A TSONGAS und S. P. KOUTSOYANNIS, Journ. of Phys. B., **2**, 437, 1969.
3. M. BORN u. J. E. MAYER, Z. f. Phys., **75**, 1, 1932; J. E. MAYER und L. HELMHOLZ, Z. f. Phys., **75**, 19, 1932.
4. J. C. SLATER und J. G. KIRKWOOD, Phys. Rev., **37**, 682, 1931.
5. U. BUCK und H. PAULY, Z. f. Phys., **185**, 155, 1965; R. J. BELL, Proc. Phys. Soc., **86**, 17, 1965; Y. M. CHAN und A. DALGARNO, Mol. Phys., **9**, 349, 1965; J. O. HIRSCHFELDER und O. LÖWDIN, Mol. Phys., **9**, 491, 1965; R. DÜREN, R. HELBING und H. PAULY, Z. f. Phys., **188**, 468, 1965; A. J. VAN DER MERWE, Z. f. Phys., **196**, 212, 1966 und Z. f. Naturf., **22a**, 593, 1967; M. O'CARROLL und J. SUCHER, Phys. Rev. Letters, **21**,

1143, 1968; SUPRIYA RAY, J. D. LYONS und T. P. DAS, Phys. Rev., **174,** 104 u. 112, 1968; J. MEHRA, Acta Phys. Austr., **27**, 341, 1968.
6. J. SOFFER und J. SUCHER, Phys. Rev., **161,** 1664, 1967.
7. Z. B. J. C. SLATER, Insulators, Semiconductors and Metals. (Quantum Theory of Molecules and Solids. Vol. 3.) McGraw-Hill Book Comp., New York, 1967. S. 318—48.
8. R. EISENSCHITZ und F. LONDON, Z. f. Phys., **60,** 491, 1930.
9. H. MARGENAU, Phys. Rev., **38,** 747, 1931.
10. L. PAULING und J. Y. BEACH, Phys. Rev., **47,** 686, 1935.
11. J. O. HIRSCHFELDER und J. W. LINNETT, J. Chem. Phys., **18,** 130, 1950.
12. N. MOORE, J. Chem. Phys., **33,** 471, 1960.
13. F. LONDON, Z. f. phys. Chem., (B) **11,** 222, 1931.
14. J. C. SLATER und J. G. KIRKWOOD, Phys. Rev., **37,** 682, 1931.
15. J. G. KIRKWOOD, Phys. Zeitschr., **33,** 57, 1932; J. P. VINTI, Phys. Rev., **41,** 813, 1932.
16. H. MARGENAU, Rev. Mod. Phys., **11,** 1, 1939.
17. TH. NEUGEBAUER und P. GOMBÁS, Z. f. Phys., **89,** 480, 1934; TH. NEUGEBAUER, Math. und Naturwiss. Anzeiger d. Ung. Akad. d. Wiss., **55,** 410, 1937 und Z. f. Phys., **107,** 785, 1937.
18. Vgl. z. B. Geiger-Scheel, Handbuch der Physik. 2. Aufl. Bd. XXIV/1, Artikel von H. BETHE, S. 433.
19. D. R. HARTREE und W. HARTREE, Proc. Roy. Soc. London (A), **156,** 45, 1936.
20. H. A. WILSON, Proc. Roy. Soc. London (A); **122,** 589, 1929. Vgl. auch P. A. M. DIRAC, Proc. Roy. Soc. London (A) **112,** 661, 1926 und **114,** 243 und 710, 1927 und W. HEISENBERG, Ann. d. Phys., **9,** 338, 1931.
21. I. M. CHAN und A. DALGARNO, Mol. Phys., **9,** 525, 1965,
22. L. JANSEN, Phys. Rev., **135,** A 1292, 1964 und Phys. Rev. Letters, **20,** 530, 1968. Vgl. ausserdem die neuesten Arbeiten von I. J. ZUCKER und G. G. CHELL, Journ. of Phys., C., **1**, 1505, 1968; Y. YASUDA, J. of the Phys. Soc. Japan, **26,** 163, 1969; A. A. LUCAS, Phys. Rev., **176**, 1093, 1968.

О ФИЗИЧЕСКОЙ РЕАЛЬНОСТИ ПОТЕНЦИАЛА ЛЕНАРДА-ДЖОНСА

Т. НАЙГЕБАУЭР

Р е з ю м е

Рассматривается вопрос, является ли потенциал Ленарда-Джонса отображением одной действительной закономерности природы, или его можно считать хорошо сохранившейся чисто эмпирической формулой. Рассматривая второй член, легко можно показать, что он — появляющееся в результате Ферми-статистики отталкивание, обусловленное перекрыванием электронного облака, тогда как первый член истолкуется как энергия Ван дер Ваальса. Часто полагается, что в данном выражении только первые члены соответствуют данным энергиям и дальнейшие члены при взаимодействии богатых в электронах атомов и в конденсированной материи настолько велики, что сделают сходимость данного ряда сомнительной. В настоящей работе показывается, что эти члены совсем не имеют физического смысла, последний был присужден им в простой теории. Обращается внимание на важность данного условия в физике твердого тела и в последнее время в молекулярной биологии.

Acta Physica Academiae Scientiarum Hungaricae, Tomus 27, pp. 421—434 (1969)

EFFECT OF TRAPS ON STEADILY TRAVELLING DOMAINS IN SEMICONDUCTORS*

By

G. PATAKI

RESEARCH INSTITUTE FOR TECHNICAL PHYSICS OF THE HUNGARIAN ACADEMY OF SCIENCES, BUDAPEST

(Received 20. II. 1969)

This paper deals with the effect of traps on the domain velocity (u_0) and total current (j_S) in the presence of steadily travelling high field domains. The treatment is applicable both for the Watkins—Gunn effect and recombination instability. The calculations are carried out without linearization of the related equations, using the method proposed in [9] for the trap-free case. The assumptions used are: (i) Only transitions leading to negative differential conductivity depend on the electric field; (ii) The relaxation times of transitions between high and low mobility states are shorter than the other characteristic times of the problem; (iii) The mobilities and diffusion coefficients are field independent; (iv) The electron concentration in the band is much lower than those of empty and filled centres.

The effect of traps on the Watkins—Gunn effect is discussed in detail and expressions for possible domain-velocity are derived. In contrast to the trap-free case the domain velocity is sensitive to the domain shape. For quadratic domains, the peak field dependence of possible domain modes is discussed.

A simple analysis shows that the applicability of the model for slowly moving domains in semi-insulating GaAs cannot be definitely decided without a knowledge of the relaxation time from low-mobility states to the traps.

1. Introduction

Since the first more detailed experimental investigations of slowly moving high field domains in Ge [1], [2], it has been suggested that the very low domain velocity might be controlled by centres (traps), which differ from those leading to negative differential conductivity. Although, to the best of our kowledge, there is no direct evidence for the existence of these centres, not even in the case of germanium, it seems reasonable to assume — especially for compensated semi-insulating materials — that the traps really contribute to the space charge density. In fact, it was proposed in [3], that the slowly moving domains in semi-insulating GaAs [4], [5], [6] can be explained by the electron transfer mechanism between valleys, rather than an impurity barrier mechanism and the velocity is controlled by the oxygen impurity. This model seems to be all the more suitable because, as shown in [7], the empty oxygen centres are electrically neutral. On the other hand, for CdS one has to assume at least two types of centres, in order to interpret the existence of domains, say, by field quenching [8].

* Dedicated to Prof. P. GOMBÁS on his 60th birthday.

In [9] and [10], we suggested a new method to determine the domain velocity (u_0) and the total current (j_s) for the case of recombination instability and the Watkins—Gunn effect, but neglecting the effect of traps. It was found in [9], that low domain velocity in Au doped Ge can be obtained if a proper (asymmetrical) domain shape is assumed. On the other hand, the Gunn domains propagate practically independently of the domain shape, and their velocity equals the *average* electron drift velocity at the peak field with good approximation.

Now, the effect of traps of a general two-state model will be investigated using the above method which, in contrast to [3], does not require the linearization of equations.

Because the calculations are now more complicated than those for the trap-free case some simplifications must be introduced to make the results easier to survey. These are: (i) Only the relaxation time responsible for the negative differential conductivity depends on the electrical field; (ii) There is a quasi-equilibrium between the low- and high-mobility states (instantaneous transitions); (iii) The mobilities and the diffusion coefficients are field independent; (iv) The electron concentration in the band is much lower than the concentrations of empty and filled centres.

Using the above assumptions an algebraic equation system is given for u_0 and j_s. Approximate expressions are derived for the possible domain velocities. The application for oxygen doped GaAs as well as the peak field dependence of domain velocities are discussed.

2. The basic equations of the model

In a general two-state model the negative differential conductivity arises from transitions of electrons from high-mobility states (index "1") to low-mobility states (index "2"). For the recombination instability the low-mobility states are actually zero-mobility states, localized in the forbidden gap. Figs. 1a and 1b refer to the Watkins—Gunn effect and recombination instability, respectively. It is assumed that only the transitions $1 \rightarrow 2$ depend on electrical field. Although the transitions $2 \rightleftarrows t$ are important for the Watkins—Gunn effect but not for recombination instability, the calculations allow these transitions, too (broken lines in Fig. 1b).

The basic equations of the model are the equations of charge continuity, the Poisson equation, the phenomenological expressions for current densities in states "1" and "2" and, finally, the reaction kinetic equations for transitions between states "1", "2" and "t".

$$\frac{\partial \varrho_1}{\partial t} - \frac{\partial j_1}{\partial x} = -\Psi_{12}(\varrho_1, \varrho_2, E) - \Psi_{1t}(\varrho_1, \varrho_t, E) \equiv \left(\frac{\partial \varrho_1}{\partial t}\right)_{\text{gen.}}, \qquad (1)$$

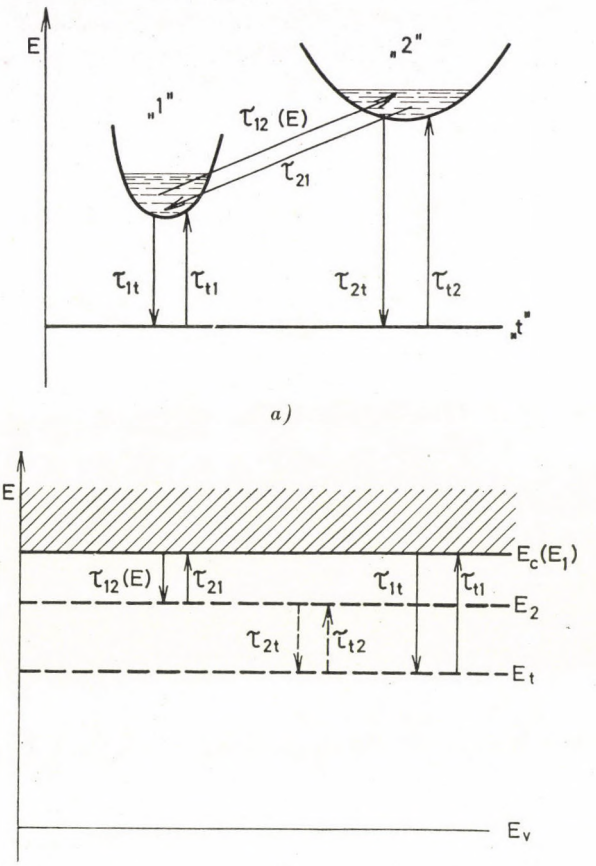

Fig. 1. Electronic transitions allowed by the model. Only the transition 1 → 2 depends on the electrical field. a) Watkins—Gunn effect; b) Recombination instability

$$\frac{\partial \varrho_2}{\partial t} - \frac{\partial j_2}{\partial x} = +\Psi_{12}(\varrho_1, \varrho_2, E) - \Psi_{2t}(\varrho_2, \varrho_t, E) \equiv \left(\frac{\partial \varrho_2}{\partial t}\right)_{\text{gen.}}, \tag{2}$$

$$\frac{\partial \varrho_t}{\partial t} = \Psi_{1t} + \Psi_{2t}, \tag{3}$$

$$\frac{\partial E}{\partial x} = \frac{4\pi}{\varepsilon}(\varrho_0 - \varrho_1 - \varrho_2 - \varrho_t) \equiv \frac{4\pi}{\varepsilon}\varrho, \tag{4}$$

$$j_i = \varrho_i \mu_i E + D_i \frac{\partial \varrho_i}{\partial x}; \ (i = 1,2). \tag{5}$$

Here the notations of papers [9] and [10] have been used. The functions ψ_{ij} can be determined easily assuming a Shockley—Read—Hall type recombination model. With a further simplification the function ψ_{ij} can be linearized with

respect to the concentrations if the electron concentration in the band is much lower than the concentrations of empty and filled centres [9]:

$$\begin{aligned} \Psi_{12} &= \varrho_1/\tau_{12}(E) - \varrho_2/\tau_{21}, \\ \Psi_{1t} &= \varrho_1/\tau_{1t} - \varrho_t/\tau_{t1}, \\ \Psi_{2t} &= \varrho_2/\tau_{2t} - \varrho_t/\tau_{t2}. \end{aligned} \tag{6}$$

The physical meaning of time constants introduced in the above equations is evident (see Fig. 1). In the following calculations the quasi-equilibrium between states "1" and "2" is assumed, which leads to $\psi_{12}=0$ and thus we have:

$$\varrho_2/\varrho_1 = \tau_{21}/\tau_{12}(E) \equiv r(E). \tag{7}$$

From Equs. (1)—(3) for space charge density ϱ and current $j = j_1 + j_2$ one obtains:

$$\frac{\partial \varrho}{\partial t} + \frac{\partial j}{\partial x} = 0, \tag{8}$$

while the definition of the total current is:

$$j_s \equiv j + \frac{\varepsilon}{4\pi} \frac{\partial E}{\partial t}. \tag{9}$$

For a steadily travelling domain the charge densities ϱ_i ($i = 1, 2, t$) and the electrical field E depend only on the variable $z = x - u_0 t$ [11] and if the derivation with respect to z is denoted by $'$ then from Equs. (1)—(4) the following differential equation system is obtained:

$$u_0 \varrho_1' + j_1' = \Psi_{12} + \Psi_{1t}, \tag{1'}$$

$$u_0 \varrho_2' + j_2' = -\Psi_{12} + \Psi_{2t}, \tag{2'}$$

$$u_0 \varrho_t' = -\Psi_{1t} - \Psi_{2t}, \tag{3'}$$

$$E' = \frac{4\pi}{\varepsilon}(\varrho_0 - \varrho_1 - \varrho_2 - \varrho_t). \tag{4'}$$

On the other hand, from Equ. (8) and definition (9) we arrive to the two important equations:

$$j' = u_0 \varrho' = \frac{\varepsilon u_0 E''}{4\pi}, \tag{10}$$

$$j = u_0 \varrho + j_s = j_s + \frac{\varepsilon u_0 E'}{4\pi}, \tag{11}$$

where the total current j_s is constant for the wave-like solution [11].

The further calculations are based on the Equs. (10)—(11). In fact, if these equations are taken at the point of electrical neutrality z_0, where $E'(z_0) = 0$, then we have:

$$j_s = \varrho_{10}(v_{10} + r_0 v_{20}) + \varrho'_{10}(D_1 + r_0 D_2), \tag{12}$$

$$u_0 S_2 = \varrho'_{10}(v_{10} + r_0 v_{20}) + \varrho_{10} \dot{r}_0 D_2 E''_0 + \varrho''_{10}(D_1 + r_0 D_2), \tag{13}$$

where $v_{i0} = \mu_{i0} E_0$; $\dot{r} = dr/dE$; and $S_i = \varepsilon/4\pi E_0^{(i)}$ $(i = 1, 2, \ldots)$ are the "domain shape parameters" introduced in [9].

3. Determination of u_0 and j_s for arbitrary domain shapes

1. General case: two-state model

According to Equs. (11) and (13) the quantities ϱ_{10}, ϱ'_{10} and ϱ''_{10} are to be determined. The functions ϱ_i $(E, E'; \ldots)$, $(i = 1, 2, t)$, can be determined relatively simply if the condition of instantaneous transitions between states "1" and "2" is valid. With the aid of Equs. (3') and (11) and using the Poisson equation repeatedly the functions ϱ'_1 and ϱ_t' can be eliminated and for ϱ_1 and ϱ_t the following equation system can be derived:

$$\begin{aligned} \varrho_1(1+r) + \varrho_t &= T, \\ L\varrho_1 - M\varrho_t &= R, \end{aligned} \tag{14}$$

where

$$\begin{aligned} T &= \varrho_0 - \varepsilon E'/4\pi; \\ L &= (v_1 + r v_2)(1+r) u_0 + (D_2 - D_1) u_0 \dot{r} E' + (D_1 + rD_2)(1/\tau_{1t} + r/\tau_{2t}); \\ M &= (D_1 + rD_2)/\tau_g; \quad 1/\tau_g = 1/\tau_{t1} + 1/\tau_{t2}; \\ R &= u_0 \left[(1+r)(j_s + \varepsilon u_0 E'/4\pi) - (D_1 + rD_2) T'\right]. \end{aligned} \tag{14'}$$

The solution of this equation system is:

$$\varrho_1 = \frac{R + TM}{L + (1+r) M}; \qquad \varrho_t = \frac{-R(1+r) + TL}{L + (1+r) M}. \tag{15}$$

With the aid of Equ. (15) the derivatives figuring in Equs. (12), (13) can be determined. In fact, with the notation $L + (1 + r)M = N$ we have

$$\varrho_{10} N_0 = R_0 + T_0 M_0, \tag{16a}$$

$$\varrho'_{10} N_0 = R'_0 + T'_0 M_0 - L'_0 \varrho_{10}, \tag{16b}$$

$$\varrho''_{10} N_0 = R''_0 + T''_0 M_0 + T_0 M''_0 - N''_0 \varrho_{10} - 2 L'_0 \varrho'_{10}. \tag{16c}$$

Here, for convenience, the quantities appearing in Equs. (16) will be given:

$$R_0' = u_0 [(1 + r_0) u_0 S_2 + (D_1 + r_0 D_2) S_3] ;$$

$$R'' = u_0 [\dot{r}_0 E_0''(j_s + D_2 S_2) + (1 + r_0) u_0 S_3 + (D_1 + r_0 D_2) S_4] ;$$

$$L_0' = (D_2 - D_1) u_0 \dot{r}_0 E_0'' ;$$

$$L_0'' = (\mu_1 + r_0 \mu_2)(1 + r_0) u_0 E_0'' + (D_2 - D_1) u_0 \dot{r}_0 E_0''' +$$
$$+ \dot{r}_0 E_0'' [u_0 (1 + r_0) v_{20} + u_0 (v_{10} + r_0 v_{20}) +$$
$$+ D_2 (1/\tau_{1t} + r_0/\tau_{2t}) + (D_1 + r_0 D_2)/\tau_{2t}] ;$$

$$T_0 = \varrho_0 ; \; T_0^{(i)} = - S_{i+1} ; \; (i = 1,2,\ldots) ; \; M_0' = 0 ; \; M_0'' = \dot{r}_0 D_2 E_0''/\tau_g ;$$

$$N_0' = L_0' ; \; N_0'' = L_0'' + (1 + r_0) M_0'' + \dot{r}_0 E_0'' M_0 ;$$

$$N_0 = (1 + r_0) [u_0 (v_{10} + r_0 v_{20}) + (D_1 + r_0 D_2)/\tau_{t0}] .$$

Here by definition:

$$\frac{1 + r_0}{\tau_{t0}} \equiv \frac{1}{\tau_{1t}} + \frac{r_0}{\tau_{2t}} + \frac{1 + r_0}{\tau_g} . \tag{17}$$

Using the above expressions, the current and the velocity can be calculated. Before doing this, it is more convenient to introduce dimensionless quantities into Equs. (12) and (13). Let $i_s = j_s/\varrho_0 v_{a0}$; where $v_{a0} = (v_{10} + r_0 v_{20}) \cdot (1 + r_0)^{-1}$ is the average electron drift velocity in the band. The average diffusion coefficient is $D_{a0} = (D_1 + r_0 D_2) \cdot (1 + r_0)^{-1}$. Assuming $S_2 \neq 0$, we have:

$$i_s = \frac{\varrho_{10}}{\varrho_0}(1 + r_0) + \frac{\varrho_{10}' D_{a0}}{v_{a0} \varrho_0}(1 + r_0) \tag{18}$$

$$x = \frac{\varrho_{10}'}{S_2}(1 + r_0) + \frac{\varrho_{10} D_2 \dot{r}_0 E_0''}{S_2 v_{a0}} + \frac{\varrho_{10}'' D_{a0}}{S_2 v_{a0}}(1 + r_0) . \tag{19}$$

In order to calculate the various term sin Equs. (18) and (19) we need the following dimensionless quantities:

$$\alpha_0 = \tau_{i0} D_{a0} E_0''/E_0 ; \; \alpha_1 = D_{a0}/v_{a0}^2 \tau_{t0} ; \; \alpha_2 = v_{a0} \tau_{t0} S_3/S_2 ;$$
$$\alpha_3 = \alpha_1 \alpha_2 ; \; \alpha_4 = \tau_{t0} D_{a0} S_4/S_2 ; \; \alpha_s = v_{a0}^2 \tau_{t0} \tau_{Ma} E_0''/E_0 ; \tag{20}$$
$$\vartheta_0 = \alpha_1 \alpha_s ; \; \alpha_g = \tau_{t0}/\tau_g ; \; \alpha_M = \tau_{t0}/\tau_{Ma} ; \; (\alpha_0 = \alpha_M \vartheta_0) ;$$
$$\gamma = E_0/r_0 \cdot (dr/dE)_0 ; \; \delta_i = D_i/D_{a0} ; \; \delta = \delta_1 - \delta_2 ;$$
$$G_0 = x + \alpha_1 ; \; \alpha_{21} = \tau_{t0} (1/\tau_{2t} - 1/\tau_{1i})$$

and here:

$$\tau_{Ma} = \varepsilon/4\pi\varrho_0 \mu_{a0} ; \; \mu_{a0} = (\mu_1 + r_0 \mu_2)(1 + r_0)^{-1} .$$

From Equ. (28) $\alpha_{i0} = (1 + r_0)^{-1}$.

First, based on Equs. (16a, b) the quantities ϱ_{10}, ϱ'_{10} will be determined. After simple calculation we have

$$\frac{\varrho_{10}}{\varrho_0}(1+r_0) = \frac{x(i_s+\vartheta_0)+\alpha_1\alpha_g}{G_0}\,; \tag{21}$$

$$\frac{\varrho'_{10}D_{a0}}{\varrho_0 v_{a0}}(1+r_0) = \frac{\vartheta_0}{G_0}\left[x(x+\alpha_3)-\alpha_1\alpha_g\right] + \frac{r_0\gamma\alpha_0\alpha_1\delta x}{G_0(1+r_0)}\cdot\frac{\varrho_{10}}{\varrho_0}, \tag{22}$$

For i_s we obtain, after multiplying by G_0 and $1/\alpha_1$:

$$i_s = \alpha_g + \alpha_s\left[x(1+\alpha_3)+x^2-\alpha_1\alpha_g\right] + r_0\gamma\alpha_0\delta x(1+r_0)^{-1}\frac{\varrho_{10}}{\varrho_0}\,. \tag{23}$$

Now, from Equs. (21) and (22) both ϱ_{10}/ϱ_0 and i_s can be expressed as:

$$i_s\bar{G}_0 = G_0\left\{\alpha_g+\alpha_s\left[x(1+\alpha_3)+x^2-\alpha_1\alpha_g\right]\right\} + \frac{r_0\gamma\alpha_0\delta x}{(1+r_0)^2}(\alpha_1\alpha_g+\vartheta_0)\,; \tag{24}$$

$$\frac{\varrho_{10}}{\varrho_0}(1+r_0)\bar{G}_0 = \alpha_0 G_0 + x\left\{\vartheta_0+\alpha_s\left[x(1+\alpha_3)+x^2-\alpha_1\alpha_g\right]\right\}, \tag{25}$$

where

$$\bar{G}_0 = G_0 - r_0\gamma\alpha_0\delta x^2(1+r_0)^{-2}\,.$$

The determination of the velocity is more complicated, because the term ϱ''_{10} also appeared in Equ. (19). First, Equ. (22) is inserted into Equ. (19), then having multiplied by G_0 and $1/\alpha_1$, we obtain the following expression:

$$x = \alpha_2 x - \alpha_g + r_0\gamma\alpha_M x\frac{\varrho_{10}}{\varrho_0} + r_0\gamma\alpha_1\alpha_M\delta_2\frac{\varrho_{10}}{\varrho_0} + \frac{\tau_{t0}\varrho''_{10}N_0}{(1+r_0)S_2 v_{a0}}\,. \tag{26}$$

Here the relation $\delta(1+r_0)^{-1}+\delta_2 = 1$ has been taken into account. The last term of Equ. (26) can be determined using Equs. (16c) and (14). First, however, the term ϱ'_{10} in (16c) is expressed with i_s from Equ. (12). After tedious calculations we have:

$$\begin{aligned} xP = &-\alpha_g F + \alpha_2 x^2 + (3-2\delta_2)(1+r_0)^{-1} r_0\gamma\alpha_M x i_s - \alpha_M K x\varrho_{10}/\varrho_0 - \\ &- r_0\gamma\alpha_1\alpha_M\left[1+\alpha_{21}(1+r_0)^{-1}\right]\varrho_{10}/\varrho_0\,, \end{aligned} \tag{27}$$

where

$$\begin{aligned} P &= 1-\alpha_2-\alpha_4-r_0\gamma(1+r_0)^{-1}\alpha_M\delta_2\vartheta_0\,; \\ F &= 1+\alpha_3-r_0\gamma\alpha_1\alpha_M(1+r_0)^{-1}\,; \\ K &= 1+r_0+r_0\gamma\left[2\delta(1+r_0)^{-1}+v_{20}/v_{a0}-\delta\alpha_3(1+r_0)^{-1}\right]. \end{aligned} \tag{27'}$$

Now, the inconvenient term ϱ_{10}/ϱ_0 in Equ. (27) can be eliminated using Equ. (21) and then the following algebraic equation for the dimensionless velocity x is obtained:

$$b_3 x^3+b_2 x^2+b_1 x+b_0 = 0\,, \tag{28}$$

where

$$b_3 = +\alpha_2\,;$$

$$b_2 = +\alpha_1\alpha_2 - P+(3-2\delta_2)\, r_0\gamma\alpha_{i0}\alpha_M i_s - \alpha_M\alpha_{i0}K\,(i_s+\vartheta_0)\,;$$

$$b_1 = -\alpha_1 P - \alpha_g F+(3-2\delta_2)\, r_0\gamma\alpha_1\alpha_{i0}\alpha_M i_s - \alpha_1\alpha_M\alpha_g\alpha_{i0}K -$$

$$- r_0\gamma\alpha_1\alpha_M\alpha_{i0}\,(1+\alpha_{21}\alpha_{i0})\,(i_s+\vartheta_0)\,;$$

$$b_0 = -\alpha_1\alpha_g\,[F+r_0\gamma\alpha_1\alpha_M\alpha_{i0}\,(1+\alpha_{21}\alpha_{i0})]\,.$$

Equs. (24) and (28) form a coupled algebraic equation system for u_0 and j_s, the roots of which can be determined, say, by numerical methods. Instead, we shall give approximate expressions for the current and velocity but, before doing this, the case of recombination instability will be treated briefly.

2. Recombination instability

For simplicity's sake, the transitions denoted by broken lines in Fig. 1b will be neglected. In other words, the characteristic times for transitions $2 \rightleftarrows t$ are much longer than any other characteristic time of the problem.

As the low-mobility electrons are localized in the forbidden gap, the average drift velocity v_a should not be introduced. Using the usual notations $D_1 = D$; $\mu_1 = \mu$; $v_1 = v$ the following quantities will be introduced: $x = (1+r_0)x'$; $i_s = (1+r_0)i_{sr}$; $\tau_M = (1+r_0)\tau_{M0}$; $\tau_{t0} = (1+r_0)\tau_0$ and here $\tau_{M0} = \varepsilon/4\pi\varrho_0\mu$. According to our assumption $1/\tau_g \equiv 1/\tau_{t_1}$ and, thus, $1/\tau_0 = 1/\tau_{1t} + (1+r_0)/\tau_{t_1}$ and $\alpha_g = (1+r_0)\tau_0/\tau_g \equiv (1+r_0)\beta_g$; while for all other α_k ($k = 0, 1, 2, 3, 4, s, M$, io;) $\alpha_k \to \beta_k$ and $\vartheta_0 \to \varphi_0$. Finally, it is easy to see that $\delta_2 = 0$; $\delta = 1 + r_0$ and $1 + \alpha_{21}\cdot\alpha_{i0} \to \beta_g(1+r_0)$.

Introducing the above notations, the following algebraic equation system results for x' and i_{sr}:

$$i_{sr}\,[G_0' - \beta_3 r_0\gamma\,(1+r_0)] = G_0'\,\{\beta_g+\beta_s\,[x'(1+\beta_3)+x'(1+r_0) - \beta_1\beta_g]\} + \tag{29}$$

$$+ r_0\gamma\beta_0\,x'(\beta_1\beta_g+x'\varphi_0)\,,$$

where $G_0' = x'(1+r_0) + \beta_1$ and

$$a_3 x'^3+a_2 x'^2+a_1 x'+a_0 = 0\,. \tag{30}$$

where the coefficients a_i are:

$$a_3 = \beta_2(1+r_0)^2;$$

$$a_2 = (\beta_1\beta_2 - P' + 3\,r_0\gamma\beta_M i_{sr})(1+r_0) - \beta_M K'[i_{sr}(1+r_0)+\varphi_0];$$

$$a_1 = -\beta_1 P' - (1+r_0)\beta_g F' + 3\,r_0\gamma\beta_1\beta_M i_{sr} - \beta_1\beta_M\beta_g K' -$$

$$- r_0\gamma\beta_1\beta_M\beta_g[i_{sr}(1+r_0)+\varphi_0];$$

$$a_0 = -\beta_1\beta_g(F' + r_0\gamma\beta_1\beta_M\beta_g)$$

and $P' = 1-\beta_2-\beta_4$; $K' = 2r_0\gamma + 1 + r_0 - r_0\gamma\beta_3$; $F' = 1 + \beta_3$.

4. Approximate expressions for u_0 and j_s

In order to give closed expressions for u_0 and j_s we make some approximations. A simple estimate shows that the diffusion component of current j_s is negligible compared with the drift term, i.e. $j_s \approx \varrho_{10}(v_{10} + r_0 v_{20})$. Using Equ. (21) one obtains for i_s

$$i_s = \alpha_g + \alpha_s x. \tag{31}$$

In the same approximation, the quantity ϱ_{10}/ϱ_0 will have the form:

$$\frac{\varrho_{10}}{\varrho_0}(1+r_0) = \alpha_g + \alpha_s x. \tag{32}$$

It is easy to see that the approximation made also involves the condition $|x| \ll 1$. This condition certainly holds if the traps influence the domain velocity and take part in the formation of the space charge. In the trap-free case the domain velocity turned out to be equal to the average drift velocity v_{a0} and thus if traps are present it should be much less than v_{a0}, i.e. $|x| \ll 1$. It is interesting to note that the approximation (31) is a good one because it gives the same result as the exact expression (24) also for $x = -\alpha_1$ ($G_0 = 0$).

This is not true for Equ. (32). The approximate equations (31) and (32) contain only one shape-dependent parameter (α_s). The exact expressions (24) and (25) depend also on α_0; α_3, but not on α_2. Now, instead of inserting Equ. (31) into coefficients b_2 and b_1 (as it was done in [9—10]), it is more convenient to use Equ. (27) directly. After simple calculations, using the relation $\delta\alpha_{i0} + \delta_2 = 1$, and Equ. (27') one obtains:

$$C_0 x^2 - P_0 x - \alpha_g F_0 = 0, \tag{33}$$

where

$$C_0 = \alpha_2 - \alpha_M \alpha_s \alpha_{i0} K_0 ;$$

$$P_0 = 1 - \alpha_2 - \alpha_4 + r_0 \gamma \alpha_1 \alpha_M \alpha_s \alpha_{i0}^2 (\delta + \alpha_{21}) + \alpha_g \alpha_M \alpha_{i0} K_0 ;$$

$$F_0 = 1 + \alpha_3 + r_0 \gamma \alpha_1 \alpha_M \alpha_{i0}^2 (\delta + \alpha_{21}) ;$$

$$K_0 = 1 + r_0 - r_0 \gamma (1 - v_{20}/v_{a0}) - r_0 \gamma \alpha_{i0} \delta \alpha_3 .$$

So, instead of the third order algebraic equation, (see Equ. (28)), we obtained an algebraic equation of second order. A simple analysis shows that the third omitted root corresponds to the case $G_0 = 0$, and hence a possible domain velocity is

$$- u_{0D} = \frac{D_{a0}}{v_{a0} \tau_{t0}} , \tag{34}$$

which will be referred to as the "diffusion mode". The two roots of Equ. (33) can be determined approximately as $-x_1 \approx \alpha_g F_0/P_0$; $x_2 \approx P_0/C_0$. The first root can be called the "drift mode". As for the existence of the second root, no theoretical or experimental evidence is known. The "drift mode" has the ollowing form:

$$- u_{0d} = v_{a0} \alpha_g \cdot \frac{1 + \alpha_3 + r_0 \gamma \alpha_1 \alpha_M \alpha_{i0}^2 (\delta + \alpha_{21})}{1 - \alpha_2 - \alpha_4 + r_0 \gamma \alpha_1 \alpha_M \alpha_s \alpha_{i0} (\delta + \alpha_{21}) + \alpha_g \alpha_M \alpha_{i0} K_0} , \tag{35}$$

which is very sensitive to the domain shape because of the asymmetry parameter α_2. Before discussing the peak field dependence of domain velocities, the signs of different terms of the denominator should be examined. If $r_0 B > \gamma$, the term K_0 is positive, more precisely: $\alpha_{i0} K_0 \approx 1$. The asymmetry parameter α_2 can drastically reduce the domain velocity, as was pointed out in [9]. As for its sign, $\alpha_2 \leq 0$, because, according to experimental observations the leading edge of the propagating domain is a depletion layer (where $E' > 0$) the slope of which is less than that of the trailing edge. For such a domain shape, as can be seen, $\alpha_2 < 0$. Despite α_s being negative its effect is negligible because it is multiplied by the very small α_1 factor. From the above consideration it follows that the denominator of Equ. (35) does not become zero. Let us investigate briefly the peak field dependence of domain velocities. Both for diffusion and drift modes we need the field dependence of the average drift velocity, v_{a0}. According to [12], v_{a0} shows saturation with increasing electrical field ($E_0 > 15$kV/cm). Although in our model $\mu_i = $ const. and thus v_{a0} does not saturate, a simple analysis shows that v_{a0} can be considered as the actual

average drift velocity. (It is not difficult to take into consideration a field dependent mobility in the upper valleys). The diffusion mode will depend essentially on the τ_{t_0}, if $E_0 > 3E_c$. The drift mode depends on the domain shape parameters. Therefore, one has to assume a concrete domain shape. According to [13] and [14], the domain may be symmetrical. Assuming a quadratic domain shape $\alpha_2 = \alpha_3 = \alpha_4 = 0$, while the term containing the parameter α_s can be neglected. Using these assumptions we have (with $\alpha_{i_0} K_0 \approx 1$):

$$-u_{0d} \approx v_{a0}\,\alpha_g \frac{1 + r_0\,\gamma\alpha_1\,\alpha_M\,\alpha_{i0}^2\,(\delta+\alpha_{21})}{1+\alpha_g\,\alpha_M} \,. \tag{36}$$

From this expression it is clear that the peak field dependence of u_{0d} is determined by v_{a0}, α_g and α_M. The average electron drift velocity saturates if $E_0 > 3E_c$. The behaviour of α_g(or τ_{t_0}) depends on the parameter $\xi \equiv \tau_{1t}/\tau_{2t}$. If $\xi = 1$, then α_g is independent from the electrical field. In this case, according to Equ. (32), the electron concentration at the point of electrical neutrality practically does not change.

If the slowly moving domains are associated with oxygen impurities in semi-insulating GaAs [4]—[6], then the following parameter values can be used. The energy level of oxygen is situated at $E_t = 0.75$ eV below the conduction band.* The effective density of states in the central valley is $N_{c_1} = 6.10^{17}$ cm^{-3}. The generation time τ_{t_1} is defined as $\tau_{t_1} = 1/C_{1t}n_1 = 1/C_{1t}N_{c_1} \exp(-E_t/kT)$, where $C_{1t} = S_{1t}v_{th}$, and S_{1t} is the electron capture cross-section for transition $1 \to t$ and v_{th} is the electron thermal velocity. According to [7] we can write $S_{1t} = 5 \cdot 10^{-15}$ cm^2 and thus $C_{1t} = 5 \cdot 10^{-15} \cdot 3.6 \cdot 10^7 = 1.8 \cdot 10^{-7}$ $\mathrm{cm}^3/\mathrm{sec}$. At room temperature $\tau_g \approx \tau_{t_1} = 20$ sec (the generation time τ_{t_2} can evidently be neglected). In order to determine the capture time constant τ_{1t} we need the concentration of empty centres because $\tau_{1t} = 1/C_{1t}p_{t_0}$. An essential simplification $n_0 < p_{t_0}, n_{t_0}$. For $n_0 = 10^7\,\mathrm{cm}^{-3}$, corresponding to the material used in [5], the ratio of empty to filled centres is $p_{t_0}/n_{t_0} = 2{,}8 \cdot 10^{-2}$, $(n_0 p_{t_0}/n_{t_0} = n_1)$. Thus, it is sufficient to assume that $p_{t_0} = 2.8 \cdot 10^{13}\mathrm{cm}^{-3}$ and $n_{t_0} \approx \varrho_0/e = 10^{15}\mathrm{cm}^{-3}$. To the author's knowledge, there is no available experimental data on the electron capture cross-section S_{2t} of oxygen centres. Therefore, in Fig. 2 the ratio $\xi = \tau_{1t}/\tau_{2t}$ is used as a parameter. If n_0 is small enough and $\alpha_g\alpha_M \ll 1$, the peak field dependence of the drift mode is determined by $v_{a0}\,\alpha_g$, or by $v_{a0}\,\tau_{t_0}$ because in the present model τ_g is independent from the field. This shows that in this respect the diffusion and drift modes behave contrarily.

* A suitable choice of the parameters is $\mu_1 = 7000$ $\mathrm{cm}^2/\mathrm{Vsec}$; $\mu_2 = B\mu_1$: $B = 0.02$ $D_1 = 182$ $\mathrm{cm}^2/\mathrm{sec}$; $D_2 = BD_1$ (in the calculations the validity of the Einstein relation was not assumed), $\varepsilon = 12.5$. The effective mass of electrons in the central valley is $m_1 = 0.071\ m_0$.

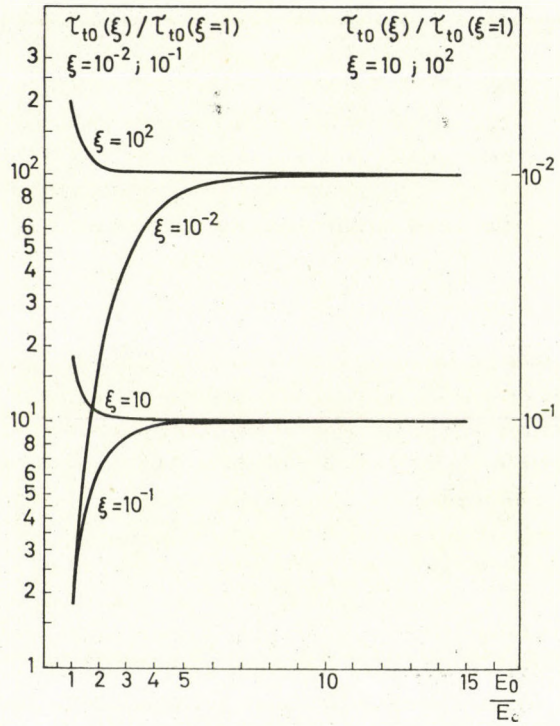

Fig. 2. Dependence of $\tau_{t0}(\xi)/\tau_{t0}(\xi = 1)$ on relative peak-field E_0/E_c for different values of $\xi = \tau_{1t}/\tau_{2t}$. The curves are plotted with parameter values given in the text ($\tau_{t0}(\xi = 1) = 2 \cdot 10^{-7}$ sec)

5. Discussion

The model presented provides a possibility to investigate the effect of traps on the recombination instability and also on the Watkins—Gunn effect. In contrast to the linear theory [3], the present treatment deals with nonlinear equations using the method proposed in [9], [10] for the trap-free case. Different domain modes are derived under the assumptions listed in the introduction. Contrary to the trap-free case the slowly moving Gunn domains are sensitive to the domain shape, at least for the drift mode. The velocity expressions derived are similar to those obtained for the recombination instability without traps [9], if the diffusion coefficient and mobility are replaced by the corresponding average quantities and the capture time constant τ_0 by an effective relaxation time τ_{t0}, containing the relaxation times between high and low mobility states (see definition (17)). In the present treatment, both the total current (j_s) and domain velocity (u_0) are expressed with quantities taken at the peak field (neutrality point). All calculations were carried out without assuming the time constants τ_{1t} and τ_{2t} to be equal. This point seems to be important,

because both the current and domain velocity will vary with a change in the parameter ξ. From this a possible determination method for ξ follows by measuring the peakfield dependence of total current and domain velocity. However, at least two effects have to be taken into account: the field dependence of v_{a0} and τ_{t0} (since v_{a0} saturates only if $E_0 > 3E_c$). By comparing the theoretical and experimental results we are trying to identify the observed domain velocity with the drift mode. Experimental studies have dealt with semi-insulating GaAs of different electron concentrations, namely $n_0 \approx 10^7 \text{cm}^{-3}$[5] and $n_0 \approx 10^{11} \text{cm}^{-3}$ [6]. In the former case, $\alpha_g \alpha_M \ll 1$ and the domain velocity is approximately $u_0 \approx -v_{a0}\alpha_g$. With a proper, but not unrealistic, choice of the parameter ξ the domain velocity will be close to the observed value: $|u_0| \approx 0.1$ cm/sec. At higher electron concentrations we have some difficulties, because the present theory is applicable only if $n_0 \ll n_{t0}, p_{t0}$. In fact, for $n_0 = 10^{11} \text{cm}^{-3}$; $p_{t0}/n_{t0} = 2.8 \cdot 10^{-6}$ and, therefore, a very high trap concentration, $n_{t0} > 10^{17}$ cm^{-3}, is required. If $n_{t0} \approx \varrho_0/e = 10^{17} \text{cm}^{-3}$, then the term $\alpha_g \alpha_M$ will predominate in the denominator of Equ. (36) and, thus, $-u_{0d} \approx v_{a0}\tau_{Ma}/\tau_{t0}$. The observed domain velocity $|u_0| \approx 3 \cdot 10^3$ cm/sec [6] can be obtained only for an extremely small value of τ_{t0} (if $\varrho_0/e = 10^{17}$ cm^{-3}, $\tau_{Ma} = 5.6 \cdot 10^{-13}$ sec, $v_{a0} = 5 \cdot 10^6$ cm/sec, then $\tau_{t0} \approx 10^{-9}$ sec.) It is obvious from the above discussion that for the time being, it cannot be definitely stated that the domains in oxygen doped semi-insulating GaAs are slowly moving Gunn domains. This is all the more true because field dependent trapping was observed in [15] and also slowly moving domains in p-type GaAs have been reported [16].

If the domains are due to an impurity barrier mechanism, say, Cu^- centres in GaAs, with a threshold field well below the threshold for the Gunn effect, then Equs. (29)—(30) can be applied.*

The situation is probably more complicated and both the field dependent trapping and an electron transfer mechanism exist simultaneously. In principle, it is not difficult to extend the present method for this case also, but without proper simplifications, calculations will be too complicated.

REFERENCES

1. B. K. Ridley and R. G. Pratt, J. Phys. Chem. Solids, **26,** 21, 1965.
2. I. A. Kurova and M. Vrana, F. T. P., **1,** 1095, 1967.
3. B. K. Ridley, Brit. Journ. Appl. Phys., **17,** 595, 1966.
4. A. Barraud, C. R. Acad. Sci. Paris, **256,** 3632, 1962.
5. D. C. Northrop, P. R. Thornton and K. E. Trezise, Solid State Electr., **7,** 17, 1964.
6. Y. Tokumaru and M. Kikuchi, Japan. J. Appl. Phys., **6,** 654, 1967, and also **7,** 95, 1968.
7. R. Williams, J. Appl. Phys., **37,** 3411, 1966.
8. K. W. Böer and G. A. Dussel, Phys. Rev., **154,** 292, 1967 and also phys. stat. sol., **21,** K145, 1967.
9. G. Pataki, Acta Phys. Hung., **24,** 119, 1968.

* *Note added in proof*: According to the recent paper by Tokumaru [17] this model seems to be convincing although the centres were not identified definitely.

10. G. Pataki, Acta Phys. Hung., **25,** 377, 1968 and Proc. of the 9th Int. Conf. on the Physics of Semiconductors, Moscow, 1968. p. 1001.
11. V. L. Bonch-Bruevich, phys. stat. sol., **22,** 267, 1967.
12. P. N. Butcher, W. Fawcett and N. R. Ogg, Brit. J. Appl. Phys., **18,** 755, 1967.
13. K.-E. Kröll, phys. stat. sol., **24,** 707, 1967.
14. G. Döhler, phys. stat. sol., **24,** 331, 1967.
15. J. S. Heeks, Trans IEEE ED—**13,** 68, 1966.
16. A. P. Kulsreshta and A. E. Yunovich, F. T. T. **8,** 353, 1966.
17. Y. Tokumaru, Japan. J. Appl. Phys., **8,** 76, 1969.

ВЛИЯНИЕ ЛОВУШЕК НА СТАЦИОНАРНО ДВИЖУЩИЕСЯ ДОМЕНЫ В ПОЛУПРОВОДНИКАХ

Г. ПАТАКИ

Резюме

В настоящей статье рассматривается влияние ловушек на скорость (u_0) стационарно движущихся доменов и на польный ток (j_s) в случае рекомбинационной неустойчивости и эффекта Уаткинса—Ганна. Расчёты проведены без линеаризации соответствующих уравнений, пользуясь методом предложенным в [9], для случая без ловушек. Для упрощения расчётов будет предположено: (i) от электрического поля зависят только переходы, ведущиеся к отрицательной дифференциальной проводимости; (ii) времена переходов между состояниями с большой и малой подвижностью являются более короткими чем другие характеристические времена проблемы; (iii) подвижности и коэффициенты диффузии не зависят от электрического поля; (iv) концентрация электронов в зоне гораздо меньше концентрации пустых и запольненных центров.

Более подробно рассмотрено влияние ловушек на эффект Уаткинса—Ганна. Получены выражения для возможных скоростей ганновских доменов при наличии ловушек. В отличии от случая без ловушек скорость оказывается чувствительной к форме домена. Обсуждена, в случае квадратичных доменов, зависимость скоростей различных мод от максимального значения поля в домене.

Простой анализ показывает, что вопрос о применимости принятой модели к медленно движущимся доменам в полуизолирующем GaAs нельзя однозначно решать без знания времени перехода электронов из состояний с малой подвижностью в ловушки.

Acta Physica Academiae Scientiarum Hungaricae, Tomus 27, pp. 435—439 (1969)

INTEGRATION OF THE DYNAMICAL SYMMETRY GROUPS FOR THE $-1/r$ POTENTIAL*

By

G. GYÖRGYI

CENTRAL RESEARCH INSTITUTE FOR PHYSICS OF THE HUNGARIAN ACADEMY OF SCIENCES, BUDAPEST

(Received 20. II. 1969)

Finite dynamical symmetry transformations of the Kepler motion are given in closed analytic form.

In recent years there has been considerable interest in the problem of dynamical groups in Classical and Quantum Mechanics. For the classical one particle problem in a $-1/r$ potential, characterized by the energy function (Hamiltonian)

$$E = \frac{p^2}{2m} - \frac{g}{r}, \tag{1}$$

two well-known vectorial constants of motion exist (see e.g., [1]): the angular momentum

$$\mathbf{L} = \mathbf{r} \times \mathbf{p}, \tag{2}$$

and the Laplace—Lenz—Runge vector

$$\mathbf{A} = \frac{mg}{p_0}\left(\frac{\mathbf{r}}{r} - \frac{\mathbf{p}\times\mathbf{L}}{mg}\right), \tag{3}$$

where

$$p_0 = \sqrt{2m|E|}. \tag{4}$$

The Poisson bracket relations of **L** and **A** coincide with the defining relations of the SO(4) and SO(3,1) Lie algebras for negative and positive energies, respectively. Higher Lie algebras can also be constructed out of the primitive dynamical variables. The pioneering work in this direction has been done by BACRY [2]. One finds (see also [3]) that the quantities

$$\mathbf{B} = r\mathbf{p}\begin{Bmatrix}\cos\\ \mathrm{ch}\end{Bmatrix}\frac{p_0(\mathbf{pr})}{mg} + \frac{mg}{p_0}\left[\frac{\mathbf{r}}{r} - \frac{(\mathbf{rp})\,\mathbf{p}}{mg}\right]\begin{Bmatrix}\sin\\ \mathrm{sh}\end{Bmatrix}\frac{p_0(\mathbf{pr})}{mg}, \tag{5a}$$

$$S = \frac{mg}{p_0}\left(1 - \frac{rp^2}{mg}\right)\begin{Bmatrix}\cos\\ \mathrm{ch}\end{Bmatrix}\frac{p_0(\mathbf{pr})}{mg} \mp \mathbf{rp}\begin{Bmatrix}\sin\\ \mathrm{sh}\end{Bmatrix}\frac{p_0(\mathbf{pr})}{mg}, \tag{5b}$$

* Dedicated to Prof. P. GOMBÁS on his 60th birthday.

as well as **L** and **A**, obey the bracket relations of the SO(4,1) and SO(3,2) Lie algebras for negative and positive energies, respectively. Further,

$$\mathbf{C} = \pm \frac{mg}{p_0}\left[\frac{\mathbf{r}}{r} - \frac{(\mathbf{rp})\,\mathbf{p}}{mg}\right]\begin{Bmatrix}\cos\\ \mathrm{ch}\end{Bmatrix}\frac{p_0(\mathbf{pr})}{mg} - r\mathbf{p}\begin{Bmatrix}\sin\\ \mathrm{sh}\end{Bmatrix}\frac{p_0(\mathbf{pr})}{mg}, \tag{6a}$$

$$T = -r\mathbf{p}\begin{Bmatrix}\cos\\ \mathrm{ch}\end{Bmatrix}\frac{p_0(\mathbf{pr})}{mg} - \frac{mg}{p_0}\left(1 - \frac{rp^2}{mg}\right)\begin{Bmatrix}\sin\\ \mathrm{sh}\end{Bmatrix}\frac{p_0(\mathbf{pr})}{mg}, \tag{6b}$$

together with **L** and **A**, obey the bracket relations of the SO(4,1) algebra for both negative and positive energies. In (5) and (6) the trigonometric functions should be taken for bound states, and the hyperbolic functions for positive energy. (The upper and lower signs refer to negative and positive energies, respectively.) Finally, one finds that **L**, **A**, **B**, S **C** and T, taken together with the new quantity

$$M = \pm\sqrt{\mp\frac{mg^2}{2E}}, \tag{7}$$

satisfy the Poisson bracket relations of the Lie algebra of the SO(4,2) group, again for both positive and negative energies [3].

The three-dimensional finite rotations generated by the angular momentum vector **L** can be immediately obtained by integration. As to the finite transformations of the dynamical variables **r** and **p** generated by the Laplace—Lenz—Runge vector **A**, it has been pointed out in [4] that these transformations are non-linear and cannot be given in explicit analytic form. In [5] it has been proved that the transformations generated by the angular momentum and the Laplace—Lenz—Runge vector **A** form, indeed, a group of canonical transformations. The finite group elements have been obtained by integration, and the global structure of this dynamical (invariance) symmetry group has been clarified; the group is isomorphic to the four-dimensional rotation group SO(4).

In what follows the dynamical invariance and non-invariance symmetry transformations will be treated in a unified and general manner. The use of the BACRY variables [3] as the basic quantities makes it possible to obtain explicit transformation formulae. Introduce the four-dimensional notation

$$B_\alpha\left[\mathbf{B}, (\pm)^{-1/2}\,S\right],\quad C_\alpha\left[\mathbf{C}, (\pm)^{-1/2}\,T\right]$$

for the quantities (5) and (6). The BACRY variables may be defined as

$$b_\alpha = \pm\, mgM^{-2}\,B_\alpha, \qquad c_\alpha = \pm\,(mg)^{-1}\,MC_\alpha; \tag{8}$$

they can be used equivalently instead of the original **r**, **p** position and momentum variables. Thus, the transformation formulae for these basic variables b_α, c_α are determined by those valid for B_α, C_α and M.

The three-dimensional rotations generated by the angular momentum vector will not be considered. For an infinitesimal canonical transformation generated by the Laplace—Lenz—Runge vector one has

$$\left.\begin{aligned}
\delta\mathbf{B} &= (\mathbf{B}, \mathbf{A}\delta\boldsymbol{\alpha}) = -S\delta\boldsymbol{\alpha}\,,\\
\delta S &= (S, \mathbf{A}\delta\boldsymbol{\alpha}) = \pm\mathbf{B}\delta\boldsymbol{\alpha}\,,\\
\delta\mathbf{C} &= (\mathbf{C}, \mathbf{A}\delta\boldsymbol{\alpha}) = -T\delta\boldsymbol{\alpha}\,,\\
\delta T &= (T, \mathbf{A}\delta\boldsymbol{\alpha}) = \pm\mathbf{C}\delta\boldsymbol{\alpha}\,,\\
\delta M &= (M, \mathbf{A}\delta\boldsymbol{\alpha}) = 0\,.
\end{aligned}\right\} \tag{9}$$

Further, for the infinitesimal canonical transformations generated by the quantities $\mathbf{B}$, S, $\mathbf{C}$ and T the following formulae hold:

$$\left.\begin{aligned}
\delta\mathbf{L} &= (\mathbf{L}, \mathbf{B}\delta\boldsymbol{\beta}) = -\mathbf{B}\times\delta\boldsymbol{\beta}\,,\\
\delta\mathbf{A} &= (\mathbf{A}, \mathbf{B}\delta\boldsymbol{\beta}) = S\delta\boldsymbol{\beta}\,,\\
\delta\mathbf{B} &= (\mathbf{B}, \mathbf{B}\delta\boldsymbol{\beta}) = \mathbf{L}\times\delta\boldsymbol{\beta}\,,\\
\delta S &= (S, \mathbf{B}\delta\boldsymbol{\beta}) = \mathbf{A}\delta\boldsymbol{\beta}\,,\\
\delta\mathbf{C} &= (\mathbf{C}, \mathbf{B}\delta\boldsymbol{\beta}) = M\delta\boldsymbol{\beta}\,,\\
\delta T &= (T, \mathbf{B}\delta\boldsymbol{\beta}) = 0\,,\\
\delta M &= (M, \mathbf{B}\delta\boldsymbol{\beta}) = \mathbf{C}\delta\boldsymbol{\beta}\,;
\end{aligned}\right\} \tag{10}$$

$$\left.\begin{aligned}
\delta\mathbf{L} &= (\mathbf{L}, S\delta\sigma) = 0\,,\\
\delta\mathbf{A} &= (\mathbf{A}, S\delta\sigma) = \mp\mathbf{B}\delta\sigma\,,\\
\delta\mathbf{B} &= (\mathbf{B}, S\delta\sigma) = -\mathbf{A}\delta\sigma\,,\\
\delta S &= (S, S\delta\sigma) = 0\,,\\
\delta\mathbf{C} &= (\mathbf{C}, S\delta\sigma) = 0\,,\\
\delta T &= (T, S\delta\sigma) = \pm M\delta\sigma\,,\\
\delta M &= (M, T\delta\sigma) = T\delta\sigma\,;
\end{aligned}\right\} \tag{11}$$

$$\left.\begin{aligned}
\delta\mathbf{L} &= (\mathbf{L}, \mathbf{C}\delta\boldsymbol{\gamma}) = -\mathbf{C}\times\delta\boldsymbol{\gamma}\,,\\
\delta\mathbf{A} &= (\mathbf{A}. \mathbf{C}\delta\boldsymbol{\gamma}) = T\delta\boldsymbol{\gamma}\,,\\
\delta\mathbf{B} &= (\mathbf{B}, \mathbf{C}\delta\boldsymbol{\gamma}) = -M\delta\boldsymbol{\gamma}\,,\\
\delta S &= (S, \mathbf{C}\delta\boldsymbol{\gamma}) = 0\,,\\
\delta\mathbf{C} &= (\mathbf{C}, \mathbf{C}\delta\boldsymbol{\gamma}) = \pm\mathbf{L}\times\delta\boldsymbol{\gamma}\,,\\
\delta T &= (T, \mathbf{C}\delta\boldsymbol{\gamma}) = \pm\mathbf{A}\delta\boldsymbol{\gamma}\,,\\
\delta M &= (M, \mathbf{C}\delta\boldsymbol{\gamma}) = \mp\mathbf{B}\delta\boldsymbol{\gamma}\,;
\end{aligned}\right\} \tag{12}$$

$$\left.\begin{aligned}
\delta\mathbf{L} &= (\mathbf{L}, T\delta\tau) = 0\,,\\
\delta\mathbf{A} &= (\mathbf{A}, T\delta\tau) = \mp\mathbf{C}\delta\tau\,,\\
\delta\mathbf{B} &= (\mathbf{B}, T\delta\tau) = 0\,,\\
\delta S &= (S, T\delta\tau) = \mp M\delta\tau\,,\\
\delta\mathbf{C} &= (\mathbf{C}, T\delta\tau) = \mp\mathbf{A}\delta\tau\,,\\
\delta T &= (T, T\delta\tau) = 0\,,\\
\delta M &= (M, T\delta\tau) = \mp S\delta\tau\,.
\end{aligned}\right\} \tag{13}$$

The integration can be easily carried out. From (9) one obtains

$$\left.\begin{aligned}
\mathbf{B}' &= \mathbf{B} - (\mathbf{Bn})\,\mathbf{n} + (\mathbf{Bn})\,\mathbf{n}\begin{Bmatrix}\cos\\ \mathrm{ch}\end{Bmatrix}\alpha - S\mathbf{n}\begin{Bmatrix}\sin\\ \mathrm{sh}\end{Bmatrix}\alpha,\\
S' &= S\begin{Bmatrix}\cos\\ \mathrm{ch}\end{Bmatrix}\alpha \pm \mathbf{Bn}\begin{Bmatrix}\sin\\ \mathrm{sh}\end{Bmatrix}\alpha,\\
\mathbf{C}' &= \mathbf{C} - (\mathbf{Cn})\,\mathbf{n} + (\mathbf{Cn})\,\mathbf{n}\begin{Bmatrix}\cos\\ \mathrm{ch}\end{Bmatrix}\alpha - T\mathbf{n}\begin{Bmatrix}\sin\\ \mathrm{sh}\end{Bmatrix}\alpha,\\
T' &= T\begin{Bmatrix}\cos\\ \mathrm{ch}\end{Bmatrix}\alpha \pm \mathbf{Cn}\begin{Bmatrix}\sin\\ \mathrm{sh}\end{Bmatrix}\alpha,\\
M' &= M
\end{aligned}\right\} \tag{14}$$

($\alpha = |\boldsymbol{\alpha}|$, $\mathbf{n} = \boldsymbol{\alpha}/\alpha$); from (10) one has

$$\left.\begin{aligned}
\mathbf{L}' &= (\mathbf{Ln})\,\mathbf{n} + [\mathbf{L} - (\mathbf{Ln})\,\mathbf{n}]\,\mathrm{ch}\,\beta - \mathbf{B}\times\mathbf{n}\,\mathrm{sh}\,\mathbf{B},\\
\mathbf{B}' &= (\mathbf{Bn})\,\mathbf{n} + [\mathbf{B} - (\mathbf{Bn})\,\mathbf{n}]\,\mathrm{ch}\,\beta + \mathbf{L}\times\mathbf{n}\,\mathrm{sh}\,\beta,\\
\mathbf{A}' &= \mathbf{A} - (\mathbf{An})\,\mathbf{n} + (\mathbf{An})\mathbf{n}\,\mathrm{ch}\,\beta + S\mathbf{n}\,\mathrm{sh}\,\beta,\\
S' &= S\,\mathrm{ch}\,\beta + \mathbf{An}\,\mathrm{sh}\,\beta,\\
\mathbf{C}' &= \mathbf{C} - (\mathbf{Cn})\,\mathbf{n} + (\mathbf{Cn})\,\mathbf{n}\,\mathrm{ch}\,\beta + M\mathbf{n}\,\mathrm{sh}\,\beta,\\
T' &= T,\\
M' &= M\,\mathrm{ch}\,\beta + \mathbf{Cn}\,\mathrm{sh}\,\beta
\end{aligned}\right\} \tag{15}$$

($\beta = |\boldsymbol{\beta}|$, $\mathbf{n} = \boldsymbol{\beta}/\beta$); from (11) one gets

$$\left.\begin{aligned}
\mathbf{L}' &= \mathbf{L},\\
\mathbf{A}' &= \mathbf{A}\begin{Bmatrix}\mathrm{ch}\\ \cos\end{Bmatrix}\sigma \mp \mathbf{B}\begin{Bmatrix}\mathrm{sh}\\ \sin\end{Bmatrix}\sigma,\\
\mathbf{B}' &= \mathbf{B}\begin{Bmatrix}\mathrm{ch}\\ \cos\end{Bmatrix}\sigma - \mathbf{A}\begin{Bmatrix}\mathrm{sh}\\ \sin\end{Bmatrix}\sigma,\\
S' &= S,\\
\mathbf{C}' &= \mathbf{C},\\
T' &= T\begin{Bmatrix}\mathrm{ch}\\ \cos\end{Bmatrix}\sigma + M\begin{Bmatrix}\mathrm{sh}\\ \sin\end{Bmatrix}\sigma,\\
M' &= M\begin{Bmatrix}\mathrm{ch}\\ \cos\end{Bmatrix}\sigma \pm T\begin{Bmatrix}\mathrm{sh}\\ \sin\end{Bmatrix}\sigma;
\end{aligned}\right\} \tag{16}$$

from (12) one has

$$\left.\begin{aligned}
\mathbf{L}' &= (\mathbf{Ln})\,\mathbf{n} + [\mathbf{L} - (\mathbf{Ln})\,\mathbf{n}] \begin{Bmatrix} \mathrm{ch} \\ \cos \end{Bmatrix} \gamma - \mathbf{C} \times \mathbf{n} \begin{Bmatrix} \mathrm{sh} \\ \sin \end{Bmatrix} \gamma , \\
\mathbf{A}' &= \mathbf{A} - (\mathbf{An})\,\mathbf{n} + (\mathbf{An})\,\mathbf{n} \begin{Bmatrix} \mathrm{ch} \\ \cos \end{Bmatrix} \gamma + T \begin{Bmatrix} \mathrm{sh} \\ \sin \end{Bmatrix} \gamma , \\
\mathbf{B}' &= \mathbf{B} - (\mathbf{Bn})\,\mathbf{n} + (\mathbf{Bn})\,\mathbf{n} \begin{Bmatrix} \mathrm{ch} \\ \cos \end{Bmatrix} \gamma - M\mathbf{n} \begin{Bmatrix} \mathrm{sh} \\ \sin \end{Bmatrix} \gamma , \\
S' &= S , \\
\mathbf{C}' &= (\mathbf{Cn})\,\mathbf{n} + [\mathbf{C} - (\mathbf{Cn})\,\mathbf{n}] \begin{Bmatrix} \mathrm{ch} \\ \cos \end{Bmatrix} \gamma \pm \mathbf{L} \times \mathbf{n} \begin{Bmatrix} \mathrm{sh} \\ \sin \end{Bmatrix} \gamma , \\
T' &= T \begin{Bmatrix} \mathrm{ch} \\ \cos \end{Bmatrix} \gamma \pm \mathbf{An} \begin{Bmatrix} \mathrm{sh} \\ \sin \end{Bmatrix} \gamma , \\
M' &= M \begin{Bmatrix} \mathrm{ch} \\ \cos \end{Bmatrix} \gamma \mp \mathbf{Bn} \begin{Bmatrix} \mathrm{sh} \\ \sin \end{Bmatrix} \gamma
\end{aligned}\right\} \tag{17}$$

($\gamma = |\boldsymbol{\gamma}|$, $\mathbf{n} = \boldsymbol{\gamma}/\gamma$); finally, from (13) it follows that

$$\left.\begin{aligned}
\mathbf{L}' &= \mathbf{L} , \\
\mathbf{A}' &= \mathbf{A}\,\mathrm{ch}\,\tau \mp \mathbf{C}\,\mathrm{sh}\,\tau , \\
\mathbf{B}' &= \mathbf{B} , \\
S' &= S\,\mathrm{ch}\,\tau \mp M\,\mathrm{sh}\,\tau , \\
\mathbf{C}' &= \mathbf{C}\,\mathrm{ch}\,\tau \mp \mathbf{A}\,\mathrm{sh}\,\tau , \\
T' &= T \\
M' &= M\,\mathrm{ch}\,\tau \mp S\,\mathrm{sh}\,\tau .
\end{aligned}\right\} \tag{18}$$

This completes the integration of the SO(4,2) full dynamical symmetry group for the classical Kepler problem. The transformation formulae (14)—(18) determine the analytic form of the transformation laws for the primitive dynamical variables b_α, c_α or $\mathbf{r}$, $\mathbf{p}$; though, the formulae cannot be solved explicitly for $\mathbf{r}'$ and $\mathbf{p}'$.

REFERENCES

1. L. D. Landau and E. M. Lifshitz: Mechanics, Oxford, 1960, p. 39.
2. H. Bacry, Nuovo Cimento, **41**, A, 222, 1966.
3. G. Györgyi, Nuovo Cimento, **53** A, 717, 1968.
4. R. U. Sexl, Acta Phys. Austriaca, **22**, 161, 1965.
5. H. Bacry, H. Ruegg and J.-M. Souriau, Commun. math. Phys., **3**, 323, 1966.

ИНТЕГРИРОВАНИЕ ДИНАМИЧЕСКИХ ГРУПП СИММЕТРИИ ДЛЯ ПОТЕНЦИАЛА — $1/r$

Г. ДЬЁРДИ

Р е з ю м е

В закрытой аналитической форме даются конечные динамические преобразования симметрии движения Кеплера.

Acta Physica Academiae Scientiarum Hungaricae, Tomus 27, pp. 441—448 (1969)

NEW FOUNDATIONS FOR THE THOMAS–FERMI MODEL*

By

R. GÁSPÁR

INSTITUTE OF THEORETICAL PHYSICS, KOSSUTH LAJOS UNIVERSITY, DEBRECEN 10

and

RESEARCH GROUP FOR THEORETICAL PHYSICS, HUNGARIAN ACADEMY OF SCIENCES, BUDAPEST

(Received 20. II. 1969)

It is demonstrated that the atomic model, in which the zero order approximations to the one electron orbitals are hydrogen like orbitals, always leads to a model which imitates very closely the Thomas—Fermi model of the statistical theory of the atoms.

The Schrödinger equation and zero order solutions

For an atom with atomic number Z the Hamiltonian has the form [1]

$$\begin{aligned}\mathbf{H} &= -\frac{\hbar^2}{2m}\sum_{i=1}^{Z}\Delta_i - Z\sum_{i=1}^{Z}\frac{e^2}{r_i} + \sum_{j>i=1}^{\cdot\cdot}\frac{e^2}{r_{ij}} = \\ &= Z^2\left\{-\frac{\hbar^2}{2m}\sum_{i=1}\Delta_{\varrho_i} - \sum_{i=1}^{Z}\frac{e^2}{\varrho_i} + \frac{1}{Z}\sum_{j>i=1}^{\cdot\cdot}\frac{e^2}{\varrho_{ij}}\right\} = Z^2\,\mathbf{H}_\varrho\,,\end{aligned} \tag{1}$$

where we have introduced the scaled coordinates with the relation [1]

$$\boldsymbol{\varrho} = \mathbf{r}Z\,. \tag{2}$$

The Schrödinger equation

$$\mathbf{H}\Psi = E\Psi \tag{3}$$

has perturbation solution with the energy

$$\frac{E}{Z^2} = W_2 + W_1\frac{1}{Z} + W_0\frac{1}{Z^2} + 0\left(\frac{1}{Z^3}\right) \tag{4}$$

in which

$$W_2 = -\frac{1}{2}\sum_{\alpha=1}^{k} q_\alpha\frac{1}{n_\alpha^2}\frac{e^2}{a_0} \tag{5}$$

* Dedicated to Prof. P. GOMBÁS on his 60th birthday.

is the sum of the hydrogenic energy terms. a_0 is the first Bohr radius in the hydrogen atom and e^2/a_0 is the atomic unit of the energy 27.23 eV; q_α is the occupation number of the states, with principal quantum number n_α. W_1 is determined by the electrostatic interaction matrix. For closed shells the occupation numbers are

$$q_\alpha = 2\, n_\alpha^2 \tag{6}$$

and the total number of electrons is

$$Z = \sum_{\alpha=1}^{k} q_\alpha = 2 \sum_{\alpha=1}^{k} n_\alpha^2 = 2\, \frac{k\,(k+1)\,(2k+1)}{6} = \frac{2}{3}\left(k+\frac{1}{2}\right)^3 - \frac{1}{6}\,k - \frac{1}{12}\,, \tag{7}$$

so that approximately

$$k = -\frac{1}{2} + \left(\frac{3}{2}\right)^{1/3} Z^{1/3}. \tag{8}$$

By inserting (6) and (8) into (5) we get

$$W_1 = \frac{1}{2} - \left(\frac{3}{2}\right)^{1/3} Z^{1/3} \tag{9}$$

which is the zeroth order approximation to E/Z^2. By investigating the case for non closed shells it turns out that equation (9) represents W_2 for non closed shells to a good approximation also.

Energy theorems

Because of the Coulomb forces in the Hamiltonian (1) the virial theorem

$$E = -\,E_k = \frac{1}{2}\,(E_p^n + E_p^e) \tag{10}$$

is valid, where we have introduced the kinetic energy E_k, the electron—nucleus interaction energy E_p^n and the electron—electron interaction energy E_p^e which add up to the total energy

$$E = E_k + E_p^n + E_p^e \tag{11}$$

with the explicit expressions as follows

$$E_p^n = -\,Ze^2 \int \frac{\varrho(\mathbf{r})}{r}\, dv\,, \tag{12}$$

$$E_k = -\,\frac{\hbar^2}{2m} \sum_{i=1}^{Z} \langle \Psi | \Delta_i | \Psi \rangle\,, \tag{13}$$

$$E_p^e = \frac{1}{2}\, e^2 \int \frac{\varrho(\mathbf{r})\varrho(\mathbf{r}')}{|\mathbf{r}-\mathbf{r}'|}\, dv\, dv'. \tag{14}$$

In a previous paper [2] we have made use of the Hellmann–Feynman theorem stating

$$\frac{\partial E}{\partial Z} = \frac{1}{Z} E_p^n \tag{15}$$

and a combination of this theorem with the virial theorem gave us for neutral atoms

$$\frac{E_p^e}{E} = -Z \frac{d}{dZ} \left\{ \log \left(\frac{-E}{Z^2} \right) \right\}_{N=Z} . \tag{16}$$

By introducing $-W_2$ i.e. the zeroth order approximation for $-E/Z^2$ we get after some manipulation

$$\frac{E_p^e}{E} = -\frac{1}{3} - \frac{1}{6\left(\frac{3}{2}\right)^{1/3}} \frac{1}{Z^{4/3}} . \tag{17}$$

The second term in (17) is negligible for greater atomic numbers and we may use

$$\frac{E_p^e}{E} = -\frac{1}{3} \tag{18}$$

as a first approximation. (18) shows us that dependence of E_p^e and E and consequently that of E_p^n on the atomic number is expressed by the same power of Z which determines the logarithmic derivative and so the ratio E_p^e/E. Therefore the equation $E_p^e/E = -1/3$ is true with a much higher accuracy. Using the virial theorem, it is easy to demonstrate that this is equivalent to

$$\frac{E_p^n}{E_p^e} = -7 \tag{19}$$

which is a well known theorem of the Thomas–Fermi theory [3].

We are going to make use of relations (18) and (19). By the aid of a scale transformation we get the following relation

$$E(\lambda) = \lambda^2 E_k^0 + \lambda E_p^{n0} + \lambda E_p^{e0} \tag{20}$$

and for the minimum value

$$\lambda_0 = -\frac{E_p^{n0} + E_p^{e0}}{2 E_k^0} \tag{21}$$

and

$$E(\lambda_0) = -\lambda_0^2 E_k^0 . \tag{22}$$

The zeroth order values are

$$E_k^0 = -W_2\,, \tag{23}$$

$$E_p^{n0} = 2W_2 = -2E_k^0 \tag{24}$$

and

$$E_p^{e0} = -\frac{1}{7}E_p^{n0}\,. \tag{25}$$

As a consequence

$$\lambda_0 = \frac{6}{7}$$

and (26a)

$$E(\lambda_0) = \left(\frac{6}{7}\right)^2 W_2 = \frac{18}{49}Z^2 - \frac{36}{49}\left(\frac{3}{2}\right)^{1/3} Z^{7/3}\,,$$

or because the first term is much smaller than the second we get by an averaging process

$$E(\lambda_0)_a = -0.712\,866\,Z^{7/3}\,. \tag{26b}$$

Scaling and invariance

In this Section we investigate the consequences of the above results. We introduce a scaling of the coordinates and the charge density by the following relations

$$\mathbf{r} = Z^a\mathbf{r}' \quad \text{and} \quad \varrho = Z^b\varrho'\,. \tag{27}$$

The primed quantities in the above and following equations denote scaled quantities.

Equations (27) lead us to a scaling of the energy and the normalization condition in the following manner. By introducing the scaled quantities according to (27) into (13) and (14) we get

$$E_p^n = Z^{1+b+2a}E_p^{n'} \tag{28}$$

and

$$E_p^e = Z^{2b+5a}E_p^{e'}\,. \tag{29}$$

The normalization condition for the charge density turns out to be

$$-Ze = -e\int \varrho\,dv = Z^{b+3a}(-e)\int \varrho'\,dv' \tag{30}$$

for neutral atoms i.e. $N = Z$. If

$$b + 3a = 1 \tag{31}$$

the normalization condition

$$\int \varrho' \, dv' = 1 \tag{32}$$

is independent of the atomic number.

We may observe that because of equation (31) we get

$$c = 1 + b + 2\,a = 2\,b + 5\,a \tag{33}$$

for any value of a and the corresponding value of b.

Because of the virial theorem there is a scaling of the kinetic energy too

$$E_k = Z^c \, E_k' \,. \tag{34}$$

The total energy has the following form

$$E = E_k + E_p^n + E_p^e = Z^c \, E', \tag{35}$$

where E' is a slowly varying function of Z. By comparing (26b) and (35) we get for the exponent the value

$$c = \frac{7}{3}, \tag{36}$$

and using this value of c in (33), combining it with (31) and solving the system of linear equations we get the constants

$$a = -\frac{1}{3} \quad \text{and} \quad b = 2. \tag{37}$$

These constants have the values well known for the scaling exponents in the Thomas–Fermi theory.

Let us make the further assumption that

$$E_k = \int \varepsilon_k(\varrho) \, dv, \tag{38}$$

i.e. the kinetic energy is expressible as a function of the particle density. If we take an energy density like

$$\varepsilon_k(\varrho) = \varkappa \varrho^{\lambda} \,, \tag{39}$$

which is the simplest possible form, we get

$$\lambda = \frac{5}{3} \tag{40}$$

if we take the scaling and (34) with the proper value of the constant c. We leave the determination of the constant $\varkappa$ to a later discussion.

The Thomas—Fermi equation

According to (35), (34), (13) and (14) the total energy of the atom may be written in the following form

$$E = \varkappa \int \varrho^{5/3}\, dv - Ze^2 \int \frac{\varrho(\mathbf{r})}{|\mathbf{r}-\mathbf{r}|}\, dv' + \frac{1}{2}\, e^2 \iint \frac{\varrho(\mathbf{r})\,\varrho(\mathbf{r}')}{|\mathbf{r}-\mathbf{r}'|}\, dv\, dv'.$$

By the aid of an argument similar to that given by GOMBÁS in his famous book [3] we get the Thomas—Fermi expression

$$\varrho = \sigma_0 (V - V_0)^{3/2}, \qquad \sigma_0 = \left(\frac{3e}{5\varkappa}\right)^{3/2} \tag{41}$$

and combining this with Poisson's equation we obtain the Thomas—Fermi equation

$$\Delta (V - V_0) = 4\pi\sigma_0\, e (V - V_0)^{3/2} \tag{42}$$

and the scaled form of this is

$$\varphi'' = \frac{\varphi^{3/2}}{x^{1/2}} \tag{43}$$

with exactly the same boundary conditions that may be found in GOMBÁS's book. We shall not repeat them here. The solution of the scaled equation (43) is the same and has been tabulated in the article [4].

In (43)

$$x = \frac{r}{\mu} \tag{44}$$

with

$$\mu = \frac{1}{(4\pi\sigma_0)^{3/2}\, eZ^{1/3}}, \tag{45}$$

and

$$\varphi(x) = \frac{r}{Ze}\,(V - V_0). \tag{46}$$

In all the above expressions $\varkappa$ is a yet undetermined constant. It is interesting that without this constant it is possible to get an equation for the determination of φ, i.e. the potential field. This is a consequence of the inhomogeneity of equations (42) and (43).

The final determination of this parameter may be achieved by the aid of the energy expression (26b) and the virial theorem. By inserting ϱ from (41) into (38) with (39) and taking into account (46), (45) and (44) we get the following expression

$$\varkappa = \frac{9}{35}(4\pi)^{2/3}\,\frac{\varphi'(0)}{-0.712\,866}\,e^2 a_0 = 3.0963\,e^2 a_0\,. \tag{47}$$

Discussion

The consequences of the change in the value of the parameter $\varkappa$ as compared to that for the free electron value

$$\varkappa_k = \frac{3}{10}(3\pi^2)^{2/3}\,e^2 a_0 = 2.871\,e^2 a_0$$

may be summarized as follows. Because μ is proportional to $\varkappa$, the density distribution gets looser giving a smaller magnitude for the potential energy of the atom and consequently reducing the average kinetic energy too. These energy reductions result in a reduction of the total energy which is very much welcome, but the reduction is not enough to get near to the experimental total energy. Naturally many of the shortcomings of the original Thomas–Fermi density distributions remain incorporated also in this model.

The main aim of this paper has been achieved, however, because we have demonstrated that we can get a model starting from the true zero-order solutions of the atomic problem, which has the main features of the original Thomas—Fermi theory without mentioning plane waves and statistics at all.

Now we are in a position to reinterpret our results in the following manner. The kinetic energy density function $\varepsilon(\varrho) = \varkappa\varrho^{5/3}$ with $\varkappa = \varkappa_k$ is a characteristic function of free electrons with mass m_0. According to the above theory a neutral atom may be believed to be composed of a nucleus and a cloud of quasi particles that imitate free electrons but with a reduced mass $m = \nu m_0$, where

$$\nu = \frac{\varkappa_k}{\varkappa} = \frac{2.871\,e^2 a_0}{3.0963\,e^2 a_0} = 0.9272\,.$$

It is interesting to note that a much better agreement for the energy of atoms may be achieved if we suppose semiempirically that the effective mass of the quasi electrons is

$$m' = \nu' m_0 \quad \text{with} \quad \nu' = \frac{2.871\,e^2 a_0}{3.51997\,e^2 a_0} = 0.8156\,.$$

LITERATURE

1. See e. g. D. LAYZER, Ann. Phys. (N. Y.) **8**, 271, 1959.
2. R. GÁSPÁR, Int. J. Quantum Chemistry, **1**, 139, 1967.
3. P. GOMBÁS: Die statistische Theorie des Atoms und ihre Anwendungen, Springer-Verlag, Wien, 1949.
4. P. GOMBÁS: Statistische Behandlung des Atoms, S. Flügge's Encyclopaedia of Physics, Bd. 36. p. 127.

НОВЫЕ ОБОСНОВАНИЯ МОДЕЛИ ТОМАСА—ФЕРМИ

Р. ГАШПАР

Р е з ю м е

Демонстрируется, что атомная модель, в которой нулевое приближение одноэлектронных орбиталей есть применение водородоподобных орбиталей, систематически ведет к модели, точно напоминающей модель Томаса—Ферми статистической теории.

Acta Physica Academiae Scientiarum Hungaricae, Tomus 27, pp. 449—466 (1969)

NEGATIVE MAGNETORESISTANCE OF COMPENSATED *n*-TYPE GaAs AT 77°K TEMPERATURE*

By

B. PŐDÖR

RESEARCH INSTITUTE FOR TECHNICAL PHYSICS OF THE HUNGARIAN ACADEMY OF SCIENCES, BUDAPEST

(Received 5. III. 1969)

The magnetoresistance of strongly compensated *n*-type GaAs doped with Cr and O has been measured at 77 °K temperature. The electron concentrations of the samples were between 3.8×10^{17} and 1.6×10^{18} cm^{-3} at room temperature. In low magnetic fields negative magnetoresistance was observed at liquid nitrogen temperature. The characteristics of this anomalous negative magnetoresistance were shown to be very similar to those observed at liquid He temperatures in heavily doped semiconductors. In weak fields the negative magnetoresistance was proportional to the square of the magnetic field, and showed saturation in the magnetic field range of 4000—6000 G. To account for the observed effects it was postulated that metal-like impurity band conduction is the dominant mechanism of the charge carrier transport in our samples. The observed features of the negative magnetoresistance are shown to be consistent with the model of scattering of electrons in the impurity band by localized magnetic moments. For the average value of the localized magnetic moments a value of the order of 2—3 Bohr magneton was deduced from the experimental data. It is shown that the strong compensation may play an important role in the formation of impurity band at 77 °K temperature and above it.

Introduction

Negative magnetoresistance is frequently observed in heavily doped semiconductors at very low (1—10 °K) temperatures. At liquid He temperature (4.2 °K) it was found in various semiconductors, notably in *n*- and *p*-type InSb, in *n*-type Ge doped with As and Sb, in *n*-type GaAs [1], [2], further in *p*-type GaAs and *n*-type CdS [1], in *n*-type Si doped with P, in *p*-type Si doped with B, in Ge doped with Cu, in *n*-type Ge doped with P, in *p*-type GaAs doped with Cd [2], and quite recently in *p*-type CdSb [3].

The existence of negative magnetoresistance in *n*-type GaAs at temperatures below 20—30 °K was established by R. BROOM et al. [4], in 1956. Their crystals were undoped, having room temperature electron concentration of the order of 10^{17} cm^{-3}, but their samples were much more contaminated judging by the comparatively low mobility values measured by them. Negative magnetoresistance of undoped and of S- and Se-doped *n*-type GaAs at very low temperatures was thoroughly investigated by O. V. EMELYANENKO et al. [5]. Their samples had electron concentrations in the range of 3×10^{15}— $2\times$ $\times10^{17}$ cm^{-3}. They have shown that the negative magnetoresistance at 4.2 °K

* Dedicated to Prof. P. GOMBÁS on his 60th birthday.

temperature was most pronounced in the electron concentration range of 10^{16}— 10^{17} cm^{-3}. J. F. Woods and C. Y. Chen have measured negative magnetoresistance in *n*-type GaAs with electron concentrations between 2×10^{15} and 3×10^{18} cm^{-3} at liquid He temperatures, and in Cd-doped *p*-type GaAs with hole concentrations of the order of 10^{17} cm^{-3} [2]. In one of their samples, with an electron concentration of 6×10^{15} cm^{-3}, the negative magnetoresistance turned to be positive above 30 °K temperature. Quite recently L. Halbo and R. J. Sladek have measured the negative magnetoresistance at 4.2 °K temperature in undoped *n*-type GaAs of comparatively high purity [6].

The above mentioned results show that the occurrence of negative magnetoresistance at very low temperatures and at moderate and high doping levels is a common phenomenon in various semiconductors. Its main features are the following.

In low magnetic fields the specific resistivity decreases. This decrease is either quadratic in the magnetic field [1], [5], [6], or approximately linear in it [2]. In certain cases anisotropy consistent with the cubic symmetry is seen in these fields. The decrease of the resistivity becomes less steep as the field is increased, and saturates at a certain magnetic field. Further increase of the magnetic field results in a reversal of this trend, and the resistivity begins to increase. In higher fields magnetoresistance turns to be positive and is proportional to the square of the magnetic field.

With increasing temperature the negative magnetoresistance decreases and at a certain temperature it completely disappears. This temperature is usually of the order of 20—30 °K.

It is supposed that the measured total magnetoresistance at low temperatures is composed of two parts. One of them is the usual positive component proportional to the square of the magnetic field, the other is the anomalous and temperature dependent component, which predominates in the lower fields and saturates at intermediate fields [1].

The appearance of negative magnetoresistance is usually accompanied by a characteristic peak in the Hall coefficient versus temperature curve. The presence of this maximum on the Hall curve, and the fact that the negative magnetoresistance is observed in crystals having high impurity concentrations indicates that this anomalous magnetoresistance is connected with the impurity conduction [1], [2], [5]. At high doping levels impurity conduction is manifested through impurity band conduction, and at lower doping levels through hopping conduction. The transition between them is not sharp [2]. According to O. V. Emelyanenko et al. [5], in highly doped *n*-type GaAs at low temperatures the impurity band conduction is the dominant mechanism of charge transport.

Up to recent times negative magnetoresistance was observed only at very low temperatures, usually below 30—50 °K. Quite recently O. V.

EMELYANENKO et al. [7], observed negative magnetoresistance and impurity conduction in n-type GaAs, compensated with Cu diffusion, up to 200 °K temperatures. At the same time B. S. LISENKER et al. [8], observed impurity band conduction in Fe-doped n-type GaAs in the temperature range of 77—200 °K. Preliminary results of observations of negative magnetoresistance in Cr-doped n-type GaAs at 77 °K temperature were reported by the author of this paper [9].

This negative magnetoresistance, which was observed at liquid nitrogen or higher temperatures only in strongly compensated n-type GaAs [7], [9], is similar to the effect found at very low temperatures. It was suggested by O. V. EMELYANENKO et al. [7] that the negative magnetoresistance at higher temperatures is connected with the impurity conduction, most probably with impurity band conduction.

In this work results of observations of negative magnetoresistance at 77 °K and higher temperatures in compensated, Cr- and O-doped n-type GaAs single crystals are presented. In the second part of this paper sample preparation and measurement methods are described. In the third part the experimental results are presented. In the fourth and last part the results of magnetoresistance measurements are discussed and compared with other results and with the existing theoretical models.

Experimental techniques

n-type GaAs crystals were prepared by the horizontal Bridgman method by E. PAPP and his coworkers at the Research Institute for Metallic Industry, Budapest [10]. According to our observations undoped crystals were of n-type, with an electron concentration of the order of 10^{17} cm^{-3}. Some crystal, were slightly doped either with Cr or with O during the growth process, buf remained of low resistivity with n-type conduction. Stronger doping with Cr produced semi-insulating crystals of high resistivity. For our measurements samples cut out from Cr- and O-doped as well as undoped n-type GaAs crystals of low resistivity were used.

Prism-shaped samples with dimensions of $12 \times 2 \times 0.5$ mm were cut from the crystals. The samples were not oriented. Electrical contacts were made by alloying 0.5 mm diameter In dots to the samples at 450 °C temperature in H_2 atmosphere [11], then 0.1 mm diameter gold wires were connected to them by the help of a micro-soldering pin. Two contacts at the ends of the samples served as current leads, and four, two on each face with dimensions of 12×0.5 mm served as potential probes. The separation between the potential probes was about 5 mm.

While the width and thickness of the samples could be easily determined with high accuracy, the determination of separation between the potential

probes, which is necessary for the evaluation of resistivity, is more uncertain because the contact dimensions are not small in comparison with contact separation, actually the former is about 10 per cent of the latter. Besides, the finite dimensions of contacts cause a distortion of current pattern in the sample resulting in errors in the measurements of the magnetoresistance. The contact separation was taken to be equal to the distance between the centres of contact dots, thus causing a maximum error of about 5 per cent in the determination of the resistivity, and an error of the order of 5—10 per cent in the determination of magnetoresistance.

Conductivity, Hall coefficient, Hall mobility and magnetoresistance were measured by the usual d.c. compensation method at 77° and 300 °K temperatures. On some of our samples these parameters were measured in the function of temperature between 77 °K and 400 °K temperatures. Measurements at 77 °K were made simply by immersing the sample into liquid N_2. Temperatures between 80° and 400 °K were produced in a cryostat, similar to the one described in [12]. The maximum magnetic field was about 8000 G, and it was measured with an estimated accuracy of 2 per cent. Four readings were taken to get each value of the Hall coefficient, properly commuting the sample current and the magnetic field. A similar method was used when measuring the magnetoresistance. The zero-field resistance was measured before the first and after the fourth measurement. In this way the accuracy of the measurements of the magnetoresistance was greatly improved. The potential measuring circuit had a sensitivity of 1—2 μV depending on the resistance of the sample and of the contacts. Magnetoresistances of the order of 5×10^{-5} could be determined without causing inadmissible power dissipation in the sample.

Experimental results

Five samples cut out from four different crystals were measured. One crystal was undoped, two were doped with Cr and the fourth was doped with O. From one of the Cr-doped crystals two samples were cut, from near to both ends of the crystals. The results of Hall and resistivity measurements are summed up in Table I. The geometry of the samples allowed to measure two Hall coefficients and two resistivities on each sample, from these values we could judge the homogeneity of our samples. The differences between the two resistivities measured on each side of the samples did not exceed 10 per cent, and the differences in the measured Hall coefficients did not exceed 10—15 per cent, except samples cut out from crystal No. 178, where they reached 20—30 per cent, showing that these two samples had a considerable inhomogeneity in macroscopic dimensions. Inhomogeneities of the same order were detected by J. F. Woods and C. Y. Chen [2], in some of their samples,

Table I

Sample N°	158/1	176	178/*a*	178/*b*	177
Dopant	—	Cr	Cr	Cr	0
Cond. type	*n*	*n*	*n*	*n*	*n*
R_H cm³/Asec $T = 300$ °K	75.0	10.1	5.3*	16.8*	3.9
μ_H cm²/Vsec T = 300 °K	3860	3700	2200	1800	1930
R_H cm³/Asec $T = 77$ °K	93.0	10.3	5.4*	17.6*	4.0
μ_H cm²/Vsec $T = 77$ °K	3960	3300	1900	1250	1350
n cm^{-3} $T = 300$ °K	8.3×10^{16}	6.2×10^{17}	1.2×10^{18}	3.8×10^{17}	1.6×10^{18}
N_d cm^{-3}	3.5×10^{17}	1.0×10^{18}	2.4×10^{18}	2.3×10^{18}	4.3×10^{18}
N_a cm^{-3}	2.6×10^{17}	0.4×10^{18}	1.2×10^{18}	1.9×10^{18}	2.7×10^{18}
K_n	0.7	0.4	0.5	0.8	0.6

* Averaged values. Measured values showed an inhomogeneity, amounting to 20—30 per cent.

not influencing, however, their measurements of negative magnetoresistance.

The electron concentration as well as the donor and acceptor concentrations can be determined approximately from the room temperature Hall coefficient and the Hall mobility values in the following way. The electron concentration and the Hall coefficient are connected through the equation $n = r/eR_H$, where r is the scattering factor, the value of which was put equal to 1 approximately. The electron concentrations estimated in this way are shown in Table I too.

Taking into account the above mentioned two scattering mechanisms, the measured mobility can be written in the usual approximation as $\mu^{-1} = \mu_I^{-1} + \mu_P^{-1}$, where μ_I and μ_P are the electron mobilities, caused by the two scattering mechanisms separately. The best theoretical value for the mobility caused by the scattering on polar optical phonons is $\mu_P = 9300$ cm²/Vs [13], [14]. This was confirmed by recent mobility measurements too [15]. With the help of this value the mobility caused by the scattering on ionized impurity atoms can be deduced for each sample. This mobility depends only on the electron concentration, the Fermi level and the ionized impurity concentration, and thus with the help of the Brooks—Herring formula (see e.g. [16], [17]) the concentration of ionized impurity atoms can be deduced. Because all impurity atoms are ionized at room temperature this gives the total impurity

concentration. Knowing the electron and impurity concentration, the donor and acceptor concentrations are easily obtained. Table I contains these values too with the compensation degree defined as $K_n = N_a/N_d$. All our samples are considerably compensated, but as we shall see later, the undoped sample did not exhibit negative magnetoresistance. Because of the exceptionally low mobilities measured at 77 °K in samples Nos. 178/a, 178/b and 177 we can presume that the compensation is caused by the presence of the Cr and O impurities, respectively. For sample No. 176 the role of the Cr dopant can be inferred only indirectly, by comparing the magnetoresistance results of the Cr-doped samples.

It is well known that Cr gives rise to a deep acceptor level in GaAs [13], at 0.81 eV below the conduction band edge [18]. Strong Cr doping produces semi-insulating GaAs [13], with room temperature resistivities of the order of 10^8 ohmcm [18]. O-doping also gives rise to high resistivity semi-insulating crystals [13]. As we have mentioned in the second part of this paper, our samples were only slightly doped with Cr and O. Stronger doping with Cr produced high resistivity crystal, with room temperature resistivities of 10^8 ohmcm. We have measured the temperature dependence of resistivity of two such samples over the temperature range of 290°—400 °K and obtained activation energies of 0.825 and 0.81 eV, respectively, which are in good agreement with the activation energy measured by G. A. ALLEN [18]. This fact confirms our arguments concerning the role of Cr impurity in our magnetoresistance samples.

The conductivity and the Hall coefficient in function of the reciprocal temperature for some of our samples is shown in Fig. 1. The Hall mobility versus temperature curves are presented in Fig. 2. The Hall coefficient versus temperature curves for Cr-doped samples Nos. 178/a and 178/b and for O-doped sample No. 177 are horizontal, not showing the characteristic maximum above 77 °K which was observed in Cu-doped n-type GaAs by O. V. EMELYANENKO et al., [7] and in Fe-doped n-type GaAs by B. S. LISENKER et al. [8].

Transversal magnetoresistances measured at room temperature in the undoped, in a Cr-doped and in the O-doped samples are shown in Fig. 3. The measurements were performed with the magnetic field perpendicular to the plane with dimensions of 12×2 mm. In accordance with other experimental results [19], the transversal magnetoresistance had not been changed by rotating the sample by 90° around an axis, parallel to the length of the sample. This agrees with the well-established model of the conduction band of GaAs having a spherical minimum in the middle of the Brillouin zone [13], [14]. It can be seen that the magnetoresistance has a quadratic dependence on the magnetic field, which is a natural consequence of the fact that the measurements were performed in small magnetic field, i.e. $\mu_H B \cong \omega_c \tau \ll 1$, where ω_c is the cyclotron frequency and τ is the relaxation time for electrons.

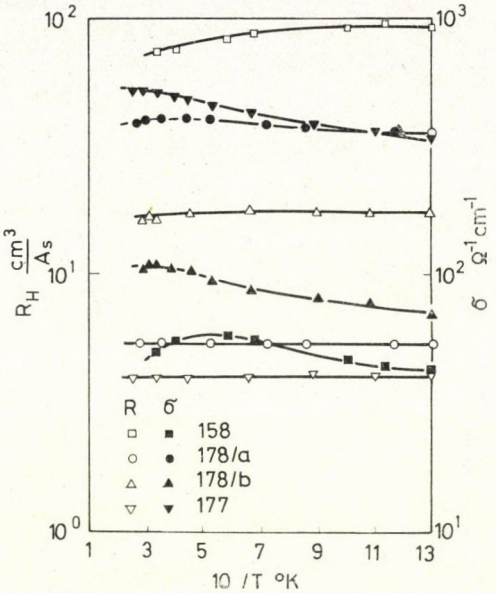

Fig. 1. Conductivity and Hall coefficient vs reciprocal temperature for undoped (No. 158), O-doped (No. 177) and Cr-doped (Nos. 178/a and 178/b) samples

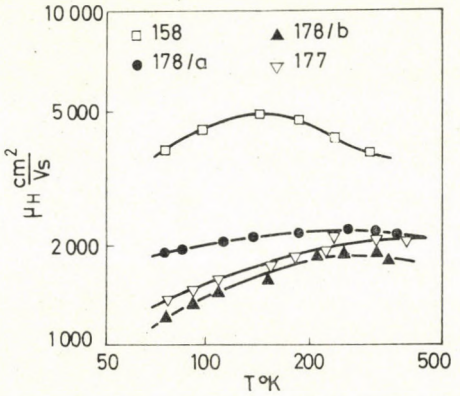

Fig. 2. Hall mobility vs temperature for undoped (No. 158), O-doped (No. 177) and Cr-doped (Nos. 178/a and 178/b) samples

Transversal magnetoresistance measured at 77 °K in the Cr-doped samples are shown in Fig. 4, the same measured on the O-doped and undoped samples are presented in Fig. 5. While the undoped sample exhibits normal positive magnetoresistance with quadratic dependence on the magnetic field, the value of which is in accordance with the prediction based on the assumption that at such low temperatures the scattering by ionized impurities determines the electron mobility as was shown in our earlier work [17], the O- and Cr-doped samples show an anomalous negative magnetoresistance.

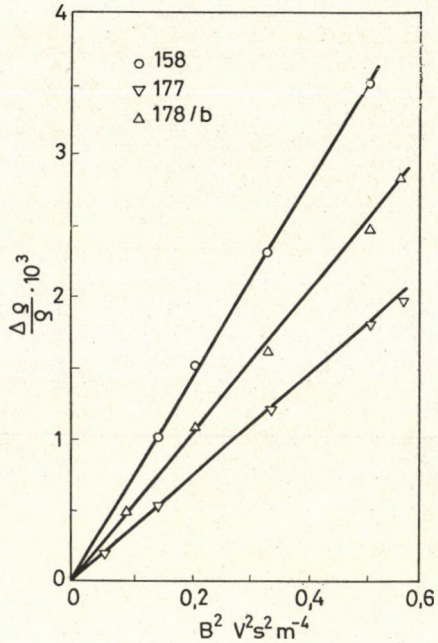

Fig. 3. Magnetoresistance vs square of the magnetic field at room temperature for undoped (No. 158), O-doped (No. 177) and Cr-doped (No. 178/b) samples

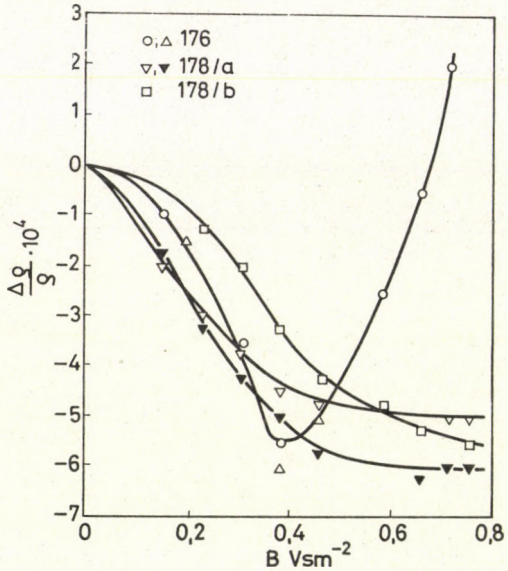

Fig. 4. Magnetoresistance of Cr-doped samples at 77 °K temperature

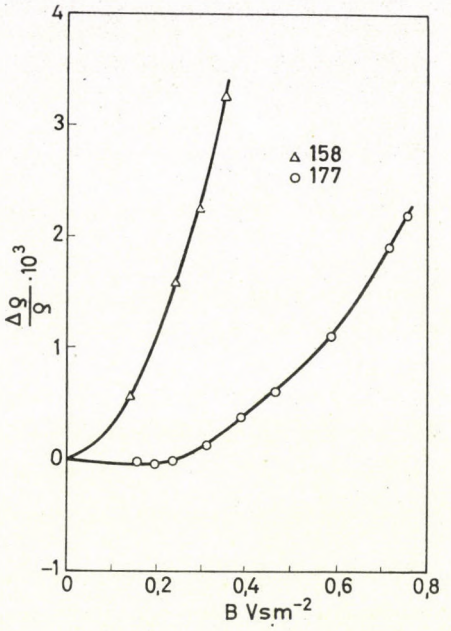

Fig. 5. Magnetoresistance of undoped (No. 158) and O-doped (No. 177) samples at 77 °K temperature

In the case of sample No. 177 which was doped with O there is a very small negative magnetoresistance for magnetic fields below 2500 G, the magnitude of which is hardly higher than the detection limit, but its presence was established beyond doubt in several independent runs of the measurement. The results of measurements were independent of the pair of potential contacts on which the magnetoresistance has been detected, or of the rotation of the sample around its length axis with 90°.

On the Cr-doped samples the negative magnetoresistance appeared quite markedly, as shown in Fig. 4. The negative magnetoresistance of samples Nos. 178/a and 176 after the initial increase with the magnetic field reached its maximum or saturated at moderate fields of 4000—6000 G, then its trend reversed and in the case of sample No. 176 it turned to be positive above 6500 G. The negative magnetoresistance of sample No. 178/b saturated at somewhat higher fields. For these samples there were occasionally slight but not significant deviations between the magnetoresistances measured on the same sample but on different pairs of contacts, or after the rotation of the magnetic field by 90°, probably due to the spurious inhomogeneities of the samples already mentioned. Such a case (No. 178/a) is shown in Fig. 4 too.

It is more interesting to note that while the initial increase of negative magnetoresistance of samples Nos. 176 and 178/b follows a quadratic dependence in the magnetic field as demonstrated in Fig. 6, where the initial part

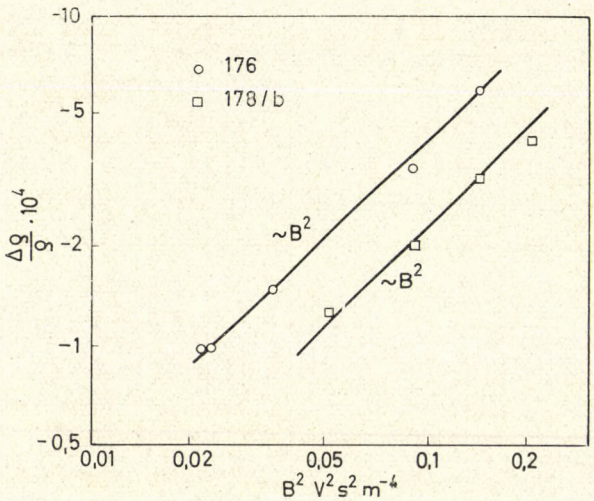

Fig. 6. Negative magnetoresistance vs square of magnetic field in Cr-doped samples at 77 °K temperature

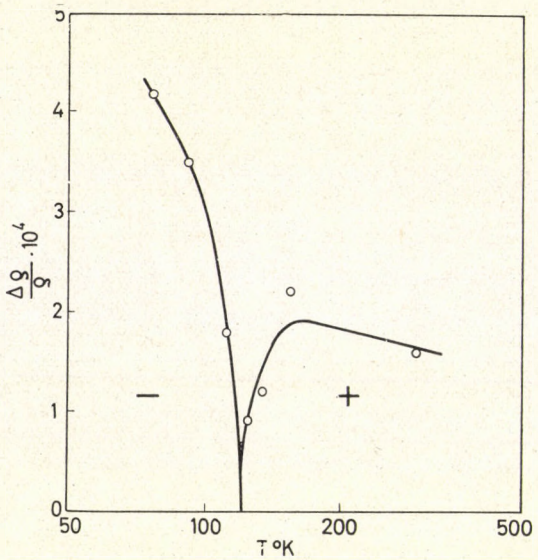

Fig. 7. Magnetoresistance of Cr-doped sample No. 176/a at 3000 Gauss vs temperature

of the magnetoresistance curves are shown on a logarithmic scale, at the same time the magnetoresistance of sample No. 178/a exhibits a dependence on the magnetic field which is nearer to the linear. The negative magnetoresistance of O-doped sample No. 177 was too small to draw conclusions concerning its dependence on the magnetic field.

The temperature dependence of magnetoresistance in sample No. 178/a is shown in Fig. 7. At about 120 °K the small field magnetoresistance changes its sign, and above this temperature it turns to be positive. Further, above 150 °K the magnetoresistance begins to be proportional to the square of the magnetic field, and is nearly independent of the temperature. This kind of temperature dependence was observed by several authors in GaAs and in other crystals [2], [4].

Interpretation of magnetoresistance results

The characteristics of negative magnetoresistance observed in our compensated *n*-type GaAs samples at 77 °K temperature are the same or very similar to the characteristic features of negative magnetoresistance at very low temperature observed by several authors in various materials including GaAs [1], [2], [3], [4], [5], [6], [7]. Only the usually occurring maximum on the Hall coefficient versus temperature curves was not present. We suppose that this is due to the fact that the values of the Hall coefficients are too low to allow to detect a small maximum, the appearance of which is less pronounced for small values of the Hall coefficient [5], [8].

On the basis of this evidence we are justified to suppose that the negative magnetoresistance observed by us in compensated *n*-type GaAs at 77°K temperature and above it is produced by the same cause, namely by the dominant role of impurity conduction in the electron transport of our samples. Now we shall proceed to discuss two interconnected questions. The first of them is the explanation of the existence and characteristic features of negative magnetoresistance observed in our samples on the basis of the various models of impurity conduction put forward in the literature, and the second is how the occurrence of negative magnetoresistance and impurity conduction at 77 °K and higher temperatures, which has been observed up to now only at very low temperatures can be explained.

A great number of theoretical [20], [21], [22], [23], [24], [25] and experimental [1], [2] investigations have shown that there are different types of impurity conduction in semiconductors depending on the concentration of impurities. At low impurity concentrations the electrons are localized at the impurity centres and electrical conduction can take place through the occasional jumps of the localized electrons to neighbouring centres (hopping), [21], with the assistance of phonons [26], if there are nearby vacant centres caused by impurity compensation. For instance, in *n*-type Ge hopping conduction can take place below donor concentrations of 10^{15}— 10^{16} cm^{-3} [27].

Increasing the impurity concentration the electron wave functions localized on different impurity centres begin to overlap with each other, and the localization of electrons becomes obscured. The energy level of impurities

splits, and the activation energy of charge carriers decreases with increasing impurity concentration as observed in n-type Ge by J. F. LE HIR [27], by P. DEBYE and E. CONWELL [28], and in n-type GaAs by O. V. EMELYANENKO et al. [5] and by D. V. EDDOLS et al. [29]. At the same time, by the overlap of impurity wave functions an impurity band is formed in which the electrons become completely delocalized and can move freely in it. The impurity band is separated from the conduction (or valence) band by an energy gap of the order of the ionization energy of impurities, but this separation decreases with increasing impurity concentration. The formation of impurity band takes place in n-type Ge between 1×10^{16} and 2×10^{17} cm^{-3} donor concentrations [27].

Above a certain critical concentration which is about 2×10^{17} cm^{-3} for n-type Ge [27], [28] and $(1—2)\times10^{16}$ cm^{-3} for n-type GaAs [5], [29], the activation energy of the impurity atoms completely disappears, and at higher concentrations the electrical resistivity is approximately independent of the temperature. At such high impurity concentrations the impurity band and the conduction band (or valence band) merge, and a new type of charge carrier conduction, the metal-like conduction of degenerate electron gas dominates the charge carrier transport mechanism [1], [27].

The transition to this metal-like electron conduction in the impurity-band is observed at impurity concentrations where the interatomic distance between majority impurities is about 2.5 time the effective Bohr radius of the hydrogen-like impurity atoms [1]. This observation is in good agreement with the estimations of N. F. MOTT [20], [30].

According to W. SASAKI [1], and to J. F. WOODS and C. Y. CHEN [2], the various observations of negative magnetoresistance at 4.2 °K were all made in the impurity conduction range of dopings and among the various materials all the three ranges of impurity conduction are represented. Notably in the case of GaAs all the three ranges were observed in [1], [2], [5] and [6].

The various possible mechanisms giving rise to negative magnetoresistance were briefly analyzed by J. F. WOODS and C. Y. CHEN [2]. According to them it seems to be only two possible kinds of mechanisms which could account for negative magnetoresistance in the impurity conduction range. Either the magnetic field gives rise to a redistribution of charge carriers among different energy states having different carrier mobility, or the magnetic field increases the mobility or hopping probability of electrons. It is not necessary for these mechanisms to be mutually exclusive, but it is probable that in the different ranges of impurity conduction (i.e. hopping conduction, transition range and impurity band conduction) different mechanisms should play the leading role.

As was shown by R. J. SLADEK and R. W. KEYES [31], and by N. MIKOSHIBA [32], the magnetic field reduces the mobility or hopping probability in the hopping (or transition) region, due to the shrinkage of wave functions

of impurities thus reducing the orbital overlap. To interpret the results of measurements in this range it seems inevitable to postulate a model with energy states having different mobilities in order to account for the observed negative magnetoresistance, at least in the absence of impurity band conduction [2]. According to J. F. WOODS and C. Y. CHEN [2], the general character of the magnetoresistance observations is consonant with a two energy state model of impurity conduction, in which the energy difference between the two states is reduced by the application of a magnetic field thus increasing the occupation probability of the higher energy states which presumably have a higher mobility than the ground states due to the greater orbital overlap of wave functions. A competing process would be the restriction of orbital overlap as shown by R. J. SLADEK and R. W. KEYES [31] thus the resistance change would be the outcome of the results of the influence of two competing processes. This model was put forward by J. F. WOODS and C. Y. CHEN [2], when interpreting their measurements of negative magnetoresistance of *n*- and *p*-type GaAs at liquid He temperatures, which in low magnetic field was approximately linear in the field, in contrast with other observations, where a quadratic dependence was found in a wide range of impurity concentrations [1], [5], [6].

A two-state model would, in general, predict a variation of the Hall coefficient with the magnetic field. However, since the Hall effect was not measured in the hopping region so far this prediction could not be verified [2]. The two-state model in principle could be applied to the impurity band conduction region too but in this range in *n*-type GaAs no significant variation of the Hall coefficient with the magnetic field could be found [2], [33]. We should like to note that in our measurements too a variation of the Hall coefficient with the magnetic field was not detected.

The only successful model of mobility increase mechanism was put forward by Y. TOYOZAWA [22], [23], which can account for the negative magnetoresistance in the impurity band and metallic conduction region [1], but it is incapable to explain the features of negative magnetoresistance in the hopping conduction region. According to this model there exist localized magnetic moments in the crystal, which obey a Curie—Weiss-type law, and the magnetic scattering of the electrons moving in the impurity band by these localized magnetic moments results in the negative magnetoresistance. For highly doped (*n*-type) semiconductors it is believed that the magnetic moments causing this behaviour are the spins of electrons semilocalized around the donor impurities [22], [23].

According to this model some impurity atoms (donors in *n*-type semiconductors) are close enough to each other so that the electronic states form an impurity band. Conduction is via electrons in this band and is limited by the scattering of electrons. Due to the random distribution of impurities, however, some impurities are far enough from each other for the electrons

to be localized around them most of the time, giving rise to localized magnetic moments around the impurity atoms, which interact with the other electrons, thus causing a scattering of charge carriers in the impurity band. In magnetic fields these magnetic moments become aligned and the amount of scattering caused by them will be reduced, and the resistivity will decrease. The resistivity change is approximately proportional to the square of the average magnetization of these impurities, i.e.

$$\frac{\Delta\varrho}{\varrho_0} = \frac{\varrho(B) - \varrho(0)}{\varrho(0)} \sim -\langle m \rangle^2,$$

where $\langle m \rangle$ is the average magnetization [22], [23]. For small and large magnetic fields, respectively, this yields

$$\frac{\varrho(B) - \varrho(0)}{\varrho(0)} \sim -\left(\frac{\mu B}{kT}\right)^2 \text{ (for small } B),$$

$$\frac{\varrho(B) - \varrho(0)}{\varrho(0)} = \text{const.} \qquad \text{(for large } B),$$

where μ is the magnetic moment localized in the impurities [22], [23]. The basic features of this model, i.e. the quadratic dependence of the negative magnetoresistance at the lowest fields, saturation in larger fields, and the increase of the negative magnetoresistance with decreasing temperature are all in good agreement with the bulk of the experimental data [1], [5], [6], [22], [23]. Because the localized magnetic moments obey a Curie—Weiss-type law, the temperature dependence of the negative magnetoresistance in this model at low temperatures is the following, [22], [23]

$$\frac{\varrho(B) - \varrho(0)}{\varrho(0)} \sim -\frac{1}{(T+\Theta)^2}.$$

The constant Θ appears due to the coupling between the magnetic moments, and its experimental values are positive, of the order of 1—2 °K, showing an antiferromagnetic interaction between the localized magnetic moments [1], [6], [22], [23].

In our samples the donor concentrations of Cr- and O-doped samples were in the range of $N_d = (1\text{—}2.4) \times 10^{18}\ \text{cm}^{-3}$, so the average distance between the donor impurities is $r_d = (3/4\pi N_d)^{1.3} = (0.45\text{—}0.65) \times 10^{-6}$ cm, while the effective Bohr radius is $r_B = a_0 \varepsilon_r m_0/m_* = 0.85 \times 10^{-6}$ cm with $a_0 = \hbar^2/m_0 e^2$ and with $\varepsilon_r = 11.5$ and $m_*/m_0 = 0.072$ [14]. Thus the average distance between the donor impurities is of the order of the effective Bohr radius, therefore our samples are all in the metal-like impurity band conduction range [1], [20], where the model of the localized magnetic moments by Y. TOYOZAWA [22], [23] can be applied [1].

The results of our measurements of negative magnetoresistance, i.e. the quadratic field dependence observed in the Cr-doped samples, the saturation at moderate fields, the steep decrease of the negative component with increasing magnetic field, all agree well with the predictions of Y. TOYOZAWA's model. This interpretation of the results for the Cr-doped samples has been already put forward by us in [9] without detailed analysis.

On the basis of the formalism developed by Y. TOYOZAWA in [23] we can estimate the average magnitude of the magnetic moments localized on the impurities, using the measured values of the weak field negative magnetoresistance, and of the saturation value of the magnetoresistance. We can make only a very crude estimation because the saturation value of the negative magnetoresistance is not very well determined, due to the presence of the common positive component of the magnetoresistance. On the other hand, the impurity concentration in our samples is somewhat greater than the impurity concentrations for which Y. TOYOZAWA's model was originally applied [23], and the strong compensation of our samples can reduce the reliability of this analysis.

For the localized magnetic moments of the impurity centres we got values of the order of 2—3 Bohr magneton. These values seem to be in good agreement with other results [23]. This analysis applied to other cases gave values for the magnetic moments of the order of 5—10 Bohr magneton [22], [23]. In his model this great value was explained by Y. TOYOZAWA [23], as being the result of the statistical distribution of the magnetic moments of localized spins due to their collective nature. According to Y. TOYOZAWA on the one hand, they are caused by the electrons which are constantly entering and leaving the magnetic sites, and on the other hand, the surrounding non-magnetic sites make an additional contribution to the magnetic moments. In our samples it is possible that the magnetic moments of the Cr impurities too play a role in determining the interaction of electrons with the localized magnetic moments.

The resistivity in the metal-like impurity band was estimated by N. F. MOTT and W. D. TWOSE [20]. The conduction electrons form a degenerate electron gas with the same density of states effective mass as that of the conduction band electrons [1]. For a degenerate Fermi gas the conductivity is

$$\sigma = \frac{ne^2 l}{vm_*},$$

where l and v are the mean free path and the electron velocity at the surface of Fermi distribution. For degenerate electron gas we have the formula

$$\frac{vm_*}{\hbar} = 2\pi \left(\frac{3n}{8\pi}\right)^{1/3}.$$

Supposing that the mean free path can be written as

$$l = \frac{p}{n^{1/3}},$$

where p is the number of interatomic distances on a mean free path. Combining these expressions we get for the conductivity

$$\sigma = \frac{n^{1/3} e^2 p}{\hbar \pi} \left(\frac{\pi}{3}\right)^{1/2}.$$

These formulas were applied by N. F. MOTT and W. D. TWOSE [20] to the case of n-type Ge with donor concentrations between 2×10^{17} and 4×10^{19} cm^{-3} at liquid He temperatures, and they have got an electron mean free path which was nearly constant in the whole range of impurity concentrations.

We have applied this model to our Cr- and O-doped samples and the results are shown in Table II. The reduced Fermi levels $\zeta = E_F/kT$ which are also shown in Table II were evaluated with the assumption that the density of states in the metal-like impurity band is the same as in the conduction band [1], to show that in our samples at 77 °K the electron gas is really degenerate. Except for sample No. 178/b we can see that the mean free path does not depend strongly on the electron donor concentrations. Apparently the assumption concerning the degeneracy does not hold for sample No. 178/b.

Our last task is to explain the occurrence of metal-like impurity band conduction and of the negative magnetoresistance in our samples at relatively high temperatures (77 °K and above). The fact that our samples were strongly compensated, presumably plays a significant role in the formation of impurity band at higher temperature than in other cases. According to O. V. EMELYANENKO et al., [7], in their n-type GaAs samples which were doped with Cu diffusion, the strong compensation produced relatively high concentrations of impurities with lower concentrations of charge carriers, thus giving rise to the formation of impurity band at higher temperatures than it is usual. The same is the case with our Cr- and O-doped and strongly compensated samples, where the metal-like conduction mechanism shows that the conduction and impurity bands merged, and most probably with the samples of B. S. LISENKER et al., [8], having Fe as the compensating impurity.

It is very interesting to note that until now the formation of impurity band and the presence of negative magnetoresistance at relatively higher temperatures (77 °K and above) have been observed only in highly compensated n-type GaAs, with compensating impurities having deep energy levels. As we have mentioned Cr creates deep acceptor levels in GaAs with energy level of 0.81 eV below the conduction band edge, Fe creates deep acceptors too with

energy level most probably at 0.52 eV but at the same time another level of 0.37 eV was observed too [18]. It seems that there are more than one deep acceptor levels associated with the Cu impurity [34], and the acceptor level connected with the O impurity lies about in the middle of the forbidden band at 0.63 eV above the valence band edge [35].

Table II

Sample No	σ Ω^{-1} cm^{-1}	n cm^{-3}	P	l cm	ζ
176	323	6.1×10^{17}	48.8	58×10^{-6}	5.3
178/*a*	358	1.2×10^{18}	43.3	41×10^{-6}	8.3
178/*b*	71	3.6×10^{17}	12.9	18×10^{-6}	3.6
177	337	1.6×10^{18}	37.1	32×10^{-6}	10.2

Finally we would like to point out that in the compensated samples the mobility at 77 °K is usually exceptionally low as observed in our samples Nos. 177, 178/a and 178/b and therefore the normal positive component of the magnetoresistance is very low too, and cannot mask the not too strong negative magnetoresistance.

Acknowledgements

I wish to express my acknowledgements to Dr. E. PAPP and to his coworkers S. ZSINDELY and T. LEGÁT of the Research Institute for Metallic Industry, Budapest, supplying us with the GaAs crystals and for the discussions concerning the properties of Cr- and O-doped crystals.

Thanks are due also to Dr. G. PATAKI and T. GESZTI for valuable discussions, to K. SOMOGYI for constructing the cryostat for Hall effect and conductivity measurements, to J. HAGYÓ for making the electrical contacts and to Dr. Z. BODÓ and B. RÖSNER for valuable discussions and for having read the manuscript before publication.

REFERENCES

1. W. SASAKI, Proc. Int. Conf. Phys. Semicond. Kyoto, p. 543, 1966.
2. J. F. WOODS and C. Y. CHEN, Phys. Rev., **135A**, 1462, 1964.
3. I. K. ANDRONIK, E. K. ARUSHANOV, O. V. EMELYANENKO and D. N. NASLEDOV, phys. stat. sol., **27**, 45, 1968.
4. R. BROOM, R. BARRIE and I. M. ROSS, Proc. Int. Coll. Semicond. and Phosphors, Garmisch-Partenkirchen, p 453, 1956.
5. О. В. Емельяненко, Т. С. Лагунова, А. Н. Наследов, Р. Н. Талалакин, ФТТ, **7**, 1315, 1965.
6. L. HALBO and R. J. SLADEK, Phys. Rev., **173**, 794, 1968.
7. О. В. Емельяненко, Э. Э. Клотыныш, Т. С. Лагунова, А. Н. Наследов, ФТП, **1**, 933, 1967.
8. Б. С. Лисенкер, И. Е. Марончук, Ю. Е. Марончук, ФТП, **1**, 929, 1967.
9. B. PŐDÖR, phys. stat. sol., **31**, K 55, 1969.
10. E. PAPP, S. ZSINDELY, T. LEGÁT, Neue Hütte, **13**, 29, 1968.

11. Л. Л. Либов, С. С. Мескин, А. Н. Наследов, В. Е. Седов, Б. В. Царенков, ПТЭ, 1965/4, 14.
12. R. W. Ure, Rev. Sci. Instr., **28,** 836, 1957.
13. C. Hilsum, Progress in Semiconductors, **9,** 135, 1967.
14. H. Ehrenreich, Phys. Rev., **120,** 1951, 1960.
15. C. S. Kang and P. E. Greene, Appl. Phys. Letters, **11,** 171, 1967.
16. E. H. Putley, The Hall Effect and Related Phenomena, London, 1960.
17. B. Pődör and C. Iványka, Acta Phys. Hung., **25,** 115, 1968.
18. G. A. Allen, Br. J. Appl. Phys., (J. Phys. D) Ser. 2. **1,** 593, 1968.
19. D. Fritsch and N. Weiss in Semiconductors and Semimetals, Vol. 1. 373. Ed. R. K. Willards, 1966.
20. N. F. Mott and W. D. Twose, Adv. Phys., **10,** 107, 1961.
21. A. Miller and E. Abraham, Phys. Rev., **120,** 745, 1960.
22. Y. Toyozawa, Proc. Int. Conf. Semicond. Phys., Exeter, 104, 1962.
23. Y. Toyozawa, J. Phys. Soc. Jap., **17,** 986, 1962.
24. Б. Л. Бонч-Бруевич, ФТТ, **4,** 2660, 1962.
25. Б. Л. Бонч-Бруевич, ФТТ, **5,** 1852, 1963.
26. J. Mycielski, Phys. Rev., **125,** 46. 1961.
27. J. F. Le Hir, Journal de Physique, **28,** 563, 1967.
28. P. Debye and E. Conwell, Phys. Rev., **93,** 693, 1954.
29. D. V. Eddols, J. R. Knight and B. L. H. Wilson, Gallium Arsenide Proc. Int. Symp. Reading, Sept. 1966. p. 3. Ed. A. C. Stickland, 1967.
30. N. F. Mott, Phil. Mag., **6,** 287, 1961.
31. R. J. Sladek and R. W. Keyes, Phys. Rev., **122,** 437, 1961.
32. N. Mikoshiba, Phys. Rev., **127,** 1962, 1962.
33. D. N. Dasledov and O. V. Emelyanenko, Proc. Int. Conf. Phys. Semicond, Exeter, p. 163, 1962.
34. C. S. Fuller, K. B. Wolfstirn and H. W. Allinson, J. Appl. Phys., **38,** 2873, 1967.
35. S. M. Sze and J. C. Irvin, Solid-State Electronics, **11,** 599, 1968.

ОТРИЦАТЕЛЬНОЕ МАГНЕТОСОПРОТИВЛЕНИЕ В КОМПЕНСИРОВАННОМ АРСЕНИДЕ ГАЛЛИЯ *n*-ТИПА ПРИ ТЕМПЕРАТУРЕ 77 °К

Б. ПЭДЭР

Р е з ю м е

Магнетосопротивление в сильно компенсированном арсениде галлия *n*-типа с примесью хрома и кислорода было измерено при температуре 77 °К. Концентрация электронов при комнатной температуре находилась в пределах от $3{,}8\times10^{17}$ до $1{,}6\times10^{18}$ $см^{-3}$. При слабых магнитных полях отрицательное магнетосопротивление было обнаружено при температуре жидкого азота. Было показано, что поведение этого аномального отрицательного магнетосопротивления очень похоже на то, которое было обнаружено в сильно дегивованных полупроводниках при гелиевых температурах. Отрицательное магнетосопротивление было пропорционально квадрату магнитного поля при слабых полях, и показало насыщение при полях 4000—6000 гаусс. Для объяснения обнаруженного эффекта было предположено, что главным механизмом переноса носителей тока в наших образцах является металлическая проводимость в примесной зоне.

Было показано, что обнаруженные характерные черты отрицательного магнетосопротивления совместимы с моделью рассеяния электронов на локализированных магнитных моментах в примесной зоне. Из экспериментальных данных среднее значение локализированных моментов составляет порядка 2—3 магнетона Бора.

Было высказано предположение, что сильная компенсация может играть существенную роль в формировании примесной зоны при температурах 77 °К и выше.

Acta Physica Academiae Scientiarum Hungaricae, Tomus 27, pp. 467—475 (1969)

ON THE NUMERICAL SOLUTION OF HARTREE–FOCK EQUATIONS INDEPENDENT OF COUPLING SCHEME*

By

R. KARAZIJA, P. BOGDANOVICIUS and A. JUCYS

INSTITUTE OF PHYSICS AND MATHEMATICS OF THE ACADEMY OF SCIENCES, LITHUANIAN SSR, VILNIUS, LITHUANIAN SSR

(Received 10. III. 1969)

The solution of Hartree—Fock equations by a numerical method on computers, type BESM, is described. The minimization of the input information is reached by using the equations independent of coupling scheme and the universal potential field for obtaining the initial radial wave functions. The results obtained are compared with those evaluated from the solutions of conventional Hartree—Fock equations.

1. Introduction

A proper theoretical investigation of atomic properties is possible only when radial wave functions are available. These are obtained, in the main, from traditional Hartree—Fock equations. Sometimes improved methods, e.g. multi-configuration approximation, extended method of calculation, incomplete separation of variables, and other methods are used. However, these latter methods are applied only for rather simple cases. Consequently, the traditional Hartree—Fock radial wave functions remain the best available, especially as concerns many-electron atoms. For this reason they are very widely used at present and the solution of Hartree—Fock equations is the problem of to-day.

The method of numerical solution of Hartree—Fock equations have been elaborated mainly by FOCK, PETRASHEN [1] and HARTREE [2]. The development of modern computing techniques provides new possibilities for obtaining the corresponding solutions in an easy way. Various programmes by different authors for carrying out the corresponding calculations have been compiled, and the tabulation of numerical functions has gradually been given up. Therefore, efforts are made to draw up programmes suitable for any atom in any state in order to provide for any problem to be solved by the wave functions.

At the present time programmes for numerical solution of Hartree—Fock equations have been given by WORSLEY [3], RIDLEY [4], PIPER [5], IVANOVA et al. [6], BRATSEV [7], HERMAN and SKILLMAN [8], FROESE [9, 10], MAYERS and O'BRIEN [11] and by others. Besides this the method of analytical solution of Hartree—Fock equations [12] is widely used as well. As far as we

* Dedicated to Prof. P. GOMBÁS on his 60th birthday.

are dealing with the methods of numerical solution we give no further references on this last very interesting approach in this paper.

The process of solution of Hartree—Fock equations is rather complicated even for powerful computing machines. For this reason simplifications are sometimes used to facilitate the numerical procedures. This is achieved by neglecting the non-diagonal Lagrange multipliers, as is done in [7], or by replacing the exchange terms by a more simple expression, as is done in [8], and so on.

In this paper we describe the method of solution of Hartree—Fock equations in which the simplification is achieved by solving the corresponding equations independent of coupling scheme instead of accurate Hartree—Fock equations and by the use of the universal potential for estimating the initial one-electron radial wave functions. Such an approach allows the "input" information to be minimized considerably.

In the next two Sections we describe the Hartree—Fock equations independent of the coupling scheme and the universal potential, correspondingly. In Section 4 we indicate the methods of numerical calculations and in Section 5 we present and discuss the results for NeII.

2. Hartree—Fock equations independent of the coupling scheme

The solutions of Hartree—Fock equations for each term of a given configuration is rarely done, because it requires a great number of operations. Therefore, it is usual to solve the equations either for the "centre of gravity" of the configuration or for one particular term of the configuration under consideration. The solutions so obtained are used to evaluate the physical quantities to be calculated.

The modification of Hartree—Fock equations we shall use are those equations which do not depend on particular coupling scheme, i.e., the equations are quite similar to those proposed by JUCYS and VIZBARAITE [13] and are obtained by making the functional stationary which is equal to the energy expression with all interactions depending on terms omitted. Such terms, besides magnetic interactions, are

I. The non-spherical part of the direct electrostatic interaction between electrons belonging to the same incomplete shell.

II. The non-spherical part of the direct electrostatic interaction between electrons belonging to different incomplete shells (when one or both shells are complete this part vanishes).

III. The non-spherical exchange electrostatic interaction between electrons belonging to different incomplete shells, under the concept of the shell being understood the group of electrons with the same set of quantum numbers *nl*.

Under these circumstances integrals $F_k(nl, nl)$ $(k > 0)$ and $G_k(nl, n'l')$ are partially neglected, integrals $F_k(nl, n'l')$ $(k > 0,\ n'l' \neq nl)$ are all omitted, nl and $n'l'$ belonging to the incomplete shells. Then we are left with the expression (in atomic units of HARTREE [2])

$$E = \sum_{nl} \Bigg\{ N_{nl}\, I(nl) + \frac{N_{nl}(N_{nl}-1)}{2} F_0(nl, nl) - \\ - \frac{N_{nl}}{4l+2} \sum_{k>0} (l\|C^{(k)}\|l)^2 F_k(nl, nl) + \\ + N_{nl} \sum_{n'l'}{}' N_{n'l'} F_0(nl, n'l') - \\ - \frac{N_{nl}}{4l+2} \sum_{n'l'}{}' \sum_k \frac{N_{n'l'}}{2l'+1} (l\|C^{(k)}\|l')^2 G_k(nl, n'l') \Bigg\}, \tag{1}$$

which is to be made stationary by FOCK's variation method [14].

N_{nl} in (1) denotes the number of electrons in the shell characterized by the quantum numbers nl. The prime to the summation symbol shows that $n'l' = nl$ is to be excluded from the summation. The radial integrals I, F_k and G_k are defined according to HARTREE [2]. $(l||C^{(k)}||l)$ is the reduced matrix element of the spherical harmonic as defined by RACAH [15]. Its numerical values can be found in Appendix 6 of [16].

The functional (1) coincides with the expression for the energy not involving magnetic interactions when only one electron is present outside the complete shells or one electron is missing as well as when the configuration contains the complete shells only. The deviation from the energy increases with increasing number of electrons in partially filled shells and increasing number of missing electrons in almost closed shells. This is true for the highest and lowest energy levels, because the functional under consideration is usually not far from the the "centre of gravity" of a given configuration. This last involves the radial integrals representing the dependence on the coupling scheme mostly with small coefficients and do not matter very much. Absence of these integrals in our functional makes it more convenient for calculation.

When applying the FOCK variation method [14] to (1) supplemented by Lagrange multipliers one obtains the equations

$$\left[\frac{d^2}{dr^2} - 2Y(nl|r) - \frac{l(l+1)}{r^2} - \varepsilon_{nlnl} \right] P(nl|r) - \\ - X(nl|r) - \sum_{n'}{}' \varepsilon_{nln'l} P(n'l|r) = 0\,, \\ \text{(for all } nl\text{)} \tag{2}$$

where

$$Y(nl|r) = \frac{1}{r}\left\{-Z + \sum_{n'l'}(N_{n'l'} - \delta_{nln'l'})\,Y_0(n'l', n'l'|r) - \right.$$
$$\left. - (2l+1)^{-1}\sum_{k=2}^{2l}(l\|C^{(k)}\|l)^2\,Y_k(nl, nl|r)\right\} \tag{3}$$

is the potential function and

$$X(nl|r) = -\frac{1}{r}\sum_{n'l'}\sum_{k}\frac{N_{n'l'}}{(2l'+1)(2l+1)}(l\|C^{(k)}\|l')^2\,Y_k(nl, n'l'|r)\,P(n'l'|r) \tag{4}$$

represents the exchange terms, the $Y_k(nl, n'l'/r)$ being radial integral functions defined by the formula 3.5 (1) of [2].

Owing to the fact that (2) does not involve terms depending on the coupling scheme it is easier to make calculations fully automatic.

3. The universal potential

Besides the configuration, there must be put into the computer initial estimates of one-electron radial wave functions from which a process of successive approximation must be started. Generally, there the complementary procedure is programmed by which the estimates mentioned are obtained automatically. Such procedures used to be of several kinds. One of them consists of using analytic hydrogen-like one-electron radial wave functions and the other in making use of the interpolations or extrapolations from the wave functions of neighbouring atoms or ions already computed. The third consists of using the Thomas—Fermi statistical potential. The first procedure is applied mostly in the case of light atoms and the second in the case of heavy ones. The procedure we are going to describe is a modification of the third approach mentioned and used in [8]. It consists of using the universal potential field derived from the statistical theory of the atom with a correction fitting it to ions as well as to neutral atoms.

The statistical theory of the atom founded by THOMAS [17] and FERMI [18] and further developed by GOMBÁS [19] allowed GÁSPÁR [20, 21] to approximate the Hartree—Fock potential by the so-called universal potential field. This universality consists in scaling the radial variable in such a way that the potential field has an expression independent of the atomic number in the periodic system of elements.

The universal potential mentioned above, giving a good approximation for neutral atoms (c.f. GÁSPÁR [22]) has been adjusted to ions as well by the use of a simplified Fermi—Amaldi correction (c.f. GOMBÁS [19] p. 65 and [21]

p. 40). The resulting expression is given by equation (5) of [23]. As far as we are interested in the first estimates of radial wave functions we neglect the exchange part and the adjustable parameter α in this last equation. Such an approach leads us to this Schrödinger equation

$$\left[\frac{d^2}{dr^2} + \frac{2I}{r} + \frac{2}{r}(Z-I)\frac{e^{-\lambda_0 r}}{1+A_0 r} - \frac{l(l+1)}{r^2} - \varepsilon_{nlnl}\right] P(nl|r) = 0\,, \qquad (5)$$

where I is the degree of ionization and

$$\lambda_0 = 0{,}2075\, Z^{1/3}, \quad A_0 = 1{,}19\, Z^{1/3}. \qquad (6)$$

Z is the nuclear charge number here as well as in the preceding Section.

For all one-electron wave functions equation (5) is the same, hence the solutions are spontaneously orthogonal. The programme for solving equation (5) was used as the complementary procedure mentioned above.

4. The process of numerical solution

The system of equations (2) was solved under well known boundary conditions [1, 2]

$$P(nl|0) = P(n, l|\infty) = 0 \qquad (7)$$

numerically following, on the whole, the methods used by FROESE [9, 10] which conforms well to the specificity of the computer.

In order to keep the intervals between adjacent points constant in the entire range of r a logarithmic mesh [2] has been used. Then

$$\varrho = \ln Zr \qquad (8)$$

s the independent variable instead of r. The last is then calculated by this simple formula

$$r_n = e^h r_{n-1}\,, \qquad (9)$$

where h is the interval between adjacent points in the logarithmic mesh, subscript n showing the ordinal number of mesh points.

The solution of equations (2) was performed with NUMEROV's formula [24]. However, for small and large values of r, the solutions are unstable. In these regions the LOCKUCIEVSKY [25] method of factorization was used as is done by FROESE [9]. The main point of this last approach is the replacement of NUMEROV's formula by two stable ones of lower order.

The calculations have been carried out by outward and inward solutions. Both solutions are connected at a fixed point in the second half of the range of r. The difference between these solutions at this point allows the correction of the diagonal Lagrange multiplier to be determined. This procedure is applied mainly in solving the equations for radial wave functions of inner shells.

As FROESE has pointed out, the method of DETTMAR and SCHLÜTER [26] is more appropriate in the case of outer shells. They suggest the expansion of the function in power series of $\varepsilon - t$, ε and t being, correspondingly, the accurate and approximate values of the diagonal Lagrange multiplier. The coefficients of such an expansion are found step by step.

An important feature of radial wave functions is their orthogonality between the shells with the same l and different n. This orthogonality is secured by the non-diagonal Lagrange multipliers which must be used when incomplete shells are present. The functions are orthogonalized by Schmidt procedure and the estimates of non-diagonal Lagrange multipliers calculated by the method of FROESE [10]. Then the solution of equations (2) is carried out using the estimated values of non-diagonal Lagrange multipliers. Afterwards, those radial wave functions are improved for which self-consistency is poor.

The degree of self-consistency is measured by the value of

$$\Delta P = \max(r)|P^i - P^{i-1}|\,, \tag{10}$$

where i indicates the iteration number, max (r) denotes the maximum value over the entire range of r. Iterations are performed until

$$\max(nl)\,\Delta P(nl) \approx 10^{-5} \tag{11}$$

is attained, max(nl) denoting the maximum over all shells of electrons.

5. The results for NeII

The numerical procedures described in the preceding Section have been programmed for computers BESM—2 and BESM—4. The programme works entirely automatically and is suitable for each atom in the periodic system of elements in any state of excitation. What initially must be known is the atomic number and the configuration. After self-consistency is attained the radial integrals are calculated and automatically printed by the output mechanism.

We are presenting some results for the configuration $1s^22s^22p^43p$ of NeII in order to see how the solutions of Hartree—Fock equations independent of

Table I

The quantities of self-consistent field independent of coupling scheme in comparison with those of accurate Hartree—Fock method

quantity A	independent of coupling scheme	differences ΔA			
		$(^3P)^2P$	$(^1D)^2P$	$(^1S)^2P$	$(^3P)^4P$
ε_{2p2p}	4.16203	0.27711	0.16449	—0.01591	0.23861
ε_{3p3p}	0.69866	0.00288	0.01088	0.02008	0.05235
$\bar{r}(2p)$	0.8141	—0.0138	—0.0097	0.0038	—0.0153
$\bar{r}(3p)$	3.958	0.056	—0.002	—0.260	—0.331
$F_2(2p, 2p)$	0.51661	0.01095	0.00682	—0.00259	0.00485
$F_2(2p, 3p)$	0.03452	—0.00467	—0.00220	—	0.01358
$G_0(2p, 3p)$	0.00977	—0.00365	—0.00227	0.00541	0.00899
$G_2(2p, 3p)$	0.00986	—0.00320	—0.00287	0.00471	0.00812
$\lambda_{2p,3p}$	—0.20366	—0.22149	—0.06382	0.1697	—

Table II

Values* of the total energy (in atomic units) for NeII $1s^22s^22p^43p$

	$(^3P)^2P$	$(^1D)^2P$	$(^1S)^2P$	$(^3P)^4P$	$(^3P)^4D$	$(^3P)^2D$	$(^3P)^2S$
E_t	—126.7163	—126.6001	—126.4200	—126.7474	—126.7364	—126.7290	—126.7215
E_{nr}	—126.7144	—126.6007	—126.4201	—126.7422	—126.7339	—126.7295	—126.7215

* E_t — from the accurate Hartree—Fock equations.
E_{nr} — from those independent of coupling scheme.

coupling scheme work as compared with the solutions of traditional Hartree—Fock equations as given by FROESE [10]. In Table I the values of Lagrange multipliers and some integrals widely used (the first two columns) and their deviations from the values as given by FROESE [10] (columns 3—6) are given. Table II contains the energy values evaluated by us (E_{nr}) and by FROESE (E_t).

The results show the well known fact that every modification of Hartree—Fock equations affects the individual quantities noticeably. However, the values of physical quantities are affected rather slightly. In our case, the non-diagonal Lagrange multipliers undergo the maximum changes. However, this deviation is less than the maximum difference between separate terms in accurate traditional Hartree—Fock equations, as is to be seen from the results of FROESE. The next quantity which is considerably affected is the radial integral G_2 and then G_0. For the term ^4P it reaches 90 per cent. Nevertheless, the difference in total energy does not exceed 0.004 per cent.

On account of the simplicity of handling and rather good final results the use of the Hartree—Fock self-consistent field equations independent of coupling scheme is justified, especially as the difference under consideration is considerably less than the difference between traditional Hartree—Fock equations and those accounting for the correlation effect. As an example we can take the method of a self-consistent field in multi-configurational approximation (cf. [27]).

The results of the theoretical calculations of the energy spectra of ZnIV isoelectronic sequence in the configuration d^8p [28] may serve as the additional confirmations of usefulness of the solutions of Hartree—Fock equations independent of coupling scheme.

The authors are very happy to take this opportunity to express their appreciation to Prof. CHARLOTTE FROESE-FISCHER for making available all information concerning the process of programming the numerical procedures.

REFERENCES

1. В. А. Фок и М. А. Петрашень, ЖЭТФ, **4**, 295, 1934.
2. D. R. HARTREE, The Calculation of Atomic Structures, New York—London, 1957.
3. E. C. RIDLEY, Proc. Cambr. Phil. Soc., **51**, 702, 1955.
4. B. WORSLEY, Canad. J. Phys., **36**, 289, 1956; Proc. Roy. Soc. **A241**, 239, 1957.
5. W. N. PIPER, Phys., Rev., **A123**, 1281, 1961.
6. А. В. Иванова, А. Н. Иванова, А. И. Прихоженко, И. И. Пятецкий-Шапиро, В. Л. Тарнопольский; Liet. fiz. rinkinys, **3**, 129, 1963.
7. В. П. Братцев, Таблицы атомных волновых функций, Наука, Москва, 1966.
8. F. HERMAN and S. SKILLMAN, Atomic Structure Calculations, Prentice-Hall Inc., Englewood Cliffs, New Jersey, 1963.
9. C. FROESE, Canad. J. Phys., **41**, 1895, 1963.
10. C. FROESE, Phys. Rev., **137**, A1644, 1965.
11. D. F. MAYERS and F. O'BRIEN, Proc. Phys. Soc., A **1**, 145, 1968.
12. C. C.J. ROOTHAAN and P. S. BAGUS, Methods in Computational Physics, Vol. II (1963), Academic Press, New York, N. Y.
13. А. П. Юцис и Я. И. Визбарайте LTSR MA Darbai, **B 1(24)**, 65, 1961.
14. V. FOCK, ZS f. Phys., **61**, 126, 1930.
15. G. RACAH, Phys. Rev., **62**, 438, (1942).
16. А. П. Юцис, А. А. Бандзайтис, Теория момента количества движения в квантовой механике, Вильнюс, 1965.
17. L. H. THOMAS. Proc. Cambr. Phil. Soc., **23**, 542, 1926.
18. E. FERMI. Rend. Lincei, **6**, 602, 1922; ZS f. Phys., **48**, 73, 1928.
19. P. GOMBÁS, Die statistische Theorie des Atoms und ihre Anwendungen, Springer-Verlag, Wien, 1949.
20. R. GÁSPÁR, Acta Phys. Hung., **2**, 151, 1952, **3**, 263, 1954; Liet. fiz. rinkinys, **3**, 41, 1963.
21. P. GOMBÁS, Pseudopotentiale, Springer-Verlag, Wien, 1967.
22. R. GÁSPÁR, Acta Phys. Hung., **6**, 105, 1956; **7**, 455, 1957; **12**, 171, 335, 1960; **15**, 257, 1963.
23. A. JUCYS, I. GLEMBOCKIS and R. GÁSPÁR, Acta Phys. Hung., **23**, 425, 1967.
24. Б. М. Нумеров, Труды Центральной Астрономической Обсерватории, **2**, 188, 1933.
25. Б. П. Демидович, И. А. Марон, Э. З. Шувалова, Численные методы анализа, Москва, 1963
26. H. K. DETTMAR and A. SCHLÜTER, Z. Angew. Math. Mech., **38**, 220, 1958.
27. А. П. Юцис, ЖЭТФ, **23**, 129, 1952.
28. Я. И. Визбарайте, Д. В. Грабаускас, А. И. Иванова, Р. И. Каразия, И. В. Рабинькина, У. И. Сафронова, А. П. Юцис, Оптика и спектроскопия, **26**, 337, 1969.

К ВОПРОСУ О РЕШЕНИИ УРАВНЕНИЙ ХАРТРИ–ФОКА, НЕ ЗАВИСЯЩИХ ОТ ТИПА СВЯЗИ, ЧИСЛЕННЫМ МЕТОДОМ

Р. И. КАРАЗИЯ, П. О. БОГДАНОВИЧУС и А. ЮЦИС

Р е з ю м е

Рассматривается методика решения уравнений Хартри–Фока численным методом и её применение к электронным вычислительным машинам типа БЭСМ. Минимизация начальной информации достигается путём использования уравнений, не зависящих от типа связи (2)–(4) и универсального потенциала (5) для получения исходных радиальных волновых функций. Результаты для NeII $1s^2 2s^2 2p^4 3p$ сравниваются с решениями уравнений Хартри–Фока для каждого терма. Обсуждается точность полученных функций и их пригодность в расчётах.

Acta Physica Academiae Scientiarum Hungaricae, Tomus 27, pp. 477—491 (1969)

MODEL AB-INITIO CALCULATIONS AND THE FOUNDATION OF THE MO—LCAO METHOD*

By

G. DEL RE

GRUPPO CHIMICA TEORICA, CONSIGLIO NAZIONALE DELLE RICERCHE, VIA CORNELIO CELSO 7, 00161 ROMA, ITALY

(Received 10. III. 1969)

A use of *ab initio* calculations that seems to have been largely overlooked because of its simplicity is the construction and analysis of simple models of the chemical bond. Such models may render enormous services both in clarifying previously known results and in suggesting new ones, and in making possible a detailed discussion of interpretation schemes and approximations. Treatments using the LCAO scheme over the valence electrons may be seriously at fault when effects like inter-shell orthogonalization are neglected. Such effects are consequences of the approximations used; nevertheless, they may be physically significant because the corresponding approximations may be essential in order to reach an understanding of the molecular reality. They include changes of the AO's with molecular geometry. The realization that a certain type of modification of the AO basis is important must be followed by a very careful analysis of the way in which such a correction should be introduced in order to preserve simplicity and physical significance.

The present article is part of a discussion of the theory of molecules started several years ago with a study of the connection between hybridization and localization [1] and continued later in various directions. The attempt will be made here to draw attention on some more points regarding the use and limitations of the molecular orbital method, in its simple LCAO versions, as a tool of theoretical physics rather than as an interpolation technique useful for chemical problems.

The fact that such pioneers as MULLIKEN [2], PAULING [3], GOMBÁS [4] have devoted much work to single-particle treatments and related aspects of the quantum theory of molecules is sufficient indication of the importance of our subject. Nevertheless, we recall some of the considerations that justify a renewed interest in methods avowedly incapable of giving exact numerical results.

One can expect two kinds of information from a theoretical treatment: very good quantitative predictions and/or an explanation of facts in the sense of a correlation of various details in a general scheme. Contrary to what was once the case, the domains where the two uses of the theory do not exclude each other are nowadays very rare. This is because the equations that govern the behaviour of most systems are very complicated, and very accurate treatments are seldom amenable to a clear physical interpretation. In fact, quali-

* Dedicated to Prof. P. GOMBÁS on his 60th birthday.

tative and even semi-quantitative understanding is often reached by simple schemes connecting the phenomena to be interpreted with some specially significant features of the general theory of matter; such in the case, for instance, with the interpretation of the excitation potentials of conjugated molecules in terms of the allowed energies of a single particle confined in a limited region of space.

Various reasons, among which the advent of large computers is very important, have led to much emphasis on the quantitative side, so that an enormous effort has been made to obtain better and better solutions of the (electronic) Schrödinger equations for larger and larger molecules. It is curious that, instead of insisting on the undeniable importance of such calculations for testing and reference purposes, many authors have defended that effort by claiming that no attempt should be made to understand molecular phenomena unless very accurate wavefunctions are available. To many a physicist, this claim must sound as a condemnation of most of theoretical physics, both pure and applied; suffice it to think of problems like particle scattering or transport phenomena in solids to realize what broad fields are based on comparatively rough approximations of the 'rigorous' equations.

I. Correlation and the MO—LCAO method in a simple model calculation

In a first part of the present article, we shall consider the above questions in some more detail, the reason being that one must somehow know where one stands when one tries to use an approximation for strictly theoretical purposes. There are two kinds of objections put forth against physical considerations on molecules based on single-particle (i.e., orbital) methods. One regards the fact that such methods are usually approximate versions of the ideal one-electron treatment given by the Hartree—Fock equations; the other is more directly concerned with the shortcomings of the one-electron scheme. We shall consider first the latter point, which goes under the name of "the correlation problem" [5].

Although there is a growing suspicion that this problem may have been overemphasized by some authors, there is no doubt that it has a perfectly sound origin. Any independent-particle treatment of a many-electron system must involve averages over all the electrons but one, thus replacing them by charge clouds. As has been known for a long time, this contradicts the inherent dualism in the nature of an electron, whose interactions are all to be described by point-particle potentials. The corrections that should be introduced in order to take into account the corpuscular nature of all the electrons are the so-called correlation corrections; evidently, they must be studied and their

importance assessed before accepting even qualitative conclusions drawn from treatments neglecting them. Now, an examination of the available data suggests that the correlation correction to the energy of a molecule is indeed very small; however, it is comparable with the dissociation energies of ordinary chemical bonds. Therefore, the argument runs, the independent-particle model is not reliable in connection with molecular physics. Of course, there is a weak point in the last part of the above considerations, because the fact that dissociation energies and correlation energies are of the same order of magnitude does not imply that one cannot obtain the former without knowing the latter; as a matter of fact, dissociation energies are differences, and, in principle, can be obtained to a good approximation from (more or less equally) incorrect quantities. This remark leads to further arguments in favour and against the supporters of correlation, all based on quantitative considerations involving mainly the expectation values of the energy. The question is how far such quantitative arguments, usually limited to energies, are significant.

With very few exceptions, highly accurate molecular calculations with correlation are not available; moreover, calculations claimed to include correlation are very complicated, and this is a serious hindrance in discussions of aspects other than energy expectation values.

Attempts to introduce simple indices of the importance of correlation for various observables, especially those using the so-called "correlation coefficients", appear to be quite promising [6], but several difficulties have still to be overcome especially as regards the application to molecules. The best alternative to rough estimates and dubious analyses of complicated situations consists in following the traditional approach of theoretical physics, namely to have recourse to a model, where the main features of the actual problem are present.

Although much has been done using the hydrogen molecule as a model, a better way of simulating very simply an ordinary chemical bond is probably to treat the states of two electrons in the field of two positive first-row ions (say, Li ones) by an LCAO-MO-CI method with a limited basis set [7, 8]. In fact, the coefficients of the linear combinations of atomic orbitals used to construct the molecular orbitals are the variational parameters which must be determined in order to reach an "optimum" one-electron description, just as the coefficients of an expansion in a complete set of orthogonal functions can be taken as the variational parameters to be determined in order to get the best one-electron scheme, namely the Hartree—Fock orbitals for the given system; and the coefficients of the linear combinations of the Slater determinants that can be constructed from the given molecular orbitals correspond to the coefficients of the expansion in a complete set of configurations obtained from the Hartree—Fock orbitals, and thus describe correlation. The definition of the latter adopted here amounts to the statement that correlation is whatever

cannot be taken into account by a single-configuration treatment carried out within the given scheme. In order to use our model for the purpose of assessing the importance of correlation in the qualitative description of bonds, we have to compare results obtained with and without single-configuration mixing.

To illustrate the above considerations, take the basis set formed by the $2s$ and $2p$ orbitals of lithium, centred on two different nuclei at a distance R [8]. Let us postpone for the moment a discussion of the importance of the existence of the inner core, and assume that the given orbitals depend on R only through their centres; this is in full accordance with the spirit of the simplest MO—LCAO method, as used by theoretical chemists. Then, the results for the ground-state energy are those summarized in Table I, where the single-

Table I

Ground-state energies of a two-electron bond between equal nuclei having effective charge 1.30 when the trial function is: (b) a single determinant over $2s$ STO's with orbital exponent 0.65; (c), a single determinant over $2s-2p$ hybrids with the same orbital exponent and an optimized s-character; (d), a linear combination of the two determinants corresponding to the bonding and antibonding MO's formed by the same hybrids. Line (e) is the percent difference between (c) and (d). All the energies are in a.u.; the distances in a.u. multiplied by 0.65 are given in line (a)

(a)	2	3	4	5	6
(b)	1.2020	1.0722	0.9613	0.8803	0.8244
(c)	1.3515	1.1199	0.9768	0.8857	0.8268
(d)	1.3519	1.1228	0.9912	0.9194	0.8795
(e)	0.03	0.26	1.45	3.63	6.00

determinant (SC) and configuration interaction (CI) approximations are compared, the SC function being optimized with respect to the degree of hybridization of the atomic orbitals, and the SC function being a linear combination of the two g determinants constructed with the bonding and antibonding bond orbitals resulting from the optimum hybrids.

Table II shows that the model used leads to the same results as analyses of the hydrogen molecule and *ab initio* all-electron calculations. In particular, the internuclear distance can be divided into three ranges: one, where the correlation effects are relatively unimportant; one, where they are very important; and one where an intermediate situation takes place. The question we are interested in is whether the picture given by the correlation energies must be understood as an indication that interpretations of facts based on the SC function are not reliable.

There is no doubt that the electron density distribution is a more sensitive and convenient quantity for assessing the validity of a given description. Therefore, we present Table II, where, in addition to the actual changes in

Table II

Analysis of electron densities for the model of Table I

(a)	2	3	4	5	6
(b)	.0004	.0029	.0144	.0337	.0527
(c)	.005	.203	.283	.341	.231
(d)	.0001	.0007	.0002	.0000	.0000
(e)	—.001	—.006	—.083	—.261	—.401
(f)	—.0001	—.0004	—.0032	—.0054	—.0043
(g)	.998	.994	.917	.740	.599

Explanation:
(a) same as line (a) of Table I;
(b) 'correlation' energies (line (d)-line(c) of Table I);
(c) and (d), relative and absolute changes in the electron densities at the nuclei;
(e) and (f), idem at the centre of the bond of Table I;
(g) corresponding weights of the ground-state configurations.

energies, the changes in the one-electron densities associated with the nuclei and the centre of the bond for various internuclear distances are compared. The changes in density at the nuclei, even though they are large fractions of the density itself, are not very important. The situation at the centre is different: the correlation correction (which tends, of course, to separate the electrons) is lower than 10% for internuclear distances R lower than ca. 6.5 a.u., but then increases rapidly, thus deepening the well between the atoms. In Table II, therefore, the three regions mentioned above appear to be for R less than 6 a.u., R larger than 8 a.u., R comprised between 6 and 8 a.u.; this partition is quite clear in the weights of the SC ground-state function in the CI functions.

In short, Table II confirms and even emphasizes the importance of correlation at large internuclear distances, but indicates that, around the internuclear equilibrium distance, that correction is relatively unimportant both on energies and on the electron densities. This conclusion can be generalized to most bonds in a very easy way, if we assume that they can be treated by at most two determinants — as is strongly indicated by the example of Li_2 and some other examples. In order to see this point, consider the secular equation associated with the Hamiltonian matrix over two configurations, and suppose that the configurations in question are determinants over bonding and antibonding orbitals, respectively. In the homonuclear case, the energies E_1, E_2 associated with the two configurations become equal when the internuclear distance tends to infinity, and, moreover, the contribution of hybridization becomes very small. Now, when the diagonal elements of a second-order matrix are nearly degenerate, the first perturbation term is proportional to the interaction element B_{12}; moreover, the coefficients of the linear combination associat-

ed with it become equal each other. On the other hand, for small internuclear distances, the separation between E_1 and E_2 is large (at least if the bond is very stable), and the first-order perturbation correction is proportional to $B_{12}^2/(E_2—E_1)$ and the contribution of the excited-state configuration is proportional to $B_{12}/(E_2—E_1)$. This result is valid for any homonuclear bond, provided the difference $E_2—E_1$ is large compared with B_{12}; this is the condition one can assume as a condition for the possibility of describing a bond by means of an MO picture [2].

The case of heteronuclear bonds involves a number of novel features. For instance, it does not necessarily require configuration mixing as a means of ensuring the correct limit at large distances. A study of these cases is rather complicated because simplifications provided by equal nuclear charges are lacking. It is very important, however, that a close similarity can be introduced between the two cases by taking into account the screening effect of the electrons: at large internuclear distances, an electron on atom A tends to see B as a singly-charged positive ion, and vice versa; therefore, as far as binding effects are concerned, the situation should be very much the same as for the homonuclear case (cfr. [9]). Further work on simple models for heteronuclear cases is in progress.

We shall assume from now on that the picture provided by the one-electron density associated with an SC (MO) calculation is sufficient for interpretation purposes in the vicinity of the equilibrium distance. The fact that correlation pushes some charge away from the centre of the bond cannot be considered very important if the corresponding change is almost negligible from a quantitative point of view. The numerical examples given above show, on the other hand, that the real shortcoming of MO 'theories' is still in the dissociation limits, as was pointed out by MOFFITT a long time ago [10]. A very urgent task of quantum chemistry seems to be, therefore, that of combining the exceptional simplicity and heuristic power of the single-electron picture at distances near the equilibrium ones with some convenient picture of the situation when the atoms are far apart; the more so, as already the interactions between non-bonded atoms in a polyatomic molecule would seem to fall in the category of molecular features not describable by an MO theory, at least as such theories stand now.

There have been suggestions that the two-particle density is a more significant function as regards the importance of correlation. As a matter of fact, the ratios between the values of P (1, 2) as obtained from a configuration interaction calculation and the corresponding values for a single-determinant approximation are all very close to unity in the case of formaldehyde in the equilibrium configuration [11]; the only important correlation appears to be 'spin' or Fermi correlation, which is already included in the single-determinant function.

II. Choice of the basis and physical significance of simple LCAO treatments. Radial distortion

The brief discussion given above may be completed by the remark that the very concept of correlation implies that the single-particle description of a molecule should be well understood and brought to its extreme consequences, so that one may be sure that certain facts cannot be explained within any consistent orbital scheme. We shall now try to indicate some of the points that must still be clarified in that connection on the basis of very simple models, especially with LCAO 'theories' [18].

The introduction of the latter answers, as was pointed out by MULLIKEN [2], to a need of simplicity and physical significance of the interpretation scheme. It may seem at first sight that the best orbital scheme is a Hartree—Fock one, where the variational principle has been used to obtain the best energy compatible with a single-particle treatment. It is now becoming clearer and clearer that the word "best" used in an ambiguous way has been the source of many difficulties. From the point of view adopted in the present article, the most important function of a theory of molecules is to make possible a complete and consistent interpretation of molecular properties, by tracing them back to very few basic statements and pictures; this goal is to be reached, if necessary, at the expense of high accuracy. Now, among other things, the pure Hartree — Fock scheme does not provide a built-in reference to the fact that atoms are the building blocks of a molecule; and much less that bonds exist at all: so that the analysis of its results requires a large amount of work to find out the way in which atoms and bonds are concealed in them [12]. This consideration is sufficient to show that the choice of atomic orbitals is a most important point in the progress toward a consistent theory of molecules [13]. The usual choice of an (AO) basis is well-known, and corresponds closely to that considered above for the Li_2 molecule: one assumes that the AO's are fixed functions of the atoms forming a molecule, and can only adjust to the specific situation through hybridization. This starting point is sound as long as the basis is complete and the treatment involves all the electrons; but we are interested precisely in the case when a limited basis is used and only a few electrons are treated, in order to keep the results as easy to interpret as possible. Under these conditions, at various internuclear distances, as can be seen when one considers a specific example (vide infra), a choice of AO's adjusted in a special way to the molecular situation is required by strictly physical considerations.

In short, if simplified schemes are necessary for interpreting molecular phenomena, and if a limited-basis MO—LCAO treatment must be taken as such a scheme (thus deserving the name of theory), a careful study of the dependence of the basis AO's on molecular geometry is essential. Of course, it would be particularly satisfying if the forms of the AO's could be left invariant; but the

very example of hybridization indicates that this is not possible. What we can (and should) do in order to put some order in our analysis is to make reference to some standard AO's to be interpreted as the entities that represent, as it were, the undisturbed atoms; and introduce corrections on them, trying to interpret them as physical effects.

Let us come back to the simple model (the two-electron model of the Li_2 molecule) which we have introduced in order to consider a case where a number of features arising from the use of a complicated basis is eliminated. Here, the reference fixed AO's are the 2*s* Slater orbitals of lithium, and a first step shows that hybridization is very important for obtaining reasonable results. Further analysis indicates that modifications of the radial parts of the AO's are necessary — still with four AO's as a basis — among other things, in order to ensure orthogonality to the inner shell [14, 15]. Finally, variation of the orbital exponents is necessary in order to satisfy the virial theorem. These modifications are not introduced just as improvements of the calculations; they must be considered as essential features of an LCAO calculation, to be added to those already discussed in [13]. We shall call them radial distortion (or, sometimes, 'promotion' [13]) and 'scaling', respectively. We emphasize that they are introduced with the tacit assumption that the unmodified AO is of the *s* type (in our model), although — as will be seen presently — not necessarily a regular Slater orbital.

The simplest kind of radial distortion in an atomic orbital participating in a bond orbital is connected with orthogonalization to the inner core. The necessity of introducing this modification in the basis orbitals was pointed out long ago [14], but has not been stressed too much in recent years, because it arises only when the valence electrons are treated separately, and becomes really evident when such a treatment is carried out at various distances; moreover, it may be very small when the inner core has a very high orbital exponent. To emphasize the importance of the condition of orthogonality to the inner shell suffice it to mention that, in its absence, the united atom limit of bond orbitals resulting from two (2*s*, 2*p*) hybrid AO's would be essentially 1*s* orbitals [8]. Therefore, in a consistent orbital theory, the corresponding modification of the atomic orbitals should be introduced as a standard effect to be treated before actual energy calculations, as could be done with hybridization [1, 15], because it is part of the preparation of the atomic orbital basis.

The problems arising in this connection are easily illustrated in the model at hand. For simplicity, suppose a treatment using only one *s*-type orbital per atom is to be carried out for the valence electrons. Then, orthogonalization to the MO to which the inner core electrons are assigned requires the introduction of atomic orbitals of the form

$$|2s_m> = N(|1s> - m|2s>), \tag{1}$$

Table III

Analysis of orthogonalization to the inner shell in a two-electron model of the Li_2 molecule for three values of the internuclear distance R.

Column (a) gives the values of $\varrho = \alpha R$, with $\alpha = 0.65$ and R in a. u. Columns (b) and (c) report the energies obtained from a Slater determinant over pure-s orbitals corresponding to Equ. (1) of the text with $m = 0$ and m such as to ensure orthogonality of the $2\sigma g$ to the $1\sigma g$ orbital, respectively. The corresponding values of m are given in column (d). Column (e) contains the values of m ensuring the same orthogonality condition when the Slater $2s$ orbital is replaced by an sp^3 hybrid, the values for hybrids with a lower p character being intermediate. Column (f) gives the values of the parameter m' for a pure-p orbital of the type of Equ. (6)

(a)	(b)	(c)	(d)	(e)	(f)
3	1.0722	.8165	2.849	2.585	.3499
4	.9613	.7675	2.923	2.859	.2614
5	.8244	.6614	2.941	2.939	.1725

where N is an appropriate normalization factor, m is a positive quantity used for ensuring orthogonality to the inner core MO (which is given by the normalized sum of the Slater $1s$ orbitals associated with the inner core of the two atoms, having exponent 2.70). The two Slater orbitals appearing in (1) are assigned the same orbital exponent, say 0.65. Some indications about the results are given in Table III, which shows that the contribution of the $1s$ orbitals is not negligible. The changes in energy reported in Table III support the physical interpretation of orthogonalization as a repulsion tending to increase the energy of the outer electrons, especially at small internuclear distances [15]. As is well known, this interpretation can be translated into a rigorous mathematical formalism by introducing appropriate pseudopotentials [4].

The kind of orthogonalization suggested here — which corresponds to forming hydrogen-like orbitals — is equivalent to the usual Schmidt orthogonalization. A study of such hydrogen-like orbitals in free atoms has been carried out [16], and has given results comparable with those of the usual Slater orbitals, thus removing the only serious objection to the use of hydrogenlike orbitals. Of course, the 'best-atom' orbital exponents are no longer very close to those given by the Slater rules. Nevertheless, they are close enough for most practical calculations.

The modification brought about by the addition of $1s$, $3s$, . . . terms to the Slater orbital may be called "promotion"; here, at variance with [13], we use the term "radial distortion" because the word 'promotion' recalls the physical interpretation of the additional terms as higher-energy orbitals of the free atom, which is not possible here (see also [2]). A physical interpretation of this distortion can only be founded on a redefinition of the reference

free-atom orbital and on a discussion of the way in which an analysis of the electron density should be carried out.

We consider now some more aspects of the question of orthogonalization to the inner shell. Suppose that, instead of considering pure-s orbitals, we wish to consider hybrids. We are then faced with two possibilities. First of all, we can write a hybrid in the form

$$|h> = N[|1s> - m(|2s> + g|2p>)] \tag{2}$$

(where g is a hybridization parameter and N a normalization factor), and then it is impossible to decide whether, by introducing the $1s$ contribution, we have modified the $2s$ or the $2p$ orbital; so that we have no longer a right to distinguish between hybridization and radial distortion. In other words, the procedure based on (2) leads to an m value which depends both on the inner core and on the degree of hybridization, but, as we have just said, it must be interpreted as a distortion of the s orbital. This point of view is perfectly reasonable, and should be completed by the decision that radial distortion of the $2p$ orbital will be introduced only if orthogonalization to orbitals resulting from p orbitals is to be carried out, as would happen in the case of, say, the Na_2 molecule. However, this leads to ambiguities in the general case of bond orbitals formed by hybrid AO's which must be orthogonalized to bond orbitals also formed by hybrid AO's. We consider here, therefore, the other possibility, namely that of orthogonalizing separately the pure-s orbital and the pure-p bond orbital to the inner core orbitals, and then building the required hybrids. The situation becomes particularly interesting when this criterion is to be applied to the general case. Let s_1, s_2, p_1, p_2 denote the subsets formed by a $1s$, a $2s$, . . . orbital with the same orbital exponent on atom 1, same on atom 2, and the subsets formed by a $1p$, a $2p$, . . . orbital on atom 1, same on atom 2, respectively. A molecular orbital $|\chi_1\rangle$ will be written in terms of a column vector C which is defined as follows

$$|\chi_1> = (s_1, s_2, p_1, p_2) \begin{vmatrix} C_{11} \\ C_{21} \\ C_{31} \\ C_{41} \end{vmatrix} \tag{3}$$

and another orbital $|\chi_2\rangle$ will be expressed through the same basis set and another column vector with subvectors C_{12}, C_{22}, etc. By definition, a mixing of orbitals of the same subset is a radial distortion or 'promotion', whereas a mixing of subsets s_i and p_i is hybridization. Now, the requirement that $|\chi_1\rangle$ and $|\chi_2\rangle$ be orthogonal to one another leaves such a freedom that we can require at the same time that only promotion be used to satisfy it. Let us assume that

$|\chi_1\rangle$ is given, and that only $|\chi_2\rangle$ must be determined. Let us denote by S_{11}, S_{12}, etc. the overlap matrices associated with the four subsets of the given AO basis. Then, the conditions we find on C_{12}, C_{22}, etc., are:

$$\sum_j C_{i2}^+ S_{ij} C_{j1} = 0. \tag{4}$$

This equation defines one element of each C_{i2}, and thus, when there is only one inner-shell orbital to which orthogonality must be ensured, the C_{i2} vectors need have only two elements. A particular case is that of the pure-*s* orbitals considered above. Another interesting case is that of pure-*p* orbitals, where the possibility of including the 1*p* orbitals in the atomic *p* subset has been considered explicitly. We comment briefly on this point because it illustrates one of the most delicate aspects of the problem at hand. There are two ways of looking at our new *s* orbitals. One, as has been mentioned, consists in assuming that we replace Slater orbitals by strictly hydrogen-like orbitals; the other consist in assuming that we have granted a certain degree of flexibility to the radial parts of our orbitals, and replaced the factor *r* of the Slater 2*s* orbital by a more general first-degree polynomial involving one parameter to be used for the orthogonality requirements. From the former point of view, the introduction of a 1*p* orbital does not appear to be justified; from the latter point of view, on the contrary, it would seem reasonable to modify the radial part of a *p* orbital exactly as has been done for its *s* counterpart. Now, it is important to keep in mind that the 1*s* orbital introduced by us in the s_l subset cannot be interpreted as something physically significant by itself, because it is not one of the functions of the basis set actually used for the calculations, but belongs to a basis set from whose *contraction* the final physically significant set is obtained; the 1*p* orbital would play the same rôle, and hence it seems advisable to use it. In short, Equ. (1) can be rewritten as

$$|2s_m\rangle = \sqrt{\frac{\alpha^3}{\pi}}\, N(m) \left(1 - \frac{m}{\sqrt{3}}\varrho\right) e^{-\varrho}\,, \tag{5}$$

where α is the orbital exponent, and $\varrho = \alpha r$ is the scaled distance from the nucleus; and, so far, it seems that the most reasonable *p* partner of the orbital (5) should be

$$|2p_{m'}\rangle = \sqrt{\frac{3\alpha^3}{\pi}}\, N(m') \left(1 - \frac{m'}{\sqrt{3}}\varrho\right) e^{-\varrho}\cos\vartheta \tag{6}$$

(m' being determined from the condition of orthogonality to the inner core MO) rather than a *p* orbital having in the radial part a second-degree polynomial in ϱ.

A simple calculation gives the values of m' reported in the last line of Table III. These data reveal that there is a weakness in the above reasoning, because they show (as can be proven algebraically) that the limit of the orbital (6) when the internuclear distance goes to infinity is a $1p$ orbital rather than the expected $2p$ orbital. This makes a physical interpretation of the orbital (6) quite difficult, and one may conclude that inclusion of a $3p$ orbital is a better choice.

A point not apparent in our simple model is that orthogonalization to the inner core involves, in principle, a doubling of the orbitals. In the homonuclear case, if one had to introduce the antibonding valence MO's one should take care that, say, the $2s$ orbitals participating in the $2\sigma u$ MO be modified so as to make it orthogonal to the $1\sigma u$ inner-shell orbital. This condition is not equivalent to that associated with the g symmetry. More generally, let the 1σ molecular orbitals be given as

$$1\sigma = (1\bar{s}_1, 1\bar{s}_2) \begin{vmatrix} q_{11} & q_{12} \\ q_{21} & q_{22} \end{vmatrix} = 1s \cdot Q(1\sigma) \tag{7}$$

nd the 2σ molecular orbitals are given as

$$2\sigma = (s_1, s_2) \begin{vmatrix} C_{11} & C_{12} \\ C_{21} & C_{22} \end{vmatrix} \cdot Q(2\sigma)\,, \tag{8}$$

where s_1 and s_2 contain, say, n elements each. Calling S the $2 \times 2n$ overlap matrix between the set $1s$ and the set $2s \equiv (s_1, s_2)$, we obtain, for the condition that 2σ be orthogonal to 1σ whatever $Q(2\sigma)$ may be,

$$Q^+(1\sigma) \cdot S \cdot C = T \cdot C = 0, \tag{9}$$

where T has been introduced as a $2 \times 2n$ matrix. As C is a $2n \times 2$ matrix, we have four conditions to be satified by $4n$—2 unknowns, and this is clearly possible with $n = 2$, as would be if we used Equ. (1). The difficulty is that we have to accept non-zero elements in C_{21} and C_{12}, thus entering the long dispute about the significance of multi-centre basis orbitals. If we wish to stay in the frame of a simple MO—LCAO scheme, it is better to require that C_{21} and C_{12} should vanish, in which case we have only $2(n - 1)$ unknowns. This means that we must have $n \geq 3$, if we wish to keep the basis set completely independent of $Q(2\sigma)$. An intermediate situation, where we can use a double basis [different values of m in (1) for the bonding and the antibonding MO's] arises if one tries to take advantage of some general property of $Q(2\sigma)$. A case in point is that of homonuclear two-centre bonds, where it is easy to define different $2s_{n\ell}$ orbitals for the g and the u 2σ MO's. If this is not done, one must use

a general form:

$$|2s_{\text{ortho}}> = N(l, lm)\,(|1s> - m|2s> + l|3s>) \tag{10}$$

exactly as would be done in the non-symmetrical case.

Conclusion

The example of radial distortion required by the orthogonality condition is a good illustration of an effect which must be included in an approximate treatment lest one should lose any hope of giving a theoretical interpretation of them. The physical significance of orthogonality originates from the fact that the limits for very large and very small internuclear distances are to satisfy certain conditions known from the theory of atoms. It is interesting to note that, as a byproduct of inter-shell orthogonalization, one can distinguish between two kinds of hybridization. When no orthogonality to the inner shell is required, an SC calculation with hybrids where the s character is a variational parameter will always give as close as possible an approximation *to the* 1σ molecular orbital; consequently, the s character tends to zero for the united-atom limit. On the other hand, at very large internuclear separations, the s character is maximum; continuity then implies an increasing p contribution as the internuclear distance tends to zero [8]. This kind of hybridization is so to say 'essential', and disappears as soon as orthogonality to the inner shell is ensured; only then whatever hybridization is found is really a feature leading to a better approximation of the actual physical situation, and hence has a real physical significance.

We shall not discuss here in detail scaling as a further modification of the basis; we only point out that it is very close to radial distortion because it is not expressible as a linear combination of the basis elements, and affects directly the radial forms of the atomic orbitals. We prefer to close the present remarks with a few words regarding the analysis of charge densities and the reference free-atom orbitals. It is clear that no theory of chemistry is possible if one has no way of comparing the molecular situation with an ideal, free-atom situation. The problem of the reference free-atom orbitals arises all the time whenever we speak of modifications of the basis AO's. In the above discussion, we have assumed that the reference orbitals in question are essentially Slater orbitals, except for the $2s$ orbital, which is supposed to be orthogonalized to the corresponding $1s$ orbital by an appropriate choice of m in Equ. (1). The path to be followed in using these reference orbitals is exemplified in our studies of the model mentioned above, where one of the intermediate calculations is over a Slater determinant with pure-s spinorbitals in no way adjusted to the molecular situation. There are several delicate points in the choices implicit in this kind of comparison, and the question is by no means settled.

Once the reference orbitals have been chosen, the question of the analysis of electron densities ceases to be meaningless. Why one should consider electron densities is nowadays clear: the analyses in terms of single indices like the various kinds of populations are much too arbitrary to be relied upon in drawing physical interpretations, and it seems that, if such indices have to be introduced, it will be best to start all over again. The analysis of electron densities could follow RUEDENBERG's very good treatment [17]. As regards the basis orbitals, one might separate the density associated with a single atomic orbital into a contribution identical with that of the free atom and an 'interference' contribution associated with each successive modification.

The questions just mentioned deserve a separate study. As a conclusion of the present article, we shall briefly summarize the main points illustrated in it [18].

First, a use of *ab initio* calculations that seems to have been largely overlooked because of its simplicity is the construction and analysis of simple models of the chemical bond. Such models may render enormous services both in clarifying previously known results and in suggesting new ones, and in making possible a detailed discussion of interpretation schemes and approximations.

Second, treatments using the LCAO scheme over the valence electrons may be seriously at fault when effects like inter-shell orthogonalization are neglected. Such effects are consequences of the approximations used; nevertheless, they may be physically significant because the corresponding approximations may be essential in order to reach an understanding of the molecular reality. They include changes of the AO's with molecular geometry.

Third, the realization that a certain type of modification of the AO basis is important must be followed by a very careful analysis of the way in which such a correction should be introduced in order to preserve simplicity and physical significance.

We hope that considerations like those given above will help to bridge the apparent gap between the work of researchers devoted to highly sophisticated *ab initio* calculations and the work of researchers interested in a simple if approximate understanding of facts.

REFERENCES

1. G. DEL RE, Theoret. Chim. Acta, **1**, 188, 1963.
2. R. S. MULLIKEN, J. Chimie Phys., **46**, 497, 1949; J. Chem. Phys., **43**, 839, 1965.
3. L. PAULING, The Nature of the Chemical Bond, Cornell, Ithaca, 1956.
4. P. GOMBÁS, Pseudopotentiale, Springer, Berlin, 1967.
5. R. K. NESBET, Adv. Chem. Phys., **9**, 321, 1965; P. O. LÖWDIN, ibid., **8**, 3, 1965; and references therein.
6. W. KUTZELNIGG, G. DEL RE and G. BERTHIER, Phys. Rev., **172**, 49, 1968.
7. G. DAS and A. C. WAHL, J. Chem. Phys., **44**, 87, 1966.

8. B. Cadioli, U. Pincelli and G. Del Re, Theoret. Chim. Acta (Berl.), **10**, 393, 1968.
9. G. Del Re and R. G. Parr, Revs. Mod. Phys., **35**, 604, 1963.
10. W. Moffitt, Proc. Roy. Soc. (London), **A—210**, 245, 1951.
11. H. Suard and G. Berthier, private communication.
12. B. Nelander and G. Del Re, to be published.
13. G. Del Re, Int. J. Quantum Chem., **1**, 293, 1967.
14. C. A. Coulson and G. R. Lester, Trans. Farad. Soc., **51**, 1605, 1955.
15. U. Pincelli, B. Cadioli and G. Del Re, Theoret. Chim. Acta (Berl.), **14**, 253, 1969.
16. A. Rastelli and G. Del Re, Int. J. Quantum Chem., in press; Ri. Sci., **38**, 769, 1968.
17. K. Ruedenberg, Revs. Mod. Phys., **34**, 326, 1962.
18. The point of view adopted in the present paper is very close to that which has inspired much work by R. S. Mulliken. Therefore, in addition to Ref. 2, at least the following articles by him should be consulted: J. Am. Chem. Soc., **88**, 1849, 1966; "Quantum Theory of Atoms, Molecules, and the Solid State", Wiley, New York 1966, p. 231; and the older series including: J. Chem. Phys., **3**, 517, 1933.

МОДЕЛЬ AB INITIO ВЫЧИСЛЕНИЙ И ОБОСНОВАНИЕ МЕТОДА MO—LCAO

ДЖУЗЕППЕ ДЭЛ РЕ

Р е з ю м е

Применение ab initio вычислений, которое оказывается тщательно проверенным благодаря его простоте, является истолкованием и анализом простых моделей химической связи. Такие модели могут оказывать огромную помощь, как при уточнении заранее известных результатов, так и при исследовании новых, далее сделают возможным подробную дискуссию интернациональных схем и приближений. Приемы, применяющие LCAO схему в случае валентных электронов, могут давать серьезно ошибочный результат, если пренебречь эффектами, обусловленными ортогонализацией внутренних оболочек. Такие эффекты следуют из примененного приближения, хотя они могут быть физически важными, так как соответствующие приближения иногда необходимы с целью обеспечения понятности молекулярной реальности. Они включают в себя изменения атомных орбит с молекулярный геометрией. За реализацией, в которой модификация базиса атомных орбит определенного типа важна, обязательно должен следовать очень тщательный анализ приема, в рамках которого имеется возможность для введения данной коррекции с целью сохранения простоты и физических характерностей.

Acta Physica Academiae Scientiarum Hungaricae, Tomus 27, pp. 493—521 (1969)

STUDY OF THE ELECTRONIC STRUCTURE OF MOLECULES. X*

GROUND STATE FOR ADENINE, CYTOSINE, GUANINE AND THYAMINE

By

E. CLEMENTI, J. M. ANDRÉ[1], M. Cl. ANDRÉ[1], D. KLINT[2] and D. HAHN[3]

IBM RESEARCH LABORATORY, MONTEREY AND COTTLE ROADS, SAN JOSÉ, CALIFORNIA 95114, USA

(Received 12. III. 1969)

All electrons SCF-LCAO-MO computations for adenine, cytosine, guanine and thyamine are reported. In addition, to compute the total energies and wave functions we have computed the relative gross charges and the dipole moment. Analysis of the orbital energy for the inner shell indicates that there are three effects which govern the orbital energies splitting for inner shell a) the gross charge, or ionicity degree, of the atom in consideration, b) its valency state, c) the neighbor atoms ionicities. The first two effects are sufficient for determining the relative location of the inner shell as well as for estimating the extrema of the splitting of the inner shell electrons of a given type of atoms.

The gross charge population was used to determine the overall flow of the σ and π charge transfer. It was found that the charge transfer flow requires direct consideration of at least next nearest neighbors to be explained. In addition, it was found that simple π electron considerations could lead to not only quantitative but even to qualitative erroneous prediction about the electronic charge distribution. For example, an atom can be positively charged, if one considers only the π electrons, and the same atom can be negatively charged, if one considers only the σ electrons. Therefore, we reiterate on the necessity of all electron computations not only for quantitative but even for qualitative studies of the electronic structure in molecules.

I. Introduction

This work was initiated the summer of 1967 by CLEMENTI and HAHN. Cytosine was computed using Version 2 of IBMOL on an IBM 360/50 and reported at the Kutna Hora meeting and at the Hungarian Summer School in 1967. The remaining molecules of this paper were computed with Version 4 of IBMOL on an IBM 360/65 computer. The four molecules are clearly of importance in biological study. However, we wish to point out that there might be a great gap between computing the electronic structure of a biologically important molecule and contributing to our understanding of biological mechanisms. Therefore, throughout this paper no further mention will be made to the possible biological implication of this work, and we shall consider these four molecules as additional compounds (containing hydrogen, carbon, nitrogen

* Dedicated to Prof. P. GOMBÁS on his 60th birthday.

[1] Present address: Laboratoire de Chimie Quantique, Kapeldreef, Egenhoven-Heverle, Belgium.

[2] Present address: Washington State University, Dept. of Chemistry, Pullman, Washington, USA.

[3] Present address: Stanford University, Department of Chemistry, Stanford, California, USA.

Table I

Orbital exponents of Gaussian functions for hydrogen, carbon, nitrogen and oxygen

	hydrogen	carbon	nitrogen	oxygen
		s-type functions		
1	4.500370	391.445	636.101	1113.12
2	0.681277	64.7358	105.386	172.260
3	0.151374	16.2247	27.5167	42.8008
4		5.33460	9.02708	13.3710
5		2.00995	3.33086	4.83970
6		0.502323	0.828625	1.07380
7		0.155139	0.243109	0.31690
		p-type functions**		
8	*	4.316130	5.19829	6.92200
9		0.873682	1.10716	1.42610
10		0.202860	0.26175	0.32120

* No *p*-type function was used for hydrogen atoms.

** The *p* functions can be either p_x or p_y or p_z; for the 3 different cases the angular part is clearly different, but the orbital exponent was kept constant.

Table II

Contracted Gaussian set for hydrogen (H), carbon (C), nitrogen (N) and oxygen (O)

1*s* (H)	$0.070480\chi_1 + 0.407890\chi_2 + 0.647669\chi_3$
1*s* (C)	$0.022220\chi_1 + 0.132968\chi_2 + 0.384690\chi_3 + 0.458385\chi_4 + 0.154547\chi_5$
2*s* (C)	$0.534240\chi_6 + 0.524992\chi_6$
2*p* (C)	$0.108451\chi_8 + 0.461164\chi_9 + 0.630435\chi_{10}$
1*s* (N)	$0.018231\chi_1 + 0.108122\chi_2 + 0.324286\chi_3 + 0.478333\chi_4 + 0.221201\chi_5$
2*s* (N)	$0.466703\chi_6 + 0.596283\chi_7$
2*p* (N)	$0.138430\chi_8 + 0.497601\chi_9 + 0.575051\chi_{10}$
1*s* (O)	$0.013221\chi_1 + 0.087629\chi_2 + 0.296295\chi_3 + 0.492042\chi_4 + 0.258935\chi_5$
2*s* (O)	$0.497086\chi_6 + 0.566094\chi_7$
2*p* (O)	$0.148880\chi_8 + 0.516709\chi_9 + 0.558700\chi_{10}$

The $\chi_1, \chi_2 \ldots$ are the Gaussian functions given in Table I. Clearly the $\chi_1 \ldots \chi_3$ to be used for the 1s(H) are those in column 2 of Table I (or the $\chi_1 \ldots \chi_5$ for oxygen are those in column 5 of Table I.)

Table III

Total energy in a.u. for the atoms using the Gaussian set of Table I and comparison to other sets

basis set	Table II	Table I	minimal Slater[a]	Hartree-Fock[b]	exact[c]
hydrogen (^2S)	— 0.4970	0.4988	— 0.5000	— 0.5000	— 0.5000
carbon (^3P)	—37.5900	—37.6296	—37.6224	—37.6886	—37.8558
nitrogen (^4S)	—54.2440	—54.3130	—54.2689	—54.4009	—54.6122
oxygen (^3P)	—74.5973	—74.6763	—74.5404	—74.8094	—75.1101

a) From E. CLEMENTI and D. RAIMONDI, J. Chem. Phys., **38**, 2686, 1963.
b) From E. CLEMENTI, Tables of Atomic Functions [8].
c) From A. VEILLARD and E. CLEMENTI, J. Chem. Phys., **49**, 2415, 1968.

and oxygen atoms) in the list of molecules previously studied in this series of papers. The work is carried out in the self-consistent field, (SCF) linear combinations of atomic orbitals (LCAO) approximation. The basis set we have used (Table I) for the H, C, N, and O atoms is the same basis set previously used. The same holds for the contraction coefficients (Table II). The reason is not that such a basis set is a particularly good one, but is the best that can be done with 7*s* type gaussians and 3*p* type gaussians. When we programmed our molecular package [1] we decided to compromise in the basis set size so as to be in a position to compute a large number of rather complex molecules within the same accuracy, so as to be in a position to compare results from molecule to molecule. At that time the above basis set did seem the best compromise, between accuracy and realistic possibility to carry out our program of study in the electronic structure of molecules. Comparison between our basis set and other more adequate is given in Table III. From these considerations it is clear that the results presented in this work are of preliminary value. The main feature in these computations is that the model used (SCF—LCAO) is very well defined, that no approximation is made in the integrals computations or even more, in the number of electrons explicitly considered for the molecular system. From previous work in this series [2] we know that the so-called π electrons cannot be considered as some separated and privileged set from the so-called σ electrons (the notation σ and π is most unfortunate since it is correct only for linear systems; however, we shall continue to use such bad notation only in deference to a careless as well as very vast body of literature). Hence, the need for all-electrons ab initio computations. From other work (to be published [3]) we know that the inner shell electrons are more important for determination of molecular geometry than previously assumed. Hence, the need for equal treatment for inner shell and valency electrons. The simple n^4 relation (where n is the basis set size for a given molecule) and required number of many-center integrals, clearly poses a practical limit in the computations [4].

II. Computational results

The geometry we have used for adenine, cytosine, guanine and thyamine (hereafter referred to as A, C, G and T) are given in Tables IV, V, VI and VII, resp ectively. Figs. 1, 2, 3 and 4 complement these tables. The total energy as well as the orbital energies are given in Tables VIII through XI for A, C, G and T, respectively.

The expansion coefficients for each orbital, obtained from the SCF procedure are too long to be reported and are available elsewhere [5]. The gross population analyses [7] are given in Table XII through XV for A, C, G and T, respectively, and the hybridization for each atom is given in Tables

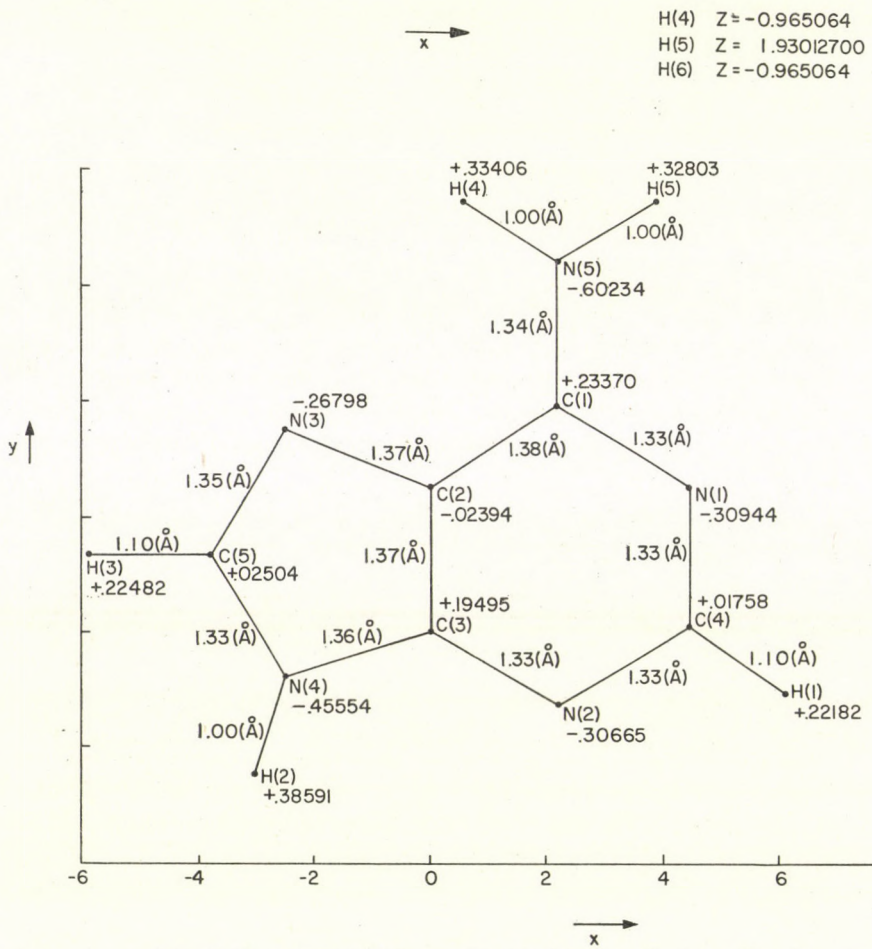

Fig. 1. Geometry and gross charges for the adenine molecule

CYTOSINE (LACTAM I) bond distances, gross charges*

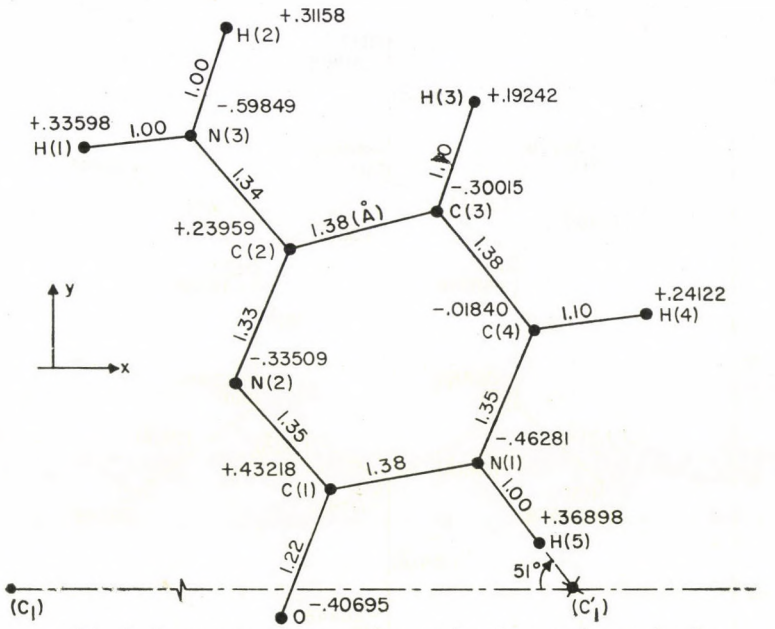

Fig. 2. Geometry and gross charges for the cytosine molecule

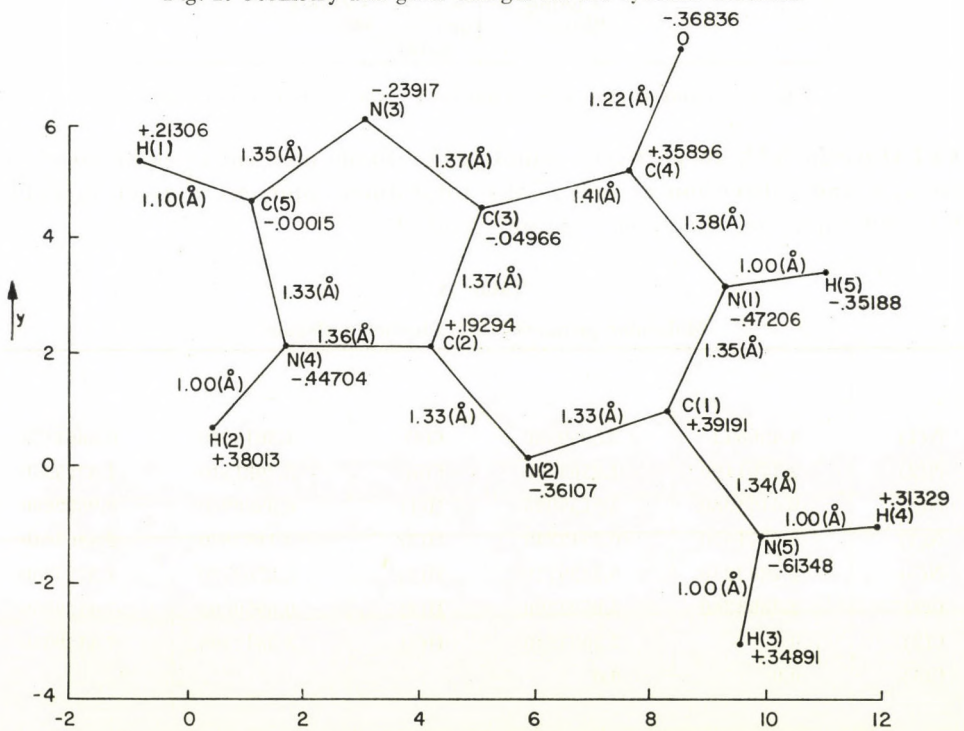

Fig. 3. Geometry and gross charges for the guanine molecule

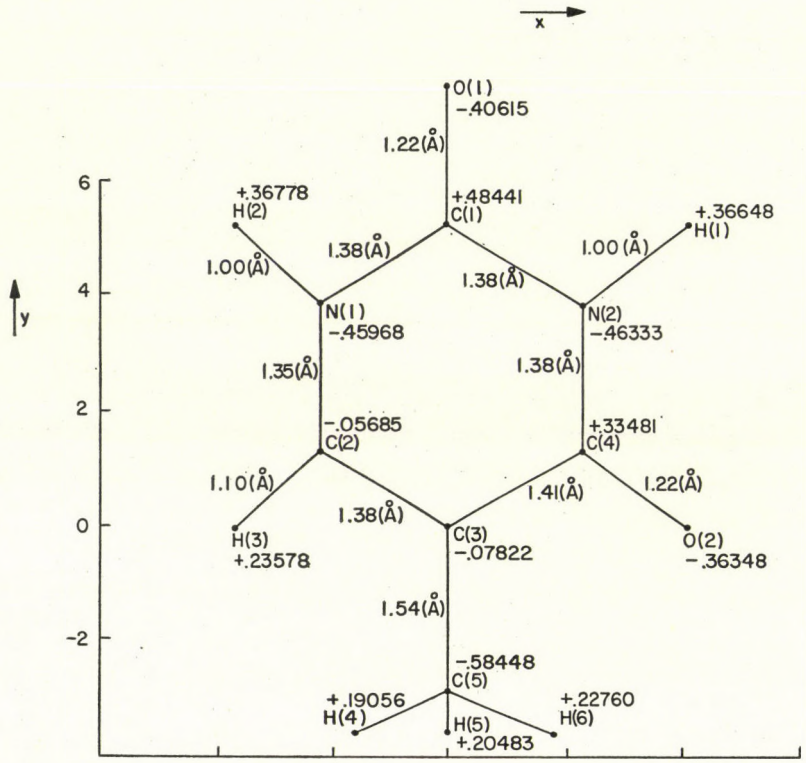

Fig. 4. Geometry and gross charges for the thyamine molecule

XVI through XIX respectively. Finally, the dipole moment in components in the x, y and z direction as well as the total dipole moment is given in Table XX. All quantities are given in atomic units [7].

Table IV

Molecular geometry for adenine molecule*

	x	y		x	y
N(1)	4.456643	2.5959530	C(4)	4.3013910	0.0864170
N(2)	2.1761190	—1.2563760	C(5)	—3.7981510	1.3725350
N(3)	—2.4164080	3.5159020	H(1)	6.0908940	—0.9682600
N(4)	—2.4571470	—0.7512240	H(2)	—3.1187670	—2.5207840
N(5)	2.2803240	6.3839750	H(3)	—5.8763680	1.3725350
C(1)	2.2803240	3.8523290	H(4)	0.6959090	7.4129050
C(2)	0.0	2.5883240	H(5)	3.8647390	7.4129050
C(3)	0.0	0.0			

* Distances are given in atomic units; the value of the z coordinate is 0.

Table V

Molecular geometry for the cytosine (lactam 1) molecule*

	x	y		x	y
0	15.682272	−0.4604511	H(1)	12.264164	7.6893053
N(1)	19.039032	2.1588593	H(2)	14.692337	9.7267876
N(2)	14.826015	3.6494255	H(3)	18.995163	8.4874620
N(3)	14.139829	7.9196091	H(4)	22.047836	4.8494406
C(1)	16.470795	1.7060061	H(5)	20.228302	0.6902478
C(2)	15.767538	5.9797821			
C(3)	18.318405	6.5219889			
C(4)	19.994705	4.5242567			

* Distances are given in atomic units; the value of the z coordinate is 0.

Table VI

Molecular geometry for the guanine molecule*

	x	y		x	y
0	8.5351915	7.3326225	C(3)	5.1557379	4.5441399
N(1)	9.2876520	3.0396242	C(4)	7.7466660	5.1661663
N(2)	5.8988562	0.1219844	C(5)	1.1614723	4.6027842
N(3)	3.1580334	6.1909208	H(1)	−0.8040018	5.2795506
N(4)	1.7482090	2.1588602	H(2)	0.5589515	0.6902482
N(5)	9.9972229	−1.2595730	H(3)	9.4605036	−3.0715036
C(1)	8.3526487	0.6659773	H(4)	11.8708070	−1.0129108
C(2)	4.3342476	2.0889683	H(5)	11.1612360	3.2862854

* Distances in atomic units; the z coordinate is 0.

III. Discussion on the orbital energies for inner shell electrons

The orbital energies of the separated atoms, namely the eigenvalues ε_i of the equation

$$F\varphi_i = \varepsilon_i \varphi_i ,$$

where φ_i is the i-th orbital, and F the Hartree—Fock operator (the field seen by φ_i) are clearly related to the orbital energies of the atoms in the molecule. However, the relation is not too immediate. First of all the field F is no longer the atomic field but the molecular field. Second, the φ_i in the molecule are not localized at the atom site, but delocalized over the entire molecular frame

Table VII

Molecular geometry for the thyamine molecule*

	x	y	z
O(1)	0.0	7.4626860	0.0
O(2)	4.1881240	0.0	0.0
N(1)	—2.2579160	3.8541470	0.0
N(2)	2.3049310	3.9391650	0.0
C(1)	0.0	5.1577550	0.0
C(2)	—2.2579160	1.3036080	0.0
C(3)	0.0	0.0	0.0
C(4)	2.307002	1.3319480	0.0
C(5)	0.0	—2.9095030	0.0
H(1)	3.9030790	5.0821840	0.0
H(2)	—3.7917320	5.0821840	0.0
H(3)	—3.9297180	0.13380900	0.0
H(4)	—1.6715400	—3.6274320	—0.96506400
H(5)	0.0	—3.6274320	1.93012700
H(6)	1.6715400	—3.6274320	—0.96506400

* Distances in atomic units

(subject to symmetry constraints). If the molecular orbitals are only slightly delocalized as compared to the atoms, and if the dominant part of the field is the atomic field, then the orbital energies in the separated atoms will resemble substantially the orbital energies in the molecule. This is the case of the inner shell electrons. The orbital energies of the $1s^2$ electrons in the carbon (^3P), nitrogen (^4S) and oxygen (^2P) atomic ground state are —11.32552 a. u., —15.62892 a. u., —20.66864 a. u., respectively [8]. With this in mind it is simple to correlate the inner shell electrons of the four molecules (Tables VIII, IX, X and XI) with the inner shell of the separated atoms. Fig. 5 makes this correlation explicit for the case of cytosine. However, the correlation is only qualitative. For instance, the spread in the orbital energies for the carbon atom goes from 11.53 a. u. to —11.44 a. u., from —11.56 a. u. to —11.41 a. u., from —11.59 a. u. to —11.40 a. u. and from —11.61 a. u. to —11.39 a. u. for A, C, G and T, respectively. In other words, there is a spread of about 3 to 6 electron volts. These fluctuations are substantial, strongly pointing against the simplifying assumption that the inner shells in molecules are as the inner shells of the corresponding separated atoms. The electronic density is very much the same, however, but since the inner shell electrons are highly energetic, a small variation in density has a large effect on the energy. For equivalent reasons, a relatively large density variation in valency electrons corresponds to a relatively

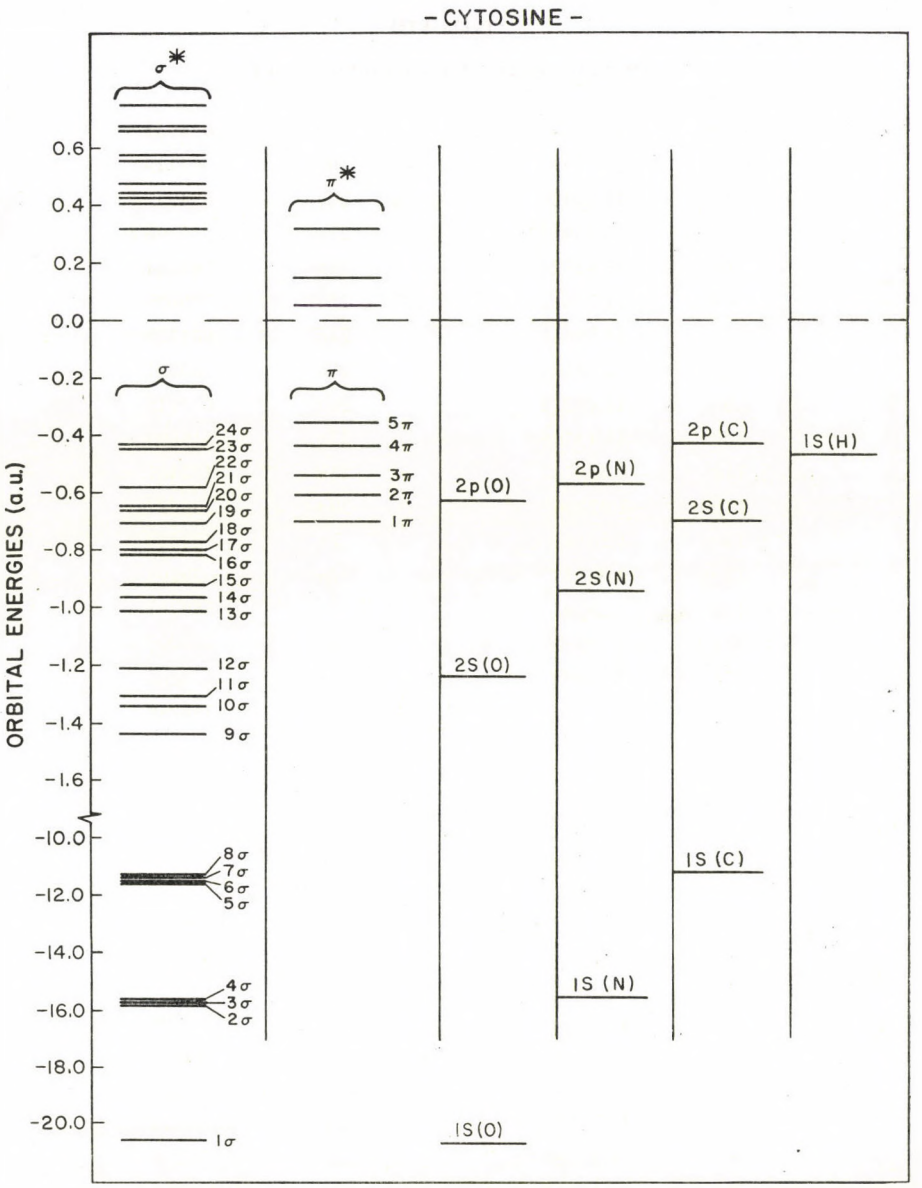

Fig. 5. Comparison of orbital energies for cytosine with the orbital energies of the component atoms in the ground state

small energy variation. Indeed, from analysis of Tables XIII through XVII, we see that the valency shell splitting in the molecular field as compared to the separated atoms is of the same order of magnitude as the inner shell splitting.

From the previous discussion it follows that we should be able to state something more quantitative about the splitting of the inner orbital energies

Table VIII

Orbital energies for adenine (in a.u.)*

1σ	−15.75998	18σ	−.924933
2σ	−15.65410	19σ	−.904119
3σ	−15.65020	20σ	−.83495
4σ	−15.63953	21σ	−.785000
5σ	−15.63526	22σ	−.743324
6σ	−11.53362	23σ	−.739640
7σ	−11.51086	24σ	−.684126
8σ	−11.49101	25σ	−.663891
9σ	−11.48222	26σ	−.647116
10σ	−11.43706	27σ	−.519899
11σ	−1.45674	28σ	−.482487
12σ	−1.37406	29σ	−.436027
13σ	−1.28443	1π	−.724339
14σ	−1.24147	2π	−.638200
15σ	−1.20797	3π	−.560701
16σ	−1.10388	4π	−.488591
17σ	−0.961035	5π	−.443605
		6π	−.366840

* Total energy = −462.55284 a. u.

Table IX

Orbital energies for cytosine (in a.u.)*

1σ	−20.487343	16σ	−0.812685
2σ	−15.729407	17σ	−0.805849
3σ	−15.661884	18σ	−0.771609
4σ	−15.595631	19σ	−0.705790
5σ	−11.569219	20σ	−0.664342
6σ	−11.533484	21σ	−0.651121
7σ	−11.517662	22σ	−0.588110
8σ	−11.407959	23σ	−0.454238
9σ	−1.443140	24σ	−0.442661
10σ	−1.341111	1π	−0.702333
11σ	−1.309476	2π	−0.609556
12σ	−1.209500	3π	−0.544552
13σ	−1.120933	4π	−0.437576
14σ	−0.960774	5π	−0.361283
15σ	−0.923618		

* Total energy −390.93564 a.u.

Table X

Orbital energies for guanine (in a.u.)*

1σ	—20.53240	21σ	—0.88660
2σ	—15.74850	22σ	—0.85184
3σ	—15.72616	23σ	—0.80546
4σ	—15.68678	24σ	—0.78431
5σ	—15.63471	25σ	—0.74539
6σ	—15.61607	26σ	—0.72761
7σ	—11.59306	27σ	—0.68175
8σ	—11.56340	28σ	—0.62823
9σ	—11.49640	29σ	—0.61354
10σ	—11.45654	30ϱ	—0.50676
11σ	—11.40342	31σ	—0.46656
12σ	—1.45529	32σ	—0.44245
13σ	—1.42078	1π	—0.72983
14σ	—1.38907	2π	—0.67628
15σ	—1.26388	3π	—0.60963
16σ	—1.25621	4π	—0.50039
17σ	—1.22620	5π	—0.49096
18σ	—1.08293	6π	—0.45257
19σ	—0.96778	7π	—0.33471
20σ	—0.93780		

* Total energy —537.13942 a.u.

as compared to the separated atoms. We shall now use this same type of reasoning adopted in the study for inner shells analysis given elsewhere [3]. From Tables XII, XIII, XIV and XV we know that the atoms are not neutral in the molecule but have excess or deficiency of electrons due to charge transfer. This fact ought to be the first order correction in the orbital energies of the inner shell. For example, the carbons in adenine have lost 0 234, 0.195, 0.018 and 0.025 electrons in C(1), C(3), C(4) and C(5) and gained 0.024 in C(2), respectively. The $C^+(^2P)$ ion has an orbital energy [8] of —11.8983 a. u. (to be compared with —11.3255 a. u. for the neutral atom in the ^3P state). If, most approximatively we assign an energy difference of —11.8983—11.3255—0.5728 a. u. for the loss of one electron and use this number for the fractional losses in the carbon atoms of adenine we obtain the orbital energies reported in Table XXI, with an energy spread of 0.1577 a. u.; this value should be compared with a spread of —11.53362+11.43706=—0.09656 a. u. given the computation reported in Table VIII. Therefore, we seem to have some quantitative understanding of the inner shell orbital energies spread.

Table XI

Orbital energies, ε, for thyamine (in a.u.)*

ε_1	−20.53970	ε_{18}	−0.82544
ε_2	−20.53656	ε_{19}	−0.81492
ε_3	−15.73519	ε_{20}	−0.75640
ε_4	−15.70864	ε_{21}	−0.73289
ε_5	−11.61562	ε_{22}	−0.68439
ε_6	−11.56386	ε_{23}	−0.64193
ε_7	−11.49468	ε_{24}	−0.63905
ε_8	−11.41183	ε_{25}	−0.63041
ε_9	−11.39018	ε_{26}	−0.61814
ε_{10}	−1.48448	ε_{27}	−0.61304
ε_{11}	−1.44039	ε_{28}	−0.58368
ε_{12}	−1.33965	ε_{29}	−0.56292
ε_{13}	−1.28092	ε_{30}	−0.49831
ε_{14}	−1.14551	ε_{31}	−0.46663
ε_{15}	−1.00557	ε_{32}	−0.44665
ε_{16}	−0.96609	ε_{33}	−0.38722
ε_{17}	−0.91973		

* Total energy −449.59107 a.u.

Having a somewhat better understanding of the spread of orbital energies, let us discuss in more detail its absolute values. We have determined the spread by comparing the neutral carbon in the ^3P state. We should not use the ^3P state, since the molecule can be envisioned to be formed by atoms in the "valency state". Most important, we should take some state that is more diffuse than the ^3P and a singlet state. If we take as basis the ^1S state of carbon, then, after having computed the splitting we should lower the orbital energy by $-11.39111+11.32552=0.065$ a. u. (where −11.39222 is the $\varepsilon(^1S)$ for $C(^3P)$ and −11.32552 is the $\varepsilon(^1S)$ for $C(^1S)$ as known from previous work [8]). We would, therefore, expect in this level of crude approximation to have the following orbital energies for the inner shell electrons of the carbon atoms in adenine: −11.534 a. u., −11.502 a. u., −11.502 a. u., −11.405 a. u., −11.404 a. u., −11.402 a. u. to be compared with these of Table VIII. Up to now we have (1) analyzed the effect of the spread of the orbital energies and (2) we have adjusted the baricent of the orbital energies manifold for the inner shells.

In Table XXI we report the orbital energies for the inner shell electrons on the carbon atoms for adenine as given in Table VIII (first column), the orbital energies we would obtain by knowledge of the ionicity on the carbon atoms (second column), the orbital energies of the second column corrected by a more adequate choice so as to approximate the valency state (^1S rather than ^3P) [9].

Table XII

Adenine — gross charges

		N(1)	
$1s$	1.99732	$1s = 1.99732$	$\delta(\sigma) = -0.13653$
$2s$	1.47328	$2s = 1.47328$	$\delta(\pi) = -0.77291$
$2p_x$	1.48730	$2p = 3.83882$	$\delta(\text{tot}) = -0.30944$
$2p_y$	1.17861		
$2p_z$	1.17291		
		N(2)	
$1s$	1.99730	$1s = 1.99730$	$\delta(\sigma) = -0.25040$
$2s$	1.45077	$2s = 1.45077$	$\delta(\pi) = -0.15625$
$2p_x$	1.02527	$2p = 3.85856$	$\delta(\text{tot}) = -0.30665$
$2p_y$	1.67704		
$2p_z$	1.15624		
		N(3)	
$1s$	1.99748	$1s = 1.99748$	$\delta(\sigma) = +0.06555$
$2s$	1.54724	$2s = 1.54724$	$\delta(\pi) = -0.33353$
$2p_x$	1.05991	$2p = 3.92321$	$\delta(\text{tot}) = -0.26798$
$2p_y$	1.52982		
$2p_z$	1.33353		
		N(4)	
$1s$	1.99729	$1s = 1.99729$	$\delta(\sigma) = -0.81401$
$2s$	1.34616	$2s = 1.34616$	$\delta(\pi) = +0.35847$
$2p_x$	1.18404	$2p = 4.11207$	$\delta(\text{tot}) = -0.45554$
$2p_y$	1.28650		
$2p_z$	1.64153		
		N(5)	
$1s$	1.99726	$1s = 1.99726$	$\delta(\sigma) = -0.79717$
$2s$	1.36749	$2s = 1.36749$	$\delta(\pi) = -0.19483$
$2p_x$	1.27738	$2p = 4.23757$	$\delta(\text{tot}) = -0.60234$
$2p_y$	1.15502		
$2p_z$	1.80517		

Table XII (continued)

C(1)

$1s$	1.99942	$1s = 1.99942$	$\delta(\sigma) = +0.14255$
$2s$	0.93633	$2s = 0.93633$	$\delta(\pi) = +0.09115$
$2p_x$	0.99680	$2p = 2.83054$	$\delta(\text{tot}) = +0.23370$
$2p_y$	0.92489		
$2p_z$	0.90885		

C(2)

$1s$	1.99902	$1s = 1.99902$	$\delta(\sigma) = +0.13066$
$2s$	0.93213	$2s = 0.93213$	$\delta(\pi) = -0.15460$
$2p_x$	0.95886	$2p = 3.09277$	$\delta(\text{tot}) = -0.02394$
$2p_y$	0.97931		
$2p_z$	1.15460		

C(3)

$1s$	1.99932	$1s = 1.99932$	$\delta(\sigma) = +0.21805$
$2s$	0.92375	$2s = 0.92375$	$\delta(\pi) = -0.02310$
$2p_x$	0.87516	$2p = 2.88196$	$\delta(\text{tot}) = +0.19495$
$2p_y$	0.98370		
$2p_z$	1.02310		

C(4)

$1s$	1.99936	$1s = 1.99936$	$\delta(\sigma) = -0.00912$
$2s$	1.02373	$2s = 1.02373$	$\delta(\pi) = +0.02670$
$2p_x$	1.05141	$2p = 2.95932$	$\delta(\text{tot}) = +0.01758$
$2p_y$	0.93461		
$2p_z$	0.97330		

C(5)

$1s$	1.99926	$1s = 1.99926$	$\delta(\sigma) = +0.00569$
$2s$	1.01971	$2s = 1.01971$	$\delta(\pi) = -0.03073$
$2p_x$	1.09616	$2p = 2.95596$	$\delta(\text{tot}) = +0.02504$
$2p_y$	0.82907		
$2p_z$	1.03073		

Table XII (continued)

		H(1)	
1*s*	0.77818		δ(tot) = +0.22182
		H(2)	
1*s*	0.61409		δ(tot) = +0.38592
		H(3)	
1*s*	0.77518		δ(tot) = +0.22482
		H(4)	
1*s*	0.66594		δ(tot) = +0.33406
		H(5)	
1*s*	0.67197		δ(tot) = +0.32803

IV. Discussion on the orbital energies of the valency electrons

The relevant features of the orbital energies of the valency electrons are those previously noted in other papers of this series [2]. The σ and π electrons (see for comparison, Fig. 6) are fully intermixed. In addition, the highest filled π orbital is always somewhat higher than the highest filled σ orbital. The spread in the π orbital energies is rather constant and this deserves some note. The four molecules contain C, N and O atoms as contributors to the π system. The orbital energies for the $2p$ electrons in the separated atoms [8] (for the ground state) are —0.43334 a. u., —0.56753 a. u. and —0.63186 a. u., respectively. However, the splitting of the π electron orbital energies seems rather independent of the original orbital energies in the separated atoms. For instance, the lowest π orbital energy is —0.724 a. u. in adenine and the lowest π orbital energy is —0.702 a. u. in cytosine. It is noted that adenine does not contain oxygen atoms whereas cytosine contains an oxygen atom. The explanation is in the delocalization of the π electrons cloud. In other words the field seen by the π electrons resembles very little the field seen by the corresponding $2p$ electron in the separated atom.

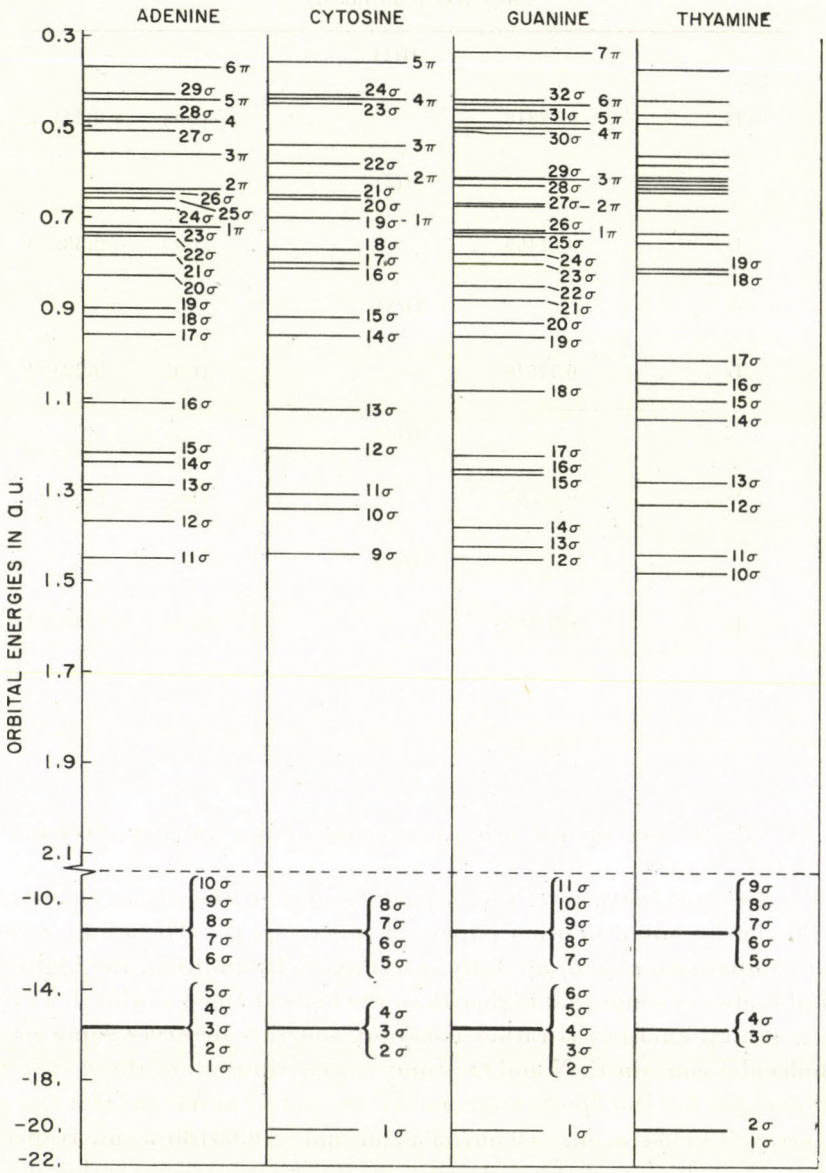

Fig. 6. Comparison of orbital energies for A, C, G, T.

V. Charge transfer

Probably one of the most interesting aspects of the electronic structure of the four molecules is its charge transfer mechanism. We find the two way charge transfer (σ in one direction and π in the opposite) as well as the one way charge transfer (σ and π in the same direction as charge transfer goes).

Table XIII

Cytosine — gross charges

		O	
$1s$	1.99761	$1s = 1.99761$	$\delta(\sigma) = -.08093$
$2s$	1.78662	$2s = 1.78662$	$\delta(\pi) = -.32602$
$2p_x$	1.82903	$2p = 4.62272$	$\delta(\text{tot}) = -.40695$
$2p_y$	1.46767		
$2p_z$	1.32602		
		N(1)	
$1s$	1.99727	$1s = 1.99727$	$\delta(\sigma) = -.78095$
$2s$	1.34673	$2s = 1.34673$	$\delta(\pi) = +.31814$
$2p_x$	1.22440	$2p = 4.11855$	$\delta(\text{tot}) = -.46281$
$2p_y$	1.21255		
$2p_z$	1.68186		
		N(2)	
$1s$	1.99727	$1s = 1.99727$	$\delta(\sigma) = -.05650$
$2s$	1.47290	$2s = 1.47290$	$\delta(\pi) = -.27859$
$2p_x$	1.59502	$2p = 3.86492$	$\delta(\text{tot}) = -.33509$
$2p_y$	.99131		
$2p_z$	1.27859		
		N(3)	
$1s$	1.99729	$1s = 1.99729$	$\delta(\sigma) = -.79299$
$2s$	1.36971	$2s = 1.36971$	$\delta(\pi) = +.19450$
$2p_x$	1.23300	$2p = 4.23149$	$\delta(\text{tot}) = -.59849$
$2p_y$	1.19299		
$2p_z$	1.80550		
		C(1)	
$1s$	1.99959	$1s = 1.99959$	$\delta(\sigma) = +.39038$
$2s$	.88488	$2s = .88488$	$\delta(\pi) = +.04180$
$2p_x$	.83823	$2p = 2.68335$	$\delta(\text{tot}) = +.43218$
$2p_y$	.88692		
$2p_z$	.95820		

Table XIII (continued)

		C(2)	
$1s$	1.99942	$1s = 1.99942$	$\delta(\sigma) = +.10616$
$2s$	.95047	$2s = .95047$	$\delta(\pi) = +.13343$
$2p_x$	1.00245	$2p = 2.81052$	$\delta(\text{tot}) = +.23959$
$2p_y$	.94150		
$2p_z$	.86657		
		C(3)	
$1s$	1.99893	$1s = 1.99893$	$\delta(\sigma) = -.08390$
$2s$	1.01854	$2s = 1.01854$	$\delta(\pi) = -.21625$
$2p_x$	.96950	$2p = 3.28268$	$\delta(\text{tot}) = -.30015$
$2p_y$	1.09693		
$2p_z$	1.21625		
		C(4)	
$1s$	1.99934	$1s = 1.99934$	$\delta(\sigma) = -.15142$
$2s$	1.06409	$2s = 1.06409$	$\delta(\pi) = +.13302$
$2p_x$	1.15816	$2p = 2.95497$	$\delta(\text{tot}) = -.01840$
$2p_y$	.92983		
$2p_z$	.86698		
		H(1)	
$1s$	.66402		$\delta(\sigma) = +.33598$
		H(2)	
$1s$	.68842		$\delta(\sigma) = +.31158$
		H(3)	
$1s$	.80758		$\delta(\sigma) = +.19242$
		H(4)	
$1s$	.75878		$\delta(\sigma) = +.24122$
		H(5)	
$1s$	.63102		$\delta(\sigma) = +.36898$

Table XIV

Guanine — gross charges

		O	
$1s$	1.99763	$1s = 1.99763$	
$2s$	1.79034	$2s = 1.79034$	$\delta(\pi) = -0.28447$
$2p_x$	1.84502	$2p = 4.58037$	$\delta(\text{tot}) = -0.36836$
$2p_y$	1.45088		
$2p_z$	1.28447		
		N(1)	
$1s$	1.99727	$1s = 1.99724$	
$2s$	1.33629	$2s = 1.33629$	$\delta(\pi) = +0.27436$
$2p_x$	1.26190	$2p = 4.13851$	$\delta(\text{tot}) = -0.47206$
$2p_y$	1.15097		
$2p_z$	1.72564		
		N(2)	
$1s$	1.99715	$1s = 1.99715$	
$2s$	1.43982	$2s = 1.43982$	$\delta(\pi) = -0.32450$
$2p_x$	1.02358	$2p = 3.92408$	$\delta(\text{tot}) = -0.36107$
$2p_y$	1.57600		
$2p_z$	1.32450		
		N(3)	
$1s$	1.99755	$1s = 1.99755$	
$2s$	1.55440	$2s = 1.55440$	$\delta(\pi) = -0.09131$
$2p_x$	1.00216	$2p = 3.68720$	$\delta(\text{tot}) = -0.23917$
$2p_y$	1.59373		
$2p_z$	1.09131		
		N(4)	
$1s$	1.99731	$1s - 1.99731$	
$2s$	1.35154	$2s - 1.35154$	$\delta(\pi) = +0.37637$
$2p_x$	1.21527	$2p - 4.09816$	$\delta(\text{tot}) = -0.44704$
$2p_y$	1.25926		
$2p_z$	1.62363		

Table XIV (continued)

		N(5)	
$1s$	1.99724	$1s$ — 1.99724	
$2s$	1.36690	$2s$ = 1.36690	$\delta(\pi)$ = +0.17522
$2p_x$	1.20866	$2p$ = 4.24931	δ(tot) = −0.61348
$2p_y$	1.21587		
$2p_z$	1.88470		
		C(1)	
$1s$	1.99953	$1s$ = 1.99953	
$2s$	0.91689	$2s$ = 0.91689	$\delta(\pi)$ = +0.11905
$2p_x$	0.94124	$2p$ = 2.69166	δ(tot) = +0.39191
$2p_y$	0.86947		
$2p_z$	0.88095		
		C(2)	
$1s$	1.99932	$1s$ — 1.99932	
$2s$	0.93123	$2s$ = 0.93123	$\delta(\pi)$ = −0.01167
$2p_x$	0.85765	$2p$ = 2.87650	δ(tot) = +0.19294
$2p_y$	1.00718		
$2p_z$	1.01167		
		C(3)	
$1s$	1.99900	$1s$ = 1.99900	
$2s$	0.93424	$2s$ = 0.93424	$\delta(\pi)$ = −0.21138
$2p_x$	0.97198	$2p$ = 3.11640	δ(tot) = −0.04966
$2p_y$	0.93304		
$2p_z$	1.21138		
		C(4)	
$1s$	1.99955	$1s$ = 1.99955	
$2s$	0.90738	$2s$ = 0.90738	$\delta(\pi)$ = +0.06713
$2p_x$	0.97524	$2p$ = 2.73409	δ(tot) = +0.35896
$2p_y$	0.82598		
$2p_z$	0.93287		

Table XIV (continued)

		C(5)	
$1s$	1.99922	$1s = 1.99922$	
$2s$	1.0113	$2s = 1.01113$	$\delta(\pi) = -0.08874$
$2p_x$	1.08504	$2p = 2.98978$	$\delta(\text{tot}) = -0.00015$
$2p_y$	0.81600		
$2p_z$	1.08874		
		H(1)	
$1s$	0.78694		$\delta(\text{tot}) = +0.21306$
		H(2)	
$1s$	0.61987		$\delta(\text{tot}) = +0.38013$
		H(3)	
$1s$	0.65109		$\delta(\text{tot}) = +0.34897$
		H(4)	
$1s$	0.68671		$\delta(\text{tot}) = +0.31329$
		H(5)	
$1s$	0.64812		$\delta(\text{tot}) = +0.35188$

It might be of interest to reconstruct the flow of electrons. For this reason we attempt to indicate the mechanism of charge transfer within the following simplifying assumption: *if a donor and an acceptor are nearest neighbors, we assume that the charges donated by the donor are accepted as fully as possible by the nearest acceptor.* Of course this assumption is arbitrary because of the indistinguishability of the electron which prevents us from labeling an electron or fraction of it. However, from a "model" view point, we would like to establish the characteristic of a "flow" in the hope that this flow of electrons would be somewhat transferable from molecule to molecule. It is noted that the arbitrariness of our assumption is the very same encountered in assigning gross populations, or in referring to atoms in a molecular system. Let us consider, for example, the case of the thyamine molecule for which we have attempted to schematically describe the total flow in Fig. 7. Let us start at the CH_3 group [designated as

Table XV

Thyamine — gross charges

		C(1)	
$1s$	1.99761	$1s = 1.99761$	$\delta(\sigma)$
$2s$	1.78892	$2s = 1.78892$	$\delta(\pi)$
$2p_x$	1.89636	$2p = 4.61960$	$\delta(\text{tot}) = -.40615$
$2p_y$	1.39083		
$2p_z$	1.33241		
		O(2)	
$1s$	1.99763	$1s = 1.99763$	$\delta(\sigma)$
$2s$	1.78963	$2s = 1.78963$	$\delta(\pi)$
$2p_x$	1.60018	$2p = 4.57620$	$\delta(\text{tot}) = -.36348$
$2p_y$	1.71878		
$2p_z$	1.25724		
		N(1)	
$1s$	1.99723	$1s = 1.99723$	$\delta(\sigma)$
$2s$	1.33487	$2s = 1.33487$	$\delta(\pi)$
$2p_x$	1.20100	$2p = 4.12756$	$\delta(\text{tot}) = -.45968$
$2p_y$	1.18685		
$2p_z$	1.73971		
		N(2)	
$1s$	1.99727	$1s = 1.99727$	$\delta(\sigma)$
$2s$	1.34414	$2s = 1.34414$	$\delta(\pi)$
$2p_x$	1.19286	$2p = 4.12190$	$\delta(\text{tot}) = -.46333$
$2p_y$	1.17377		
$2p_z$	1.75527		
		C(1)	
$1s$	1.99959	$1s = 1.94959$	$\delta(\sigma)$
$2s$	0.88761	$2s = 0.88761$	$\delta(\pi)$
$2p_x$	0.87002	$2p = 2.62838$	$\delta(\text{tot}) = +.48441$
$2p_y$	0.84593		
$2p_z$	0.91243		

Table XV (continued)

		C(2)	
$1s$	1.99930	$1s = 1.99930$	$\delta(\sigma)$
$2s$	1.04733	$2s = 1.04733$	$\delta(\pi)$
$2p_x$	1.14671	$2s = 1.04733$	$\delta(\text{tot}) = -.05685$
$2p_y$	0.92605		
$2p_z$	0.93744		
		C(3)	
$1s$	1.99903	$1s = 1.99903$	$\delta(\sigma)$
$2s$	0.98034	$2s = 0.98034$	$\delta(\pi)$
$2p_x$	0.95068	$2p = 3.09882$	$\delta(\text{tot}) = -.07822$
$2p_y$	1.01028		
$2p_z$	1.13786		
		C(4)	
$1s$	1.99951	$1s - 1.99951$	$\delta(\sigma)$
2s	0.91281	$2s = 0.91281$	$\delta(\pi)$
$2p_x$	0.95053	$2p = 2.75285$	$\delta(\text{tot}) = +.33481$
$2p_y$	0.87210		
$2p_z$	0.93022		
		C(5)	
$1s$	1.99898	$1s = 1.99898$	$\delta(\sigma)$
$2s$	1.21868	$2s = 1.21868$	$\delta(\pi)$
$2p_x$	1.18437	$2p = 3.36681$	$\delta(\text{tot}) = -.58448$
$2p_y$	1.00724		
$2p_z$	1.17520		
		H(1)	
$1s$	0.63352		$\delta(\text{tot}) = +.36648$
		H(2)	
$1s$	0.63222		$\delta(\text{tot}) = +.36778$

Table XV (continued)

		H(3)	
1*s*	0.76422		δ(tot) = +.23578
		H(4)	
1*s*	0.80944		δ(tot) = +.19056
		H(5)	
1*s*	0.79517		δ(tot) = +.20483
		H(6)	
1*s*	0.77240		δ(tot) = +.22760

C(5) and H(4), H(5) and H(6)]. The three hydrogens donate the charges given in the Figure. However, the sum of the donated charges is 0.623 of an electron and C(5) accepts only 0.584 charges. The charge excess 0.623—0.584=0.039 is therefore transferred over to the C(3) site. The remaining charge for C(3) is assumed to be supplied by the H(3) site. This way we can construct the flow of charges as given in Fig. 7.

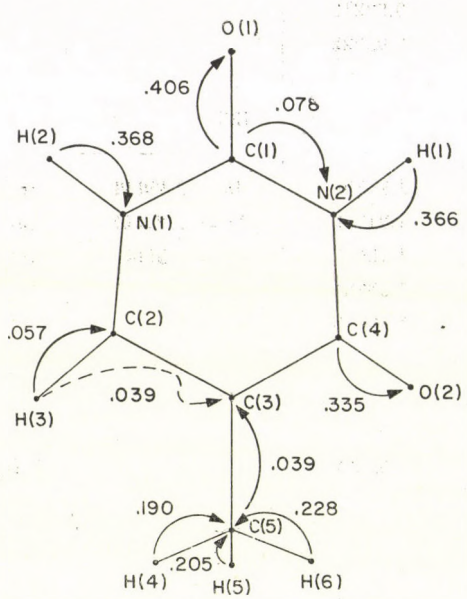

Fig. 7. Charge transfer of σ and π electrons in thyamine

Table XVI

Hybridization: adenine

atom	1s	2s	$2p_\sigma$	$2p_\pi$
N(1)	1.997	1.437	2.666	1.173
N(2)	1.997	1.451	2.702	1.156
N(3)	1.997	1.547	2.590	1.334
N(4)	1.997	1.346	2.470	1.641
N(5)	1.997	1.367	2.432	1.805
C(1)	1.999	0.936	1.922	0.909
C(2)	1.999	0.932	1.938	1.155
C(3)	1.999	0.924	1.859	1.023
C(4)	1.999	1.024	1.986	0.973
C(5)	1.999	1.020	1.925	1.031
H(1)	0.778		*	*
H(2)	0.614		*	*
H(3)	0.775		*	*
H(4)	0.666		*	*
H(5)	0.672		*	*

* Data not available at present due to choice of basis set.

Table XVII

Hybridization: cytosine

atom	1s	2s	$2p_\sigma$	$2p_\pi$
O	1.998	1.787	3.297	1.326
N(1)	1.997	1.347	2.437	1.682
N(2)	1.997	2.473	2.586	1.278
N(3)	1.997	1.370	2.426	1.805
C(1)	1.999	0.885	1.725	0.958
C(2)	1.999	0.950	1.944	0.866
C(3)	1.999	1.018	2.066	1.216
C(4)	1.999	1.064	2.088	0.867
H(1)	0.664		*	*
H(2)	0.688		*	*
H(3)	0.806		*	*
H(4)	0.759		*	*
H(5)	0.631		*	*

* Data presently not available due to choice of basis set.

Table XVIII
Hybridization: guanine

atom	1s	2s	$2p_\sigma$	$2p_\pi$
O	1.998	1.790	3.296	1.284
N(1)	1.997	1.336	2.413	1.726
N(2)	1.997	1.440	2.599	1.324
N(3)	1.997	1.554	2.596	1.091
N(4)	1.997	1.352	2.474	1.624
N(5)	1.997	1.367	2.424	1.824
C(1)	1.999	0.917	1.811	0.881
C(2)	1.999	0.931	1.865	1.012
C(3)	1.999	0.934	1.905	1.211
C(4)	1.999	0.907	1.801	0.933
C(5)	1.999	1.011	1.901	1.089
H(1)	0.787		*	*
H(2)	0.620		*	*
H(3)	0.651		*	*
H(4)	0.687		*	*
H(5)	0.648		*	*

* Data presently not available due to choice of basis set.

Table XIX
Hybridization: thyamine

atom	1s	2s	$2p_\sigma$	$2p_\pi$
C(1)	1.999	0.887		0.912
C(2)	1.999	1.047		0.937
C(3)	1.999	0.980		1.139
C(4)	1.999	0.913		0.930
C(5)	1.999	1.219		1.175
N(1)	1.997	1.335		1.740
N(2)	1.997	1.344		1.755
O(1)	1.998	1.789		1.332
O(2)	1.998	1.790		1.257
H(1)				
H(2)				
H(3)				
H(4)				
H(5)				
H(6)				

Table XX

Dipole moment (a. u.)

molecule	x component	y component	z component	total
adenine	1.0230	0.0975	0.0	1.0277
cytosine	−1.5835	−1.9576	0.0	2.5179
guanine	−0.6270	2.6577	0.0	2.7307
thyamine	1.2922	0.0647	0.0034	1.2938

Table XXI

Computed and rationalized orbital energies for the carbon inner shell of adenine molecule

atom	(a)	(b)	(c)
C(1)	−11.5336	−11.4595	−11.5345
C(3)	−11.5109	−11.4372	−11.5022
C(5)	−11.4910	−11.3396	−11.4046
C(4)	−11.4822	−11.3367	−11.4017
C(2)	−11.4371	−11.3118	−11.3768

(a) Computed as for Table VIII
(b) Computed from the ionic character and with $\varepsilon(1S)$ of ^3P in carbon as reference.
(c) Computed from the ionic character and with $\varepsilon(1S)$ of the ^1S in carbon as reference.
The remaining discrepancy between column (a) and (c) is attributed to neighboring atoms effect, primarily their ionic character.

There are, of course, several possible ways to draw such flow paths; *but the essential feature we obtain is that there is no way to draw such flow paths by limiting ourselves to nearest neighbors; we need to go at least to the next nearest neighbors.* Indeed, the path we have chosen can now be properly balanced unless we assume that H(3) transfers 0.028 and 0.019 of an electron to O(2) and N(2), respectively.

Let us now consider the cytosine molecule and investigate the σ charge transfer first, the π charge transfer second and the total charge transfer at last. The effect of the σ transfer is to have the C(1) and the N(2) atoms positive (donors) and all the other atoms negative (acceptors), of course neglecting the hydrogen atoms, which are donors. On the other hand, the effect of the π charge transfer is to have the C(1), N(1), C(2) and N(3) positive (donors) and all the other atoms acceptors. Therefore, in the π approximation (namely in those computational models, where only the π electrons are explicitly considered) the result one would obtain can be even *qualitatively* in disagreement with all-electron computations. Similar conclusions can be drawn by considering the charge transfer data for guanine and thyamine (Table XII to Table XV).

VI. Hybridization

Much of chemistry is based on the concept of valency, i.e., the ability to bind in a defined number of ways as well as a defined, directional way. The concept of valency was then translated into the concept of hybridization, or possibly, in the concept of valency state as first step, and hybridization as a second step. However, in so doing we have to complicate our model by thinking in terms of covalent and ionic structures in the traditional valency bond approach. The concept of charge transfer used within the Molecular Orbital approximation (as we did in the second paper of this series) allows us to incorporate the ionic character of a molecule with the concept of hybridization. Let us examine Tables XVI to XIX and let us consider the carbon atoms in adenine molecule. These are clearly sp^2 hybridized, to a first approximation. However, there are important deviations 1) in the 1 : 2 ratio of the hybrid and 2) in the fact that the sum of the hybridized electrons deviates from three. The deviation from the ratio 1 : 2 can be taken as a first effect, namely the precise hybridization ratio for pairs of atoms still considered as neutral. The deviation from 3 corresponds to the second effect, namely the introduction of ionic character, via intramolecular charge transfer.

VII. Conclusions

It is expected that in time, with more computational data of the type reported here, we should be in a position to assign quite precisely the hybridization ratio as well as the amount of electrons donated (as well as accepted) within a given molecule solely on the basis of geometrical considerations. To state this goal differently, we expect that knowledge of structure alone will suffice to determine accurate charge distribution in a molecule, both in terms of hybridization and intramolecular charge transfer.

REFERENCES

1. E. CLEMENTI and D. DAVIS, J. Comp. Phys., **1**, 223, 1966.
2. E. CLEMENTI, J. Chem. Phys., **46**, 3842, 1967; 3851, 1967; 4725, 1967; 4731, 1967; 4737, 1967; ibid. **47**, 2323, 1967; 3837, 1967; 4485, 1967.
3. E. CLEMENTI, V. COIRO and E. RUSCONI, J. Chem. Phys., Study in the Electronic Structure of Molecules. XII, Inner Shells and Aufbau Principle (to be published).
4. Somewhat parenthetically we would like to note that the $\sim n^4$ number (more accurately $(N^2 + N)/2$, where $N = (n^2 + n)/2$ if n is the basis set size) is most definitely only an upper limit. The larger the molecule (say 5 to 6 first row atom and up), the more the above statement is true since a large (up to 50 to 90%) number of integrals is exceedingly small (of the order of equal or less than 10^{-8} atomic units).
5. Appendix to IBM Technical Report: Study in the Electronic Structure of Molecules. X. Ground State Functions for adenine, cytosine, guanine and thyamine.

6. The gross population analysis is computed according to R. S. MULLIKEN, J. Chem. Phys., **23**, 1833, 1841, 2243, 1955. See in addition the first paper in this series (E. CLEMENTI, J. Chem. Phys., **46**, 3842, 1967).
7. The atomic unit for energy corresponds to 27.2098 e.v. for length to 0.5292 Å, for dipole moments to 2.5416 debyes.
8. E. CLEMENTI, Tables of Atomic Functions. Supplement to a paper by E. CLEMENTI, IBM Journal of Res. and Dev., **9**, 2, 1965.
9. Let us now take into consideration the neighbors effect. This effect has been taken into consideration indirectly, by using the ionic charges. Clearly, the charge transfer takes place because there are neighbors. However, we wish to take into account the nearest neighbors more directly. In other words, the field F of the equation $F\Phi_i = \varepsilon_i \Phi_i$ is the field of the atom (after loss or gain of charges because of charge transfer) plus the field of the neighboring atoms, i.e., $F = F_I + F_N$, where F_I is the local (nearly atomic field) and F_N the neighbors field. This will affect the $_i$ which can be obtained by perturbation of the ε_{ic} where ε_{il} is the orbital energy of the separated atoms, with correct ionic character and in the valency state. A positive charge in the neighborhood of an atom will affect its inner shell by polarizing the inner shell electrons toward that charge and will increase (absolute value) its energy. A negative charge in the neighborhood of an atom will affect its inner shell by polarizing the inner shell electrons away from that charge and will likely affect its energy less than for positive charges. A systematic study of point charge variation on the orbital energies restricted however, to CN^- molecules, seems to support this point [10]. The inner shell variation due to presence of point charges (positive or negative) in the CN^- system is of the order of few hundreds of an atomic unit or sufficient to bring the data of column three in better agreement with those of column one (in Table XX). At this stage we can only content ourselves with having established a reason for the magnitude of the splitting and in having correlated correctly the relative position of the computed orbital energies with our ionic model. Point charge perturbations are in progress to elucidate the neighboring charges effect.
10. E. CLEMENTI and D. KLINT, Study in the Electronic Structure of Molecules, IX. The Cyano Group (J. Chem. Phys. in press).

ИЗУЧЕНИЕ ЭЛЕКТРОННОЙ СТРУКТУРЫ МОЛЕКУЛ, X.

ОСНОВНОЕ СОСТОЯНИЕ ДЛЯ АДЕНИНА, ЦИСТОЗИНА, ГУАНИНА И ТИАМИНА

Э. КЛЕМЕНТИ, Й. М. АНДРЕ, М. КЛ. АНДРЕ, Д. КЛИНТ и Д. ХАН

Р е з ю м е

Излагаются все электроны, определенные методом SCF-LCAO-MO, для аденина, цистозина, гуанина и тиамина. С целью вычисления полной энергии и волновых функций определены относительно большие заряды и дипольный момент. Анализ орбитальной энергии для внутренних оболочек показывает, что имеется три эффекта, которые оказывают влияние на орбитальные энергии по отношению внутренних оболочек а) полный заряд, или степень ионизации исследуемого атома; б) его валентное состояние; в) ионизации соседних атомов. Первые два эффекта достаточны для определения относительного расположения внутренней оболочки, для оценки экстремума расщепления электронов внутренних оболочек атомов данного типа.

Полная зарядная населенность использовалась для определения универсального потока переноса заряда δ и π. Найдено, что поток переноса заряда требует непосредственного рассмотрения по крайней мере следующих самых близких соседей. Наконец, показывается что рассмотрения просто π-электронов могут проводить не только к качественному, но и к количественному ошибочному предсказанию о распределении электронного заряда. Например, атом может быть заряжен положительно, если рассматриваются только — электроны, и тот же атом может иметь отрицательный заряд, если рассматриваются лишь δ-электроны. На основе этого мы подчеркиваем необходимость принятия во внимание всех электронов при вычислениях не только с целью количественного, но даже и качественного изучения электронной структуры молекулы.

Acta Physica Academiae Scientiarum Hungaricae, Tomus 27, pp. 523—548 (1969)

SOME PROBLEMS OF INVESTIGATING PERIODICITIES OF COSMIC RAY TIME SERIES*

By

J. KÓTA and A. SOMOGYI

CENTRAL RESEARCH INSTITUTE OF PHYSICS, BUDAPEST

(Received 13. III. 1969)

A generalization of the method of the analysis of variance is given to investigate the existence and the shape of a periodicity with given length of period. Allowance is made for slow variations of the intensity of cosmic rays as well as for meteorological effects. In addition to the exact test of the existence of the periodicity, maximum likelihood estimates both of the constants characterizing the shape of the periodicity and of the mean square amplitude of the periodic function are given, together with their respective statistical errors, in the case of an arbitrary number of meteorological factors affecting the intensity of the cosmic radiation.

Disadvantages in applying the Fourier method when investigating a periodicity with given length of period are pointed out as well as the fact that the determination of meteorological coefficients, if done statistically, must not be separated from the analysis of the periodicity.

I. Introduction

§ 1. It is known long since that the intensity of cosmic radiation shows periodic variations. Three kinds of periodic variations have, up to now, been demonstrated without doubt. The lengths of periods of these are one solar day, about 27 days, and about 11 years, respectively. The shapes of these periodicities are not constant, especially large variations may be observed in the case of the shape of the 27 day variation.

The aim of this paper is to give a statistically correct method, making use of the full information available, to detect or else to contest the existence of a periodicity with given length of period and strictly constant shape, as well as to determine the shape of such a periodic change.

§ 2. The Fourier method, i.e. that of expressing the shape of the periodicity to be investigated by means of a trigonometrical polynome, has almost exclusively been used to investigate periodicities in the intensity of cosmic rays with given lengths of period. This method has, however, two serious shortcomings:

2.1. If the question to be decided upon is whether a periodicity with given length of period does exist or not, it is not sufficient to content oneself with determining the first few Fourier coefficients or, as it is sometimes done, the amplitude of the first harmonic, rather should the maximum possible number of Fourier amplitudes be taken into consideration so as to make use

* Dedicated to Prof. P. GOMBÁS on his 60th birthday.

of the maximum amount of information available in the form of the measured data. To calculate the maximum possible number of Fourier coefficients requires, however, rather tedious calculations. It will be shown that exactly the same amount of information can be gained on the basis of the same measured data in a way much simpler than that of calculating Fourier coefficients.

2.2. If, in addition to proving the existence of the periodicity, the shape of the periodic function is also to be determined, the application of the Fourier method may lead to difficulties. The Fourier method is justified only in the case when the periodic function is really a trigonometrical polynome. If a function other than a trigonometrical polynome is approximated by trigonometric polynomes, the approximation obtained bears only a weak resemblance to the function to be determined and, in addition to this, the coefficients of the polynome approximating the unknown function are "void" in the sense that they do not have any direct physical meaning, when considered individually; right on the contrary, they may be misleading sometimes. Variations of the cosmic ray intensity may often be sinusoidal and the second harmonic may also have physical meaning in certain cases. Fourier coefficients of the higher order have, however, no direct physical meaning in cosmic ray variations; at least, as for the present there has been no reason to attribute them any.

§ 3. Both disadvantages mentioned in the preceding paragraph are get rid of when approximating the unknown periodic function by means of a simple step function instead of a trigonometrical polynome. Numerical calculation of the heights of the maximum possible number of steps is a task by far simpler than that of calculating the maximum possible number of Fourier coefficients. In addition to this, the heights of the individual steps have straightforward physical meanings, i.e. they are equal to the mean values of the intensity during the time intervals corresponding to the widths of the steps.

Although the special conditions encountered in cosmic ray investigations are born in mind throughout this paper, the methods outlined and the results obtained apply to a large variety of other problems as well.

II. Formulation of the problem. Basic notations

§ 4. Let us denote by $n_\nu (\nu = 1,2, \ldots, N)$ the rates of a certain kind of cosmic ray particles as observed during N consecutive unit time intervals. Let us assume that the measured $n_\nu (\nu = 1,2, \ldots, N)$ values are not affected by any *systematic* errors, i.e. that $\langle n_\nu \rangle$, the expected value of n_ν, is equal to the mean value of the intensity during the unit time interval.

Furthermore, let us assume that the stochastic variables $n_\nu (\nu = 1,2, \ldots N)$ are independent of each other and are distributed normally. These condi-

tions are generally not met rigorously, they, however, can be regarded as sufficiently good approximations in many cases.

Let us temporarily assume that the variances of all the variables n_ν are equal to σ^2. In Section VI the more general case with variables n_ν having different variances σ_ν^2 will also be dealt with.

§ 5. We have to test the hypothesis that, apart from certain types of changes, the intensity be a periodic function of time with a given period length, q. Furthermore, if this hypothesis turns out to be true, the shape of the periodic function is to be determined.

The unit of time should be chosen in such a way that q should be an integer, and the total number of measurements, N, should be $N = pq$, where p denotes an integer number. The case with p being a non-integer value is dealt with in Section VI.

The measured data, n_ν ($\nu = 1,2, \ldots, N$) should then be arranged to form a matrix $\mathbf{n}(p, q) = \mathbf{n}$ with p rows and q columns in such a way that the elements n_{ij} of the matrix should be equal to n_ν in the following order:

$$n_{ij} = n_\nu \qquad \text{if} \qquad \nu = (i-1)\,q+j$$

$$(i = 1, 2, \ldots, p \qquad j = 1, 2, \ldots, q \qquad \nu = 1, 2, \ldots, pq)$$

$p \geqq 2$ and $q \geqq 2$ will be assumed throughout this paper.

§ 6. A few more notations:

a) Matrices will always be denoted by bold characters. Upper indices written in brackets and applied to a matrix symbol denote the numbers of rows and columns, respectively, of the matrix. These indices will be dropped if no ambiguity arises by doing so.

b) A dot on the place of a running index denotes the arithmetic mean of the quantities involved, when the index replaced by the dot runs through its usual range.

E.g.
$$n_{\cdot i} = \frac{1}{p} \cdot \sum_{i=1}^{p} n_{ij},$$

$$n_{\cdot\cdot} = \frac{1}{pq} \sum_{i=1}^{p} \sum_{j=1}^{q} n_{ij}, \qquad \text{and so on.}$$

c) Two identical running indices within a single term denote summation extended over the usual range of the identical indices.

d) A bar over a symbol denotes the estimated (measured) value of an unknown parameter. Thus symbols with bars represent always stochastic variables.

e) The variance of a stochastic variable x will be denoted by σ_x^2. (The estimated value of σ_x^2 will be denoted by $\bar{\sigma}_x^2$). σ^2 and $\bar{\sigma}^2$ without any index denote the variance of the stochastic variable n_{ij} and its estimated value, respectively.

III. The simple step function method in the case of a "pure" periodicity

§ 7. Let us assume for the moment that the intensity has no changes except of the hypothetical periodicity with the period length of q. This case will be referred to as the case of a "pure" periodicity. The mean values of the intensity during the subsequent unit time intervals within the length of a period should be denoted by $a_j (j = 1,2, \ldots, q)$. The periodicity does exist, if at least two of the a_j $(j = 1,2, \ldots q)$ values are not equal to each other. Clearly

$$\langle n_{ij} \rangle = a_j \qquad \begin{matrix} (i = 1, 2, \ldots, p \\ j = 1, 2, \ldots, q) . \end{matrix} \tag{1}$$

$\langle n_{ij} \rangle$ is independent of the row index, that means periodicity.

We are thus facing the following problems:

7.1 $\bar{a}_j (j = 1,2, \ldots, q)$ i.e. the estimated values of the parameters $a_j (j = 1,2, \ldots, q)$ are to be determined, together with the estimated values of their respective statistical errors, $\overline{\sigma^2_{a_j}}$.

7.2 The probability ε that the deviations of all the $\bar{a}_j (j = 1,2, \ldots, q)$ values from each other are due only to statistical fluctuations is to be determined. If this probability turns out to be very small, the existence of the periodicity may be regarded as proved.

7.3. $\bar{a}^2$ i.e. the estimated value of

$$a^2 = \frac{1}{q} \sum_{j=1}^{q} (a_j - a.)^2$$

is to be determined, together with its statistical error, $\bar{a}^2$ is the estimated value of the mean square amplitude of the periodic step function.

§ 8. Problems 7.1 and 7.2 are basic problems of the analysis of variance. Their solutions, which can be found in text books, are as follows (see e.g. [1]):

8.1

$$\bar{a}_j = n._{j.} \tag{2}$$

Let us introduce the following notations:

$$\left.\begin{aligned} p' &= q(p-1) , \\ Q_1 &= \sum_{j=1}^{q} (\bar{a}_j - \bar{a}.)^2 , \\ Q_2 &= \sum_{i=1}^{p} \sum_{j=1}^{q} (n_{ij} - \bar{a}_j)^2 . \end{aligned}\right\} \tag{3}$$

Since

$$\sigma^2_{\bar{a}_j} = \frac{\sigma^2}{p} \tag{4a}$$

we have

$$\overline{\sigma^2_{\bar{a}_j}} = \frac{\bar{\sigma}^2}{p} = \frac{Q_2}{pp'} . \tag{4b}$$

8.2 Introducing the notation

$$x = \frac{1}{2} \ln \left(\frac{pp'}{q-1} \frac{Q_1}{Q_2} \right)$$

the probability, ε, that the deviations of the quantities $\bar{a}_j (j = 1,2, \ldots, q)$ from each other are due exclusively to statistical fluctuations is given by

$$\varepsilon = P_{q-1,p'} (\zeta > x),$$

where $P_{\nu,\mu}(\zeta > x)$ stands for FISHER's z distribution with μ and ν degrees of freedom.

8.3

$$\overline{a^2} = \frac{1}{q} \left[Q_1 - \frac{q-1}{pp'} Q_2 \right]. \tag{5}$$

The problem of determining $\overline{\sigma^2_{a^2}}$ is not treated in the literature. According to calculations outlined in Appendix II we have

$$\overline{\sigma^2_{a^2}} = \frac{2Q_2}{pp'q^2} \left[2\,Q_1 - \frac{(q-1)^2}{pp'(p'+2)} \left(\frac{p'}{q-1} - 1 \right) Q_2 \right]. \tag{6}$$

If $p \gg 2$, this turns into

$$\overline{\sigma^2_{a^2}} = \frac{2\,Q_2}{pp'\,q} \left(\frac{Q_1}{q} + \overline{a^2} \right). \tag{6*}$$

IV. Comparison of the simple step function method and the Fourier method in the case of pure periodicity

§ 9. The Fourier method is based on the hypothesis that the intensity $I(t)$, as a function of time, t, has the form of a trigonometric polynome.

$$I(t) = A_0 + \sum_{\mu=1}^{m} A^*_\mu \cos \left(\mu \frac{2\pi}{q} t \right) + \sum_{\mu=1}^{m'} B^*_\mu \sin \left(\mu \frac{2\pi}{q} t \right) . \tag{7}$$

The expected values of the measured data are equal to the mean values of $I(t)$ as taken during subsequent unit time intervals:

$$\langle n_{ij}\rangle = \int_{\nu-1}^{\nu} I(t)\,dt = A_0 + \sum_{\mu=1}^{m} A_\mu \cos\left[\mu\frac{2\pi}{q}\left(j-\frac{1}{2}\right)\right] + \sum_{\mu=1}^{m'} B_\mu \sin\left[\mu\frac{2\pi}{q}\left(j-\frac{1}{2}\right)\right] \tag{8}$$

$$(i=1,2,\ldots,p;\ j=1,2,\ldots,q;\ |m-m'|\leq 1),$$

where ν stands for $(i-1)q+j$ and

$$\frac{A_\mu}{A_\mu^*} = \frac{B_\mu}{B_\mu^*} = \frac{\sin(\mu\pi/q)}{(\mu\pi/q)}\,.$$

The estimated values of the Fourier coefficients $A_\mu(\mu=1,2,\ldots,m)$ and $B_\mu(\mu=1,2,\ldots,m)$ have to be determined. The maximum possible number of the parameters which can be determined is equal to* q; in particular

$$m\leq E\left[\frac{q-1}{2}\right] \quad \text{and} \quad m'\leq E\left[\frac{q}{2}\right],$$

where $E[x]$ stands for the largest integer number not larger than x.

It is well known that the estimated values of the Fourier coefficients and their statistical errors are the following:

$$\left.\begin{aligned}
&\bar{A}_0 = n_{\cdot\cdot}\,, && \overline{\sigma^2_{\bar{A}_0}} = \frac{\overline{\sigma^2}}{pq}\\
&\bar{A}_\mu = \frac{2}{q}\sum_{j=1}^{q} n_{\cdot j}\cos\left[\mu\frac{2\pi}{q}\left(j-\frac{1}{2}\right)\right], && \overline{\sigma^2_{\bar{A}_\mu}} = \frac{2\overline{\sigma^2}}{pq}\\
&\qquad\left(\mu=1,2,\ldots,m\leq E\left[\frac{q-1}{2}\right]\right)\\
&\bar{B}_\mu = \frac{2}{q}\sum_{j=1}^{q} n_{\cdot j}\sin\left[\mu\frac{2\pi}{q}\left(j-\frac{1}{2}\right)\right], && \overline{\sigma^2_{\bar{B}_\mu}} = \frac{2\overline{\sigma^2}}{pq}\\
&\qquad\left(\mu=1,2,\ldots,m'\leq E\left[\frac{q-1}{2}\right]\right)
\end{aligned}\right\} \tag{9}$$

If $q=2m'$, then

$$\left.\begin{aligned}
&\bar{B}_{m'} = \frac{1}{q}\sum_{j=1}^{q}(-1)^j n_{\cdot j}\,, && \overline{\sigma^2_{\bar{B}_{m'}}} = \frac{\overline{\sigma^2}}{pq}
\end{aligned}\right\}$$

* Compare, however, [2], where this fact is disregarded.

It should be pointed out that also the expression (8) has the form of a step function. The step function representation of $\langle n_{ij} \rangle$ is inevitable since the number of measurements during a period is by all means finite. Expression (8) is, however, considerably more complicated than the simple expression (1) on which the method outlined in Section III was based. The question arises, whether the much more complicated method based on expression (8) yields statistically more information as to the existence of the periodicity, than does the simple step function method based on (1). It will be shown, in what follows, that the answer is negative.

Let be

$$m = E\left[\frac{q-1}{2}\right] \quad \text{and} \quad m' = E\left[\frac{q}{2}\right], \tag{9*}$$

i.e.

$$m + m' + 1 = q.$$

It will be shown that, in this case, the Fourier procedure is statistically equivalent to the simple step function method based on (1).

§ 10. First it will be shown that the estimated value of the mean square amplitude as obtained by the Fourier method and the simple step function method are exactly the same, i.e. they are identical second order expressions of the quantities n_{ij}.

A simple calculation shows that the mean square amplitude of the function (8) is equal to

$$A^2 = \frac{1}{2}\left[\sum_{\mu=1}^{m} A_\mu^2 + \sum_{\mu=1}^{m'} B_\mu^2\right] + \varepsilon_q B_{m'}^2, \tag{10}$$

where

$$\varepsilon_q = E\left[\frac{q}{2}\right] - \frac{q-1}{2}.$$

In order to determine $\overline{A^2}$ it should be noted that

$$\overline{A_\mu^2} = \bar{A}_\mu^2 - \overline{\sigma_{A\mu}^2} \qquad (\mu = 1, 2, \ldots, m),$$

and

$$\overline{B_\mu^2} = \bar{B}_\mu^2 - \overline{\sigma_{B\mu}^2} \qquad (\mu = 1, 2, \ldots, m').$$

Furthermore, it can be shown by rather longish elementary calculations that

$$\frac{1}{2}\left[\sum_{\mu=1}^{m} \bar{A}_\mu^2 + \sum_{\mu=1}^{m'} \bar{B}_\mu^2\right] + \varepsilon_q \bar{B}_{m'}^2 = \frac{1}{q}\sum_{j=1} (n_{\cdot j} - n_{\cdot\cdot})^2$$

whence, on the basis of (10), (2), and (5), it can be seen that

$$\overline{a^2} = \overline{A^2},$$

i.e. the estimated values of the mean square amplitude of the periodic function as obtained on the basis of (1) or (8) are identical expressions of the n_{ij} data.

§ 11. We proceed with showing that the simple step function method based on (1), and the Fourier method based on (8) reduce the (empirical) mean square deviation of the n_{ij} values from their mean to exactly the same extent. The reduced mean square deviation divided by $p' = q(p-1)$ gives the value of $\overline{\sigma^2}$. Thus both procedures lead exactly the same value of $\overline{\sigma^2}$

$\overline{\sigma^2}$ as determined on the basis of (1) is given by

$$\overline{\sigma^2} = \frac{Q_2}{p'}. \tag{11}$$

(The notations are explained in Equs. (3)). In the case of the Fourier method we have, on the other hand,

$$\overline{\sigma^2} = \frac{1}{p'} \sum_{i=1}^{p} \sum_{j=1}^{q} \left\{ n_{ij} - \bar{A}_0 - \sum_{\mu=1}^{m} \bar{A}_\mu \cos\left[\mu \frac{2\pi}{q}\left(j - \frac{1}{2}\right)\right] - \right. \\ \left. - \sum_{\mu=1}^{m'} \bar{B}_\mu \sin\left[\mu \frac{2\pi}{q}\left(j - \frac{1}{2}\right)\right] \right\}^2. \tag{12}$$

It can be shown by direct calculation that the right hand sides of Equs. (11) and (12) are identical second order expressions of the values n_{ij} if (9*) is true.

§ 12. It seems to be worth while to emphasize that the unbiased estimate of the mean square amplitude of the periodic function (8) is given by

$$\overline{A^2} = \frac{1}{2}\left[\sum_{\mu=1}^{m} \overline{A_\mu^2} + \sum_{\mu=1}^{m'} \overline{B_\mu^2}\right] + \varepsilon_q \overline{B_{m'}^2},$$

i.e. *not* by the expression

$$U^2 = \frac{1}{2}\left[\sum_{\mu=1}^{m} \bar{A}_\mu^2 + \sum_{\mu=1}^{m'} \bar{B}_\mu^2\right] + \varepsilon_q \bar{B}_{m'}^2,$$

which is used in many cases in spite of the fact that U^2 is *not* an *unbiased* estimate of A^2. It can be easily seen that in all cases (except that of $n_{ij} =$ constant)

$$U^2 > \overline{A^2} \quad \text{and thus} \quad \langle U^2 \rangle > A^2.$$

The difference $U^2 - A^2$ is large just in the delicate cases when the statistical errors of the coefficients $\bar{A}_\mu$, B_μ are large and the existence of the periodicity is questionable. The incorrect value U^2 unjustly favours the hypothesis that the periodicity exists.

V. The simple step function method in the case of mixed periodicity

§ 13. The intensity of any component of the cosmic radiation shows, in all cases, also systematic variations others than the periodicity to be investigated (cases of "mixed" periodicity). There are systematic variations like the absorption effect or the decay effect, which depend on quantities, like the barometric pressure or the height of a certain isobaric level, which in principle, can be measured regularly and have thus known values β_{ijk} ($i = 1,2, \ldots, p$; $j = 1,2, \ldots q$; $k = 1,2, \ldots, r$) during the time interval (i, j). (Let us take e.g. β_{ij1} to be the average barometric pressure during the time interval (i, j), β_{ij2} the average height of the 100 mb isobaric level during the name interval, and so on.) Supposing that the intensity be a linear function of the quantities $\beta_{ijk}(k = 1,2, \ldots, r)$ we have, in the case of a periodicity with the period length q

$$\langle n_{ij} \rangle = a_j + \beta_{ijk} b_k \qquad (i = 1, 2, \ldots, p;\ j = 1, 2, \ldots, q;\ k = 1, 2, \ldots, r) \tag{13}$$

where $b_k(k = 1,2, \ldots, r)$ are unknown parameters, e.g. b_1 the partial barometric coefficient, b_2 the decay coefficient, and so on.

It can always be assumed, without any restriction of generality, that the (sum of any type of the quantities β_{ijk} taken for the total time of measurement is zero i.e.

$$\beta_{..k} = 0 \qquad (k = 1, 2, \ldots, r).$$

Note, however, that generally

$$\beta_{.jk} \neq 0\,, \qquad \beta_{i\cdot k} \neq 0.)$$

It would be *incorrect* to determine the values $\bar{b}_k(k = 1,2, \ldots, r)$ separately, on the basis of the equations

$$\langle n_{ij} \rangle = \beta_{ijk} b_k^*$$

and then to use the "corrected" values $n_{ij}^* = n_{ij} - \beta_{ijk} \bar{b}_k^*$ to determine $\bar{a}_j(j = 1,2, \ldots, q)$ on the basis of

$$\langle n_{ij}^* \rangle = a_j^*$$

since in general

$$b_k^* \neq b_k \quad \text{and} \quad a_j^* \neq a_j$$

and the values $b_k^*(k = 1,2, \ldots, r)$ and $a_j^*(j = 1,2, \ldots, q)$ have no physical meaning.

Sometimes it may be of advantage to use corrected values $n_{ij} - \beta_{ijk}\bar{b}'_k$ with predetermined $\bar{b}'_k$. This may be the case when the total time of measurement is short and there are previous measurements available with considerably longer duration thus yielding considerably more exact values $\bar{b}'_k$. It is, however, indispensable that these predetermined coefficients should have been calculated on the basis of equations allowing also for the periodicity in question, i.e.

$$\langle n'_{ij} \rangle = a'_j + \beta'_{ijk} b'_k$$

$$(i = 1, 2, \ldots, p'; \quad j = 1, 2, \ldots, q'; \quad k = 1, 2, \ldots, r'$$

with

$$p' \geqslant p, \quad q' = q, \quad r' = r),$$

where n'_{ij} are the results of the older measurements and β'_{ijk} are the meteorological factors pertaining to them.

§ 14. Problems of the type of Equ. (13) have also been dealt with in the literature (see e.g. [3]). The solutions found are, however, incomplete in the sense that they do not give answers to all questions raised in cosmic ray investigations.

A full treatment of the problem will be given in what follows. The method applied will be that of the maximum likelihood which allows a compact treatment of the problem on the one hand, and may be used also in cases, when the n_{ij} variables are not distributed normally, on the other.

§ 15. The problem must be formulated in a more general way than that indicated in Equ. (13) so as to allow for systematic variations which are not of the type $\beta_{ijk} b_k$. There may be e.g. periodic variations with a period length other than q or aperiodic changes, like a slow recovery after a Forbush effect. The general character of these systematic variations must be known a priori or, at least, a reasonable hypothesis must be made as to the general trend of these variations. New terms containing some unknown parameters must then be inserted into Equ. (13). The estimated values of these parameters can be determined by means of the maximum likelihood method as discussed below.

No special hypothesis has to be made as to the general character of the remaining systematic variations if these are "slow", i.e. the changes due to them during the time q are small as compared to $\sqrt{a^2}$ where a^2 stands for

$$\frac{1}{q} \sum_{j=1}^{q} (a_j - a.)^2$$

as before. "Slow" systematic variations can be approximated by a step function in which the width of the steps are equal to q. Denoting the heights

of the steps by c_i Equ. (13) becomes

$$\langle n_{ij} \rangle = c_i + a_j + \beta_{ijk} b_k, \qquad (14)$$
$$c_1 = 0 \ *), \qquad \beta_{..k} = 0,$$
$$(i = 1, 2, \ldots, p; \quad j = 1, 2, \ldots, q; \quad k = 1, 2, \ldots, r)$$

or, in a more symmetric form:

$$\langle n_{ij} \rangle = A + c_i + a_j + \beta_{ijk} b_k,$$
$$c_. = 0 \ *, \qquad a_. = 0 \ *, \qquad \beta_{..k} = 0, \qquad (15)$$
$$(i = 1, 2, \ldots, p; \quad j = 1, 2, \ldots, q; \quad k = 1, 2, \ldots, r).$$

If the systematic variation characterized by the constants c_i is slow enough, then the width of the steps may be chosen to be larger than q, e.g. an arbitrary integer multiple of q. Alternatively, a "slow" variation can be approximated also by a polygonal line connecting equidistant points separated by the distance q or an arbitrary integer multiple of q. The most suitable hypothesis as to the form of the slow variation must be chosen individually in each case on the basis of careful consideration of the circumstances.

The problem as specified by Equ. (15) will be dealt with in what follows. It can be seen that

$$\langle n.. \rangle = A,$$

i.e. A is the average intensity as taken during the total time of measurement.

Again the problem is a threefold one:

(I) Unbiased estimated values of the parameters A,

$$A, c_i \ (i = 1, 2, \ldots, p), \quad a_j \ (j = 1, 2, \ldots, q), \quad b_k \ (k = 1, 2, \ldots, r)$$

have to be determined together with their respective statistical errors and covariances.

(II) The probability has to be calculated, that the deviation from zero of the estimated values $\bar{a}_j (j = 1,2, \ldots, q)$ are due to statistical fluctuations alone.

(III) An unbiased estimated value of the quantity

$$a^2 = \frac{1}{q} \sum_{j=1}^{q} a_j^2,$$

i.e. the mean square amplitude of the periodicity in question, has to be determined together with its statistical error.

* Without this (these) assumption(s) the problem would become indeterminate.

§ 16. Let us introduce the following notations:

$$\delta_{mn} = 1 \quad \text{if} \quad m = n \quad \text{and} \quad \delta_{mn} = 0 \quad \text{if} \quad m \neq n .$$

The transpose of the matrix $\mathbf{M}^{(m,n)}$ should be denoted by $\tilde{\mathbf{M}}^{(n,m)}$.

The inverse of the matrix $\mathbf{M}$ consisting of the elements M_{ij} should be denoted by $\mathbf{M}^{+}$, the elements of $\mathbf{M}^{+}$ by $\mathbf{M}_{ij}^{+}$.

$\mathbf{J}^{(m)}$ should denote a unit matrix with m rows and columns.

$\mathbf{J}^{(m,n)}$ should denote a matrix whose elements are all equal to 1, and $\mathbf{O}^{(m,n)}$ a matrix with elements all equal to 0.

$\mathbf{B} = \mathbf{B}^{(r,r)}$ should denote the matrix with elements $B_{kk'} = \beta_{ijk}\beta_{ijk'}$,

$\mathbf{B}^{*} = \mathbf{B}^{*(r,r}$ should denote the matrix with elements $B^{*}_{kk'} = B_{kk'} - p\beta_{\cdot ijk}\beta_{\cdot jk'} - q\beta_{i\cdot k}\beta_{i\cdot k'}$,

$\mathbf{N} = \mathbf{N}^{(r,1)}$ should denote the matrix with elements $N_k = n_{ij}\beta_{ijk} - pn_{\cdot j}\beta_{\cdot jk} - qn_{i\cdot}\beta_{i\cdot k}$,

$\mathbf{B}_c = \mathbf{B}_c^{(p,r)}$ should denote the matrix with elements $B^{c}_{ik} = \beta_{i\cdot k}$,

$\mathbf{B}_a = \mathbf{B}_a^{(q,r)}$ should denote the matrix with elements $B^{a}_{jk} = \beta_{\cdot jk}$,

$\mathscr{B}_c = \mathscr{B}_c^{(p,r)}$ should denote the matrix with elements $\mathscr{B}^{c}_{ik} = \beta_{i\cdot k'} B^{*+}_{k'k}$,

$\mathscr{B}_a = \mathscr{B}_a^{(q,r)}$ should denote the matrix with elements $\mathscr{B}^{a}_{jk} = \beta_{\cdot jk'} B^{*+}_{k\,k'}$,

$\mathscr{B}_{cc} = \mathscr{B}_{cc}^{(p,p)}$ should denote the matrix with elements $\mathscr{B}^{cc}_{ii'} = \beta_{i\cdot k}\mathscr{B}^{c}_{i'k} + \dfrac{1}{q}\delta_{ii'} - \dfrac{1}{pq}$,

$\mathscr{B}_{ac} = \mathscr{B}_{ac}^{(p,q)}$ should denote the matrix with elements $\mathscr{B}^{ac}_{ij} = \beta_{i\cdot k}\mathscr{B}^{a}_{jk} = \beta_{\cdot jk}\mathscr{B}^{c}_{ik}$,

$\mathscr{B}_{aa} = \mathscr{B}_{aa}^{(q,q)}$ should denote the matrix with elements $\mathscr{B}^{aa}_{jj'} = \beta_{\cdot jk}\mathscr{B}^{a}_{j'k} + \dfrac{1}{p}\delta_{jj'} - \dfrac{1}{pq}$.

It can be seen easily that all quadratic matrices defined above are symmetrical.

§ 17. (Problem I of § 15).

According to the method of maximum likelihood, unbiased estimates of the parameters A, c_i, a_j, b_k can be obtained (see e.g. [4]) as the solutions

of the simultaneous equations

$$\left.\begin{aligned}
&\frac{\partial P}{\partial A} = 0 \\
&\frac{\partial P}{\partial c_i} = 0 \quad (i = 1, 2, \ldots, p) \\
&\frac{\partial P}{\partial a_j} = 0 \quad (j = 1, 2, \ldots, q) \\
&\frac{\partial P}{\partial b_k} = 0 \quad (k = 1, 2, \ldots, r) \\
&\frac{pq}{\sigma^2} c. = 0 \\
&\frac{pq}{\sigma^2} a. = 0
\end{aligned}\right\}, \tag{16}$$

where

$$P = \ln P^* - \frac{pq}{\sigma^2}\lambda_c c. - \frac{pq}{\sigma^2}\lambda_a a. ,$$

with

$$\frac{pq}{\sigma^2}\lambda_c \quad \text{and} \quad \frac{pq}{\sigma^2}\lambda_a$$

denoting Lagrange multipliers, and

$$P^* = \prod_{i=1}^{p} \prod_{j=1}^{q} \frac{1}{\sqrt{2\pi\sigma^2}} \exp\left[-\frac{1}{2\varkappa^2}(n_{ij} - \langle n_{ij}\rangle)^2\right],$$

i.e. P^* stands for the joint distribution of the stochastic variables $n_{ij}(i = 1,2, \ldots, p; j = 1,2, \ldots, q)$. If the variables n_{ij} are not independent and normal, P^* has another form which, at any rate, must be known. The explicit formulae given in what follows refer to the case when n_{ij} are independent and normal.

The solution of the simultaneous equations are the following:

$$\left.\begin{aligned}
&\bar{A} = n.. \\
&\bar{c}_i = n_{i\cdot} - n.. - \beta_{i\cdot k} B^{*+}_{kk'} N_{k'} \\
&\qquad (i = 1, 2, \ldots, p) \\
&\bar{a}_j = n._j - n.. - \beta._{jk} B^{*+}_{kk'} N_{k'} \\
&\qquad (j = 1, 2, \ldots, q) \\
&\bar{b}_k = B^{*+}_{kk'} N_{k'} \\
&\qquad (k = 1, 2, \ldots, r) \\
&\lambda_a = \lambda_c = 0 .
\end{aligned}\right\}. \tag{17}$$

In order to obtain the statistical errors and covariances of the estimated values as indicated in Equs. (17), let us write down the matrix of the simultaneous equations (16) multiplied by —1. This is a matrix of $p + q + r + 3$ rows and columns and is composed of submatrices in the following way:

$$\mathbf{M} = \frac{1}{\sigma^2} \left\| \begin{array}{cccccc} pq & q\mathbf{J}^{(1,p)} & p\mathbf{J}^{(1,q)} & \mathbf{O}^{(1,r)} & O & O \\ q\mathbf{J}^{(p,1)} & q\mathbf{I}^{(q)} & \mathbf{J}^{(p,q)} & q\mathbf{B}_c^{(p,r)} & q\mathbf{J}^{(p,1)} & \mathbf{O}^{(q,1)} \\ p\mathbf{J}^{(q,1)} & \mathbf{J}^{(q,p)} & p\mathbf{I}^{(q)} & p\mathbf{B}_a^{(q,r)} & \mathbf{O}^{(q,1)} & p\mathbf{J}^{(q,1)} \\ \mathbf{O}^{(r,1)} & q\tilde{\mathbf{B}}_c^{(r,p)} & p\tilde{\mathbf{B}}_a^{(r,q)} & \mathbf{B}^{(r,r)} & \mathbf{O}^{(r,1)} & \mathbf{O}^{(r,1)} \\ O & q\mathbf{J}^{(1,p)} & \mathbf{O}^{(1,q)} & \mathbf{O}^{(1,r)} & O & O \\ O & \mathbf{O}^{(1,p)} & p\mathbf{J}^{(1,q)} & \mathbf{O}^{(1,r)} & O & O \end{array} \right\| .$$

The inverse of $\mathbf{M}$ is

$$\mathbf{M}^+ = \sigma^2 \left\| \begin{array}{cccccc} \frac{1}{pq} & \mathbf{O}^{(1,p)} & \mathbf{O}^{(1,q)} & \mathbf{O}^{(1,r)} & -\frac{1}{pq} & -\frac{1}{pq} \\ \mathbf{O}^{(p,1)} & \mathscr{B}_{cc}^{(p,p)} & \mathscr{B}_{ac}^{(p,q)} & -\mathscr{B}_c^{(p,r)} & \frac{1}{pq}\mathbf{J}^{(p,1)} & \mathbf{O}^{(p,1)} \\ \mathbf{O}^{(q,1)} & \mathscr{B}_{ac}^{(q,p)} & \mathscr{B}_{aa}^{(q,q)} & -\mathscr{B}_a^{(q,r)} & \mathbf{O}^{(q,1)} & \frac{1}{pq}\mathbf{J}^{(q,1)} \\ \mathbf{O}^{(r,1)} & \mathscr{B}_c^{(r,p)} & -\mathscr{B}_a^{(r,q)} & \mathbf{B}^{*+(r,r)} & \mathbf{O}^{(r,1)} & \mathbf{O}^{(r,1)} \\ -\frac{1}{pq} & \frac{1}{pq}\mathbf{J}^{(1,p)} & \mathbf{O}^{(1,q)} & \mathbf{O}^{(1,r)} & O & O \\ -\frac{1}{pq} & \mathbf{O}^{(1,p)} & \frac{1}{pq}\mathbf{J}^{(1,q)} & \mathbf{O}^{(1,r)} & O & O \end{array} \right\|$$

The meanings of the symbols can be found in § 16.

Let $\mathscr{M}^+$ be the matrix obtained when deleting the last two rows and columns in $\mathbf{M}^+$ · $\mathscr{M}^+$ is, of course, degenerate because of $c. = a. = 0$ and is of the rank $p + q + r - 1$. Let s' and s be integer numbers such that $1 \leq s' \leq p$ and $1 \leq s \leq q$. Let us omit the rows and columns of $\mathscr{M}^+$ standing on the places numbered $1 + s'$ and $1 + p + s$. The resulting matrix, $\mathscr{M}^+_{s's}$ is the covariance matrix of the variables $\bar{A}$, $\bar{c}_i (i = 1,2, \ldots, s' - 1, s' + 1, \ldots, p)$, $\bar{a}_j (j = 1,2, \ldots, s - 1, s + 1, \ldots, q)$, $\bar{b}_k (k = 1,2, \ldots, r)$.

It can thus be seen that $\bar{A}$ is independent of the measured values of all remaining parameters and has the estimated variance

$$\overline{\sigma^2_{\bar{A}}} = \frac{1}{pq}\overline{\sigma^2}.$$

The estimated values of the parameters $\bar{c}_i$, $\bar{a}_j$, $\bar{b}_k$ are not independent of each other. Their estimated variances are the diagonal elements of the matrices $\overline{\sigma^2}\,\mathscr{B}_{cc}$, $\overline{\sigma^2}\,\mathscr{B}_{aa}$ and $\overline{\sigma^2}\,\mathscr{B}^{*+}$ respectively; i.e.

$$\left.\begin{aligned} \overline{\sigma^2_{\bar{c}_i}} &= \mathscr{B}^{cc}_{ii'}\,\overline{\sigma^2} \qquad (\text{with } i' = i) \\ \overline{\sigma^2_{\bar{a}_j}} &= \mathscr{B}^{aa}_{jj'}\,\overline{\sigma^2} \qquad (\text{with } j' = j) \\ \overline{\sigma^2_{\bar{b}_k}} &= \mathscr{B}^{*+}_{kk'} \qquad (\text{with } k' = k) \end{aligned}\right\}. \tag{18}$$

It can be easily seen that the estimated value of σ^2 is

$$\begin{aligned} \overline{\sigma^2} &= \frac{1}{q'}\,(n_{ij} - \bar{n}_{ij})\,(n_{ij} - \bar{n}_{ij}) = \\ &= \frac{1}{q'}\,[n_{ij}\,n_{ij} - pq\,\bar{A}^2 - qn_{i\cdot}\,\bar{c}_i - pn_{\cdot j}\,\bar{a}_j - n_{ij}\beta_{ijk}\,\bar{b}_k]\,, \end{aligned} \tag{19}$$

where $q' = (p-1)(q-1) - r$ and

$$\bar{n}_{ij} = \bar{A} + \bar{c}_i + \bar{a}_j + \beta_{ijk}\,\bar{b}_k\,.$$

The quantity $q'\,\overline{\sigma^2}/\sigma^2$ is a stochastic variable with a χ^2 distribution of q' degrees of freedom.

On the basis of the identity

$$\sum_{i=1}^{p}\sum_{j=1}^{q}(n_{ij} - n_{\cdot\cdot})^2 = \sum_{i=1}^{p}\sum_{j=1}^{q}(n_{ij} - \bar{n}_{ij})^2 + \sum_{i=1}^{p}\sum_{j=1}^{q}(\bar{c}_i + \bar{a}_j + \beta_{ijk}\,\bar{b}_k)^2$$

making use of the theorem of COCHRAN [5] and FISHER's lemma, it can be seen that all quantities $n_{ij} - \bar{n}_{ij}$ $(i = 1,2,\ldots,p;\ j = 1,2,\ldots,q)$ are independent of $\bar{A}$, $\bar{c}_i$ $(i = 1,2,\ldots,p)$ $\bar{a}_j (j = 1,2,\ldots,q)$ and $\bar{b}_k (k = 1,2,\ldots,r)$ Thus, e.g., $(n_{ij} - \bar{n}_{ij})(n_{ij} - \bar{n}_{ij})$ is independent of $f(\bar{a}_1, \bar{a}_2, \ldots, \bar{a}_q)$, this latter being an arbitrary function of the variables $\bar{a}_1, \bar{a}_2, \ldots, \bar{a}_q$.

§ 18. (Problem II of § 15). In order to calculate the probability ε that the deviations from zero of the values $\bar{a}_j (j = 1,2,\ldots,q)$ are due to statistical fluctuations alone, let us introduce the following notations:

$\bar{\mathbf{a}}_s$ should denote the matrix

$$\bar{\mathbf{a}}_s^{(1,q-1)} = \|\bar{a}_1, \bar{a}_2, \ldots, \bar{a}_{s-1}, \bar{a}_{s+1}, \ldots, \bar{a}_q\|$$

with s being an integer number chosen arbitrarily within the interval

$$1 \leq s \leq q.$$

$\mathscr{B}_s^{q-1,q-1}$ should be the matrix obtained when omitting the row and column in the matrix $\mathscr{B}_{aa}^{(q,q)}$ numbered s.

First, let us calculate the probability ε_s that the deviations from zero of the elements of $\bar{\mathbf{a}}_s$ are due only to statistical fluctuations.

The covariance matrix of the elements of $\bar{\mathbf{a}}_s$ is $\sigma^2\mathscr{B}_s$. Assuming $a_j = \langle\bar{a}_j\rangle = 0$ $(j = 1,2, \ldots, q)$ the joint distribution function of the elements of $\bar{\mathbf{a}}_s$ is given by

$$S(\bar{\mathbf{a}}_s) = \frac{\sqrt{D_s^+}}{(2\pi)^{q-1/2}} \exp\left[-\frac{1}{2\sigma^2}\bar{\mathbf{a}}_s\mathscr{B}_s^+\tilde{\bar{\mathbf{a}}}_s\right],$$

where D_s^+ stands for the determinant of the matrix

$$\frac{1}{\sigma^2}\mathscr{B}_s^+.$$

It is well known that the quantity

$$Q_s = \frac{1}{\sigma^2}\bar{\mathbf{a}}_s\mathscr{B}_s^+\tilde{\bar{\mathbf{a}}}$$

is distributed according to a χ^2 distribution with $q-1$ degrees of freedom. As it was shown at the end of § 17 $(n_{ij} - \bar{n}_{ij})(n_{ij} - \bar{n}_{ij})$ is independent of any function of $\bar{a}_1, \bar{a}_2, \ldots, \bar{a}_q$ thus $\overline{\sigma^2}$ and Q_s are independent of each other. As a consequence, the quantity

$$y_s = \frac{1}{2}\ln\frac{1}{q-1}\,\frac{\bar{\mathbf{a}}_s\mathscr{B}_s^+\tilde{\bar{\mathbf{a}}}}{\overline{\sigma^2}}$$

is distributed according to FISHER's z distribution with $q-1$ and q' degrees of freedom. Denoting this latter distribution by $P_{q-1,q'}$ $(\zeta > z)$ the result is obtained that

$$\varepsilon_s = P_{q-1,q}\,(\zeta > y_s). \tag{20}$$

Applying the theorem proved in Appendix III it can be seen that $\bar{\mathbf{a}}_s\mathscr{B}_s^+\tilde{\bar{\mathbf{a}}}$, is independent of s and, as a consequence, the same is true also for y_s and ε_s It is therefore justified to regard the value $\varepsilon_1 = \varepsilon_2 = \ldots = \varepsilon_q = \varepsilon$ as being the probability that the deviations from zero of the values $\bar{a}_j$ $(j = 1,2, \ldots, q)$ are due to statistical fluctuations alone. The value of $\varepsilon = \varepsilon_s$ is thus determined by Equs. (20).

§ 19. (Problem III of § 15). Since

$$\overline{a_j^2} = \overline{a_j^2} - \overline{\sigma_{aj}^2} \qquad (j = 1, 2, \ldots, q),$$

therefore, taking into account Equ. (18), an unbiased estimate of a^2 is

$$\overline{a^2} = \frac{1}{q}(\bar{a}_j \bar{a}_j - \mathcal{B}_{jj}^{aa}\,\overline{\sigma^2}). \tag{21}$$

Calculations outlined in Appendix II show that the estimated value of the variance of $\overline{a^2}$ is equal to

$$\overline{\sigma_{a^2}^2} = \frac{2\,\overline{\sigma^2}}{q^2}\left[2\,\bar{a}_j \mathcal{B}_{jj'}^{aa}, \bar{a}_{j'} - \frac{\overline{\sigma^2}}{q'+2}(q'\,\mathcal{B}_{jj'}^{aa}\mathcal{B}_{jj'}^{aa} - \mathcal{B}_{jj}^{aa}\mathcal{B}_{j'j'}^{aa})\right] \tag{22}$$

the value of $\overline{\sigma^2}$ being given with Equ. (19).

VI. The case of the incomplete matrix n with elements of unequal variances*

§ 20. It may happen that the measurement of the intensity $\langle n_{ij}\rangle$ and/or some of the quantities β_{ijk} was interrupted during certain intervals (i, j), and thus the corresponding n_{ij} and/or β_{ijk} values are missing. It may also happen that the variances of the measured quantities n_{ij} are not equal to each other. The solutions of the three problems formulated in § 15 may then be found on the following lines.

Let us denote the variance of n_{ij} by

$$\sigma_{ij}^2 = \sigma^{2*}/w_{ij},$$

where the factors $1/w_{ij}$ must be known a priori and σ^{2*} is to be determined.

Furthermore, let be

$\Delta_{ij} = w_{ij}$ if the values $n_{ij}, \beta_{ij_2}, \beta_{ij_2}, \ldots, \beta_{ijr}$ are all available,

$\Delta_{ij} = 0$ if at least one of the values $n_{ij}, \beta_{ij_1}, \beta_{ij_2}, \ldots, \beta_{ijr}$ is missing.

If among the values $\Delta_{i_1}, \Delta_{i_2}, \ldots, \Delta_{iq}$ there is not more than one different from zero, the ith rows of the matrices** $\mathbf{n}$ and $\beta_k (k=1,2,\ldots,r)$ should be deleted and the numeration of the rows should be rearranged accordingly.

If not more than one among the quantities $\Delta_{1j}, \Delta_{2j}, \ldots, \Delta_{pj}$ is different from zero, the measurement must be continued until at least two of the $\Delta_{1j}, \Delta_{2j}, \ldots, \Delta_{pj}, \Delta_{p+1,j}, \ldots, \Delta_{p+p^*,j}$ values becomes different from zero, and the value $p + p^*$ should then be denoted by p.

Thus at least two elements in each row and column of the matrix $\Delta_{(p,q)}$ are different from zero.

* Identical indices do *not* mean summation in this chapter.

** $\beta_k^{(p,q)}$ stands for the matrix with elements β_{ijk} $(i = 1,2,\ldots, p;\ j = 1,2,\ldots,q)$

The values $n_{ij}, \beta_{ijk} (k = 1,2, \ldots, r)$ will, in what follows, never occur without being multiplied by Δ_{ij}. Thus arbitrary values (e.g. 0) may be written in the place of n_{ij} and β_{ijk} $(k = 1,2, \ldots, r)$ if $\Delta_{ij} = 0$. This way the blank places in the matrices $\mathbf{n}$ and $\mathbf{\beta}_k$ $(k = 1,2, \ldots, r)$ can be filled in. This is also the case when the total time of measurement (N) is not an integer multiple of q; the last row can be completed arbitrarily only that the corresponding Δ_{pj} values must be put equal to 0. It will be assumed in what follows that there are no blank places in the matrices $\mathbf{n}$ and $\mathbf{\beta}_k$ $(k = 1,2, \ldots, r)$.

It can be assumed without restriction imposed upon the factors β_{ijk} that

$$\sum_{i=1}^{p} \sum_{j=1}^{q} \Delta_{ij} \beta_{ijk} = 0 \qquad (k = 1, 2, \ldots, r).$$

The sum of the elements of the matrix $\mathbf{\Delta}$ should be denoted by Δ and the number of elements in $\mathbf{\Delta}$ which are different from 0 should be N_0. $(N_0 \leqslant pq$ is thus the total number of useful measurements.) The product of all non-zero values Δ_{ij} should be denoted by $\pi(\Delta)$.

§ 21. The basic assumption as to the form of the change of the intensity (Equs. (14)) may remain unchanged, neither does change the principle of deriving the equations for determining the estimated values of the parameters (Equs. (16)). The particular form of Equs. (16) will, however, be different from that in § 17. The matrix of the system of linear equations (multiplied by —1) will, in this case, be the following:

$$\mathbf{M} = \frac{1}{\sigma^{2*}} \left\| \begin{array}{cccccc} \Delta & \Delta_c^{(1,p)} & \Delta_a^{(1,q)} & \mathbf{0}^{(1,r)} & 0 & 0 \\ \Delta_a^{(p,1)} & \Delta_{cc}^{(p,p)} & \Delta^{(p,q)} & \mathbf{B}_c^{(p,r)} & q\mathbf{J}^{(p,1)} & \mathbf{0}^{(p,1)} \\ \tilde{\Delta}_a^{(q,1)} & \tilde{\Delta}^{(q,p)} & \Delta_{aa}^{(q,q)} & \mathbf{B}_a^{(q,r)} & \mathbf{0}^{(q,1)} & p\mathbf{J}^{(q,1)} \\ \mathbf{0}^{(r,1)} & \tilde{\mathbf{B}}_c^{(r,p)} & \tilde{\mathbf{B}}_a^{(r,q)} & \mathbf{B}^{(r,r)} & \mathbf{0}^{(r,1)} & \mathbf{0}^{(r,1)} \\ 0 & q\mathbf{J}^{(1,p)} & \mathbf{0}^{(1,q)} & \mathbf{0}^{(1,r)} & 0 & 0 \\ 0 & \mathbf{0}^{(1,p)} & p\mathbf{J}^{(1,q)} & \mathbf{0}^{(1,r)} & 0 & 0 \end{array} \right\|, \tag{23}$$

where

$\Delta_c^{(1,p)}$	stands for the matrix with elements	$\sum_{j=1}^{q} \Delta_{ij}$	$(i = 1, 2, \ldots, p)$
$\Delta_a^{(1,q)}$	stands for the matrix with elements	$\sum_{i=1}^{p} \Delta_{ij}$	$(j = 1, 2, \ldots, q)$
$\Delta_{cc}^{(p,p)}$	stands for the diagonal matrix with diagonal elements	$\sum_{j=1}^{q} \Delta_{ij}$	$(i = 1, 2, \ldots, p)$
$\Delta_{aa}^{(q,q)}$	stands for the diagonal matrix with diagonal elements	$\sum_{i=1}^{p} \Delta_{ij}$	$(j = 1, 2, \ldots, q)$

$\mathbf{B}_c^{(p,r)}$ stands for the matrix with elements $\sum_{j=1}^{q} \Delta_{ij}\beta_{ijk}$ $(i = 1, 2, \ldots, p$ $k = 1, 2, \ldots, r)$

$\mathbf{B}_a^{(q,r)}$ stands for the matrix with elements $\sum_{i=1}^{p} \Delta_{ij}\beta_{ijk}$ $(j = 1, 2, \ldots, q$ $k = 1, 2, \ldots, r)$

$\mathbf{B}^{(r,r)}$ stands for the matrix with elements $\sum_{i=1}^{p}\sum_{j=1}^{q} \Delta_{ij}\beta_{ijk}\beta_{ijk'}$ $(k,k' = 1, 2, \ldots, r)$.

Δ is explained in § 20, **O** and **J** have the same meaning as in § 16.

In general, no simple expressions can be derived for the estimated values of the parameters which can, in principle, be calculated by inverting the matrix (23). If this has been done, every question can be answered exactly as it has been done in Section V. Note, however, that the estimated value of σ^2 will be

$$\overline{\sigma^{2*}} = \frac{1}{N_0 - p - q - r + 1} \sum_{i=1}^{p}\sum_{j=1}^{q} \Delta_{ij}(n_{ij} - \bar{n}_{ij})^2.$$

Equations (20), (21), (22) remain valid if

$$q' = N_0 - p - q - r + 1 \text{ (instead of } (p-1)(q-1) - r),$$

and $\sigma^{2*}\mathscr{B}_{jj'}^{aa}$ denotes the covariance of $\bar{a}_j$ and $\bar{a}_{j'}$, and $\sigma^{2*}\mathscr{B}_s$ stands for the matrix obtained by omitting the row and column numbered s in the covariance matrix of the $\bar{a}_s$ quantities.

§ 22. Sometimes it may be almost impossible to calculate the inverse of the matrix (23) even by means of electronic computers. This is the case if p is very large (e.g. ≥ 200), i.e. the matrix **n** consists of very many rows and thus there are lots of parameters c_i characterizing the slow change of the intensity. The inversion of the whole matrix (23) can, however, be avoided in the following way:

Let us introduce the following notations:

$$\left.\begin{aligned} \Delta_i &= \sum_{j=1}^{q} \Delta_{ij} \\ n_{\cdot}^{i} &= \frac{1}{\Delta_i} \sum_{j=1}^{q} \Delta_{ij} n_{ij} \\ a_{\cdot}^{i} &= \frac{1}{\Delta_i} \sum_{j=1}^{q} \Delta_{ij} a_j \\ \beta_{\cdot k}^{i} &= \frac{1}{\Delta_i} \sum_{j=1}^{q} \Delta_{ij} \beta_{ijk} \\ \beta'_{ijk} &= \beta_{ijk} - \beta_{\cdot}^{i} \\ d_i &= A + c_i + a_{\cdot}^{i} + \beta_{\cdot k}^{j} b_k \end{aligned}\right\}. \qquad (24)$$

Note that

$$\left.\begin{aligned} &\sum_{j=1}^{n} \Delta_{ij}(n_{ij} - n^i_{\cdot}) = 0 \qquad (i = 1, 2, \ldots, p) \\ &\sum_{j=1}^{q} \Delta_{ij}(a_j - a^i_{\cdot}) = 0 \qquad (i = 1, 2, \ldots, p) \\ &\sum_{j=1}^{q} \Delta_{ij}\beta'_{ijk} = 0 \qquad \begin{matrix}(i = 1, 2, \ldots, p \\ k = 1, 2, \ldots, r)\end{matrix} \end{aligned}\right\}. \tag{24a}$$

The basic assumption as to the change of the intensity can thus be written in the form

$$\langle n_{ij} \rangle = d_i + a_j - a^i_{\cdot} + \beta'_{ijk} b_k$$

$$(a_{\cdot} = 0\,, \quad 1 = 1, 2, \ldots, p; \quad j = 1, 2, \ldots, q; \quad k = 1, 2, \ldots, r)$$

which is identical with the form as expressed by Equ. (14).

Regarding the quantities $d_i (i = 1,2, \ldots, p)$, $a_j (j = 1,2, \ldots, q)$ and $b_k (k = 1,2, \ldots, r)$ as unknown parameters the normal equations for determining $\bar{d}_i$, $\bar{a}_j$ and $\bar{b}_k$ will be the following:

$$\frac{\partial P}{\partial d_i} = \frac{1}{\sigma^{2*}} \sum_{j=1}^{q} \Delta_{ij}(n_{ij} - \bar{d}_i) = 0\,, \quad (i = 1, 2, \ldots, p) \tag{25}$$

$$\left.\begin{aligned} &\frac{\partial P}{\partial a_j} = \frac{1}{\sigma^{2*}} \sum_{j=1}^{p} \Delta_{ij}(n_{ij} - n^i - \bar{a}_j + \bar{a}^i - \beta'_{ijk}\bar{b}_k) = 0 \\ &\qquad\qquad (j = 1, 2, \ldots, q) \\ &\frac{\partial P}{\partial b_k} = \frac{1}{\sigma^{2*}} \sum_{i=1}^{p} \sum_{j=1}^{q} \Delta_{ij}\beta'_{ijk}(n_{ij} - n^i - \bar{a}_j + \bar{a}^i - \beta'_{ijk'}\bar{b}_{k'}) = 0 \\ &\qquad \sum_{j=1}^{q} \bar{a}_j = 0\,. \end{aligned}\right\}, \tag{26}$$

It can be seen that Equs. (25) and (26) do not have common variables and

$$\bar{d}_i = n^i_{\cdot} \qquad (i = 1, 2, \ldots, p)\,.$$

The system (26) consists of only $q + r + 1$ equations the matrix of which can be inverted much easier than the matrix (23), and the covariance matrix of the quantities $\bar{a}_j (j = 1, 2, \ldots, q)$ and $\bar{b}_k (k = 1,2, \ldots, r)$ can thus be determined.

The estimated values of the quantities $A + c_i (i = 1, 2, \ldots, p)$ can be obtained on the basis of $\bar{a}_j$, $\bar{b}_k$ and Equ. (24). The variances involving $\bar{A} + \bar{c}_i$ $(i = 1,2, \ldots, p)$ can also be calculated on the basis of (24) and of the fact that the $\bar{d}_i (i = 1,2, \ldots, p)$ are independent of $\bar{a}_j (j = 1,2, \ldots, q)$ and $\bar{b}_k (k = 1,2, \ldots, r)$, E.g.

$$\text{covariance of } (\bar{A} + \bar{c}_i, \bar{a}_j) = -\text{ covariance of } (\bar{a}^i_{\cdot}, \bar{a}_j) - \sum_{k=1}^{r} \text{covariance of } (\beta^i_{\cdot k}\bar{b}_k, \bar{a}_j).$$

VII. Concluding remarks

§ 23. It has been shown that the representation

$$\langle n_{ij} \rangle = A + c_i + a_j + \beta_{ijk} b_k$$
$$(i = 1, 2, \ldots, p; \quad j = 1, 2, \ldots, q; \quad k = 1, 2, \ldots, r) \tag{27}$$
$$a_\cdot = c_\cdot = 0$$

may be very often preferred to that of the Fourier type. Assuming n_{ij} to be independent Gaussian variables, explicite expressions have been given for the maximum likelihood estimations of the parameters A, c_i, a_j, b_k together with the variances and covariances of the estimates. The probability that the deviations of the values $\bar{a}_j$ $(j = 1,2,\ldots, q)$ from zero are due to statistical fluctuations only has been derived as well as an unbiased estimated value of the mean square amplitude

$$a^2 = \frac{1}{q} \sum_{j=1}^{q} a_j^2$$

and the variance of this estimate.

The advantage of the representation (27) is that

a) it does not involve the assumption that the periodic function be a trigonometric polynome, and

b) the numerical calculations required are by far simpler than those involved in a Fourier representation with the same number of parameters.

There are cases when the first and may be also the second Fourier components have direct physical meanings and should be estimated. In such cases the Fourier method and the simple step function method may be combined to yield the estimated values of the amplitudes of the first and second harmonics and the rest may be investigated by the step function representation.

§ 24. The existence of a slow variation of the intensity, i.e. the probability ε_c that the deviations from zero of the estimated values $\bar{c}_i$ $(i = 1,2, \ldots, p)$ are due to statistical fluctuations alone, can be determined just in the same way as it has been done in the case of the periodic part of the variation. All what we have to do is to change the notations referring to "a" into those referring to "c". We thus have

$$\varepsilon_c = P_{p-1,q'}(\zeta > y_c)$$

with

$$y_c = \frac{1}{2} \ln \frac{1}{p-1} \frac{\bar{\mathbf{c}}_s \mathscr{B}^{+}_{sc} \tilde{\bar{\mathbf{c}}}_s}{o^2},$$

where $\mathscr{B}_{sc}$ stands for the matrix obtained when omitting the row and column numbered s in the matrix $\mathscr{B}_{cc}$ (see § 18).

The unbiased estimated value of

$$c^2 = \frac{1}{p} \sum_{i=1}^{p} c_i^2$$

the mean square amplitude of the slow variation and the variance of this estimate can also be obtained by using the formulae referring to a^2 and changing the notations accordingly.

§ 26. Applications of some parts of the results reported on in this paper may be found in [6] and [7]. Full applications will be published later on.

Acknowledgements

The authors are indebted to Professor L. JÁNOSSY for many illuminating and encouraging discussions on the subject. The helpful cooperation of Mr. F. TELBISZ and Mr. T. SÁNDOR at the early stage of the work is gratefully acknowledged.

Appendix I

If the variables $x_i (i = 1,2, \ldots, n)$ are distributed normally according to the joint density function

$$\frac{\sqrt{\det (A_{ik})}}{(2\pi)^{n/2}} \exp\left[-\frac{1}{2} A_{ik} (x_i - a_i)(x_k - a_k) \right],$$

$$(i, k = 1, 2, \ldots, n)$$

then the variable

$$u = \sum_{i=1}^{n} (x_i - x.)^2$$

has the expected value

$$\langle u \rangle = A_i A_i + A_{ii}^{*}, \tag{A1}$$

and the variance

$$\sigma_u^2 = 2 A_{ij}^{*} (A_{ij}^{*} + 2 A_i A_j), \tag{A2}$$

where

$$A_i = a_i - a$$

and

$$A_{ij}^{*} = A_{ij}^{+} - A_{i.}^{+} - A_{.j}^{+} + A_{..}^{+} . \tag{A3}$$

Proof. The quantities

$$x_i' = x_i - x. \qquad (i = 1, 2, \ldots, n)$$

have the expected values

$$\langle x_i' \rangle = A_i$$

and their covariance matrix is composed of the elements $A_{ij}^*(i, j = 1,2, \ldots, n)$, It can be shown by means of simple calculations that the quantity

$$u = x_i' x_i'$$

has the expected value and variance as given by Equs. (*A*1) (*A*2), respectively.

Appendix II

The variables $x_i\,(i = 1,2, \ldots, n)$ should be distributed normally with

$$\langle x_i \rangle = a_i \qquad (i = 1, 2, \ldots, n)$$

and

$$\langle (x_i - a_i)(x_j - a_j \rangle = \sigma^2 A_{ij}, \qquad (i, j = 1, 2, \ldots, n)\,,$$

where the A_{ij} elements are known, the rank of the matrix $|| A_{ij} ||$ is at least $n - 1$, a_i and σ^2 are unknown, but σ^2 has a known estimate $\overline{\sigma^2}$, such that $p'\overline{\sigma^2}/\sigma^2$ is distributed according to χ^2 with p' degrees of freedom, and $\overline{\sigma^2}$ is independent of $\chi_i(i = 1,2, \ldots, n)$.

Clearly the value

$$\overline{a^2} = \frac{1}{n}\,[x_i x_i - A_{ii}\,\overline{\sigma^2}] \tag{A4}$$

is an unbiased estimate of

$$a^2 = \frac{1}{n}\,a_i a_i.$$

It will be shown that the estimated variance of $\overline{a^2}$ is

$$\overline{\sigma_{a^2}^2} = \frac{2\overline{\sigma^2}}{n^2}\left[2Q_3 - \frac{\overline{\sigma^2}}{p'+2}\,(p' A_{ij} A_{ij} - A_{ii} A_{jj})\right], \tag{A5}$$

where

$$Q_3 = x_i A_{ij} x_j.$$

According to Appendix I

$$\sigma_{x_i x_i}^2 = 2\,\sigma^2 A_{ij}\,(\sigma^2 A_{ij} + 2\,a_i a_j).$$

Taking into account that

$$\overline{(\sigma^2)^2} = \frac{p'}{p'+2}\,(\overline{\sigma^2})^2$$

and

$$\overline{\sigma^2_{\sigma^2}} = \frac{2}{p'}\,\overline{(\sigma^2)^2} = \frac{2}{p'+2}\,(\overline{\sigma^2})^2,$$

furthermore that $x_i x_i$ is independent of $\overline{\sigma^2}$, and that the estimated value of $a_i a_j \sigma^2$ is

$$x_i\, x_j\, \overline{\sigma^2} - \frac{p'}{p'+2} A_{ij}\,(\overline{\sigma^2})^2.$$

Equs. (A5) can be obtained without difficulty.

Appendix III

A one-row matrix $\mathbf{b}^{(1,n)}$ with elements $b_i (i = 1,2, \ldots, n)$ all different from zero should be given together with a one-column matrix $\mathbf{a}^{(n,1)}$ with elements $a_i (i = 1,2, \ldots, n)$, and a symmetric matrix $\mathbf{D}^{(n,n)}$ of the rank $n - 1$. Each diagonal submatrix of $\mathbf{D}$ with $n - 1$ rows and $n - 1$ columns should be of the rank $n - 1$. The elements of $\mathbf{a}$ and $\mathbf{D}$ should satisfy the equations

$$\mathbf{ba} = \mathbf{0}^{(1,1)} = O \quad \text{i.e.} \quad b_i\, a_i = O \tag{A6}$$

and

$$\mathbf{D}\tilde{\mathbf{b}} = \mathbf{0}^{(n,1)}, \quad \text{i.e.} \quad D_{ij}\, b_j = O \quad (i = 1, 2, \ldots, n). \tag{A7}$$

Let us denote by $\mathbf{a}_r^{(n-1,1)}$ the one-column matrix with elements $a_1, \ldots, a_{r-1}, a_{r+1}, \ldots, a_n$ and by $\mathbf{D}_r^{(n-1,n-1)}$ the matrix with elements $D_{ij} (i,j = 1, \ldots, r-1, r+1, \ldots, n)$.

It will be shown that the quantity

$$Q_r = \tilde{\mathbf{a}}_r\, \mathbf{D}_r^{+}\, \mathbf{a}_r \tag{A8}$$

is independent of r. This can be done as follows:

If the one-column matrix $\mathbf{y}_0^{(n,1)}$ is a solution of the equation

$$\mathbf{D}\mathbf{y}_0 = \mathbf{a}, \tag{A9}$$

then all solutions of (A9) may be written in the form

$$\mathbf{y} = \mathbf{y}_0 + \lambda\tilde{\mathbf{b}},$$

where λ denotes an arbitrary scalar quantity. Introducing the notation

$$\mathbf{z}_r^{(n-1,1)} = \mathbf{D}_r^{+}\, \mathbf{a}_r, \tag{A10}$$

it can be seen that

$$\mathbf{D}_r z_r = \mathbf{a}_r . \tag{A11}$$

Let us denote the elements of $\mathbf{z}_r$ by $z_1, z_2, \ldots, z_{r-1}, z_{r+1}, \ldots, z_n$ and let us denote by $\mathbf{z}_r'^{(n,1)}$ the matrix consisting of the elements $z_1, \ldots, z_{r-1}, O, z_{r+1}, \ldots, z_n$. It follows from (A6), (A7), and (A11) that $\mathbf{z}_r'$ is a solution of (A9), may thus be written in the form

$$\mathbf{z}_r' = \mathbf{y}_0 + \lambda_r \tilde{\mathbf{b}} . \tag{A12}$$

Making use of Q_r may be expressed by means of $\mathbf{z}_r'$ in the form

$$Q_r = \tilde{\mathbf{a}} \mathbf{z}_r' . \tag{A13}$$

Let us now investigate another quantity (A8), e.g.

$$Q_s = \tilde{\mathbf{a}}_s \mathbf{D}_s^+ \mathbf{a}_s .$$

Repeating the considerations above we arrive at

$$\mathbf{z}_s' = \mathbf{y}_0 + \lambda_s \tilde{\mathbf{b}} \tag{A14}$$

and

$$Q_s = \tilde{\mathbf{a}} \mathbf{z}_s' . \tag{A15}$$

On the basis of (A12) — (A15), and (A6) we have

$$Q_r - Q_s = (\lambda_r - \lambda_s) \tilde{\mathbf{a}} \tilde{\mathbf{b}} = 0$$

what was to be shown.

REFERENCES

1. H. Cramér, Mathematical Methods of Statistics, Princeton Univ. Press, 1946, pp. 537—541.
2. S. Chapman and J. Bartels, Geomagnetism, Oxford, Clarendon Press, 1951, p. 563.
3. H. Scheffé, The Analysis of Variance, John Wiley and Sons, New York, 1959, pp. 207—213.
4. L. Jánossy, Theory and Practice of the Evaluation of Measurements, Oxford, Clarendon Press, 1965, pp. 230—253.
5. See [1], p. 117.
6. T. Sándor, A. Somogyi and F. Telbisz, Il Nuovo Cimento, **24**, 316, 1962.
7. N. Ahababian, B. Betev, S. Kavlakov, T. Sándor and A. Somogyi: Proceedings of the International Conference on High-Energy Physics, Tihany, 1962; Hungarian Academy of Sciences, Budapest, 1963, p. 243.

НЕКОТОРЫЕ ПРОБЛЕМЫ ИССЛЕДОВАННОЙ ПЕРИОДИЧНОСТИ ВРЕМЕННОЙ СЕРИИ КОСМИЧЕСКИХ ЛУЧЕЙ

Й. КОТА и А. ШОМОДИ

Р е з ю м е

Дается обобщение метода анализа расхождения с целью исследования существования и вида периодичности с данной длиной периода. Принимаются во внимание как переменные изменения интенсивности космических лучей, так и метеорологические эффекты. Далее, кроме точного исследования существования периодичности излагаются максимальные вероятные оценки как для постоянных, характеризующих вид периодичности, так и для главной квадратичной амплитуды периодической функции вместе с их относительной статистической ошибкой в случае произвольного числа метеорологических факторов, влияющих на интенсивность космического излучения.

Показываются невыгоды применения метода Фурье в исследовании периодичности с определенной длиной периода Наконец, показывается, что факт статистического определения метеорологических коэффициентов нельзя отделять от анализа периодичности.

Acta Physica Academiae Scientiarum Hungaricae, Tomus 27, pp. 549—558 (1969)

TWO-TRIPLET MODEL OF "DIRECT" MUON PRODUCTION*

By

K. LADÁNYI

RESEARCH GROUP FOR THEORETICAL PHYSICS OF THE HUNGARIAN ACADEMY OF SCIENCES, BUDAPEST

(Received 18. III. 1969)

A particular two-triplet model of "direct" lepton productions is suggested by assuming that both leptons and hadrons belong to representations of the six-dimensional rotation group SO_6.

I. Introduction

Considerable interest has recently been attached to the deep-mine experiment of BERGESON et al. [1, 2] which indicates a failure of the $\sec\Theta$ law in the energy domain 10^3—10^4 GeV. This implies either direct production of cosmic-ray muons of $\gtrsim 10^3$ GeV or production via a very short-lived parent. Similar production of high-energy electrons has also been proposed [2] in order to explain some mu-less shower data. On the other hand, the Brookhaven experiment [3] verified the $\sec\Theta$ law below 300 GeV. In addition, the data re-examined by NASH and WOLFENDALE [4] imply no evidence for direct muon production in the energy domain 500—1000 GeV. The reported experiments indicate, if all the data are correct, the absence of a transition region between pure pion and kaon parentage below 10^3 GeV and "direct" lepton production above this energy. To explain this situation BJORKEN et al. [5] suggested some theoretical models involving the strong production of a massive particle X which is stable under strong and electromagnetic interactions and decays with high probability into a state containing a muon. According to the most popular assumptions the X particle could be an intermediate boson, produced strongly in pairs, along the lines suggested by OKUBO, MARSHAK and coworkers [6]. The experiment of BERGESON et al. seems to indicate, however, that the vertical muon intensity arises entirely from "direct" production and that the conventional flux of pions and kaons has effectively vanished [7].

As a second theoretical possibility one may conjecture that the X particles are strongly interacting heavy triplets with integral charge [5, 8—11]. This interpretation is favoured by a recent underground experiment of DARDO, PENENGO and SITTE [12]. Two distinct kinds of strongly interacting particles

* Dedicated to Prof. P. GOMBÁS on his 60th birthday.

have been observed. The first group has all the characteristics of pions, the second appears only with short delays after the triggering muons. To explain the data DARDO at al. suggested that the delayed events are due to particles of a mass about 10 $\sim$ 15 GeV, possibly heavy triplet particles of unit charge. The apparent discrepancy between these conclusions and those of earlier experiments [13] may be explained by the differences in the triggering conditions, if the following assumptions are satisfied. (a) The heavy triplet particles are created in processes involving dissociation of the colliding primaries. (b) The unstable members of the triplets have a dominant decay mode leading directly, without intermediate strongly interacting particles, to energetic muons. This production mechanism seems to be compatible with the results of BERGESON et al. On the other hand, the reported "direct" production of leptons does not follow directly, without additional assumptions, from "conventional" triplet models with integer charge. Although confirmation of the effect and further experimental details are needed, the theoretical study of the problem may lead to useful points of view. In this paper a particular two-triplet model of direct lepton production will be proposed by assuming that both leptons and hadrons belong to representations of the rotation group SO_6.

II. Two-triplet model of leptons. "Direct" production

An interesting two-triplet model of hadrons has been proposed by BACRY, NUYTS and VAN HOVE [9, 10]. In this scheme the hadrons are assigned into representations of the symplectic group Sp_6. In two previous papers [14, 15] we have discussed some general dynamical and symmetry properties of the two-triplet model by assuming that hadrons belong to representations of the six-dimensional rotation group SO_6. The basic representation 6 of the rank-three group SO_6 contains two SU_3 triplets with integer charge. The members of the triplets are the trions denoted by

$$t_1 = T^+,\ t_2 = T^0,\ t_3 = T'^0,\ t_4 = \Theta^0,\ t_5 = \Theta^+,\ t_6 = \Theta'^+. \tag{1}$$

The trions are characterized by spin 1/2 and internal quantum numbers Z, Q, Y, I, I_3, where Z is a new quantum number, related to the supercharge [9]. (Q, Y, I and I_3 denote the electric charge, the hypercharge, the isospin assignment and the third component of isospin, respectively). In addition, the fermion number N of trions is fixed by $N = 1$. These quantum numbers are identical with those of trions belonging to the basic representation 6 of Sp_6 [9]. The state assignments of trions are summarized in Table I. We shall assume that the trions t_m are created by the six-component trion field $\mathbf{t}_m$. Within the framewok of the SO_6 model the known baryons may be regarded

Table I

Quantum numbers of trions

	I_3	I	Y	Z	Q	N
T^+	$\frac{1}{2}$	$\frac{1}{2}$	$\frac{1}{3}$	$\frac{1}{3}$	1	1
T^0	$-\frac{1}{2}$	$\frac{1}{2}$	$\frac{1}{3}$	$\frac{1}{3}$	0	1
T'^0	0	0	$-\frac{2}{3}$	$\frac{1}{3}$	0	1
Θ^0	$-\frac{1}{2}$	$\frac{1}{2}$	$-\frac{1}{3}$	$-\frac{1}{3}$	0	1
Θ^+	$\frac{1}{2}$	$\frac{1}{2}$	$-\frac{1}{3}$	$-\frac{1}{3}$	1	1
Θ'^+	0	0	$\frac{2}{3}$	$-\frac{1}{3}$	1	1

as $TT\bar{\Theta}$ systems with $Z = 1$, $N = 1$. In addition, the known mesons are supposed to be $t\bar{t}$ states of $Z = 0$, $N = 0$.

The classification of leptons into the SO_6 scheme is provided by the new quantum number Z. We now put the positron e^+ and the positron-neutrino $\bar{\nu}_e$ into the basic representation 6 of SO_6 by assuming that they are created by "elementary" fields. Thus, e^+ and $\bar{\nu}_e$ are supposed to have the assignments $|Z| = 1/3$ and $N = 1$. If this is so, we have to require exact Z conservation in order to guarantee the conservation of baryons with $Z = 1$ and $N = 1$. In addition, only the approximate hypercharge conservation may lead to an apparent conservation of muon number within the framework of this model. Before considering this problem we shall discuss the e^+, $\bar{\nu}_e$ doublet. Let us call the known leptons $e^{\pm}$, $\bar{\nu}_e$, ν_e and $\mu^{\mp}$, ν_μ, $\bar{\nu}_\mu$ normal fermions of $|Z| = 1/3$, $|N| = 1$. The other particles with $Z \neq N$ will be called exotic particles. We now fix the quantum number Z of e^+ and $\bar{\nu}_e$ by assuming that all the exotic fermions and bosons are unstable particles with a mass $\gtrsim 5$ GeV. By this assumption one obtains $Z = +1/3$ for e^+ and $\bar{\nu}_e$, which can be easily seen as follows. Due to the assignments $Z = 1/3$ and $N = 1$ of e^+ and $\bar{\nu}_e$, the exotic fermions of $Z = 1/3$, $N = 1$ are unstable e g. by hypercharge violating processes. In addition, the exotic fermions with $Z = -1/3$, $N = 1$ (e.g. the trions Θ^0, Θ^+, Θ'^+) may have a Z-conserving decay mode of the type

$$\Theta \to \bar{B} + L + L', \tag{2}$$

where $\bar{B}$ is an antibaryon, represented by a $\Theta\bar{T}\bar{T}$ system with $Z = -1$, $N = -1$, and the particles L and L' may be identified with leptons of $Z = 1/3$, $N = 1$

(e.g. e^+ or $\bar{\nu}_e$). On the other hand, the assignments $Z = -1/3$, $N = 1$ of e^+ and $\bar{\nu}_e$ are excluded by our assumptions, because one of the exotic particles (e.g. a trion T of $Z = 1/3$, $N = 1$) would be absolutely stable in this case.

Summarizing, the members of the T-triplet and the leptons e^+ and $\bar{\nu}_e$ have the common quantum numbers $Z = 1/3$, $N = 1$ in our scheme. However, the constituents T of hadrons are supposed to be collective excitations generated by a self-consistent *nonperturbative* mechanism of strong interactions [15]. The effective masses and couplings of these states may be quite different from those of free leptons. The strong interaction between hadron constituents may be connected with the large "bare" coupling constants obtained in previous dynamical calculations [15]. These "bare" coupling constants are defined by integrals of the spectral functions appearing in the effective interaction kernel. Electrons and neutrinos have no strong couplings to a known boson. Thus, in this model, their large "bare" coupling constants must arise from contributions of the continuous spectrum at very high energies.

The SO_6 properties of leptons will be fixed according to the Cabibbo universality of leptonic and semileptonic weak processes. As a first step we shall construct the weak hadronic current in terms of the six-component trion field $\mathbf{t}$ by generalizing the corresponding expressions of the quark model. In order to ensure universality, one has to assign the weak trion current to the regular representation 15 of SO_6. Compared with the weak quark current, the explicit form of the weak trion current is less trivial because the SO_6 hadrons contain two fermions T and the antifermion $\bar{\Theta}$ simultaneously. For example, let us consider the SO_6 structure of the nucleon doublet* p, n given by [16, 17] (spinor indices are omitted)

$$\mathbf{p} \sim \frac{1}{\sqrt{3}} \left[\overline{\Theta^0} (\mathbf{T}^0 \mathbf{T}^+ - \mathbf{T}^+ \mathbf{T}^0) \right], \tag{3}$$

$$\mathbf{n} \sim \frac{1}{\sqrt{3}} \left[\overline{\Theta^+} (\mathbf{T}^0 \mathbf{T}^+ - \mathbf{T}^+ \mathbf{T}^0) \right]. \tag{4}$$

It follows that the nuclear β decay is due to a weak decay of the anti-Θ ($\bar{\Theta}$) constituents of nucleons in this model. Consequently, the weak trion current, belonging to the regular representation 15 of SO_6, must have the $V + A$ form according to the $V - A$ coupling observed in semileptonic weak processes of

* The familiar SU_6 results for the baryon magnetic moments may be recovered by assuming that the magnetic moments $\mathbf{M}^{(tH)}$ of the trion constituents of hadrons transform like $\mathbf{M}^{(tH)} \sim \sim \mathbf{I}_3 + (1/2)\,\mathbf{Y}$. In this case the SO_6 transformation properties of $\mathbf{M}^{(tH)}$ are different from those of the electric charge $\mathbf{Q}$.

nucleons. We now can construct the weak Cabibbo current J^μ of trions in a straightforward way. One obtains

$$J^\mu = \bar{\mathbf{t}}\gamma^\mu(1+\gamma_5)\, V^{(+|15)}(\Theta_c)\mathbf{t}, \tag{5}$$

$$V^{(\pm|15)}(\Theta_c) = \frac{\bar{\lambda}^{1(15)} \pm i\bar{\lambda}^{2(15)}}{2}\cos\Theta_c + \frac{\bar{\lambda}^{4(15)} \pm i\bar{\lambda}^{5(15)}}{2}\sin\Theta_c, \tag{6}$$

where $\gamma_5 = i\gamma^5 = i\gamma^0\gamma^1\gamma^2\gamma^3$, Θ_c is the Cabibbo angle and the matrices $\bar{\lambda}^{j(15)}$ are generators of the group SO_6. [15] contains the complete list of the matrices $\bar{\lambda}^{j(15)}$. The weak current (5) may be written as

$$\mathbf{J}^\mu = \bar{\boldsymbol{l}}\gamma^\mu(1+\gamma_5)\, V^{(+|15)}(0)\boldsymbol{l}, \tag{7}$$

where

$$V^{(\pm|15)}(0) = (1/2)\,(\bar{\lambda}^{1(15)} \pm i\bar{\lambda}^{2(15)})$$

and

$$\boldsymbol{l} = \boldsymbol{U}(\Theta_c)\mathbf{t}, \tag{8}$$

$$U(\Theta_c) = \exp\,[i\Theta_c\bar{\lambda}^{7(15)}] = \begin{pmatrix} 1 & 0 & 0 & 0 & 0 & 0 \\ 0 & \cos\Theta_c & \sin\Theta_c & 0 & 0 & 0 \\ 0 & -\sin\Theta_c & \cos\Theta_c & 0 & 0 & 0 \\ 0 & 0 & 0 & 1 & 0 & 0 \\ 0 & 0 & 0 & 0 & \cos\Theta_c & \sin\Theta_c \\ 0 & 0 & 0 & 0 & -\sin\Theta_c & \cos\Theta_c \end{pmatrix}. \tag{9}$$

The unitary transformation (8) defines a weak SO_6 space and, in particular, the weak hypercharge Y' and the weak isospin I' in a straightforward way. By this definition the weak quantum numbers Y', I' and I'_3 of l_m are identical with the corresponding (strong) SO_6 quantum numbers Y, I and I_3 of t_m ($m = 1, \ldots 6$). In addition, l_n and t_m have a common quantum number Z.

The simplest weak isodoublets of $Z = +1/3$ are given by

$$\boldsymbol{l}_1 \sim \mathbf{T}^+, \tag{10}$$

$$\boldsymbol{l}_2 \sim \mathbf{T}^0\cos\Theta_c + \mathbf{T}'^0\sin\Theta_c, \tag{11}$$

and the "Ξ-type" members of a (weak) SU_3 15-plet

$$\mathbf{M}^0 \sim [\boldsymbol{l}_3\boldsymbol{l}_3\bar{\boldsymbol{l}}_2], \tag{12}$$

$$\mathbf{M}^- \sim [\boldsymbol{l}_3\boldsymbol{l}_3\bar{\boldsymbol{l}}_1] \tag{13}$$

with $\boldsymbol{l}_3 = -\mathbf{T}^0\sin\Theta_c + \mathbf{T}'^0\cos\Theta_c$. Table II contains the relevant quantum numbers of the particles l_1, l_2 M^0 and M^- created by the operators $\boldsymbol{l}_1$, $\boldsymbol{l}_2$, $\mathbf{M}^0$ and $\mathbf{M}^-$, respectively. It should be noted that the structures (12)—(13) imply an SO_6 representation mixing due to the T—Θ effective-mass difference.

Table II

The quantum numbers of l_1, l_2, M^0 and M^-

	I'_3	I'	Y'	Z	Q	N
l_1	$\frac{1}{2}$	$\frac{1}{2}$	$\frac{1}{3}$	$\frac{1}{3}$	1	1
l_2	$-\frac{1}{2}$	$\frac{1}{2}$	$\frac{1}{3}$	$\frac{1}{3}$	0	1
M^0	$\frac{1}{2}$	$\frac{1}{2}$	$-\frac{5}{3}$	$\frac{1}{3}$	0	1
M^-	$-\frac{1}{2}$	$\frac{1}{2}$	$-\frac{5}{3}$	$\frac{1}{3}$	−1	1

If both leptons and hadrons belong to representations of SO_6, then the sum of leptonic and hadronic weak currents may be reduced to the single trion current (5). The choice of leptonic state assignments is restricted by the following empirical facts. (a) Baryon and lepton conservation. (b) Electron—muon symmetry and the apparent conservation of muon number. (c) V—A structure of leptonic interactions in the conventional form. (d) Cabibbo reduction of the weak coupling strength in semileptonic weak processes. We observe that these conditions are satisfied if the leptons are identified by

$$e^+ = l_1, \quad \bar{\nu}_e = l_2, \quad \nu_\mu = M^0, \quad \mu^- = M^- \tag{14}$$

with (10)—(13) (ν_μ and μ^- denote the muon-neutrino and the muon, respectively, which are assumed to be tightly bound states). In this way baryon and lepton conservations are due to the exact conservation of Z and N. The particles $e^+, \bar{\nu}_e$ and ν_μ, μ^- form two distinct isodoublets in the weak SO_6 space and the apparent conservation of muon number is connected with the (approximate) conservation of the weak hypercharge Y'. We may write the leptonic piece of the weak current (5) in terms of the doublets ν_e, e^- and ν_μ, μ^-. In this conventional form we recover the well known V—A structure which follows from the SO_6 properties (10)—(14) of leptons.

A unified two-triplet model of leptons and hadrons has already been proposed by KLEIN [18]. In his model a single four-component neutrino ν, e^- and μ^- are identified with the antitrions $\overline{\Theta}^0$, $\overline{\Theta^+}$ and $\overline{\Theta'^+}$, respectively. Other triplet models for leptons have also been discussed in the literature, some papers are listed in [19].

Motivated by the structure of leptonic and semileptonic weak interactions, we now suggest that the symmetry properties of leptonic states are fixed by relations (10)—(14). In addition, our model may lead to direct lepton production by a dissociation of colliding hadrons. This process occurs only at

very high energies, if the lowest Θ mass is sufficiently large. On the other hand, no absolutely stable exotic particles are to be expected according to the present experimental situation. The simplest Z-conserving dissociation process of two colliding baryons B and B' may be written in the schematic form

$$B + B' = (TT\bar{\Theta}) + (TT\bar{\Theta})' \to L_A + L_B + \bar{\Theta} + L'_A + L'_B + \bar{\Theta}' + \text{photons}, \quad (15)$$

where the common notation L is used for the leptons (14) which are characterized by $Z = 1/3$, $N = 1$ (The corresponding antiparticles of $Z = -1/3$, $N = -1$ will be denoted by $\bar{L}$). Due to the Z-conservation, the lowest antitrion $\bar{\Theta}$ cannot decay by emission of known bosons with $Z = 0$, $N = 0$. The only Z-conserving decay modes of $\bar{\Theta}$ lead to a baryon B_f and two leptons $\bar{L}$ with $Z = -1/3$, $N = -1$. These processes are assumed to be mediated by bosons Φ_x, with $Z = 2/3$, $N = 0$ and integer charge, possibly members of an undiscovered SU_3 triplet or sextet. Both representations 15 and 20″ of SO_6 contain bosons of this type [15]. We may now write the Z-conserving $\bar{\Theta}$-decays in the form

$$\bar{\Theta} \to \bar{L} + \Phi_x \longrightarrow \bar{L}' + B_f. \quad (16)$$

In particular, let us consider the decay of the $\bar{\Theta}^0$ constituents of protons by assuming that $\Phi_x = T'^0\overline{\Theta'^+}$ which is the isosinglet member of an SU_3 sextet. In this case the dominant decay modes involve processes of the type

$$\bar{\Theta}^0 \to \mu^+ + \underbrace{(T'^0\,\overline{\Theta})}_{\longrightarrow\ e^- + \Xi^0}, \quad (17)$$

$$\bar{\Theta}^0 \to \mu^+ + \underbrace{(T'^0\,\overline{\Theta'^+})}_{\longrightarrow\ \nu_e + \Xi^-}, \quad (18)$$

according to the approximate hypercharge conservation. Summarizing, "direct" lepton production involves the dissociation (15) of colliding hadrons. The subsequent decays of the $\bar{\Theta}$ constituents lead directly, without the well known intermediate particles π, K . . ., to energetic leptons and a baryon B_f (e.g. Ξ^0 or Ξ^-). The baryon B_f has, in general, conventional decay modes mediated by pions, kaons etc. resulting in muons and other well known particles. We may tentatively assume that processes of the type (15)—(18) leave no energy for a muon production of pion or kaon parentage within the energy region covered by the experiment of BERGESON et al. On the other hand, processes (15)—(18) represent simple possibilities for the X processes indicated by experiments of BERGESON et al. and DARDO et al. In this way the X particles might be identified with the antitrions $\bar{\Theta}$ and the bosons Φ_x.

III. Leptonic and semileptonic weak processes

We next add some remarks to the two-triplet model of conventional leptonic and semileptonic weak interactions. Within the dynamical framework of our previous paper [15], the most simple explanation involves the hypothetical intermediate bosons $W^{\pm}$ which are supposed to be bound trion—antitrion systems. We shall not assume any strong quadratic interactions of W's with hadrons.

In [15] we suggested a relativistic field equation for trions, which governs the dynamics of the model. This equation is covariant under transformations of the Poincaré and SO_6 groups ($P \otimes SO_6$). We now suppose that the weak violations of SO_6 and parity are connected with the asymmetries of the intermediate boson states $|W^{\pm}>$, possibly due to a spontaneous mixing. As a first step of self-consistent calculations, the symmetry structure of W's will be fixed by the following requirement. The intermediate boson W^{+} must be coupled to the weak trion current (5) by the universal (P and SO_6 covariant) interaction of trions. We propose that this interaction be given by the nonlinear term of the field equation (1) of [15]. According to our requirement, the symmetry structure of W's is fixed by the following Bethe—Salpeter amplitudes

$$\begin{aligned} &\langle 0 \,|\, T\mathbf{t}_m(x\alpha)\, \bar{\mathbf{t}}_n(y\beta) \,|\, W^{\pm}\rangle = \\ &\quad = \exp\left[- iq \cdot \frac{1}{2}(x-y)\right] \varphi^{\mu(W^{\pm})}_{\alpha m \beta n}(q; x-y)\, \tau\big(q\mu(W^{\pm})\big)\,, \end{aligned} \tag{19}$$

where α, β are spinor indices, q is the four-momentum of the state $|W^{\pm}>$ τ is the conventional one-boson amplitude of W's, satisfying $q^{\mu}\tau(q\mu(W^{\pm})) \sim 0$ and the leading term of φ has the form

$$\varphi^{\mu(W^{\pm})}_{\alpha m \beta n}(q; z) = [(1+\gamma_5)\,\gamma^{\mu}]_{\alpha\beta}\, V^{(\pm|15)}_{mn}(\Theta_c)\, f^{1(W^{\pm})}\big(q^2, z^2, (qz)^2\big) + \ldots\,. \tag{20}$$

Note that the function $f^{1(W^{\pm})}$ depends only on q and the relative coordinat $z = x—y$. (The matrix $V^{(\pm|15)}$ is defined by Equ. (6)). By substituting the amplitude (20) into Equ. (70) of [15] we observe that the contribution of W's corresponds to the effective interaction Lagrangian

$$L_W = g_W\, \bar{\mathbf{t}}\, \gamma^{\mu}(1+\gamma_5)\, V^{(+|15)}(\Theta_c)\, \mathbf{t} W^{(+)}_{\mu} + H.C. \tag{21}$$

with

$$g_W = -\,4\sqrt{2}\, G f^{1(W^{\pm})}(m_W^2, 0, 0)\,, \tag{22}$$

where m_W is the W mass and G denotes the coupling constant in the underlying field equation (1) of [15]. The form (21) verifies the structure (19)—(20) of intermediate bosons according to our requirement imposed previously. By an empirical fit of g_W and m_W the Lagrangian (21) may be regarded as a semi-

phenomenological basis of the CP conserving weak interactions in our SO_6 model.

Let us consider amplitudes (19)—(20). We observe that the intermediate bosons $W^{\pm}$ are of mixed parity leading to the well known parity violations in weak processes. In addition, W^+ and W^- are the charged members of an isotriplet in the *weak* SO_6 space (cf. Equs. (5)—(7)). This results in hypercharge violating weak interactions of the trion constituents of hadrons which are placed in the *strong* SO_6 space. In Fig. 1 the dynamical mechanism of the model is exemplified by a schematic diagram of the process $n + \nu_\mu \to p + \mu^-$.

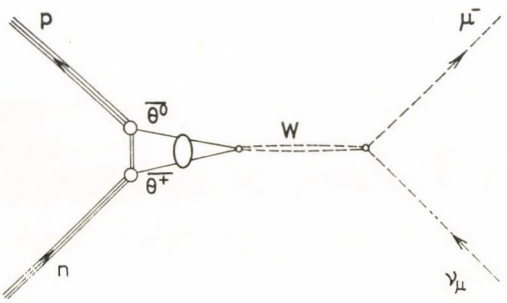

Fig. 1. Schematic diagram of the process $n + \nu_\mu \to p + \mu^-$

Finally, we shall point out some details. According to BACRY et al. [9] and GERSTEIN and WHIPPMANN [20] the known pseudoscalar bosons are to be assigned to the coregular representation 20′′ in the SO_6 model. Therefore, it is convenient to express the axial vector part of the matrix elements $\langle \Theta' | J^\mu | \Theta \rangle$, contributing to the simplest β processes, in terms of the matrices $\bar{\lambda}^{j(20'')}$ which belong to representation 20′′ of SO_6. These matrices are explicitly listed in [15]. We obtain

$$\begin{aligned} &\langle \Theta' | \bar{\mathbf{t}} \gamma^\mu (1+\gamma_5) V^{(\pm|15)}(\Theta_c) \mathbf{t} | \Theta \rangle = \\ &\quad = \langle \Theta' | \left[\bar{\mathbf{t}} \gamma^\mu V^{(\pm|15)}(\Theta_c) \mathbf{t} - \bar{\mathbf{t}} \gamma^\mu \gamma_5 V^{(\pm|20'')}(\Theta_c) \mathbf{t} \right] | \Theta \rangle \end{aligned} \tag{23}$$

with

$$V^{(\pm|20'')}(\Theta_c) = \frac{\bar{\lambda}^{1(20'')} \pm i \bar{\lambda}^{2(20'')}}{2} \cos \Theta_c + \frac{\bar{\lambda}^{4(20'')} \pm i \bar{\lambda}^{5(20'')}}{2} \sin \Theta_c . \tag{24}$$

By considering the (formal) current densities

$$\mathcal{F}^{j\mu} = \bar{\mathbf{t}} \frac{\bar{\lambda}^{j(15)}}{2} \gamma^\mu \mathbf{t} , \tag{25}$$

$$\mathcal{F}_5^{j\mu} = \bar{\mathbf{t}} \frac{\bar{\lambda}^{j(20'')}}{2} \gamma^\mu \gamma_5 \mathbf{t} \tag{26}$$

for $j = 1 \ldots 8$, we may recover the chiral $SU_3 \times SU_3$ algebra in a straightforward way.

We conclude that the two-triplet model may be a useful tool for the study of various leptonic and semileptonic processes including a direct production of leptons at very high energies.

Acknowledgement

The author is very indebted to Dr. A. SOMOGYI for a valuable discussion on the Utah experiment.

REFERENCES

1. H. E. BERGESON, J. W. KEUFFEL, M. O. LARSON, E. R. MARTIN and G. W. MASON, Phys. Rev. Letters, **19**, 1487, 1967.
2. H. E. BERGESON, J. W. KEUFFEL, M. O. LARSON, G. W. MASON and J. L. OSBORNE, Phys. Rev. Letters, **21**, 1089, 1968.
3. R. J. STEFANSKI, R. K. ADAIR and H. KASHA, Phys. Rev. Letters, **20**, 950, 1968.
4. W. F. NASH and A. W. WOLFENDALE, Phys. Rev., Letters, **20**, 698, 1968.
5. J. D. BJORKEN, S. PAKVASA, W. SIMMONS and S. F. TUAN, quoted in [2].
6. C. RYAN, S. OKUBO, R. E. MARSHAK, Nuovo Cimento, **34**, 753, 1964; S. V. PEPPER, C. RYAN, S. OKUBO and R. E. MARSHAK, Phys. Rev., **137B**, 1959, 1965; S. OKUBO, Nuovo Cimento, **57A**, 794, 1968, earlier papers are quoted there.
7. W. R. SHELDON, W. G. CANTRELL and N. M. DULLER, Phys. Rev. Letters, **22**, 312, 1969.
8. Y. HARA, Phys. Rev., **134B**, 701, 1964.
9. H. BACRY, J. NUYTS and L. VAN HOVE, Nuovo Cimento, **35**, 510, 1965.
10. L. VAN HOVE in: Preludes in Theoretical Physics (Amsterdam, 1965).
11. F. GÜRSEY, T. D. LEE and M. NAUENBERG, Phys. Rev., **125B**, 467, 1964.
12. M. DARDO, P. PENENGO and K. SITTE, Nouvo Cimento, **58A**, 59, 1968.
13. E. g. J. BJORNBOE et al., Proc. Intern. Conf. Cosmic Rays, Calgary, 1967; H. KASHA and J. STEFANSKI, Phys. Rev., **172**, 1297, 1968.
14. K. LADÁNYI, Nuovo Cimento, **45**, 289, 1966.
15. K. LADÁNYI, Nuovo Cimento, **48**, 927, 1967.
16. T. D. LEE, Nuovo Cimento, **35**, 933, 1965.
17. K. MORITA, Progr. Theor. Phys., **38**, 681, 1967.
18. O. KLEIN, Phys. Rev. Letters, **16**, 63, 1966.
19. A. GAMBA, R. E. MARSHAK and S. OKUBO, Proc. Natl. Acad. Sci., **45**, 881, 1959; M. GELL-MANN, California Institute of Technology Report CTSL—20, 1961; R. GATTO, Nuovo Cimento, **27**, 313, 1963; V. GUPTA, Phys. Rev., **135B**, 783, 1964; S. OKUBO, C. RYAN and R. E. MARSHAK, Nuovo Cimento, **34**, 759, 1964; T. DAS and K. T. MAHANTHAPPA, Nuovo Cimento, **44A**, 469, 1966.
20. I. S. GERSTEIN and M. L. WHIPPMANN, Phys. Rev., **137B**, 1522, 1965.

ДВУХТРИПЛЕТНАЯ МОДЕЛЬ «НЕПОСРЕДСТВЕННОЙ» ПРОДУКЦИИ МЮОНОВ

К. ЛАДАНЬИ

Резюме

Предлагается особенная двухтриплетная модель «непосредственных» продукций лептонов, предполагая, что и лептоны и гадроны принадлежат к представлениям шестимерной ротационной группы SO_6.

Acta Physica Academiae Scientiarum Hungaricae, Tomus 27, pp. 559—563 (1969)

COMMUNICATIO BREVIS

ON A SIMPLE CONFIGURATION INTERACTION METHOD USING NON-ORTHOGONAL BASIS FUNCTIONS*

By

L. URBÁN

RESEARCH GROUP FOR THEORETICAL PHYSICS OF THE HUNGARIAN ACADEMY OF SCIENCES. BUDAPEST

(Received 10. IX. 1968)

In the classical configuration interaction (CI) method [1] we write the approximate state fuction of an N-body problem as a linear combination of the configurations Φ_i

$$\Psi = \sum_i c_i \Phi_i , \tag{1}$$

The configurations Φ_i are built up from one-particle functions φ_i in such a way that the symmetry properties of the Hamiltonian and the state function are taken into account. We determine Ψ from the requirement

$$(\Psi|\mathscr{H}|\Psi) = \sum_{i,k} c_i^* c_k (\Phi_i|\mathscr{H}|\Phi_k) = \min \tag{2}$$

with the constraint

$$(\Psi|\Psi) = \sum_{i,k} c_i^* c_k (\Phi_i|\Phi_k) = 1 . \tag{3}$$

From requirement (2) we get a system of linear homogeneous equations and we determine the approximate energy E by solving the secular equation of the system.

In the CI method some mathematical difficulties have to be overcome. One of these is connected with the construction of the symmetry-adapted configurations. This construction is laborious if the number of particles is $N > 2$ [2]. Other complications are introduced if we use non-orthogonal orbitals [3]. In this paper we propose a method where these difficulties do not arise. In the proposed method we have to construct only one symmetry-adapted configuration and we can handle the non-orthogonal orbitals easily.

The main features of this method are as follows.

* Dedicated to Prof. P. GOMBÁS on his 60th birthday.

1. We choose a state function Ψ_0 as a zeroth approximation and determine the energy E_0 in this approximation

$$E_0 = \frac{(\Psi_0|\mathscr{H}|\Psi_0)}{(\Psi_0|\Psi_0)} .$$

2. We define a derivative along the direction Ψ of the functional $E(\Psi)$ in the "point" Ψ_0 and we determine the state $\overline{\Psi}$ where the derivative is minimal.

3. From the states Ψ_0 and $\overline{\Psi}$ we determine the first approximation Ψ_1 and $E_1 < E_0$, etc.

Let us introduce the following notations:

$\mathscr{H}$ is the Hamiltonian of the N-particle system,

Λ is a constant of motion i.e. $[\Lambda, \mathscr{H}] = 0$,

$\varphi_1, \varphi_2, \ldots, \varphi_r$ is the one-particle basis,

$\Phi_1, \Phi_2, \ldots, \Phi_s$ is the N-particle basis constructed from the one-particle functions and

L_Φ is the subspace of the Hilbert space determined by N-particle basis.

We do not require the orthogonality of φ_i-s and Φ_i-s, and we do not assume that Φ_i-s are symmetry-adapted. But we require that φ_i-s and Φ_i-s have to form a basis, i.e. they have to be linear independent. We can formulate our problem in the following way: Find the minimum of the expectation value

$$E(\Psi) = \frac{(\Psi|\mathscr{H}|\Psi)}{(\Psi|\Psi)} \tag{4}$$

with the constraint*

$$\Lambda\Psi = \lambda\Psi , \quad \text{where} \quad \Psi \in L_\Phi .$$

As a zeroth approximation we construct a state function Ψ_0 with the properties

$$\begin{aligned} &(\Psi_0|\Psi_0) = 1 , \\ &\Lambda\Psi_0 = \lambda\Psi_0 , \\ &\Psi_0 \in L_\Phi . \end{aligned} \tag{5}$$

The last condition can be written as

$$\Psi_0 = \sum_i c_{0i} \Phi_i . \tag{6}$$

* We work here with one constant of motion but the generalization for the case of more constants of motion is trivial.

The energy in this approximation is

$$E_0 = (\Psi_0|\mathscr{H}|\Psi_0) .$$

Let us define the derivative along the direction Ψ of the functional $E(\Psi)$ in the "point" Ψ_0 as [4]

$$\frac{dE}{d\Psi} = \lim_{\alpha \to 0} \frac{E(\Psi_0 + \alpha\Psi) - E(\Psi_0)}{\alpha \|\Psi\|} . \tag{7}$$

Using (4) we get from (7)

$$\frac{dE}{d\Psi} = \frac{(\Psi|\mathscr{H} - E_0|\Psi_0) + (\Psi_0|\mathscr{H} - E_0|\Psi)}{\|\Psi\|} . \tag{8}$$

We can show easily that (8) is really a derivative. If α is a positive infinitesimal quantity we can write

$$\begin{aligned} E(\Psi_0 + \alpha\Psi) &= \frac{(\Psi_0 + \alpha\Psi|\mathscr{H}|\Psi_0 + \alpha\Psi)}{(\Psi_0 + \alpha\Psi|\Psi_0 + \alpha\Psi)} = \\ &= E_0 + \alpha \frac{(\Psi|\mathscr{H} - E_0|\Psi_0) + (\Psi_0|\mathscr{H} - E_0|\Psi)}{\|\Psi\|} , \end{aligned} \tag{9}$$

i.e. $dE/d\Psi$ is a derivative.

It can be seen from Equ.(9) that in the case $dE/d\Psi < 0$, $E(\Psi_0 + \alpha\Psi)$ decreases when α increases. We use this fact to construct the first approximation.

Note that the derivative $dE/d\Psi$ does not depend on $\|\Psi\|$; we can choose $\|\Psi\| = 1$.

We write $\Psi \in L_\Phi$ as a linear combination of the basis elements

$$\Psi = \sum_i x_i \Phi_i . \tag{10}$$

Let us introduce the following notations

$$\begin{aligned} (\Phi_i|\Phi_k) &= \mathscr{M}_{ik}, \\ (\Phi_i|\mathscr{H}|\Phi_k) &= \mathscr{H}_{ik} . \end{aligned} \tag{11}$$

Using (8), (10) and (11) we get

$$\frac{dE}{d\Psi} = \sum_{i,k} \{x_i^*(\mathscr{H}_{ik} - E_0 \mathscr{M}_{ik}) c_{0k} + c_{0k}^* (\mathscr{H}_{ki} - E_0 \mathscr{M}_{ki}) x_i\} . \tag{12}$$

We are looking for the minimum value of $dE/d\Psi$ with the condition

$$(\Psi|\Psi) = \sum_{i,k} x_i^* \mathscr{M}_{ik} x_k = 1 . \tag{13}$$

The minimum is determined by the system of linear inhomogeneous equations

$$\sum_k \mathscr{M}_{ik} x_k = \frac{1}{\mu} \sum_k (\mathscr{H}_{ik} - E_0 \mathscr{M}_{ik}) c_{0k}, \tag{14}$$

where μ is the Lagrange multiplier determined by (13), or in matrix form

$$\boldsymbol{MX} = \frac{1}{\mu} (\boldsymbol{H} - E_0 \boldsymbol{M}) \boldsymbol{c}_0 . \tag{15}$$

The solution of (15) is

$$\boldsymbol{X} = \frac{1}{\mu} (\boldsymbol{M}^{-1} \boldsymbol{H} - \boldsymbol{E}_0) \boldsymbol{c}_0$$

and from (13)

$$\mu = \pm \sqrt{\boldsymbol{c}_0^+ \boldsymbol{H} \boldsymbol{M}^{-1} \boldsymbol{H} \boldsymbol{c}_0 - E_0^2}. \tag{16}$$

We get the minimum value of (12) with the minus sign in (16)

$$\frac{dE}{d\Psi_{\min}} = -2 \sqrt{\boldsymbol{c}_0^+ \boldsymbol{H} \boldsymbol{M}^{-1} \boldsymbol{H} \boldsymbol{c}_0 - E_0^2}. \tag{17}$$

It can easily be seen that

$$\boldsymbol{c}_0^+ \boldsymbol{H} \boldsymbol{M}^{-1} \boldsymbol{H} \boldsymbol{c}_0 - E_0^2 \geqslant 0 ,$$

where the equality is valid only if

$$\mathscr{H} \Psi_0 = E_0 \Psi_0$$

holds, i.e. Ψ_0 is an eigenfunction of $\mathscr{H}$. If the equality is valid we know the exact eigenfunction of $\mathscr{H}$. If that is not the case we determine the state

$$\overline{\Psi} = \sum_i x_i \Phi_i ,$$

which has the property that $E(\Psi_0 + \alpha\overline{\Psi})$ decreases when α increases from zero to α_0, where α_0 is the smallest positive root of the equation

$$\frac{d}{d\alpha} E(\Psi_0 + \alpha\overline{\Psi}) = 0 . \tag{18}$$

Let

$$\Psi_1 = \frac{\Psi_0 + \alpha_0 \overline{\Psi}}{\|\Psi_0 + \alpha_0 \overline{\Psi}\|}, \tag{19}$$

then

$$E_1 = (\Psi_1|\mathscr{H}|\Psi_1) < E_0 \tag{20}$$

iholds.

We take Ψ_1 as the first approximation, and from it we determine the second approximation in the same way, etc. In this way we get a set of energies $E_0, E_1, E_2, \ldots$ and

$$E_0 > E_1 > E_2 > \ldots \tag{21}$$

holds.

Now we examine the symmetry properties of the state functions Ψ_0, Ψ_1, etc.

Introducing the operator P projecting on the subspace L_Φ

$$P = \sum_{i,k} |\Phi_i) \mathscr{M}^{-1}_{ik} (\Phi_k| \tag{22}$$

the state $\overline{\Psi}$ can be written as

$$\overline{\Psi} = (P\mathscr{H} - E_0)\, \Psi_0. \tag{23}$$

Using the fact that Λ is a constant of motion and from Equ. (5)

if

$$\begin{aligned} \Lambda\overline{\Psi} &= \lambda\overline{\Psi} \\ P\Lambda - \Lambda P &= 0 \end{aligned} \tag{24}$$

is valid. If we choose the basis in such a way that

$$\Lambda\Phi_i = \sum_{k=1}^{s} c_{ik} \Phi_k \tag{25}$$

holds for every i, condition (24) is fulfilled and the symmetry remains in every approximation.

Applications based on this method will be published in a subsequent paper.

The author would like to thank Prof. P. GOMBÁS for his kind interest in this work. Thanks are also due to Dr. D. KISDI for his valuable help and advice.

REFERENCES

1. R. DAUDEL, R. LEFEBVRE and C. MOSER. Quantum Chemistry, Interscience Publishers, Inc. New York, 1959.
2. J. L. CALAIS, Uppsala preprint, No. 52. 1960.
3. H. SHULL and P. O. LÖWDIN, J. Chem. Phys., **23,** 1362, 1955; P. O. LÖWDIN and H. SHULL, Phys. Rev., **101,** 1730, 1956.
4. KANTOROWICH—AKILOW: Funktionalanalysis in normierten Räumen, Akademie Verlag, Berlin, 1964.

INDEX

I. Kovács: General Form of the Centrifugal Term in the Rotational Spectra. — *И. Ковач:* Общая форма центробежного члена в ротационном спектре 5

F. Csikor and *K. Nagy:* Radiative Corrections to Muon Decay with Finite Neutretto Mass. — *Ф. Чикор* и *К. Надь:* Радиационные коррекции к распаду мюонов с конечными массами нейтретто 11

A. Veres and L. Lakosi: Measurement of the Cross Section for the Isomeric Activation of ^{115}In by γ-Rays from ^{24}Na Source — *А. Вереш* и *Л. Лакоши:* Измерение эффективного сечения активации ядерного изомера ^{115}In γ-лучами ^{24}Na 19

I. Gaál, Z. Morlin and *I. Tarján:* On the Kinetics of the Phase Transformation of CsCl-Crystals II. — *И. Гал, З. Морлин* и *И. Тарьян:* О кинематике фазового перехода кристаллов CsCl II. 25

L. Jánossy: The Hydrodynamical Model of Wave Mechanics. The Many Body Problem. *Л. Яноши:* Гидродинамическая модель волновоймеханики. Задача многих тел .. 35

L. Pál: First-Order Magnetic Phase Transitions. — *Л. Пал:* Магнитные фазовые переходы первого рода 47

A. Frenkel and G. Marx: Millistrong C Violation and η Decay — *А. Френкель* и *Г. Маркс:* Миллисильное нарушение C симметрии и распад η мезона 87

J. I. Horváth and *I. K. Gyémánt:* On the Theory of Fermion Density Operators. I. The Definition of the One-Particle States and Cluster Expansions of the Density Operators — *Я. И. Хорват* и *И. К. Дьемант:* О теории операторов плотности фермионов I. Определение одночастичных состояний и кластерное разложение операторов плотности 111

F. Berencz: Berechnungen der Zustände $1sns\ ^1\Sigma_g^+$ des Wasserstoffmoleküls auf Grund der Methode der korrelationsmässigen Molekülbahnen. — *Ф. Беренц:* Вычисление состояния $1sns\ ^1\Sigma_g$ молекулы водорода на основе метода корреляционно-умеренных молекулярных орбит 131

C. Sándorfy: On the Structure and Spectra of σ-Electron Systems — *Ц. Шандорфи:* О структуре и спектре σ-электронных систем 151

T. Tietz and *S. Krzemiński:* Quantum and Correlation Corrections to the Thomas—Fermi Potential — *Т. Титц* и *С. Крземинский:* Квантовые и корреляционные поправки к потенциалу Томаса—Ферми 161

A. Lemberger and *R. Pauncz:* Remarks Concerning the Theoretical Explanation of Hund's Rule — *А. Лембергер* и *Р. Паунц:* Примечания относительно теоретического толкования правила Гунда 169

E. Kapuy: Developments in the Separated Pair Theory — *Э. Капуи:* Развития в разделенной парной теории 179

H. Preuss: Einige Bemerkungen zum kombinierten Näherungsverfahren und zum effektiven Potential — *Г. Прайс:* Некоторые замечания к комбинированным приближенным методам и эффективным потенциалам 191

V. Fock: On the Canonical Transformation in Classical and Quantum Mechanics. — *В. Фок:* О каноническом преобразовании в классической и квантовой механике 219

N. Grün und *B. Kockel:* Vergleich einer LCAO-MO- und einer VB-Zustandsfunktion des Li_2-Moleküls. — *Н. Грюн* и *Б. Кокель:* Сравнение функций состояния LCAO-MO и VB 225

A. J. R. Prentice and *D.ter Haar:* Cosmic Rays and the Origin of the Solar System. — *А. Й. Р. Прентис* и *Д. Тер Хар:* Космические лучи и начало солнечной системы 231

R. Gáspár and *I. Tamássy-Lentei:* Polynomial Wave Functions in Elliptical Coordinates for Molecules. — *Р. Гашпар* и *И. Тамаши-Лентеи:* Полиномиальные волновые функции в эллиптических координатах для молекул 237
W. Kołos: Some Accurate Results for Three-Particle Systems. — *В. Колос:* Несколько точных результатов для систем трех частиц 241
K. L. Nagy: Lee Model as a Z Limit. — *К. Л. Надь:* Модель Ли как Z-предел 253
M. Süveges: Is Poincaré Invariance Compatible with General Relativity? — *М. Шювегеш:* Инвариантность Пуанкаре совместима с общей теорией относительности? 261
I. Abonyi: Small Amplitude Waves and Weak Discontinuities in the Relativistic Hydrodynamics of an Ideal Fluid. — *И. Абони:* Волны небольших амплитуд и слабые разрывы в релятивистической гидродинамике идеальной жидкости 269
R. Voszka and *A. Watterich:* Study of V-Centres Stable at Room Temperature in NaCl(Ca) Crystals. — *Р. Воска* и *А. Ваттерих:* Исследование V-центров, стабильных при комнатной температуре, в кристаллах NaCl(Ca) 277
D. Kisdi: A Simplified Method for Calculating the Internal Structure of Neutron Stars. — *Д. Кишди:* Упрощенный метод для определения внутренней структуры нейтронных звезд 289
P. Szépfalusy: Sum Rules and Their Application in the Theory of Superfluid Helium. — *П. Сепфалуши:* Правила сумм и их применение в теории сверхтекучего гелия 299
G. Roth: Oscillations of a Relativistic Electron Plasma in an External Magnetic Field. — *Г. Рот:* Колебания релятивистической электронной плазмы во внешнем магнитном поле 309
W. A. Bingel, R.-J. Koch and *W. Kutzelnigg:* Simulation of the Influence of Core Electrons by a Pseudopotential II. — *В. А. Бингел, Р. Й. Кох* и *В. Куцельниг:* Подражение влияния электронов атомного остатка псевдопотенциалом II. 323
C. A. Coulson: Further Note on the Saddle-Point Character of Hartree—Fock Wave Functions. — *К. А. Кульсон:* Дальнейшие замечания о седловоточечном характере волновых функций Хартри—Фока 345
В. В. Толмачев: Интерпретация метода Хартри—Фока как метода частичного суммирования атомных Фейнмановских диаграмм — *V. V. Tolmachev:* Interpretation of the Hartree—Fock Method as the Method of Partial Summation of Atomic Feynman Diagrams 351
R. Janoschek: Wellenmechanische Strukturuntersuchung am Li_4. — *Р. Яношек:* Волновомеханическое исследование структуры Li_4 373
M. Schoenborn and *I. G. Csizmadia:* Vibrational Analysis of ab Initio Potential Energy Surfaces for Nitryl Fluoride. — *М. Шэнборн* и *И. Г. Чизмадия:* Вибрационный анализ поверхностей ab initio потенциальной энергии для нитрилофлуорида 377
W. H. E. Schwarz: Das kombinierte Näherungsverfahren II. — *В. Г. Э. Шварц:* Комбинированное приближение II. 391
Th. Neugebauer: Über die physikalische Realität des Lennard-Jonesschen Potentials. — *Т. Найгебауэр:* О физической реальности потенциала Ленарда—Джонса 405
G. Pataki: Effect of Traps on Steadily Travelling Domains in Semiconductors. — — *Г. Патаки:* Влияние ловушек на стационарно движущиеся домены в полупроводниках 421
G. Györgyi: Integration of the Dynamical Symmetry Groups for the $-1/r$ Potential. — *Г. Дьерди:* Интегрирование динамических групп симметрии для потенциала $-1/r$ 435
R. Gáspár: New Foundations for the Thomas—Fermi Model. — *Р. Гашпар:* Новые обоснования модели Томаса—Ферми 441
B. Pődör: Negative Magnetoresistance of Compensated n-Type GaAs at 77 °K Temperature. — *Б. Пэдэр:* Отрицательное магнетосопротивление в компенсированном арсениде галлия n-типа при температуре 77 °К 449
R. Karazija, P. Bogdanovicius and *A. Jucys:* On the Numerical Solution of Hartree—Fock Equations Independent of Coupling Scheme. — *Р. И. Каразия, П. О. Богдановичус* и *А. Юцис:* К вопросу о решении уравнений Хартри—Фока, не зависящих от типа связи, численным методом 467
G. Del Re: Model ab Initio Calculations and the Foundation of the MO-LCAO Method. — *Джузеппе Дэл Ре:* Модель ab initio вычислений и обоснование метода MO-LCAO 477

E. Clementi, J. M. André, M. Cl. André, D. Klint and *D. Hahn:* Study of the Electronic Structure of Molecules. X. Ground State for Adenine, Cytosine, Guanine and Thyamine. — *Э. Клементи, Й. М. Андре, М. Кл. Андре, Д. Клинт* и *Д. Хан:* Изучение электронной структуры молекул. X. Основное состояние для аденина, цистозина, гуанина и тиамина 493

J. Kóta and *A. Somogyi:* Some Problems of Investigating Periodicities of Cosmic Ray Time Series. — *Й. Кота* и *А. Шомоди:* Некоторые проблемы исследованной периодичности временной серии космических лучей 523

K. Ladányi: Two-Triplet Model of "Direct" Muon Production. — *К. Ладаньи:* Двухтриплетная модель «непосредственной» продукции мюонов..... 549

COMMUNICATIO BREVIS

L. Urbán: On a Simple Configuration Interaction Method Using Non-Orthogonal Basis Functions 559

Printed in Hungary

A kiadásért felel az Akadémiai Kiadó igazgatója — Műszaki szerkesztő: Farkas Sándor
A kézirat nyomdába érkezett: 1969. V. 5. — Terjedelem: 49,50 (A/5) ív, 105 ábra

69.67592 Akadémiai Nyomda, Budapest — Felelős vezető: Bernát György

The *Acta Physica* publish papers on physics, in English, German, French and Russian
The *Acta Physica* appear in parts of varying size, making up volumes.
Manuscripts should be addressed to:

Acta Physica, Budapest 502, P. O. B. 24.

Correspondence with the editors and publishers should be sent to the same address.
The rate of subscription to the *Acta Physica* is 165 forints a volume. Orders may be placed with "Kultúra" Foreign Trade Company for Books and Newspapers (Budapest I., Fő u. 32. Account No. 43-790-057-181) or with representatives abroad.

Les *Acta Physica* paraissent en français, allemand, anglais et russe et publient des travaux du domaine de la physique.
Les *Acta Physica* sont publiés sous forme de fascicules qui seront réunis en volumes.
On est prié d'envoyer les manuscrits destinés à la rédaction à l'adresse suivante:

Acta Physica, Budapest 502, P. O. B. 24.

Toute correspondance doit être envoyée à cette même adresse.
Le prix de l'abonnement est de 165 forints par volume.
On peut s'abonner à l'Entreprise du Commerce Extérieur de Livres et Journaux «Kultúra» (Budapest I., Fő u. 32. — Compte-courant No. 43-790-057-181) ou à l'étranger chez tous les représentants ou dépositaires.

«*Acta Physica*» публикуют трактаты из области физических наук на русском, немецком, английском и французском языках.
«*Acta Physica*» выходят отдельными выпусками разного объема. Несколько выпусков составляют один том.
Предназначенные для публикации рукописи следует направлять по адресу:

Acta Physica, Budapest 502, P. O. B. 24.

По этому же адресу направлять всякую корреспонденцию для редакции и администрации.
Подписная цена «*Acta Physica*» — 165 форинтов за том. Заказы принимает предприятие по внешней торговле книг и газет «*Kultúra*» (Budapest I., Fő u. 32. Текущий счет: № 43-790-057-181) или его заграничные представительства и уполномоченные.

213,— Ft

Reviews of the Hungarian Academy of Sciences are obtainable at the following addresses:

ALBANIA

Ndermarja Shtetnore e Botimeve
Tirana

AUSTRALIA

A. Keessing
Box 4886, GPO
Sydney

AUSTRIA

Globus Buchvertrieb
Salzgries 16
Wien I

BELGIUM

Office International de Librairie
30, Avenue Marnix
Bruxelles 5

Du Monde Entier
5, Place St. Jean
Bruxelles

BULGARIA

Raznoiznos
1, Tzar Assen
Sofia

CANADA

Pannonia Books
2, Spadina Road
Toronto 4, Ont.

CHINA

Waiwen Shudian
Peking
P. O. B. 88

CZECHOSLOVAKIA

Artia
Ve Směčkách 30
Praha 2

Poštovní novinová služba
Dovoz tisku
Vinohradská 46
Praha 2

Mad'arská Kultura
Václavské nám. 2
Praha I

Poštová novinová služba
Dovoz tlače
Leningradská 14
Bratislava

DENMARK

Ejnar Munksgaard
Nörregade 6
Copenhagen

FINLAND

Akateeminen Kirjakauppa
Keskuskatu 2
Helsinki

FRANCE

Office International de Documentation et Librairie
48, rue Gay Lussac
Paris 5

GERMAN DEMOCRATIC REPUBLIC

Deutscher Buch-Export und Import
Leninstraße 16
Leipzig 701

Zeitungsvertriebsamt
Fruchtstrasse 3—4
1004 Berlin

GERMAN FEDERAL REPUBLIC

Kunst und Wissen
Erich Bieber
Postfach 46
7 Stuttgart S.

GREAT BRITAIN

Collet's Holdings Ltd.
Dennington Estate
London Rd.
Wellingborough. Northants.

Robert Maxwell and Co. Ltd.
Waynflete Bldg. The Plain
Oxford

HOLLAND

Swetz and Zeitlinger
Keizersgracht 471—487
Amsterdam C.

Martinus Nijhof
Lange Voorhout 9
The Hague

INDIA

Current Technical Literature
Co. Private Ltd.
India House OPP
GPO Post Box 1374
Bombay I

ITALY

Santo Vanasia
Via M. Macchi 71
Milano

Libreria Commissionaria Sansoni
Via La Marmora 45
Firenze

JAPAN

Nauka Ltd.
92, Ikebukur O-Higashi 1-chome
Toshima-ku
Tokyo

Maruzen and Co. Ltd.
P. O. Box 605
Tokyo-Central

Far Eastern Booksellers
Kanda P. O. Box 72
Tokyo

KOREA

Chulpanmul
Phenjan

NORWAY

Johan Grundt Tanum
Karl Johansgatan 43
Oslo

POLAND

RUCH
ul. Wronia 23
Warszawa

ROUMANIA

Cartimex
Str. Aristide Briand 14—18
Bucureşti

SOVIET UNION

Mezhdunarodnaya Kniga
Moscow G—200

SWEDEN

Almquist and Wiksell
Gamla Brogatan 26
Stockholm

USA

Stechert Hafner Inc.
31, East 10th Street
New York, N. Y. 10003

Walter J. Johnson
111, Fifth Avenue
New York, N. Y. 10003

VIETNAM

Xunhasaba
19, Tran Quoc Toan
Hanoi

YUGOSLAVIA

Forum
Vojvode Mišića broj 1
Novi Sad

Jugoslovenska Knjiga
Terazije 27
Beograd